1992

Palynological investigations of Cenomanian chalks and marls from England

Duane, Ailbhe Maire

Palynological investigations of Cenomanian chalks and marls from England

by

Ailbhe Maire Duane B.A. Mod. (Hons), M.Sc.

Thesis submitted in partial fulfillment for the Degree of Doctor of Philosophy to the Council for National Academic Awards

Research conducted at Polytechnic South West

May 1992

in collaboration with the British Geological Society

ABSTRACT

Palynological investigations of Cenomanian chalks and marls from England

Ailbhe Maire Duane

The palynological analysis of chalk and marl samples from Cenomanian sections sampled at high resolution has yielded largely diverse and abundant, well-preserved microplankton assemblages. Four sections have been investigated, three from the Dover-Folkestone Warren area, south-east England and the fourth from South Ferriby, South Humberside, north-east England. The dinoflagellate cysts present accord well with previously described Cenomanian microplankton assemblages from western Europe, and are assignable to the established *Litosphaeridium siphonophorum* Zone of Davey (1970). Full descriptions of all dinoflagellate cyst species found have been included. A new species, *Litosphaeridium* sp. A is believed to be indicative of latest Cenomanian to earliest Turonian in England. A new status is suggested for *Pterodinium cingulatum polygonalis* and *Palaeohystrichophora pauciestosa* is believed to be a junior synonym of *P. infusorioides.*

Dinoflagellate cysts assemblages have been investigated with the purpose of reconstructing the palaeoenvironment of the Cenomanian Chalk Sea. To this aim, samples were prepared qualitatively and quantitatively and data produced from normal logging techniques were investigated using several statistical techniques. Finally, such palynological data were integrated in a multidiscipline geological framework in order to interpret the data further.

The application of quantitative preparation techniques has shown that the introduction of an oxidation stage causes mechanical loss of a significant proportion of the palynological residue. A further outcome of such quantitative techniques is the recognition that marl samples consistently yield more abundant palynological residues than do marly chalk and chalk lithologies, based on counts of dinoflagellate cysts per gramme of sediment.

Statistical techniques such as diversity indices, cluster analysis and fourier analysis (spectral analysis) were applied to palynological data sets. As a result it is suggested that the percentage presence of certain dinoflagellate cysts species is strongly dependent on lithology and thus allows recognition of the lithological rhythmicity. Other key dinoflagellate cysts species appear to be controlled by palaeotemperature. *Palaeohystrichophora infusorioides* is therefore recognised as a slightly cooler water cyst (23°C), while *Cleistosphaeridium huguoniotii* and *Cyclonephelium distinctum* both are interpreted as being slightly warmer water cysts (25°C). Cluster analysis has successfully identified the existence of two dinoflagellate cyst associations in the Middle Cenomanian, which are linked to the Mid-Cenomanian non-sequence of Carter and Hart (1977) as they occur immediately above and below the non-sequence. Statistical interpretation of the Late Cenomanian dinoflagellate cyst assemblage of South Ferriby confirms that it records stressed palaeoenvironmental conditions.

LIST OF CONTENTS

LIST OF FIGURES

List of Tables

List of accompanying material

ACKNOWLEDGEMENTS

I am grateful to all those who have assisted in the production of this thesis however, some deserve special thanks.

Many members of staff of the Polytechnic South West have been helpful to me while carrying out this thesis. Both the academic and technical staff of the Dept. of Geological Sciences are thanked for all their assistance, especially Drs S.A. Caswell and B.A. Tocher. Also thanked are the staff of Media Services and Dr. T.J. Green of Computing Services.

Prof. M.B. Hart and Dr. R. Harland are both sincerely thanked for their help, inspiration and guidance throughout the many stages of metamorphosis of this thesis.

My thanks to Dr. P. Ditchfield and P. Dodsworth for the provision of samples and much information relating to this project.

I would like to mention my postgraduate colleagues at Plymouth, and the camaraderie experienced there. R.D. Eddies and A.R. Wooler are thanked for their substantial computing assistance. My special thanks to M.E.J. FitzPatrick for her companionship and the sharing of her palynological knowledge.

Finally, I would like to pay special thanks to my parents for their continued support and encouragement throughout. Also, my thanks to Alexander for being so supportive and helping me keep things in perspective.

This research was carried out during the tenure of a Polytechnic South West Research Assistantship.

DECLARATION

This is to certify that work submitted for the Degree of Doctor of Philosophy under the title "Palynological investigations of Cenomanian chalks and marls from England" is the result of original work.

All authors and works consulted are fully acknowledged. No part of this work has been accepted in substance for any other degree and is not currently being submitted in candidature for any other degree.

During the tenure of this thesis, one paper has been published:

Hart, M.B., Dodsworth, P., Ditchfield, P.W., Duane, A.M. and Orth, C.J. 1991. The Late Cenomanian event in eastern England. *Historical Biology*, vol. 5, pp. 339-354.

Candidate

Ailbhe M. Duane

A.M. Duane

Research supervisor

Malcolm Hart

Prof. M.B. Hart

Chapter 1

INTRODUCTION

1.1. General introduction

This study deals with the palaeo-oceanographical implications derived from the dinoflagellate cyst assemblages present within Cenomanian strata from specific sections of south and north-eastern England.

During the mid-Cretaceous this area of Western Europe was positioned between 30° and 40°N palaeolatitude. Between the Late Jurassic and Early Cretaceous, this region comprised a more or less land-locked epeiric sea. To the south lay the Tethys, to the west the North Atlantic was opening, to the east the Precambrian and Palaeozoic massifs of Central Europe, and to the north-west lay the North American shield areas of Scotland and Greenland.

From Albian times onwards within the Cretaceous period, this area of Western Europe experienced a period of tectonic quiescence. Broadly speaking therefore, sedimentation within this region can be simplistically interpreted as an interaction of the tectonic framework and the transgressive history (Reyment and Bengtson, 1985).

The Cretaceous Chalk sea is believed (Hancock, 1976) to have been a sea of normal salinity experiencing average temperatures of about 30°C (Scholle, 1974), and which was between 100-600 m. deep. Individual basins, perhaps 100's of kilometers wide existed within this Chalk seaway which were themselves divided into troughs and highs (Hancock, 1976).

1.2. Dinoflagellate biology

Dinoflagellates are a group of microplankton present in both ancient and modern seas and oceans. Dinoflagellates are opportunistic aquatic algae which occupy a variety of habitats. They are known to exist in the surface waters of the open ocean and in the seas of the continental margin as well as from freshwater lakes and bogs. The greatest number of dinoflagellate cyst producing species today occur on the continental margin in habitats ranging from coastal lagoons and bays to the continental slope.

Factors which influence the distribution of dinoflagellates in the oceans are as follows; temperature, salinity, water depth,

ocean currents, hydrodynamics, nutrient supply, amount of suspended matter (Williams, 1971a). Also, with increased distance from a terrigenous supply, the proportion of terrestrial palynomorphs within the marine realm decreases and that of the marine microplankton, including dinoflagellates, increases.

Dinoflagellates are mostly autotrophic but some are known to display a heterotrophic mode of life. Autotrophic dinoflagellates occupy a position within the photic zone and most dinoflagellates are found between 18-90 m. water depth. Dinoflagellates display marked seasonal fluctuations in numbers, typically blooming in late Spring or Summer. Heterotrophic dinoflagellates tend to follow the maximum diatom bloom. Dinoflagellates are major primary producers, second only to the diatoms.

Dinoflagellates are unicellular organisms and are believed to exhibit a mesokaryotic biological state (Dodge, 1965), an intermediary evolutionary position between prokaryotic and eukaryotic cell types. This mesokaryotic status implies that dinoflagellates are evolutionarily, very primitive algae.

There are four stages in the life cycle of dinoflagellates. The encystment stage occurs when the resting cyst or hypnozygote is produced. The dinoflagellate cyst can act as a reproductive, protective, propagative or dispersal mechanism (Lentin and Williams, 1980). Encystment is believed by many to be induced by the onset of adverse conditions, however, this is perhaps an over-simplistic viewpoint. More probably, the resting cyst represents an adaptive link between sexual reproduction and survival strategy, whereby dinoflagellates can therefore cope with seasonal and temporary unfavourable conditions for prolific vegetative growth (Evitt, 1985).

1.3. Dinoflagellate cysts and their palaeoenvironmental implications

Dinoflagellate cysts, as well as most other palynomorphs are of the coarse silt size fraction. However, because of their low density they behave hydrodynamically as medium silt-sized sedimentary particles or finer (Harker *et al.*, 1990). Their eventual site of deposition is determined by their size, density and floatation characteristics.

Factors affecting deposition and preservation of dinoflagellate cysts within the sediment are primarily linked to their supply in the water above the sediment body, the sediment type being

deposited and the oceanographic forces acting in the water body.

Even after successful incorporation of dinoflagellate cysts within the deposited sediment, factors such as post-depositional biological decay and oxidation can destroy all or part of the dinoflagellate cyst assemblage. Certain physical, post-depositional features such as current winnowing or reworking of the sediment supply can also result in the varying degrees of loss of the dinoflagellate cyst content.

However, only a small proportion (10-15%) of modern dinoflagellates produce fossilisable organic-walled cysts, *i.e.* are meroplanktic (Wall and Dale, 1968; Dale, 1976; Evitt, 1970; Davey, 1975). Therefore, the exact composition of the original population of dinoflagellates cannot be determined from analysis of the cyst association (Dale, 1976).

The incubation studies of Wall and Dale (1968) and Dale (1983) have provided the first data sets that link living thecate dinoflagellates with dinoflagellate cysts. These studies have shown that certain living dinoflagellate species, e.g. *Protoperidinium compressum* (Abé) Balech, 1974 produce one dinoflagellate cyst species *Stelladinium stellatum* (Wall and Dale, 1968) Reid, 1977. However, the living dinoflagellate *Gonyaulax spinifera* (Claparède and Lachmann 1859) Diesing 1886 appears to produce a variety of six different dinoflagellate cyst morphologies, some of which have differing, but related archaeopyle types. Therefore, estimations of dinoflagellate population size and composition as derived from the analysis of the dinoflagellate cyst assemblages is not as straight forward as it would immediately seem (see Evitt, 1985)

Also, Dale (1976) and Wall *et al.* (1977) have shown that in tropical oceanic and higher latitude waters a directly proportional relationship does not exist between the number of species of dinoflagellate cysts and living dinoflagellate species. Care must therefore be taken with respect to interpretations on primary productivity of the original water mass based on counts of numbers of dinoflagellate cysts contained within a sediment. However, all things considered, it is accepted that interpretations of, and comparisons based upon, counts of individuals and species of dinoflagellate cysts have great potential in the study of local sections over relatively short intervals of time, Evitt (1985).

Dinoflagellate cysts represent the organisms which once existed within the marine microplankton community which developed and changed within the water mass with respect to space and time. Thus, although dinoflagellate cyst assemblages are filtered through and are therefore the result of many depositional and preservational processes, they are the only record of dinoflagellate assemblages available for investigation. Therefore, bearing all limitations in mind, it is not unreasonable to assume that the data yielded by the analysis of dinoflagellate cyst assemblages is not a quirk but is a true representation of the palaeo-oceanography of the water mass as it existed at the time, given the limitations discussed above.

The analysis of the distribution of dinoflagellate cysts present in Recent sediments is particularly successful with respect to depositional palaeoenvironmental interpretations, as many fossil Recent cysts have modern living counterparts. Recent sediments have been analysed with respect to the distribution of dinoflagellates cysts (Davey, 1971; Williams, 1971b; Reid, 1972, 1974, 1975; Davey and Rogers, 1975; Wall *et al.*, 1977; Morzadec-Kerfourn, 1977, 1979; Harland, 1977, 1983). These authors have shown that Recent dinoflagellate cyst distributions are influenced by two features, an inshore-offshore gradient and a latitudinal control. Wall *et al.* (1977) stated that the thanatocoenosis of dinoflagellate cysts was controlled dominantly by climatical, ecological and hydrodynamical factors, and also documented that dinoflagellate cyst diversity increased with increasing depth seawards.

Many investigations into the distribution of fossil marine microplankton within pre-Quaternary sediments with respect to palaeoenvironmental reconstructions have been carried out. Such investigations can be summarised by the basis of the approach taken. Many have evolved from the comparison of detailed analyses of the dinoflagellates cysts and their associations with the already known sedimentological and lithological features of the sections studied (Scull *et al.*, 1966; Davey, 1970; Downie *et al.*, 1971; Harland, 1973; Lentin and Williams, 1980; Hultberg and Malmgren, 1986; Köthe, 1990; Harker *et al.*, 1990). Common to all these investigations is the identification of associations of dinoflagellate cysts and certain distinctive morphological features of dinoflagellate cysts, which appear to be dependant on the depositional setting of particular types

of sediment. Certain key dinoflagellate cysts, whose presence typify the dinoflagellate cyst assemblage are chosen as the characterising cysts of a particular dinoflagellate association, which individually are distinctive of a particular depositional environment (Scull *et al.*, 1966; Lentin and Williams, 1980; Hultberg and Malmgren, 1986; Köthe, 1990; Harker *et al.*, 1990). Others have involved palaeoenvironmental interpretations made from comparisons with the modern dinoflagellate cyst communities (Harland, 1973; Goodman, 1979). More commonly in recent publications, palynological data have been manipulated by the application of varied statistical techniques to identify associations or trends within the dinoflagellate cyst assemblages present in fossil sediments (Brideaux, 1971b; Goodman, 1979; Boulter and Hubbard, 1982; Davies *et al.*, 1982; Hultberg and Malmgren, 1986; Harker *et al.*, 1990). Combinations of all the above techniques yield the most meaningful and significant results.

Certain morphological features of dinoflagellate cysts appear to be under palaeoenvironmental control. For example, it has been interpreted that dinoflagellate cyst spines and processes appear to be buoyancy devices, which become larger and elaborate in more open marine conditions. Also, it has been postulated that thick-walled, cavate dinoflagellate cysts characterise unstable, higher energy, inner neritic conditions, whereas thin walled chorate cysts typify more stable, reduced energy, open marine conditions (Scull *et al.*, 1966; Downie *et al.*, 1971; Harker *et al.*, 1990).

Davey (1970) noted that similar aged samples of Albian-Cenomanian deposits from different geographical locations contained dinoflagellate cyst associations which were dominated by cysts of differing morphologies. This was interpreted by Davey (1970) as being due to temperature control, as chorate cysts were more dominant in warmer waters, with few proximate and cavate cysts. The colder water assemblage was typically dominated by cavate cysts, with minor proportions of proximate cysts.

Harland (1973), by comparison with the modern open marine environment, recognised a parameter termed the Gonyaulacacean ratio. He noted that gonyaulacacean species were more numerous than peridinacean species in the modern open marine setting. Thus, Harland (1973) postulated that the higher the ratio, the more open marine the environment. However, the Gonyaulacacean ratio is based on number of

species and does not take account of numbers of individuals. It is also dependant on the interpretation of cyst affinity. Therefore, it is now accepted that the predominance of gonyaulacacean cyst species indicates a more open marine situation and that a dominance of peridinacean dinoflagellate cyst species is indicative of a nearer-shore and perhaps reduced salinity environment (Harland, 1991 *pers. comm.;* Harker *et al.*, 1990).

Goodman (1979) also made comparisons to Quaternary dinoflagellate cyst distributions in order to identify dinoflagellate cyst "communities" within Lower Eocene sediments in America. Six diagnostic dinoflagellate communities were identified on the basis of such comparisons and also from information available from the sedimentology and lithology of the sediments. Statistical methods such as absolute abundance, rank abundance analyses and cluster analysis were employed and confirmed the identification of the communities. Three of these communities were characterised by higher species diversity and lower relative species dominance and were interpreted as representing a more offshore environment. The remaining three cyst communities exhibited lower species diversity and higher relative dominance of cyst species, which is postulated to be typical of more inshore or perhaps estuarine conditions.

The application of statistical analysis in the interpretation of palynological data has been carried out by many workers (Brideaux , 1971a; Goodman, 1979; Boulter and Hubbard, 1982; Davies *et al.*, 1982; Hultberg and Malmgren, 1986; Harker *et al.*, 1990).

Brideaux (1971a), in his investigation of Albian dinoflagellate assemblages of Canada, documented the presence and distribution of recurrent groups of dinoflagellate cysts and acritarchs by the use of the binomial test. These recurrent groups are believed by Brideaux (1971a) to be the result of sedimentary and palaeoenvironment change.

The application of multivariate statistical analysis to terrestrial palynomorph assemblages from the Eocene of Britain was carried out by Boulter and Hubbard (1982). The specific techniques used, principal component analysis and cluster analysis, allowed the reconstruction of Tertiary palaeoclimatical changes within the Eocene versions of deciduous, fern and conifer, and paratropical rain forest.

A review of statistical applications made to palynological data with respect to palaeoenvironmental reconstructions was carried out by Davies *et al.* (1982). Such applications were grouped into four categories; absolute abundance of dinoflagellate cysts, relative abundance of dinoflagellate cysts, species diversity and dominance and dinoflagellate cyst assemblage composition.

Hultberg and Malmgren (1986) carried out an investigation of the distribution of dinoflagellate cysts and planktonic foraminifera from the Boreal Maastrichtian which involved the use of several statistical computations based on abundance and diversity. Identified trends within these two groups of microfossils were explained by comparison to the known sedimentology and lithology of the areas under investigation. These trends were postulated to be linked to lowering of sea-level and as a result certain dinoflagellate cyst species were interpreted as being useful as palaeobathymetrical indices within the uppermost Cretaceous of the Boreal realm.

The Late Campanian microplankton assemblages of areas within North America were investigated using cluster analysis techniques by Harker *et al.* (1990). This technique proved useful in the identification of species associations and groups of assemblages deposited within similar palaeoenvironmental conditions. The dominant palaeoenvironmental forcing mechanism within these assemblages is believed to be that of differential salinity. Thus, it was recognised that proximate cysts, particularly peridinioid cysts, together with thin-spined acritarchs, appear to be indicative of marginal marine or reduced salinity conditions. Chorate and proximochorate cysts with thick and elaborately branched processes and gymnodinioid cysts are typical of more open marine environments. Variations in the parameters of microplankton:spore-pollen ratio and of diversity and equitability indices appear to have resulted from changes in depositional environment.

1.4. The project and its aims

This project on the palynology of selected Cenomanian successions in south-eastern and north-eastern England evolved out of the work of others. Samples were collected and investigated mainly by two colleagues, see Chapter 3. Three of the sections (Site 3a, TBB and MCB) were the basis of an investigation into the stable isotopic

signature of the same sections as examined palynologically herein. The third section (SFE) was investigated as a broad-based geological approach, which dealt with many aspects such as stable isotopes, rare earth element geochemistry and palynology (herein). The high resolution sampling interval necessary for the application of many of the above disciplines is a feature common to all sections except one (TBB), and is seen to have great potential with respect to palynological interpretations.

Because of the sporadic distribution and limited vertical coverage of the Cenomanian successions examined herein, a comprehensive investigation of the biostratigraphical distributions of Cenomanian palynomorphs was not attempted. Indeed, the stratigraphical distribution of the palynomorphs of the Cenomanian of the Anglo-Paris Basin and the north of England is already comprehensively known and well documented, see Chapter 6. For the same reasons, it was felt that a detailed taxonomic investigation of the palynomorphs was not within the scope of this study as indeed this aspect of the Cenomanian palynology of England is already sufficiently well known and understood (Chapter 7). Therefore, this project is neither biostratigraphically nor taxonomically orientated, and no attempt has been made to update the known biostratigraphy and systematic palynology of Cenomanian dinoflagellate cysts. However, the known dinoflagellate cyst biostratigraphies and systematics proved readily applicable to all the successions studied.

One key to the potential within this project has been the high resolution sampling interval used through-out almost all sections. As a consequence of this, a quantitative approach was applied in the processing of all samples, in order that real interpretations on abundance and relative abundance of samples could be made. This quantitative technique is much the same as that employed in the processing of Quaternary palynological samples, as learned by the author during a Quaternary palynological M.Sc. project (Duane, 1988). Within the palynological analysis of Quaternary marine sediments, the sampling interval is commonly at a high resolution and counts of the number of dinoflagellate cysts per gramme of sediment have proven very useful tools in the interpretation of abundance (Harland, 1984a, 1984b; 1988a; 1988b; Turon and Londeix, 1988). Therefore, it was felt that a quantitative approach should be applied

here as it provides very useful data as the result of little extra processing and observational effort. However, the potential distortional effects of differential sedimentation rates and compaction must be borne in mind in the interpretation of abundance values yielded by counts of pre-Quaternary dinoflagellate cyst assemblages.

As a result of the high resolution sampling interval of the successions studied herein, it was decided to attempt palaeoenvironmental interpretations based on the palynological content of the samples, but much aided by statistical manipulation of the raw data. By and large, trends now identified as being associated with palaeoenvironmental changes were not obvious within the raw palynological data but were only identified and confirmed by statistical applications, see Chapters 7, 8, 9. The application of multivariate statistical techniques has proven successful in the synthesis of palaeoenvironmental interpretations based on palynological data, as has been outlined above. The particular palaeoenvironmental features which characterise these Cenomanian successions have been identified by the application of other geological disciplines, see Chapter 2. Therefore, this project provides the opportunity to introduce the palynological data into the broader geological equation. Also, bearing in mind the fact that the Cenomanian represents a time of relative tectonic quiescence, such sediments are highly suitable for the investigation of palaeo-oceanographical forces as these will be the major features affecting the sedimentary deposition within the basin.

The application of a multi-disciplinary approach to palaeoenvironmental interpretations has heralded much success in the geological analysis of Quaternary marine deposits. The linking of palynological and stable isotopic data (de Vernal and Hillaire-Marcel, 1987a; 1987b; Hillaire-Marcel and de Vernal, 1989; Turon and Londeix, 1988; Harland, 1992) and other geological disciplines such as foraminiferal analysis, sedimentology, geochemistry, major element analysis, seismic characteristics (Long *et al.*, 1986; de Vernal *et al.*, 1987; Morton *et al.*, 1988; Aksu *et al.*, 1989; Hillaire-Marcel *et al.*, 1989; Stoker *et al.*, 1991) has enabled the erection of a climatostratigraphy for the Quaternary marine sediments examined. This climatostratigraphy is the basis for the chronostratigraphy of

the Quaternary sediments for much of the North and South Atlantic oceans, North Sea and the Mediterranean. In the light of this, it was realised that this project dealing with the analysis of the palynological content of Cenomanian sediments linked into an already established multi-disciplinary geological project, should therefore have great potential.

Therefore, the aims of this project are to attempt a reconstruction of the marine environment in which the living dinoflagellates existed during selected intervals during the Cenomanian, based on the dinoflagellate cyst assemblages present within the deposited sediments. Interpretation and manipulation of this data are carried out by normal palynological observational techniques and by the use of multivariate statistical methods, respectively. Final palaeoenvironmental interpretations are then made, drawing on all other geological information available from the same sections.

Chapter 2

STRATIGRAPHY AND LITHOLOGICAL DESCRIPTION OF THE CENOMANIAN CHALK

2.1. STRATIGRAPHY

The history of the stratigraphy of the British Upper Cretaceous Chalk deposits started in the early 19th Century, and has continued with much gusto ever since. The name Chalk was derived from the German word 'kalk', and was initially used to describe the soft white or whitish limestone found in the south-east of England.

2.1.1. Chronostratigraphy

The Cenomanian Stage is within the Upper Cretaceous Series. The stage boundaries, its type locality and characteristic index fossils are all defined by Birkelund *et al.* (1984). The stage was originally proposed by d'Ordigny in 1847 with a type locality of Le Mans (Roman Cenomanum) in Sarthe, France, however, he did not designate a type section.

2.1.2. Lithostratigraphy

2.1.2a. Introduction

Inherent in any stratigraphical study of the Chalk, is the considerable confusion introduced by many workers of the past and present with the divisions of the Chalk. In past literature the aim of the work was often to erect a stratigraphy. However, the larger lithostratigraphical or chronostratigraphical units were subdivided into sub-units, and this was sometimes carried out on the basis of palaeontology. Therefore, stratigraphical schemes became a mixture of chrono, litho and bio -stratigraphies. Thus, the present stratigraphy of the Chalk is unfortunately a relic of its confused past.

The most important lithostratigraphical schemes most relevant to this project are as follows. The lithostratigraphy of southern England is documented first, followed by that of northern England. The decision to deal with the lithostratigraphy separately on this geographical basis is because the traditional lithostratigraphical tripartite sub-divisions of the Chalk of southern England cannot be applied in northern England on the basis of either lithostratigraphical or macropalaeontological grounds. Citations for

STAGES

	Phillips 1821 (Dover)		Mantell 1822 (Sussex)	Woodward 1833 (Norfolk)	Dixon 1850 (Sussex)	Jukes-Browne 1880 (Cambridgeshire)	Zones
SENONIAN	The Chalk with numerous flints	with few organic remains	Upper Chalk with numerous beds of flint	Upper Chalk	Upper soft white chalk, containing flints	Upper Chalk	*Micraster cor-bovis*
		with interspersed flints					Chalk Rock
TURONIAN	The Chalk with few flints		Lower Chalk with few flints	Median Chalk with few flints		Middle Chalk	*Holaster planus*
							Terebratulina gracilis
							Rhynchonella cuvieri
							Melborn Rock
CENOMANIAN	The Chalk without flints	with numerous and thin beds of organic remains		Lower Chalk without flints	Lower hard grey chalk, without flints	Lower Chalk	*Holaster subglobosus*
		with few organic remains					Totternhoe Stone
							Chalk Marl
	The Grey Chalk		Grey Chalk Marl	Chalk Marl	Chalk Marl		Cambridge Greensand
ALBIAN			Blue Chalk Marl	Red Chalk			

Figure 2.1 Summary of the stratigraphical schemes for the Chalk of England.

each area are listed in chronological order for convenience. There are also corresponding diagrams, Figures 2.1, 2.2 and 2.3, detailing these various schemes and their possible correlation.

2.1.2b. Lithostratigraphy of southern England (Figures 2.1, 2.2)

Phillips (1818, 1821) was the first to attempt a sub-division of the Chalk. His sub-divisions were based on the differing Chalk lithologies of the London Basin, Isle of Wight and Dover successions respectively. The Chalk of Sussex was sub-divided by Mantell (1822) on the basis of both its lithological and palaeontological content. Woodward (1833) sub-divided the Chalk of Norfolk on lithological grounds. Dixon (1850) also working on the Chalk of Sussex sub-divided it lithologically. From a palynological view point Dixon's paper (1850), is of particular interest as he makes reference to Prof. Ehrenberg's "Observations of the Cretaceous period" (1840) where he quotes the first mention of "Cretaceous siliceous Infusoria", now known as dinoflagellates.

These lithological sub-division schemes are either tripartite; Phillips (1818, 1821) and Woodward (1833) or bipartite; Mantell (1822) and Dixon (1850), but all share the common theme of being based on lithological variation and presence or absence of flints within the chalk.

The French scientist d'Orbigny in 1847 first defined the Cenomanian Stage, after a study of its ammonite and rudist content. D'Orbigny (1842) had previously erected the Turonian Stage and in this later work (1847) he used this new stage, the Cenomanian, to redefine the lower part of his original Turonian.

Between 1850 and 1876 the Phillips (1821) scheme was redeveloped and expanded by successive workers. Dowker (1870) working on the Chalk of Kent, and Whitaker *et al.* (1872) based on the Chalk of the London Basin assigned new names to Phillips' (1821) units. Evans (1870) in his paper on Surrey and Sussex Railways, and Barrois' (1876) analysis of the British and Irish Chalk deposits, documented new palaeontological data on the Chalk, thus expanding Phillips' (1921) sub-divisions within a new biostratigraphical framework.

Jukes-Browne (1880), working on the Chalk of Cambridgeshire deposits and Jukes-Browne and Hill (1903) in their summary of the "Cretaceous Rocks of Britain", supported a tripartite division of the

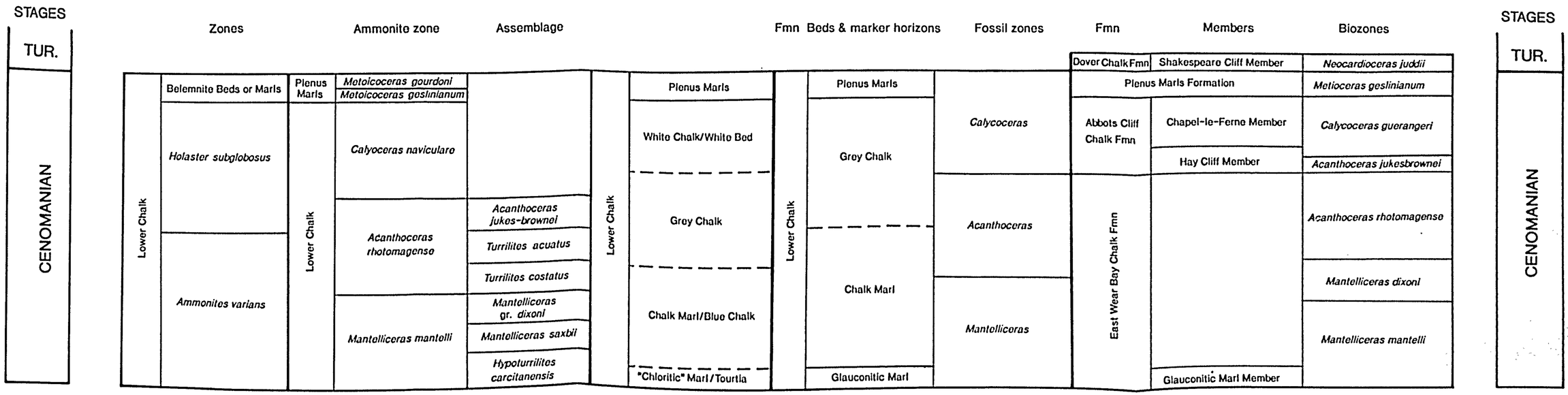

Figure 2.2 Comparison of the Lower Chalk stratigraphical zonation schemes for south-east England.

Chalk into Lower, Middle and Upper, and documented further biostratigraphical sub-divisions of these main divisions. They also attempted a correlation between the Lower, Middle, and Upper Chalk and the Cenomanian, Turonian and Senonian of d'Orbigny (1852). Jukes-Browne and Hill (1903) identified biozones within their tripartite lithological division of the Chalk, each of which was individually characterised by zonal fossils.

Hereafter, only the specific stratigraphy of the Cenomanian Chalk or Lower Chalk will be discussed.

The detailed stratigraphy of the *Actinocamax plenus* Sub-Zone of the Anglo-Paris Basin was first erected by Jefferies (1963). This has now become known as the *Plenus* Marls Formation. In the field, the top of this formation is broadly taken to mark the lithological boundary between the Cenomanian and Turonian Stages.

Kennedy (1967a) documented the diagnostic features of the Lower Chalk of the Eastbourne area. He was the first to mention "the rhythmic alterations of more or less argillaceous chalk" within the Lower Chalk. He also attempted the successful subdivision of the Lower Chalk and the *Plenus* Marls of south-east England on the basis of their ammonite content (Kennedy, 1969). Within the Lower Chalk he erected three ammonite Zones, two of which were subsequently divided into three assemblage sub-zones. The *Plenus* Marls were divided into two ammonite Zones. Kennedy (1969) also recognised fourteen bands which were localised sub-divisions of the Lower Chalk, identified from an idealised Folkestone section.

Destombes and Shephard-Thorn (1971) in their investigation of the Channel Tunnel, identified the Lower Chalk and sub-divided it into four stratigraphical units. Reference was also made to the corresponding French unit, the Cenomanian. They too recognised the lithological alterations of chalks and marls within the Lower Chalk.

Mortimore (1983) working on the Chalk in Sussex erected a lithostratigraphical scheme for the Lower Chalk Formation, within the Cenomanian Stage. He identified four lithological beds or marker horizons within the Lower Chalk and they were assigned to Kennedy's biozones (1969). He too documented the lithological rhythmicity of the chalks and marl seams.

The lithostratigraphy of the Lower Chalk of the North Downs was erected by Robinson (1986a). He stated that the traditional

tripartite division of the Chalk based on lithology of Jukes-Browne and Hill (1903) is too simplified for lithostratigraphical correlation purposes. He formally proposed a new lithostratigraphical scheme, where five new formations were proposed for the Chalk. Within the Cenomanian he identified three complete formations, of which the lower two contain members. He also assigned biozones to all these sub-divisions, based on their ammonite content. Each lithological unit was defined and described. This lithostratigraphical scheme of Robinson (1986a) is the one applied during this project.

2.1.2c. Lithostratigraphy of northern England (Figure 2.3)

The history of research into the lithostratigraphy of the Chalk of northern England began with Woodward (1833). He sub-divided the Chalk of Norfolk on lithological grounds into lower, middle and upper parts.

In a Memoir of the Geological Survey, Dakyns, Fox-Strangways and Cameron (1866) looked at the Chalk of East Yorkshire, and again divided it in a tripartite manner, but with a basal Red Chalk included.

Blake (1878) in his discussion of the chalk of Yorkshire, proposed a stratigraphy for the area based on lithological and palaeontological grounds.

Jukes-Browne and Hill (1903) in their famous account of the Cretaceous Rocks of Britain, applied a tripartite division of the Chalk to the Chalk deposits of Lincolnshire. Within the Lower Chalk of Lincolnshire the upper zone of the Lower Chalk, the *Holaster subglobosus* Zone was replaced by the *Offaster sphaericus* Zone due to the extended range of *Holaster subglobosus* in Lincolnshire and Yorkshire.

Wright and Wright (1942) made a significant contribution to the knowledge of the northern Chalk deposits however, no detailed sections were ever published.

Further information on the Cenomanian chalk deposits of eastern England was given by Jeans (1973, 1980). This work involved the detailed measuring of sections, followed by subsequent detailed geochemical investigations.

In his detailed account of the lithostratigraphy of the *Actinocamax plenus* Subzone of the Anglo-Paris basin, Jefferies (1963) makes reference to the corresponding unit in northern England at South

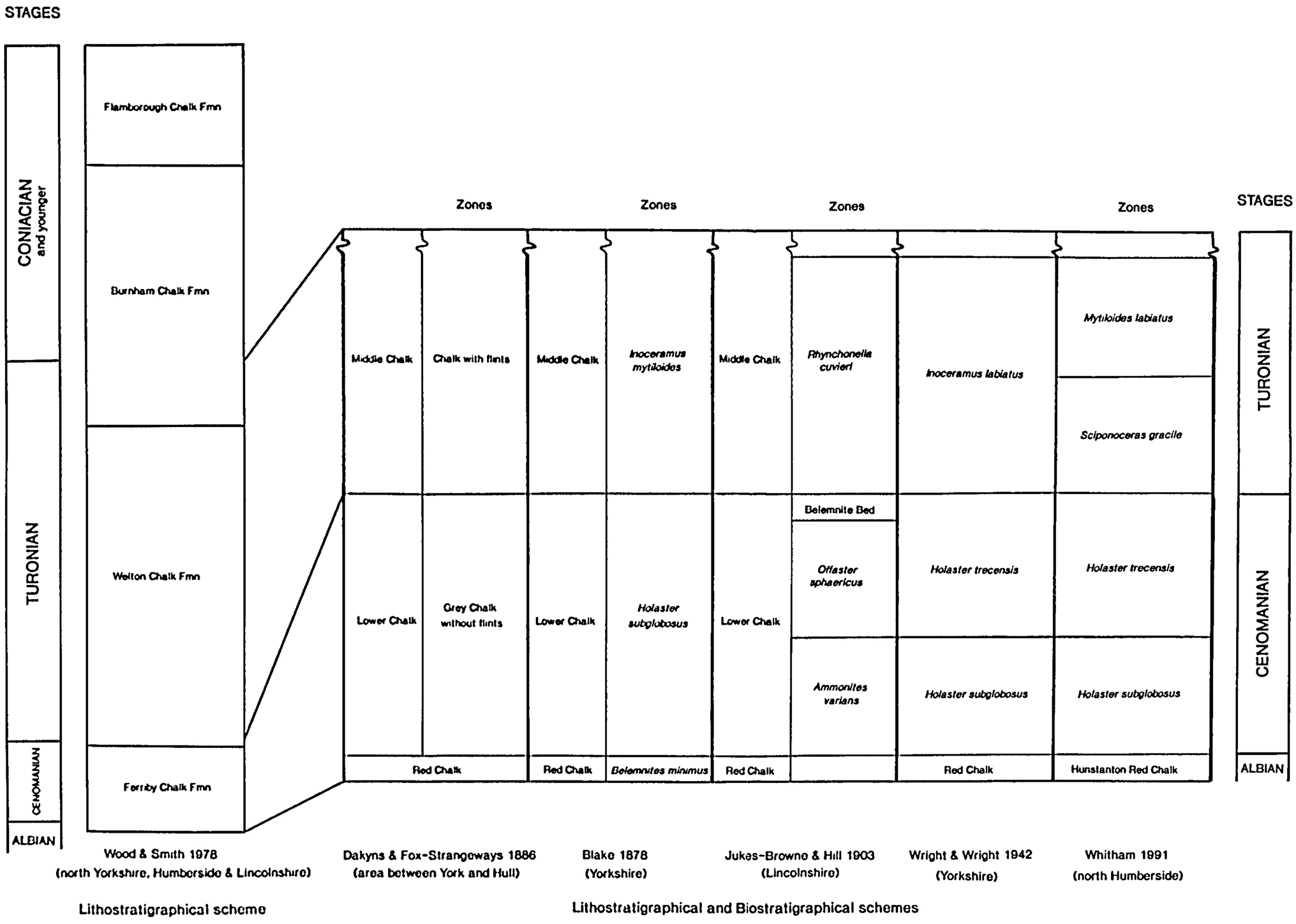

Figure 2.3 Comparison of the Lower Chalk stratigraphical schemes for northern England.

Ferriby and Buckton Cliffs.

Wood and Smith (1978) erected a new lithostratigraphical scheme for the Chalk of North Yorkshire, Humberside and Lincolnshire, as they claimed that the traditional tripartite sub-division of the Chalk (based on southern England) could not be applied in these areas from the point of view of both lithology and macropalaeontology. Indeed, the lithology and macropalaeontology of the southern and northern Chalk deposits are sufficiently different, that Wood and Smith (1978) stated that they were two separate depositional and faunal provinces. Thus, they divided the Chalk group of northern England into four formations. The lower two formations, the Ferriby Chalk Formation and the Flamborough Chalk Formation are without flints, whereas the succeeding Welton Chalk Formation has flints and the upper Burnham Chalk Formation is characterised by tabular and related types of flints. This lithostratigraphical scheme of Wood and Smith (1978) is the one applied to the succession studied in this project.

Whitham (1991) documented new exposures of Ferriby, Welton and Burnham formations of Upper Cretaceous Chalk Group in areas north of the River Humber and in north-east England. The investigation of these exposures provided the basis for a more complete lithostratigraphical scheme to be developed. Within this scheme, the lithological sequences examined, provided a framework for the first detailed account of the distribution of the major elements of the macropalaeontological content of the upper Cretaceous Chalk of northern England. Also, an informal subdivision of the *Hagenowia rostrata* Biozone is suggested.

2.2. LITHOLOGICAL DESCRIPTION OF THE CENOMANIAN CHALK

A detailed investigation of the petrology of the Cretaceous Chalk was carried out by Hancock (1976). He describes the Chalk as a biomicritic limestone, made up largely of coccolith debris, and as a result it is composed of almost 100% calcium carbonate. It was deposited originally as Low-Mg calcite in a sea of normal salinity and temperatures about 30° (Scholle, 1974), which was usually 100-600m. deep. However, Burnaby (1961) claimed the Chalk sea was only 9m. deep on the basis of a study of the benthonic foraminifera, a view refuted

by Hart (1992, *pers. comm.)*. Hancock (1976) also investigated syn- and post-depositional features of the Chalk. Very little early lithification occurred in the Chalk as a whole and this is particularly true of the Cenomanian chalk. Post-depositional diagenesis resulted in the formation of flints and hardgrounds, features which normally characterise the post-Cenomanian chalks.

Hancock (1976) also investigated the palaeogeography of the Cretaceous Chalk sea. The Chalk was deposited in broad basins, perhaps 100's of kilometers wide, but which also contained troughs.

The Cenomanian chalk is characterised by a chalk-marl facies. The different lithologies seen within this facies are defined and documented by many authors; Hancock (1976), Wood and Smith (1975) Mortimore (1983) and Robinson (1986a). As Robinson's (1986a) lithostratigraphic scheme is the one applied in this project, his definitions of the various lithologies of the Cenomanian Chalk are used and are as follows:

White chalk:

(i) This term is also used by Hancock (1976) and corresponds to the terms "massive chalk", Wood and Smith (1978) and "featureless chalk" Mortimore (1983).

(ii) It is soft, white fine grained and homogeneous, and is dominantly composed of coccoliths and their debris, with 10% foraminiferal remains, Hart (1990 *pers. comm.)*

(iii) *Thalassinoides* burrows are common and the chalk is in general well bioturbated.

Marly chalk:

(i) This term is also used by Wood and Smith (1978) and Jarvis and Woodroof (1984).

(ii) It is grey and intensely bioturbated.

(iii) There is a high clay content and in the Lower Cenomanian this non-carbonate component may form 60% of the sediment (Kennedy, 1967b).

(iv) The clay minerals are dominantly smectites.

Marl seam:

(i) Thin (1-5cm) greenish-grey marl beds with high non-carbonate content (15-35%).

(ii) Non-carbonate component: 75% Clay minerals (Smectites)
10% Quartz (sand grade), often as agglutinated foraminifera Hart (1990 *pers. comm.)*

15% Quartz (silt grade)

(iii) They are laterally very persistent.

(iv) It has been suggested that they may be of volcanic origin, Pacey (1984) and Leary and Wray (1989)

2.2.1. Particular features of the Cenomanian Chalk under investigation

Certain aspects of the Cenomanian which are to be examined in detail within this project are as follows.

2.2.1a. Rhythmic bedding of the Cenomanian chalks and marls

It is well established that the Cenomanian chalk consists of alternating chalks and marls (Kennedy, 1967a; Destombes and Shephard-Thorn, 1971; Lott, 1982; Mortimore, 1983; Robinson, 1986a; Hart, 1987) The Cenomanian can be divided into three parts on the basis of this rhythmic bedding, as the lower part has smaller scale bedding, the middle section has larger scale bedding, whereas the upper portion is more massively bedded.

Kennedy (1967a) when describing the Lower Chalk of the Folkestone area, stated that "the sequence can be interpreted as rhythmic alterations of more or less argillaceous chalk". On the basis of these alterations Kennedy (1967a) divided up the Lower Chalk into three parts. The lower part in which the marls are 45-60cm. and the chalks 15-30cm. thick, the middle part with chalks 15-30cm. thick and an upper portion where the marl content is so low that the alterations are barely visible. Kennedy (1967a) noticed that the base of the marl bed is a sharp one whereas there is a transitional junction between the marl and the chalk. Kennedy (1967a) did not allude to any origin of this rhythmicity.

During their initial investigation of the Channel Tunnel site, Destombes and Shephard-Thorn (1971) also documented the presence of rhythms within the Cenomanian Lower Chalk. The lowest unit, the Chalk Marl displays 1m. rhythms of dark grey chalky marl with pale harder beds, followed by the Grey Chalk which displays rhythmic alterations on a 1m scale of pale to medium grey, more or less marly chalk. The upper White bed or White Chalk is a homogeneous unit of marly chalk, Destombes and Shepard-Thorn (1971).

Lott (1982) also recognised rhythms within the Lower Chalk of the Winterbourne Kingston borehole in Dorset, where minor

sedimentary cycles occur due to the variations in the clay content.

Mortimore (1983) described the rhythmicity of the Cenomanian Lower Chalk of Sussex. The lower Chalk Marl exhibits beds of pale grey chalks (0.3m. thick) alternating with bands of marl (0.7m thick). The succeeding grey Chalk is massively bedded white chalk which has interspersed thin marl seams.

When Robinson (1986a) erected his lithostratigraphical scheme for the North Downs, he included information on the rhythmicity of the Cenomanian chalk facies. The lower East Wear Bay Formation is characterised by sedimentary rhythms up to 3m. thick. Within each individual rhythm and through-out the formation as a whole the clay minerals and non-carbonate mineral content decrease upwards. The Abbots Cliff Chalk Formation Robinson (1986a) is characterised by "apparently featureless chalk" which is massively bedded. However, under closer investigation it appears to be bioturbated by numerous *Thalassinoides* and *Chondrites* burrows, Robinson (1986a).

On a smaller scale, Robinson (1986b) identified fining upwards microrhythms within the Upper Cretaceous Chalks of the North Downs. These microrhythms within the Cenomanian to Campanian chalks are on a 0.2 - 0.3m. scale. Robinson (1986b) suggested that such microrhythms are caused by the change from high to low energy conditions within the water mass, which is in an erosive state at the beginning of the rhythm and changes to winnowing and finally to a still-stand state by the end of the microrhythms. Within the Cenomanian the microrhythms correspond to the marl-chalk alterations and both rhythms share the same base. Robinson (1986b) interpreted these microrhythms as being caused by variations in the tidal current strength controlled by the Earth's 21,000 year obliquity cycle of Milankovitch (1962).

Hart (1987) also documents the lithological rhythmicity of the Cenomanian Chalk in his analysis of the chalk facies of Britain. The Lower Chalk succession of the Isle of Wight was measured in detail and histograms of the various cycle thicknesses were plotted. The analysis shows that the cycle data provided some form of variable time scale which would appear to be the result of orbital variations on the 23,000 and 41,500 year cycle, Hart (1987). Theses cycles of 23,000 and 41,500 years may be linked to the precession and obliquity cycles of Milankovitch (1941).

Gale (1989a) defined a detailed cyclostratigraphy for the rhythmically bedded Cenomanian chalks of the northern Anglo-Paris Basin which he postulated could be correlated over 100,000 km^2. He suggested that the individual decimeter-scale couplets probably represented the precessional cycle which can themselves be grouped into sets averaging five, indicative of the eccentricity cycle.

2.2.1b. The Mid-Cenomanian non-sequence

The presence of a non-sequence in the Middle Cenomanian indicated by a dramatic microfaunal change in the planktonic to benthonic foraminiferal ratio was documented by Carter and Hart (1977) as the Mid-Cenomanian non-sequence. This event would appear to be geographically widespread as it is recorded within the foraminferal populations of the Middle Cenomanian of southern England, Carter and Hart (1977) and the western interior of the United States, Eicher (1969). Across this Middle Cenomanian interval there is a sudden change from a predominantly benthonic foraminiferal population to a dominantly planktonic one, Carter and Hart (1977). Also, the appearance of one particular planktonic foraminifera, *Rotalipora cushmani* (Morrow 1934) picks out the non-sequence particularly well. This species increases numerically at the non-sequence and dominates the planktonic fauna at certain horizons above it (Carter and Hart, 1977).

Jeans (1968) identified a brachiopod 'pulse-fauna' occurring at this level in the Middle Cenomanian of the Lower Chalk of England. Gale (1989a) has also recognised such 'pulse-faunas' and states that they may be used to correlate individual beds between different geographical locations.

Although there is no widespread unique sedimentological expression of this non-sequence across the Chalk basin, there are areas where the non-sequence dominates the mid Cretaceous stratigraphy. For example in some areas of Dorset the Mid Cenomanian non-sequence is coincident with the base of the Chalk.

It would appear that this faunal non-sequence can be related to an increase in the water depth of the Cenomanian sea, which may be related to the development of the Atlantic ocean (Carter and Hart, 1977). However, changing water depth alone cannot be the only major controlling influence as there is no distinctive sedimentological

change, corresponding to this planktonic/benthonic ratio change. Also Carter and Hart (1977) stated that if water depth was the only forcing mechanism then the total number of planktonic foraminifera would decrease towards the edge of the basin, and this is not so. It is suggested that periodic changes in the water mass between alternating colder and warmer water within a deepening basin could perhaps provide the mechanism to cause the Middle-Cenomanian non-sequence.

The Middle Cenomanian of north-west Europe is also characterised by a carbon stable isotope excursion. This carbon excursion is not associated with the Mid-Cenomanian non-sequence of Carter and Hart (1977) as the excursion occurs stratigraphically below the non-sequence (Figure 8.14). Ditchfield *et al. (in prep.)* have investigated this carbon stable isotope excursion, studying the carbon and oxygen stable isotope signature, lithostratigraphy, sedimentology, biostratigraphy and cyclostratigraphy of five sections from three separate depositional basins within this area. Three of the sections are from the Anglo-Paris Basin, and the remaining two are from the Cleveland and Münsterland Basins. The carbon isotopic signature for all five sections is similar, with a double-peaked excursion in which the second peak is larger, and has a maximum shift of 1°/oo PDB. Ditchfield *et al. (in prep.)* believe that this excursion is unlikely to be diagenetic in origin and is most likely to be associated with variations in the Cenomanian sea water, which are probably caused by burial of organic sediments (possibly in the North Atlantic). However, because the excursion is not associated with any significant faunal change it is interpreted by Ditchfield *et al. (in prep.)* that any expansion in the oxygen minimum zone must have been relatively minor. Nevertheless, the identification of this carbon stable isotopic excursion is a tool to be used in conjunction with biostratigraphy and cyclostratigraphy for the correlation of Middle Cenomanian successions from different basins.

2.2.1c. Cenomanian-Turonian boundary event of South Ferriby, north-eastern England

The South Ferriby quarry in South Humberside exposes a Cenomanian-Turonian boundary section marked by a reduced *Plenus* Marls sequence (Jefferies, 1963). This particular part of the sequence comprises the uppermost part of the Ferriby Chalk Formation and the

lowermost portion of the Welton Chalk Formation (Wood and Smith, 1978) (Figure 2.3).

The *Plenus* Marls sequence is the basal unit of the Welton Chalk Formation (Wood and Smith, 1978), and its base is marked by the sub-*Plenus* erosion surface. After this erosion surface follows Beds i-vi of the *Plenus* Marls, Jefferies (1963). These beds are believed by Jefferies (1963), on the basis of their macropalaeontological content, to be the upper part of the *Plenus* sub-Zone. Within these beds is the "Black Band", a very distinctive marker within the South Ferriby quarry and elsewhere where it is exposed in northern England. This Black Band was first mentioned by Blake in 1878. Wood and Smith (1978) described the "Black Band" as a dark laminated marl up to 7cm. thick or more lying in the middle of The *Plenus* Marls, which they describe as a complex of marls and silty chalks. At South Ferriby there is a localised development of a second thin black band at the top of Bed iv, but the remainder of the Welton Chalk Formation consists of massive or thickly bedded chalks (Wood and Smith, 1978).

A detailed investigation of the "Black Band" was carried out using various techniques by Hart *et al.* (1991). Careful examination of this horizon has revealed that the black marls are interlaminated with paler-coloured marls. The "Black Band" was examined using the scanning electron microscope (SEM) and this has shown that it consists of finely disseminated clay minerals, which in the very organic-rich mudstones are devoid of visible calcareous fossils.

The Cenomanian-Turonian boundary sequence in much of north-west Europe is associated with a $\delta^{13}C$ excursion; Schlanger and Jenkyns (1976), Scholle and Arthur (1980) and Schlanger *et al.* (1987). Sediments of this horizon are associated with exceptionally high ratios of ^{13}C:^{12}C. Normal $\delta^{13}C$ values in chalks range from +1.5 to $+2^{o}/_{oo}$ (Pomerol, 1984) whereas during this event itself values increase to $+4^{o}/_{oo}$ (Schlanger *et al.*, 1987) and $+3.4^{o}/_{oo}$ (Jarvis *et al.*, 1988a). These values were both taken from samples within the Melbourne Rock. This ^{13}C enrichment is due to the preferential extraction of ^{12}C by marine plankton whose organic components are not recycled back into overall oceanic circulation due to an enhanced organic carbon burial, Scholle and Arthur (1980) and Arthur *et al.* (1987).

This event is also expressed by anomalous geochemical

(Jarvis *et al.*, 1988a; Farrimond *et al.*, 1990; Crumière *et al.* 1990) and biotic characteristics (Hart and Bigg, 1981; Jarvis *et al.*, 1988a; Hart and Leary, 1989; Leary *et al.*, 1989; Corfield *et al.*, 1990). All these characteristics are indicative of the Cenomanian-Turonian oceanic anoxic event, when there was believed to be expansion of the oxygen minimum zone in the ocean and/or increased dysaerobic bottom waters, Jarvis *et al.* (1988a), Corfield *et al.* (1990) and Crumière *et al.* (1990).

A discussion of the all currently available knowledge of this event was carried out by Hancock (1989) in relation to the sea level changes during the Late Cretaceous. Hancock (1989) also documented the various theories on the forcing mechanisms thought to be involved in this oceanic anoxic event. The majority of these theories involve a rise in sea level associated with a major transgression, Schlanger and Jenkyns (1976), Fischer and Arthur (1977), Jenkyns (1980) and Schlanger *et al.* (1987); whereas Jarvis *et al.* (1988a) favour an upwelling mechanism which caused an increase in ocean-surface productivity. Crumière *et al.* (1990) believe that the late Cenomanian-early Turonian event to be time of rising sea-level on the European margin of the Tethys Ocean. This resulted in a progressive drowning of the Provence platform, in successive breaks in marine sedimentation and also in the initiation of deep water dysaerobia. They postulate that palaeogeographical and structural features may have controlled the regional extent of the oxygen minimum layers, the distribution of laminated and organic-rich sediments and the regional duration of this worldwide oceanic anoxic event.

A further detailed investigation of the geochemistry of the *Plenus* Marls of Dover carried out by Jeans *et al.* (1991) has concluded that the Cenomanian-Turonian $\delta^{13}C$ anomaly is due to glacial influence. These sediments were deposited in an increasingly shallowing sea during a major regressional phase in the Chalk Sea in Europe (Jeans *et al.* 1991). The high clay content of the *Plenus* Marls is explained by Jeans *et al.* (1991) as having arisen from the post-depositional argillization of unstable silicate detritus introduced by rejuvenating river systems. Jeans *et al.* (1991) state that dysaerobic and anaerobic water conditions were completely absent and that the level of oxygenation increased in parallel within the shallowing water and the enhanced $\delta^{13}C$ excursion. The anomalous geochemical features of

the *Plenus* Marls at Dover are interpreted by Jeans *et al.* (1991) as being the result of redeposition of Flixton-type coccolith-rich chalk and the occasional introduction of cold northern bottom waters enriched in ^{13}C. The Flixton *Plenus* Marls section in east Yorkshire is recognised by Jeans *et al.* (1991) as showing evidence of restricted faunas typical of deposition under anoxic conditions. Jeans *et al.* (1991) suggest that the *Plenus* Marls $\delta^{13}C$ excursion is a worldwide event which reflects the waxing and waning of polar glaciation which is supported by other evidence such as widespread regression, restricted ocean circulation, lower ocean temperatures, enhanced input of terrestrial organic matter and the presence of dropstones.

Chapter 3

SAMPLES

3.1. Introduction

The palynological samples studied herein are from four sections within chalk of Cenomanian age, three of which are from south-east England and one from north-east England. A summary diagram showing the relative positions of the four sections within a litho- and bio-stratigraphical framework is given in Figure 3.1. The samples from all four sections were collected by persons other than myself, and I am grateful to those who contributed to their collection. As a result, I am dependent on the work of others with respect to the lithological, sedimentological and petrological descriptions of all sections which follow. All such descriptions of sections Site 3A, TBB and MCB are from Ditchfield (1990 unpublished Ph.D. Thesis). The South Ferriby section (SFE) is described by Dodsworth (1990 unpublished undergraduate project) and in Hart *et al.* (1991).

3.2. Site 3a section

3.2.1. Introduction

The location for Site 3A is in the Dover Warren-Folkestone area (Grid reference TR 260384) (Figure 3.2). This section is of Middle Cenomanian age and is sited 5m. below the Hay Cliff Member (Robinson 1986a), which is equivalent to bed 13 of Kennedy (1969). The base of the Hay Cliff Member is marked by a strong laterally persistent marly unit. The samples lie within the *Acanthoceras rhotomagense* zone of Kennedy (1969) and within the foraminiferal zone 1111 of Carter and Hart (1977). Photographs showing the Site 3a section aregiven in Figure 3.3 and 3.4.

This sampled section continues upwards for 1.25m. above the Hay Cliff Member (Robinson 1986a), sampling continuously every 5cm (Figure 3.5).

3.2.2. Style of Bedding

Dark grey, marly chalks, up to 60 cm. thick grade upwards into light grey, less clay-rich, chalks, up to 1m. thick. These light grey

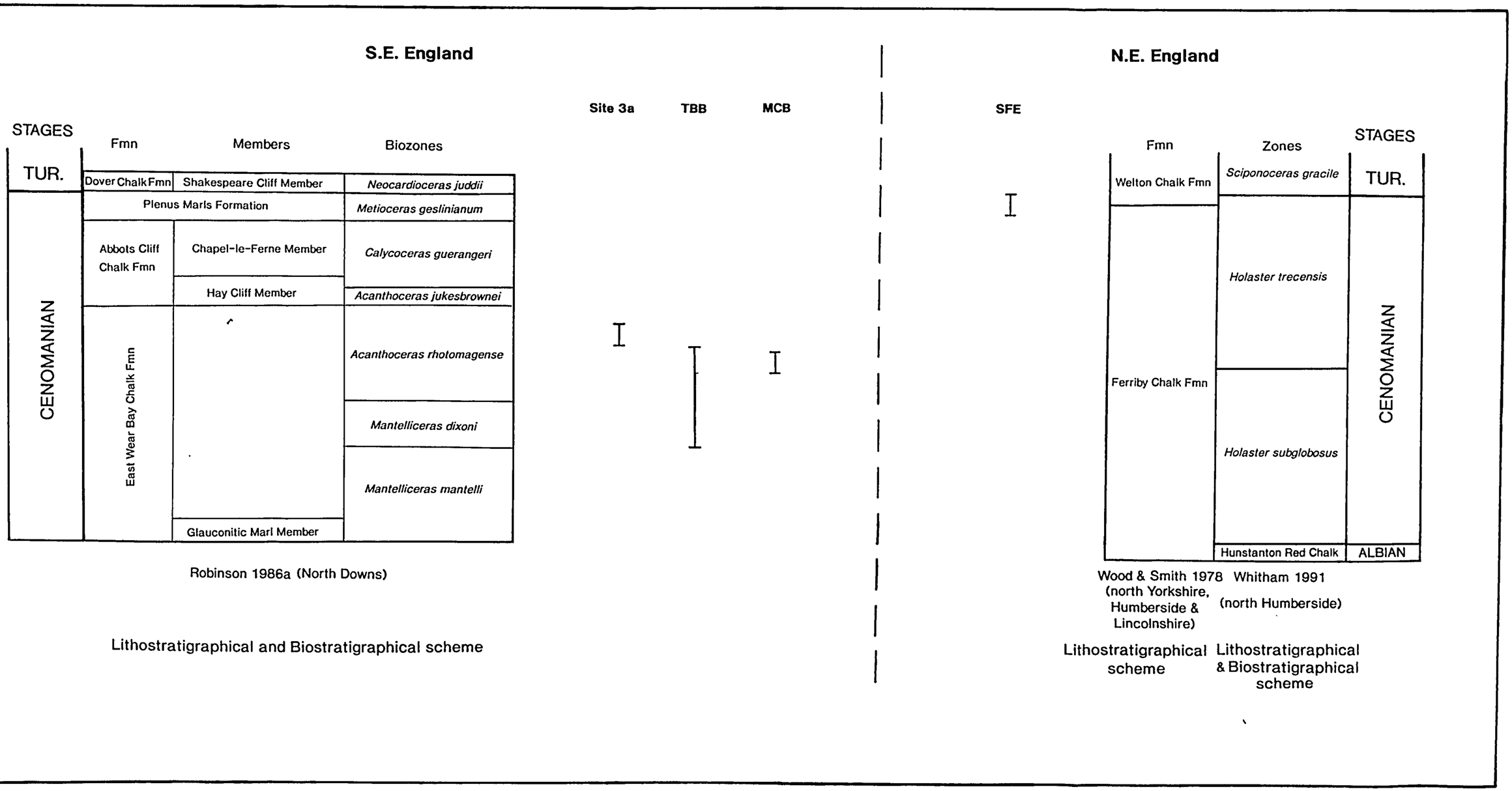

Figure 3.1 Schematic representation of sections studied showing their relative positions within a stratigrapical framework.

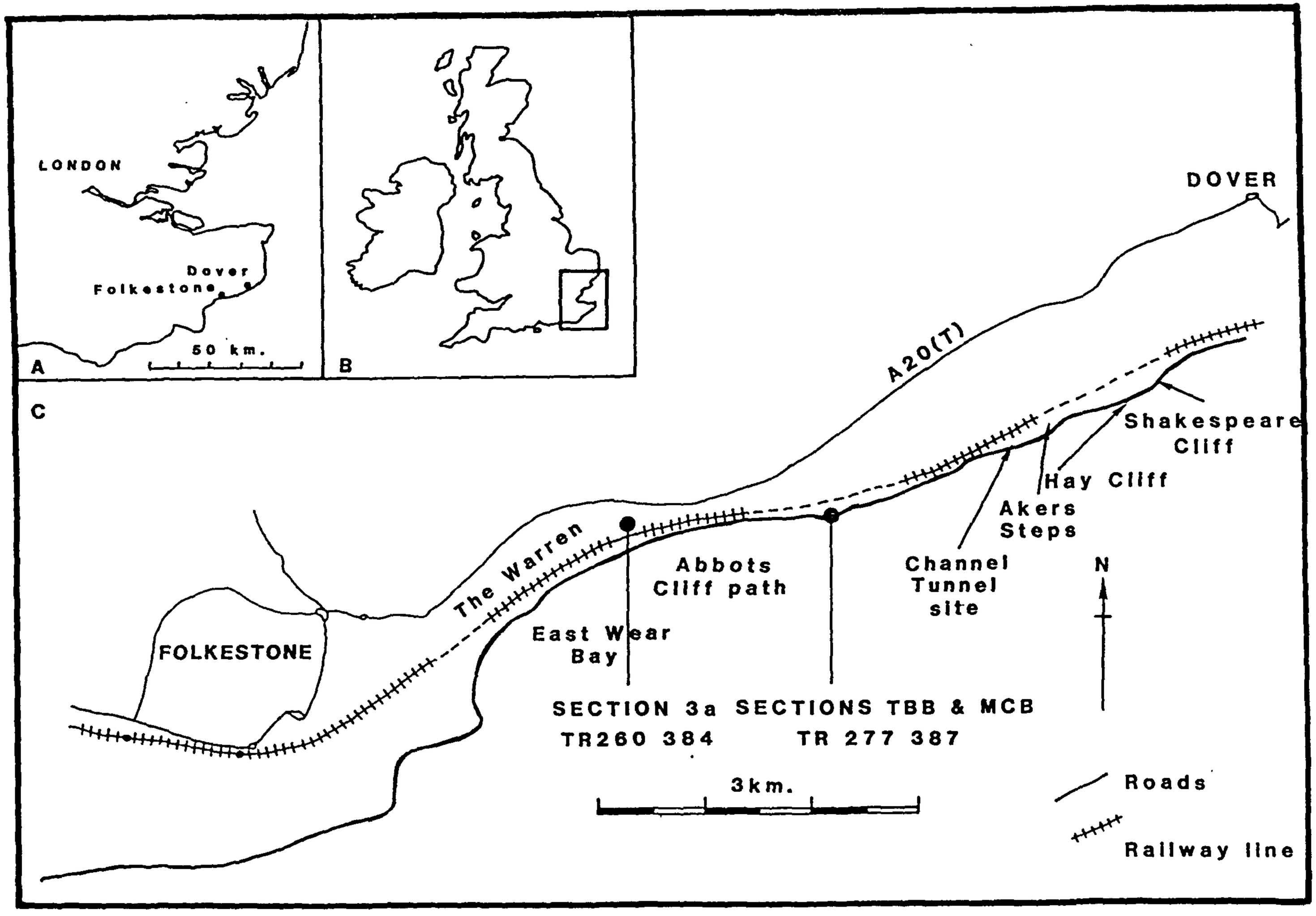

Figure 3.2 Location map for sections Site 3a, TBB and MCB from the Dover - Folkestone Warren area of south-east England.

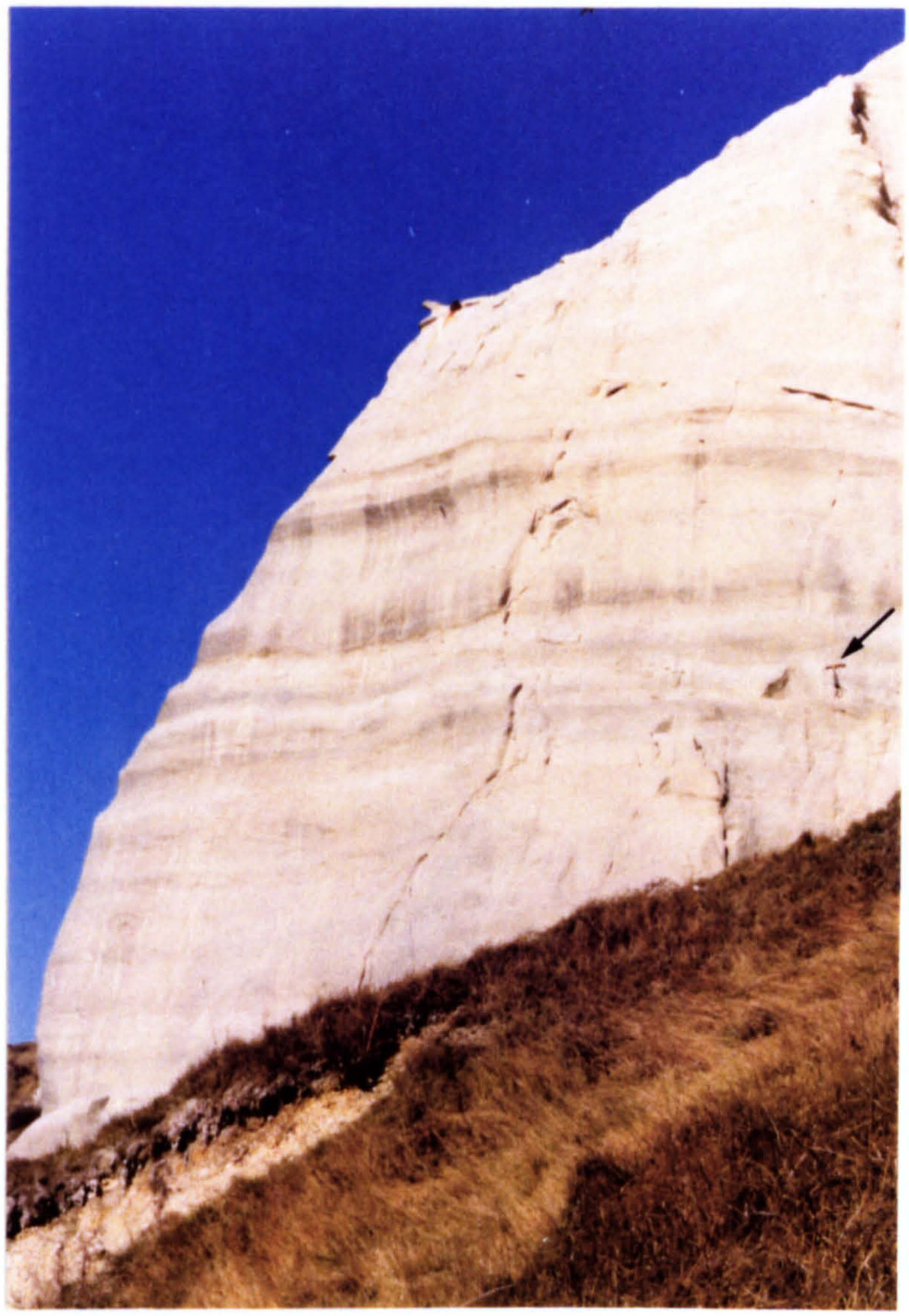

Figure 3.3 Photograph of cliff section which includes the Site 3a section, Dover - Folkestone Warren area, south-east England. See hammer (marked by arrow) for scale.

Figure 3.4 Close-up photograph of Site 3a section. Base of hammer marks the base of the section.

chalks are often terminated by a sharp, though burrowed surface. Bioturbation is conspicuous throughout the section with a different suite of trace fossils found in each lithology. These trace fossils provide good evidence that differences between successive beds are primary as the overlying bed is invariably found piped down along burrows into the underlying lithology. Rare calcarenite filled scours are present, becoming more common towards the top of the section. These scour fills may be up to 60 cm. wide and 15 cm. deep. They are larger but much less frequent than the calcarenite scour fills that characterise the overlying Hay Cliff Member (Robinson 1986a). Both the chalk and marl lithologies are sparse biomicrites containing up to 20% bioclasts, mostly calcispheres, shell fragments and foraminiferan tests, set in a micritic matrix composed largely of nannofossil debris and varying amounts of clay. Acid insoluble residues for bulk rock samples dissolved in 10% hydrochloric acid solution range from 5.2% to 19.5%. Both chalk and marl samples are poorly consolidated and their porosities are high.

3.2.3. Petrology

Petrographic analysis was carried out using both standard light microscopy of stained acetate peels and scanning electron microscopy (SEM) of fractured rock fragments.

All samples from this section, Site 3A were found to be sparse biomicrites under the Folk (1959) classification scheme, containing up to 20% bioclasts most commonly calcispheres, bivalve fragments, and foraminiferan tests. The micritic matrix in all samples was composed of non-ferroan calcite (stained pink), with varying amounts of clay. Rare non-ferroan and ferroan calcite cements were found. However, these were restricted to specific micro-environments, such as inside the chambers of foraminiferal tests. These cements were very rare and showed no systematic variation in abundance with respect to lithology.

Further petrographic analysis was carried out under the SEM to assess the degree of compaction, and to discover to what extent cementation by microspar had taken place. This investigation proved that there was very little evidence of compaction beyond that associated with initial dewatering. This is consistent with the minimum diagenetic alteration observed by Scholle (1974) in the chalks

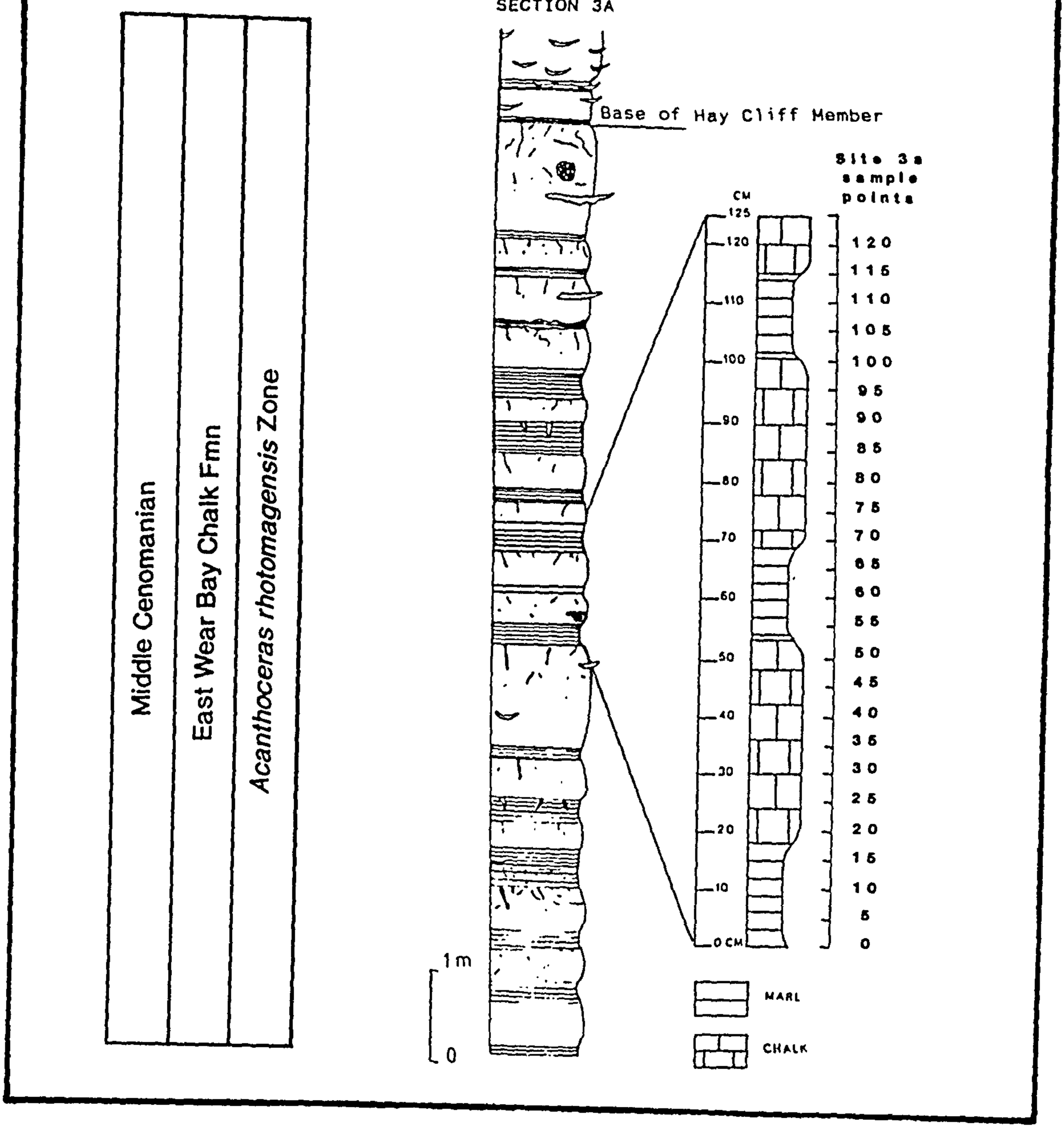

Figure 3.5 Lithological log of section Site 3a showing sample positions

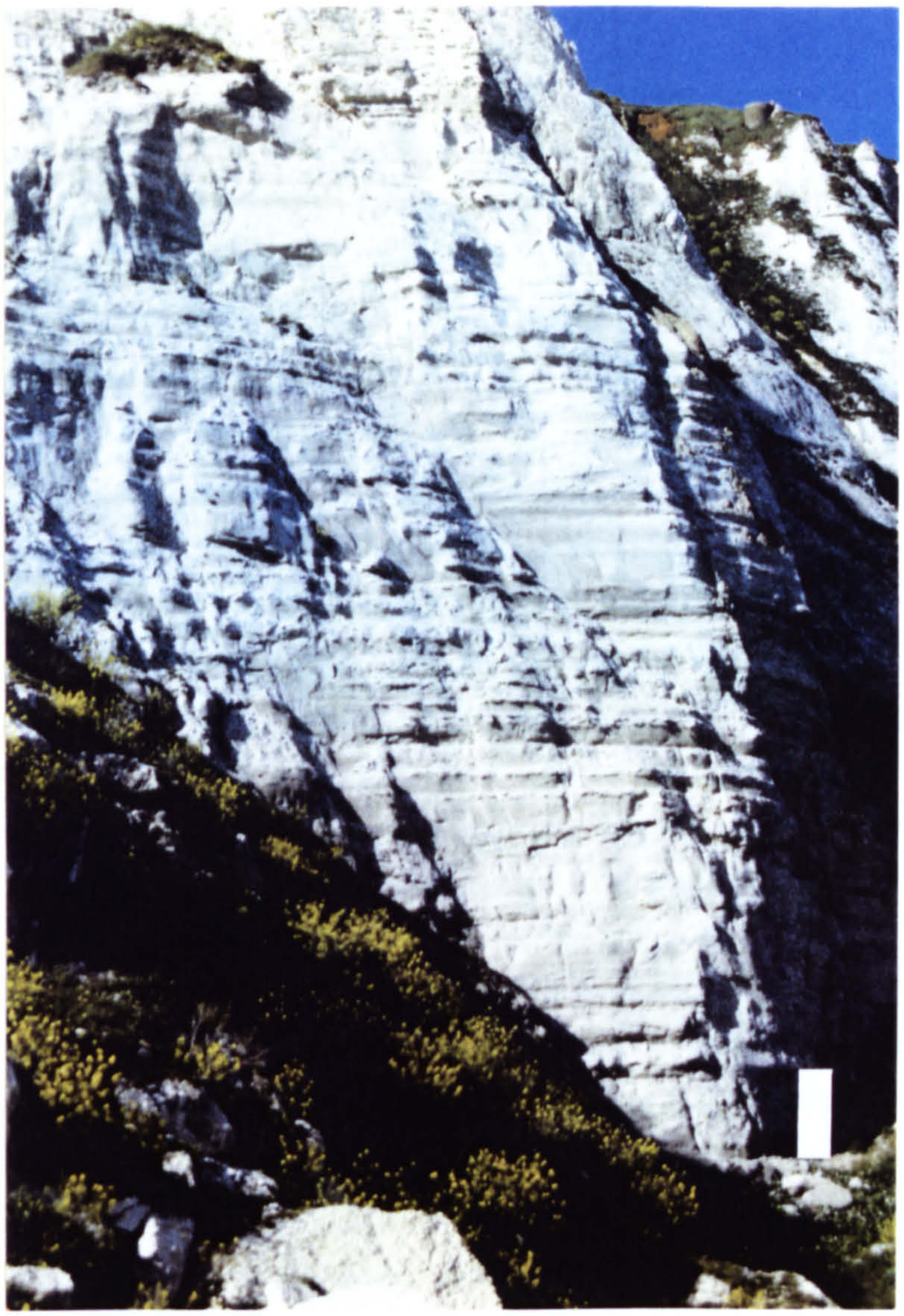

Figure 3.6 Photograph of TBB and MCB sections, Dover - Folkestone Warren area, south-east England. Scale bar 2m.

of south-east England.

3.3. Sections TBB and MCB

3.3.1. Introduction

Section TBB is a composite section taken from several closely spaced outcrops in the cliffs between Folkestone and Dover, in the immediate area of a large cliff fall (Grid reference TR 277387) (Figure 3.2). Section MCB samples a sub-section of the TBB section. Both TBB and MCB sections are of Middle Cenomanian age and are within the *Acanthoceras rhotomagense* ammonite zone of Kennedy (1969) and also within the foraminiferal zone 1li of Carter and Hart (1977). A photograph of both the TBB and MCB sections is given in Figure 3.6 and a close-up shot of the MCB section is given in Figure 3.7.

The section TBB samples approximately 17 m. of chalk, marl and marly chalk lithologies, and each sample is taken at a sampling interval of 1m (Figure 3.8). The MCB section is taken across the Mid-Cenomanian planktonic/benthonic foraminiferal non-sequence of Carter and Hart (1977). MCB samples are taken continuously every 5cm and the sampled section spans 1m. across the Mid-Cenomanian non-sequence (Carter and Hart, 1977) (Figure 3.9).

As well as the Mid-Cenomanian non-sequence (Carter and Hart 1977) the TBB section contains several lithostratigraphical and biostratigraphical marker horizons, including beds which contain 'pulse faunas' (Gale 1989a). A method of numbering the chalk/marl couplets which characterise the Middle Cenomanian chalks of south-east England, has been developed by Gale (1989 *pers. comm.*) and this method has been included herein.

The Mid-Cenomanian non-sequence (Carter and Hart 1977) occurs at the top of a prominent, indurated chalk bed which can be identified easily in the field as it is the top most of five relatively prominent chalk beds. These five chalk beds are relatively thin and are separated by well developed marl beds forming a conspicuous feature in outcrop (Figure 3.8). Although the Mid-Cenomanian non-sequence may represent a very short break in the succession it does not form an obvious erosive contact. Approximately 5m. below the Mid-Cenomanian non-sequence (Carter and Hart 1977) is

Figure 3.7 Close-up photograph of MCB section. The arrow marks the Mid Cenomanian non-sequence.

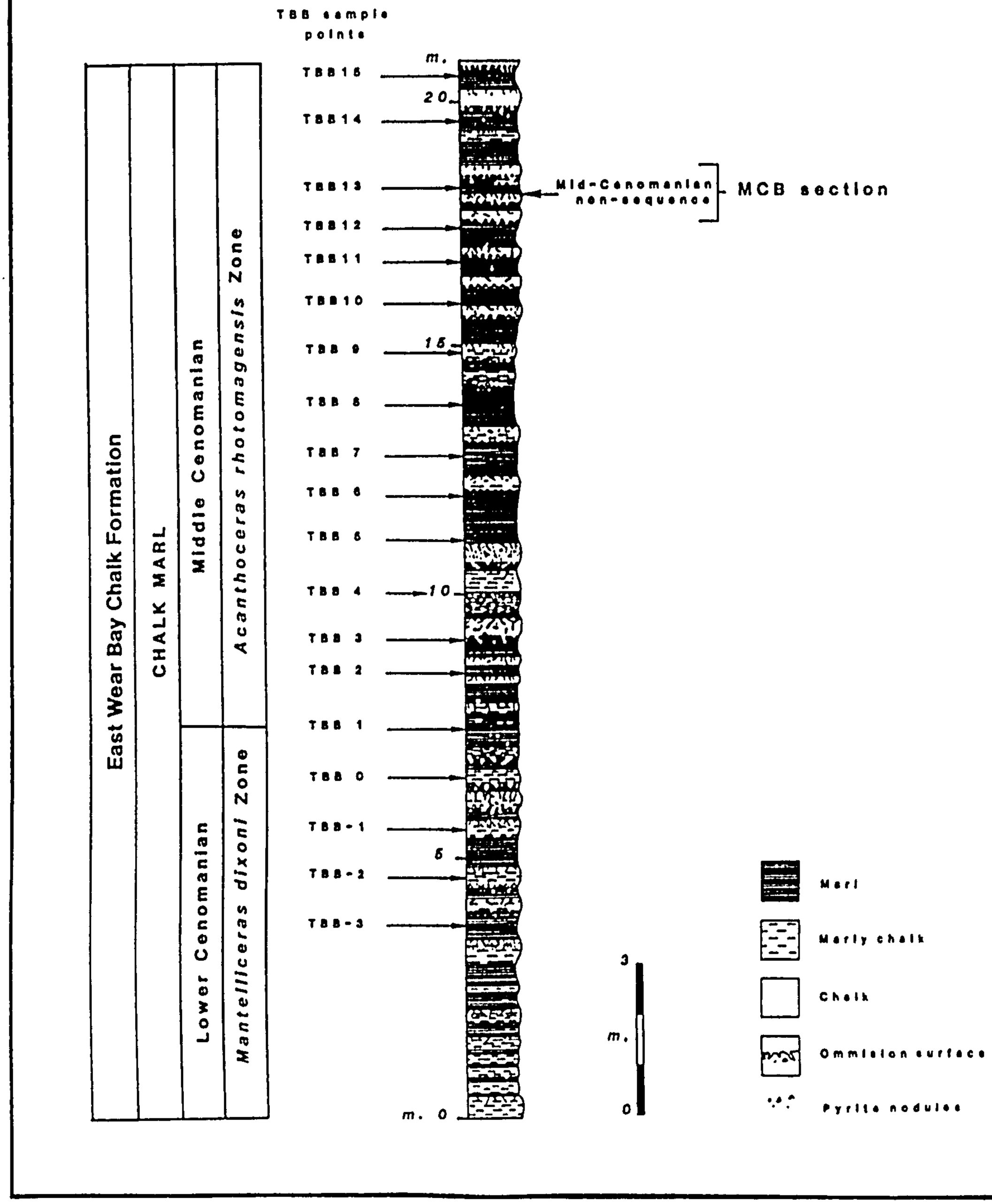

Figure 3.8 Lithological log of section TBB showing sample positions. Log taken from Gale (1989b).

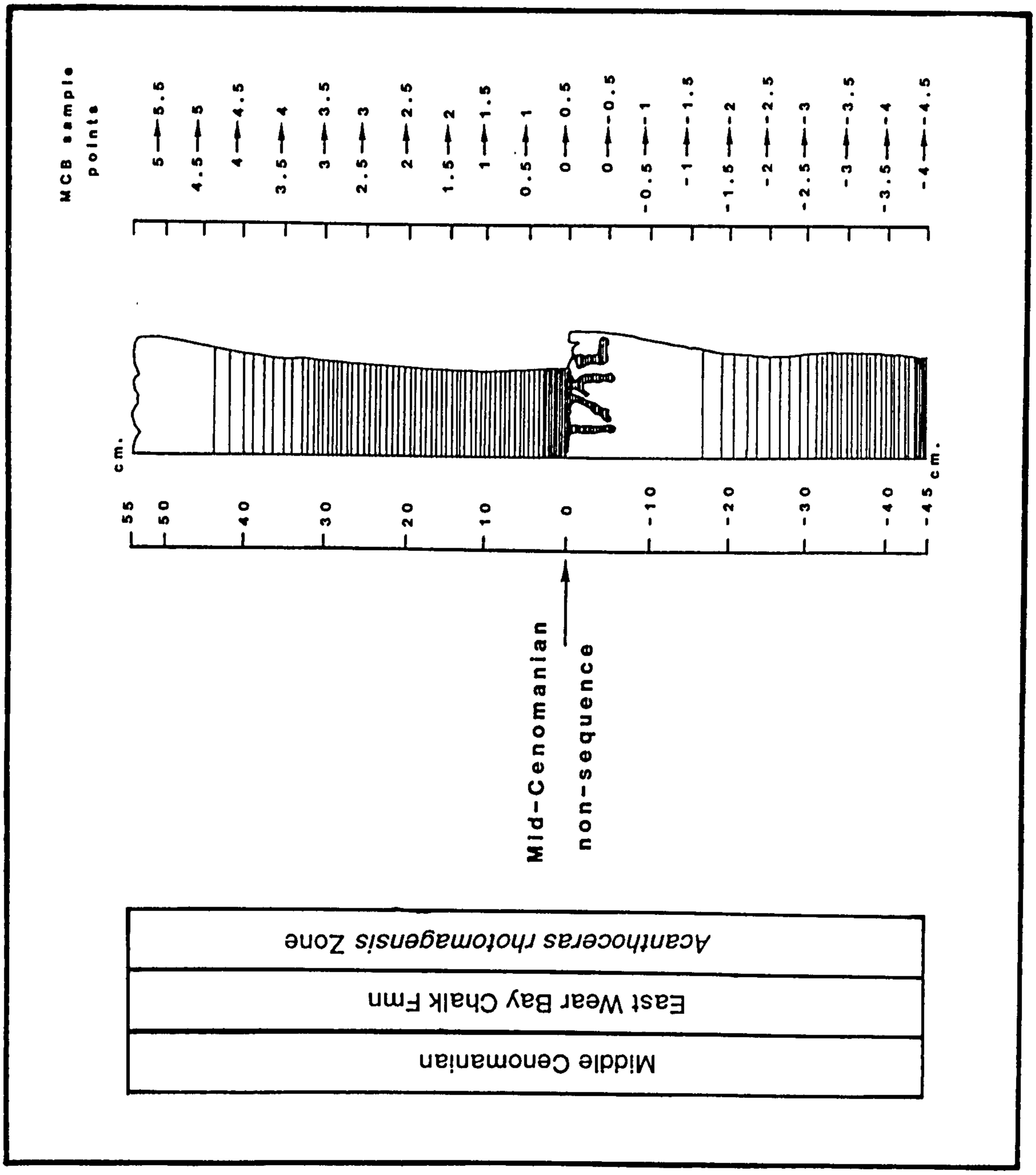

Figure 3.9 Lithological log for section on MCB showing sample positions

the next lithological marker, a 1m. thick buff to dark grey, silty marl unit (ie the marl of couplet C1 (Gale 1989 *pers. comm.*)). It contains abundant limonite coated moulds of aragonitic shelled molluscs, and is equivalent to the Cast bed of Price (1877). At the base of the Cast bed equivalent is a very prominent, hard, white, chalk bed (chalk of couplet B43 (Gale 1989 *pers. comm.*)). This prominent chalk bed is separated from a second hard chalk bed by approximately 1.5m. of more marly material. Together, these two hard white chalk beds form a very prominent and easily recognisable feature in outcrop, and are probably equivalent to the two white-weathering limestones described by Kennedy (1969). Underlying the base of the lower of these prominent chalk beds is a very dark marly bed (the marl of couplet B41 (Gale 1989 *pers. comm.*)), which contains a distinct fauna with abundant *Aequipecten arlesiensis.*

3.3.2. Style of Bedding

The TBB section is conspicuously rhythmic, consisting of alterations of clay-rich marl and clay-poor chalks which together form chalk/marl couplets. The clay-rich marl beds grade upwards into the clay-poor chalk beds, which are usually terminated by a sharp, though burrowed upper surface. There are considerable differences in the bed thickness and clay content between successive beds. This results in grouping or bundling of a number of consecutive couplets together, and differentiating a particular bundle from other bundles above or below it.

Superimposed on the bed by bed, and bundle by bundle variation in clay content, there is a general trend of decreasing clay content upwards within the section. A further marked change in clay content occurs at the top of the third rhythm above the Mid-Cenomanian non-sequence (Carter and Hart 1977), which is equivalent to couplet C14 (Gale 1989 *pers. comm.*). As this forms a prominent feature in this section and other equivalent sections within the Anglo-Paris basin such as Southerham in Sussex and Cap Blanc-Nez in France, this 'calcimetry break' must represent a widespread event affecting the supply of terrigenous clay to the whole of the basin.

All the beds within the TBB section are generally thoroughly bioturbated such that many of the boundaries are diffuse or gradational. Again the infilling of burrows with material from the

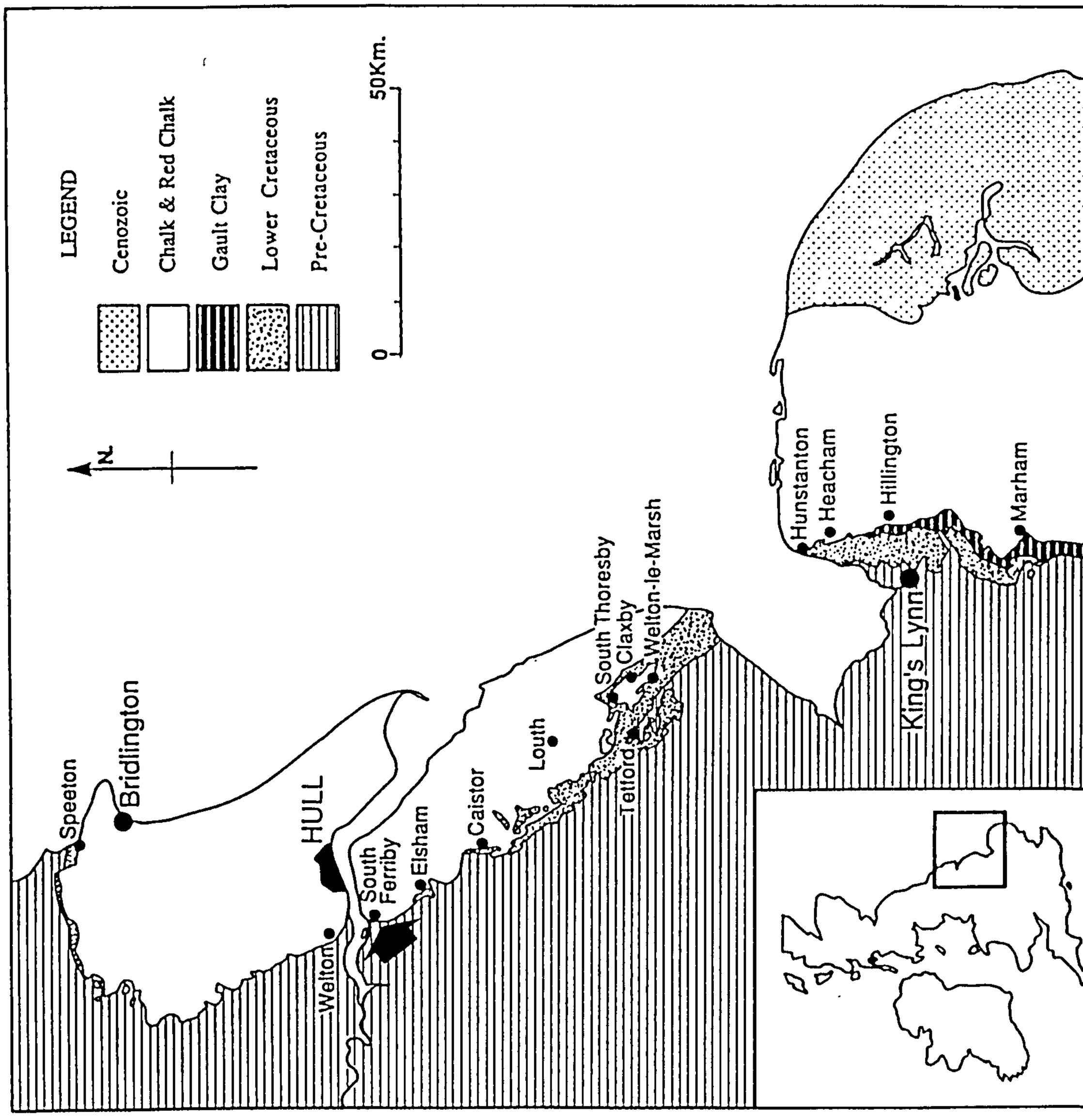

Figure 3.10 Location map for section SFE at South Ferriby, South Humberside, north-eastern England.

overlying lithology provides good evidence of primary sedimentological differences between successive beds. Many large burrow systems are well preserved and in some cases have considerable local effect on early diagenesis. Large open burrow systems, such as *Bathichus*, have locally promoted early pre-compaction cementation, to form a cement halo around the vertical burrow.

3.3.3. Petrography

As with the Site 3a section, samples from the TBB and MCB sections underwent petrographic analysis using standard light microscopy and scanning electron microscopy.

The petrographic results of these two sections are broadly similar to those of the Site 3A section. The rhythms consist of alternations of argillaceous and less argillaceous biomicrites (marls and chalks).

There is little evidence of compactional fracturing of the bioclasts examined from the stained peels, but some compactional fracturing of coccoliths was evident under the SEM. This fracturing was more common in the well developed marl beds adjacent to indurated chalk beds. There is no macroscopic evidence of pressure dissolution.

3.4. South Ferriby section, (SFE)

The South Ferriby site is in South Humberside, north-east England, (Grid reference TA 450420) (Figure 3.10). This site is a Rugby Group Cement quarry, exposing substantial thicknesses of Jurassic and Cretaceous strata. A photograph of the SFE section together with a close-up shot of the Black band horizon are given in Figure 3.11.

The section under particular investigation herein, is the Cenomanian-Turonian boundary sequence. The boundary sequence in this area of north-east England is recorded by a reduced *Plenus* Marls sequence, Jefferies (1963).

The SFE section is composed of 1.5m. of continuous sampling across and including the *Plenus* Marls (Jefferies 1963) (Figure 3.12). All samples within the SFE section lie within the *Holaster trecensis* Zone (Wright and Wright, 1942) (Figure 3.13). The lowermost four samples are taken from the uppermost part of the Ferriby Chalk

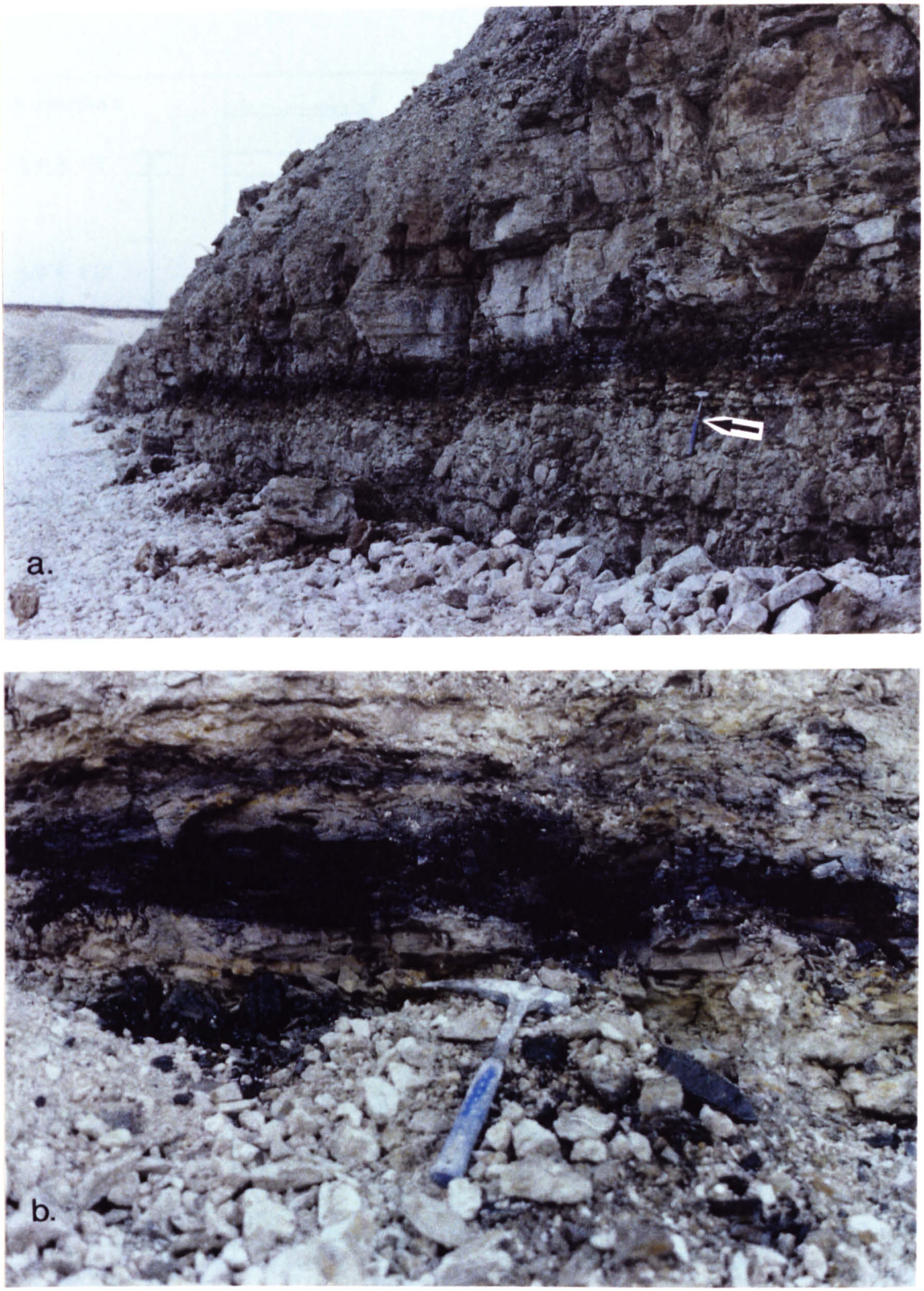

Figure 3.11 Photograph of SFE section, South Ferriby, South Humberside, north-east England, showing the Black Band. a. General shot of SFE section, see hammer (marked by arrow) for scale. b. Close-up shot of the Black Band horizon.

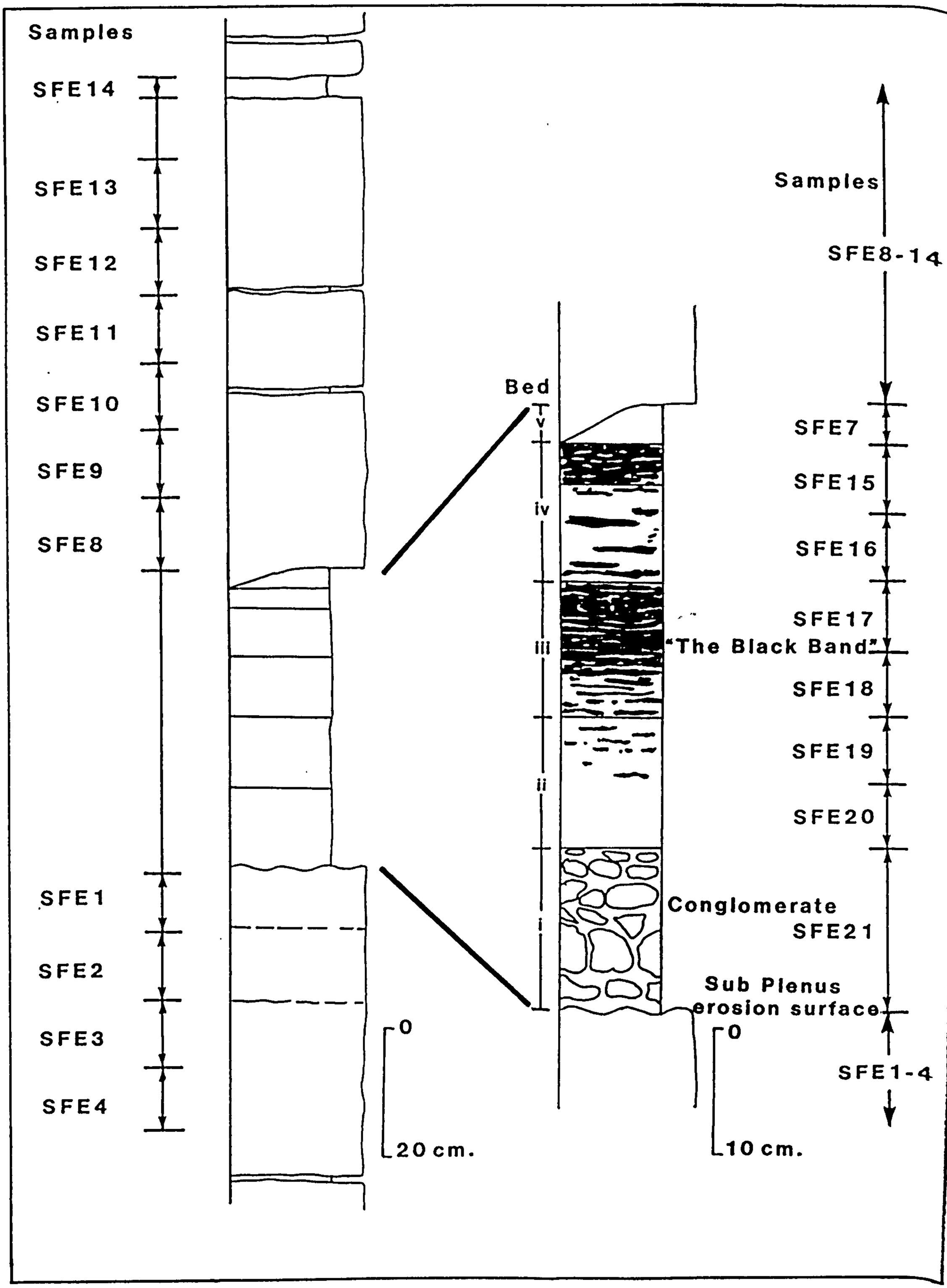

Figure 3.12 Lithological log of section SFE showing sample positions.

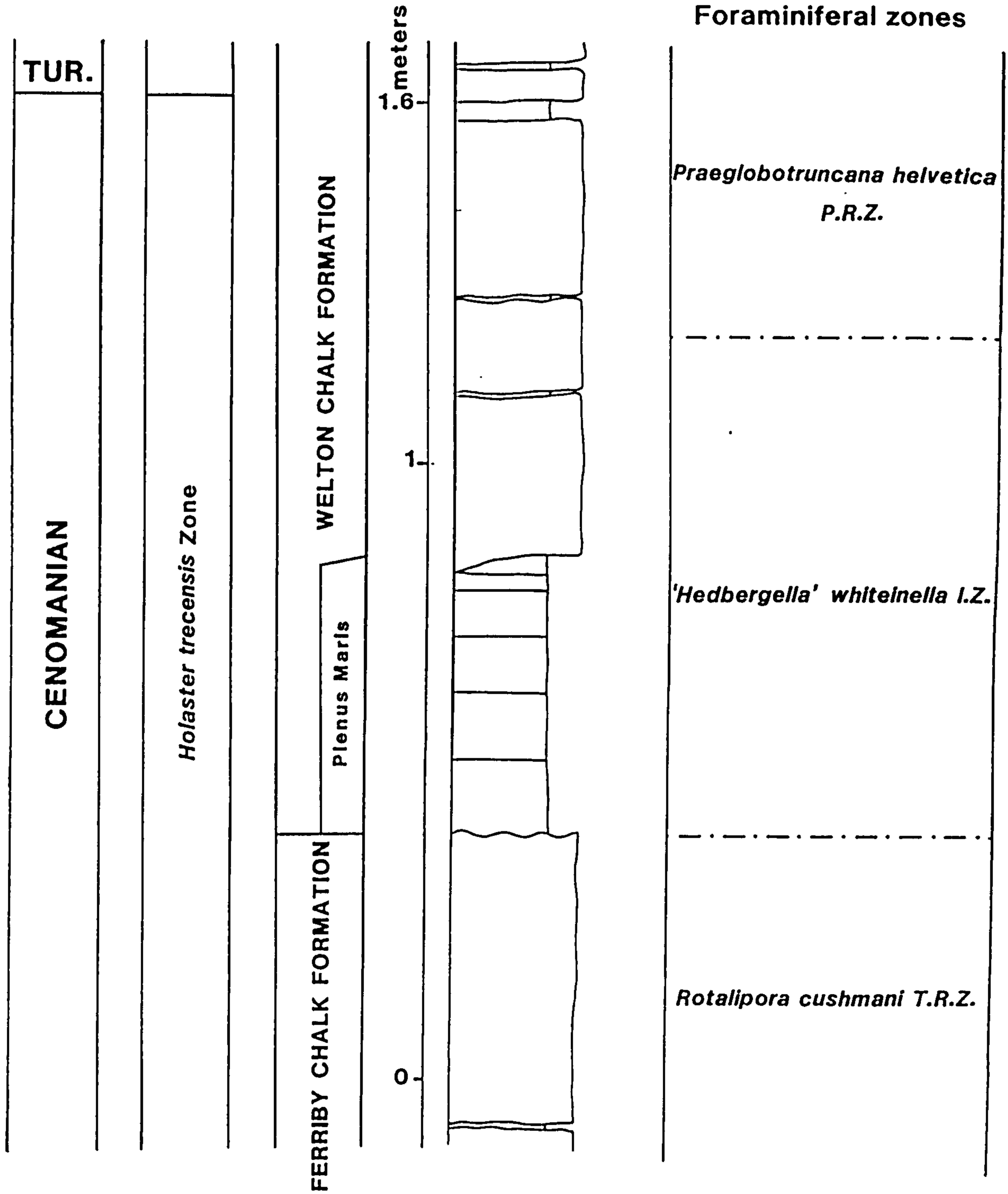

Figure 3.13 Litho- and bio-stratigraphical zonation scheme for South Ferriby section. Foraminiferal zonation taken from Hart and Leary (1989).

Formation (Wood and Smith, 1978). This part of the section corresponds to the foraminiferal zone the *Rotalipora cushmani* Total Range Zone (T.R.Z.), Hart and Leary (1989), (Figure 3.13). This part of the sequence is largely composed of massive, homogeneous chalks with thin interlaminated marls (Hart *et al.*, 1991). The South Ferriby quarry is the type section of the Ferriby Chalk Formation (Wood and Smith, 1978). Samples within this part of the SFE section are taken every 10cm.

There is a significant hiatus between the eroded top of the Ferriby Chalk Formation and the overlying basal Welton Chalk Formation (Wood and Smith, 1978). This hiatus is known as the sub-*Plenus* erosion surface. The erosion surface is picked out by a conglomerate of phosphatised chalk pebbles which rests on a slight angular unconformity. This feature is interpreted by Hart *et al.* (1991) as being indicative of long periods of exposure on the sea-floor. The sub-*Plenus* erosion surface marks the boundary between two foraminiferal zones, the lower being the *Rotalipora cushmani* T.R.Z. and the upper being the *'Hedbergella' whiteinella* Interval Zone (I.Z.), Hart and Leary (1989), (Figure 3.13).

The *Plenus* Marls sequence is the basal unit of the Welton Chalk Formation and is referred to as the "Black Band" succession by Hart *et al.* (1991). The *Plenus* Marls of South Ferriby are characterised by the presence of the "Black Band" which is a marl band which is interlaminated with paler-coloured marls, Hart *et al.* (1991). Above and below the "Black Band" the proportion of these paler laminae becomes greater than that of the black laminae. Individual laminae have been distorted and truncated by de-watering and compaction processes, Hart *et al.* (1991). Also, within the South Ferriby quarry there is a localised development of a second thinner black band at the top of Bed iv. Samples within the *Plenus* Marls sequence are taken continuously every 5cm.

The remaining seven samples are within the succeeding part of the Welton Chalk Formation and are taken at a sampling interval of every 10cm. The uppermost two samples of the SFE section are taken from the part of the section which corresponds to the *Praeglobotruncana helvetica* Partial Range Zone (P.R.Z.), Hart and Leary (1989), (Figure 3.13).

Chapter 4

MATERIAL AND METHODS

4.1. Introduction

In palynological processing the use of acids is employed to concentrate the organic fraction of the rock. This involves the digestion of acid-soluble mineral matter and the removal of non-soluble mineral matter by mechanical means. Also a quantitative approach was applied to all samples to ensure the quantity of material was precisely known initially and remains as constant as possible throughout the processing and slide making techniques. Meaningful interpretations on the quantitative analysis of the samples are then possible.

All samples were given a standard palynological treatment as outlined in Barss and Williams (1973) and Phipps and Playford (1984). However, due to the nature of the lithology of the rocks involved and their resultant residue, a standard oxidation stage was rarely if ever employed. Indeed, following the oxidation of only four samples in the whole project (TBB -3, -1, 13, 15), it has been conclusively shown herein that introducing a stage of oxidation reduces the resultant number of cysts per gramme of sediment (see section on Oxidation within this chapter).

Samples were initially crushed in a strong plastic bag with a hammer, to yield a fine grained powdered sample. A sub sample of this was then taken, placed in a polypropylene tripore beaker and weighed. Sample weights varied between 20 and 60 grammes which proved ample for both chalk and marl samples. The accurate weight of each sample was precisely recorded. The weight of each sample was given the notation "a", which is used later in the quantitative analysis. Some distilled water was added to dampen the sample so as to prevent air-borne contamination in the laboratory. Each sample was then covered with a plastic circular watch glass top.

It was necessary to use distilled water throughout all stages of the processing as tap water is supplied from reservoirs from the neighbouring Dartmoor. As a result the water is contaminated with modern spores and pollen and is frequently dirty.

4.2. Acid treatment

Concentrated hydrochloric acid (HCl 36%) was added to all samples to remove the carbonate content of the rock. As is to be expected with chalk and marl samples, there is a high carbonate content and, therefore, all samples reacted vigorously with each HCl addition. It became obvious that the HCl should be added very carefully, as there was always a very vigorous reaction. The technique of pouring the HCl down a glass rod into the sample proved useful in maximising the amount of HCl added in each individual addition. Frequently there was a vigorous reaction with HCl, especially during the first additions, and these were dampened down with water added from a squeeze bottle, a technique which also prevents sample loss. Samples were then left to continue reacting with the HCl and were stirred daily. Usually a further 3 - 6 additions of HCl were made, before all the carbonate was successfully removed. Complete carbonate removal was indicated when there is no further reaction with any additional HCl. Samples were then neutralised using distilled water by successive decantations until the remaining residue was neutral.

After neutralisation concentrated hydrofluoric acid (HF 60%) was added to all samples, to remove the silica content of the residues. This proved a shorter process than the HCl stage as little silica was present in any sample. Usually a single addition of HF was sufficient to remove all the silica. However, after this single addition, samples were stirred daily for a couple of days to reactivate the HF. Those few samples which still remained "gritty" on stirring were subjected to another addition of HF. After complete silica removal, samples were again neutralised with successive decantations of distilled water.

4.3. Sieving

At this stage of the procedure all samples were sieved through a plastic nest which encloses a 20μm nylon sieve mesh. Plenty of distilled water was filtered through the residue, to remove all the unwanted <20μm fines. This stage is deemed to be complete when the filtered water is clear, and for the first time the sample can be examined by the microscope, to examine its quality and content.

4.4. Mechanical removal methods

With the majority of samples it became necessary to sieve the resultant post-acid residue through a 250μm and very rarely through a 150μm mesh sieve. The latter sieve was only used with TBB samples -3, 9, 13, 15. This stage in the procedure removes any unwanted large particles (>250μm and >150μm) from the residue, such as fibres and large crystals. The resultant >250μm and >150μm fraction was always checked to see if any of the palynological content had been removed, however, loss by this means was always negligible. The >250μm and >150μm fractions were kept and bottled separately. Also, if heavy mineral particles were present in the residue, they were removed by panning. This technique concentrates the heavy particles which fall to the bottom of the pan, allowing the floating lighter particles including the palynomorphs, to be poured off. Again, the "heavys" were checked to ensure no palynological loss. This separation technique was only employed for sample TBB6, as there were no facilities for the use of Heavy liquid separating techniques. However, the panning technique proved perfectly adequate.

4.5. Staining

Fortunately, all the palynomorphs recovered had sufficient inherent colour from maturation and/or normal body colour, that staining was not required.

4.6. Oxidation

The inclusion of an oxidation stage within the palynological preparation was only necessary in the case of four samples; TBB -3, -1, 13, 15. These samples contained higher proportions of the kerogen type amorphogen. These samples underwent slight oxidation in order to remove this unwanted organic material. They were exposed to 2 - 5 minutes in nitric Acid (63% HNO_3) and were immediately diluted in distilled water and sieved again through a 20μm mesh nylon sieve, until neutral.

After quantitative analysis of the oxidised samples (TBB -3, -1, 13, 15) it became apparent that the values of number of cysts per gramme of sediment for these four samples were anomalously low when compared to the other TBB samples. Subsequently, to check and substantiate these findings aliquot slides were made of the

palynofacies/non-oxidised portion of all the samples in question. This exercise proved that there was substantial loss of palynomorphs due to the addition of an oxidation stage, as number of cysts per gramme rose by 30 to 210%, see below;

	Number of cyst/gramme of sediment	
	Oxidised sample	Unoxidised sample
TBB -3	198	616
TBB -1	225	511
TBB 13	311	412
TBB 15	309	412

I believe the resultant loss caused by oxidation was not due to chemical degeneration of the palynomorphs, but rather mechanical loss due to the introduction of an extra stage of sieving etc. Thus, this extra stage in the preparation proceedure introduces unwanted bias.

4.7. Quantitative techniques

The organic residues of all samples were centrifuged for 5 -10 minutes at 2,000 r.p.m. until a small pellet of residue forms. The water above the pellet was pipetted off and the residue accurately made up to 5 ml. using distilled water. The residue was then thoroughly mixed to ensure even dispersal of the organic residue within the water.

4.8. Slide preparation

Two types of slides were prepared; aliquot slides for quantitative work and ordinary strewn mounts for logging purposes. The aliquot method involves the use of a micropipette to withdraw a measured aliquot of 0.05ml. of the residue.

Glycerine jelly is the mounting medium used and it was prepared using the following recipe; 50g. Gelatine granules and 350g. Glycerol mixed together in 300ml. of distilled water. This mixture was dissolved by heating, but never boiled, and at this stage a few drops of concentrated Phenol were added to preserve the medium. To mount the slides the mounting medium was placed in a bath of hot water which was itself placed on the hot plate to allow it to melt.

The glass slides for both methods were labelled with a

diamond-tipped pencil and placed on a warm hot plate (25°C) on a stack of three other glass slides to prevent convection currents developing. In the case of the aliquot slide, a single drop of the mounting medium was pipetted onto the glass slide whereas three drops were pipetted onto the strewn slides. These were then left to cure for about two minutes until the jelly was semi-flowing. The measured aliquot of the residue was pipetted into the mounting medium on the aliquot slide and usually three drops of residue were pipetted into the mounting medium of the strewn slide. These were then mixed thoroughly to ensure maximum dispersal of the residue within the jelly. The slides were left for another couple of minutes to ensure maximum water evaporation from the residue. Care was taken throughout to ensure that there were no air bubbles trapped in the jelly. Finally, a glass cover slip was carefully lowered on top of the residue plus jelly mixture. The slides were left to stand on the hot plate for a few more minutes, removed and placed inverted on a rack for 24 hours to encourage the palynomorphs to settle in one focal plane within the mounting medium.

Any mounting medium which had extruded beyond the cover slip on to the surrounding slide was cleaned off using Methylated spirit and a scalpel. The edges of the cover slide were then painted with nail varnish to preserve the glycerine jelly. Each slide was then labelled with an adhesive label.

A couple of drops of HCl (36%) were added to all remaining residues, to prevent fungal growth.

4.9. Logging techniques

The palynological content of both strewn mount and aliquot slides was recorded, see Appendices 1-4. Counts of the total content of the aliquot slides were made with respect to the total number of palynomorphs present and to the various palynological groups present (dinoflagellates cysts, spores, pollen, acritarchs and fossil prasinophytes). Because a strict quantitative procedure was employed in the preparation of all samples, these data gave information on the number of cysts per gramme of sediment or abundance of samples. Counts of approximately 300 palynomorphs were made of the strewn mount slides with any additional occurrences of previously unrecorded palynomorphs being noted. However, no percentage values are attached to these additional occurrences.

4.10. FootNote

Site 3A samples were processed by the palynology technician of the Department of Geological Sciences, Polytechnic South West. As a result of this, aliquot slides of this section were prepared after the strewn mount slides were made. Site 3A values of number of cysts per gramme of sediment therefore read slightly lower than is anticipated.

1. Crush samples
2. Weigh samples and record result (gives "a")
3. Standard palynological preparation techniques
   - (i) Acid treatment
   - (ii) Sieving
   - (iii) Mechanical removal methods
   - (iv) Oxidation
4. Quantitative techniques

   Number of cysts per gramme calculated as follows:

   Number of cysts counted on aliquot slide (gives "b")

$$\text{Cysts/gm.} = \frac{b \times 100}{a} \qquad \text{Cysts/gm.} = \frac{\text{Aliquot} \times 100}{\text{dry weight of sample}}$$

5 Slide preparation

Table 1 Flow chart for quantitative palynological processing of chalks and marls.

Chapter 5

SYSTEMATIC PALYNOLOGY

5.1. Introduction

Genera are grouped into three families; GONYAULACACEAE, PERIDINIACEAE and CERATIACEAE within the Order PERIDINIALES. Cysts with unknown affinities are placed in INCERTAE-SEDIS. Within these families species are ordered alphabetically. Basic citation reference is given on each genus, its generic synopsis and type species. An effort was made to quote all important synonymies of the species. The synonymies contain reference to the original citation, subsequent taxonomic and systematic change and to the more important citations; it is not a monographic treatment. Junior synonyms are included and are indicated by being placed in inverted commas. Synonymies from unpublished Ph.D theses are indicated by the letter 'T', in the left hand margin.

The original description and subsequent emendations of all the species recovered were consulted. Information on the holotype and original dimensions is also included. However, a systematic description based upon the specimens observed herein is included under the title Description. Within such descriptions, the morphological terms applied are those defined by Williams *et al.* (1978), Evitt, (1985) and Jan du Chêne *et al.* (1986). The Kofoidian nomenclature system is used to define paratabulation patterns. Measurements are also included from the examined material; the minimum, mean (indicated in brackets) and maximum values are given, unless otherwise stated. Lengths are measured from apex to antapex and breadths are measured across the maximum width of the paracingulum, except where otherwise stated. The known stratigraphic range of all taxa is given as indicated by Lentin and Williams (1989), unless indicated otherwise. Although the term Senonian is used by Lentin and Williams (1989), it is realised herein that the use of this term was discussed by the IUGS Stratigraphic Sub-commission for the Cretaceous at Münster in April 1978. One of the resolutions of this meeting was that use of Senonian was to be discouraged. The stratigraphic occurrence of all species within all sections studied is recorded. All slides are held in the Department of Geological Sciences, Polytechnic South West.

5.2. Taxonomy

Division PYRRHOPHYTA Pascher 1914

Class DINOPHYCEAE Fritsch 1929

Order PERIDINIALES Haeckel 1894

Family GONYAULACACEAE Lindemann 1928

Genus *Achomosphaera* Evitt 1963

Generic Synopsis: Stover and Evitt 1978, p. 138

Type Species: *Achomosphaera ramulifera* (Deflandre 1937) Evitt 1963.

Achomosphaera neptuni (Eisenack 1958) Davey and Williams 1966a

Pl. 1, Fig. 1.

1958 *Baltisphaeridium neptuni* Eisenack, p. 399, pl. 26, figs 7,8; text-fig. 8.

1966a *Achomosphaera neptuni* (Eisenack) Davey and Williams, p. 51, fig. 7; pl. 9, fig. 11.

1978 *Achomosphaera ? neptuni* (Eisenack) Davey and Williams, Stover and Evitt, p. 139.

Original Description: Eisenack 1958, p. 399, pl. 26, fig. 7,8; text-fig. 8.

Holotype: Eisenack 1958, pl. 26, fig. 7.

Original Dimensions:

Diameter of cyst	40 - 60µm
Whole diameter	75 - 95µm
Holotype	48 - 88µm

Description: Skolochorate, medium sized, ellipsoidal cyst, with reticulate endophragm and gonal processes, which both bifurcate and trifurcate. Cyst shape varies very slightly from being ellipsoidal to ovoidal. The central body is sub-spherical to ovoidal. The two walls are closely adpressed over much of the cyst, except at the base of the processes in the paracingular and antapical areas. The central body has a distinctive reticulate ornament. Parasutural markings are rarely present. Processes are gonal and typically bifurcate and trifurcate with their tips closed distally. Processes in the antapical and paracingular regions are diagnostic of this species. Those in the paracingular area fuse proximally to form thick based

processes and these in the antapical area are large and symmetrically positioned. A sexiform antapical arrangement is present. There is a reduced precingular archaeopyle (Type P) which represents the camerate 3" paraplate and this together with the sexiform antapex are the only signs of paratabulation seen.

Remarks: Stover and Evitt (1978) designated this species as a provisionally accepted species within the genus *Achomosphaera* based upon the re-examination of the holotype which showed it to have an apical archaeopyle and multifurcate intratabular processes. In this study the species is easily identified on the basis of its original and emended description and the commonly occurring precingular archaeopyle. Therefore, I would favour the retention of *Achomosphaera neptuni* within this genus.

Dimensions:		
	Overall length of cyst	48 (56.8) 70µm
	Length of inner body	28 (34.4) 42µm
	Breadth of inner body	26 (30.1) 38µm
	Maximum height of antapical processes	10 (13.5) 18µm
	Number of specimens measured	20

Known stratigraphic range: Early Cretaceous

Occurrences:

Site 3A 0, 5, 20, 50 to 80, 100, 120

TBB -3 to 6, 8 to 13, 15

MCB -4.5 --> -4 to -2 --> -1.5, -0.5 -->1 to 5 -->5.5

SFE 16 to 18

Achomosphaera ramulifera (Deflandre 1937) Evitt 1963

Pl.1, Fig.2.

1935 *Hystrichosphaera* cf. *ramosa* (Ehrenberg) Deflandre, p. 5, fig.3

1937 *Hystrichosphaeridium ramuliferum* Deflandre, p. 74, pl. 14, figs 5,6; pl. 17, fig, 10.

1959 *Hystrichosphaeridium rehdense* Maier, p. 317, pl. 32, figs 3,4.

1963 *Baltisphaeridium ramuliferum* (Deflandre) Downie and Sarjeant, p. 32.

1963 *Achomosphaera ramulifera* (Deflandre) Evitt, p. 163

1981 *"Homotryblium distinctum"* Salujha and Kindra, p. 51, pl. 2, figs 45, 46.

Original Description: Deflandre 1937, p. 74, pl. 14, figs 5,6; pl. 17, fig. 10.

Holotype: Deflandre 1937, pl. 14, fig. 5.

Original Dimensions: Shell only (without appendages) 35 -45μm
Shell width with appendages reaches 90 - 100μm

Description: Ellipsoidal skolochorate cyst with a large, quite angular central body. The cyst is composed of two wall layers, which are separated only at the base of the processes in the apical, antapical and paracingular areas. Both periphragm and endophragm are smooth. The central body has a characteristic polygonal outline. The processes are gonal in position, large and hollow with typically trifurcating and bifurcating long tips. The bases of the processes at the paracingulum and antapex fuse, almost to form membranes. Antapical arrangement is sexiform. A reduced precingular archaeopyle (Type P) is usually present, formed by the loss of a camerate 3" paraplate. These latter two characteristics are the only signs of paratabulation seen on the cyst. Operculum is free.

Dimensions:

Overall length of cyst	50	(59.2)	70μm
Length of central body	30	(32)	40μm
Breadth of central body	24	(27.7)	36μm
Maximum process length	12	(18.2)	36μm
Number of specimens measured	20		

Known stratigraphic range: Late Cretaceous.

Occurrence:

Site 3A all samples

TBB all samples

MCB all samples

SFE no occurrence

Achomosphaera cf. *ramulifera*

Pl. 1, Figs 4-8.

1967 *Achomosphaera ramulifera* (Deflandre) Evitt, Clarke and Verdier, pl. 8, fig. 1.

T1973 *Achomosphaera ramulifera* (Deflandre) Evitt, Wilson, pl. 24, figs 11, 12.

1974 *Achomosphaera ramulifera* (Deflandre) Evitt, Kjellström, p. 10, fig. 2.

Description: Large elongate skolochorate cysts, with large strong *Achomosphaera* type processes. Central body sub-circular to oval. Periphragm and endophragm usually separated at the base of the processes in the paracingular, apical and antapical areas of the cyst. The degree of separation between these two wall layers varies considerably from cyst to cyst, depending on the elaborateness of the development of the processes. The more elaborate the processes are the more angular the cyst shape becomes (Pl. 1, Fig. 8). Both the periphragm and the endophragm are smooth. Processes are non-tabular, and are randomly distributed over the whole cyst and therefore do not denote a paratabulation pattern. Process size and morphology varies quite considerably intraspecifically and to a smaller extent, there is some variation depending on the position of the process on the cyst. However, all processes have either bifurcated or trifurcated tips. These tips may be produced into pointed spines or may be quite robust, like grapnel tips. Processes in the precingular and postcingular areas are usually simple, fine and parallel-sided with bifurcated and trifurcated tips. Those processes in the apical, paracingular and antapical areas are typically large, broad-based and appear biconvex in cross-section. They are terminated by distal bifid or trifid tips. Very often in these areas the bases of neighbouring processes merge to form a thick membrane from which the processes emanate. This membranous development is a highly variable characteristic of this cyst, as it may be developed to a greater or lesser extent. Where this characteristic is strongly developed the precingular and postcingular areas can appear devoid of processes (Pl. 1, Fig. 8). No parasutural features are present and therefore a paratabulation pattern is not obvious. A reduced precingular archaeopyle, Type P is present, representing the 3" paraplate, but it is not commonly seen. Operculum is free.

Remarks: *Achomosphaera* cf.*ramulifera* bears a strong resemblance to type *Achomosphaera ramulifera*. However, the former is larger in size and has a more robust, angular appearance, due to the development of some of its processes. This extreme development of the apical, antapical and paracingular processes clearly separates this species from typical *A. ramulifera*.

Clearly, in the past cysts of this type have been identified as *A. ramulifera*, see synonym list. However, it would appear that

cysts of this type are considerably different than type *A. ramulifera*, and they may be sufficiently different to validate the formation of a new species?

Dimensions:	Overall length	60 (72.1) 80µm
	Overall breadth	60 (68.5) 78µm
	Length of central body	30 (40) 48µm
	Breadth of central body	30 (32.6) 40µm
	Number of specimens measured	20

Occurrence:

Site 3A 0 to 10, 25, 35, 45 to 55, 75, 80, 95, 105, 110

TBB all samples

MCB all samples except 3.5 --> 4

SFE 16, 18

Achomosphaera reginensis Corradini 1973

Pl. 1, Fig. 3

1973 *Achomosphaera reginensis* Corradini, p. 171, pl. 27, fig. 2; text-fig. 8.

Original Description: Corradini 1973, p. 171, pl. 27, fig. 2; text-fig. 8.

Holotype: Corradini 1973, pl. 27, fig. 2.

Original Dimensions:	Holotype	Range
Diameter of central body	54 x 66µm	39 (48) 60 x 48 (55) 62µm
Length of processes	20 - 30µm	18 (28) 34µm

Description: Simple, spherical to ovoidal cyst with thin, highly furcate processes and smooth central body. Periphragm and endophragm are closely adpressed over the whole cyst. Processes are always single and neither their bases nor tips ever fuse. This species is characterised by thin delicate processes, which bifurcate and trifurcate about half way along the shaft, to give rise to long slender tips. Archaeopyle is rarely seen, but is a reduced precingular, (Type P) representing the 3" paraplate. Occasionally, faint parasutural lines are seen, but paratabulation is impossible to define as they occur haphazardly on different areas of the cyst, and from specimen to specimen.

Dimensions:	Length of central body	28	(33)	38µm
	Breadth of central body	24	(28.7)	35µm
	Maximum length of processes	12	(13.3)	20µm
	Number of specimens measured	20		

Known stratigraphic range: Senonian

Occurrences:

Site 3A 5 to 20, 30, 50 to 85, 95 to 120

TBB all samples except 14

MCB all samples

SFE 15, 16, 17, 18

Achomosphaera sagena Davey and Williams 1966a

Pl.1, Figs 9,10.

1955 *"Hystrichosphaera crassipellis"* Deflandre and Cookson, p. 265, pls 2,3; text-fig. 20

1966a *Achomosphaera sagena* Davey and Williams, p. 51, pl. 2, figs 1,2.

1967 *Achomosphaera "reticulata"* Clarke and Verdier, p. 41, pl. 8, figs 2,3; text-fig. 16.

Original Description: Davey and Williams 1966a, p. 51, pl. 2, figs 1,2.

Holotype: Davey and Williams 1966a, pl. 2, figs 1,2.

Original Dimensions:	Holotype	Range
Diameter of central body	48µm	35 - 59µm
Length of processes up to	20µm	28µm

Description: Large, ellipsoidally shaped cysts with reticulate, sub-spherical to ellipsoidal central body. The two wall layers are closely adpressed over much of the central body, except to a small extent in the paracingular areas. The wall of the central body is finely to densely reticulate, and this is very diagnostic of the species. Indeed, this reticulation may extend onto the periphragm at the base of the processes. Processes are hollow, thick and robust, and are gonal in position with bifurcate and trifurcate tips. A reduced precingular archaeopyle (Type P), formed by the loss of a camerate 3" paraplate. No sign of paratabulation besides that of the archaeopyle is seen. Operculum is free.

Dimensions:			
	Overall length of cyst	66	(74.2) 90µm
	Length of central body	40	(48.1) 57µm
	Breadth of central body	30	(43.5) 58µm

Maximum process length 22 (26.1) 33µm

Number of specimens measured 20

Known stratigraphic range: Cenomanian

Occurrences:

Site 3a all samples

TBB all samples

MCB -4.5 --> -4 to -1 --> -0.5, 0 --> 0.5, 0.5 --> 1, 2 --> 2.5, 3 -->3.5 to 5 -->5.5

SFE 16, 18

Genus *Apteodinium* Eisenack 1958

Generic Synopsis: Stover and Evitt, 1978.

Junior Synonyms: *Coniferatium* Burgess, 1971.

Dodekovia Dörhöfer and Davies, 1980

Emslandia Gerlach, 1961.

Type Species: *Apteodinium granulatum* Eisenack 1958

Apteodinium deflandrei (Clarke and Verdier 1967) emend. Lucas-Clarke, 1987

Pl. 2, Fig. 1

1967 *Gardodinium deflandrei* Clarke and Verdier 1967, p. 26, pl. 3, figs 10-12; text-fig. 10.

1978 *Aldorfia deflandrei* (Clarke and Verdier) Stover and Evitt 1978, p. 140.

1987 *Apteodinium deflandrei* (Clarke and Verdier) Lucas-Clarke, p. 172, pl. 5, figs 1-6, 8-10; text-fig. 6.

Original Description: Clarke and Verdier 1967, p. 26, pl. 3, figs 10-12; text-fig. 10.

Holotype: Clarke and Verdier 1967, pl. 3, fig. 10.

Original Dimensions:

	Holotype	Range
Overall length	52µm	52 - 56µm
Overall breadth	40µm	40 - 48µm
Length of inner body	36µm	36 - 43µm
Breadth of inner body	34µm	34 - 41µm
Length of apical horn	8µm	8 - 10µm
Length of pillars	1.5 - 4µm	1.5 - 4.5µm

Description: Medium sized, proximate ovoidal cyst with apical projection. Cyst possesses two wall layers, the endophragm and

periphragm are separated over the whole cyst. The resultant pericoel is filled with small pillar-like projections, which appear to support the outer membrane. In rare specimens, these pillars are replaced by muri. The endophragm is reticulate. The apical projection is formed of periphragm only and is conical in shape with a blunt top. Paratabulation is indicated only by the presence of a paracingulum, where the pillars are aligned to denote the paracingulum. A large reduced precingular archaeopyle (Type P) is present, formed by the loss of a camerate shaped 3" paraplate. Operculum is free.

Remarks: When *A. deflandrei* is observed in an apical - antapical compression, it may be confused with *Cleistosphaeridium huguoniotii* (Valensi) Davey. However, the smaller pillar-like projections and reticulate inner body of *A. deflandrei* are diagnostic and allow its differentiation from *C. huguoniotii*.

Dimensions: Overall length 38 (45.1) 52µm
Overall breadth 32 (37.9) 46µm
Number of specimens measured 20

Known stratigraphic range: Cenomanian to Santonian

Occurrence:

Site 3a 15, 35, 50, 65, 70, 85 to 95, 105 to 115
TBB -2, 1, 4, 12 to 14
MCB -4.5 --> -4 to 1 --> 1.5, 2.5 -->3, 3.5 --> 4, 4.5 --> 5, 5 --> 5.5
SFE 15, 16, 17, 18

Apteodinium maculatum Eisenack and Cookson 1960

Pl. 2, Fig. 2

1960 *Apteodinium maculatum* Eisenack and Cookson, p. 4, pl. 2, figs 1-3.

1960 *Apteodinium "conjunctum"* Eisenack and Cookson, p. 5, pl. 1, figs 7,8.

1984 *"Cribroperidinium conjunctum"* (Eisenack and Cookson) Helenes, p. 121, pl. 1, figs 7-14; text.fig. 5, A-D.

1988 *Apteodinium maculatum* Eisenack and Cookson, Backhouse, p. 74, pl.18, figs 1-3.

Original Description: Eisenack and Cookson 1960, p. 4, pl. 2, figs 1-3.

Holotype: Eisenack and Cookson 1960, pl. 2, fig. 1 and Jan du Chêne

et al. 1986, pl. 14, figs 6,7.

Original Dimensions:

	Holotype	Range
Length	88µm	74 - 105µm
Breadth	78µm	70 - 105µm

Description: Large oval proximate cyst with a small apical horn. Cyst shape varies slightly from ovoidal to sub-spherical. Typically the width across the paracingulum is approximately equal to the length of the body, excluding the apical horn. The apical horn is sub-conical in shape and is short and pointed. Autophragm only is present, and is shagreenate to finely granulate. A precingular archaeopyle is always present which is formed by the loss of a large camerate 3" paraplate. The archaeopyle is the only representation of paratabulation. Operculum is free.

Remarks: It is acknowledged that the previously accepted stratigraphic range for this species is that it is restricted to the Albian. The occurrence of this species within the Cenomanian herein is believed to be real.

Dimensions:

Length	60 (66.6)	80µm
Breadth	40 (53)	64µm

Number of specimens measured 5

Known stratigraphic range: Albian

Occurrence:

Site 3A 50, 55, 65 to 80, 90, 105, 120

TBB -3, -1 to 1, 2, 3, 8, 9, 11, 12, 14, 15

MCB -4.5 --> -4, -3 --> -2.5, -2.5 --> -2, -1 --> -0.5, 0 --> 0.5, 0.5 --> 1.

SFE 16, 17, 18

Genus *Callaiosphaeridium* Davey and Williams 1966a; emend. Below 1981

Generic Synopsis: Stover and Evitt 1978, p. 202.

Emended Generic Diagnosis: Below 1981, p. 27

Junior Synonym: *Hexasphaera* Clarke and Verdier 1967.

Type Species: *Callaiosphaeridium asymmetricum* (Deflandre and Courtville 1939) Davey and Williams 1966a.

Callaiosphaeridium asymmetricum (Deflandre and Courtville 1939) Davey and Williams 1966a.

Pl. 2, Fig. 3

1939 *Hystrichosphaeridium asymmetricum* Deflandre and Courtville p. 100, pl. 4, figs 1,2.

1966a *Callaiosphaeridium asymmetricum* (Deflandre and Courtville) Davey and Williams, p. 104, pl. 8, figs 9, 10; pl. 9, fig. 2.

1967 *"Hexasphaeridium asymmetrica"* (Deflandre and Courtville) Clarke and Verdier, p. 43, pl. 7, figs 1-3; text-fig. 17.

Original Description: Deflandre and Courtville 1937, p. 100, pl. 4, figs 1,2.

Holotype: Deflandre and Courtville 1937, pl. 4, fig. 1.

Original Dimensions: Diameter of shell 40µm
Length of tubular appendages 32 - 34µm

Description: Large, chorate, spherical cyst, characterised by bimorphic processes. Paratabulation is easily discernable. Typical mode of preservation is as an apical-antapical compression. The periphragm is finely reticulate. The epicyst possesses ?6 slender to slightly thicker solid intratabular precingular processes (6"), which are interconnected proximally by parasutural ridges. Forming a prominent flange around the equator of the cyst are 6 distinctive penitabular paracingular processes (6c). These processes are hollow and tubular, with broad bases, parallel sides and flared aculeate open distal margins, which are produced into furcated fine tips. The 5 intratabular postcingular processes (5"') again are slender to broad, solid and are distally furcate, reminiscent of *Spiniferites*. Parasutural ridges connect these postcingular processes, and are ornamented by raised beads. Parasutural ridges between apicals are weakly expressed and those in the pre- and post-cingular areas disappear towards the paracingulum. In antapical view the parasutural ridges outline a sexiform antapical arrangement. Reflected paratabulation pattern is ?', ?6", 6c, 5"', 1"". The archaeopyle is a compound epicystal type, formed by the loss of apical and precingular paraplates, however, it is only rarely seen.

Dimensions:			
Inner body diameter	32	(46.1)	52µm
Length of paracingular processes	20	(25)	30µm
Length of other processes	16	(20.1)	24µm
Number of specimens measured	15		

Known stratigraphic range: Senonian

Occurrences:

Site 3A 0, 5, 15 to 50, 60 to 120

TBB 9, 11, 12, 14, 15

MCB -4.5 --> -4 to -2 --> -1.5, -0.5 --> 0 to 0 --> 0.5, 1 --> 1.5, 2 --> 2.5, 3 --> 3.5 to 4.5 --> 5

SFE 18

Genus *Canningia* Cookson and Eisenack 1960b; emend. Helby 1987.

Generic Synopsis: Stover and Evitt 1978, p. 24.

Emended Generic Diagnosis: Helby 1987, p. 321.

Junior Synonym: *Hashenia* Yu Jingxian and Zhang Wangbing 1980.

Type Species: *Canningia reticulata* Cookson and Eisenack 1960b; emend. Below 1981; emend. Helby 1987.

Remarks: The genus *Canningia* has been included in the family *Gonyaulacaceae* following the recommendation of Dörhöfer and Davies (1980, p. 14) and Evitt (1985, p. 213).

Canningia colliveri Cookson and Eisenack 1960b

Pl. 2, Fig. 4

1960b *Canningia colliveri* Cookson and Eisenack, p. 251, pl. 38, figs 3,4.

1988 "*Canninginopsis colliveri*" (Cookson and Eisenack) Backhouse, p. 77, pl. 2, figs 7-9.

Original Description: Cookson and Eisenack, 1960b, p. 251, pl. 38, figs 3,4.

Holotype: Cookson and Eisenack 1960b, pl. 38, figs 3,4.

Original Dimensions:

	Holotype	Paratype
Length	107µm	106µm
Breadth	100µm	90µm

Description: Medium to large proximate cysts. Ovoidal shaped cyst, almost as broad as is long. Occasionally slight antapical bulges are present, giving the cyst a more angular shape. Autophragm is fine granular yielding a finely pitted appearance. Paracingulum is sometimes obvious, and is indicated by a indentation at the area of maximum width of the cyst. No other surface expression of paratabulation is seen. An apical archaeopyle (Type $\overline{tA}$) is present, and the archaeopyle margin has strong accessory archaeopyle sutures, giving the cyst a zig-zag margin after archaeopyle loss. The shape of

the precingular paraplates is as follows; 3", 4", 6" are camerate and 2" and 5" are planate. There is also a prominent sulcal notch which is offset to the left on the ventral surface. The latter two characteristics are the only form of paratabulation seen. Operculum is characteristically free.

Remarks: Backhouse (1988) transferred *Canningia colliveri* to the genus *Canninginopsis*. However, in his remarks (p. 78) he stated that *Canninginopsis colliveri* can be distinguished "by the absence of paratabular features". He includes that "faint partial paratabulation is expressed on only a few specimens by narrow strips devoid of normal, fine surface granulation". Therefore, Backhouse (1988) himself invalidates his own transfer of *Canningia colliveri* to *Canninginopsis colliveri*; the two genera are separated on the basis that *Canningia* has no parasutural features except a paracingulum, whereas *Canninginopsis* has both. The transfer of *Canningia colliveri* to the genus *Canninginopsis* is therefore rejected. It is felt that the occurrence of this species within the Cenomanian is real, and therefore extends the known stratigraphic occurrence of this species from the Aptian (see below) to include the Cenomanian.

Dimensions: Length from archaeopyle margin to cyst base 52 (59.6) 70μm

Breadth	52 (60.4) 66μm
Number of specimens measured	10

Known stratigraphic range: Aptian

Occurrences:

Site 3A 5, 10, 30, 40

TBB 2, 3

MCB -1.5 --> -1 to -0.5 --> 0, 0.5 --> 1, 2 --> 2.5, 4 --> 4.5

SFE 15, 16, 17, 18

Canningia reticulata Cookson and Eisenack 1960b; emend. Helby 1987.

Pl. 2, Fig. 5

1960b *Canningia reticulata* Cookson and Eisenack, p. 251, pl. 38, figs 1,2.

1981 *Canningia reticulata* Cookson and Eisenack, Below p. 32, pl. 4, figs 12-14; pl.12, figs 13-15.

1987 *Canningia reticulata* Cookson and Eisenack, Helby, p. 332, fig.27A - J.

Original Description: Cookson and Eisenack 1960b, p. 251, pl. 38,

fig. 1,2.

Holotype: Cookson and Eisenack 1960b, pl. 38, fig. 1, and Helby 1987, fig.27J.

Original Dimensions:	Holotype	Paratype	Range
Length	100µm	95µm	94 - 108µm
Breadth	86µm	98µm	74 - 98µm

Description: Medium to large ovoidal to sub-angular proximate cysts. Cyst wall is thick and densely granular and appears 'spongy' as the ectophragm seems to be differentated into two layers. The cyst appears to bulge in the paracingular area. Paratabulation is not expressed on the cyst surface, except sometimes the paracingulum is faintly indicated by an indentation at the cyst margin. This species exhibits an apical archaeopyle (Type $\overline{tA}$). Also present are marked accessory archaeopyle sutures, giving a zig-zag margin to the remaining cyst, after archaeopyle opening. Thus, it is observed that the 6 precingular paraplates have the following shape; 3", 4", 6" are camerate and 2" and 5" are planate. Also, the sulcal notch is offset to the left when the ventral surface is seen. These two latter characteristics are the only form of paratabulation seen. Operculum is characteristically free.

Discussion: Cookson and Eisenack (1960a), when erecting the new genus *Canningia*, stated it to have an apical archaeopyle which is lost, *i.e.* the operculum is free. However, in his emendation of the genus Below (1981) documented that the operculum is simple, enlarged but attached. If this characteristic of an adnate operculum is displayed by *Canningia* spp., then it is impossible to speciate *C. reticulata* from *Kallosphaeridium ? ringnesiorum* (Manum and Cookson, 1964) Helby 1987. Thus, I favour the emendation by Helby (1987) of the *Canningia* genus. See *K ? ringnesiorum* Discussion for further details.

Dimensions:	
Length from archaeopyle margin to base of cyst	70 (75) 84µm
Breadth	70 (86) 97µm
Number of specimens measured	10

Known stratigraphic range: Tithonian

Occurrences:

Site 3A 5, 15, 35

TBB -3, 4, 6 to 13

MCB -3.5 --> -3, -1 --> -0.5, 4 --> 4.5, 5 --> 5.5

SFE 15, 16, 17, 18

Genus *Carpodinium* Cookson and Eisenack 1962;
emend. Leffingwell and Morgan 1977

Generic Synopsis: Stover and Evitt, 1978, p. 145.

Type Species: *Carpodinium granulatum* Cookson and Eisenack 1962

Carpodinium obliquicostatum Cookson and Hughes 1964
Pl. 2, Fig. 6

1964 *Carpodinium obliquicostatum* Cookson and Hughes, p. 48, pl.6, figs 1-6.

Original Description: Cookson and Hughes, p. 48, pl. 6, figs 1-6.

Holotype: Cookson and Hughes 1964, pl. 6, figs 1-6.

Original Dimensions:

	Holotype	Range
Length	73μm	59 - 80μm
Breadth	50μm	36 - 50μm

Description: Medium sized elongate proximate suturocavate cyst with an apical horn and characteristic endophragm ornamentation. Cyst composed of periphragm and endophragm closely adpressed except at the apical horn and where the periphragm develops high parasutural ridges. Apical horn is composed of periphragm only, is sub-conical in shape and has a blunt top. Endophragm is ornamented by geometrically arranged anastomosing grooves, which grouped together give a triangular pattern. These grooves run obliquely to the long axis of the cyst. The paracingulum is marked by an indentation of the parasutural ridges. In addition, cyst carries parasutural ridges that outline the paratabulation and they reach their highest elevation at the paracingulum [10 (14.4) 20μm]. The distal margin of these ridges is serrate to denticulate. The sigmoidal relationship of the paracingulum and parasulcus implies that it has an S-type ventral organisation. Paratabulation is indicated by the parasutural crests. The reflected paratabulation pattern is typically gonyaulacacean and the formula is; 4', 6", 6c, 5", 1p, 1"". A large reduced precingular archaeopyle (Type P) is shown, representing the 3" paraplate. Operculum is free.

Dimensions:

Overall length of cyst	62 (68.1) 82μm
Length of central body	48 (56.10 70μm
Maximum paracingular breadth	34 (41.1) 50μm

Breadth of central body	24	(28)	36μm
Length of apical horn	8	(9.6)	12μm
Maximum height of parasutural crests	10	(14.4)	20μm
Number of specimens measured	20		

Known stratigraphic range: Late Albian to Early Cenomanian

Occurrences:

Site 3A 0 to 35, 60 to 120

TBB 0 to 5, 11 to 15

MCB -4 --> -3.5, -3 --> -2.5, -1 --> -0.5, 4 --> 4.5, 5 --> 5.5

SFE 17

Genus *Chlamydophorella* Cookson and Eisenack 1958; emend. Duxbury 1983

Generic Synopsis: Stover and Evitt 1978, p. 27.
Duxbury 1983, p. 41.

Type Species: *Chlamydophorella nyei* Cookson and Eisenack 1958

Remarks: Three species of the genus *Chlamydophorella* have been recorded herein; *C. discreta, C. nyei* and *C. ? urna.* In dorso-ventral compression, identification of these three species types is based on the presence or absence of an apical horn and paracingulum. It is necessary to refer to individual species descriptions for the details of each species respectively. In antapical view these cysts cannot be confidently assigned to any of the three species mentioned because the diagnostic characters are hidden in this orientation. Identification and allocation of the recorded species of *Chlamydophorella* was therefore only made when cysts were preserved in dorso-ventral compression.

Chlamydophorella discreta Clarke and Verdier 1967

Pl. 3, Fig. 1

1967 *Chlamydophorella discreta* Clarke and Verdier, p. 24, pl. 2, figs 9-10; text-fig. 9.

Original Description: Clarke and Verdier 1967, p. 24, pl. 2, figs 9-10; text-fig. 9.

Holotype: Clarke and Verdier 1967, pl. 2, fig. 10.

Original Dimensions:

	Holotype	Range
Overall diameter	33μm	29 - 35μm

Description: Small, spherical to sub-spherical proximate cyst with pillar-like structures between wall layers. Two wall layers are

present, the endophragm is produced into pillar-like processes with capitate to buccinate tops that appear to support the smooth periphragm. Maximum pillar height is 3μm. Pillar distribution is non-tabular and therefore paratabulation is not discernable. No apical horn or paracingulum was observed. An apical archaeopyle is present (Type $\overline{tA}$). Operculum is free.

Remarks: *Chlamydophorella discreta* is differentiated from *C. neyi* and *C. ? urna* by its lack of an apical projection and paracingulum. See initial Remarks on the genus *Chlamydophorella* for further discussion.

Dimension:		
	Length	34 (36.5) 40μm
	Breadth	30 (34.3) 40μm
	Number of specimens measured	20

Known stratigraphic range: Cenomanian

Occurrences:

Site 3A 5, 20, 30, 35, 45 to 55, 65 to 80, 110 to 120

TBB -3 to 6, 8 to 13, 15

MCB -4.5 --> -4 to 0 --> 0.5, 1.5 --> 2 to 2.5 --> 3, 3.5 --> 4 to 4.5 --> 5

SFE no occurrence

Chlamydophorella nyei Cookson and Eisenack 1958

Pl. 3, Fig. 2

1955 Hystrichosphaeridae vel Dinoflagellata Deflandre and Cookson, pl. 7, fig. 12

1958 *Chlamydophorella nyei* Cookson and Eisenack, p. 56, pl. 11, figs 1-3.

1970 *Chlamydophorella "apiculata"* Cookson and Eisenack, p. 150, pl.13, fig. 3.

1970 *Chlamydophorella "lagena"* Cookson and Eisenack, p. 151, pl. 13, fig. 4.

Original Description: Cookson and Eisenack 1958, p. 56, pl. 11, figs 1-3.

Holotype: Cookson and Eisenack 1958, pl. 11, fig. 1.

Original Dimensions:	Holotype	Range
Overall dimensions	48 x 43μm	48 x 43μm
Shell dimensions	38 x 35μm	
Appendage length	2.5 - 5μm	

Description: Small sub-spherical to oval proximate cyst with pillar-like structures and apical prominence. These structures terminate with capitate to buccinate tops which appear to support the periphragm. Apical horn is small and has a gentle rounded apex. A paracingulum is indicated by an indentation of the outer margin of the cyst and this is the only form of paratabulation seen. This indentation is accentuated as the largest processes are on either side of it. Apical archaeopyle is rarely seen, Type $\overline{tA}$.

Remarks: *Chlamydophorella nyei* can be distinguished from *C. discreta* and *C. ? urna* on the basis of its apical prominence and a paracingular indentation. See initial Remarks on the genus for further discussion.

Dimensions:		
	Length	36 (39.8) 45µm
	Breadth	32 (35.4) 40µm
	Number of specimens measured	20

Known stratigraphic range: Aptian to Turonian

Occurrences:

Site 3A no occurrence

TBB -3, -2, 0, 3, 11

MCB -1.5 --> -1, -0.5 --> 0, 5 --> 5.5

SFE no occurrence

Chlamydophorella ? urna Cookson and Eisenack 1960a

Pl. 3, Figs 3,4

1960a *Chlamydophorella urna* Cookson and Eisenack, p. 10, pl. 3, fig. 7.

1978 *Chlamydophorella ? urna* Cookson and Eisenack, Stover and Evitt, p. 28.

Original Description: Cookson and Eisenack 1960a, p. 10, pl. 3, fig. 7.

Holotype: Cookson and Eisenack 1960a, pl. 3, fig. 7.

Original Dimensions:	Holotype	Range
Length	39µm	29 - 43µm
Breadth	30µm	24 - 38µm

Description: Small, spherical to sub-spherical proximate cyst with short pillar-like structures between wall layers. These structures are parallel sided with capitate to buccinate tops that give the appearance of supporting the outer membrane. This external wall appears very thin and unornamented. A paracingulum is indicated by an

indentation of the external membrane in the paracingular areas and this is the only form of paratabulation seen. An archaeopyle is not observed.

Remarks: *Chlamydophorella ? urna* may be differentiated from *C. discreta* by the presence of a paracingulum and from *C. neyi* by the absence of an apical prominence. See initial Remarks on genus for further discussion.

Dimensions:	Length	30 (35.7) 40µm
	Breadth	30 (33.8) 40µm
	Number of specimens measured	20

Known stratigraphic range: Late Albian to Cenomanian

Occurrences:

Site 3A 10, 20, 50 to 75, 85, 95 to 110

TBB 6, 8, 9, 14

MCB -3.5 --> -3, -2.5 --> -2, -2 --> -1.5, -1 --> -0.5, 1.5 --> 2

SFE no occurrence

Genus *Cleistosphaeridium* Davey *et al.* 1966

Generic Synopsis: Stover and Evitt 1978, p. 31.

Junior Synonym: *Laticavodinium* Wilson and Sarjeant *in* Sarjeant 1984b

Type Species: *Cleistosphaeridium diversispinosum* Davey *et al.* 1966

Cleistosphaeridium armatum (Deflandre 1937) Davey 1969a

Pl. 3, Figs 5,6

1937 *Hystrichosphaeridium armatum* Deflandre, p. 76, pl. 16, figs 6,7.

1963 *Baltisphaeridium armatum* (Deflandre) Downie and Sarjeant, p. 91.

1967 *Baltisphaeridium armatum* (Deflandre) Clarke and Verdier, p. 71, pl. 13, fig. 3.

1969a *Cleistosphaeridium armatum* (Deflandre) Davey, p. 153, pl. 8, figs 1,2,12.

Original Description: Deflandre 1937, p. 76, pl. 16, figs 6,7.

Holotype: Deflandre 1937, pl. 16, fig. 6.

Original Dimensions: Body length approximately 25µm

Breadth 18 - 20µm

?Horn vary between 10 and 15µm, rarely longer.

Description: Medium sized, sub-spherical chorate cyst with numerous

long processes. Autophragm is densely granular, giving the surface a "diffuse-fuzzy" appearance. Processes are hollow, non-tabular and rigid. They are parallel-sided and gradually taper distally, but do not form a point. No paratabulation is seen apart from the presence of an archaeopyle which is only observed on some specimens. The archaeopyle is apical, Type $\overline{tA}$. Operculum is free.

Remarks: Specimens of *C.armatum* conform to the original description of Deflandre (1937), and the expanded description of Davey (1969a). However, herein processes on one individual and from specimen to specimen, are always simple and taper distally without giving rise to short spines, see Davey (1969a).

Dimensions:		
Diameter of central body	24 (28.9)	36µm
Maximum process length	10 (11.1)	14µm
Number of specimens measured	20	

Known stratigraphic range: Late Senonian

Occurrence:

Site 3A all samples

TBB all samples

MCB all samples

SFE 16, 17

Cleistosphaeridium clavulum (Davey 1969a) Below 1982

Pl. 3, Figs 7,8

1964 *Hystrichosphaeridium recurvatum* subsp. *polypes* Cookson and Eisenack, Cookson and Hughes, p. 47, pl. 9, fig. 14.

1969a *Cleistosphaeridium polypes* var *clavulum* Davey, p. 154, pl. 6, figs 9,10.

1973 *Bacchidium polypes* subsp. *clavulum* (Davey) Lentin and Williams, p. 24

1982 *Cleistosphaeridium clavulum* (Davey) Below, p. 15.

Original Description: Davey 1969a, p. 154, pl.6, figs 9,10.

Holotype: Davey 1969a, pl. 6, fig. 9.

Original Dimensions:	Holotype	Range
Diameter of central body	29 x 32µm	29 (31.5) 39µm
Length of processes	12 - 13µm	13 (14.5) 15µm

Description: Medium sized, spherical to sub-spherical chorate cysts with numerous fine processes. Autophragm is finely granular. Processes are solid, long and non-tabular. They are parallel-sided

and gradually taper distally to form a blunt to capitate top, giving them a pin-head-like appearance. Archaeopyle is rarely seen but is probably apical, Type $\overline{tA}$.

Dimensions: Diameter of central body 30 (35.6) 40μm
Maximum process length 10 (11.5) 14μm
Number of specimens measured 20

Known stratigraphic range: Cenomanian

Occurrence:

Site 3A 0, 10, 25, 35, 55 to 65, 75 to 85, 95, 105 to 120
TBB all samples
MCB all samples
SFE 16, 17, 18

Cleistosphaeridium huguoniotii (Valensi 1955a) Davey 1969a

Pl. 3, Figs 9,10

1955a *Hystrichosphaeridium huguonioti* Valensi p. 38, text-fig. 2A

1960a *Hystrichosphaeridium ancoriferum* Cookson and Eisenack, p. 8, pl. 2, fig. 11.

1963 *Baltisphaeridium huguonioti* (Valensi) Downie and Sarjeant, p. 91.

1963 *Hystrichosphaeridium ancoriferum* Cookson and Eisenack, Balteş, p. 586, pl. 6, fig. 13.

1964 *Hystrichosphaeridium ancoriferum* Cookson and Eisenack, Cookson and Hughes, p. 47, pl. 9, fig. 7.

1966 *Cleistosphaeridium ancoriferum* (Cookson and Eisenack) Davey *et al.* p. 167, pl. 9, fig. 1.

1967 *Hystrichosphaeridium ancoriferum* Cookson and Eisenack, Balteş, p. 330, pl. 4, figs 9-12.

1967 *Hystrichosphaeridium huguonioti* Valensi, Clarke and Verdier, p. 54, pl. 11, figs 4,5.

1969a *Cleistosphaeridium huguonioti* (Valensi) Davey, p. 155, pl. 7, fig. 10.

1974 *Cleistosphaeridium ancoriferum* (Cookson and Eisenack) Cookson and Eisenack, p. 66.

1978 *Chlamydophorella huguoniotii* Davey, p. 893.

1978 *Cleistosphaeridium huguoniotii* (Valensi) Davey, Stover and Evitt, p. 32.

1980 *Cleistosphaeridium ancoriferum* (Cookson and Eisenack) Davey

et al., Morgan, p. 19, pl. 6, figs 1-7.

1981 *Polysphaeridium ambigum* (Deflandre) Yun, p. 44, pl. 3, fig. 16.

Original Description: Valensi 1955a, p. 38, text-fig. 2A.

Holotype: Valensi 1955a, text-fig. 2A.

Original Dimensions:

Length of central body	29 - 33µm
Breadth of central body	25 - 29µm
Total breadth	33 - 41µm
Length of processes	4 - 7µm

Description: Small spherical to sub-spherical chorate cyst with numerous processes. Cyst wall is smooth to finely granulate. Processes are non-tabular and are buccinate or "anchor-shaped". These processes are hollow, but do not connect proximally with the central body and radiate perpendicularly about the central body. Processes may be distally linked by thin spines. If this latter characteristic is well developed, the cyst appears to be enveloped in a thin transparent membrane, which is apparently supported by the processes. An apical archaeopyle is nearly always exhibited, Type $\overline{tA}$. Operculum is free but is not regularly found as a separate entity.

Discussion: There has been much discussion to clarify the taxonomic position of *Cleistosphaeridium huguoniotii* and *C. ancoriferum*, and the relationship they have one to other; see Clarke *et al.* (1968) and Stover and Evitt (1978). Prior to these two publications, workers would either identify cysts of this type as belonging to one or other of these two cyst species, ie. *C. huguoniotii* and *C. ancoriferum* were never identified as occurring together. Clarke *et al.* (1968) thought that prevalent feeling was that these species were synonymous. However, because of the nature of the preservation of the holotype of *C. huguonioti* this could not be demonstrated conclusively. Stover and Evitt (1978) because of this preservation difficulty stated that the name *C. huguoniotii* should only be applied to its type specimens only. Later Morgan (1980) agreed with Cookson and Eisenack (1974) to retain *C. ancoriferum* separately from *C. huguoniotii*. However, having translated the relevant passage of Cookson and Eisenack (1974 p. 66) in which they discuss the confusion associated with these two species, it does not state that the two are separate species.

Throughout this investigation it has been found both the original description of Valensi (1955) and the subsequent description

by way of a new combination by Davey (1969a), together with their corresponding illustrations are of sufficient quality to facilitate easy identification of *C. huguoniotii*. This, together with the fact that *C. ancoriferum* should be a junior synonym of *C. huguoniotii* under the systematic laws of antecedence, were the reasons for attribution of these cysts types to *C. huguoniotii*.

Dimensions:	Diameter of central body	26 (32) 38µm
	Maximum process height	4 (5.3) 8µm
	Number of specimens measured	20

Known stratigraphic range: Late Cretaceous

Occurrence:

Site 3A all samples

TBB all samples

MCB all samples

SFE 16, 17, 18

Genus: *Coronifera* Cookson and Eisenack, 1958; emend. Mao Shaozhi and Norris, 1988.

Generic Synopsis: Stover and Evitt, 1978, p. 148.

Emended Generic Description: Mao Shaozhi and Norris, 1988, p. 35.

Type Species: *Coronifera oceanica* Cookson and Eisenack, 1958, emend. May, 1980.

Coronifera oceanica Cookson and Eisenack 1958, emend. May, 1980.

Pl. 3, Fig. 11

1958 *Coronifera oceanica* Cookson and Eisenack, p. 45, pl. 12, figs 5,6.

1980 *Coronifera oceanica* Cookson and Eisenack, May, p. 48

Original Description: Cookson and Eisenack, 1958, p. 45, pl. 12, figs 5,6.

Holotype: Cookson and Eisenack, 1958, pl. 12, fig. 6.

Original Dimensions:	Holotype	Specimen in pl. 12, fig.5
Overall	90 x 81µm	105 x 86µm
Shell (without horn)	57 x 48µm	76 x 36µm
Hollow horn	17µm	14µm

Description: Intermediate sized, sub-spherical to oval chorate cyst with a distinctive antapical process. Endophragm and periphragm closely adpressed over much of the body, except at apical and

antapical areas. The endophragm is smooth but is wrinkled due to the presence of low, non-tabular ridges. However, on either side of the paracingulum these ridges seem to denote parasutures. Paratabulation is not otherwise recognised. All the processes, apart from the apical and antapical processes are aciculate, fine and non-tabular, and give the cyst a fibrous or hairy appearance. The apical processes are quite small and conical in shape. The antapical process is large, tubular and is distally flared with a denticular margin. Specimens exhibiting both precingular, Type P (3" paraplate) and combination archaeopyles Type t$\overline{Aa}$ + P are observed, however the former type is more common.

Dimensions:	Length of central body	40 (46.6) 52µm
	Breadth of central body	36 (41.5) 48µm
	Length of antapical process	10 (14.2) 16µm
	Length of other processes	10 (12.2) 16µm
	Number of specimens measured	10

Known stratigraphic range: Albian

Occurrences:

Site 3A 10, 15

TBB 3, 4, 9, 10, 14

MCB -4.5 --> -4 to -1.5 --> -1, 0 --> 0.5, 0.5 --> 1, 1.5 --> 2, 2.5 --> 3

SFE 15

Genus *Cribroperidinium* Neale and Sarjeant, 1962; emend. Helenes, 1984.

Generic Synopsis: Stover and Evitt, 1978, p.149.

Emended Generic Description: Helenes, 1984, p. 112.

Junior Synonyms: *Meristaulax* Sarjeant, 1984a.
Millioudodinium Stover and Evitt, 1978.

Type Species: *Cribroperidinium sepimentum* Neale and Sarjeant, 1962

Cribroperidinium cooksoniae Norvick, 1976.
Pl. 4, Figs 1-7

1976 *Cribroperidinium cooksoniae* Norvick, p. 36, pl. 1, figs 1-3; text-fig. 13.

1984 *Cribroperidinium cooksoniae* Norvick, Helenes, p. 121.

Original Description: Norvick 1976, p. 36, pl. 1, figs 1-3;

text-fig. 13.

Holotype: Norvick 1976, pl. 1, fig. 2 and Jan du Chêne, *et al.*, 1986, pl. 31, fig. 7.

Original Dimensions:	Holotype	Range
Overall length	81μm	58 (72) 95μm
Width	67μm	

Description: Large, ovoidal to ellipsoidal, proximate acavate cyst, with characteristic parasutural ridges. Shape of cyst in dorso-ventral compression can vary from ovoidal to even rhomboidal. This variation depends on the extremity of the difference between the minimum breadth, at the apex and antapex, and the maximum paracingular breadth. The epicyst has a more angular appearance than the rounded hypocyst. Autophragm only present. Apical horn is hollow and usually stout, conical in shape, and tapers to form a blunt top. The paracingulum is broad helicoid and laevorotatory, but there are no individual paracingular paraplates. The parasulcus is also obvious as a depression/indentation in the outline of the cyst, especially noticeable on the hypocyst. Paratabulation is indicated by low parallel pairs of parasutural ridges (Pl. 4, Fig. 2). The parasutural ridges are unornamented. The inferred paratabulation is ?4', 6", 6c, 6"', 1p, 1"". An L-type ventral organisation is present. There is a sexiform antapical arrangement. However, in my experience, only the pre- and post-cingular areas show any clear indications of paratabulation. The autophragm is differentiated into a lower homogeneous layer and an outer vesicular or "fuzzy" looking outer layer. A precingular archaeopyle is exhibited, Type P, formed by the loss of the 3" paraplate. This is an enlarged archaeopyle giving this paraplate a camerate shape but with a more gently rounded geniculate boundary. Operculum is free.

Remarks: Under higher magnifications specimens of *C. cooksoniae* become out of focus or "fuzzy" because of the nature of the autophragm. This causes difficulties in identifying paraplates and thus defining paratabulation and also carrying out higher magnification photography. This "fuzziness" is believed to be due to the vesicular nature of the outer portion of the autophragm.

Dimensions:		
Length including the apical horn	64 (73.4) 92μm
Length excluding apical horn	60 (68.5) 82μm
Heigth of apical horn	4 (5.2) 10μm

	Maximum breadth	50 (63.1) 74µm
	Number of specimens measured	20

Known stratigraphic range: Cenomanian

Occurrences:

Site 3A all samples

TBB -3 to -1, 4 to 15

MCB -4.5 --> -4 to -3.5 --> -3, -2 --> -1.5, 0 --> 0.5, 0.5 --> 1, 1.5 --> 2 to 4.5 --> 5

SFE no occurrence

Cribroperidinium edwardsii (Cookson and Eisenack 1958) Davey, 1969a.

Pl. 5, Figs 1-6

1958 *Gonyaulax edwardsi* Cookson and Eisenack, p. 32,, pl. 3, figs 5,6; text-fig. 7.

1967 *Gonyaulacysta edwardsi* (Cookson and Eisenack) Clarke and Verdier, p. 31, pl.5, fig. 1.

1969a *Cribroperidinium edwardsi* (Cookson and Eisenack) Davey, p. 128.

1984 *Cribroperidinium edwardsii* (Cookson and Eisenack) Davey, Helby, p. 125.

Original Description: Cookson and Eisenack, 1958, p.32, pl.3, figs 5,6; text-fig. 7.

Holotype: Cookson and Eisenack, 1958, pl. 3, fig. 6, text-fig. 7 and Jan du Chêne *et al.*, 1986, pl. 33, fig. 3.

Original Dimensions: Holotype 143 x 125µm

Description: Large sub-spherical to ovoidal proximate acavate cyst with strong apical horn and prominent parasutural ridges. Epicyst is characterised by the apical horn, which is hollow, broad based and tapers distally to a rounded point. Length of the horn varies from 10 - 30µm with a mean value of 19µm. Autophragm is granular to coarsely granular, appears thick and is dark brown in colour. Paracingulum is helicoid and laevorotatory. Paracingular paraplates are hinted at by faint parasutures. Parasulcus is represented by an indentation of the cyst on the ventral surface. Diagnostic parasutural ridges are present indicating a paratabulation pattern of; 4', 6", 6c, 6"', 1p, 1"". Antapical paraplate arrangement is sexiform. The distal margin of the parasutural ridges are serrate to denticulate. An enlarged precingular archaeopyle (Type P) is present formed by the loss of a

large 3" camerate paraplate which has a rounded geniculate paraplate boundary. Operculum is free.

Remarks: Specimens of *C. edwardsii* were often broken.

Dimensions:			
Length including apical horn	112	(126.8)	144µm
Length excluding apical horn	94	(107.8)	126µm
Height of apical horn	10	(19)	20µm
Maximum breadth	80	(101.6)	122µm
Number of specimens measured	10		

Known stratigraphic range: Albian to early Turonian

Occurrences:

Site 3A no occurrence

TBB -3 to 4, 11

MCB no occurrence

SFE no occurrence

Genus *Cyclonephelium* Deflandre and Cookson, 1955;
emend. Stover and Evitt, 1978.

Generic Synopsis: Stover and Evitt, 1978, p. 35.

Type Species: *Cyclonephelium compactum* Deflandre and Cookson, 1955.

Remarks: The genus *Cyclonephelium* is included in the family *Gonyaulacaceae* following the recommendation of Dörhöfer and Davies (1980, p.14) and Evitt (1985, p. 212).

Cyclonephelium distinctum Deflandre and Cookson, 1955.
Pl. 6, Fig. 1

1955 *Cyclonephelium distinctum* Deflandre and Cookson, p. 285, pl. 2, fig. 14; text-figs 47,48.

1986 *Circulodinium distinctum* (Deflandre and Cookson) Jansonius, p.204.

Original Description: Deflandre and Cookson 1955, p. 285, pl. 2, fig. 14; text-figs 47,48.

Holotype: Deflandre and Cookson 1955, pl. 2, fig. 14.

Original Dimensions:		
Diameter of shell	65 - 97µm	
Length of appendages	2.5 - 18µm	

Description: Large proximochorate cyst, typically dorso-ventrally compressed and thus sub-circular to sub-polygonal in outline. Shape of the hypocyst varies from being rounded to possessing slight antapical bulges, the former is most common. Autophragm has a

granular to punctate appearance. The numerous processes are non-tabular, solid and usually short. The distal apices of the processes are variable from simple to capitate to buccinate. Processes are usually single but, rarely one or two are linked proximally to form a mini lamella. Processes distribution as is typical for the genus *Cyclonephelium* is concentrated at the periphery of the cyst and are lacking in the mid dorsal and ventral areas. An apical archaeopyle, Type $\overline{tA}$ is present. Operculum is always detached leaving a characteristic zig-zag suture margin indicating a tetra-meta apical arrangement of paraplates. After archaeopyle loss the shape of the precingular paraplates is seen as follows; 1", 2", 4" planate and 3", 5", 6" camerate. The parasulcal notch is offset to the left on the ventral surface. These latter characteristics are the only signs of paratabulation seen.

Remarks: Specimens of *C. distinctum* are nearly always found having lost their operculum.

Discussion: Jansonius (1986) appears to have transferred *C. distinctum* to *Circulodinium distinctum* for no apparent reason. However, *C. distinctum* conforms in all aspects to the generic description of *Cyclonephelium*, Stover and Evitt (1978), and I see no justification to transfer this species. Thus, I reject Jansonius (1986) transfer of *Cyclonephelium distinctum* to *Circulodinium*.

Dimensions:			
	Width of central body	54 (64.2)	74µm
	Length of central body	50 (57)	62µm
	Maximum height of processes	8 (10.4)	14µm
	Number of specimens measured	20	

Known stratigraphic range: Senonian

Occurrence:

Site 3A all samples

TBB all samples

MCB all samples

SFE 17, 18

Cyclonephelium membraniphorum Cookson and Eisenack 1962

Pl. 6, Figs 2-5

1962 *Cyclonephelium membraniphorum* Cookson and Eisenack, p. 495, pl. 6, figs 8-14.

1981 "*Maghrebinia membraniphora*" (Cookson and Eisenack) Below, p.

Original Description: Cookson and Eisenack 1962, p. 495, pl. 6, figs 8-14.

Holotype: Cookson and Eisenack 1962, pl. 6, fig. 9.

Original Dimensions:	Holotype	Range
Length	127µm	
Breadth	108µm	73 - 128µm
Width of wing-like membranes		6 - 22µm

Description: Large proximochorate, sub-circular to sub-angular shaped cyst, with elaborate parasutural membranes. Autophragm is smooth to fine punctate. As is typical of the genus *Cyclonephelium* the mid-dorsal and mid-ventral areas are devoid of the parasutural membranes as they are concentrated around the periphery of the cyst. Processes are highly developed to form flamboyant parasutural membranes or muri which have the overall morphology of being box or funnel-shaped. Neighbouring membranes connect to give the periphery of the cyst a very membranous appearance. Occasionally on certain cysts these parasutural membranes denote the position of paraplates, thus indicating a partial paratabulation pattern (Pl. 6, Figs 4, 5). This feature is most obvious in the paracingular and parasutural areas on the ventral surface of the cysts, where individual paraplates can be identified. There is an L-type ventral arrangement to the paracingulum and parasulcus. A large 1p paraplate is present. An apical archaeopyle is present, Type $t\overline{A}$. After archaeopyle loss the remaining cyst has a zig-zag archaeopyle margin due to the presence of slight accessory archaeopyle sutures, indicating a tetra-meta apical paraplate arrangement. The shape of the precingular paraplates is as follows; 3", 5", 6" are camerate shaped and 1", 2", 4" are planate shaped. Also, the sulcal notch is offset to the left on the ventral surface. These latter characteristics are the only signs of paratabulation seen. Operculum is free.

Remarks: Below (1981) transferred *C. membraniphorum* to his new genus *Maghrebinia*, on the basis that it exhibits some parasutural features. During this investigation, only occasional cysts of this type are found to exhibit clear parasutural features, thus indicating paratabulation. However, the majority of cysts have parasutural membranes which cannot be resolved to indicate any form of paratabulation (Pl. 6, Figs 2, 3). Hence, *C. membraniphorum* is

retained in the genus *Cyclonephelium.*

Also, within the South Ferriby section, a distinctive *C. compactum-membraniphorum* complex is seen. Although the parasutural membranes of the *C. membraniphorum* end-member of the complex never reach the elaborateness of type *C. membraniphorum* found elsewhere herein, this end-member and type *C. membraniphorum* clearly show strongest affiliations to the *Cyclonephelium* genus.

Dimensions:

Overall length of cyst (including membranes)	54	(71.4)	90μm
Length of cyst (excluding membranes)	40	(55)	64μm
Overall width of cyst (including membranes)	40	(63.2)	80μm
Width of cyst (without membranes)	30	(48.6)	64μm
Maximum height of membranes	8	(10.2)	14μm
Number of specimens measured	20		

Known stratigraphic range: Albian to Cenomanian

Occurrence:

Site 3a 0, 25, 35, 90, 100, 120

TBB -2, 0, 1, 3, 5, 8, 10 to 12, 14, 15

MCB -3.5 --> -3, -1.5 --> -1, -1 --> -0.5, 0.5 --> 1, 1 --> 1.5, 2 --> 2.5, 4 --> 4.5, 5 --> 5.5

SFE no occurrence

Cyclonephelium compactum-membraniphorum complex

Marshall and Batten, 1988

Pl. 6, Figs 6-8

1988 *Cyclonephelium compactum-membraniphorum* complex Marshall and Batten, 1988, p. 90, pl. 1, figs 3-7.

Original Remarks: Marshall and Batten, 1988, p.90, pl. 1, figs 3-7.

Type Examples: Marshall and Batten, 1988, pl. 1, figs 3-7.

Descriptions: Large proximate to proximochorate, sub-circular to sub-polygonal cyst, with variable process morphology. Autophragm slightly punctate. Shape of the hypocyst varies from essentially rounded to possessing antapical projections. Process distribution is characteristic of the genus *Cyclonephelium* as processes are concentrated towards the periphery of the cyst and less in the mid dorsal and ventral areas. Process morphology is very varied from one cyst to another within the complex. One end member of process morphology is like that of *C. compactum*; processes short and joined

proximally to form lamella or trabeculae (Pl. 6, Fig. 7). The other extreme is like that of *C. membraniphorum*, when processes are highly developed into parasutural membranes, which are box or funnel-shaped and are very broad based (Pl. 6, Fig. 8). The distal margin of these membranes is irregular. Individual parasutural membranes are never linked distally. There are also members of the complex with very short verrucate type processes which compare neither to *C. compactum* nor *C. membraniphorum*. An apical archaeopyle is present, Type $\overline{tA}$. After archaeopyle loss the remaining cyst has a zig-zag margin, due to the presence of strong accessory archaeopyle sutures, which denotes a tetra-meta apical paraplate arrangement. The shape of the precingular paraplates is also indicated; 3", 5", 6" are camerate and 1", 2", 4" are planate. Parasulcal notch is offset to the left on the ventral surface. Operculum is free.

Remarks: The development of the membranes exhibited by the *C. membraniphorum* end member of the complex never reaches the flamboyant elaborateness of *C. membraniphorum* found elsewhere throughout this investigation. Every gradation in between the examples given is seen and thus identification and differentiation into separate species is impossible and thus the erection of a *C. compactum-membraniphorum* complex is unavoidable.

Dimensions:			
Length, from archaeopyle margin to cyst base	46	(55.8)	70µm
Breadth of central body	56	(62.5)	74µm
Height of processes	3	(7.3)	20µm
Number of specimens measured	20		

Known stratigraphic range: Latest Cenomanian to Early Turonian (Marshall and Batten 1988).

Occurrence:

Site 3A no occurrence

TBB no occurrence

MCB no occurrence

SFE 15, 16, 17, 18

Genus *Dapsilidinium* Bujak *et al.*, 1980.

Generic Synopsis: Stover and Evitt, 1978, p. 69.

Type Species: *Dapsilidinium pastielsii* (Davey and Williams 1966b) Bujak *et al.* 1980.

Dapsilidinium laminaspinosum (Davey and Williams 1966b)
Lentin and Williams, 1981.
Pl. 7, Fig. 1

1966b *Polysphaeridium laminaspinosum* Davey and Williams, p. 94, pl. 8, fig. 8.

1981 *Dapsilidinium laminaspinosum* (Davey and Williams) Lentin and Williams, p. 69.

Original Description: Davey and Williams 1966b, p. 94, pl. 8, fig. 8.

Holotype: Davey and Williams 1966b, pl. 8, fig. 8.

Original Dimensions:	Holotype	Range
Diameter of central body	27 x 27µm	23 - 28µm
Length of processes	11 - 15µm	11 - 17µm
Number of processes	36	

Description: Small, spherical to sub-spherical skolochorate cyst with numerous tubular processes. Endophragm is granular to reticulate. The processes are hollow, non-tabular and open distally. Processes are parallel sided, but flared distally and have a serrate to denticulate margin. Apical archaeopyle present, Type $\overline{tA}$. Operculum is free.

Dimensions:		
	Diameter of central body	24 (27.1) 32µm
	Length of processes	10 (11.9) 14µm
	Number of processes	29 (29.8) 34
	Number of specimens measured	20

Known stratigraphic range: Cenomanian

Occurrences:

Site 3A 5, 20, 30 to 40, 50, 60 to 120

TBB -3, 1 to 3, 5, 7 to 9, 12

MCB -3.5 --> -3, -0.5 --> 0, 0.5 --> 1 to 1.5 --> 2, 2.5 --> 3, 4 --> 4.5, 5 --> 5.5

SFE 16

Genus: *Dinopterygium* Deflandre 1935; emend. Stover and Evitt, 1978.

Generic Synopsis: Stover and Evitt,1978, p. 204.

Junior Synonym: *Oodnadattia* Eisenack and Cookson, 1960.

Type Species: *Dinopterygium cladoides* Deflandre, 1935.

Dinopterygium cladoides Deflandre, 1935

Pl. 7, Fig. 2

1935 *Dinopterygium cladoides* Deflandre, p. 231, pl. 8, fig. 6.

1960a *"Toolongia medusoides"* Cookson and Eisenack, p. 14, pl. 3, figs 11,12.

1978 *"Dinopterygium medusoides"* (Cookson and Eisenack) Stover and Evitt, p. 205.

1981 *"Dinopterygium medusoides"* (Cookson and Eisenack) Stover and Evitt, Yun, p.71.

Original Description: Deflandre, 1935, p. 231, pl. 8, fig. 6.

Holotype: Deflandre, 1935, pl. 8, fig. 6.

Original Dimensions: (none given with original description)

Description: Medium to large proximochorate, spherical to sub-spherical cyst, with elaborate parasutural septa. Central body usually spherical, finely granular and sometimes bears tubercules. Parasutural septa are developed and appear fine. They reflect a paratabulation formula; 4', 6", ?c, 6"', 1p, 1"", 1ps. A combination archaeopyle is present, Type $\overline{\text{tAtP}}$, although it was rarely observed within this analysis.

Dimensions:

Total cyst diameter	64	(68.5)	74µm
Breadth of central body	40	(42.5)	50µm
Maximum height of parasutural septa	14	(17)	20µm
Number of specimens measured	5		

Known stratigraphic range: Senonian

Occurrences:

Site 3A 5, 30, 55, 70 to 85, 105, 115, 120

TBB -3, 9

MCB no occurrence

SFE 16, 18

Dinopterygium medusoides (Cookson and Eisenack 1960a) Stover and Evitt, 1978

Pl. 7, Fig. 3

1960a *"Toolongia medusoides"* Cookson and Eisenack, p. 14, pl. 3, figs 11,12.

1978 *Dinopterygium medusoides* (Cookson and Eisenack) Stover and Evitt, p. 205.

1981 *Dinopterygium "medusoides"* (Cookson and Eisenack) Stover and

Evitt, Yun, p. 71.

Original Description: Cookson and Eisenack, 1960a, p. 14, pl. 3, figs 11,12.

Holotype: Cookson and Eisenack, 1960a, pl. 3, fig. 11.

Original Dimensions:

	Holotype	Range
Overall diameter	90 x 100μm	80 - 120μm

Description: Medium to large proximochorate sub-spherical to sub-polygonal cysts, with strong parasutural septa. The spherical central body is granular and possesses tubercules. The parasutural septa are strongly developed and give the cyst a polygonal outline. Septa are supported by processes, such that the highest part of the septa is at the process and it is at its lowest mid way between two processes. Because of the highly compressed mode of preservation of these cysts, exact identification of paratabulation pattern was very difficult. A combination archaeopyle, Type $\overline{tAtP}$, is rarely observed.

Remarks: *D. medusoides* may be differentiated from *D. cladoides* by the robustness of the parasutural septa and the nature of their supporting processes. I therefore support the retention of *D. medusoides* as a separate species, and reject that it is a junior synonym of *D. cladoides* Yun, (1981).

Dimensions:				
	Total cyst diameter	60	(69.6)	84μm
	Breadth of central body	40	(44.4)	52μm
	Maximum height of parasutural septa	10	(16)	20μm
	Number of specimens measured	5		

Known stratigraphic range: Senonian

Occurrences:

Site 3A 55, 70 to 85, 115, 120

TBB 0, 2, 3, 9, 11, 12, 14

MCB -0.5 --> 0, 0 --> 0.5, 1--> 1.5, 4 --> 4.5

SFE 18

Genus: *Ellipsoidinium* Clarke and Verdier, 1967.

Generic Synopsis: *Ellipsoidinium rugulosum* Clarke and Verdier, 1967.

Type Species: *Ellipsoidinium rugulosum* Clarke and Verdier, 1967.

Ellipsoidinium rugulosum Clarke and Verdier, 1967

Pl. 7, Fig. 4

1967 *Ellipsoidinium rugulosum* Clarke and Verdier, p. 69, pl 14,

figs 4-6; text-fig. 29.

1967a *"Chelinocysta lita"* Sarjeant, p.327.

1968 *Ellipsoidinium rugulosum* Clarke and Verdier, Clarke *et al.*, p.182.

Original Description: Clarke and Verdier, 1967, p. 69, pl. 14, figs 4-6; text-fig. 29.

Holotype: Clarke and Verdier, 1967, pl. 14, fig. 6.

Original Dimensions:

	Holotype	Range
Length	40µm	35 - 45µm
Breadth	39µm	33 - 40µm
Height of ledges	up to 1.5µm	1 - 3µm

Description: Medium-sized elongate proximochorate cyst, with characteristic longitudinal ridges. Autophragm is ornamented by many long, discontinuous parasutural ridges. These ridges are parallel and run from apex to antapex. Their distal margin is denticular to undulate. The longitudinal ridges are irregularly connected by short perpendicular ridges. The paracingulum is obvious as it is indented and interrupts the longitudinal ridges. No other form of paratabulation is present. A reduced precingular archaeopyle is present, Type P, formed by the loss of the 3" paraplate, which is camerate in shape but, with a more rounded, genicular plate boundary. Operculum is free.

Dimensions:

Length of cyst	30 (39.5) 56µm
Breadth of cyst	28 (33.5) 46µm
Height of ridges	2 (2.4) 4µm
Number of specimens measured	20

Known stratigraphic range: Cenomanian to Santonian

Occurrences:

Site 3A 10 to 25, 35, 50 to 120

TBB -3 to 4, 7, 9, 11, 12, 14, 15

MCB -4.5 --> -4 to 2.5 --> 3, 3.5 --> 4 to 5 --> 5.5

SFE 18

Genus: *Endoscrinium* (Klement 1960) Vozzhennikova 1967

Generic Synopsis: Vozzennikova 1967, p. 174.

Type Species: *Endoscrinium galeritum* (Deflandre 1938) Vozzehennikova, 1967.

Endoscrinium campanula (Gocht 1959) Vozzhennikova, 1967

Pl. 7, Figs 5, 6

1959 *Scriniodinium campanula* Gocht, p. 61, pl. 4, fig. 6; pl. 5, fig. 1.

1967 *Endoscrinium campanula* (Gocht) Vozzhennikova, p. 272, pl. 98, figs 1-3.

1971b *"Gonyaulacysta fragosa"* Brideaux, p. 83, pl. 23, fig. 42; pl. 24, figs 44, 45; text-fig. 8 c-d.

1978 *Scriniodinium campanula* Gocht, Stover and Evitt, p. 187.

1981 *Endoscrinium campanula* (Gocht) Vozzhennikova, Lentin and Williams, p. 96.

1986 *Scriniodinium campanula* Gocht, Jan du Chêne *et al.*, p. 315, pl. 110, figs 1-5.

Original Description: Gocht 1959, p. 61, pl. 4, fig. 6; pl. 5, fig. 1.

Holotype: Gocht 1959, pl. 5, fig. 1 and Jan du Chêne *et al.*, 1986, pl. 110, figs 1-5.

Original Dimensions:

	Holotype	Range
Length	104µm	85 - 100µm
Breadth	91µm	74 - 91µm
Apical horn	16µm	

Description: Large, elongate polygonal to rhomboidal circumcavate cyst. Epicyst carries a pointed conical apical prominence and is smaller than the hypocyst. The hypocyst is more rounded. Distance from the paracingulum to the antapical margin is characteristically long, giving the cyst its elongate shape. Both periphragm and endophragm are smooth. Low relief parasutural ridges/crests are sometimes seen on periphragm which gives an indication of the paratabulation. Paracingulum is indicated by a thickened folded area across the median of the cyst. This pronounced paracingulum appears to extend far beyond the limit of the central body, thus maximising the paracingular width. There is an L-type pattern to the alignment of the parasulcus and the paracingulum. A claustra/pylome is usually present in the periphragm of the hypocyst (Pl. 7, Fig. 6). A precingular archaeopyle, Type P is present, representing a camerate 3" paraplate. Operculum is free.

Remarks: The occurrence of this species within the Cenomanian palynological assemblages studied herein is believed to be real, which

thus extends tha range of this cyst species from the Hauterivian (see below) to the Cenomanian.

Dimensions:	Overall length	68 (81.5) 92μm
	Overall breadth	60 (67.5) 74μm
	Number of specimens measured	20

Known stratigraphic range: Hauterivian

Occurrence:

Site 3A all samples

TBB 3, 5 to, 15

MCB -4 --> -3.5 to -2 --> -1.5, -1.5 --> -1, -1 --> -0.5, 0.5 --> 1 to 5 --> 5.5

SFE 16, 17, 18

Genus: *Exochosphaeridium* Davey *et al.*, 1966

Generic Synopsis: Stover and Evitt, 1978, p. 154.

Type Species: *Exochosphaeridium phragmites* Davey *et al.*, 1966.

Exochosphaeridium cf. *arnace* Davey and Verdier, 1973

Pl. 8, Figs 3, 4

1967 *Baltisphaeridium whitei* (Deflandre and Courtville) Clarke and Verdier, p. 76, pl. 16, figs 1,2.

1966 *Exochosphaeridium phragmites* Davey *et al.*, p. 7, fig. 5.

1973 *Exochosphaeridium arnace* Davey and Verdier, p. 184, pl. 1, figs 3,6.

Original Description: Davey and Verdier, 1973, p. 184, pl. 1, figs 3,6.

Holotype: Davey and Verdier, 1973, pl. 1, figs 3,6.

Original Dimensions:	Holotype	Range
Central body length	45μm	45 (48) 52μm
Central body breadth	36μm	36 (39) 42μm
Process length	10 - 15μm	12 - 15μm (max)

Description: Medium-sized spherical to sub-spherical skolochorate cyst with highly fibrous processes. Central body is spherical and composed of autophragm only, which has a slightly pitted appearance. Processes are non-tabular and are broad based. They are highly fibrous and this characteristic is so developed that they appear to anastomose together, giving the cyst a very hairy appearance, as if forming a fringe. A precingular archaeopyle is probably present (Type

P) representing a very large camerate 3" paraplate, but it may be of a different type altogether. No other form of paratabulation is seen. Operculum is free.

Remarks: The highly fibrous to "hairy" nature of the processes seems to be developed to such a degree that this characteristic differentiates these cysts from type *C. arnace*, as its original description does not allow for such elaborateness.

Dimensions:		
Total cyst diameter	60 (73.7) 84µm	
Diameter of central body	38 (45) 56µm	
Maximum height of fibrous processes	16 (28.4) 40µm	
Number of specimens measured	20	

Occurrences:

Site 3A 0 to 35, 45 to 120

TBB -2 to 3, 6 to 15

MCB -4.5 --> -4 to -1.5 --> -1, -0.5 --> 0 to 0.5 --> 1, 1.5 --> 2 to 2.5 --> 3, 3.5 --> 4, 4.5 --> 5

SFE no occurrence

Exochosphaeridium bifidum (Clarke and Verdier, 1967)
Clarke *et al.*, 1968
Pl. 8, Fig. 5

1967 *Baltisphaeridium bifidum* Clarke and Verdier, p. 72, pl. 17, figs 5-6; text-fig. 30.

1968 *Exochosphaeridium bifidum* (Clarke and Verdier) Clarke *et al.*, p. 182.

Original Description: Clarke and Verdier, 1967, p. 72, pl. 17, figs 5-6; text-fig. 30.

Holotype: Clarke and Verdier, 1967, pl.17, fig. 5.

Original Dimensions:	Holotype	Range
Diameter of body	66µm	44 - 72µm
Length of processes	22µm	13 - 34µm

Description: Intermediate sized spherical to sub-spherical skolochorate cyst with long thin processes. The central body is spherical and is finely granular. The long processes are non-tabular and solid. Apical processes are typically larger than other processes. The distal margins of the processes flare slightly to form a small bifurcated top. Processes are also expanded distally. A precingular archaeopyle, Type P is present, formed by the loss of the

3" paraplate.

Remarks: In certain orientations *E. bifidum* may be confused with *Pervosphaeridium pseudhystrichodinium* (Deflandre 1937) Yun 1981. However, the Type P archaeopyle of *E. bifidum* readily distinguishes it from *P. pseudhystrichodinium*, which has a Type 2P archaeopyle.

Dimensions:		
	Length of central body	40 (45.1) 52μm
	Breadth of central body	30 (39.3) 46μm
	Maximum length of processes	12 (15.5) 22μm
	Number of specimens measured	15

Known stratigraphic range: Cenomanian to Campanian

Occurrences:

Site 3A 20, 50 to 105, 115, 120

TBB -3 to 3, 5, 7, 11, 12, 14, 15

MCB -4 --> -3.5 to -1.5 --> -1, -0.5 --> 0, 1 --> 1.5 to 3 --> 3.5, 4 --> 4.5, 4.5 --> 5

SFE 16

Exochosphaeridium phragmites Davey *et al.*, 1966

Pl. 8, Fig. 6

1966 *Exochosphaeridium phragmites* Davey *et al.*, p. 165, pl.2, figs 8-10.

Original Description: Davey *et al.*, 1966, p. 165, pl.2, figs 8-10.

Holotype: Davey *et al.*, 1966, pl.2, figs 9, 10.

Original Dimensions:	Holotype	Range
Diameter of central body	49 x 56μm	33 x 36μm
Length of processes	up to 22μm	22μm

Description: Spherical to sub-spherical skolochorate cyst of medium size, with numerous long solid processes. Central body is spherical and is composed of autophragm only, which has a pitted ornamentation. Processes are non-tabular, long and fibrous. They are broad based; some are simple but others divided half way along the shaft. They are acuminate in shape. No paratabulation pattern is discernable, but sometimes the apical processes are distinctive as they are large and divided medianly. A precingular archaeopyle is seen, Type P. Operculum is free.

Remarks: Like *E. bifidum*, *E. phragmites* may sometimes be confused with *Pervosphaeridium pseudhystrichodinium*, but they may be readily distinguished apart by the presence of a Type P archaeopyle in

Exochosphaeridium.

Dimensions: Length of central body 32 (43.1) 62μm
Breadth of central body 38 (44.4) 52μm
Maximum height of processes 12 (16.2) 20μm
Number of specimens measured 15

Known stratigraphic range: Cenomanian

Occurrences:

Site 3A 5, 95, 105

TBB -3, 1 to 14

MCB -4.5 --> -4, -4 --> -3.5, -3 --> -2.5 to -2 --> -1.5, -1 --> -0.5, -0.5--> 0, 2 --> 2.5, 3 --> 3.5, 4 --> 4.5 to 5 --> 5.5

SFE 18

Genus: *Florentinia* Davey and Verdier, 1973; emend. Duxbury, 1980.

Generic Synopsis: Stover and Evitt, 1978, p.155.

Emended Generic Description: Duxbury, 1980, p. 119.

Junior Synonym: *Silicisphaera* Davey and Verdier, 1976.

Type Species: *Florentinia laciniata* Davey and Verdier, 1973.

Florentinia deanei (Davey and Williams, 1966b) Davey and Verdier, 1973

Pl.9, Fig. 1

1966b *Hystrichosphaeridium deanei* Davey and Williams, p. 58, pl.6, figs 4, 8.

1973 *Florentinia deanei* (Davey and Williams) Davey and Verdier, p. 187, pl. 1, fig. 9.

Original Description: Davey and Williams, 1966b, p. 58, pl. 6, figs 4, 8.

Holotype: Davey and Williams, 1966b, pl. 6, fig. 8.

Original Dimensions:	Holotype	Range
Diameter of central body	46 x 47μm	41 - 54μm
Width of antapical process	31μm	
Length of antapical process	35μm	
Length of other processes	15 - 30μm	15 - 45μm
Number of processes	21	

Description: Skolochorate medium sized cyst with spherical to ovoidal central body and characteristic large antapical process. Central body is smooth. Process morphology is variable, but reflects the paratabulation pattern, as there is one process per paraplate.

Reflected paratabulation pattern is 4', 6", 6c, 5"', 1p, 1"". Processes are all long, hollow and tubular to lagenate, with flared distal margins, which may be serrate. Apical processes are narrower than the precingular processes, which are more squat. Paracingular processes are thin, whereas the postcingular processes are large, but not as large as the antapical one. This antapical process is characteristically much larger and wider than the other processes and is lagenate to sub-conical in shape,with a serrate to denticulate distal margin. A combination archaeopyle Type tA + P is formed. The apical operculum usually remain attached but the 3" paraplate is typically lost.

Remarks: There seems to be two distinct, mutually exclusive size groupings of *F. deanei* cysts. The larger group's central body diameter ranges from 40 -(42.8)- 48µm, whereas the smaller group varies between 30 -(33.1)- 36µm. All other morphological characteristics are the same, the division is purely one of size.

Dimensions:

Central body diameter	30 (40)	48µm
Length of antapical process	16 (26.6)	38µm
Maximum length of other processes	16 (19.2)	24µm
Number of specimens measured	20	

Known stratigraphic range: Cenomanian

Occurrences:

Site 3A 0, 15 to 30, 50 to 105, 115, 120

TBB -3 to 5, 7 to 15

MCB -4.5 --> -4 to -3 --> -2.5, -2 --> -1.5, -1.5 --> -1, 1 --> 1.5 to 3 --> 3.5, 4 --> 4.5, 4.5 --> 5

SFE 15, 16, 17

Florentinia ferox (Deflandre 1937) Duxbury, 1980

Pl. 9, Fig. 2

1937 *Hystrichosphaeridium ferox* Deflandre, p. 72, pl. 14, figs 3,4

1967 *Baltisphaeridium ferox* (Deflandre) Clarke and Verdier, p. 73, pl. 15, fig. 4.

1967 *"Hystrichosphaeridium ferox"* (Deflandre) *in* Evitt, p. 19, pl. 8, figs 1-5.

1969a *"Hystrichokolpoma ferox"* (Deflandre) Davey, p. 159, pl.9, figs 5-7.

1971 *Hystrichosphaeridium ferox* (Deflandre) Foucher, p.106, pl.9, figs 11,12; pl. 10, figs 1,2.

1973 *"Hystrichokolpoma ferox"* (Deflandre) Davey, Davey and Verdier, p. 192.

1976 *"Silicisphaera ferox"* (Deflandre) Davey and Verdier, p. 322, pl. 3, figs 1, 2; text-fig. 4.

1980 *Florentinia ferox* (Deflandre) Duxbury, p. 121.

Original Description: Deflandre, 1937, p. 72, pl. 14, figs 3, 4.

Holotype: Deflandre, 1937, pl. 14, fig. 3.

Original Dimensions: Holotype

Length of the central body	46µm
Width of the central body	36µm
Total length	78µm
Length of processes	15 - 17µm

Description: Sub-spherical to ovoidal shaped cyst with long processes. Central body is sub-spherical with densely granulate endophragm. Processes are varied but there is only one process per paraplate, they are thin walled, appear transparent, are broad based and taper distally. Three types of processes were seen. Firstly, there are simple elongate conical to tubular processes which taper distally to a point; typical of the apical, paracingular, sulcal and antapical processes. Secondly there are the larger compound, medianly bifurcating tubular precingular processes. Thirdly, there are the largest compound processes which are medianly trifurcate, arising from the five postcingular paraplate areas. Reflected process formula is therefore, 4', 6", 6c, 5"', 1"", ?s. The antapical process is not distinctively large. A compound archaeopyle is formed, Type tA + P. The precingular paraplate involved in the archaeopyle formation is the 3". The apical opercula usually remain attached but the 3" paraplate is lost.

Remarks: *Florentinia ferox* may be differentiated from the similar *F. resex* Davey and Verdier 1976, by the granular nature of the central body and by the absence of a large antapical process.

Dimensions:

Central body diameter	36 (38.9) 40µm
Length of processes	14 (16.7) 18µm
Number of specimens measured	10

Known stratigraphic range: Senonian

Occurrences:

Site 3A 5, 10, 20, 40, 50, 55, 65 to 95, 105 to 120

TBB -2, 3, 5, 11

MCB -4.5 --> -4, -3.5--> -3, 2 --> 2.5, 3 --> 3.5, 4 --> 4.5, 4.5 --> 5

SFE 15, 16, 17, 18

Florentinia laciniata Davey and Verdier 1973

Pl. 9, Fig. 3

1973 *Florentinia laciniata* Davey and Verdier, p. 186, pl. 2, figs 1, 3, 6, 7, 9.

Original Description: Davey and Verdier 1973, p. 186, pl. 2, figs 1, 3, 6, 7, 9.

Holotype: Davey and Verdier 1973, pl. 2, figs 1, 3.

Original Dimensions:

	Holotype	Range
Central body diameter	36 x 44µm	36 (46) 55µm
Process length	15 - 30µm	26 (36) 49µm

Description: Skolochorate medium sized cyst, with spherical to sub-spherical central body and variable process morphology. Central body is finely granular. Processes are intratabular and show three types of morphology as follows:

1. Simple elongate tubular processes which are either single or more commonly distally bifurcated and always produced into a point. These are typical of the apical, paracingular and parasulcal processes.
2. Large compound tubular processes, which are broad based and medianly branch to form multifurcate tips. These processes represent the precingular and postcingular processes and are distinctively large.
3. The antapical process is long and sub-conical in shape. It is very broad based and tapers markedly towards the distal margin, where it forms a constricted circular opening. This margin is usually entire, but in some rare cases it is serrate.

Reflected process formula is probably ?4', 4", ?c, 5"', 1p, 1"", ?s, but is usually difficult to determine as specimens are usually very squashed. A combination archaeopyle is present, Type $\overline{tA}$ + P, where 3" is the precingular paraplate involved. Operculum is free.

Dimensions:	Central body diameter	38 (26) 30µm
	Central body length	40 (42) 44µm
	Number of specimens measured	5

Known stratigraphic range: Late Albian to Early Cenomanian

Occurrence:

Site 3a 10, 70, 120

TBB no occurrence

MCB 1.5 --> 2

SFE no occurrence

Florentinia mantellii (Davey and Williams 1966b)

Davey and Verdier 1973.

Pl. 9, Fig. 4

1966b *Hystrichosphaeridium mantelli* Davey and Williams, p. 66, pl. 6, fig. 6.

1973 *Florentinia mantellii* (Davey and Williams) Davey and Verdier, p. 187, pl. 1, figs 1, 4, 7; pl. 4, figs 1, 3.

Original Description: Davey and Williams 1966b, p. 66, pl. 6, fig. 6.

Holotype: Davey and Williams 1966b, pl. 6, fig. 6.

Original Dimensions:

	Holotype	Range
Diameter of central body	41 x 42µm	36 - 45µm
Length of processes	13 x 21µm	13 - 26µm
Number of processes	25	

Description: Medium-sized skolochorate cyst, with highly variable process morphology. Central body spherical to sub-spherical in shape and is smooth. The intratabular processes show three types of morphologies as follows:

1. Simple acuminate tubular processes which taper distally to form a point. This morphology is typical of the apical, paracingular and parasulcal processes.

2. Large compound tubular processes with broad bases, which are medianly bifid or trifid. These processes are typical of pre- and post-cingular areas. The precingular processes are typically smaller and less furcated than the postcingular ones, which are much larger. Occasionally, some precingular processes have a simple acuminate morphology, but they are large and have a broad base, which distinguishes them from the apical, paracingular and parasulcus simple processes.

3. One large antapical process, which is conical in shape. This process is very broad-based and tapers considerably towards its distal margin, which is usually serrate.

Reflected process formula is ?4', 4", ?c, 5"', 1p, 1"", ?s. A combination archaeopyle is present, Type $\overline{tA}$+ P, where the precingular paraplate involved is the 3" one. Operculum is free.

Dimensions:	Diameter of central body	38 (41.5) 44µm
	Length of processes	12 (16.4) 18µm
	Length of antapical process	16 (20) 24µm
	Number of specimens measured	5

Known stratigraphic range: Late Cenomanian

Occurrence:

Site 3a 65, 110, 115, 120

TBB -3, 2,

MCB -3 --> -2.5

SFE no occurrence

Florentinia resex Davey and Verdier, 1976

Pl. 9, Fig. 5

1976 *Florentinia resex* Davey and Verdier, p. 319, pl. 4, figs 1-3; text-fig. 2.

Original Description: Davey and Verdier, 1976, p. 319, pl. 4, figs 1-3; text-fig. 2.

Holotype: Davey and Verdier, 1976, pl. 4, fig. 1.

Original Dimensions:	Holotype	Paratype	Range
Central body diameter	38 x 39µm	43 - 51µm	38 - 51µm
Length of processes	7 - 13µm	12 - 23µm	7 - 23µm

Description: Spherical to sub-spherical skolochorate medium sized cyst, with numerous long processes. The central body is spherical, is usually smooth but occasionally is finely granular. Processes are numerous, implying more than one process per paraplate, and are variable in morphology. Some are simple, elongate and acuminate. Others, the pre- and post-cingular processes, are medianly bifid. The large antapical process is distinctive as is tubular, sub-conical with a flared finely serrate distal margin. The archaeopyle appears to be precingular (Type P) with the loss of the 3" paraplate which often remains attached.

Remarks: *Florentinia resex* may be distinguished from *F. ferox* by its

smooth to only finely granular central body, and a distinctively large tubular antapical process.

Dimensions:	Central body diameter	30 (36.2) 40μm
	Length of antapical process	12 (15.9) 20μm
	Number of specimens measured	10

Known stratigraphic range: Turonian

Occurrences:

Site 3A 0, 20, 35, 45 to 55, 65, 70, 80, 90

TBB -2 to 7, 9, 11, 12, 14, 15

MCB -4.5 --> -4 to -3.5 --> -3, -2 --> -1.5

SFE 15, 16

Genus: *Fromea* Cookson and Eisenack, 1958; emend. Yun, 1981

Generic Synopsis: Stover and Evitt, 1978, p. 47.

Emended Generic Description: Yun, 1981, p. 55.

Type Species: *Fromea amphora* Cookson and Eisenack, 1958.

Fromea amphora Cookson and Eisenack 1958

Pl. 9, Fig. 6

1958 *Fromea amphora* Cookson and Eisenack, p. 56, pl. 5, figs 10, 11.

1972 *"Fromea warlinghamensis"* Gitmez and Sarjeant, p. 188, pl. 1, figs 6,8; pl. 9, figs 5-8.

Original Description: Cookson and Eisenack, 1958, p. 56, pl. 5, figs 10, 11.

Holotype: Cookson and Eisenack, 1958, pl. 5, fig. 10.

Original Dimensions:

	Holotype	Range
Dimensions	81 x 62μm	62 - 95 x 47 - 81μm
Apertures	33μm	

Description: Large oval to ellipsoidal single layered cyst, which is characteristically dark brown. Cyst wall generally smooth, but some isolated areas may be granulate to pitted. Archaeopyle is apical but its type is uncertain. These cysts are always found having lost their archaeopyle, yielding a weakly concave aperture. The area of maximum width of the cyst is half way along the cyst length and this width is typically twice to $^{2}/_{3}$ the width of the archaeopyle margin. No indication of a paracingulum is present. Arcuate, obliquely transverse folds are nearly always present. Operculum is always free.

Dimensions:	Length of cyst	60 (72.3) 80µm
	Breadth of cyst	46 (58.1) 70µm
	Number of specimens measured	20

Known stratigraphic range: Albian to Cenomanian

Occurrence:

Site 3A 30 to 40, 50, 65 to 85, 95, 105, 120

TBB 6, 8, 11, 13, 14

MCB -4.5 --> -4, -2.5 --> -2, -1.5 --> -1 to -0.5 --> 0, 0.5 --> 1, 1 --> 1.5, 2 --> 2.5, 2.5 --> 3, 3.5 --> 4, 4.5 --> 5

SFE 16, 17, 18

Genus *Gonyaulacysta* Deflandre 1964; emend. Sarjeant, 1982.

Generic Synopsis: Stover and Evitt, 1978, p. 157.

Emended Generic Description: Sarjeant, 1982, p. 27.

Type Species: *Gonyaulacysta jurassica* (Deflandre 1938) Norris and Sarjeant, 1965.

Gonyaulacysta cassidata (Eisenack and Cookson 1960) Sarjeant, 1966

Pl. 10, Figs 1, 2

1960 *Gonyaulax helicoidea* subsp. *cassidata* Eisenack and Cookson, p. 3, pl. 1, figs 5,6.

1962 *Gonyaulax cassidata* Eisenack and Cookson, Cookson and Eisenack, p. 486, pl. 2, figs 11, 12.

1966 *Gonyaulacysta cassidata* (Eisenack and Cookson) Sarjeant, p. 125, pl. 14, figs 3,4; text-fig. 31.

Original Description: Eisenack and Cookson, 1960, p. 3, pl. 1, figs 5, 6.

Holotype: Eisenack and Cookson, 1960, pl. 1, fig. 5 and Jan du Chêne *et al.*, 1986, pl. 40, figs 6, 7.

Original Dimensions:

	Holotype	Range
Length	83µm	71 - 95µm
Breadth	52µm	47 - 57µm

Description: Elongate to ovoidal, large, bicavate proximate cyst. There is a conspicuous apical horn and antapical parasutural crests, giving the cyst an angular polygonal shape. Central body is sub-spherical. Pericoel is at its greatest extent at the apical horn and in the antapical area. Apical horn is intermediate in size and has either a rounded point at its apex or is capped by a large

nipple-like thickening. Epicyst is larger and more pointed than the hypocyst. Paracingulum strongly developed and is broad, strongly helicoid and laevorotatory. Parasulcus is evenly distributed between the epicyst and the hypocyst and is of the S-type arrangement. Paratabulation is indicated by the high relief parasutural crests, all paraplates are easily seen. The reflected paratabulation pattern is, 4', 1a, 6". 6c, 6"', 1p, 1"", ?s. There is a sexiform antapical arrangement. Parasutural crests are high, may be entire or carry a serrate to denticulate to machicolate distal margin. There is no regularity in the distribution of the indentations along the parasutural crests but, it is typically more non-entire closer to the paracingulum. Intratabular areas between the parasutural crests are ornamented by tubercules whose number and distribution varies from specimen to specimen. Archaeopyle is precingular, Type P representing an elongate camerate 3" paraplate. Operculum is free.

Remarks: At first glance, *G. cassidata* may be confused with *Psaligonyaulax deflandrei* Sarjeant 1966. However, *P. deflandrei* is more strongly bicavate than *G. cassidata*. Using this criterion it became obvious that cysts of this type fall easily into one of these two species with no intermediate groups being observed. However because of the overall similarity of morphology, these two species may be closely related; see Stover and Evitt (1978) and Sarjeant (1982) for further details.

Dimensions:		
	Total length of cyst	52 (65.3) 75µm
	Length of central body	35 (41.8) 54µm
	Breadth of cyst	36 (41.4) 46µm
	Length of apical horn	6 (11.8) 18µm
	Number of specimens measured	10

Known stratigraphic range: Aptian to Cenomanian

Occurrences:

Site 3A 20, 30, 50, 60 to 85, 100, 105, 115, 120

TBB -3, 0 to 10, 12, 14,15

MCB -3.5 --> -3, -3 --> -2.5, -0.5 --> 0, 0.5 --> 1 to 3.5 --> 4, 4.5 --> 5

SFE no occurrence

Gonyaulacysta whitei Sarjeant 1966

Pl. 10, Figs 3, 4

1966 *Gonyaulacysta whitei* Sarjeant, p. 126, pl. 14, fig. 2; text-fig. 32.

1978 *Impagidinium ? whitei* (Sarjeant) Stover and Evitt, p.166

1982 *"Rhynchodiniopsis whitei"* (Sarjeant) Sarjeant, p.36.

1986 *Impagidinium ? whitei* (Sarjeant) Stover and Evitt, Jan du Chêne *et al.*, p. 169, pl. 54, figs 17-19.

Original Description: Sarjeant 1966, p. 126, pl. 14, fig. 2; text-fig. 32.

Holotype: Sarjeant, 1966, pl. 14, fig. 2.

Original Dimensions:

Holotype	
Overall length	62μm
Overall breadth	49μm
Shell length	53μm
Shell breadth	45.5μm
Length of horn	9μm

Description: Ovoidal proximate medium-sized cyst, with a prominent apical horn and parasutural ridges. A small pericoel is developed and is most noticeable in the antapical area of the hypocyst. Apical horn is large and has a gently rounded apex. This apex seems to be thickened into a node as if a plug is present. Epicyst and hypocyst equally large. Both periphragm and endophragm are smooth, transparent and unornamented. Central body is oval with a slight bulge into the apical horn area. Paracingulum is obvious and is strongly helicoid and laevorotatory. Parasulcus is also conspicuous, occurs evenly on the epicyst and hypocyst, but no individual sulcal paraplates are indicated. An S-type ventral arrangement is present. Paratabulation is clearly indicated by parasutural ridges that are low to medium relief features with an entire rounded margin. There is a sexiform antapical arrangement. Reflected paratabulation pattern is 3', 1a, 6", 6c, 6"', 1p, 1"". A precingular archaeopyle is present formed by the loss of a camerate shaped 3" paraplate. Operculum is free.

Remarks: I would favour the retention of this species *G. whitei* within this genus for the following reasons. It possesses a strong apical horn, it is bicavate, and the parasutures are always complete and give a full representation of the paratabulation.

Dimensions:	Total length of cyst	44 (57.2) 66µm
	Length of central body	32 (42.5) 50µm
	Total breadth of cyst	38 (43.8) 50µm
	Breadth of inner body	28 (38.3) 44µm
	Height of apical horn	7 (10.6) 16µm
	Number of specimens measured	15

Known stratigraphic range: Cenomanian

Occurrences:

Site 3A 85, 95, 105, 110, 120

TBB -1, 14, 15

MCB 2.5 --> 3, 3.5 --> 4, 5 --> 5.5

SFE no occurrence

Genus: *Hystrichodinium* Deflandre, 1935; emend. Sarjeant 1966

Generic Synopsis: Stover and Evitt, 1978, p. 161.

Emended Generic Diagnosis: Sarjeant 1966, p. 140.

Junior Synonym: *Heliodinium* Alberti, 1961; emend. Sarjeant, 1966.

Type Species: *Hystrichodinium pulchrum* Deflandre, 1935.

Hystrichodinium pulchrum Deflandre 1935

Pl.10, Fig. 5; Pl. 11, Fig. 5

1935 *Hystrichodinium pulchrum* Deflandre, p. 229, pl. 5, fig. 1; text-figs 9-11.

Original Description: Deflandre, 1935, p. 229, pl. 5, fig. 1; text-figs 9-11.

Holotype: Deflandre, 1935, p. 5, fig. 1.

Original Dimensions: (None given with original description)

Description: Sub-polygonal medium to large skolochorate cyst, with numerous long processes. Epicyst and hypocyst equal in size and shape. Shape of cyst is geometrical as epicyst possess shoulders and hypocyst has corners. The length of the central body [40 (51.20) 58µm] is nearly always equal to the paracingular width [40 (50.7) 60µm]. Autophragm only present and is finely granular but, with irregularly distributed tubercules. Paracingulum is indicated by a thickening of the autophragm, and is weakly helicoid. Typically there is a fold in the cyst about this area. Parasulcus not present. Processes are non-tabular, long and flattened, with a pointed tip and are typically recurved or bent distally. They are $^{2}/_{3}$ to $^{3}/_{4}$ the

width of the paracingulum in length, and may join up proximally to give a faint indication of paratabulation. These parasutural indications are strongest where the pre and post -cingular paraplates meet the paracingulum but, elsewhere they are absent. A full paratabulation pattern is not discernable but, there are probably six precingular (6") and six postcingular (6"') paraplates. A precingular archaeopyle is present (Type P) which represents the 3" paraplate, which has a camerate shape. Operculum is free.

Dimensions: Length of central body 40 (51.2) 58µm
Breadth of central body 40 (50.7) 60µm
Length of processes 22 (27.1) 32µm
Number of specimens measured 20

Known stratigraphic range: Senonian

Occurrences:

Site 3A all samples

TBB all samples

MCB all samples

SFE 16, 17

Genus: *Hystrichosphaeridium* Deflandre 1937; emend. Davey and Williams 1966b

Generic Synopsis: Stover and Evitt, 1978, p. 55.

Type Species: *Hystrichosphaeridium tubiferium* (Ehrenberg 1838) Deflandre, 1937; emend. Davey and Williams, 1966b.

Hystrichosphaeridium bowerbankii Davey and Williams, 1966b

Pl. 10, Fig. 6

1966b *Hystrichosphaeridium bowerbanki* Davey and Williams, p.69, pl. 8, figs 1,4.

Original Description: Davey and Williams, 1966b, p. 69, pl.8, figs 1,4.

Holotype: Davey and Williams, 1966b, pl.8, fig. 4.

Original Dimensions:	Holotype	Range
Overall diameter	58 x 78µm	60 - 85µm
Diameter of central body	39 x 29µm	29 - 40µm
Length of processes	24 - 26µm	21 - 26µm
Number of processes	24	

Description: Elongate skolochorate cyst of medium size and with intratabular processes with recurved to orthogonal distal margins. Central body thin walled, smooth and typically transparent. Processes are cylindrical with distinctively parallel sides, but taper slightly towards their distal margins. This distal margin is recurved and typically possesses 4 - 7 short spines. The bases of the processes widen slightly as they meet the central body and diagnostically at this junction there appears to be a little circle where the periphragm is thickened slightly. Process length varies from being equal to $^{5}/_{6}$ of the diameter of the central body. In rare cases the process length may be greater than the body diameter. Process distribution is such that there is one per paraplate, including each precingular paraplate. Thus the reflected paratabulation pattern is 4', 6", 6c, 5"', 1p, 1"", ?5s. Number of processes varies between 22 to 28, with a mean value of 25. An apical archaeopyle, Type $\overline{tA}$ is always seen. The remaining cyst has a zig-zag margin due to the presence of slight accessory sutures. Operculum is free.

Remarks: *Hystrichosphaeridium bowerbankii* is similar in morphology and process style to *Oligosphaeridium prolixispinosum* Davey and Williams 1966b. The two are differentiated on the basis of process number with *H. bowerbankii* carrying 22 (24.8) 28 processes and *O. prolixispinosum* only having 14 (16.2) 18 processes; the difference due to the lack of paracingular processes in *O. prolixispinosum*

Dimensions: Length of cyst	46 (54.6)	68µm
(From archaeopyle margin to tip of 1"" process)		
Length of cyst	30 (34.2)	38µm
(From aracheopyle margin to base of central body)		
Breadth of cyst	20 (27)	32µm
(Paracingular breadth)		
Breadth of cyst	36 (67.4)	82µm
(From tip of processes either side of the paracingulum)		
Maximum length of processes	19 (22.3)	26µm
Number of spines on process tip	4 (5.4)	7
Number of processes	22 (24.8)	28
Number of specimens measured	20	

Known stratigraphic range: Cenomanian

Occurrences:

Site 3A 0 to 40, 50, 55, 65 to 75, 90 to 110, 120

TBB -3 to 2, 4, 5, 8 to 12

MCB -4.5 --> -4 to -2.5 --> -2, -1 --> -0.5, -0.5 --> 0, 0.5 --> 1 to 2 --> 2.5, 3.5 --> 4 to 5 --> 5.5

SFE no occurrence

Hystrichosphaeridium tubiferum (Ehrenberg 1838) Deflandre, 1937; emend. Davey and Williams, 1966b.

Pl. 10, Fig. 7

1838 *Xanthidia tubiferum* Ehrenberg, pl. I, fig. 16.

1904 *Ovum hispidium (Xanthidia tubiferum)* Ehrenberg, Lohmann, p. 21.

1937 *Hystrichosphaeridium tubiferum* (Ehrenberg), Deflandre, p. 68, pl. 13, figs 2,4,5.

1966 *Hystrichosphaeridium tubiferum* (Ehrenberg) Deflandre, Davey *et al.*, p. 56, pl. 6, figs 1,2; pl. 8, fig. 5; pl. 10, fig. 2; text-fig. 13.

First Description: Deflandre, 1937, p. 68, pl. 13, figs 2,4,5.

Holotype: Ehrenberg, 1838, pl. I, fig. 16.

First Dimensions: Deflandre, 1937, p. 68.

Central body 40µm

Total breadth reaches and often exceeds 100-150µm

Description: Spherical to sub-spherical medium sized skolochorate cyst, with long, intratabular processes. Central body is spherical and is composed of smooth endophragm. The periphragm however, is slightly granular. The processes are tubiform with slightly wider bases and flared distal margins, edged by small spines. At the bases of the processes is a characteristic circular mark. Processes are of variable width and size, dependent on their position on the cyst. Parasulcal processes and the 1" paraplate are smaller and thinner than the larger, sturdier pre and post -cingular processes. A reflected paratabulation pattern is as follows; 4', 6", 6c, 5"', 1p, 1"", 2-5s. Number of processes varies from 22 - 24. An apical archaeopyle is present, Type $\overline{tA}$. There is a zig-zag margin to the remaining cyst, after archaeopyle loss, due to the presence of slight accessory archaeopyle sutures. These latter characteristics imply there is a tetra-ortho apical arrangement of paraplates, with camerate shaped 1", 3", 5", 6" and planate shaped 2", 4". Operculum is free.

Dimensions: Length of central body 30 (35.1) 38µm

Breadth of central body 24 (27.2) 30µm

Length of processes		10 (15.9) 18μm
Number of specimens measured		20

Known stratigraphic range: ? Late Cretaceous

Occurrences:

Site 3A 5, 10, 20, 30 to 85, 100, 110 to 120

TBB all samples

MCB -4.5 --> -4 to -0.5 --> 0, 0.5 --> 1 to 3 --> 3.5, 4.5 --> 5 to 5 --> 5.5

SFE no occurrence

Genus: *Hystrichostrogylon* Agelopolos, 1964;
emend. Stover and Evitt, 1978

Generic Synopsis: Stover and Evitt, 1978, p. 164.

Junior Synonym: *Diaphasiosphaera* Duxbury, 1980.

Type Species: *Hystrichostrogylon membraniphorum* Agelopolos, 1964.

Hystrichostrogylon membraniphorum Agelopolos, 1964
Pl. 10, Fig. 8

1964 *Hystrichostrogylon membraniphorum* Agelopolos, p. 674, pls 1,2.

1976 *"Achomosphaera membraniphora"* (Agelopolos) Eaton, p.237.

Original Description: Agelopolos, 1964, p.674, pls 1,2.

Holotype: Agelopolos, 1964, pl. 1.

Original Dimensions:	Holotype	Remaining examples
Central body length	45μm	35 - 57μm
Central body width	40μm	
Length of supports	13 - 29μm	
Width of supports	2 - 6μm	

Description: Medium to large camocavate skolochorate spherical to ovoidal cyst, with characteristic ventro-antapical membrane. Central body is spherical. Periphragm and endophragm are smooth and transparent. Membranes are closely adpressed over the cyst, except in the antapical portion of the hypocyst, where a pericoel is developed. Processes are gonal and intergonal in position, and are long, thin and solid with long trifurcating and bifurcating tips respectively, resembling *Spiniferites* process morphology. Some faint parasutural markings are sometimes present, but paratabulation is rarely distinct. A precingular archaeopyle is present (Type P), representing the

reduced 3" camerate paraplate. Operculum is free.

Remarks: The occurrence of this species within the Cenomanian herein, is believed to be real, and therefore extends the known straigraphic range of this species from the Late Eocene (see below) down to the Cenomanian.

Dimensions:

Total length of cyst including AA membrane	58 (66.8) 76µm
Length of central body	30 (33.9) 44µm
Length of AA membrane	22 (29.6) 38µm
Breadth of central body	32 (39.4) 44µm
Maximum length of processes	12 (14.7) 18µm
Number of specimens measured	20

Known stratigraphic range: Late Eocene

Occurrences:

Site 3A 0, 10, 15, 25, 35, 45 to 75, 90, 95, 105 to 120

TBB -3 to 0, 2, 4, 6 to 13

MCB - 4.5 --> -4, -3.5 --> -3 to -2 --> -1.5, -1 --> - 0.5, 0.5 --> 0, 0.5 --> 1 to 3.5 -> 4, 4.5 --> 5, 5 --> 5.5

SFE no occurrence

Genus: *Kallosphaeridium* De Coninick 1969;
emend Jan du Chêne *et al.* 1985.

Generic Synopsis: Stover and Evitt 1985, p. 58.

Type Species: *Kallosphaeridium brevibarbatum* De Coninick 1969; emend Jan du Chêne *et al.* 1985.

Kallosphaeridium ? ringnesiorum (Manum and Cookson 1964) Helby 1987
Pl.11, Fig. 1

1964 *Canningia ringnesii* Manum and Cookson, p. 15, pl. 2, fig. 10.

1980 *Chytreoisphaeridia ringnesiorum* (Manum and Cookson) Morgan, p. 19.

1980 *Batiacasphaera ringnesii* (Manum and Cookson) Dörhöfer and Davies, p. 40.

1981 *Canningia ringnesiorum* Manum and Cookson Below, p. 33.

1987 *Kallosphaeridium ? ringnesiorum* (Manum and Cookson) Helby, p. 325.

1987 *Kallosphaeridium ringnesiorum* (Manum and Cookson) Helby, Tocher and Jarvis, p. 325, pl. 9.2, fig. 3.

Original Description: Manum and Cookson 1964, p. 15, pl. 2, fig. 10.

Holotype: Manum and Cookson 1964, pl. 2, fig. 10.

Original Dimensions:	Holotype	Range
Length	92µm	64 - 102µm
Breadth	93µm	57 - 100µm

Description: Medium to large proximate cyst, with adnate archaeopyle. Cyst is sub-spherical to spherical in shape, is typically almost as broad as it is long and has a well rounded antapical margin with no antapical lobes present. The cyst is composed of autophragm only, which is densely reticulate to tuberculate. No sign of paratabulation is present on the cyst. Archaeopyle is apical (Type $\overline{tA}$) and characteristically the operculum remains attached.

Discussion: Cysts of this type were first assigned to the genus *Cannigia* by Manum and Cookson (1964). This species was subsequently incorrectly assigned to two other genera, see synonym list for details. Helby (1987) questionably included this species in the genus *Kallosphaeridium*. Tocher and Jarvis (1987) unquestionably transferred this species to this genus again on the basis of "its sub-spherical shape, non-tabular tuberculate surface ornament and apical archaeopyle with attached operculum".

However, when Below (1981) emended the genus *Cannigia*, he stated that it exhibits an apical archaeopyle and the operculum is simple, attached and enlarged. Also Below (1981) in his emendation of *C. reticulata* states it to have an attached operculum (Type $\overline{tAa}$). If this is the case, there is thus great difficulty in differentiating between *C. reticulata* and *K. ringnesiorum,* as all other characteristics of these cysts; shape, size, surface ornament, are similar.

Remarks: It is believed that the occurrence of this species within the Cenomanian is real, as is documented herein and also by Tocher and Jarvis (1987) and Jarvis *et al.* (1988a). Therefore, it is suggested that the stratigraphic range of this spcies should be extended to include the Cenomanian (see below).

Dimensions:		
Length of cyst	58 (64.4) 74µm
Breadth of cyst	52 (61.8) 72µm
Number of specimens measured	20

Known stratigraphic range: Campanian to Maastrichtian

Occurrence:

Site 3a no occurrence

TBB no occurrence

MCB no occurrence

SFE 15, 16, 17, 18

Genus: *Kleithriasphaeridium* Davey, 1974

Generic Synopsis: Stover and Evitt, 1978, p.167.

Junior Synonym: *Diversispina* Benson, 1976.

Type Species: *Kleithriasphaeridium corrugatum* Davey, 1974.

Kleithriasphaeridium readei (Davey and Williams, 1966b)
Davey and Verdier, 1976
Pl. 11, Figs 2, 3

1966b *Hystrichosphaeridium readei* Davey and Williams, p. 64, pl. 6, fig. 3.

1976 *Kleithriasphaeridium readei* (Davey and Williams) Davey and Verdier, p. 314, pl. 4, fig. 8.

Original Description: Davey and Williams, 1966b, p. 64, pl. 6, fig. 3

Holotype: Davey and Williams, 1966b, pl. 6, fig. 3.

Original Dimensions:

	Holotype	Range
Diameter of central body	41 x 45µm	31 - 54µm
Length of processes	23 - 29µm	20 - 35µm
Number of processes	24	

Description: Spherical to sub-spherical medium sized skolochorate cyst, with distinctive morphological processes. Central body is spherical to sub-spherical. Endophragm and periphragm closely adpressed over the whole central body. Both endophragm and periphragm are smooth. Periphragm is produced into long tubular hollow processes. There are usually between 24 - 27 processes, implying one per paraplate. Processes have a flared open distal margin which is aculeate to secate with tiny spines. Along the shaft of the processes are fibrous longitudinal ribs that extend to the base of the processes and connect along the cyst to the base of a neighbouring process. This gives the surface of the cyst an appearance of having a geometrical arrangement of septa between the process bases. The sulcal processes are usually slightly smaller than the others. Reflected process formula is 4', 6", 6c, 5"',1p, 1"", 2s. A

precingular archaeopyle is present, formed by the loss of a camerate 3" paraplate which is reduced giving the archaeopyle a more rounded geniculate boundary. Operculum is free.

Dimensions:	Diameter of central body	38 (42.6) 52μm
	Maximum process height	26 (31.1) 35μm
	Number of specimens measured	20

Known stratigraphic range: Cenomanian

Occurrences:

Site 3A 0, 20, 50, 65, 75

TBB -3, -2, 0 to 6, 8, 10 to 12, 14

MCB -2 --> -1.5 to -1 --> -0.5, 1 --> 1.5 to 2 --> 2.5, 3 --> 3.5, 4 --> 4.5, 4.5 --> 5

SFE no occurrence

Genus: *Leberidocysta* Stover and Evitt, 1978.

Generic Synopsis: Stover and Evitt, 1978, p. 59.

Type Species: *Leberidocysta chlamydata* (Cookson and Eisenack 1962) Stover and Evitt, 1978.

Leberidocysta chlamydata (Cookson and Eisenack 1962) Stover and Evitt, 1978.

Pl. 11, Fig. 4

1962 *Hexagonifera chlamydata* Cookson and Eisenack, p. 496, pl. 7, figs 1-3, 5-8.

1978 *Leberidocysta chlamydata* (Cookson and Eisenack) Stover and Evitt, p. 60.

Original Description: Cookson and Eisenack, 1962, p. 496, pl.7, figs 1-2, 5-8.

Holotype: Cookson and Eisenack, 1962, pl. 7, fig. 2.

Original Dimensions:	Holotype	Range
Overall length	75μm	ca. 69 - 75μm
Width	76μm	ca. 42 - 54μm
Shell	60 x 50μm	56 - 68 x 42 - 54μm

Description: Large elongate to oval cavate cyst. Central body oval and densely granular to verrucate. Periphragm smooth, transparent and appears thin and fragile. Irregular folds present in the periphragm, alter the shape of the cyst. Pericoel present over majority of the cyst, except at the apical archaeopyle margin where the periphragm and

endophragm are closely adpressed together. No sign of paratabulation is seen except for the apical archaeopyle, Type $\overline{tA}$. Operculum is free.

Remarks: *Leberidocysta chlamydata* may be distinguished from *L. defloccata* (Davey and Verdier, 1973) Stover and Evitt 1978, on the basis of its densely verrucate central body.

Dimensions:		
	Overall diameter	50 (63.3) 75µm
	Diameter of central body	34 (46.2) 54µm
	Overall length	64 (72.4) 82µm
	Number of specimens measured	10

Known stratigraphic range: Albian to Cenomanian

Occurrences:

Site 3A all samples

TBB -3, -2, 0 to 2, 4, 5, 7, 8, 10 to 15

MCB -4.5 --> -4, -3.5 --> -3 to 5 --> 5.5

SFE 15, 18

Leberidocysta defloccata (Davey and Verdier 1973)
Stover and Evitt, 1978
Pl. 11, Fig. 6

1973 *Hexagonifera defloccata* Davey and Verdier, p.198, pl. 3, figs 6,8.

1976 *"Thalassiphora defloccata"* (Davey and Verdier) Lentin and Williams, p. 85.

1978 *Leberidocysta defloccata* (Davey and Verdier) Stover and Evitt, p. 60.

1981 *"Disphaeria defloccata"* (Davey and Verdier) Yun, p. 70.

1984 *"Craspedodinium defloccatum"* (Davey and Verdier) Mehrotra and Sarjeant, p.49.

1985 *Leberidocysta defloccata* (Davey and Verdier) Lentin and Williams, p. 214.

Original Description: Davey and Verdier, 1973, p.198, pl. 3, figs 6,8.

Holotype: Davey and Verdier, 1973, pl. 3, fig. 8.

Original Dimensions:	Holotype	Paratype	Range
Inner body diameter	38 x 41µm	42 x 44µm	37 (44) 57µm
Overall diameter	68 x 90µm	48 x 52µm	48 (65) 90µm

Description: Large elongate cavate cysts, with oval central body.

Pericoel present over majority of the cyst, but periphragm and endophragm joined only at the archaeopyle margin. Both periphragm and endophragm are smooth. Periphragm is thin, transparent and often folded causing its shape to vary quite considerably. An apical archaeopyle, Type $\overline{tA}$ is present. No other sign of paratabulation is present. Operculum is free.

Remarks: *Leberidocysta defloccata* may be distinguished from *L. chlamydata* by the presence of a smooth central body.

Dimensions:

Overall length	62	(70.8)	80μm
Length of central body	40	(44.30	50μm
Overall breadth	54	(64.3)	80μm
Breadth of central body	38	(45)	48μm
Number of specimens measured	10		

Known stratigraphic range: Late Albian to Early Cenomanian

Occurrences:

Site 3A 5, 15, 20, 55 to 90, 100 to 120

TBB 11, 15

MCB -3 --> -2.5, -2 --> -1.5, -0.5 --> 0

SFE no occurrence

Genus: *Litosphaeridium* Davey and Williams 1966b; emend. Lucas-Clark, 1984.

Generic Synopsis: Stover and Evitt, 1978, p. 61.

Emended Generic Description: Lucas-Clark, 1984, p. 181.

Type Species: *Litosphaeridium siphonophorum* (Cookson and Eisenack 1958) Davey and Williams, 1966b, emend. Lucas-Clark, 1984.

Litosphaeridium siphonophorum (Cookson and Eisenack 1958) Davey and Williams, 1966b, subsp. *glabrum* Lucas-Clark, 1984.

Pl. 13, Figs 1-4

T1967 *Litosphaeridium siphonophorum* (Cookson and Eisenack 1958) Davey and Williams "subsp. *glabrum*" Warren, pp.205-207, pl. 18, figs 1,2

1984 *Litosphaeridium siphonophorum* (Cookson and Eisenack) Davey and Williams subsp. *glabrum* Lucas-Clark, p. 186, pl. 1, figs 1-11; pl. 2, fig. 2.

Original Description: Lucas-Clark, 1984, p. 186, pl.1, figs 1-11; pl. 2, fig. 2.

Holotype: Lucas-Clark, 1984, pl. 1, figs 2,3.

Original Dimensions:	Holotype	Paratype #1	Paratype #2	Range
Overall diameter	42µm	/	/	/
Diameter of central body	28µm	25µm (without operculum)	37µm	20 - 35µm
Process length	ca. 14µm	ca.12µm	ca.10µm	8 - 20µm
Total length (including apical process)	/	/	/	40 - 50µm

Description: Small spherical to sub-spherical skolochorate cyst, with intratabular processes of distinctive morphology and smooth periphragm. Periphragm and endophragm closely adpressed over the whole cyst. Endophragm ornament only visible beneath the process bases, and appears shagreenate to spongy. Periphragm is smooth, fine and unornamented and seems almost transparent in the processes There is one process per paraplate, except for the paracingular and parasulcal plates, which are not represented. The reflected process formula is 3', 6", 0c, 5"', 1p, 1"", 0s. Processes are hollow, closed and curved at their base, but have an open distal margin. The apical processes have closed tips and form a blunt, slightly flared distal point or top. Process shape varies intraspecifically from conical to sub-conical to sub-cylindrical to cylindrical to lagenate to bulbous to "semi-circular" (Pl. 13, Figs 1-4). Process shafts are circular to sub-circular in cross section. Process distal margin, depending on the processes shape is entire to serrate or wavy and may be thickened to form a rim. An apical archaeopyle is seen, Type $\overline{tA}$, leaving a characteristic zig-zag margin to the remaining cyst. Slight accessory archaeopyle sutures are sometimes visible, as is a sulcal notch. Specimens are rarely found with their archaeopyle intact. Operculum is free.

Remarks: *Litosphaeridium siphonophorum glabrum* may be distinguished from *Litosphaeridium siphonophorum* (Cookson and Eisenack 1958) Davey and Williams, 1966b subsp. *siphonophorum* Lucas-Clark, 1984 on the the following characteristics. *Litosphaeridium siphonophorum glabrum* is smaller than *L. siphonophorum siphonophorum* with a central body diameter of 22 (29.2) 38µm compared with 28 (33.4) 42µm for *L. siphonophorum siphonophorum.* Secondly, the periphragm of *L. siphonophorum glabrum* is smooth and unornamented, whereas that of *L. siphonophorum siphonophorum* is granular such that *L. siphonophorum glabrum* is always more transparent than the other subspecies, which are always darker and more opaque. Thirdly, the variation of process

morphology of *L. siphonophorum glabrum* is slighly more conservative and process size is smaller than that of *L. siphonophorum siphonophorum.* Maximum processes size of *L. siphonophorum glabrum* is 6 (10.6) 14µm and that of *L. siphonophorum siphonophorum* is 11 (14.2) 18µm.

Dimensions: Diameter of central body 22 (29.2) 38µm
Maximum length of processes 6 (10.6) 14µm
Minimum length of processes 4 (7.9) 12µm
Number of specimens measured 20

Known stratigraphic range: Albian to Cenomanian

Occurrences:

Site 3A all samples

TBB all samples

MCB all samples except 5 --> 5.5

SFE no occurrence

Litosphaeridium siphonophorum (Cookson and Eisenack 1958) Davey and Williams, 1966b subsp. *siphonophorum* Lucas-Clark, 1984

Pl. 12, Figs 1-6

1958 *Hystrichosphaeridium siphonophorum* Cookson and Eisenack, p. 44, pl. 11, figs 8-10.

1966b *Litosphaeridium siphonophorum* (Cookson and Eisenack) Davey and Williams, p. 80, pl. 7, figs 7,8; text-figs 16,17.

1972 *Litosphaeridium siphonophorum* Auct. non. (Cookson and Eisenack) Davey and Williams, Habib, pl.16, fig. 8.

1984 *Litosphaeridium siphonophorum* (Cookson and Eisenack) Davey and Williams subsp. *siphonophorum* Lucas-Clark, p. 186, pl. 1, figs 1,3,4.

Original Description: Cookson and Eisenack, 1958, p. 44, pl. 11, figs 8-10.

Emended Description: Lucas-Clark, 1984, p. 186, pl. 2, figs 1,3,4.

Holotype: Cookson and Eisenack, 1958, pl. 11, fig. 8.

Original Dimensions: Davey and Williams, 1966b, p. 80-81.

	Holotype	Paratype	Range of British Cenomanian forms
Overall diameter	76µm	69µm	/
Diameter of central body	43µm	33µm	22 (34) 47µm
Length of processes	14-24µm	14µm	4 - 25µm

Description: Medium sized spherical to sub-spherical skolochorate

cyst, with intratabular processes of characteristic morphology and a granular periphragm. Endophragm and periphragm closely adpressed over the whole cyst. The shagreenate to spongy nature of the endophragm is only visible at the process bases. The periphragm is finely to densely granular giving the cyst a light to dark brown colour. There is one process per paraplate, except for the paracingular and parasulcal plates, which are unrepresented. Process formula is therefore 3', 6", 0c, 5"', 1p, 1"", 0s. Processes are hollow and have closed curved bases, but an open distal margin. The apical processes are closed distally and form a blunt top, like that of a pin-head. In cross-section, process shafts are circular to sub-circular. The distal margin of the processes may be entire to serrate or wavy, depending on the particular process morphology. Often the distal margin is thickened to form a rim or a lip. Process shape is intraspecifically variable, it may be conical to sub-conical to sub-cylindrical to cylindrical to lagenate to "flask-shaped" (Pl. 12, Figs 1-6). An apical archaeopyle is exhibited, Type $\overline{tA}$, which when lost gives the remaining cyst a zig-zag margin. Slight accessory archaeopyle sutures are seen occasionally between the precingular paraplates. A sulcal notch is also present. Complete specimens with their archaeopyle intact are rare. Operculum is free.

Remarks: *Litosphaeridium siphonophorum siphonophorum* may be differentiated from *L. siphonophorum glabrum* in a number of ways, see Remarks of *L. siphonophorum glabrum* for more complete details. In summary however, *L. siphonophorum siphonophorum* is bigger than *L. siphonophorum glabrum*, appears darker, has a granular periphragm, and exhibits a more variable process morphology and larger maximum process size.

Dimensions:

Diameter of central body	28	(33.4)	42µm
Maximum length of processes	11	(14.2)	18µm
Minimum length of processes	8	(9.7)	12µm
Number of specimens measured	20		

Known stratigraphic range: Albian to Cenomanian

Occurrences:

Site 3A all samples

TBB all samples

MCB all samples

SFE no occurrence

Litosphaeridium sp. A

Pl. 13, Figs 5-7

T1983 *Litosphaeridium chlidanum* Marshall, p. 80, pl. 13, figs 16-18; text-fig. 18

1985 *Litosphaeridium* sp. A Marshall and Batten, p. 92, pl. 1, fig. 9.

Original Description: Marshall 1983, p. 80, pl. 13, figs 16-18; text-fig. 18.

Holotype: Marshall 1983, pl. 13, fig. 17.

Original Dimensions:

	Range
Body diameter	36 - 49µm
Maximum process length	19 - 26µm

Description: Medium sized spherical to sub-spherical skolochorate cysts, with characteristic goblet shaped process morphology and smooth periphragm. The periphragm and endophragm are closely adpressed. The periphragm is smooth and unornamented, and appears finely transparent. The processes are intratabular and there is one process per paraplate, except for the paracingular and parasulcal plates which are not represented. Inferred paratabulation pattern is 3', 6", 0c, 5"', 1p, 1", 0s. Processes are formed of smooth periphragm. In cross section the process shafts are circular to sub-circular. They are hollow, with a closed curved base and open distal margin. Process shape is fairly uniform within a specimen and intraspecifically. They are either sub-cylindrical, with a gradual flaring along the whole shaft length, or they are goblet shaped, with a cylindrical lower half and flared upper portion. The distal margin is denticulate to scalloped, frilled or frayed, and is never thickened or produced into a rim or lip. An apical archaeopyle is present (Type $\overline{tA}$). The operculum is free.

Remarks: This species was first recorded by Marshall (1983) who named it *L. chlidanum*. Marshall and Batten (1988) also recognised this cyst type but recorded it as a *Litosphaeridium* type cyst, calling it *Litosphaeridium* sp. A.

This cyst type is a *Litosphaeridium* cyst on the basis of its size, shape, intratabular processes and paratabulation pattern. It bears some similarities to *L. siphonophorum* subspecies in that it is without paracingular and parasulcal processes and has a free

archaeopyle, but its overall morphology and process shape set it apart from *L. siphonophorum.* Its smooth unornamented periphragm is similar to that of *L. siphonophorum glabrum*, but its goblet shaped processes are more similar to those of *L. bacar* Lucas-Clark, 1984. Therefore, it would seem to be a new species of *Litosphaeridium.*

Dimensions: Diameter of central body 34 (39.7) 46µm
Maximum process length 12 (18.3) 20µm
Number of specimens measured 10

Known stratigraphic range: Latest Cenomanian to Early Turonian (Marshall and Batten, 1988).

Occurrences:

Site 3A no occurrence

TBB no occurrence

MCB no occurrence

SFE 16, 18

Genus: *Microdinium* Cookson and Eisenack, 1960a; emend. Stover and Evitt, 1978.

Generic Synopsis: Stover and Evitt, 1978, p. 65.

Type Species: *Microdinium ornatum* Cookson and Eisenack, 1960a

Microdinium ? crinitum Davey, 1969a

Pl. 14, Figs 1, 2

1967 *Cometodinium obscurum* Deflandre and Courtville, Clarke and Verdier, p. 35, pl. 10, fig. 3; pl. 11, fig. 9.

1969a *?Microdinium crinitum* Davey, p.137, pl. 2, figs 7,8.

1987 *"?Phanerodinium crinitum"* (Davey) Below, p. 38.

Original Description: Davey, 1969a, p. 137, pl. 2, figs 7,8.

Holotype: Davey, 1969a, pl. 2, fig. 8.

Original Dimensions:	Holotype	Range
Shell diameter	27 x 28µm	24 (30.1) 38µm
Length of spines	ca. 12µm	6 - 19µm

Description: Small spherical to sub-spherical proximate cyst, with granular ornament and fibrous processes. The epicyst is much reduced in comparison with the hypocyst. Central body has granular to densely granular ornamented autophragm. Numerous non-tabular processes are present which are very fine and fibrous, giving the cyst a 'hairy' appearance. These processes become aligned along low relief

parasutural ridges, denoting some paratabulation. These ridges are best developed along the paracingulum and in the pre- and post -cingular areas, indicating there are 6 pre- and 6 post-cingular paraplates. There is a partiform antapical arrangement. An apical archaeopyle is present, Type $\overline{tA}$, but specimens are typically found with their archaeopyle intact. Operculum is free.

Dimensions:		
Overall length	34 (40.6) 44µm	
Length of central body	26 (29.8) 32µm	
Paracingular width	26 (28.2) 30µm	
Maximum height of ridges	5 (7.1) 10µm	

Number of specimens measured 20

Known stratigraphic range: Cenomanian

Occurrence:

Site 3A 0, 5, 10, 15, 30, 60, 65, 75, 85 to 95, 105 to 120

TBB all samples

MCB -4.5 --> -4 to 0.5 --> 1, 3 --> 3.5, 3.5 --> 4

SFE 16

Microdinium distinctum Davey, 1969a

Pl. 14, Figs 4,5

1967 *Microdinium ornatum* Cookson and Eisenack, Clarke and Verdier, p. 66, pl. 5, figs 11, 12.

1969a *Microdinium distinctum* Davey, p. 133, pl. 2, figs 9-11; text-figs 13 D, E, I.

1987 *"Phanerodinium distinctum"* (Davey) Below, p. 38.

Original Description: Davey 1969a, p. 133, pl. 2, figs 9-11; text-figs 13 D, E, I.

Holotype: Davey 1969a, pl. 2, fig. 9, 10; text-fig. 13 D, E.

Original Dimensions:	Holotype	Range
Shell length	36µm	29 - 36µm
Shell width	37µm	30 - 37µm
Height of crests ca. 2µm		2 - 2.5µm

Description: Small sub-spherical proximate cyst, with characteristic parasutural ridges. Epicyst much smaller than the hypocyst. Autophragm appears robust and thick, it is smooth and is typically pale brown in colour. Paracingulum and parasulcus are delimited by the parasutural crests, but no individual paracingular nor parasulcal plates are indicated. Paracingulum is broad and straight. Parasulcus

is wide and is present almost entirely in the hypocyst. Parasutural ridges or crests are well developed, denoting the almost complete paratabulation pattern, 4', 6", 0c, 6"', 1p, 1"", 0s. Typically the postcingular paraplates are larger than the precingular ones. There is a partiform antapical arrangement. The distal margin of the parasutural crests is entire or produced into small beads; ie machicolate, or is denticulate. In some rare specimens there are occasional intratabular tubercules. Archaeopyle is apical, Type $\overline{tA}$. Operculum is adnate dorsally.

Remarks: *Microdinium distinctum* and *M. ornatum* Cookson and Eisenack 1960a appear similar. The absence of paracingular sutural crests in *M. distinctum* is the most useful characteristic that distinguishes it from *M. ornatum*. However, it has been noticed that *M. distinctum* is typically a darker brown colour than *M. ornatum*, which is usually paler and more transparent.

Dimensions:		
	Length of cyst	30 (33.2) 38µm
	Breadth of cyst	31 (33.5) 38µm
	Number of specimens measured	10

Known stratigraphic range: Early Cenomanian

Occurrence:

Site 3A 5, 10, 35, 40, 60 to 70, 80, 85, 105, 110, 120

TBB 3, 5, 6

MCB -2 --> -1.5, -1.5 --> -1

SFE no occurrence

Microdinium ornatum Cookson and Eisenack 1960a

Pl. 14, Fig. 3

1960a *Microdinium ornatum* Cookson and Eisenack, p. 6, pl. 2, figs 3-8; text-figs 2-4.

1987 *"Phanerodinium ornatum"* (Cookson and Eisenack) Below, p. 38.

Original Description: Cookson and Eisenack 1960a, p. 6, pl. 2, figs 3-8; text-figs 2-4.

Holotype: Cookson and Eisenack 1960a, pl. 2, figs 3,4; text-fig. 2.

Original Dimensions:	Holotype	Range
Length	29µm	28 - 38µm
Breadth	27µm	27 - 36µm

Description: Small sub-spherical proximate cyst, with distinctive parasutural crests. Epicyst larger than hypocyst. Autophragm is

smooth, pale and transparent. Tubercules are irregularly distributed in the intratabular areas. The position of the paracingulum and parasulcus is clearly denoted by parasutural crests. The paracingulum is broad and planar and divided by individual paracingular plates are present. Parasulcus occurs largely in the hypocyst. No individual parasulcal plates were identified. There is a partiform antapical arrangement. Parasutural crests are low relief features with an entire margin or one which is produced into beads; ie machicolate or finely denticulate. The non-entire portion of these crests may be concentrated in the median area, whereas the ends of the crests are entire. Reflected paratabulation pattern is 4', 6", 6c, 6"', 1p, 1"", Os. Precingular paraplates are typically smaller than the postcingular ones. An apical archaeopyle is present, Type $\overline{tA}$. Operculum is adnate dorsally.

Remarks: *Microdinium ornatum* is similar to *M. distinctum.* The two may be distinguished on the basis that *M. ornatum* possesses individual paracingular plates and is paler, and more transparent almost than *M. distinctum.*

Dimensions:	Length of cyst	30 (34.6) 40μm
	Breadth of cyst	30 (33.4) 38μm
	Number of specimens measured	10

Known stratigraphic range: Albian to Turonian

Occurrence:

Site 3A 65, 115

TBB -3 to 0, 3, 4, 13, 15

MCB no occurrence

SFE 15, 17, 18

Microdinium setosum Sarjeant 1966, emend. Below 1987

Pl. 14, Figs 6, 7

1966 *Microdinium setosum* Sarjeant, p. 151, pl. 16, figs 9, 10; text-fig.39.

1967 *"Microdinium echinatum"* Clarke and Verdier, p.64, pl. 1, figs 9, 10; text-fig. 26.

1987 *"Phanerodinium setosum"* (Sarjeant) Below, p. 53, pl. 15, figs 6-10.

Original Description: Sarjeant 1966, p.151, pl. 16, figs 9, 10; text-fig. 39.

Holotype: Sarjeant 1966, pl. 16, figs 9, 10.

Original Dimensions:

	Holotype	Range
Overall length	35μm	33 - 38μm
Overall breadth	30μm	24 - 37μm
Shell length	33μm	
Shell breadth	24μm	

Description: Small sub-spherical to ovoidal proximate cyst, with denticulate parasutural crests. Hypocyst is larger than epicyst. Autophragm is densely granular. Paracingulum and parasulcus are well represented by the parasutural crests. Paracingulum is broad and very weakly laevorotatory. The parasulcus is larger in the hypocyst than the epicyst, but distinct parasulcal paraplates are not obvious. Parasutural crests are well developed and are of medium relief. Crests have a denticulate to echinate non-entire distal margin. Height of this crest varies between 2 - (4.1) - 6μm. Postcingular paraplates are bigger than the precingular paraplates. There is a partiform antapical arrangement. Reflected paratabulation is 4', 6", 6c, 6"', 1p, 1"", 0s. An apical archaeopyle is present. Operculum may remain attached dorsally

Dimensions:			
Length of cyst	27	(31)	34μm
Breadth of cyst	28	(30.7)	34μm
Maximum height of ridges	2	(4.1)	6μm
Number of specimens measured	20		

Known stratigraphic range: Cenomanian

Occurrence:

Site 3A 0, 10, 20, 30 to 45, 55 to 100, 110 to 120

TBB no occurrence

MCB -4.5 --> -4 to 3 --> -2.5, -2 --> -1.5 to -1 --> -0.5, 0 --> 0.5, 3.5 --> 4 to 4.5 --> 5

SFE no occurrence

Genus: *Nematosphaeropsis* Deflandre and Cookson, 1955; emend. Williams and Downie, 1966

Generic Synopsis: Stover and Evitt, 1978, p. 176.

Junior Synonym: *"Trabeculidinium"* Duxbury, 1980

Type Species: *Nematosphaeropsis labyrinthus* (Ostenfeld 1903) Reid, 1974.

Nematosphaeropsis densiradiata (Cookson and Eisenack 1962)
Stover and Evitt, 1978.
Pl. 14, Figs 8, 9

1962 *Cannosphaeropsis densiradiata* Cookson and Eisenack p. 493, pl. 4, figs 5-7.

1978 *Nematosphaeropsis densiradiata* (Cookson and Eisenack) Stover and Evitt, p. 176.

Original Description: Cookson and Eisenack, 1962, p. 493, pl. 4, figs 5-7.

Holotype: Cookson and Eisenack 1962, pl. 4, figs 5,6.

Original Dimensions:	Holotype	Paratype
Overall diameter	ca.70μm	ca.78μm
Shell	38μm	35μm

Description: Small spherical proximochorate cyst, with processes having distal trabeculae. Central body is spheroidal to ovoidal in shape and is composed of smooth to finely granular endophragm. The periphragm is developed into numerous gonal and intersutural penitabular processes, which envelope the central body. The shafts of the processes are circular in cross-section and robust. Tips of the processes bifurcate and trifurcate and each is connected to its neighbouring process by single trabeculae. These trabeculae are also circular in cross-section. Faint parasutural markings are present at the bases of the processes, but paratabulation cannot be deciphered properly. Archaeopyle is thought to be precingular, Type P representing the 3" paraplate, however it is rarely seen. Operculum is free.

Dimensions:			
Diameter of whole cyst	32	(40.9)	50μm
Diameter of central body	20	(20.8)	24μm
Maximum height of trabeculae	6	(9.2)	12μm
Number of specimens measured	10		

Known stratigraphic range: Cenomanian

Occurrence:

Site 3A 20, 30 to 45, 55 to 65, 75, 85 to 95

TBB 3 to 6, 8 to 11

MCB -4.5 --> -4 to -3.5 --> -3, -2.5 --> -2 to -1 --> -0.5, 2 --> 2.5, 2.5 --> 3, 4 --> 4.5

SFE no occurrence

Genus: *Oligosphaeridium* Davey and Williams 1966b; emend. Davey 1982

Generic Synopsis: Stover and Evitt 1978, p. 68.

Emended Generic Diagnosis: Davey 1982, p. 13.

Type Species: *Oligosphaeridium complex* (White 1842) Davey and Williams 1966b.

Oligosphaeridium complex (White 1842) Davey and Williams 1966b

Pl. 16, Figs 3-5

1842 *Xanthidium tubiferum complex* White, p. 39, pl. 4, div. 3, fig. 11.

1848 *Xanthidium complexum* (White) Bronn, p. 1375.

1940 *"Hystrichosphaeridium elegantulum"* Lejeune-Carpentier, p. 22, text-figs 11,12.

1946 *Hystrichosphaeridium complex* (White) Deflandre, p. 11.

1966b *Oligosphaeridium complex* (White) Davey and Williams, p. 71, pl. 7, figs 1,3; pl. 10, fig. 3; text-fig. 14.

1970 *"Oligosphaeridium cephalum"* Sah *et al.*, p. 147, pl. 2, figs 22,23.

1981 *"Hystrichosphaeridium himalayense"* Mehrotra and Sinha, p. 152, pl. 1, figs 7-9.

Original Description: White 1842, p. 39. pl. 4, div. 3, fig. 11.

Holotype: White 1842, pl. 4, div. 3, fig. 11 (Specimen lost)

Neotype: Davey and Williams 1966b, pl. 7, fig. 1.

Original Dimensions: White 1842, p. 39

Average diameter is $^{1}/_{300}$ to $^{1}/_{100}$ of an inch

First detailed Dimensions: Davey and Williams 1966b, p. 72.

	Neotype	Range
Diameter of central body	35 x 35µm	34 - 35µm
Length of processes	22 - 25µm	22 - 43µm

Description: Medium sized spherical skolochorate cyst, with intratabular processes. Endophragm and periphragm are smooth and unornamented. The two wall layers are closely adpressed over the whole cyst except at the process bases. Process distribution is intratabular, one per paraplate, but absent on paracingular and parasulcal plates. Processes are formed of periphragm and are cylindrical to infundibular. They are closed at their base, where there is a distinctive circular mark. Their distal margin is typically flared with an aculeate to secate to orthogonal margin. The

distal aculei and secae are either simple or branched to form a fork. The process formula is indicated by the intratabular processes and is, 4', 6", 0c, 6"', 1p, 1"", 0s. The paracingulum is indicated by a lack of processes in between the pre- and post-cingular processes. There is probably a sexiform antapical arrangement. An apical archaeopyle is present, Type $\overline{tA}$. After archaeopyle loss the remaining cyst has a zig-zag outline and strong accessory archaeopyle sutures are present. These latter two characteristics indicate the apical arrangement is tetra-ortho and that the paraplates 2", 4" and 5" are planate and 1", 3" and 6" are camerate in shape. Also a sulcal notch is noticeable which is offset to the left on the ventral surface. There is a simple operculum which is always free and is regularly found (Pl. 16, Fig. 5).

Remarks: It has been observed that there appears to be two mutually distinct size groupings of *O. complex*. The larger group exhibits values of central body diameter of between 40 - (44.4) - 51μm. The smaller groups values vary between 30 - (36) - 38μm. The larger group is the more common group of the two. All other characteristics of the two groups are identical.

Dimensions:		
Diameter of central body	30 (41.1) 51μm	
Maximum process length	20 (28.5) 40μm	
Number of specimens measured	20	

Known stratigraphic range: Senonian

Occurrence:

Site 3A 5, 10, 20, 30, 50 to 85, 100 to 120

TBB all samples

MCB -4.5 --> -4 to 2.5 --> 3, 3.5 --> 4 to 5 --> 5.5

SFE 15, 16, 18

Oligosphaeridium prolixispinosum Davey and Williams 1966b

Pl. 16, Fig. 6

1966b *Oligosphaeridium prolixispinosum* Davey and Williams, p. 76, pl. 8, figs 2,3.

Original Description: Davey and Williams 1966b, p. 76, pl. 8, figs 2,3.

Holotype: Davey and Williams 1966b, pl. 8, fig. 3.

Original Dimensions:	Holotype	Range
Overall width	64µm	
Diameter of central body	40 x 24µm	33 - 43 x 20 - 29µm
Length of processes	18 - 24µm	18 - 29µm
Number of processes	17	

Description: Elongate skolochorate cyst of intermediate size, with intratabular processes which taper distally and have a distal margin with spines. Endophragm and periphragm are smooth and unornamented, and are closely adpressed over much of the cyst. Number of processes (calculated from cysts after archaeopyle loss) varies from 14 - (16.2) - 18 indicating there is one process per paraplate except for the paracingulum plates. Paracingulum is without processes but is indicated by a lack of processes in that area. Process formula is (4'), 6", 0c, 6"', 1p, 1"", 0-4s. There is possibly a sexiform antapical arrangement. Processes are cylindrical with parallel sides, but taper slightly distally. The distal margin is open and may be aculeate to recurved to orthogonal. Typically 4-8 long spines are present at the distal margin. Where the periphragm of the process meets the endophragm of the central body, there is a distinctive circular mark which is the closed base of each process. Process length is typically equal to or rarely almost equal to the central body diameter. An apical archaeopyle is present, Type $\overline{tA}$, and the remaining cyst has a zig-zag margin due to the presence of slight accessory archaeopyle sutures. Operculum is free but is not observed occurring separately.

Remarks: *Oligosphaeridium prolixispinosum* is very similar to *Hystrichosphaeridium bowerbankii*. However, the two species may be differentiated by the fact that *O. prolixispinosum* has fewer processes [14 (16.2) 18] than *H. bowerbankii* [18 (16.2) 22].

Dimensions: (From archaeopyle margin to cyst base)	
Overall cyst length	34 (37.4) 44µm
Diameter of cyst	28 (23.1) 30µm
Maximum process length	18 (23.5) 27µm
Number of processes	14 (16.2) 18
Number of specimens measured	20

Known stratigraphic range: Cenomanian

Occurrence:

Site 3A 20, 50 to 120

TBB -3, -1, 0, 2, 4 to 9, 11 to 15

MCB -4 --> -3.5, -3.5 --> -3, 0 --> 0.5, 1 --> 1.5, 1.5 --> 2, 2.5 --> 3, 3 --> 3.5, 4.5 --> 5, 5 --> 5.5

SFE no occurrence

Genus: *Pervosphaeridium* Yun 1981

Generic Synopsis: Stover and Williams 1987, p. 175.

Type Species: *Pervosphaeridium pseudhystrichodinium* (Deflandre 1937) Yun 1981

Pervosphaeridium cenomaniense (Norvick 1976) Below 1982

Pl. 17, Fig. 4

1958 *Hystrichosphaeridium* cf. *H. hirsutum* Ehrenberg 1938, Cookson and Eisenack, p. 44, pl. 11, figs 5,6.

1976 *Exochosphaeridium cenomaniense* Norvick, p. 52, pl. 4, figs 4,8.

1982 *Pervosphaeridium cenomaniense* (Norvick) Below, p. 27.

Original Description: Norvick 1976, p. 52, pl. 4, figs 4,8.

Holotype: Norvick 1976, pl. 4, fig. 4.

Original Dimensions:

	Range
Overall diameter	51 (74) 97µm
Process length reaches	18µm

Description: Large skolochorate two-walled cyst, with numerous non-tabular squat processes. Central body spherical and is made up of both endophragm and periphragm. Periphragm densely granular to reticulate. Both wall layers are closely adpressed over much of the cyst except where the periphragm is produced into the processes. Processes are broad based, hollow, and conical. They often appear triangular in outline. The process shafts are usually striated to fibrous. No form of paratabulation is present and the processes are never aligned to denote parasutural features. Characteristically there is a Type 2P precingular archaeopyle, formed by the loss of camerate shaped 3" and 4" paraplates. Opercula are free.

Remarks: *Pervosphaeridium cenomaniense* may be distinguished from species of this genus by its smaller triangular/conical processes.

Dimensions:

Diameter of central body	52 (59.8) 70µm
Maximum length of processes	7 (8.8) 10µm
Number of specimens measured	10

Known stratigraphic range: Cenomanian

Occurrences:

Site 3A 0 to 15, 25 to 45, 65, 70, 90, 95, 105, 120

TBB -3, -2, 0, 4 to 6, 8, 9, 12

MCB -4.5 --> -4, -3.5 --> -3, -1.5 --> -1, 0 --> 0.5, 1 --> 1.5

SFE no occurrence

Pervosphaeridium pseudhystrichodinium (Deflandre 1937) Yun 1981

Pl. 17, Fig. 5

1937 *Hystrichosphaeridium pseudhystrichodinium* Deflandre, p. 73, pl.12, figs 3,4.

1939 *"Hystrichodinium palmatum"* Deflandre and Courtville, p. 101, pl. 3, fig.1.

1963 *Baltisphaeridium pseudhystrichodinium* (Deflandre) Downie and Sarjeant, p. 92.

1969a *Exochosphaeridium pseudhystrichodinium* (Deflandre) Davey, p. 163, pl. 11, figs 4,5.

1969 *?Exochosphaeridium pseudhystrichodinium* (Deflandre) Davey *et al.*, p. 16

1978 *"Exochosphaeridium ? palmatum"* (Deflandre and Courtville) Stover and Evitt, p. 154

1981 *Pervosphaeridium pseudhystrichodinium* (Deflandre) Yun, p. 29, pl. 5, figs 1, 2, 4, 6, 7.

Original Description Deflandre 1937, p. 73, pl. 12, figs 3, 4.

Holotype: Deflandre 1937, pl. 12, fig. 3.

Original Dimensions:		
	Diameter of central body	38 - 45µm
	Length without processes	49 - 54µm
	Total length	80 - 90µm

Description: Skolochorate sub-spherical cyst, of large size, bearing numerous, long non-tabular processes. Central body is composed of granular to perforate endophragm, giving the cyst surface a rough appearance. Processes are numerous, usually about 2 or 3 per paraplate; process number varies between 55 and 68. Process bases are broad and gives rise to long hollow, gradually tapering to acuminate processes. Occasionally the bases of neighbouring processes merge together. The distal margin of the processes is closed and may be blunt or pointed. Some processes are medianly bifurcate, giving rise to a dual pointed process. This larger type of process is typically found in the apical and antapical areas of the cyst. No sign of

parasutural alignment of these processes is present, therefore paratabulation is not obvious. A precingular archaeopyle is present, Type 2P. This represents two large camerate shaped paraplates 3" and 4". Opercula are free.

Remarks: *Pervosphaeridium pseudhystrichodinium* may be differentiated from other *Pervosphaeridium* species by its very much longer processes. Confusion with *Exochosphaeridium* species is possible but, these two genera are distinguished on the basis that *Pervosphaeridium* has a Type 2P archaeopyle, whereas *Exochosphaeridium* a Type P archaeopyle.

Dimensions:			
	Diameter of central body	46 (57.3)	68µm
	Maximum length of processes	14 (18.5)	24µm
	Number of processes	55 (57.3)	68
	Number of specimens measured	20	

Known stratigraphic range: Late Cretaceous

Occurrence:

Site 3A all samples

TBB all samples

MCB all samples

SFE 16, 17, 18

Pervosphaeridium truncatum (Davey 1969a) Below 1982

Pl. 17, Fig. 6

1969a *Exochosphaeridium striolatum* (Deflandre 1937) var. *truncatum* Davey, p. 164, pl. 7, figs 1-3.

1973 *Exochosphaeridium striolatum* (Deflandre) subsp. *truncatum* Lentin and Williams, p. 56.

1978 *Exochosphaeridium truncatum* (Davey) Stover and Evitt, p. 154

1982 *Pervosphaeridium truncatum* (Davey) Below, p. 27.

Original Description: Davey 1969a, p. 164, pl. 7, figs 1-3.

Holotype: Davey 1969a, pl. 7, fig. 2.

Original Dimensions:	Holotype	Range
Diameter of central body	66 x 67µm	34 (56.1) 81µm
Length of processes	17 - 22µm	6 (17.8) 27µm

Description: Large sub-spherical to ovoidal skolochorate cyst, with numerous non-tabular medium length processes. Both endophragm and periphragm present, the latter being finely reticulate to pitted. Number of processes present implies there are 2 to 3 processes per paraplate. Processes are broad based and are closed distally and

adjoining processes may occasionally join at their bases. Processes are of medium length. The shape of the processes varies from tapering to acuminate, with a blunt or pointed top. Very occasionally the process shaft may divide medianly. Paratabulation is never indicated by any alignment of the processes. A large precingular archaeopyle is present, Type 2P, formed by the loss of the 3" and 4" camerate paraplates. Opercula are free.

Remarks: *Pervosphaeridium truncatum* may be distinguished from *P. pseudhystrichodinium* and *P. cenomaniense* on the basis that its process length is intermediary between the other two species mentioned. Its Type 2P archaeopyle clearly distinguishes it from the similar genus *Exochosphaeridium*, which has a Type P archaeopyle.

Dimensions:			
Overall length of cyst with processes	66	(72)	80µm
Length of central body	50	(55.5)	64µm
Diameter of central body	52	(59.4)	72µm
Maximum Length of processes	8	(10.4)	12µm
Number of specimens measured	20		

Known stratigraphic range: Cenomanian

Occurrence:

Site 3A 0 to 20, 35, 50 to 80, 90 to 100, 115, 120

TBB -3, -1, 0, 2, 3, 5, 9, 10, 12, 15

MCB -4 --> -3.5, -2.5 --> -2, -1.5 --> -1 to 5 --> 5.5

SFE 16, 18

Genus: *Prolixosphaeridium* Davey *et al.* 1966; emend. Davey 1969a

Generic Synopsis: Stover and Evitt 1978, p. 77.

Type Species: *Prolixosphaeridium parvispinum* (Deflandre 1937) Davey *et al.*, 1969.

Prolixosphaeridium conulum Davey 1969a

Pl. 18, Figs 1, 2

1969a *Prolixosphaeridium conulum* Davey, p. 160, pl. 8, figs 5, 6.

Original Description: Davey 1969a, p. 160, pl. 8, fig. 5.

Holotype: Davey 1969a, pl. 8, fig. 5.

Original Dimensions:	Holotype	Range
Shell length	47µm	38 (43.8) 50µm
Shell width	27µm	20 (25.9) 29µm

Length of processes	11 - 16μm	11 (15.1) 18μm
Number of processes		45 - 60

Description: Elongate, ellipsoidal, medium sized skolochorate cyst, with numerous non-tabular processes. Central body is elongate with a rounded antapical base and an angular apex due to archaeopyle loss. Autophragm densely granular giving the surface of the cyst an irregular appearance. Processes are smooth and moderately wide based. Typically there is a circular mark at their base on the surface of the central body. Processes acuminate, tapering distally to form a closed sharp point. There is some alignment of these processes transversely and longitudinally on the cyst, but this does not appear to indicate a paratabulation. An apical archaeopyle, Type $\overline{tA}$ is present, and all specimens found were without their operculum. Operculum is free.

Remarks: *Prolixosphaeridium conulum* may sometimes be confused with *Tanyosphaeridium variecalamus* Davey and Williams 1966b. However, the former has more numerous processes [35 (40.6) 47], which taper distally to a point, in contrast to *T. variecalamus* has fewer processes [20 (25.4) 30], with flared distal tips.

Dimensions:		
	Length of cyst	40 (47.4) 54μm
	Diameter of cyst	24 (28) 30μm
	Maximum length of processes	10 (12.3) 14μm
	Number of processes	35 (39.6) 47
	Number of specimens measured	10

Known stratigraphic range: Cenomanian

Occurrence:

Site 3A 10, 25, 30, 55, 70, 75, 85, 95, 110 to 120

TBB -3, -1, 0, 2, 3, 5, 9, 10, 12, 15

MCB -4.5 --> -4, -3.5 --> -3, -2.5 --> -2, -2 --> -1.5, -0.5 --> 0, 1.5 --> 2, 4 --> 4.5, 4.5 --> 5

SFE 16, 18

Genus: *Psalligonyaulax* Sarjeant 1966; emend. Sarjeant 1982

Generic Synopsis: Stover and Evitt 1978, p. 182.

Emended Generic Synopsis: Sarjeant 1982, p. 44.

Type Species: *Psalligonyaulax deflandrei* Sarjeant 1966; emend. Sarjeant 1982.

Psaligonyaulax deflandrei Sarjeant 1966; emend. Sarjeant 1982

Pl. 18, Figs 3, 4

1966 *Psaligonyaulax deflandrei* Sarjeant, p. 137, pl. 14, figs 7,8; text-fig. 35.

1967 *"Gonyaulacysta extensa"* Clarke and Verdier, p. 30, pl. 4, figs 7-9; text-fig. 11.

1982 *Psaligonyaulax deflandrei* Sarjeant, Sarjeant, p. 45, pl. 11, figs 1-3; text-fig. 6.

Original Description: Sarjeant 1966, p. 137, pl. 14, figs 7,8; text-fig. 35.

Holotype: Sarjeant 1966, pl. 14, figs 7,8; text-fig.35 and Jan du Chêne *et al.*, 1986, pl. 85, figs 3,4; pl. 86, figs 1-3.

Original Dimensions:

	Holotype	Range
Overall length	75µm	72 - 82µm
Overall breadth	44µm	43 - 60µm
Length of inner body	35µm	
Breadth of inner body	40µm	

Description: Elongate to ellipsoidal, large, bicavate, proximate cyst. Central body is spheroidal to ovoidal. The cyst has strongly developed pericoel in the apical and antapical areas. Typically the epipericoel is larger than the hypopericoel. Apical horn is large, broad based and narrows distally into an elongate rounded tip. Endocyst appears to sit within the hypopericoel area, where the periphragm is shaped into a "collar" around the base of the endocyst. The periphragm is smooth to finely granular. Paracingulum is broad and strongly helicoid laevorotatory. Parasulcus broadens considerably on the hypocyst and demonstrates an S-type ventral arrangement with the paracingulum. Paratabulation is obvious and is indicated by distinctive parasutural flanges/crests. Paratabulation pattern is, 4', 6", 6c, 6"', 1p, 1"". There is a sexiform antapical arrangement. Parasutural crests are high and typically have denticulate to vaguely machicolate, non-entire distal margins. Characteristically these indentations to the distal margin are more common in the central area of the parasutural crest. Irregularly distributed trabeculae are found in the intratabular areas. A reduced precingular archaeopyle, Type P is present, formed by the loss of an elongated camerate shaped 3" paraplate. Operculum is free.

Remarks: *Psaligonyaulax deflandrei* may be distinguished from the

similar *G. cassidata* by its larger periepicoel and perihypocoel. See *G. cassidata* Remarks for further details.

Dimensions:		
	Overall length of pericyst	64 (74.1) 87μm
	Overall breadth of pericyst	40 (47.9) 62μm
	Length of endocyst	40 (44.3) 58μm
	Breadth of endocyst	36 (41.9) 50μm
	Number of specimens measured	20

Known stratigraphic range: Cenomanian

Occurrence:

Site 3a 0 to 45, 55 to 85, 100 to 120

TBB all samples

MCB -4.5 --> -4 to -0.5 --> 0, 0.5 --> 1 to 2 --> 2.5, 3 --> 3.5, 3.5 --> 4, 4.5 --> 5, 5 --> 5.5

SFE no occurrence

Genus: *Pterodinium* Eisenack 1958; emend. Yun 1981

Generic Synopsis: Stover and Evitt 1978, p. 182.

Emended Generic Diagnosis: Yun 1981, p. 12.

Type Species: *Pterodinium aliferum* Eisenack 1958; emend. Sarjeant 1985.

Remarks: See Lentin and Williams (1989, p. 309) for a review of the emendations to the genus.

Pterodinium cingulatum (O. Wetzel 1933b)
subspecies *cingutatum* Below 1981.
Pl. 18, Figs 5, 6

1933a *Cymatiosphaera cingulata* O. Wetzel, p.28, pl. 4, fig.10.

1955 *Hystrichosphaera cingulata* (O. Wetzel) Deflandre and Cookson, p. 267, pl. 6, figs 4,5.

1958 *"Cymatiosphaera pterota"* Cookson and Eisenack, p. 50, pl. 11, fig. 7.

1966a *"Spiniferites crassimurata"* Davey and Williams, p. 39, pl.1, fig. 11.

1967 *Hystrichosphaera cingulata* (O. Wetzel) var. *cingulata* Clarke and Verdier, p. 45, pl. 8, figs 9,10.

1970 *"Spiniferites cingulatus"* (O. Wetzel) Sarjeant, p. 76.

1970 *"Spiniferites pterotus"* (Cookson and Eisenack) Sarjeant, p. 76.

1970 *"Spiniferites crassimuratus"* (Davey and Williams) Sarjeant, p. 76.

1971 *Spiniferites cingulatus* (O. Wetzel) var. *cingulata* Davey and Verdier, p. 32.

1978 *"Spiniferites cingulata* (O. Wetzel) subspecies *cingulata"* Lentin and Williams, p. 190.

1981 *Pterodinium cingulatum* (O. Wetzel) subspecies *cingulatum* Below, p. 114, pl. 9, figs 10, 12, 13, 15; text-figs 74, 75.

Original Description: O. Wetzel 1933a, p. 28, pl. 4, fig. 10.

Holotype: O. Wetzel 1933a, pl. 4, fig. 10.

Original Dimensions: Measurements about 50µm : 42µm : ?50µm

Description: Medium sized murochorate cyst which has a spheroidal central body and high parasutural septa. Endophragm is smooth and unornamented. Periphragm is also smooth, but is produced into high relief parasutural crests. These crests denote the paratabulation of 4', 6", 6c, 5"', 1p, 1"", 0-3s. Both paracingulum and parasulcus are clearly indicated and they demonstrate an S-type ventral arrangement. Height of the parasutural crests varies from being highest at the gonal positions and lowest in the mid-gonal areas, giving the parasutural crest a slightly concaved upper margin. Maximum parasutural crest height varies between 7 - (9.7) - 12µm. The distal margin of the crests is usually straight and entire, but in some rare cases it is machicolate. There is a reduced precingular archaeopyle Type P, representing a camerate shaped 3" paraplate. Operculum is free.

Dimensions:

Overall length of cyst	50	(59.3)	66µm
Overall breadth of cyst	46	(55.2)	60µm
Length of central body	38	(45)	52µm
Breadth of central body	34	(39.4)	48µm
Maximum height of parasutural crests	7	(9.7)	12µm
Number of specimens measured	20		

Known stratigraphic range: Senonian

Occurrence:

Site 3A all samples

TBB all samples

MCB all samples

SFE all samples

Pterodinium cingulatum subspecies *granulatum*
(Clarke and Verdier 1967) Lentin and Williams 1981
Pl. 18, Figs 7, 8

1933b *Cymatiosphaera cingulata* O. Wetzel, p. 28, pl. 4, fig. 10.

1967 *Hystrichosphaera cingulata* var. *granulata* Clarke and Verdier, p. 45, pl. 8, figs 9-10.

1970 *"Spiniferites cingulatus"* (O. Wetzel) Sarjeant, p. 76.

1973 *"Spiniferites cingulatus* (O. Wetzel) Sarjeant subspecies *granulatus"* (Clarke and Verdier) Lentin and Williams, p. 127

1981 *Pterodinium cingulatum* subsp. *granulatum* (Clarke and Verdier) Lentin and Williams, p. 238.

Original Description: Clarke and Verdier 1967, p.45, pl. 9, figs 5,6; text-fig. 18.

Holotype: Clarke and Verdier 1967, pl. 9, fig. 5 and Jan du Chêne *et al.*, 1986, pl. 88, figs 5-8.

Original Dimensions:

	Holotype	Range
Overall length	51µm	48 - 56µm
Overall breadth	49µm	43 - 50µm
Height of ledges	8µm	5 - 8µm

Description: A sub-species of *P. cingulatum* which differs from *P. cingulatum cingulatum* in having a positive granulate endophragm and from other sub-species of *P. cingulatum* in being somewhat smaller. See measurements below for details.

Dimensions:

Overall length of cyst	48	(51.6)	56µm
Overall breadth of cyst	42	(47.2)	52µm
Length of central body	36	(42.8)	48µm
Breadth of central body	36	(39.5)	44µm
Maximum height of parasutural crests	8	(9.6)	12µm
Number of specimens measured	10		

Known stratigraphic range: Cenomanian

Occurrence:

Site 3A 15, 30, 35, 50 to 120

TBB all samples

MCB -4.5 --> -4, -3.5 --> -3 to -2 --> -1.5, -1 --> -0.5 to 2.5 --> 3, 3.5 --> 4 to 5 --> 5.5

SFE 16, 17, 18

Pterodinium cingulatum subspecies *reticulatum*
(Davey and Williams 1966a) Lentin and Williams 1981
Pl. 18, Fig. 9; Pl. 19, Figs 1, 2

1966a *Hystrichosphaera cingulata* var. *reticulata* Davey and Williams, p. 2, pl. 1, fig. 10; pl. 2, fig. 4.

1967 *"Hystrichosphaera* cingulata var. *perforata"* Clarke and Verdier, p. 46, pl. 9, figs 2-4; text-fig. 19.

1971 *"Spiniferites cingulatus* var. *reticulatus"* (Davey and Williams) Davey and Verdier, p. 33.

1973 *"Spiniferites cingulatus* subspecies *reticulatus"* (Davey and Williams) Lentin and Williams, p. 127.

1981 *Pterodinium cingulatum* subsp. *reticulatum* (Davey and Williams) Lentin and Williams, p. 328.

Original Description: Davey and Williams 1966a, p. 39, pl. 1, fig. 10; pl. 2, fig. 4.

Holotype: Davey and Williams 1966a, pl. 1, fig. 10.

Original Dimensions:

	Holotype	Range
Diameter of central body	40 x 55µm	33 - 59µm
Height of crests	up to 14µm	up to 17µm

Description: A subspecies of *P. cingulatum* with thick negative reticulate endophragm.

Dimensions		
Overall length of cyst	48 (58.1)	64µm
Overall breadth of cyst	46 (53.6)	66µm
Length of central body	36 (42.8)	48µm
Breadth of central body	36 (39.5)	44µm
Maximum height of parasutural crests	8 (9.6)	12µm
Number of specimens measured	10	

Known stratigraphic range: Cenomanian

Occurrence:

Site 3A 0, 10, 25 to 50, 60, 65, 75 to 110, 120

TBB all samples

MCB -4.5 --> -4, -3.5 --> -3 to 0 --> 0.5, 1.5 --> 2, 2.5 --> 3, 3.5 --> 4 to 5--> 5.5

SFE 15, 18

Pterodinium cingulatum subspecies *polygonalis* (Clarke and Verdier 1967) Lentin and Williams 1973 *stat. nov.*
Pl. 19, Figs 3-5

1866a *"Hystrichosphaera crassimurata"* Davey and Williams, p. 39, pl. 1, fig. 10; pl.2, fig. 4.

1967 *Hystrichosphaera cingulata* var. *polygonalis* Clarke and Verdier, p. 47, pl. 8, figs 7,8; text-fig. 20.

1968 *"Hystrichosphaera crassimurata"* Davey and Williams, Clarke *et al.*, p. 181.

1970 *"Hystrichosphaera crassimurata"* Davey and Williams, Davey, p. 391.

1970 *"Spiniferites cingulatus"* (O. Wetzel) Sarjeant, p.76.

1970 *"Spiniferites crassimuratus"* (Davey and Williams) Sarjeant, p. 76.

1973 *"Spiniferites cingulatus* subspecies *polygonalis"* (Clarke and Verdier) Lentin and Williams, p. 127.

1973 *"Spiniferites pterotus"* (Cookson and Eisenack) Sarjeant, Kjellström, p. 44.

1986 *Pterodinium cingulatus* subsp *cingulatus* (O.Wetzel) Below, Jan du Chêne *et al.*, pl. 89, figs 7-9.

Original Description: Clarke and Verdier 1967, p.47, pl. 8, figs 7, 8; text-fig. 20.

Holotype: Clarke and Verdier 1967, pl. 8, fig. 7.

Original Dimensions:	Holotype	Range
Overall length	60µm	55 - 65µm
Overall breadth	50µm	50 - 58µm
Height of ledges	8µm	8 - 11µm

Description: Sub-spherical to ovoidal, medium sized proximochorate cyst, with distinctive parasutural crests. Endophragm is smooth. Periphragm is thick and forms the parasutural crests. The crests are highest at the gonal positions, and lowest in the mid-gonal parts. Maximum height of the crests ranges between 8 (10.4) 12µm. The distal margin of the crests is usually entire but may be slightly undulate in places. Reflected paratabulation pattern is, 4', 1a, 6", 6c, 5"', 1p, 1"", 0-3s. The most distinctive characteristic feature of this subspecies is that the intratabular areas between the parasutural crests are thickened to yield a polygonal pattern bounded by the crests. A reduced precingular archaeopyle is exhibited (Type P), formed by the loss of a camerate 3" paraplate. Operculum is free.

Discussion: Davey and Williams (1966a) first identified this cyst as a new species of *Hystrichosphaera,* and named it *H. crassimurata.*

Clarke and Verdier (1967) recognised this cyst as a variety of the species *H. cingulata*, calling it *H. cingulata* var. *polygonalis*. However, Clarke *et al.* (1968) recognised *H. cingulata* var *polygonalis* as a junior synonym of *H. crassimuratus* and rejected the former name. Both *H. cingulata* and *H. crassimurata* were transferred to *Spiniferites* by Sarjeant (1970). Later, Lentin and Williams (1973) raised *S. cingulatus* var *polygonalis* to a subspecies level, thus calling it *S. cingulatus* subsp. *polygonalis*. However, Kjellström (1973) considered *S. crassimuratus* to be a junior synonym of *S. pterotus*. Below (1981) in his new combination of *Pterodinium cingulatum cingulatum*, did not document this morphotype as being a subspecies of the species *P. cingulatum*. Below (1981) also considered *S. pterotus* to be a junior synonym of *P. cingulatum cingulatum*.

I recognise *P. cingulatum* subspecies *polygonalis* on the presence of the distinctive polygonal shaped thickenings of the periphragm in the intratabular areas between the parasutural crests.

Dimensions:	Overall length of cyst	50 (59.2) 66μm
	Overall breadth of cyst	42 (50.1) 56μm
	Length of central body	36 (42.7) 50μm
	Breadth of central body	30 (35.4) 40μm
	Maximum height of parasutural crests	8 (10.4) 12μm
	Number of specimens measured	20

Occurrence:

Site 3A 15 to 35, 50, 65 to 90, 100, 120

TBB all samples except 3

MCB -4.5 --> -4 to 1 --> 1.5, 2 --> 2.5, 2.5 --> 3, 3.5 --> 4 to 5 --> 5.5

SFE no occurrence

Pterodinium ? cornutum Cookson and Eisenack 1962

Pl. 19, Figs 6, 7

1962 *Pterodinium cornutum* Cookson and Eisenack, p. 490, pl.3, figs 1-4.

1978 *Pterodinium ? cornutum* Cookson and Eisenack, Stover and Evitt, p.183.

1981 *"Gonyaulacysta cornuta"* (Cookson and Eisenack) Yun, p.10.

1986 *Pterodinium ? cornutum* Cookson and Eisenack, Jan du Chêne *et al.*, p.133, pl.90, fig. 1.

Original Description: Cookson and Eisenack 1962, p. 490, pl. 3, figs 1-4.

Holotype: Cookson and Eisenack 1962, pl. 3, figs 1-3.

Original Dimensions:	Holotype	Range
Overall length	83µm	78 - 86µm
Overall breadth	76µm	70 - 76µm
Shell	62 x 48µm	52 - 62 x 48 - 58µm

Description: Medium to large ovoidal proximochorate cyst, with characteristic parasutural crests and apical horn. Central body is sub-spherical to ovoidal. Apical horn is conical, with a pointed tip and gives the epicyst a pointed appearance. Both periphragm and endophragm are smooth, unornamented and transparent. Parasutural crests are medium to high relief features, and characteristically reach their highest extent at the gonal positions and are lowest mid way between two gonal processes. Paracingulum is indicated by such parasutural crests. There is an S-type ventral arrangement to the parasulcus and paracingulum. Archaeopyle is reduced precingular, Type P, representing a camerate 3" paraplate. Operculum is free.

Remarks: *Pterodinium ? cornutum* cysts recorded herein are found to be consistently smaller than that cited in the original description and measurements (Cookson and Eisenack, 1962). However, all other characteristics imply that they are indeed *P. ? cornutum*. *Pterodinium ? cornutum* is distinguished from similar *P. cingulatum* subspecies by the presence of an apical horn and by its larger size. It is believed that the occurrence of this species within the Cenomanian is a real occurrence, thus extending its range from the Apto/Albian to the Cenomanian.

Dimensions:		
Overall length of cyst		46 (57.5) 68µm
Overall breadth of cyst		40 (50.2) 56µm
Length of central body		38 (43.7) 52µm
Breadth of central body		30 (36.6) 44µm
Maximun height of parasutural ridges	8	(9.2) 12µm
Number of specimens measured	20	

Known stratigraphic range: Aptian - ?Albian

Occurrence:

Site 3a 10, 30, 65 to 80, 90, 100

TBB -3, to 4, 7 to 15

MCB -4.5--> -4 to 2--> 2.5, 3.5--> 4, 4.5--> 5

SFE no occurrence

Genus: *Rhiptocorys* Lejeune-Carpentier and Sarjeant 1983

Generic Synopsis: Stover and Evitt, 1978, p. 187.

Type Species: *Rhiptocorys veligera* (Deflandre 1937) Lejeune-Carpentier and Sarjeant 1983.

Rhiptocorys veligera (Deflandre 1937) Lejeune-Carpentier and Sarjeant 1983

Pl. 19, Figs 8, 9

1937 *Michrystridium veligerum* Deflandre, p. 81, pl. 7, fig. 9.

1943 *Ceratocorys veligera* (Deflandre) Lejeune-Carpentier, p. B24, pls 1-6.

1967 *"Microdinium irregulare"* Clarke and Verdier, p. 65, pl. 7, figs 5-8; text-fig. 27.

1967 *"Ceratocorys smolenskiense"* Vozzhennikova, p. 93, pl. 35, figs 1-6; pl. 35, fig. 6; pl. 36, fig. 4.

1969a *Microdinium veligerum* (Deflandre) Davey, p. 136, p. 3, fig. 6; pl. 4, fig. 4.

1973 *"Microdinium smolenskiense"* (Vozzhennikova) Lentin and Williams, p. 95.

1983 *Rhiptocorys veligera* (Deflandre) Lejeune-Carpentier and Sarjeant, p. 5, pl. 2, figs 2-7; text-figs 4-8.

1983 *"Phanerodinium veligerum"* (Deflandre) Below, p. 38

Original Description: Deflandre 1937, p. 81, pl. 7, fig. 9.

Holotype: Deflandre 1937, pl. 7, fig. 9.

Original Dimensions: Diameter without the crest 18µm
Diameter with the crest ca.25µm

Description: Small spherical to sub-polygonal proximochorate cyst, with parasutural septa. The epicyst is characteristically about half the size of the hypocyst. Two wall layers are present and are closely adpressed over the whole cyst except at the base of the septa. Surface of the cyst is densely granulate to areolate. The paracingulum and parasulcus are indicated by parasutural crests. Paracingulum is broad and weakly helicoid to straight. Parasulcus occurs only on the hypocyst, where it expands quite considerably to form a large postsulcal paraplate (ps). Individual paracingular and

parasulcal plates are only hinted at. Paraplates on the epicyst are very vague, and are usually absent due to archaeopyle loss. However, those on the hypocyst are clearly delimited by the parasutural crests. Paratabulation pattern where visible is, ?', ?", 6c, 6"', 1p. 1"", ?s. There is a partiform antapical arrangement. The parasutural crests are high relief features, relative to the size of the cyst, with distal margin of the crests at their highest extent at parasutural junctions. Archaeopyle is presumed to be epicystal, but precise type is uncertain. Operculum is free.

Dimensions:	Length of cyst (from archaeopyle margin to base)	28 (32.5) 36µm
	Diameter of cyst	30 (32.5) 38µm
	Number of specimens measured	20

Known stratigraphic range: Senonian

Occurrence:

Site 3A 5 to 120

TBB all samples

MCB -4.5 --> -4 to 0 --> 0.5, 1.5 --> 2, 2 --> 2.5, 3 --> 3.5, 3.5 --> 4, 4.5 --> 5, 5 --> 5.5

SFE no occurrence

Genus: *Spiniferites* Mantell 1850; emend. Sarjeant 1970

Generic Synopsis: Stover and Evitt 1978, p. 189.

Junior Synonyms: *Hystrichosphaera* O. Wetzel 1833b; emend Deflandre 1937.

Hystrichokibotium Klumpp 1953.

Type Species: *Spiniferites ramosus* (Ehrenberg 1838) Loeblich and Loeblich 1966.

Remarks: Hystrichospheres were first discovered by Ehrenberg (1838) who considered them to be siliceous Desmid zygospores of the genus *Xanthidium*. Mantell (1845) realised that these fossil forms were organic and not siliceous and on the basis of this, their morphology and habitat, he suggested that they were not Desmids. To distinguish them, Mantell (1850) created the new genus *Spiniferites*. Otto Wetzel (1933b) transferred some fossil cysts from the misidentifed *Xanthidium* genus to his new genus *Hystrichosphaera*. The genus *Hystrichosphaera* was to be realised as a junior synonym to *Spiniferites* as Sarjeant (1964) rediscovered the forgotten genus *Spiniferites* Mantell (1850). Subsequently Sarjeant (1970) expanded the generic diagnosis to include

all thus transferred *Spiniferites* species. The taxonomic approach to the genus *Spiniferites* Mantell (1850) taken herein is that of Davey and Williams (1966a).

Spiniferites ? dentatus (Gocht 1959) Lentin and Williams 1973;
emend Duxbury 1977.
Pl. 20, Figs 1, 2

1959 *Hystrichosphaera ? dentata* Gocht, p. 75, pl. 4, fig. 11; pl. 7, fig. 19.

1973 *Spiniferites dentatus* (Gocht) Lentin and Williams, p. 128.

1977 *Spiniferites dentatus* (Gocht) lentin and Williams, Duxbury, p. 49.

Original Description: Gocht 1959, p. 75, pl. 4, fig. 11; pl. 7, fig. 19.

Holotype: Gocht 1959, pl. 4, fig. 11.

Original Dimensions:

	Holotype	Other figured specimen	Other examples
Length	73µm	78µm	57 - 85µm
Breadth	70µm	70µm	
Central body	55:47µm		
Width of ridge/crest	5-15µm	19µm	

Description: Ellipsoidal to ovoidal proximochorate cyst, which is of medium to large size and possesses typical *Spiniferites* type processes. Epicyst more pointed than the hypocyst, suggesting a possible apical projection. Central body is sub-spherical to ovoidal and is composed of thin, smooth endophragm. Periphragm is also smooth and relatively transparent. Both wall layers are closely adpressed over much of the central body, except at processes bases and beneath parasutural crests. Processes are gonal and intergonal in position, are of moderate length and have bifurcated and trifurcated tips. Between the gonal processes run parasutural crests, which are ornamented distally with smaller bifurcating and trifurcating processes. These parasutural crests indicate the position of the parasulcus and the paracingulum, which is weakly helicoid laevorotatory ie. S-type. The reflected paratabulation pattern is 3', 5", 6c, 5"', 1p, 1"", ?s. There is a sexiform antapical arrangement. Archaeopyle is reduced precingular Type P, formed by the loss of a camerate 3" paraplate. Operculum is free.

Remarks: The occurrence of *S. ? dentatus* within the Cenomanian microplankton assembalges herein is believed to be real, thus extending the known range of this species from the Late Hauterivian (see below) upwards to include the Cenomanian.

Dimensions:		
Overall length of cyst	54 (59.8)	66µm
Length of central body	38 (42.9)	48µm
Breadth of central body	32 (36.9)	40µm
Maximum length of processes	8 (9.4)	12µm
Number of specimens measured	20	

Known stratigraphic range: Late Hauterivian

Occurrence:

Site 3A 10 to 90, 100, 110 to 120

TBB all samples

MCB -4.5 --> -4 to -3 --> -2.5, -2 --> -1.5 to 0 --> 0.5, 1 --> 1.5 to 5 --. 5.5

SFE no occurrence

Spiniferites multibrevis (Davey and Williams 1966a) Below 1982

Pl. 20, Figs 3, 4

1955b *Hystrichosphaera furcata* (Ehrenberg) Valensi, p. 586, pl. 4, fig. 4; pl.5, fig. 12.

1958 *Hystrichosphaera furcata* (Ehrenberg) Eisenack, p. 406, pl. 25, figs 4-8.

1959 *"Galea twistringiensis"* Maier, p. 309, pl. 30, figs 3, 4.

1966a *Hystrichosphaera ramosa* var. *multibrevis* Davey and Williams, p. 35, pl. 1, fig. 4; pl. 4, fig. 6; text-fig. 9.

1973 *Spiniferites ramosus* subspecies *multibrevis* (Davey and Williams) Lentin and Williams, p. 130.

1978 *"Spiniferites cambrus"* (Sah *et al.* 1970) Stover and Evitt, p. 190.

1982 *Spiniferites multibrevis* (Davey and Williams) Below, p. 35.

Original Description: Davey and Williams 1966a, p. 35, pl. 1, fig. 4; pl. 4, fig 6; text-fig. 9.

Holotype: Davey and Williams 1966a, pl. 4, fig. 6.

Original Dimensions:

	Holotype	Range of Hauterivian specimens	Range of Cenomanian specimens
Diameter of central body	35x44.5µm	34 - 47µm	35 - 46µm

Length of processes up to 16μm up to 12μm up to 19μm

Description: Medium sized ovoidal to sub-spherical proximochorate cyst, with very short *Spiniferites* type processes. Epicyst has a slightly angular apex, whereas the hypocyst is well rounded. Periphragm and endophragm are closely adpressed over much of the cyst, except at the base of the processes and beneath the parasutural ridges. Processes are solid and made of unornamented periphragm, which appears transparent at the extremities of the processes. Processes are gonal and intergonal in position and are characteristically short and appear stunted. Process height ranges between 6 to 10μm, with a mean value of 8.5μm. The tips of the processes are typically bifid or trifid, and these terminations are very short indeed. The position of the parasutural ridges denotes the presence of a offset laevorotatory paracingulum and vague parasutural areas. There is an S-type ventral organisation to the parasulcus and paracingulum. The reflected paratabulation pattern is, 3', 5", 6c, 5"', 1p, 1"" ?s. There is a sexiform antapical arrangement. Archaeopyle is reduced precingular, Type P representing a large 3" paraplate which is camerate in shape. Operculum is free.

Remarks: The occurrence of this species within the Cenomanian microplankton assemblages herein is believed to be real, which therefore extends the known range of *S. multibrevis* from the Hauterivian (see below) into the Cenomanian.

Dimensions:

Overall length of cyst	48 (55.1) 66μm
Length of central body	32 (40.30 50μm
Breadth of central body	30 (36.9) 45μm
Maximum length of processes	6 (8.5) 10μm
Number of specimens measured	20

Known stratigraphic range: Hauterivian

Occurrence:

Site 3A 0, 10, 15, 25 to 45, 60, 65, 75, 80, 90, 100, 120

TBB -3 to 8, 11 to 15

MCB -4.5 --> -4 to -0.5 --> 0, 1 --> 1.5 to 5 --> 5.5

SFE 15, 16, 17, 18

Spiniferites ramosus (Ehrenberg 1838) Loeblich and Loeblich 1966 subspecies *gracilis* (Davey and Williams 1966a) Lentin and Williams 1973

Pl. 21, Fig. 3

1966a *Hystrichosphaera ramosus* (Ehrenberg) var. *gracilis* Davey and Williams, p. 34, pl. 1, fig. 5; pl. 5, fig. 6.

1966 *Spiniferites ramosus* (Ehrenberg) Loeblich and Loeblich, p. 56

1973 *Spiniferites ramosus* (Ehrenberg) Loeblich and Loeblich subspecies *gracilis* (Davey and Williams), Lentin and Williams, p.130.

Original Description: Davey and Williams 1966a, p. 34, pl. 1, fig. 5; pl. 5, fig. 6.

Holotype: Davey and Williams 1966a, pl. 5, fig. 6.

Original Dimensions:	Holotype	Range of London Clay specimens	Range of Cenomanian specimens
Diameter of central body	35 x 43µm	32 - 61.5µm	28 - 33µm
Length of processes	17 - 23µm	up to 29µm	up to 20µm

Description: Ovoidal to sub-angular, medium to large proximochorate cyst possessing long slender *Spiniferites*-like processes. The endophragm and periphragm are closely adpressed over the cyst except at process bases and beneath the parasutural ridges. Central body is ovoidal, smooth and unornamented. Paracingulum is broad and helicoid laevorotatory. Individual paracingular plates are obvious, being hexagonal lozenge shaped. Sometimes individual parasulcal plates are seen. Parasulcus broadens considerably on the hypocyst and exhibits an S-type arrangement with the paracingulum. Processes are either solid or hollow, but are all long and slender, appearing somewhat delicate in comparison with other *S. ramosus* subspecies. Process length is either $^{1}/_{2}$ or slightly over $^{1}/_{2}$ the precingular width of the cyst. Processes are both gonal and intergonal in position, with long bifurcating and trifurcating tips. Parasutural ridges are present extending between the gonal processes denoting the paratabulation pattern of, 3', 5", 6c, 5"', 1p, 1"",?s. There is a sexiform antapical arrangement. A reduced precingular archaeopyle is present, Type P representing the camerate shaped 3" paraplate. Operculum is free.

Dimensions:		
	Overall length of cyst	70 (78.9) 90µm
	Length of cyst	40 (45.2) 58µm
	Breadth of cyst	36 (38.6) 44µm

Maximum process height 18 (22.8) 26μm

Number of specimens measured 10

Known stratigraphic range: Cenomanian to Eocene

Occurrence:

Site 3A 10, 20 to 40, 50 to 90, 105, 110, 120

TBB -3 to 10, 13 to 15

MCB - 4.5 --> -4, -2 --> -1.5, -1 --> -0.5 to 2 --> 2.5, 3.5 --> 4

SFE 15, 16, 17, 18

Spiniferites ramosus (Ehrenberg 1838) Loeblich and Loeblich 1966
subspecies *ramosus* Davey and Williams 1966a
Pl. 20, Figs 5-8

1838 *Xanthidium ramosum* Ehrenberg, p. 1, figs 1, 2, 5.

1838 *Xanthidium furcatum* Ehrenberg, pl.1, figs 12, 14.

1932 *Hystrichosphaera furcata* (Ehrenberg) O. Wetzel, p. 136.

1932 *Hystrichosphaera ramosa* (Ehrenberg) O. Wetzel, p. 144.

1959 *"Areoligera birama"* Maier, p. 304, pl. 29, fig. 2.

1959 *"Areoligera dermatica"* Maier, p. 305, pl. 29, fig. 3.

1959 *"Hystrichosphaeridium echinoides"* Maier, p. 318, pl. 32, figs 5, 6.

1966 *Spiniferites ramosus* (Ehrenberg) Loeblich and Loeblich, p. 56.

1966a *Hystrichosphaera ramosa* (Ehrenberg) var. *ramosa* Davey and Williams, p. 33, pl. 1, figs 1, 6; pl. 3, fig. 1; text-fig. 8

1981 *"Homotryblium distinctum"* Salujha and Kindra, p. 51, pl. 2, fig. 45.

Original Description: Davey and Williams 1966a, p. 33, pl. 1, fig. 1, 6; pl. 3, fig. 1; text-fig. 8

Holotype: Ehrenberg (1838) did not specify a holotype. Davey and Williams (1966a) designated the specimen figured by Ehrenberg (1838), pl. 1, fig. 5 as a lectotype.

Original Dimensions: Davey and Williams (1966a)

	Holotype	Range of Lower Cretaceous specimens	Range of Cenomanian specimens	Range of London Clay specimens
Diameter of central body	42 x 48μm	34 - 41μm	30 - 50μm	32 - 56μm
Length of processes	13 - 25μm	5 - 13μm	7 - 27μm	11 - 20μm

Description: Ellipsoidal to ovoidal, polygonal, medium sized proximochorate cyst with typical *Spiniferites* type processes. Central body surface is smooth. Both wall layers are closely adpressed over much of the cyst, except at the process bases and beneath the parasutural ridges. Paracingulum is broad and strongly helicoid laevorotatory and divided by individual hexagonal-lozenge shaped paracingular plates. Parasulcus is well developed and some individual paraplates are obvious like the large posterior sulcal plate (ps). There is an S-type ventral arrangement of the parasulcus with the paracingulum. Processes are solid, erect and strong. They are gonal and intergonal in position but the latter are not very common. The tips of the processes are bifid or trifid, producing long tips. Parasutural ridges are developed between the gonal processes. These ridges denote the paratabulation pattern, 3', 5", 6c, 5"', 1p, 1"", ?s. A sexiform antapical arrangement is present. There is a reduced precingular archaeopyle is seen, Type P, formed by the loss of a camerate 3" paraplate. Operculum is free.

Remarks: There is some variability in the morphology and sizes of *S. ramosus ramosus* recorded herein. Central body shape seems to be either ovoidal or more angular, even polygonal. Therefore, so as to differentiate these two groups, those with the ovoidal central bodies were logged as *S. ramosus ramosus* (ovoidal) and those with the angular/polygonal body central bodies recorded as *S. ramosus ramosus* (angular). Even within these two groups there is still a large variation in size of these cysts. The central body length for the *S. ramosus ramosus* (ovoidal) group ranges from 39-(46.6)-54μm and that of the *S. ramosus ramosus* (angular) group varies from 34-(40.3)-48μm. Also, highly variable through-out is the style of preservation as it is either such that the cysts appear transparent or dark brown in colour.

Dimensions: Measurements of the two groups of *S. ramosus ramosus* as outlined are as follows:

	Spiniferites ramosus ramosus (ovoidal) group	*Spiniferites ramosus ramosus* (angular) group
Length of central body of cyst	39 (46.6) 54μm	34 (40.3) 48μm
Diameter of central body	36 (41) 46μm	28 (35) 46μm
Maximum process height	12 (15.4) 20μm	10 (13.7) 18μm
Number of specimens measured	20	20

Known stratigraphic range: Late Cretaceous

Occurrence:

Site 3A all samples

TBB all samples

MCB all samples

SFE all samples

Spiniferites ramosus (Ehrenberg 1838) Loeblich and Loeblich 1966 subsp. *reticulatus* (Davey and Williams 1966a) Lentin and Williams 1973

Pl. 21, Figs 1.2

1966a *Hystrichosphaera ramosus* (Ehrenberg) var. *reticulata* Davey and Williams, p. 38, pl. 1, figs 2, 3.

1966 *Spiniferites ramosus* (Ehrenberg) Loeblich and Loeblich, p. 56.

1971 *Spiniferites ramosus* (Ehrenberg) Loeblich Loeblich var. *reticulatus* (Davey and Williams) Davey and Verdier, p. 34.

1973 *Spiniferites ramosus* (Ehrenberg) Loeblich and Loeblich subspecies *reticulatus* (Davey and Williams) Lentin and Williams, p. 130.

Original Description: Davey and Williams 1966a, p. 38, pl. 1, figs 2,3

Holotype: Davey and Williams 1966a, pl. 1, figs 2, 3.

Original Dimensions:	Holotype	Range
Diameter of central body	36 x 42µm	35 - 59µm
Length of processes	up to 14µm	up to 17µm

Description: Medium to large, ovoidal proximochorate cyst, with reticulate central body and typical *Spiniferites* style processes. Central body is ovoidal and characteristically reticulate to densely reticulate, giving the cyst a dark brown colour. Periphragm and endophragm closely adpressed over the cyst except beneath the processes and parasutural ridges. Paracingulum is broad and helicoid laevorotatory. Hexagonal lozenge shaped paracingular plates are visible. Parasulcus broadens considerably in the hypocyst and its relationship with the paracingulum denotes an S-type pattern. Processes are medium to long, are solid and appear quite robust. Process tips bifurcate and trifurcate to form short distal tips. Gonal and intergonal processes are present although the former are much more common. Parasutural ridges of low relief extend between

these gonal processes, indicating a paratabulation pattern, 3', 5", 6c, 5"', 1p, 1"", ?s. There is a sexiform antapical arrangement. Archaeopyle is reduced precingular, Type P representing a camerate 3" paraplate. Operculum is free.

Dimensions:		
	Overall length of cyst	60 (70.3) 80μm
	Length of central body	38 (47.9) 54μm
	Breadth of central body	33 (39.2) 52μm
	Maximum process height	12 (14.3) 18μm
	Number of specimens measured	20

Known stratigraphic range: Cenomanian

Occurrence:

Site 3A 10, 15, 30, 40, 45, 105

TBB -2 to 13, 15

MCB all samples

SFE no occurrence

Genus: *Stephodinium* Deflandre 1936a; emend. Davey 1970

Generic Synopsis: Stover and Evitt 1978, p. 192

Type Species: *Stephodinium coronatum* Deflandre 1936a

Stephodinium coronatum Deflandre 1936a

Pl. 21, Figs 4-6

1936a *Stephodinium coronatum* Deflandre, p. 58, text-fig. 104.

1962b *"Stephodinium australicum"* Cookson and Eisenack, p. 491, pl.2, figs 5-10.

1964 *"Stephodinium europacium"* Cookson and Hughes p. 50, pl. 8, figs 9-17.

Original Description: Deflandre 1936a, p. 58, text-fig. 104.

Holotype: Deflandre 1936a, text-fig. 104.

Original Dimensions: Not given in original description.

First Dimensions: Deflandre 1936b, p. 171.	
Length of body (including the horn)	56μm
Width without the ring	38μm
Width with ring	70μm

Description: A large camocavate or pterocavate cyst with large circumferential pericoel. Central body is composed of smooth unornamented endophragm and is spheroidal to ovoidal in shape. Periphragm is smooth. Endophragm and periphragm adpressed together in

the apical, antapical and ventral areas of the cyst. Elsewhere, at the paracingulum and dorsal areas they are separated by a large pericoel. The cyst in dorso-ventral orientation appears as the central body surrounded by a ring (Pl. 21, Figs 5, 6). This orientation displays a large strong apical horn, which is broad based, sub-conical and has a blunt top. Parasutural ridges are present and they are low relief features, with an entire distal margin, that give some indication of paratabulation. The paracingulum is thus indicated and is broad and straight to very weakly helicoid laevorotatory. The parasulcal area is indicated in apical-antapical compressional views (Pl. 21, Fig. 4), as the area where the periphragm and endophragm are closely adpressed, such that no pericoel is present. The deducible paratabulation pattern is ?', 5", ?6c, 5"', 1"", ?s. The pre and post -cingular paraplates are fairly large. The 1"" antapical paraplate is very large and is six-sided, therefore there is a sexiform antapical arrangement. A large precingular archaeopyle Type P is present, representing a camerate shaped 3" paraplate. Operculum is always free and is commonly found inside the endocyst.

Remarks: Apical-antapical and dorso-ventral compressions of *S. coronatum* were observed. The former compressional style is marginally more common than the latter.

Dimensions:

Overall length of cyst (including apical horn)	52	(57.9)	64µm
Length of endocyst	44	(47.4)	52µm
Maximum width of pericoel	64	(73.9)	84µm
Diameter of endocyst	40	(47.7)	56µm
Distance from ventral to dorsal sides	54	(60.1)	70µm
Number of specimens measured	20		

Known stratigraphic range: Senonian

Occurrence:

Site 3A 20, 30, 55, 65 to 95, 105 to 120

TBB -2, 0, 4, 6 to 14

MCB -4.5 --> -4 to -1 --> -0.5, 0 --> 0.5 to 2 --> 2.5, 3 --> 3.5 to 5 --> 5.5

SFE no occurrence

Genus: *Surculosphaeridium* Davey *et al.* 1966; emend. Davey 1982

Generic Synopsis: Stover and Evitt 1978, p. 83.

Emended Generic Diagnosis: Davey 1982, p. 15.

Type Species: *Surculosphaeridium cribrotubiferum* (Sarjeant 1960) Davey *et al.* 1966.

Surculosphaeridium longifurcatum (Firtion 1952) Davey *et al.* 1966

Pl. 22, Fig. 2

1952 *Hystrichosphaeridium longifurcatum* Firtion, p. 157, pl. 9, fig. 1; text-figs 1, H, K, L, M.

1963 *Baltisphaeridium longifurcatum* (Firtion) Downie and Sarjeant, p. 91.

1966 *Surculosphaeridium longifurcatum* (Firtion) Davey *et al.*, p. 163, pl. 8, figs 7, 11; text-figs 43, 44.

1978 *Surculosphaeridium ? longifurcatum* (Firtion) Davey *et al.*, Stover and Evitt, p. 83.

Original Description: Firtion 1952, p. 157, pl. 9, fig. 1; text-figs 1, H, K, L, M.

Holotype: Firtion 1952, pl. 9, fig. 1.

Original Dimensions: Diameter of the ?body 40.6µm
Length of appendages 20.4µm

Description: Spherical to sub-spherical proximochorate cyst which is of medium to large size, with long solid processes. Central body, which is composed of smooth endophragm, is spherical to sub-spherical. Endophragm and periphragm are closely adpressed over the whole cyst except where the periphragm forms the processes. Periphragm is smooth and unornamented. Processes are all solid and appear robust and rigid structures. Processes are medianly bifurcate with subsequently furcate tips, or more commonly they are complexly branched. The complex processes usually branch in the distal third of the process and result in multifurcate tipped processes. Type of process varies irregularly, regardless of position on the cyst, however the precingular processes are consistently more robust and trifurcate half-way along their shafts. Apical, precingular, postcingular, parasulcal and antapical processes are all intratabular and there is one process per paraplate. However, the cingular paraplates appear to have two slightly smaller processes and their bases are so closely juxtaposed that it may appear that bases join. The reflected paratabulation pattern is thus 4', 6", 6c, 1p, 1"", 1-5s. No other sign of paratabulation is apparent. Archaeopyle is apical, Type $\overline{tA}$.

A distinct parasulcal notch is present. Operculum is free.

Discussion: Stover and Evitt (1978) stated that *S. longifurcatum* was a provisionally accepted species of *Surculosphaeridium,* because "its archaeopyle may be precingular rather than apical; if so process distribution requires reinterpretation". Firtion (1952) in his original description of *S. longifurcatum* did not include any information on the archaeopyle type and from his illustrated specimen (pl. 9, fig. 1) the archaeopyle position cannot be determined. However, Davey *et al.* (1966) when re-assigning this cyst to the genus *Surculosphaeridium* stated it to have an apical archaeopyle and Davey (1982) published the archaeopyle type as Type $\overline{tA}$.

Current observations confirm the more comprehensive redescription of *S. longifurcatum* by Davey (1982) and the nature of the apical archaeopyle (Type $\overline{tA}$). Thus, I would favour the full retention of this species within the genus *Surculosphaeridium.*

Dimensions:

Diameter of central body	30	(38.2)	48µm
Length of cyst after archaeopyle loss	28	(35)	40µm
Maximum process length	16	(20)	29µm
Number of specimens measured	20		

Known stratigraphic range: Cenomanian

Occurrence:

Site 3A 20, 35 to 50, 60, 65, 85, 95

TBB -2 to 15

MCB all samples

SFE 16, 17, 18

Surculosphaeridium spinicongregatum Yun 1981

Pl. 22, Fig. 4

1981 *Surculosphaeridium spinicongregatum* Yun, p. 40, pl. 16, figs 2, 6.

Original Description: Yun 1981, p. 40, pl. 16, figs 2, 6.

Holotype: Yun, pl. 16, fig. 6.

Original Dimensions:

	Holotype	Range
Maximum diameter of central body		42 - 52µm
Diameter of central body	42 x 42µm	
Length of processes	12µm	12 - 15µm

Description: Medium sized proximochorate cyst, with thickly-set squat processes. Central body spherical to sub-spherical and composed

of dark granulate endophragm. Central body is generally broader than long. Periphragm is smooth and more transparent than the endophragm. Both wall layers are closely adpressed over the whole cyst, but the periphragm is produced into the processes. Processes are solid, do not connect with the endocyst and are broad based, low relief features which have cylindrical shafts and flared distal portions. The distal portion is bifurcate or multifurcate, forming hooked tips, somewhat like grapnel-tips. Position and number of the processes may denote some form of paratabulation, but an exact pattern was not discernable. An apical archaeopyle, presumably Type $\overline{tA}$, is present but is rarely seen. Operculum is free.

Remarks: Specimens of *S. spinicongregatum* were usually badly broken and/or squashed, such that the elucidation of an exact paratabulation was impossible and good photography made quite difficult. Because of the badly preserved state of speciemens of this species, it cannot be definitely suggested that its occurrence within the Cenomanian microplankton assemblages herein is real, which would therefore extend its range lower than previously recorded, into the Cenomanian.

Dimensions:

Diameter of central body	40 (41.5) 46µm
Length of cyst after archaeopyle loss	40 (47.5) 56µm
Maximum length of processes	10 (14.4) 20µm
Number of specimens measured	10

Known stratigraphic range: Early Santonian

Occurrence:

Site 3A 10, 20, 55 to 65, 75 to 85, 100 to 120

TBB -3 to 13

MCB -4.5 --> -4 to -1.5 --> -1, -0.5 --> 0, 0.5 --> 1, 2.5 --> 3, 3.5 --> 4 to 5 --> 5.5

SFE no occurrence

Genus: *Tanyosphaeridium* Davey and Williams 1966b

Generic Synopsis: Stover and Evitt 1978, p. 85.

Type Species: *Tanyosphaeridium variecalamus* Davey and Williams 1966b.

Tanyosphaeridium variecalamus Davey and Williams 1966b

Pl. 22, Fig. 3

1966b *Tanyosphaeridium variecalamum* Davey and Williams, p. 98, pl. 6, fig. 7; text-fig. 20.

Original Description: Davey and Williams 1966b, p. 98, pl. 6, fig. 7; text-fig. 20.

Holotype: Davey and Williams 1966b, pl. 6, fig. 7; text-fig. 20.

Original Dimensions:

	Holotype	Range
Length of central body	34µm	30 - 34µm
Breadth of central body	14µm	14 - 20µm
Length of processes	12 - 16µm	12 - 24µm
Number of processes	26	20 - 31

Description: Elongate, ellipsoidal, medium sized skolochorate cyst, with non-tabular processes. The central body, which is composed of granular endophragm, is elongate with a rounded antapical base and a concave upper margin caused by operculum loss. The processes which are composed of smooth periphragm are closed at their base where there is a circular mark on the central body, where the periphragm and endophragm come together. Processes are tubiform to buccinate as at their distal ends they thin slightly before forming a small, flared cup-like termination. This distal margin may posses small spines or may be serrate. The paracingulum is indicated by a transverse gap between the processes in that area, and processes either side are aligned parallel to it. Paratabulation pattern is difficult to discern as number of processes per paraplate varies from one to two, according to the position of the process on the cyst. An apical archaeopyle, Type $\overline{tA}$ is always seen. Operculum is free.

Remarks: *Tanyosphaeridium variecalamus* may be differentiated from the similar *P. conulum* on the basis of the number of processes and nature of distal tip termination. *Tanyosphaeridium variecalamus* has fewer processes [20 (25.4) 30] and an open flared cup-shaped distal termination. In contrast *P. conulum* has more numerous processes [35 (40.6) 47] and has distally pointed closed processes.

Dimensions:

Length of cyst	28 (33.1) 38µm
Diameter of cyst	13 (16.8) 20µm
Maximum process length	10 (11.5) 15µm
Number of processes	20 (25.4) 30
Number of specimens measured	10

Known stratigraphic range: Cenomanian

Occurrence:

Site 3A no occurrence

TBB -3, -1, 0

MCB -4.5 --> -4 to -0.5 --> 0, 1 --> 1.5, 1.5 --> 2, 4 --> 4.5, 4.5 --> 5

SFE no occurrence

Genus: *Trichodinium* Eisenack and Cookson 1960; emend. Clarke and Verdier 1967

Generic Synopsis: Stover and Evitt 1978, p. 196.

Type Species: *Trichodinium pellitum* Eisenack and Cookson 1960.

Trichodinium castanea (Deflandre 1935) Clarke and Verdier 1967

Pl. 22, Figs 5, 6

1935 *Palaeoperidinium castanea* Deflandre, p. 229, pl. 6, fig. 8.

1936b *Palaeoperidinium castanea* Deflandre, Deflandre, p. 29, pl. 6, figs 1-4.

1959 "*Apteodinium ciliatum*" Gocht, p. 65, pl. 8, figs 5, 6.

1967 *Trichodinium castanea* (Deflandre) Clarke and Verdier, p. 19, pl. 1, figs 9, 10.

Original Description: Deflandre 1935, p. 229, pl. 6, fig. 8.

Holotype: Deflandre 1935, pl. 6, fig. 1 and Jan du Chêne *et al.*, 1986, pl. 122, figs 9, 10.

First Dimensions: Deflandre 1936b, p. 30. (Translation)

"In general the least deformed specimens measure approximately 45µm in diameter. However, because of the broken or flattened nature of some, the dimensions 45 to 65µm can be acceptable for the group."

Description: Sub-spherical to ellipsoidal proximochorate cyst of medium size possessing a small apical prominence. Autophragm only present. The epicyst has an apical prominence giving it a more angular appearance than the hypocyst. Both epicyst and hypocyst are of equal size. Cyst is covered with numerous dense non-tabular spines. These spines are short, solid and form a point or have a capitate top. Paracingulum is devoid of spines and indicated by an alignment of the spines in this area. The paracingulum is broad and is slightly helicoid laevorotatory. Parasulcus is indicated by an area with few spines. Occasionally spines may have an alignment elsewhere on the cyst, thus giving faint indications of parasutures. However, an discernable paratabulation pattern is not obvious. A ?enlarged precingular archaeopyle is present, Type P, formed by the loss of

camerate 3" paraplate. Operculum is free.

Remarks: This species has been previously recorded in Cenomanian deposits of England, northern France and North America by Davey (1969), Davey and Verdier (1973) and Foucher and Taugourdeau (1975), which confirms its real occurrence within the Cenomanian microplankton assemblages herein.

Dimensions:			
	Length of central body	46 (51.3)	60µm
	Diameter of central body	40 (46)	54µm
	Maximum height of spines	3 (3.7)	6µm
	Number of specimens measured	20	

Known stratigraphic range: Erratic ?Senonian

Occurrence:

Site 3A 0 to 15, 25 to 90, 100 to 120

TBB all samples

MCB -4.5 --> -4 to -0.5 --> 0, 0.5 --> 1 to 2.5 --> 3, 3.5 --> 4 to 5 --> 5.5

SFE 16, 17

Genus: *Valensiella* Eisenack 1963

Generic Synopsis: Stover and Evitt 1978, p. 86.

Junior Synonym: *Favilarnax* Sarjeant 1963

Type Species: *Valensiella ovulum* (Deflandre 1947) Eisenack 1963

Valensiella ovulum (Deflandre 1947) Eisenack 1963

Pl. 22, Figs 7, 8

1947 *Membranilarnax ovulum* Deflandre, p. 9, text-figs 22, 23.

1963 *Valensiella ovulum* (Deflandre) Eisenack, p. 102.

1963 *"Favilarnax ovulum"* (Deflandre) Sarjeant, p. 720.

Original Description: Deflandre 1947, p. 9, text-figs 22, 23.

Holotype: Deflandre 1947, text-fig. 22.

Original Dimensions:		
	Length of central body	48 - 55µm
	Breadth of central body	37 - 45µm
	Overall length	55 - 65µm
	Overall breadth	44 - 55µm

Description: Large elongate proximate holocavate cyst of ovoidal to ellipsoidal shape, carrying low relief ectophragmal ridges/crests. Central body is composed of finely granular autophragm and is ovoidal

to sub-ovoidal in shape. The smooth ectophragm is produced into a series of medium to large muri giving the appearance of a large reticulum. The lumina are sub-circular to polygonal and vary considerably in size. Maximum height of of the muri is in the central area and varies from 4 (8.8) 12μm. No sign of paratabulation is present as the muri are non-tabular. An apical archaeopyle, Type $\overline{tA}$ is present. After archaeopyle loss the remaining cyst has a slight zig-zag margin and a parasulcal notch is also present. Operculum is free.

Remarks: Due to the consistent occurrence of this species within the microplankton assemblages examined herein, it is believed that the occurrence of this species within the Cenomanian is real. Therefore, the range of this species should be extended upwards to include the Cenomanian.

Dimensions:		
	Overall length of cyst	46 (54.2) 64μm
	Overall diameter of cyst	38 (51.1) 58μm
	Length of central body	34 (44.8) 53μm
	Diameter of central body	32 (41.8) 52μm
	Maximum height of muri	4 (8.8) 12μm
	Number of specimens measured	20

Known stratigraphic range: Bajocian

Occurrences:

Site 3A 0 to 100, 110 to 120

TBB -3, -1 to 6, 8 to 15

MCB -4.5 --> -4 to -3 --> -2.5, -2 --> -1.5 to 0 --> 0.5, 1 --> 1.5 to 2 --> 2.5, 3.5 --> 4 to 5 --> 5.5

SFE 16, 17, 18

Genus: *Wallodinium* Loeblich and Loeblich 1968

Generic Synopsis: Stover and Evitt 1978, p. 87.

Type Species: *Wallodinium glaessneri* (Cookson and Eisenack 1960) Loeblich and Loeblich 1968.

Wallodinium anglicum (Cookson and Hughes 1964)
Lentin and Williams 1973
Pl. 23, Fig. 1

1964 *Diplotesta anglicum* Cookson and Eisenack, p. 56, pl. 11, figs 1-5.

1973 *Wallodinium anglicum* (Cookson and Hughes) Lentin and Williams, p. 140.

Original Description: Cookson and Hughes 1964, p. 56, pl. 11, figs 1-5.

Holotype: Cookson and Hughes 1964, pl. 11, fig. 2.

Original Dimensions:	Holotype	Range
Length	126µm	34 - 80µm
Breadth	44µm	29 - 44µm
Capsule length	52µm	25 - 54µm
Capsule breadth	24µm	17 - 23µm

Description: Large elongate lunate cavate cyst. This cyst is almost circumcavate but the endocyst touches the pericyst in the mid (?)ventral region. Large pericoel developed in the apical and antapical areas and a substantial one is developed in the (?)dorsal area. Dorsal and ventral sides of the cyst cannot be confidently assigned as there is no indication of paratabulation. Endocyst is an elongate lozenge shape and is much smaller than the pericyst, with one straight side on the (?)ventral side where it is in contact with the pericyst. Both apical and antapical areas of the endocyst are rounded and the (?)dorsal side is strongly concave. Periphragm is shagreenate to scabrate. The apex always possesses an archaeopyle. The antapex tapers distally to a narrow blunt point. Both dorsal and ventral sides of the pericyst are concave, the (?)dorsal side being more strongly concave. An archaeopyle, probably apical is developed in all cysts, but its exact type is uncertain. Archaeopyle loss leaves the apex of the cyst with a curious arcuate, gently curved margin. Operculum is free.

Dimensions:				
	Length of pericyst	90	(100.3)	112µm
	Breadth of pericyst	35	(44.4)	57µm
	Length of endocyst	54	(68.3)	92µm
	Breadth of pericyst	22	(35.5)	57µm
	Number of specimens measured	10		

Known stratigraphic range: Late Albian to Early Cenomanian

Occurrence:

Site 3A 70

TBB -3, 15

MCB -2.5 --> -2, -1 --> -0.5, 1 --> 1.5

SFE no occurrence

Genus: *Xiphophoridium* Sarjeant 1966

Generic Synopsis: Stover and Evitt 1978, p. 88.

Junior Synonym: *Pyramidinium* Clarke and Verdier 1967

Type Species: *Xiphophoridium alatum* (Cookson and Eisenack 1962) Sarjeant 1966

Xiphophoridium alatum (Cookson and Eisenack 1962) Sarjeant 1966

Pl. 23, Figs 3, 4

1962 *Hystrichodinium alatum* Cookson and Eisenack, p. 487, pl.2, figs 1-4.

1966 *Xiphophoridium alatum* (Cookson and Eisenack) Sarjeant, p. 147, pl. 16, fig. 11.

1967 *"Pyramidinium alatum"* (Cookson and Eisenack) Clarke and Verdier, p. 40.

1968 *Xiphophoridium alatum* (Cookson and Eisenack) Sarjeant, Clarke *et al.*, p. 182.

1981 *"Oodnadattia alata"* (Cookson and Eisenack) Below, p. 107.

Original Description: Cookson and Eisenack 1962 p. 487, pl. 2, figs 1-4.

Holotype: Cookson and Eisenack 1962, pl. 2, fig. 1.

Original Dimensions:

	Holotype	Range
Overall length	125µm	100 - 120µm
Overall breadth	96µm	92 - 100µm
Shell	ca.70 x 52µm	

Description: Large sub-polygonal proximochorate pterate cyst, with highly developed parasutural septa. Autophragm only present. When seen in apical-antapical view the cyst appears almost circular in outline due to the presence of the paracingular circumferential sutural flange. Central body is angular to polygonal in shape and it possesses strong shoulders in the epicyst and corners in the hypocyst. Epicyst and hypocyst are almost equal in size. The cyst is divided transversely in two by a weakly helicoid laevorotatory paracingulum. The paracingulum is marked by a depression bounded by parasutural crests on both sides. Parasulcus is not expressed. There is a diagnostic development of the parasutural septa into high relief crests which carry acuminate processes or spines distally. The distal margin of these septa thus have a frayed 'fringe-like' appearance.

These parasutural flanges denote the paratabulation pattern of 4', 1a, 6", ?c, 6"', ?1p, 1"", 0s. Intratabular areas are ornamented with irregularly distributed tubules (Pl. 23, Fig. 3). Apical archaeopyle is present, Type $\overline{tA}$, leaving the cyst with a slightly zig-zag margin. There is possibly also a parasulcal notch. Operculum is free.

Dimensions:	Overall length (including parasutural septa)	70	(82.4)	100µm
	Overall width (")	70	(81.8)	95µm
	Length of central body	40	(47.2)	58µm
	Width of central body	40	(47.7)	60µm
	Maximum length of processes	15	(21.5)	28µm
	Number of specimens measured	20		

Known stratigraphic range: Albian to Cenomanian

Occurrence:

Site 3A 0 to 60, 80, 85, 95 to 120

TBB -3 to 0, 2, 3, 5 to 15

MCB -4.5 --> -4 to -2.5 --> -2, -1.5 --> -1, 0 --> 0.5 to 5 --> 5.5

SFE 17, 18

Xiphophoridium sp. A

Pl. 23, Figs 5-7

Description: Very large sub-polygonal proximochorate pterate cyst, which has strongly developed parasutural crests. This cyst is typically broader than long. When seen in apical - antapical view the cyst is circular to sub-circular in outline (Pl. 23, Fig. 5). Central body is angular in shape as it possesses strong shoulders and corners to the epicyst and hypocyst respectively. Epicyst and hypocyst are almost equal in size. Autophragm only present and it is densely granular, giving the cyst a very dark brown colour. Parasutural crests are highly developed and are high relief features with wavey to entire distal margins. Unlike *X. alatum*, they are not produced distally into spines. The paracingular parasutural crests are the most strongly developed ones on the cyst. The parasulcus is not indicated. However, in apical-antapical view there is an area of indentation of the circumferential parasutural crests, which may denote the position of the parasulcus. The crests denote the position of the paraplates in the pre- and post-cingular areas. The inferred paratabulation pattern is ?', 6", 6c, 6"', ?1"". Archaeopyle type is uncertain.

Dimensions:	Length of central body	58 (65)	70μm
	Breadth of central body	70 (75.5)	80μm
	Maximum height of crest	12 (15.3)	18μm
	Number of specimens measured	10	

Occurrence:

Site 3A 5, 10, 30, 45, 55, 60, 100

TBB 4, 6 to 8

MCB -2 --> -1.5, 0.5 --> 1 to 2 --> 2.5, 3.5 --> 4, 4 --> 4.5, 5 --> 5.5

SFE no occurrence

Family PERIDINIACEAE Ehrenberg 1832

Genus: *Epelidosphaeridia* Davey 1969a

Generic Synopsis: Stover and Evitt 1978, p. 46.

Type Species: *Epelidosphaeridia spinosa* (Cookson and Hughes 1964) Davey 1969a

Epelidosphaeridia spinosa (Cookson and Hughes 1964) Davey 1969a

Pl. 7, Figs 7, 8

1964 *Palaeoperidinium spinosum* Cookson and Hughes, p. 49, pl. 8, figs 6-8.

1969a *Epelidosphaeridia spinosa* (Cookson and Hughes) Davey, p. 143, pl. 3, figs 10-12.

Original Description: Cookson and Hughes 1964, p. 49, pl. 8, figs 6-8.

Holotype: Cookson and Hughes 1964, pl. 8, fig. 8.

Original Dimensions:

	Holotype	Range
Overall length	55µm	55 - 67µm
Overall breadth	46µm	38 - 50µm

Description: Medium-sized sub-polygonal proximochorate cyst. The epicyst has a slight apical projection, which is conical in shape and pointed. The hypocyst possesses a slight projection on the left side of the cyst, giving it an asymmetrical appearance. Periphragm is ornamented by short spines, which taper distally either to a blunt or capitate or buccinate top. The paracingulum is indicated by a distinct pair of raised parasutural lines of spines. The parasulcal area is denoted by a paucity of spines in the mid-ventral area. Paratabulation pattern is implied by grouping or alignment of the spines, but a clear paratabulation pattern is not clearly defined. An apical archaeopyle is present but its exact type is uncertain as intercalary paraplates may, or may-not, be involved. Operculum is free.

Remarks: *Epelidosphaeridia spinosa* is nearly always found having lost its archaeopyle. Indeed complete specimens are only found in 10% of the *E. spinosa* cysts seen.

Dimensions:

Length of cyst from archaeopyle margin to base 38 (43.7) 52µm

Length of cyst with archaeopyle intact	64 (65)	66µm
Paracingular width	34 (43)	56µm
Number of specimens measured	20	

Known stratigraphic range: Early Cenomanian

Occurrence:

Site 3A 0, 10, 40, 45, 55 to 85, 95 to 120

TBB all samples except 2

MCB all samples

SFE no occurrence

Genus: *Eurydinium* Stover and Evitt 1978.

Generic Synopsis: Stover and Evitt 1978, p. 104.

Type Species: *Eurydinium ingramii* (Cookson and Eisenack 1970) Stover and Evitt 1978.

Eurydinium saxoniensis Marshall and Batten 1988

Pl. 8, Figs 1, 2

1988 *Eurydinium saxoniensis* Marshall and Batten, p. 92, pl. 1, figs 10-12.

Original Description: Marshall and Batten 1988, p. 92, pl. 1, figs 10-12.

Holotype: Marshall and Batten 1988, pl. 1, figs 10, 11.

Original Dimensions:	
Pericyst length	52 - 66µm
Pericyst breadth	37 - 54µm
Endocyst length	34 - 55µm
Endocyst breadth	32 - 45µm

Description: Typically peridinoid, sub-polygonal to ovoidal shaped medium-sized proximochorate cyst. Pericyst and endocyst present, separated by a pericoel which is most developed at the apex and antapex. Pericyst has an apical horn and a pointed left antapical horn. Endocyst is rounded to sub-spherical and is without apical or antapical projections. Both periphragm and endophragm are smooth to scabrate and the endophragm is typically a dark brown. Folds are present, usually two longitudinal and one transverse, the latter indicating the paracingulum, but no other sign of paratabulation is seen. Archaeopyle is intercalary, formed by the loss of a large hexa 2a paraplate. Commonly the operculum is adnate along its posterior margin.

Remarks: Examples of *E. saxoniensis* herein show variation in shape from highly polygonal typically peridinoid to more ovoidal, less "pointed" shape. Also there is a considerable variation in size, see Dimensions below. *Eurydinium saxoniensis* may be confused with *Isabelidinium acuminatum* (Cookson and Eisenack 1958) Stover and Evitt 1978 and with *Subtilisphaera pontis-marie* (Deflandre 1936b) Lentin and Williams 1976. However *E. saxoniensis* is easily distinguished by its larger size and the presence of a distinct paracingulum.

Dimensions:

Length of pericyst	56	(64.2)	72μm
Length of endocyst	45	(53)	61μm
Breadth of pericyst	42	(50.1)	60μm
Breadth of endocyst	41	(46)	53μm
Number of specimens measured	20		

Known stratigraphic range: Late Cenomanian to Early Turonian

Occurrence:

Site 3A no occurrence

TBB no occurrence

MCB no occurrence

SFE 15, 16, 17, 18

Genus: *Isabelidinium* Lentin and Williams 1977

Generic Synopsis: Stover and Evitt 1978, p. 108.

Type Species: *Isabelidinium korojonense* (Cookson and Eisenack 1958) Lentin and Williams 1977.

Nomen substitum: *Isabelia* Lentin and Williams 1976

Isabelidinium acuminatum (Cookson and Eisenack 1958)
Stover and Evitt 1978
Pl. 10, Fig. 9

1958 *Deflandrea acuminata* Cookson and Eisenack, p. 27, pl. 4, figs 5-8.

1976 *"Alterbia acuminata"* (Cookson and Eisenack) Lentin and Williams, p. 48.

1977 *"Senegalinium acuminatum"* (Cookson and Eisenack) Loeblich and Tappan. p. 368.

1978 *Isabelidinium acuminatum* (Cookson and Eisenack) Stover and Evitt, p. 109.

Original Description: Cookson and Eisenack 1958, p. 27, pl. 4, figs

5-8.

Holotype: Cookson and Eisenack 1958, pl. 4, fig. 5.

Original Dimensions:	Holotype	Range
Theca	85 x 62μm	66 - 99 x 52 - 62μm
Capsule	48 x 48μm	38 - 47 x 38 - 47μm

Description: Small circumcavate elongate to pentagonal proximate cyst. Epicyst has a narrow, conical, pointed apical horn and hypocyst has a left antapical pointed horn. Central body is sub-spherical to ovoidal in outline. It is in only slight contact with the outer pericyst at the paracingulum. Periphragm and endophragm are separated by a pericoel which is at its greatest extent in the apical and antapical areas. Periphragm and endophragm are both thin, smooth, transparent and are without any parasutural markings. Paracingulum is not usually indicated but may be indicated by a faint thickening. An intercalary archaeopyle, Type I or Ia is sometimes present. Operculum can be free or adnate.

Dimensions:		
	Length of pericyst	40 (47.6) 52μm
	Breadth of pericyst	32 (35.4) 40μm
	Length of endocyst	28 (29.6) 32μm
	Breadth of endocyst	28 (31) 36μm

Number of specimens measured 10

Known stratigraphic range: Cenomanian to Early Turonian

Occurrence:

Site 3A no occurrence

TBB no occurrence

MCB no occurrence

SFE 15, 16, 17, 18

Genus: *Palaeohystrichophora* Deflandre 1935; emend. Deflandre and Cookson 1955

Generic Synopsis: Stover and Evitt 1978, p. 234.

Type Species: *Palaeohystrichophora infusorioides* Deflandre 1935

Palaeohystrichophora infusorioides Deflandre 1935

Pl. 17, Figs 1-3

1935 *Palaeohystrichophora infusorioides* Deflandre, p. 230, pl. 8, fig. 4.

1936b *Palaeohystrichophora infusorioides* Deflandre, Deflandre, p.

186, pl. 9, figs 5-10.

1943 *Palaeohystrichophora pauciestosa* Deflandre, p. 507, text-fig. 26.

1970 *Palaeohystrichophora infusorioides* Deflandre, Davey, p. 346, pl. 3, fig. 2,6.

1979 *Palaeohystrichophora infusorioides* Deflandre, Harker. p.369, pls 1,2.

Original Description: Deflandre 1935, p. 230, pl. 8, fig. 4.

Holotype: Deflandre 1935, pl. 8, fig. 4 and Deflandre 1936b, pl. 9, fig. 7.

Original Dimensions: Not given with original description

Description: Medium sized bicavate, typically peridinoid shaped thin-walled cyst, with numerous non-tabular spines. Preservation of this cyst is typically as a dorso-ventral compression. Pericyst has one conical, pointed large apical horn and a pointed antapical area. Endocyst is sub-spherical to ellipsoidal. Maximum extension of the pericoel is in the apical and antapical areas. The periphragm and endophragm are in contact only in the paracingular area. Both periphragm and endophragm are smooth and diagnostically appear pale to transparent. Cyst carries short stiff spines, which form a point distally and are distributed randomly over the cyst. However, they are typically aligned along raised ridges either side of the paracingulum. The paracingulum is broad and straight and may also be indicated by a thickening or fold in this area. The parasulcus may occur as a gap or depression in the mid-paracingular area and it extends posteriorly onto the hypocyst. No other sign of paratabulation is seen. Spines may be concentrated together due to their high numbers, or may be very sparse and occur irregularly and sporadically over the cyst, with every gradation in between. When few spines are present they are usually concentrated at the apex and paracingular areas (Pl. 17, Fig. 3). Archaeopyle type is unknown, but it said to be precingular Davey (1970), or combination (intercalary + precingular) Harker (1979).

Discussion: The differentiation and recognition of the two species *P. infusorioides* and *P. pauciestosa* is very difficult indeed, and seems to be arbitrarily based on the number of spines.

Deflandre (1943) when he created the new species *P. pauciestosa* stated that it was characterised by "spine or bristles

reduced in number and situated in a restricted area either side of the paracingulum" and that "spines are apparently stiffer than those of *P. infusorioides*, which has hairs instead". Deflandre (1943) also indicated another uniquely diagnostic feature of *P. pauciestosa* and that was that the internal body did not touch the paracingulum. However, in his illustration in text-fig. 26, the endocyst is shown to touch the periphragm at one side of the paracingulum.

Davey (1970), when discussing *P. infusorioides* stated that "occasionally the inner body is thicker and the spines less numerous". He accepted that "the reduced number of spines is reminiscent of *P. pauciestosa*, but in this latter species the spines are stiff and the inner body is not in contact with the outer membrane". Stover and Evitt (1978) believed *P. pauciestosa* to be an accepted species of *Palaeohystrichophora* but that it "probably falls within the range of variability for *P. infusorioides*".

Clearly there is some confusion with speciation based subjectively on the abundance or scarcity of spines; all other characteristics are the same, including the process morphology.

I believe that there is a morphological continuum between *P. pauciestosa* and *P. infusorioides* whereby the process number is scarce for the former and much more numerous for the latter, with every gradation in between. To differentiate between *P. infusorioides and P. pauciestosa* is impossible as it is too subjectively based. Hence, I would favour the same conclusion of Stover and Evitt (1978). That is, that *P. pauciestosa* should be included within the variability exhibited by *P. infusorioides*. Therefore, *P. pauciestosa* is a junior synonym of *P. infusorioides*.

Dimensions:		
	Length of pericyst	32 (40.2) 50µm
	Breadth of pericyst	26 (32) 44µm
	Length of endocyst	30 (31.8) 36µm
	Breadth of endocyst	4 (5.8) 8µm
	Number of specimens measured	20

Known stratigraphic range: ?Senonian

Occurrence:

Site 3A all samples

TBB all samples

MCB all samples

SFE 15, 16, 17

Genus: *Subtilisphaera* Jain and Millepied 1973;
emend Lentin and Williams 1976

Generic Synopsis: Stover and Evitt 1978, p. 238.

Type Species: *Subtilisphaera senegalensis* Jain and Millepied 1973.

Subtilisphaera pontis-mariae (Deflandre 1936b) Lentin and Williams 1976
Pl. 22, Fig. 1

1936b *Gymnodinium pontis-mariae* Deflandre, p. 167, p. 2, figs 7-9.
1966 *Ascodinium pontis-mariae* (Deflandre) Deflandre, p. 3.
1970 *Deflandrea pontis-mariae* (Deflandre) Davey, p. 341.
1975 *Subtilisphaera pontis-mariae* (Deflandre) Lentin and Williams, p. 119

Original Description: Deflandre 1936b, p. 167, pl. 2, figs 7-9.

Holotype: Deflandre 1936b, pl. 2, fig. 7.

Original Dimensions: Length 42 - 52μm
Breadth 24 - 26μm

Description: Medium sized, elongate to ovoidal, bicavate, proximate cyst with pericoels developed at the apex and antapex. Epicyst is somewhat bigger than the hypocyst. Endocyst is sub-spherical to ovoidal and is composed of finely granulate endophragm. Periphragm is smooth and transparent. Apical and antapical horns are present and the pericoel is at its largest extent in these areas. Both horns are sharply pointed and typically the antapical horn is asymmetrically positioned. The length of the horns varies between $^{1}/_{2}$ to $^{1}/_{3}$ the length of the endocyst. Paracingulum is indicated by a transverse indentation in the periphragm. No other form of paratabulation is present. No archaeopyle has been observed.

Dimensions:		
Length of pericyst	50 (64.2)	60μm
Length of endocyst	30 (30.9)	32μm
Breadth of cyst	28 (33)	36μm
Number of specimens measured	10	

Known stratigraphic range: ?Senonian

Occurrence:

Site 3A 60, 75, 115

TBB no occurrence

MCB no occurrence

SFE 16, 17, 18

Family CERATIACEAE Lindemann 1928

Genus: *Odontochitina* Deflandre 1935; emend Bint 1986

Generic Synopsis: Stover and Evitt 1978, p. 67.

Emended Description: Bint 1986, p. 138.

Type Species: *Odontochitina operculata* (O. Wetzel 1933a) Deflandre and Cookson 1955.

Odontochitina costata Alberti 1961; emend. Clarke and Verdier 1967

Pl. 15, Figs 1-3

1961 *Odontochitina costata* Alberti, p. 31, pl. 6, figs 10-13.

1962 *"Odontochitina striatoperforata"* Cookson and Eisenack, p. 490, pl. 3, figs 14-19.

1967 *Odontochitina costata* Alberti, emend. Clarke and Verdier, p. 58, pl. 13, figs 4-6.

Original Description: Alberti 1961, p. 31, pl. 6, figs 10-13.

Holotype: Alberti 1961, pl. 6, fig. 12.

Original Dimensions:

Total length	522µm
Length of inner body	88µm
Breadth of inner body	70µm
Length of apical projection	324µm
Length of antapical projections	103 & 110µm

Other processes show a total length of 480 - 620µm

Description: Large cornucavate typically ceratioid shaped cysts, with three long horns and an endocyst. Endocyst is spherical to sub-spherical in outline. Endophragm and periphragm present and separate at the horns to form a pericoel which is most pronounced in the antapical region. Both endophragm and periphragm are smooth and have an unornamented texture. Three horns are present; apical [237 (273.2) 375µm] which is the largest, an antapical horn [106 (117.8) 130µm] and the smallest right lateral horn [90 (108.1) 122µm]. The endocyst extends into the apical and right lateral horns where it may form a nipple-like projection just at the base of the horn. The apical horn is usually broad and has a blunt termination. The antapical and right lateral horns may end bluntly, but usually form a distal point. The surfaces of the horns have longitudinal ribs. Also a pylome may be present in the apical horn, typically in the middle

portion. Paratabulation is not expressed except for the apical archaeopyle, Type $\overline{tA}$ giving a slightly angular archaeopyle margin to the remaining cyst. Sulcal notch is off-set to the left on the ventral surface. Operculum is free and is regularly found occurring separately (Pl. 15, Fig. 2).

Remarks: The majority of *O. costata* cysts found were without their operculum. Very occasionally however, intact cysts were found with their archaeopyle still intact. These cysts are usually quite crumpled or squashed.

Dimensions:	Overall length (from archaeopyle margin to tip of AA horn)	152	(170.4)	185µm
	Length of endocyst	50	(59.1)	76µm
	Breadth of endocyst	56	(72.2)	90µm
	Length of apical horn	237	(273.2)	375µm
	Length of antapical horn	106	(117.8)	130µm
	Length of right lateral horn	90	(108.1)	122µm
	Number of specimens measured	20		

Known stratigraphic range: Cenomanian to Turonian

Occurrence:

Site 3A 0 to 10, 20 to 110, 120
TBB -2 to 2, 4, 5, 7 to 15
MCB all samples
SFE 16, 17

Odontochitina operculata (O. Wetzel 1933a) Deflandre and Cookson 1955
Pl. 15, Fig.4; Pl. 16, Figs 1,2

1933a *Ceratium* subgenus *Euceratium operculatum* O. Wetzel, p. 170, pl. 2, figs 21, 22; text-fig. 3.

1935 *"Odontochitina silicornum"* Deflandre, p. 234, pl. 9, figs 8-10.

1955 *Odontochitina operculata* Deflandre and Cookson, p. 291, pl. 3, figs 5, 6.

Original Description: O. Wetzel 1933a, p. 170, pl. 2, figs 21, 22; text-fig. 3.

Holotype: O. Wetzel 1833a, pl. 2, fig. 21.

Original Dimensions:

Specimen of pl. 2, figs 21, 22:

Whole body : 210 x 170 x 50µm

Middle body : 52 x 44 x 50µm

Suture cavity : 28μm diameter

Horns for example : 102, 88, and 51μm

Rugen specimen:

Length : 160μm

Width : 140μm

Middle body : 68μm

Horn length : 68μm

Description: Large, cornucavate, typically-ceratioid shaped cyst, with three long horns and a endocyst. Endocyst is sub-spherical and may be produced slightly into the antapical horn. Both endophragm and periphragm are smooth and unornamented. The pericoel is most noticeable at the base of the two hypocystal horns. Three horns are present, the largest being the apical one [110 (156.6) 190μm], with an intermediary-sized antapical horn [75 (94.2) 106μm], and a slightly smaller right lateral horn [70 (85) 100μm]. All horns are straight sided, unornamented and reach a distal point. No sign of paratabulation is present. An apical archaeopyle, Type $\overline{tA}$ is present. The resultant archaeopyle suture is slightly angular and a slight sulcal notch is present sometimes, which is offset to the left when seen in ventral orientation. Operculum is free and is regularly found occurring individually (Pl. 16, Fig. 2).

Remarks: There seems to be two distinct size groupings of *O. operculata* cysts seen. There is a larger group with length of cyst measured from the archaeopyle margin to the tip of the antapical horn ranging between 140 - (143.5) - 150μm. The smaller group ranges from 116 - (128) - 136μm. These two size groupings appear to be mutually exclusive, all other characteristics appear to be the same. Perhaps the smaller group appears more fragile than the more robust larger group. Also, neither size group appears to dominate numerically over the other. Similar size groupings have been observed by FitzPatrick (1990, *pers. comm.*) in Turonian specimens of *O. operculata* from south-east England.

Dimensions:

Length of cyst (from archaeopyle margin to tip of antapical horn)	116	(136.5)	150μm
Length of endocyst	40	(43.5)	50μm
Breadth of endocyst	40	(46.1)	52μm
Length of apical horn	110	(156.6)	190μm
Length of antapical horn	75	(94.2)	106μm

Length of right lateral horn	70	(85)	100μm
Number of specimens measured	20		

Known stratigraphic range: Senonian

Occurrence:

Site 3A all samples except 115

TBB all samples

MCB all samples

SFE all samples

Genus: *Xenascus* Cookson and Eisenack 1969; emend. Yun 1981

Generic Synopsis: Stover and Evitt 1978, p. 87.

Type Species: *Xenascus ceratioides* (Deflandre 1937) Lentin and Williams 1973.

Xenascus esbecklanus Yun 1981

Pl. 23, Fig. 2

1981 *Xenascus esbecklanus* Yun, p. 61, pl. 14, figs 2-4, 6.

Original Description: Yun 1981, p. 61, pl. 14, figs 2-4, 6.

Holotype: Yun 1981, pl. 14, fig. 3.

Original Dimensions:		
Length of central body	60 -	66μm
Length of cyst without archaeopyle	84 -	126μm
Breadth of cyst	80 -	88μm
Length of antapical horn	60 -	80μm
Length of lateral horn	50 -	54μm
Diameter of archaeopyle	56 -	60μm

Description: Large typically ceratioid-shaped cornucavate cyst, with three horns of unequal size and shape. Central body is sub-spherical to ovoidal. Periphragm and endophragm both granular. On the surface of the body are longitudinal ribs of thickened periphragm. Periphragm is developed into three horns; apical, antapical and lateral. The apical horn is never seen as all cysts observed were without their archaeopyle. The antapical horn is larger than the lateral one. Both taper distally to form a blunt point. No secondary spines are developed on these horns. At the base of these horns a pericoel is developed and is sometimes seen. An apical archaeopyle, Type $\overline{tA}$, leaving the cyst with a slightly angular archaeopyle margin. This is the only indication of paratabulation seen on the cyst. Operculum is always free and all cysts were without their archaeopyle.

Remarks: Specimens of this cyst species observed herein appear to be consistently smaller in all dimensions in comparison to the type material. Due to the rare occurrence of specimens of this species within the Cenomanian microplankton assemblages observed herein, it cannot be definitely stated that these occurrences are real. Therefore, an extension of the stratigraphic range of this species into the Cenomanian (see below) is not suggested.

Dimensions:			
	Length of central body	58 (60)	62µm
	Width of central body	55 (56.7)	58µm
	Width of cyst	68 (71)	75µm
	Length of antapical horn	53 (54.3)	56µm
	Length of lateral horn	42 (44.3)	47µm
	Number of specimens measured	5	

Known stratigraphic range: Early Santonian

Occurrence:

Site 3A 30, 65

TBB no occurrence

MCB -1 --> -0.5

SFE no occurrence

Cyst Type A

Pl. 24, Figs 1-3

1988 ?Cyst form A Marshall and Batten, p. 94, pl. 1, fig. 13.

Description: Medium sized proximate cyst with densely granulate surface. Cyst is ovoidal to sub-ellipsoidal is always longer than it is broad and is devoid of apical or antapical features. Paratabulation is not indicated. Densely granulate to verrucate autophragm, with longitudinal folds. There are usually two longitudinal folds on the right and left side of the cyst, which extend more or less from the apex to the antapex. Occasionally one or two transverse folds are present, but do not coincide with the paracingulum. No archaeopyle is observed. However, this may be the endocyst of a proximate dinoflagellate cyst which has lost its outer pericyst, perhaps due to mechanical degradation.

Remarks: In broad morphological terms, together with the granulate ornament, Cyst Type A resembles *Canningia colliveri*. However, this species does not have an apical archaeopyle like that of *C. colliveri*. Cyst Type A also is similar to Cyst form A Marshall and Batten (1988), due to the latter's granulate to bacculate ornamentation. However, Cyst form A of Marshall and Batten (1988) has two wall layers and is circumcavate.

Dimensions:			
	Length of cyst	50 (54.2)	60µm
	Breadth of cyst	40 (45)	50µm
	Number of specimens measured	10	

Occurrence:

Site 3A no occurrence

TBB no occurrence

MCB no occurrence

SFE 15, 16, 17, 18

? Cyst Type B

Pl. 23, Figs 4-6

Description: This is questionably included as a dinoflagellate cyst. It is a medium sized longer than broad, sub-spherical proximate cyst. Autophragm only present, which is typically dark brown and is produced

into large ?bulbous processes. These ?processes are non-tabular. Typical mode of preservation is as an apical-antapical compression. No indication of paratabulation is present. Archaeopyle is formed in the apical region and is therefore presumed to be apical, but its exact type is uncertain. Operculum is free. Specimens are always found without their archaeopyle.

Dimensions:	Length of cyst	50µm (only one specimen)
	Breadth of cyst	38 (47) 56µm
	Number of specimens measured	10

Occurrence:

Site 3A no occurrence

TBB no occurrence

MCB no occurrence

SFE 16, 17, 18

Chapter 6

PREVIOUS PALYNOLOGICAL RESEARCH ON THE CENOMANIAN OF ENGLAND

6.1. Introduction

As the geological sections studied are from England, the previous palynological analyses which proved most useful for comparison were those concerned with the microplankton assemblages of the Anglo-Paris Basin. A brief summary of these now follows, firstly those specifically dealing with the English Upper Cretaceous followed by those on the French Upper Cretaceous deposits of the Anglo-Paris Basin. Finally, there is an account of the most up-to-date biostratigraphical information available based on dinoflagellate cysts.

6.2. Palynological research on the English Upper Cretaceous deposits of the Anglo-Paris Basin

Observations on the microplankton assemblages of the Upper Cretaceous chalks of Britain were first made by a group of amateur geologists/microscopists, several of which have been honoured by more recent workers naming new species after them. Many of these pioneering workers examined specimens of dinoflagellate cysts which were embedded in flints. The first of these, the Rev. Reade (1839), looked at Upper Cretaceous flints and was the first to describe and figure dinoflagellates in English flints. In three successive papers Bowerbank (1841a; 1841b; 1841c) documented the presence of dinoflagellates in the Chalk of England and was the first to record their presence in the Upper Greensand. White (1842) gave very detailed descriptions and measurements of several new dinoflagellate and acritarch species in flints from England (Sarjeant, 1991) and in 1849 Dean recorded dinoflagellates from the Chalk near Dover. Mantell in the mid-nineteenth century (1845, 1850) made further detailed descriptions of dinoflagellate assemblages from the Chalk of England and, finally, Wilkinson (1849) made observations and descriptions of two species of dinoflagellate from Upper Cretaceous flints from England.

After this preliminary work, Cookson and Hughes (1964) were the first to undertake a comprehensive investigation into the

microplankton assemblages of the Chalk of the Anglo-Paris Basin. Their work investigated the Cambridge Greensand from which eight new species of dinoflagellate cysts were identified and several other, previously known species were recorded for the first time in Europe, and detailed stratigraphical information was included. This paper also included the first photomicrographs of the microplankton observed.

Davey *et al.* (1966) in their "Studies on Mesozoic and Cainozoic dinoflagellate cysts" gave comprehensive and detailed systematic and biostratigraphical accounts of the dinoflagellate cyst assemblages of the Cretaceous and Eocene of England. Many new genera and species were described and several new emendations to existing genera and species were included as well as some generic transfers of species. Detailed morphological descriptions were made of all the above taxa using new morphological terms. Also, emphasis was placed on the broad morphological groupings of dinoflagellate cysts into cavate, proximate and chorate groups, with some interpretation as to their different modes of formation. Detailed information on the stratigraphical occurrence of all dinoflagellate species described was included and thus, the great potential of the use of dinoflagellate cysts as stratigraphical markers was first properly realised.

The microplankton assemblages of the Cenomanian to Campanian deposits of the Isle of Wight were investigated by Clarke and Verdier (1967). Four new genera and twenty-one new species were erected and described. The first sub-division of the Cenomanian to Campanian interval was proposed based on the dinoflagellate cyst assemblages. Two stratigraphical subdivisional schemes were suggested, one which divided this time period into five zones with five subsequent subzones and the second which was based on seven stratigraphical 'intervals'. The use of these stratigraphical schemes was postulated to have basin-wide potential.

Davey (1969a, 1970) concentrated on the Cenomanian microplankton assemblages of England and northern France, with comparisons made to those of North America. Seven new genera, thirty-five new species and varieties were described. Additional detailed information as to the biostratigraphical potential of dinoflagellate cysts was given and their use in intra- and inter-regional stratigraphical correlations was first suggested.

Davey (1970) stated that the Cenomanian constituted a single zone and he named it the *Litosphaeridium siphonophorum* Zone, as this species was found to occur distinctively within the Cenomanian. The commencement of the Cenomanian was signaled by the first appearance of *Palaeohystrichophora infusorioides* Deflandre 1935 and its termination by the disappearance of *Cleistosphaeridium huguoniotii* (Valensi) Davey 1969a. He also divided the Cenomanian into three subzones, all of which are named after their distinctive dinoflagellate cyst species. The lower subzone, the *Dinopterygium perforatum* subzone (now *Maghrebinia perforata* (Clarke and Verdier) Below 1981) which Davey (1970) regarded as not having as wide an application as the other two subzones, is characterised by this cyst, but other distinctive species of this zone are *Rhiptocorys veligera* (Deflandre) Lejeune-Carpentier and Sarjeant 1983, *Canningia reticulata* Cookson and Eisenack; emend. Helby 1987 and *Pterodinium cingulatum* subspecies *granulatum* (Clarke and Verdier) Lentin and Williams 1981. The *Epelidosphaeridia spinosa* subzone is the Middle Cenomanian subzone and its boundaries are defined as follows. The base is indicated by the first appearance of *"Hystrichosphaeridium crassimurata"* (*Pterodinium cingulatum* subspecies *polygonalis* herein) and its top by the last appearance of *Epelidosphaeridia spinosa* (Cookson and Hughes) Davey 1969a. The *Cleistosphaeridium huguoniotii* subzone is the uppermost subzone and the top of this subzone, which coincides with the top of the Cenomanian, is marked by the disappearance of six distinctive dinoflagellate cyst species, most notable of which are *C. huguoniotii, L. siphonophorum* (Cookson and Eisenack) Davey and Williams 1966b; emend. Lucas-Clark 1984 and *Microdinioum setosum* Sarjeant 1966; emend. Below 1987.

Davey and Verdier (1976), during their study of Cretaceous sediments of eastern England and northern France, erected one new genus and five new species of dinoflagellate cyst, the ranges of which have stratigraphical significance.

Marshall (1983), in his Ph.D. thesis documented the dinoflagellate cyst assemblages of selected Cenomanian-Coniacian sections of England and northern Germany. He described five new species and gave informal descriptions of other species belonging to a further six genera. As part of this study, Marshall (1983) investigated the dinoflagellate cyst assemblages of some "black shale"

sequences of England (South Ferriby) and Germany (Helgoland, Misburg and Wunstorf), where he recognised two dinoflagellate cyst associations. One of these associations is jointly characterised by one of his new species, *Eurydinium saxoniensis* Marshall and Batten, 1988 and another new species *Litosphaeridium chlidanum* Marshall, 1983 is only found occurring within these "black shale" sequences. Marshall (1983) postulated that the two identified dinoflagellate associations appear to characterise restricted, possibly anoxic, marine conditions.

As a follow-up to the work of Marshall (1983), Marshall and Batten (1988) formally described and documented the two dinoflagellate cyst associations of the Cenomanian-Turonian "black shale" sequences of northern Europe, first recognised by Marshall (1983).

Tocher, together with other workers, has carried out detailed investigations into the biostratigraphy and other significant aspects of the Cenomanian-Turonian boundary sequence of southern England (Tocher and Jarvis, 1987; Jarvis *et al.*, 1987; Jarvis *et al.*, 1988a; Jarvis *et al.*, 1988b; Leary *et al.*, 1989). A palynostratigraphy of the Cenomanian-Turonian sequence is formulated as part of an integrated group of analyses (micropalaeontology, sedimentology, geochemistry, stable isotopes), and an interpretation into its formation is made in relation to the $\delta^{13}C$ excursion and the oceanic anoxic event which characterises the Cenomanian-Turonian boundary sequence of north-west Europe.

6.3. Palynological research on the French Upper Cretaceous deposits of the Anglo-Paris Basin

Investigations specifically into the French Cenomanian deposits of the Anglo-Paris Basin began with Deflandre (1936b, 1937). He investigated the microfossils of the Upper Cretaceous and made detailed descriptions of several dinoflagellate cyst and acritarch species, many of which he described for the first time. Firtion (1952) was the first to document the palynological content of the Upper Cretaceous of the northern part of France.

Davey and Verdier (1973) examined the Albian and basal Cenomanian deposits of France and Switzerland. The dinoflagellate stratigraphy of the Albian-Cenomanian boundary was documented and comparisons were made between this work and previous analyses of

coeval deposits.

The microplankton assemblages of the Aptian to Cenomanian of the Wissant section in northern France were investigated by Verdier (1975). This section was a crucial one as it covered a gap in the dinoflagellate record. Verdier (1975) proposed a dinoflagellate cyst stratigraphy of the mid-Cretaceous and compared it to the corresponding ammonite and foraminiferal biostratigraphies.

Fauconnier (1975) also studied the Cenomanian deposits of the Wissant section in conjunction with Albian sections elsewhere in the Anglo-Paris Basin. She documented for the first time that the distribution of some of the peridinacean dinoflagellate cysts found, was linked to the sedimentological nature of the deposits.

In her doctoral thesis, Fauconnier (1977) investigated the the stratigraphical range of the dinoflagellate cysts of the Albian and Lower Cenomanian of the Paris Basin and identified links between the phytoplankton and sedimentological characteristics. On the basis of the dinoflagellate cyst assemblages, she erected a palynostratigraphy for the basin. Fauconnier (1977) developed the theory (Fauconnier, 1975) that dinoflagellate richness seemed to be related to the lithology and total organic content of the sediment. She suggested there was a possible link between dinoflagellate cyst abundance and the presence of phosphate and glauconite.

Foucher (1979, 1980, 1981, 1983) together with other authors (Foucher and Taugourdeau, 1975) carried out comprehensive investigations into both the morphological descriptions and biostratigraphical distributions of the microplankton assemblages of the French Cenomanian deposits of the Anglo-Paris Basin.

Foucher and Taugourdeau (1975) carried out preliminary analysis into the dinoflagellate cyst assemblages of the Upper Albian to Cenomanian of the northern part of the Paris basin.

Foucher (1979) investigated the stratigraphical distribution of the microplankton assemblages of the Upper Cretaceous deposits of the Anglo-Paris Basin and northern Europe. Within this analysis there was a brief discussion of the Cenomanian dinoflagellate cyst assemblages.

In 1980 Foucher, together with other workers, made a detailed examination of the Aptian to Santonian biostratigraphy of the Boulonnais area, based on both macro- and microfossils. Analysis of

the microplankton assemblages enabled the division of this interval into eight dinoflagellate zones, which are characterised by the occurrence of particular dinoflagellate cysts species.

The dinoflagellate cyst biostratigraphy of Albian to Turonian deposits of the Boreal realm of Europe was suggested by Foucher (1981). This time interval was divided into six dinoflagellate interval zones, and they were correlated with the equivalent ammonite biostratigraphy. One of these zones, the *Litosphaeridium siphonophorum* Interval Zone characterises the Cenomanian. Also, the significant revival of dinoflagellate cysts in the Late Albian was recorded.

Foucher (1983) carried-out a review of all the known dinoflagellate cyst stratigraphies of the Middle and Late Cretaceous of the Anglo-Paris Basin. He indicated that a stratigraphical scheme such as this based on dinoflagellate cyst assemblages was particularly useful for dating and correlation within the same basin. Also mentioned was the potential use of dinoflagellate cysts in palaeogeographical reconstructions.

6.4. Summary of dinoflagellate cyst biostratigraphy for western Europe and worldwide for the Late Cretaceous

Harker and Sarjeant (1975) compiled and critically assessed all biostratigraphical information available prior to 1974 which was based on organic walled dinoflagellate cysts of Cretaceous and Tertiary age worldwide. Based on this information, they presented reliable stratigraphical ranges of taxa to formation and stage level within both the Cretaceous and Tertiary. Such stratigraphical ranges were presented under different geographical headings such as Europe, North America, Australasia and worldwide and within the following morphological groupings; proximate, proximo-chorate, chorate and cavate.

In a recent publication, Costa and Davey (1992) reviewed Cretaceous biostratigraphy of western Europe based on dinoflagellate cyst assemblages. Costa and Davey (1992) stated that within the Mesozoic, the Cenomanian dinoflagellate cyst assemblages are among the richest and most diverse. The dinoflagellate cyst assemblages of the Lower and Middle Cenomanian are remarkably uniform within this area of western Europe. However, by the Upper Cenomanian, more marked

composition differences are apparent between the assemblages of the Chalk Province and those of the Shetland Group of the northern North Sea. Within the Upper Cenomanian, the Shetland group assemblages are dominated by the deflandreoid dinoflagellate cysts, whereas this group of dinoflagellate cysts are uncommon in the Chalk Group assemblages.

Costa and Davey (1992) documented some biostratigraphically significant dinoflagellate cyst species from the Cenomanian of western Europe. *Epelidosphaeridia spinosa* and *Endoceratium dettmanniae* (Cookson and Hughes) Stover and Evitt (1978) (both of which first occur in the Late Albian) are typically present in the Early, Middle and Late Cenomanian. *Litosphaeridium siphonophorum* which also has its first occurrence in the Late Albian, continues through-out and to the top of the Cenomanian or Early Turonian. Costa and Davey (1992) note that the first occurrence of *P. infusorioides* is often regarded as indicating the base of the Cenomanian, however, they documented that this species is sometimes difficult to differentiate from another specimen of similar morphological form which occurs in the latest Albian. Dinoflagellate cysts which do not range above the Cenomanian-Turonian boundary include *Apteodinium granulatum* Eisenack 1958; emend Sarjeant 1985, *C. huguoniotii, Cribroperidinium exilicristatum* (Davey) Stover and Evitt 1978, *Cribroperidinium edwardsii* (Cookson and Eisenack) Davey 1969a and *Gonyaulacysta cassidata* (Eisenack and Cookson) Sarjeant 1966. Taxa which first appear within the Cenomanian are as follows, *Heterosphaeridium ? heteracanthum* (Deflandre and Cookson) Eisenack and Kjellström 1971, *Isabelidinium magnum* (Davey) Stover and Evitt 1978, *Palaeoperidinium pyrophorum* (Ehrenberg) Sarjeant 1967b, *Trithyrodinium suspectum* (Manum and Cookson) Davey 1969b and the genus *Chatangiella* Vozzhennikova 1967; emend Lentin and Williams 1976.

Chapter 7

STATISTICAL ANALYSIS

7.1. Introduction

As outlined previously within the Material and Methods chapter, samples were prepared for both qualitative and quantitative purposes. Statistically precise interpretations may then be made from analysis of the aliquot slides. The strewn mount slide is made from an exact and known quantity of residue which is itself produced from an exact and known quantity of bulk rock. The resultant residue, from which the slides are made, is suspended within the same quantity of water for each sample. Therefore, even on a strewn mount slide real results on presence/absence, numbers present, abundance and diversity are produced and can be compared and contrasted with other samples and data sets from other sections, as all samples have been subjected to the same, stringent, quantitative preparation conditions. Also, to avoid the introduction of bias by any microscopy sampling procedure, logging counts of at least 300 individual palynomorphs are made on each slide. The raw data produced from such counts are given in Appendices 1-4. Within palynological and micropalaeontological analysis this figure of 250-300 has been shown statistically (Buzas, 1979) to produce a representative population which confidently replicates the natural population of which it is a sub-sample. All subsequent interpretations herein, statistical and otherwise, are based on this statistically representative population of 300 palynomorphs. Some statistical techniques may be biased if no account has been taken of sample size whether it be that of the original bulk rock, amount of residue used or number of counted palynomorphs on a slide. Thus, such bias introduced by sampling is effectively eliminated in this study.

Various statistical methods were applied to the raw data produced from standard logging of strewn mount slides from each studied section. However, because of the enormity of the data sets produced in this way, certain inherent features and trends, etc. can remain hidden unless statistical techniques are applied. A brief description of the statistical techniques employed for the data herein is as follows. Where possible, use of available customised

statistical packages was made, eg. SPSS® (Statistical Package for Social Scientists), but the majority of the statistical programmes were written by others specifically for this project.

7.1.1. Diversity

Diversity takes two factors into account: species richness or overall richness; that is the number of species present and, secondly, the relative abundance of those species, known as evenness or equitability (Magurran, 1988). There are numerous methods of measuring diversity, but overall richness (S) is the most widely applied diversity index (Magurran, 1988). Herein information on this measurement of diversity based on overall richness (S) is given in different forms as follows. Number of species of dinoflagellate cysts is a calculation based on those cysts recorded from the logged portion of the strewn mount slide (300 count) plus those new species recorded outside this count. Those recorded outside the count are only noted on a presence basis, ie there is no information on their proportional presence. Also, information on the total number of palynomorphs present on the slide as a whole is included based on number of dinoflagellate species present as outlined above, plus number of individuals recorded from the following groups; spores, bisaccate pollen, *Veryhachium* spp., *Michrystridium* spp., *Pterospermopsis* spp. and *Tasmanites* spp. Diversity information on both these groupings (dinoflagellate cyst species and palynomorph types) is given in the format of minimum, mean (indicated in brackets) and maximum values.

The Shannon Index, H', is an index based on the proportional abundance of species and thus combines richness and evenness into a single figure (Magurran, 1988). It is widely recommended to be the most successful diversity index within palynological and micropalaeontological analysis Ramsbottom (1987, *pers.comm.*). Shannon and Wiener independently derived the function (Magurran, 1988) which is now known as the Shannon Index H':

$$H' = -\sum p_i \ln p_i$$

H': Shannon Index

p_i: Proportion of ith species, defined as $p_i = \frac{n_i}{N}$

n_i: Number of individual species in the ith species

The Shannon Index assumes that individuals are randomly sampled from an "indefinitely large" ie. effectively infinite population (Pielou, 1975). The index measures relative diversity but it is also linked to species abundance as it takes into account the evenness of the abundance of species (Peet, 1974). H' values are usually between 1.5 and 3.5 and only rarely exceed 4.5 (Margalef, 1972). This index is known to be sensitive to large variations in sample size (Kempton, 1979) however, this is not an issue herein as sample sizes, as explained below are more or less consistent through-out.

Shannon Index (H') calculations are carried out on the data sets produced from logged counts of 300, plus all new palynomorphs recorded after these counts as outlined previously in description of overall richness (S) calculations.

7.1.2. Cluster analysis, Dice co-efficient

Cluster analysis is a method applied in the interpretation of complex multivariate data such as that presented by the analysis herein. Similarity co-efficients, on which cluster analysis is based, measure degrees of similarity between organisms (R-mode) or between sample assemblages (Q-mode), based on various parameters. The R-mode of cluster analysis has been carried out on palynological data by various workers such as Goodman (1979) and Harker *et al.* (1990) and has been very successful in the identification of dinoflagellate cyst associations which also have palaeoenvironmental significance. However, herein the Q-mode of cluster analysis, based on the Dice Co-efficient (D) is applied to the palynological data due to the nature of the sections studied, as recommended by Ramsbottom (1987, *pers. comm.*).

$$D = \frac{2C}{N_1 + N_2}$$

D: Dice Co-efficient

C: Number of taxa present in both units compared

N_1: Number of taxa present in first unit

N_2: Number of taxa present in second unit

The Dice Co-efficient emphasises similarity between samples but also takes differences into account. A dendrogram can be constructed from the co-efficient matrices, which gives a graphic representation of similarity/dissimilarity between samples within a section's data set.

Cluster analysis calculations are based on the data sets produced by the 300 count plus all new palynomorphs recorded outside the count, as outlined before in the section dealing with overall richness.

7.1.3. Fourier analysis

Fourier analysis is a type of spectral analysis. A detailed account of Fourier theory is not included as such information is given by Lighthill (1958) and Hatton *et al.* (1986). Briefly, however, Fourier theory states that any periodic waveform may be split up into a series of sine (or cosine) waves whose frequencies are integer multiples of the basic repetition frequency ($^1/_T$), known as the Fundamental frequency. Also, as well as defining the frequency of each component, it is possible to define its phase and amplitude. Thus, Fourier analysis is very useful in identifying and quantifying cyclicity or rhythmicity within a data set. Fourier analysis can confidently identify cycles or rhythms of differing frequency occurring in a data set.

A periodic waveform or time series can be expressed in both the time domain, which expresses the wave amplitude as a function of time, and the frequency domain, expressing the amplitude and phase of its constituent sine waves as a function of the frequency.

The specific method of Fourier analysis employed herein is that of the Fast Fourier Transform (FFT) algorithm (Brigham, 1974), which converts a time function $q(t)$ into its equivalent amplitude $A(f)$ and phase $\phi(f)$ spectra, or into a complex function of frequency $G(f)$, known as the Frequency spectrum.

$$G(f) = A(f)e^{i\phi(f)}$$

When dealing with spectral analysis of any type, the Nyquist frequency (f_N) must be calculated which is based on the sampling interval value. The Nyquist frequency delimits statistically

significant trends calculated by the Fourier algorithm, as only those with a frequency greater than or equal to the Nyquist frequency are real (Press *et al.*, 1986).

$$f_N = {}^1/_2\ \Delta t$$

f_N: Nyquist frequency

Δt: Sampling interval

The FFT algorithm was performed only on one section within this study (Site 3a), as this is the only data set under investigation for the identification of cyclicity. For this purpose, palynological data based on the 300 count were collated and calculated into several different groupings. The first group of data is that of percentage occurrences of individual dinoflagellate cyst species and the second is a group of data sets of dinoflagellate cyst morphogroups, see Chapter 8 for more details.

7.1.4. Autocorrelation

The autocorrelation function measures the degree of similarity between a time series or data set and a shifted copy of itself as a function of that shift. This feature is very useful in identifying cyclicity or rhythmicity within the data set. The discrete autocorrelation (r_k) of a data set (x_t) is assumed to have zero mean and is defined as follows:

$$r_k\ (x) = \frac{1}{N} \sum_{t=0}^{N-k-1} \bar{x}_t .\ x_{t+k}$$

N: Number of samples from k = 0, 1,....., N - 1

$\bar{x}$: The complex conjugate

k: The lag

However, there are certain limitations in the use of autocorrelation for the identification of cycles or rhythms within a data set. Autocorrelation of data sets containing too few samples causes inconclusive and ambiguous results, where much can be interpreted that is not statistically significant, Hatton *et al.*, (1986). Also, although autocorrelation can identify cyclicity or periodicity within a data set, it cannot determine if cycles of

differing frequency are present or whether they are occurring due to the multiple effect. For example, if autocorrelation identifies cyclicities of 10, 20 and 40 cm. within a data set, the latter two may have resulted from the multiple effect of the former.

Autocorrelation is carried out on the same groupings of data as indicated in the section on FFT.

Statistical Results

7.2. Site 3a section

7.2.1. Diversity

S - Overall richness

Overall richness varies quite considerably within this section. The number of dinoflagellate cyst species ranges from 39 (52.2) to 66 and the number of total number of palynomorphs ranges from 42 (54.96) to 70 (Figure 7.1). These variations are not linked to lithology as values of dinoflagellate cyst species diversity and total palynomorph diversity are very similar for both lithologies; chalks, 39 (52.31) 66 and 42 (54.88) 68 respectively and marls, 42 (52) 66 and 43 (54.89) 70 respectively. Neither is this variation linked to any trend or characteristic identified in the overall palynological analysis of the dinoflagellate cyst assemblages. The most characteristic feature of this section is the presence of cycles within this data set identified by Fast Fourier Transform analysis. However, overall richness calculations show no link to these cyclical characteristics.

H' - Shannon Index

Shannon indices values for Site 3a vary between 1.39 (2.35) 2.67 and are shown in Figure 7.2 . These values are low to average values as H' values usually fall between 1.5 - 3.5 (Magurran, 1988). Shannon indices show some direct relationship to number of cysts per gramme of sediment (Figure 8.2), whereby increased number of cysts is matched by an increase in H' values. The Shannon index values do not show any strong relationship to lithology, although the two lowest H' values (1.4, 1.39) are yielded by chalk samples (Site 3a, 45cm. and 100cm.). This measurement of diversity does not show any link to the

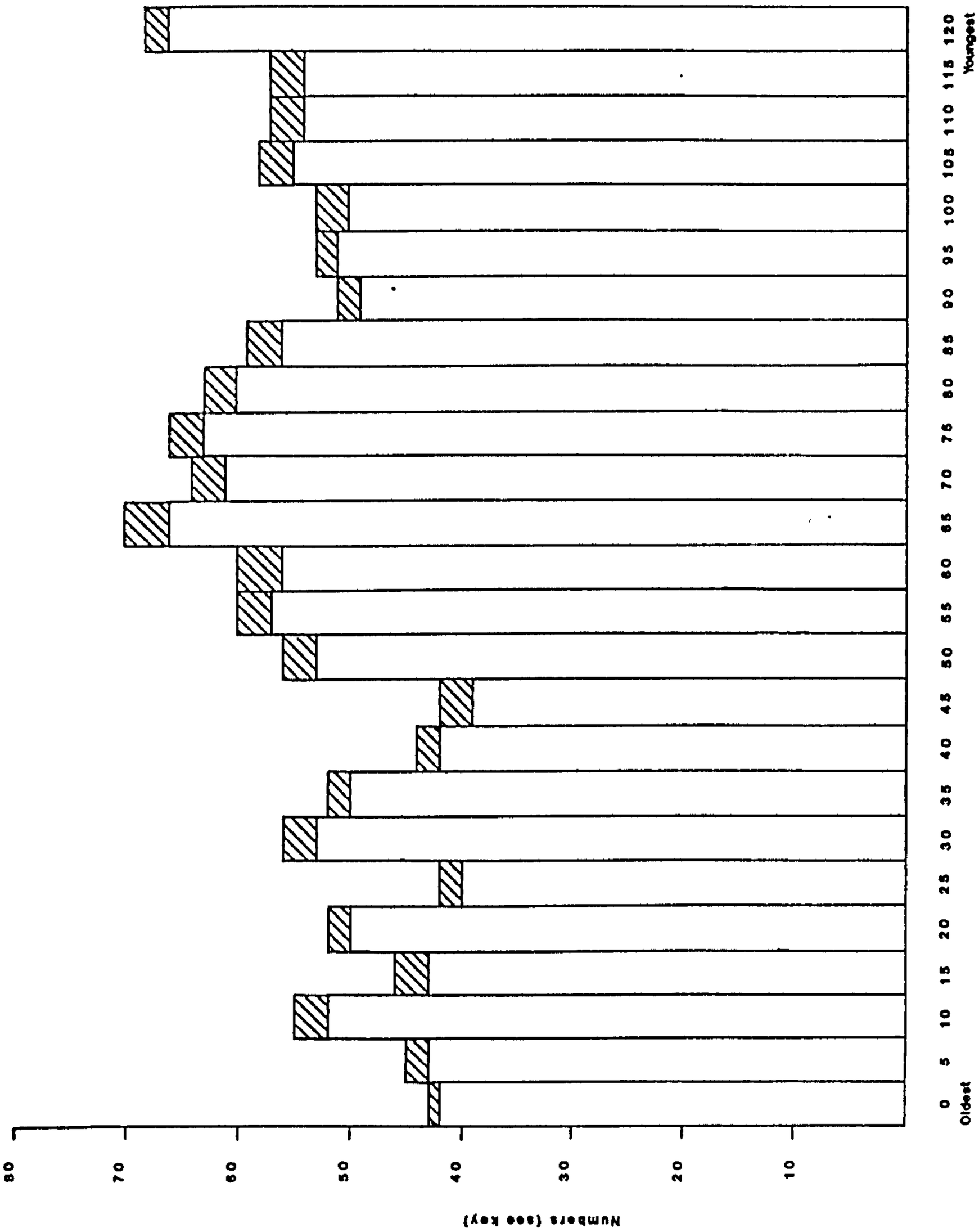

Figure 7.1 Species diversity for Site 3a samples based on overall richness index values (S).

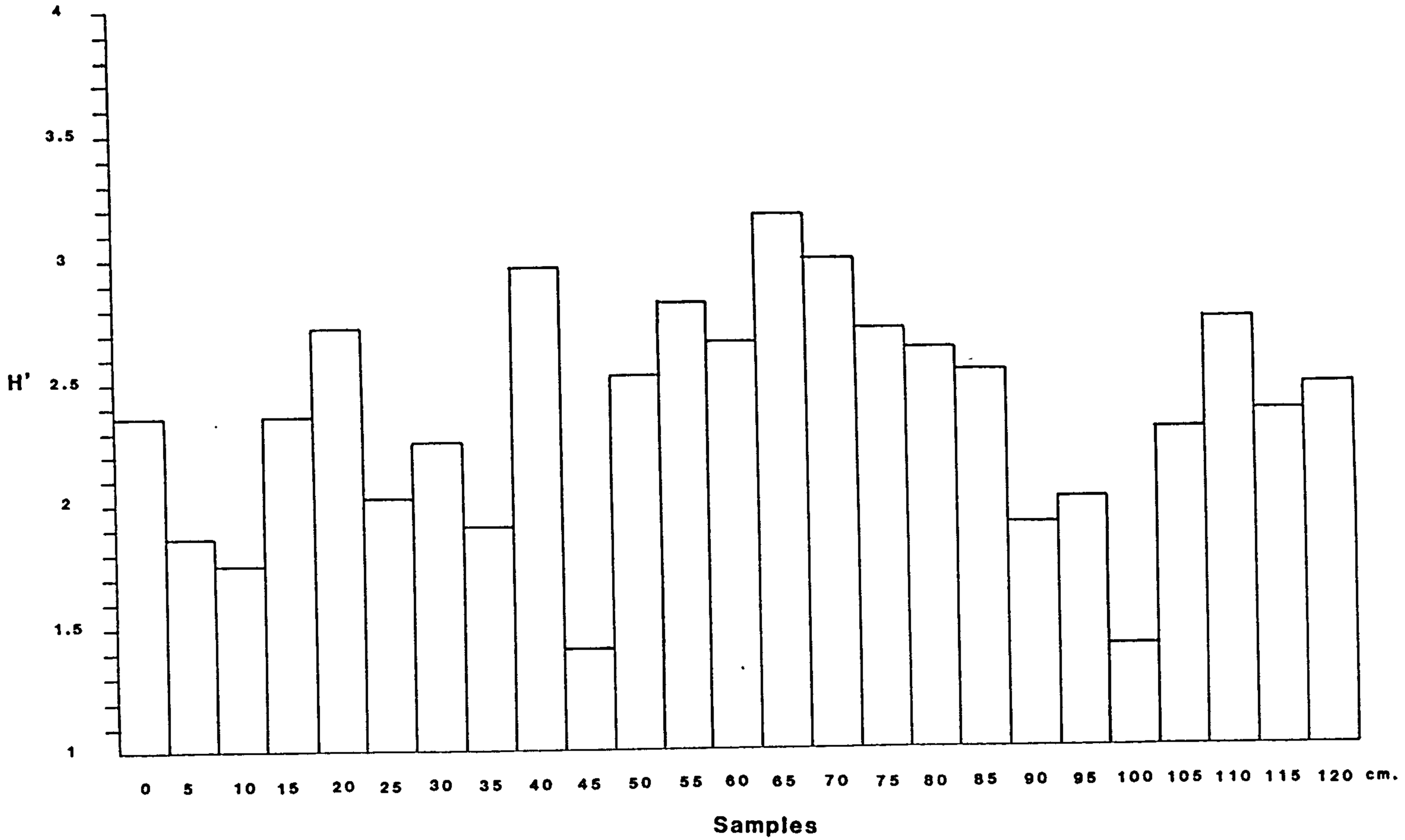

Figure 7.2 Species diversity for dinoflagellate cysts from Site 3a samples based on Shannon index values (H').

cyclical/rhythmic feature of the dinoflagellate cyst assemblages.

7.2.2. Cluster analysis D - Dice co-efficient

The dendrogram constructed from the Dice co-efficient values is shown in Figure 7.3. Broadly speaking, there is a high degree of similarity between all Site 3a samples. Cluster analysis does show that the Site 3a data set is broadly divided up into two groups, Site 3a, 0 to 45 with the exception of one sample, Site 3a, 20 and Site 3a, 50 to 120 inclusive and including Site 3a, 20. These two groups identified by the Dice co-efficient cannot be explained on the basis of lithological differences as both include chalk and marl samples. Rhythms nor cycles within the Site 3a data set are not picked out by cluster analysis.

7.2.3. Fourier analysis

The specific Fast Fourier Transform (FFT) programme (Appendix 5) used herein was written by Mr. R.D. Eddies for analysis of geophysical seismic traces (Press *et al.*, 1986). This same programme proved very applicable to the palynological data sets produced by the 300 count method. However, one slight modification had to be made to all data sets and that was to pad them out with zeros at either side, so as to increase the time series from only 25 data points (samples) to N^2, where N equals the number of data points within a data set. This is a legitimate and recommended technique for over-coming the problem of FFT carried out on small data sets and does not include or induce any errors as a result of the modification, Press *et al.*, (1986).

The Nyquist frequency (f_N) for Site 3a is 10cm., therefore no cycle with a frequency of less than 10cm. is statistically significant. The programme calculates the Nyquist frequency and does not present values lower than it.

FFT output of some of the thirty-one data sets investigated (as discussed previously) is given in Figures 7.4 to 7.14, and is given in Frequency domain *i.e.* amplitude (*y-axis*) 'v' frequency (Log_{10}) (*x-axis*). The frequency axis also has indications of corresponding centimeter values for ease of interpretation. As can be seen from these figures the FFT algorithm is successful and confidently indicates the presence of cycles of different frequencies within the Site 3a section. Figures 7.4 to 7.8 demonstrate cyclicity

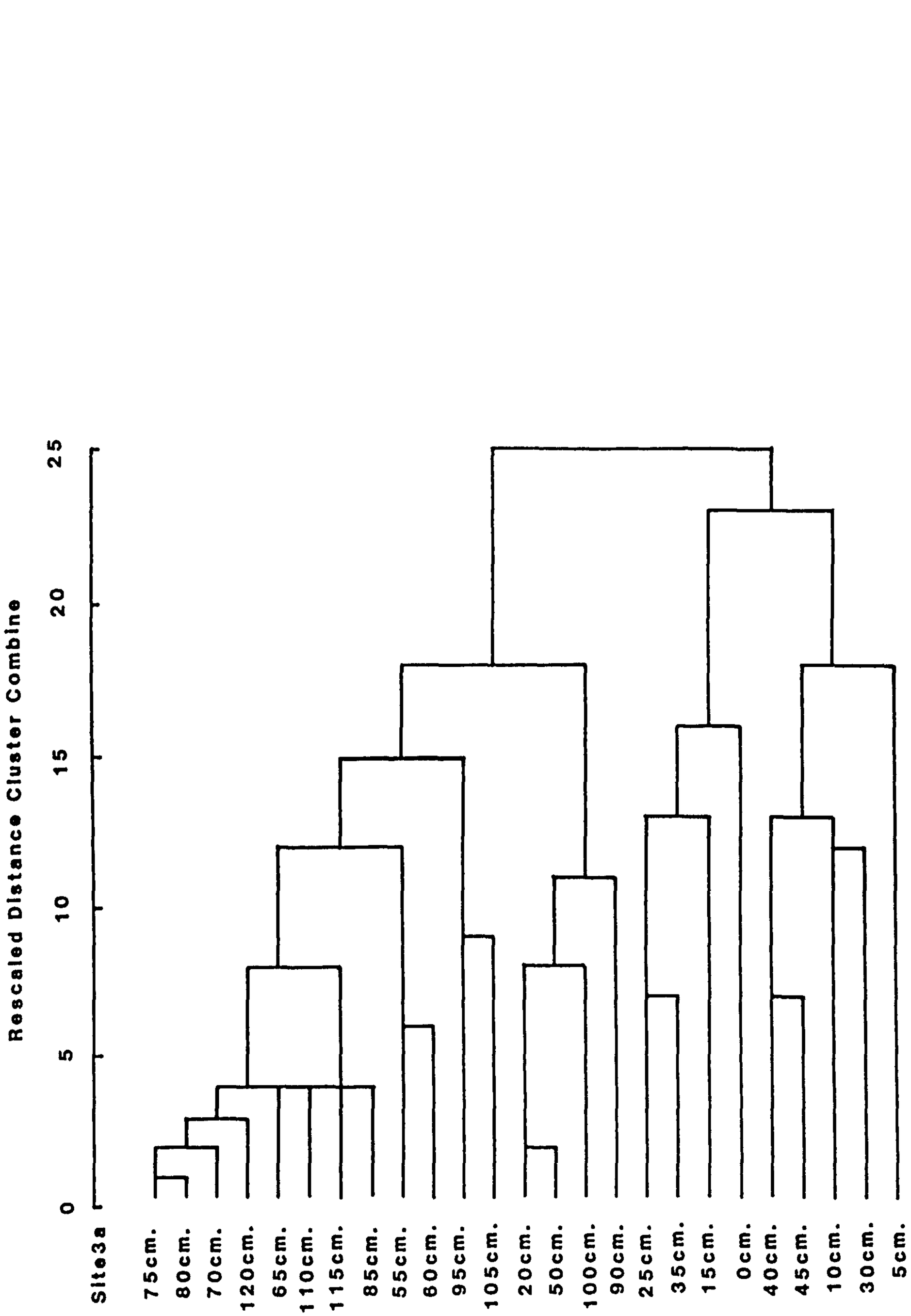

Figure 7.3 Dendrogram based on Cluster analysis of Site 3a samples.

frequencies of both 20 and 40 cm. and Figures 7.9 to 7.12 illustrate a cyclicity of 20 cm. Figures 7.13 and 7.14 are included so as to demonstrate the frequency 'v' amplitude spectra of certain data sets which fail to indicate any definable trends or cyclicity. A summary of the FFT results is as follows:

Individual dinoflagellate species percentage occurrence data sets (A)

48% of data sets exhibit cycles of both 20 and 40cm. frequencies
11% " " " " " " 20cm. frequency
5% " " " " " " 40cm. "
36% " " " " " " other frequencies

Morphological Groupings (B)

28% of data sets exhibit cycles of both 20 and 40cm. frequencies
56% " " " " " " 20cm. frequency
3% " " " " " " 40cm. "
13% " " " " " " other frequencies

Summary (A) + (B)

38% of data sets exhibit cycles of both 20 and 40cm. frequencies
34% " " " " " " 20cm. frequency
4% " " " " " " 40cm. "
24% " " " " " " other frequencies

The cycle frequencies identified by FFT are highly significant as the 20 and 40cm. cyclicity is caused by the bed thicknesses of the two lithologies present within this section. Individual chalk beds are typically 40cm. thick and 20cm. is the typical thickness of a marl. This reinforces the overall conclusion derived from analysis of the dinoflagellate cyst associations present in Site 3a section, that dinoflagellate cyst presence and distribution is linked to lithology. Also, Hart (1987) and Gale (1989a) have suggested that the 40cm. cyclicity present within the Cenomanian chalk is forced by the 21,000 years, precessional cycle (Milankovitch, 1941). However, more detailed accounts of the above conclusions are available in Chapter 8, in the section dealing with Site 3a.

Text cut off in original

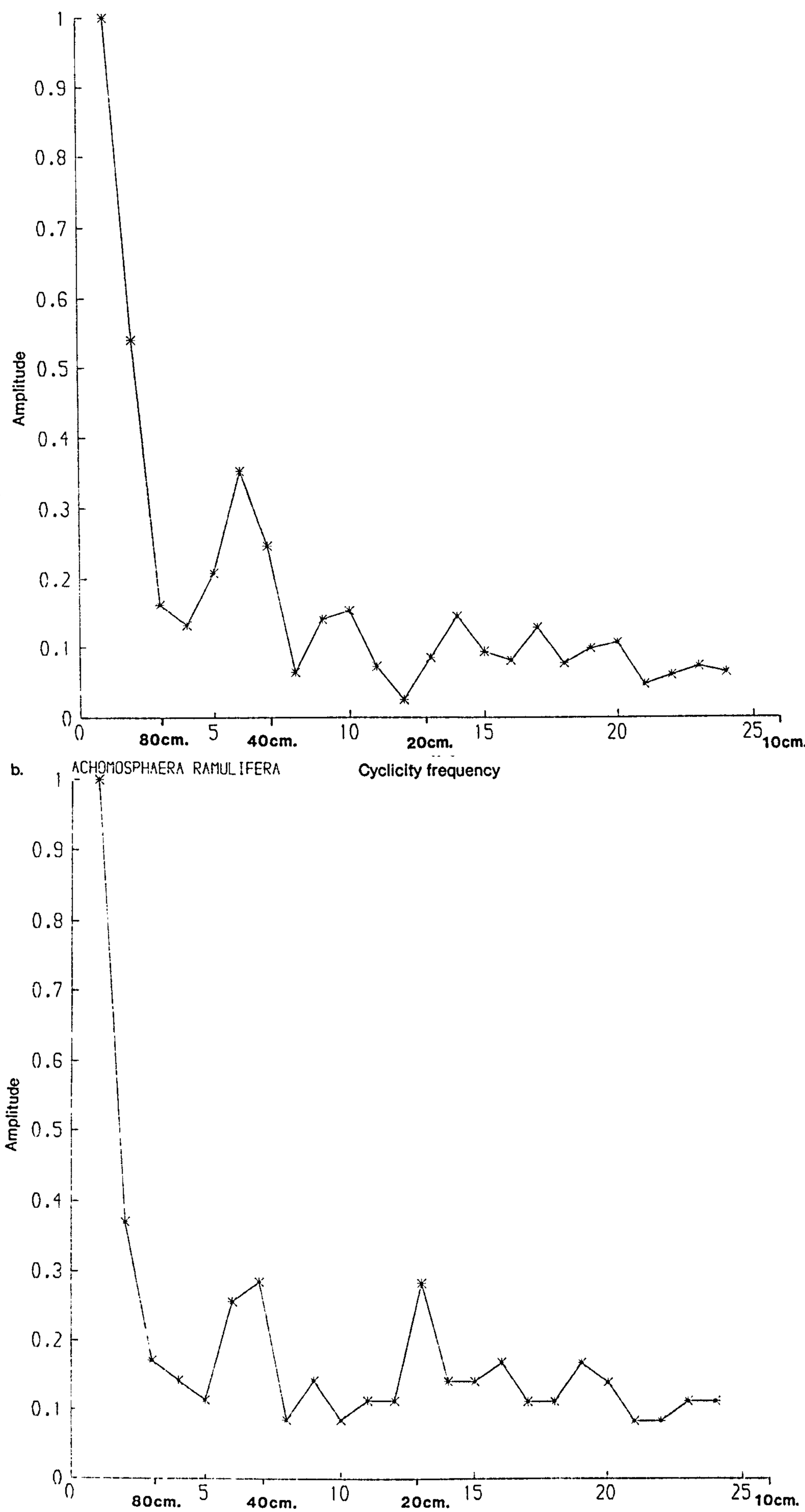

Figure 7.4 Fourier analysis frequency (f) 'v' amplitude (a) spectrum for Site 3a samples based on the FFT algorithm.

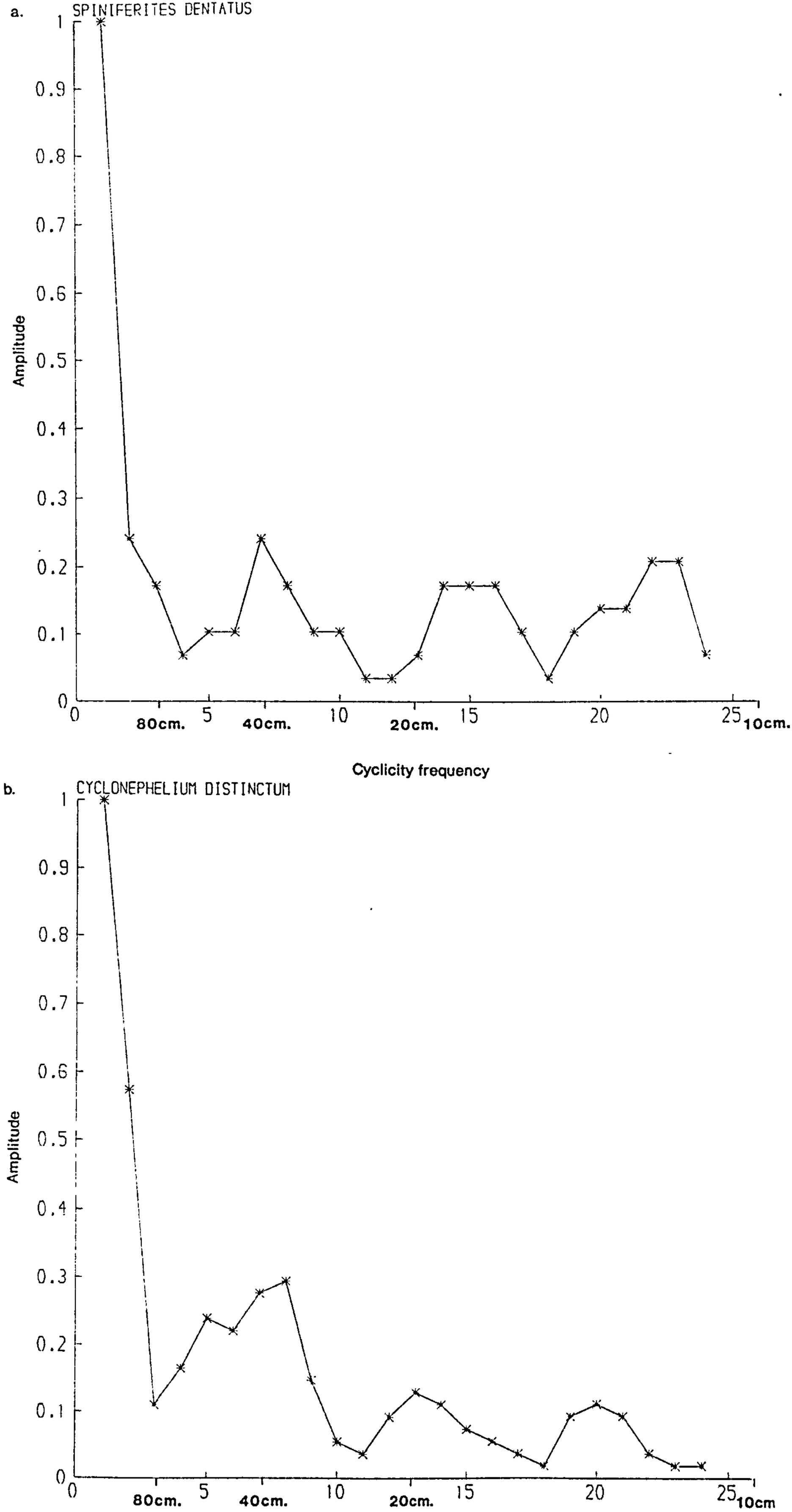

Figure 7.5 Fourier analysis frequency (f) 'v' amplitude (a) spectrum for Site 3a samples based on the FFT algorithm.

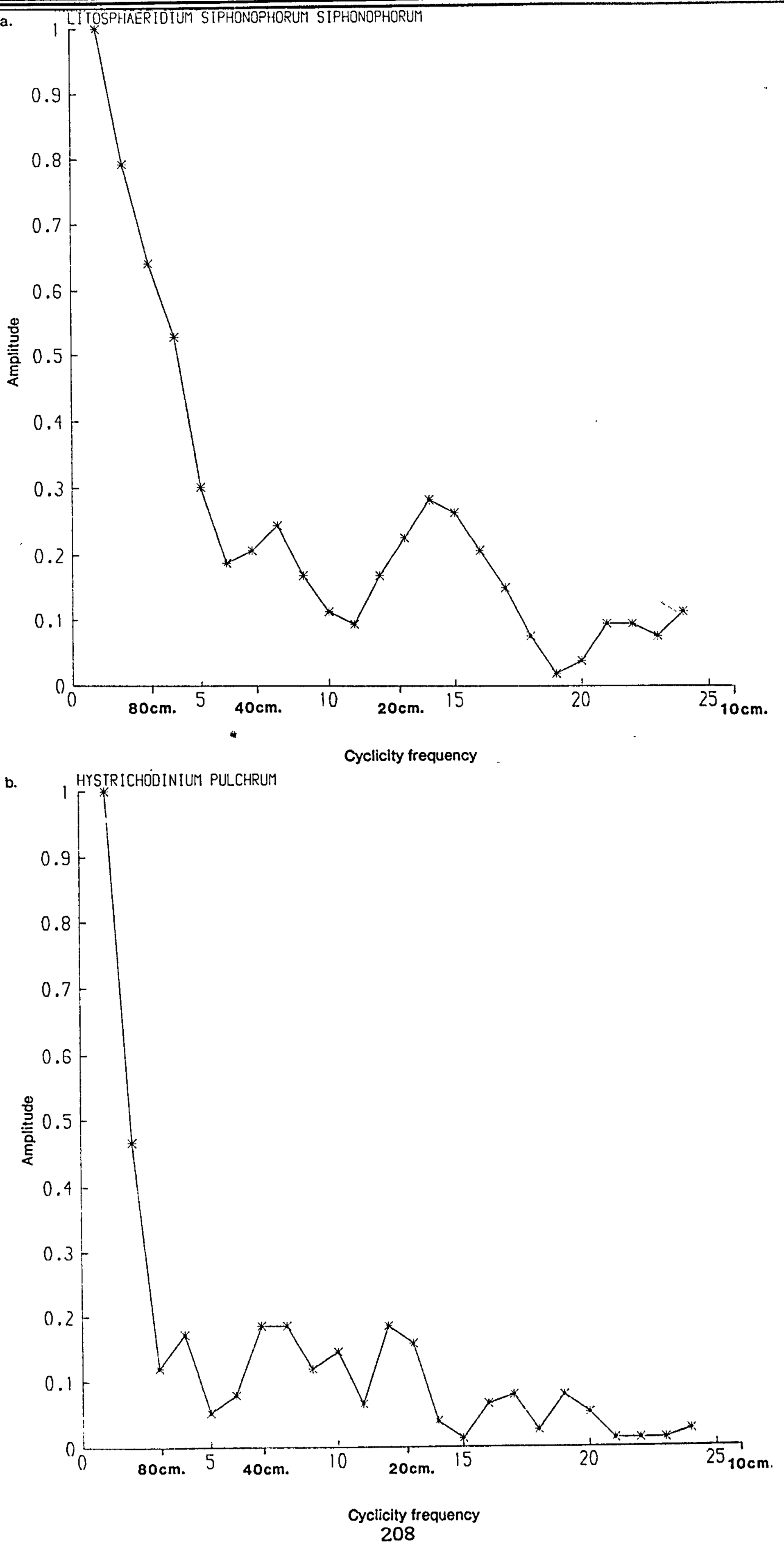

Figure 7.6 Fourier analysis frequency (f) 'v' amplitude (a) spectrum for Site 3a samples based on the FFT algorithm

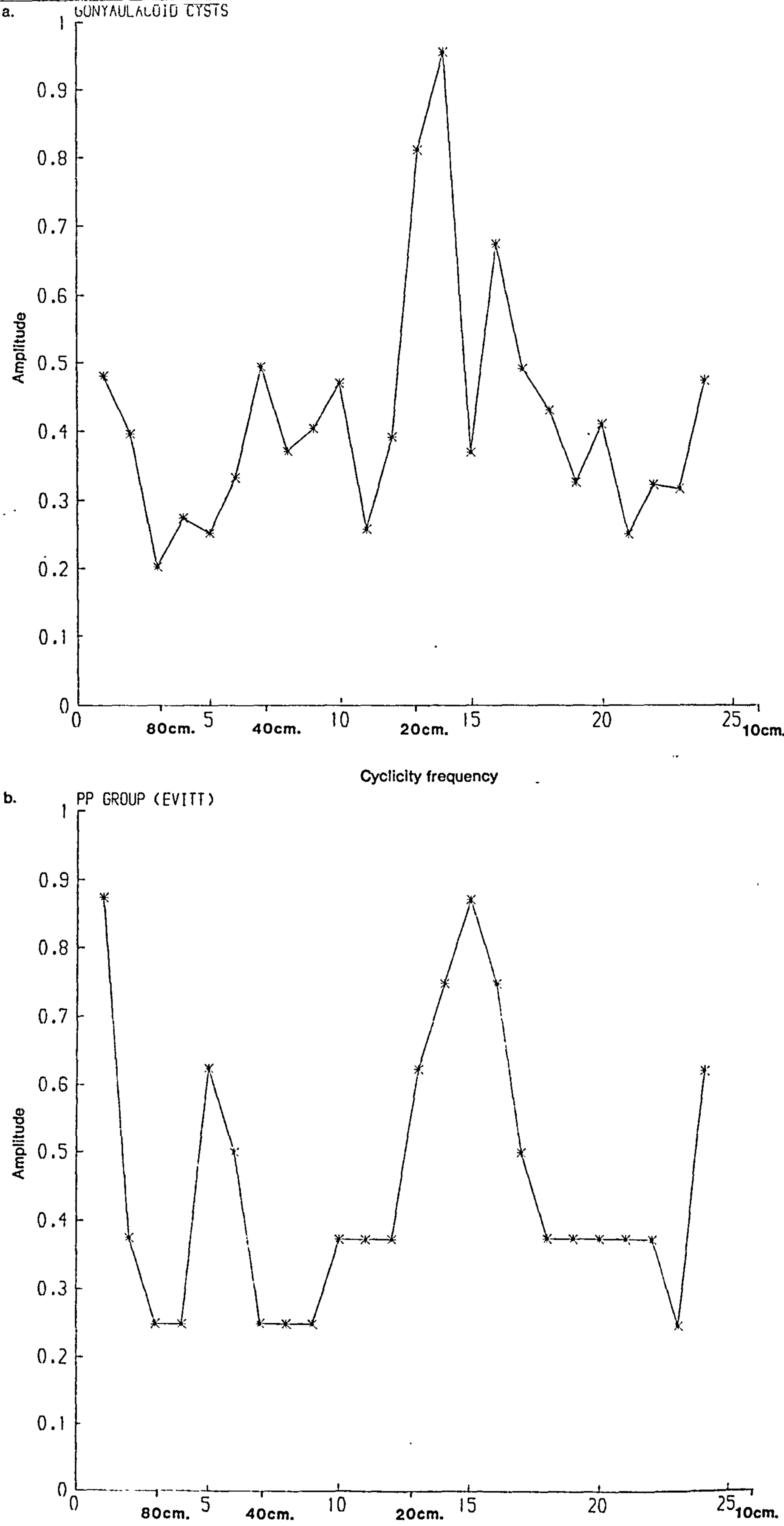

Figure 7.7 Fourier analysis frequency (f) 'v' amplitude (a) spectrum for Site 3a samples based on the FFT algorithm. for Site 3a samples based on the rri algorithm.

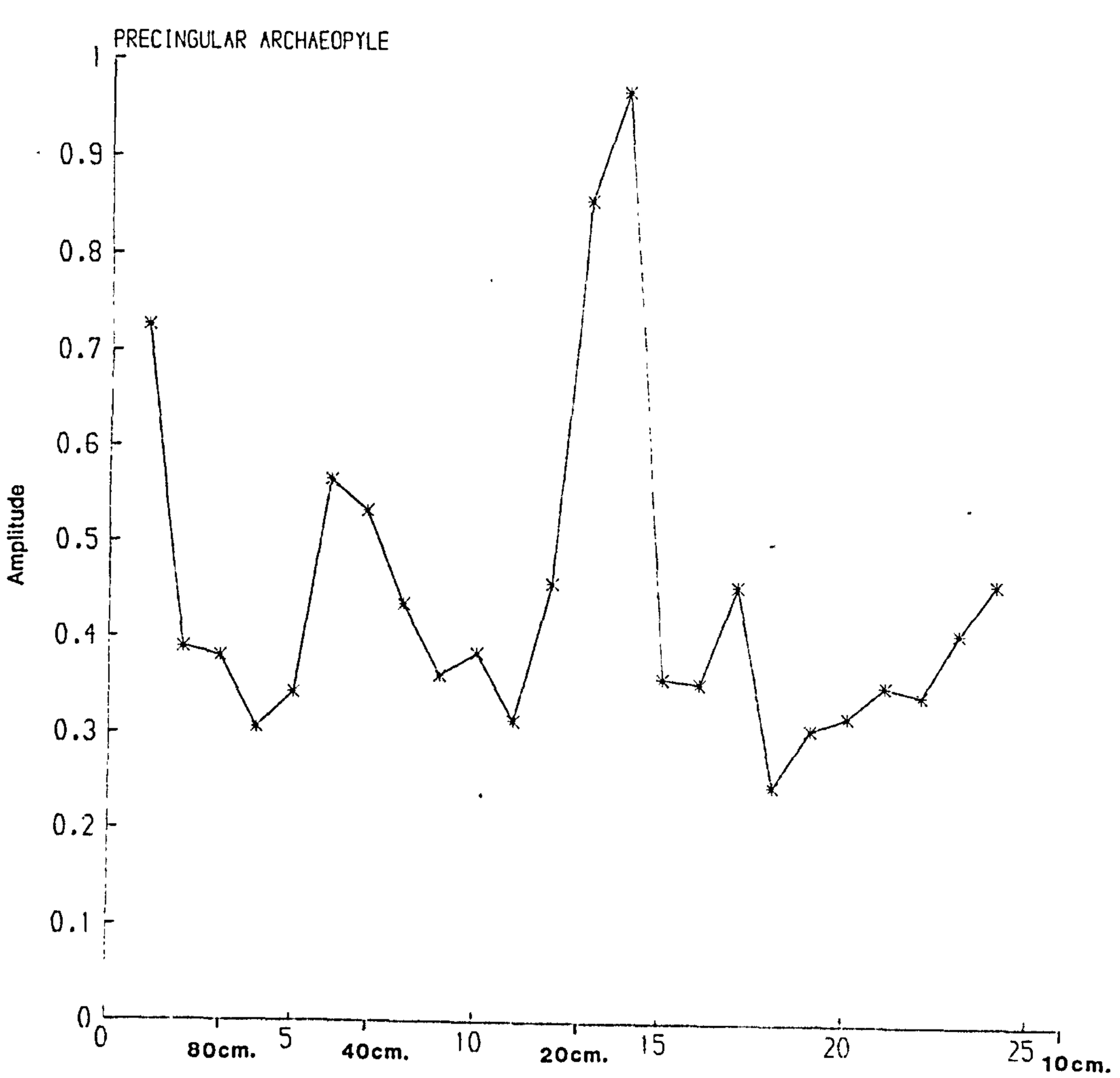

Figure 7.8 Fourier analysis frequency (f) 'v' amplitude (a) spectrum for Site 3a samples based on the FFT algorithm.

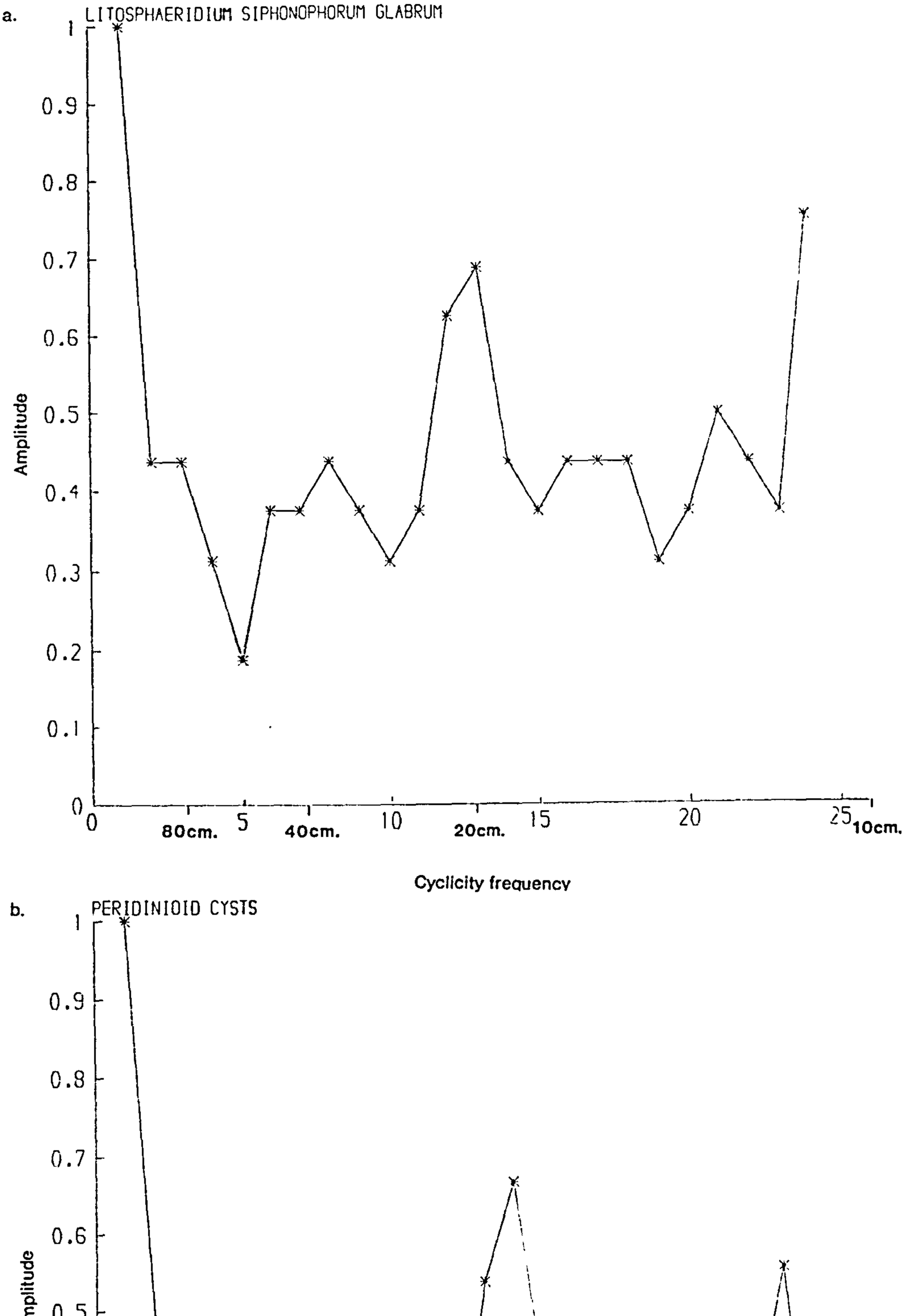

Figure 7.9 Fourier analysis frequency ('v') amplitude (a) spectrum for Site 3a samples based on the FFT algorithm.

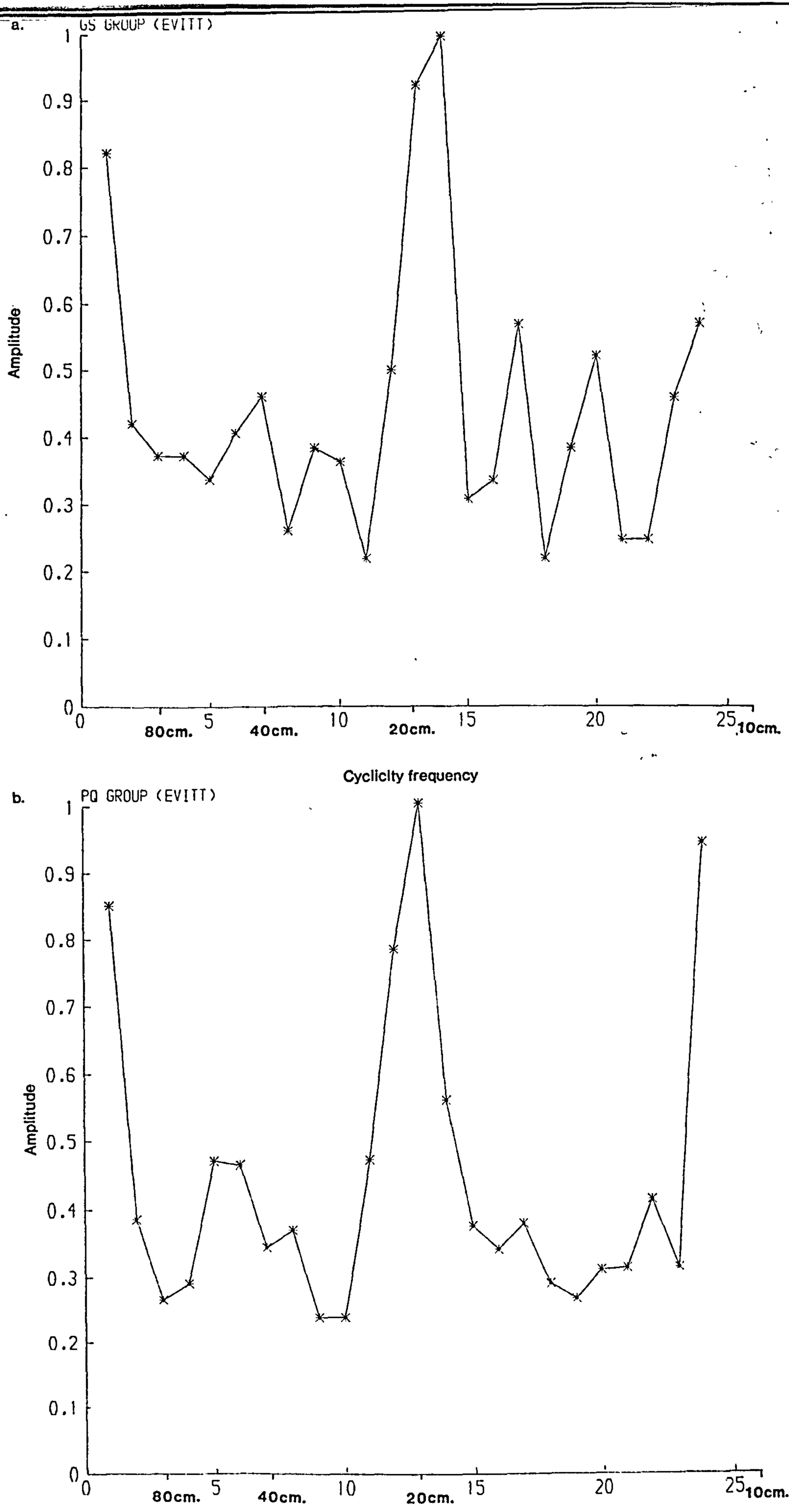

Figure 7.10 Fourier analysis frequency (f) 'v' amplitude (a) spectrum for Site 3a samples based on the FFT algorithm.

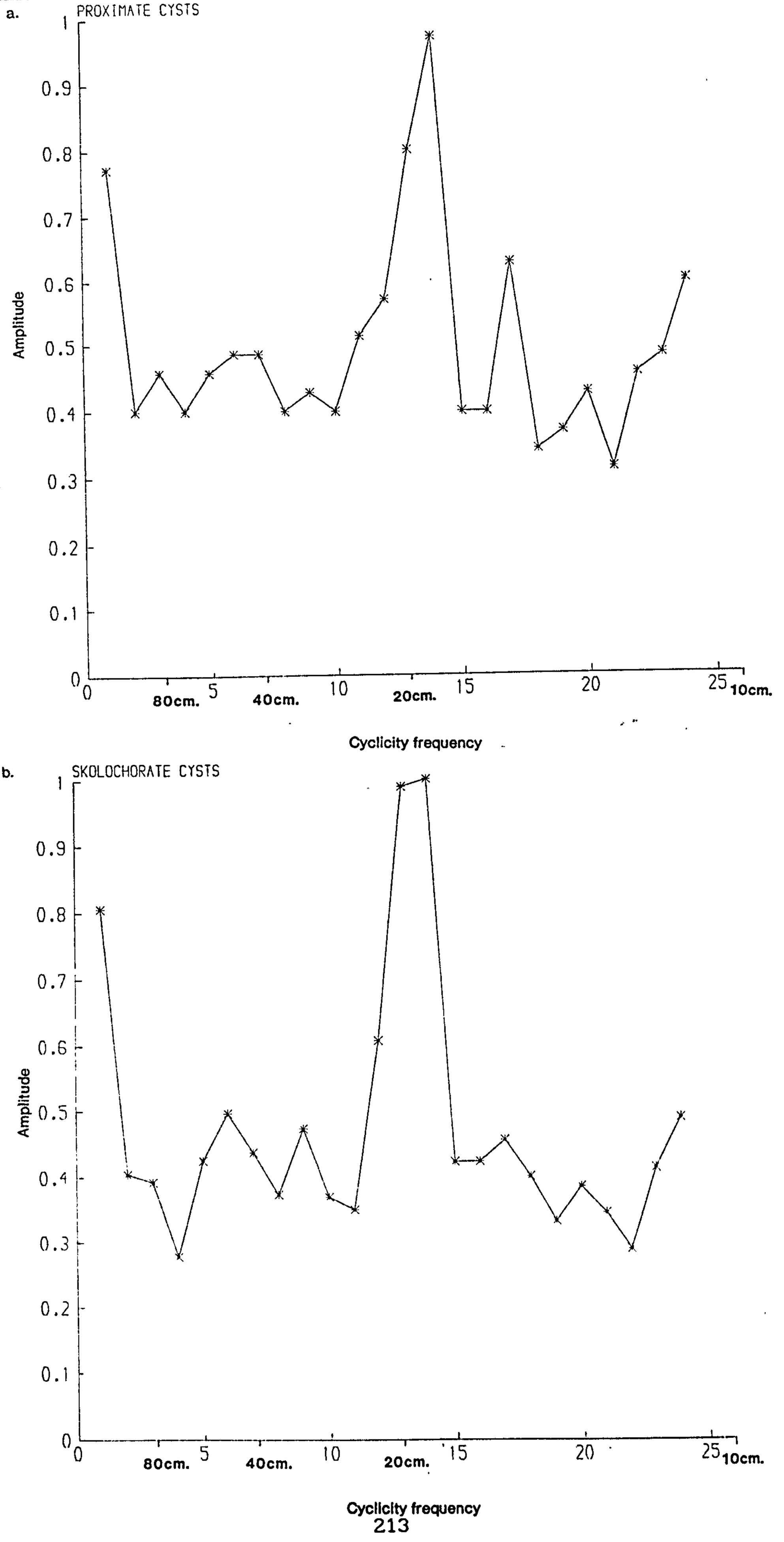

Figure 7.11 Fourier analysis frequency (f) 'v' amplitude (a) spectrum

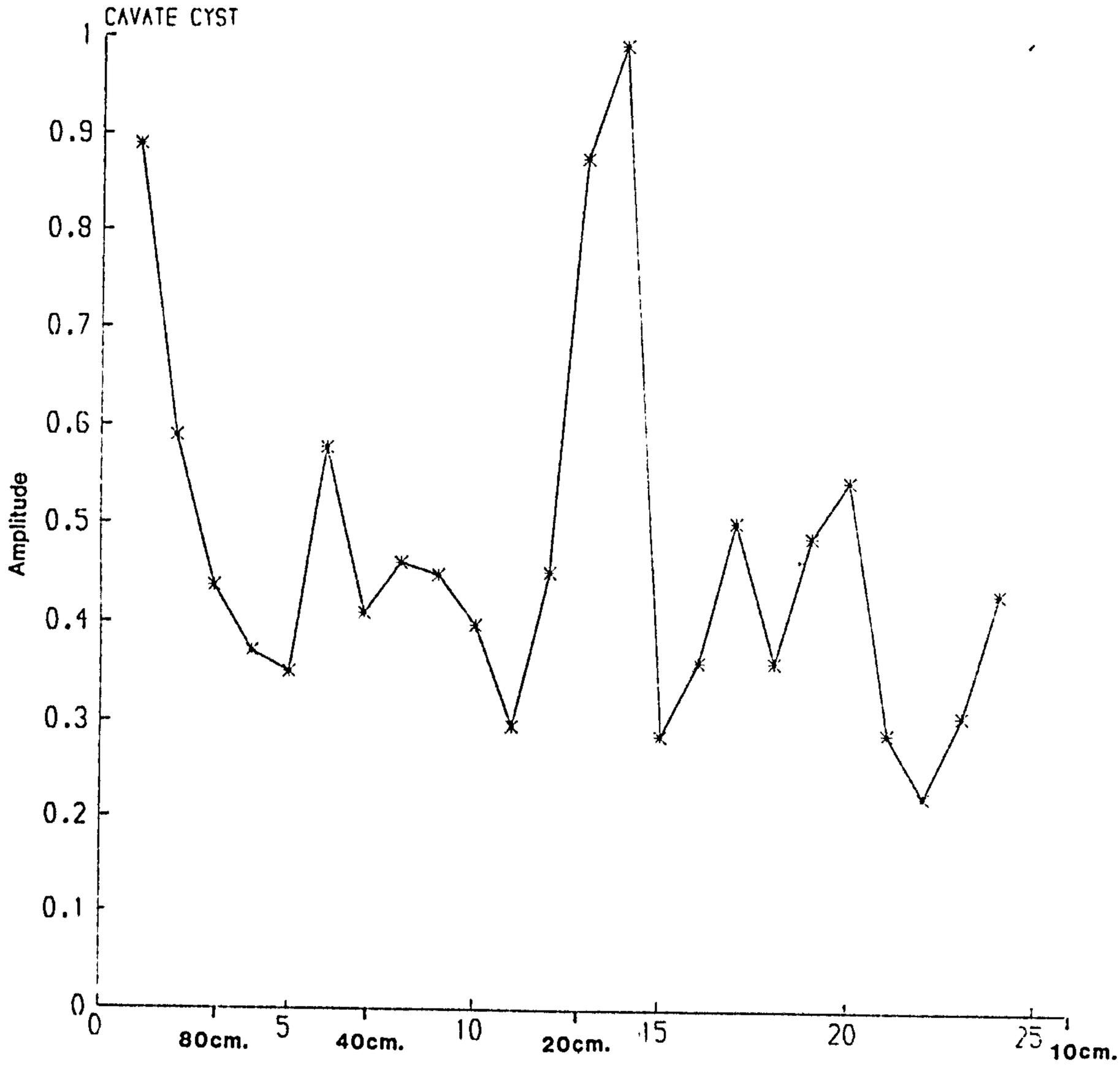

Figure 7.12 Fourier analysis frequency (f) 'v' amplitude (a) spectrum for Site 3a samples based on the FFT algorithm.

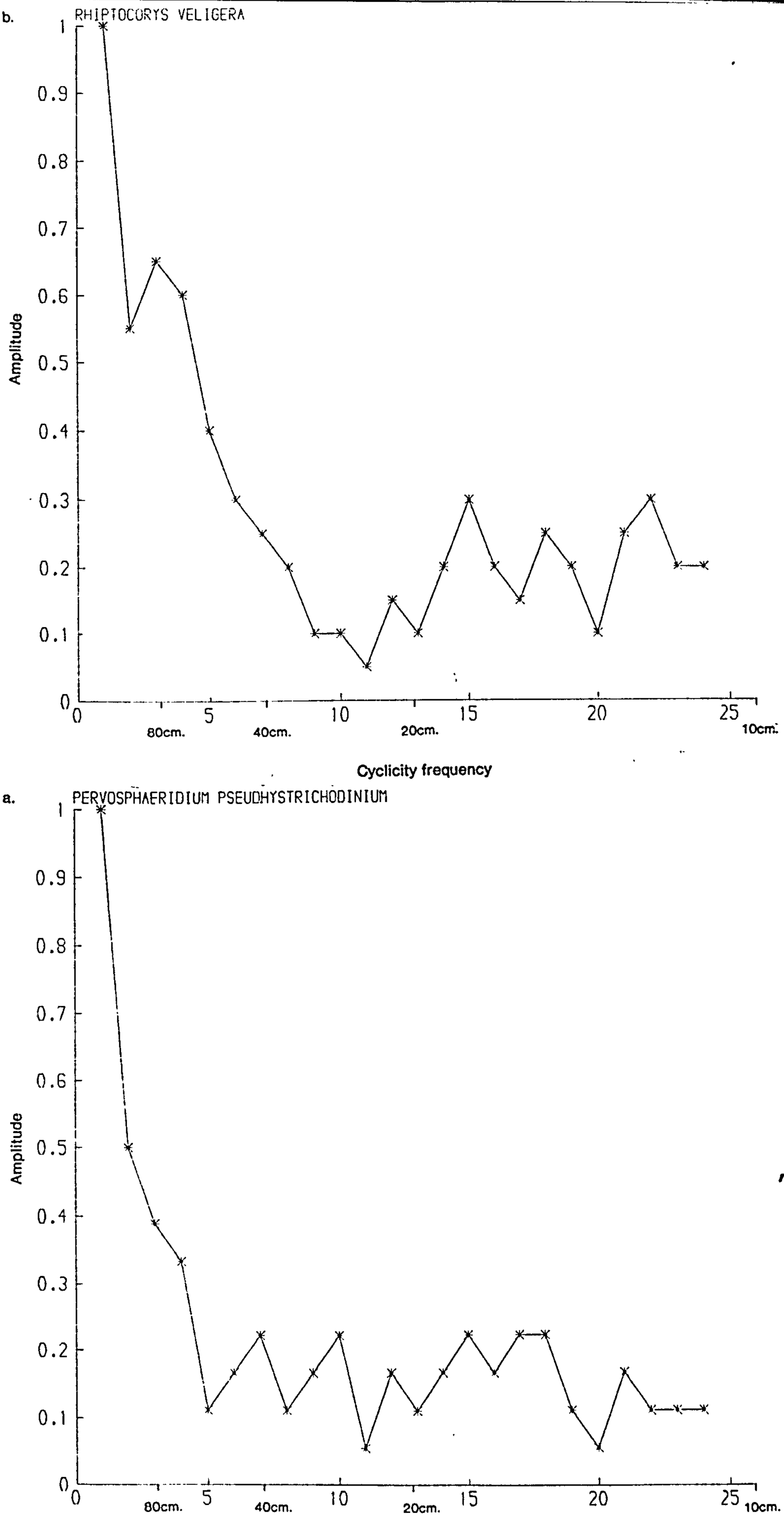

Figure 7.13 Fourier analysis frequency (f) 'v' amplitude (a) spectrum for Site 3a samples based on the FFT algorithm.

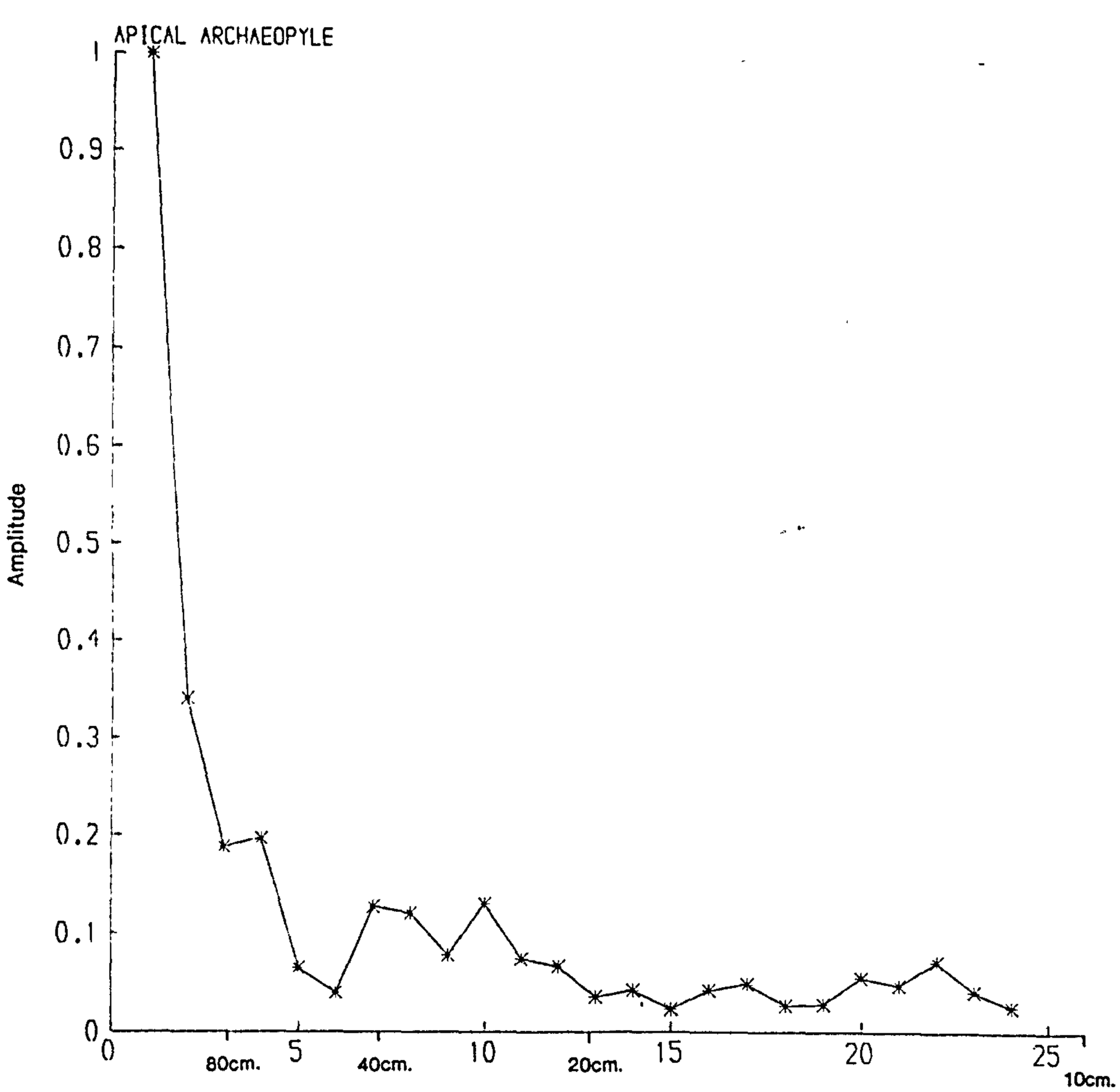

Figure 7.14 Fourier analysis frequency (f) 'v' amplitude (a) spectrum for Site 3a samples based on the FFT algorithm.

7.2.4. Autocorrelation

Although autocorrelation was carried out on the Site 3a data, it is not included as it is proved statistically spurious and thus inconclusive due to the small size of the data sets.

7.3. TBB section

7.3.1. Diversity

S - Overall richness

Values of overall richness, expressed as dinoflagellate species diversity and total palynomorphs shows this section to be consistently richer than Site 3a. Number of dinoflagellate cyst species varies from 53 (58.32) 65 and total palynomorph values range from 56 (62) 69 (Figure 7.15), both implying high species diversity. Neither of these indications of diversity show any relationship to number of dinoflagellate cysts per gramme of sediment nor to lithology. However, both estimations of diversity/richness show troughs around sample TBB7, the sample which displays the $\delta^{13}C$ excursion (Ditchfield, 1990) one of the features of interest within this section, see Chapters 2 and 8, for more details. Also, dinoflagellate cyst species diversity is higher ($\bar{x}$ = 59.2) in post-TBB7 samples, with species diversity values pre-TBB7 only reaching an average of 57.5.

H' - Shannon Index

Shannon index values shown in Figure 7.16 range from 2.36 (2.98) 3.42 and are consistently higher than those of Site 3a, a feature also implied by the overall richness characteristics as outlined previously. Thus, considering that H' values normally range between 1.5 - 3.5 (Magurran, 1988) this TBB section records a high diversity assemblage. There is a strong and direct relationship between H' values and number of dinoflagellate cysts per gramme of sediment (Figure 8.13). Indeed, Shannon index values are somewhat anomalously low for samples TBB -3, -1, 13, 15, which are the only samples within this section to be oxidised, a feature which is shown also by the number of dinoflagellate cysts per gramme distribution. H' values distribution is also similar to that of the cyst species diversity. H' values when compared to lithology show that chalk samples range

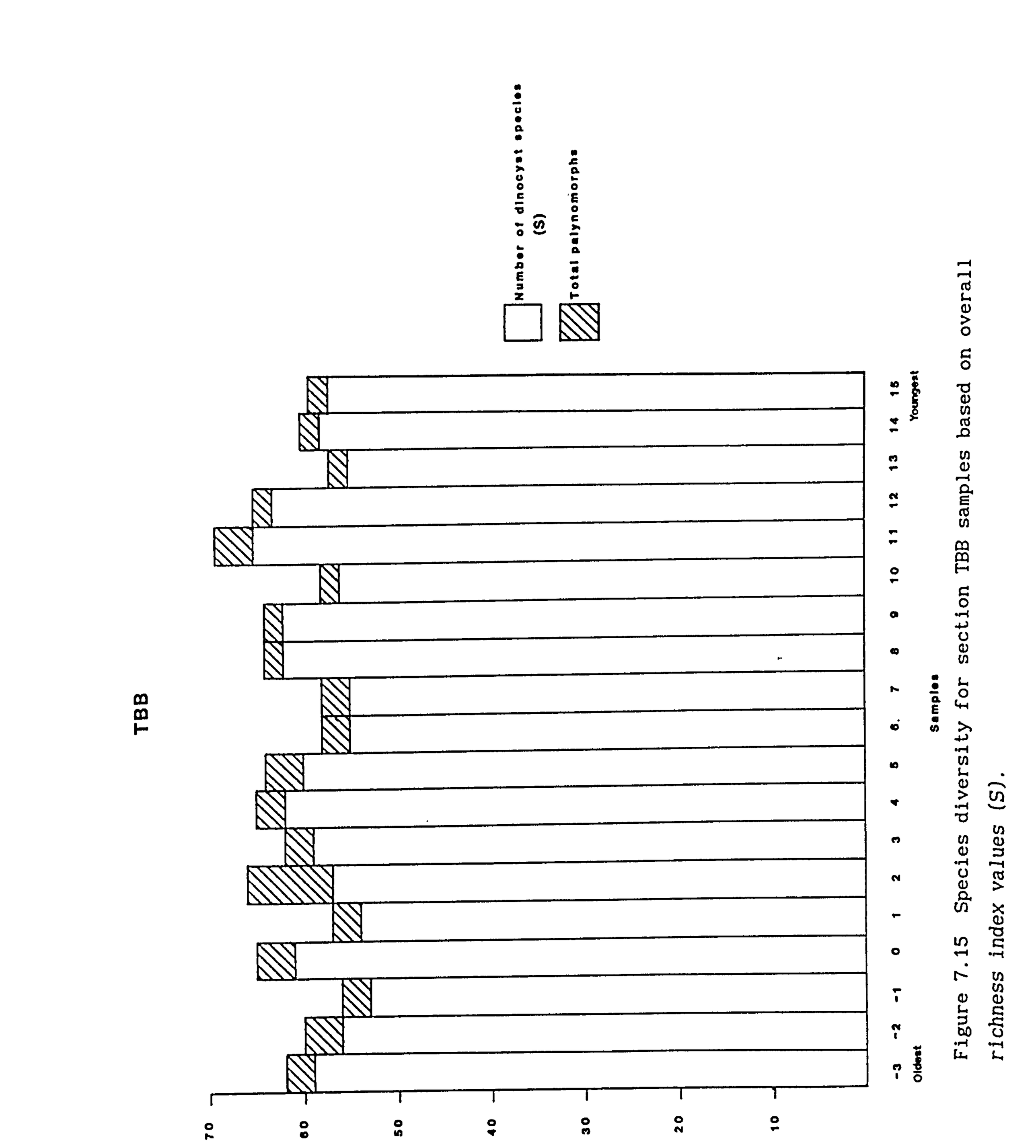

Figure 7.15 Species diversity for sections TBB samples based on overall richness index values (S).

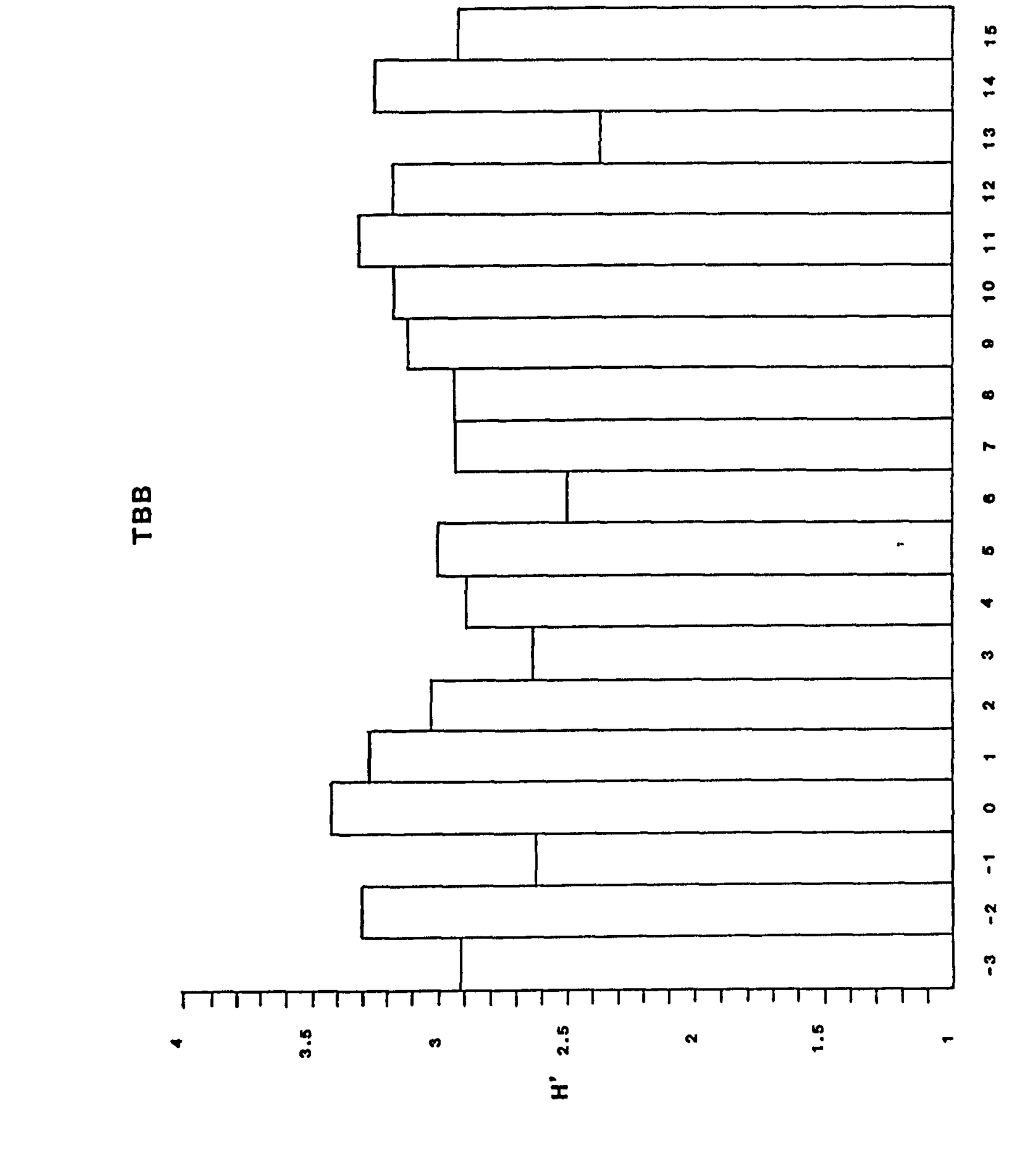

Figure 7.16 Species diversity for dinoflagellate cysts from section TBB samples based on Shannon index values (H').

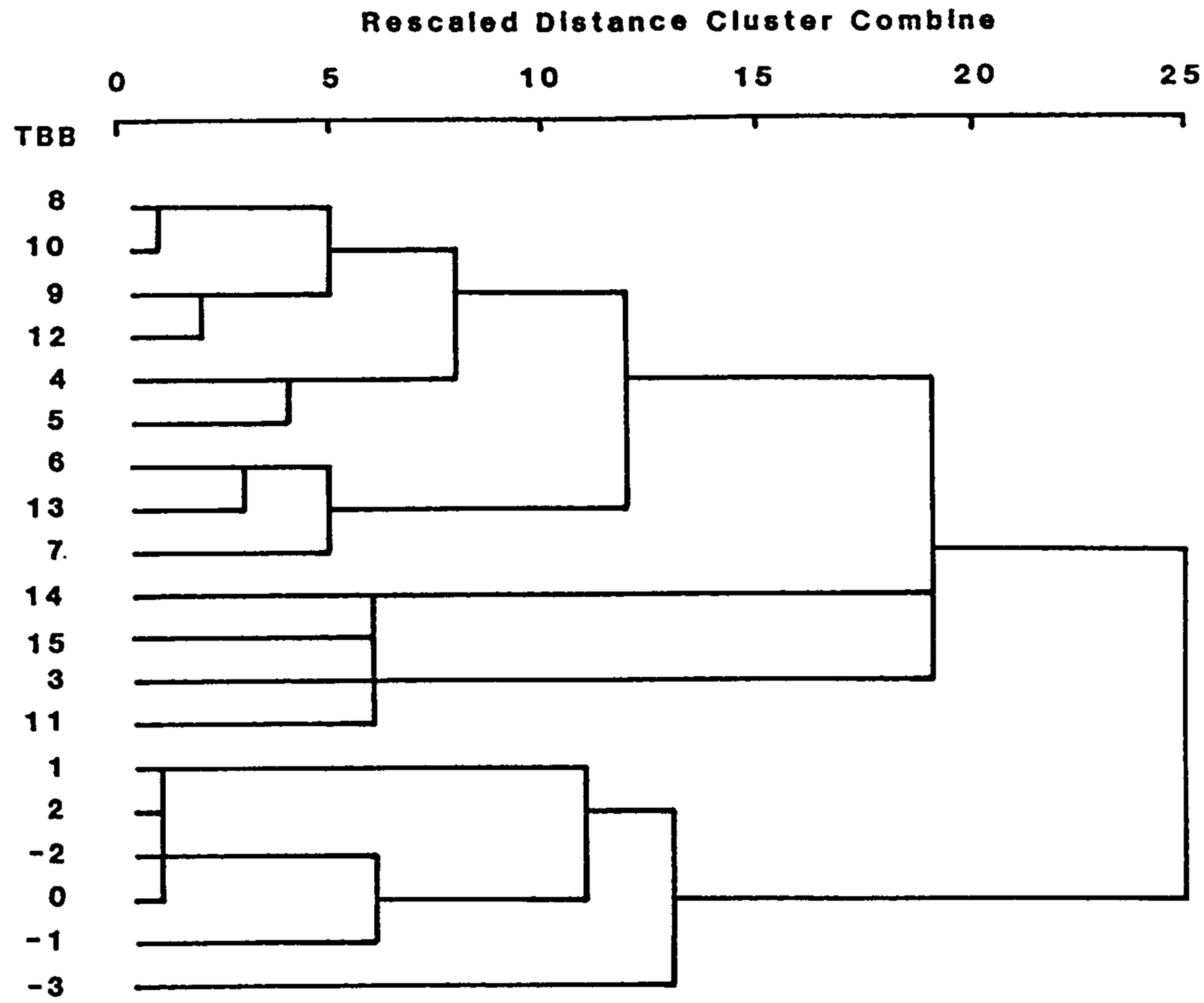

Figure 7.17 Dendrogram based on Cluster analysis of TBB samples.

between 2.62 (3.07) 3.42, marl samples between 2.63 (3.03) 3.31 and marly chalk lithologies vary between 2.36 (2.92) 3.27 implying that marly chalk lithology exhibits consistently lower species diversity values than both chalk and marl lithologies, which record similar values. As mentioned previously, one of the features of interest within this section is the presence of a $\delta^{13}C$ excursion recorded in sample TBB7 (Ditchfield, 1990). The distribution of H' values appears to be weakly linked to this feature as samples pre-TBB7 have lower average H' values [2.49 (2.95) 3.42] whereas post-TBB7 samples exhibit consistently higher H' values [2.36 (3.01) 3.31]. In summary, Shannon index diversity analysis successfully substantiates characteristics and features identified by the palynological analysis of the TBB section.

7.3.2. Cluster analysis D - Dice co-efficient

A dendrogram has been constructed on the basis of the co-efficient matrices of TBB samples and is shown in Figure 7.17. Analysis of the dendrogram shows that similarities identified by the Dice co-efficient method of cluster analysis do not bear any relationship to lithology. Also, this method of cluster analysis does not indicate the occurrence of associations caused by the presence of the $\delta^{13}C$ excursion (Ditchfield, 1990). In broad terms cluster analysis indicates the presence of two assemblages, TBB -3 to 2 and TBB 3 to 15, with many sub-associations within each. Indeed, the discrimination of these two associations does seem to be substantiated by comparison with the palynofacies analysis of this section, see Chapter 8 for more detail.

7.4. MCB section

7.4.1. Diversity

S - Overall richness

Diversity values for this MCB section range between 44 (55.85) 63 for species diversity and 47 (58.8) 67 for total palynomorphs (Figure 7.18). These values imply that it records a high diversity assemblage, similar to the diversity levels exhibited by the preceding TBB section. These estimates of diversity do not bear any relationship to number of dinoflagellate cysts per gramme of sediment

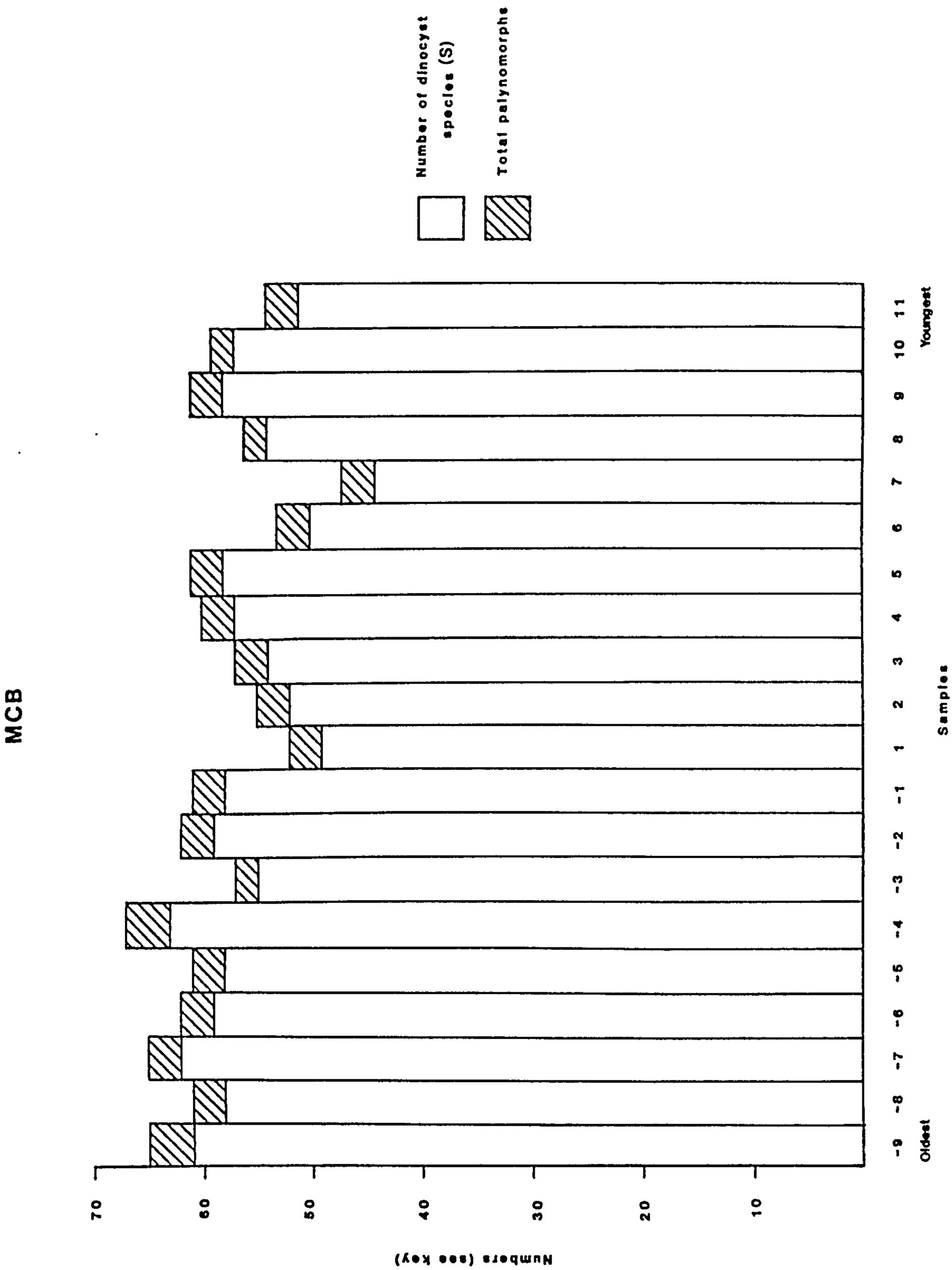

Figure 7.18 Species diversity for section MCB samples based on overall richness index values (S). The abbreviated sample numbering system shown above corresponds to the following sample numbers:

-9 = -4.5-->-4, -8 = -4-->-3.5, -7 = -3.5-->-3, -6 = -3-->-2.5,
-5 = -2.5-->-2, -4 = -2-->-1.5, -3 = -1.5-->-1, -2 = -1-->-0.5,
-1 = -0.5--> 0, 1 = 0--> 0.5, 2 = 0.5--> 1, 3 = 1--> 1.5,
4 = 1.5--> 2, 5 = 2--> 2.5, 6 = 2.5--> 3, 7 = 3--> 3.5,
8 = 3.5--> 4, 9 = 4--> 4.5, 10 = 4.5--> 5, 11 = 5--> 5.5

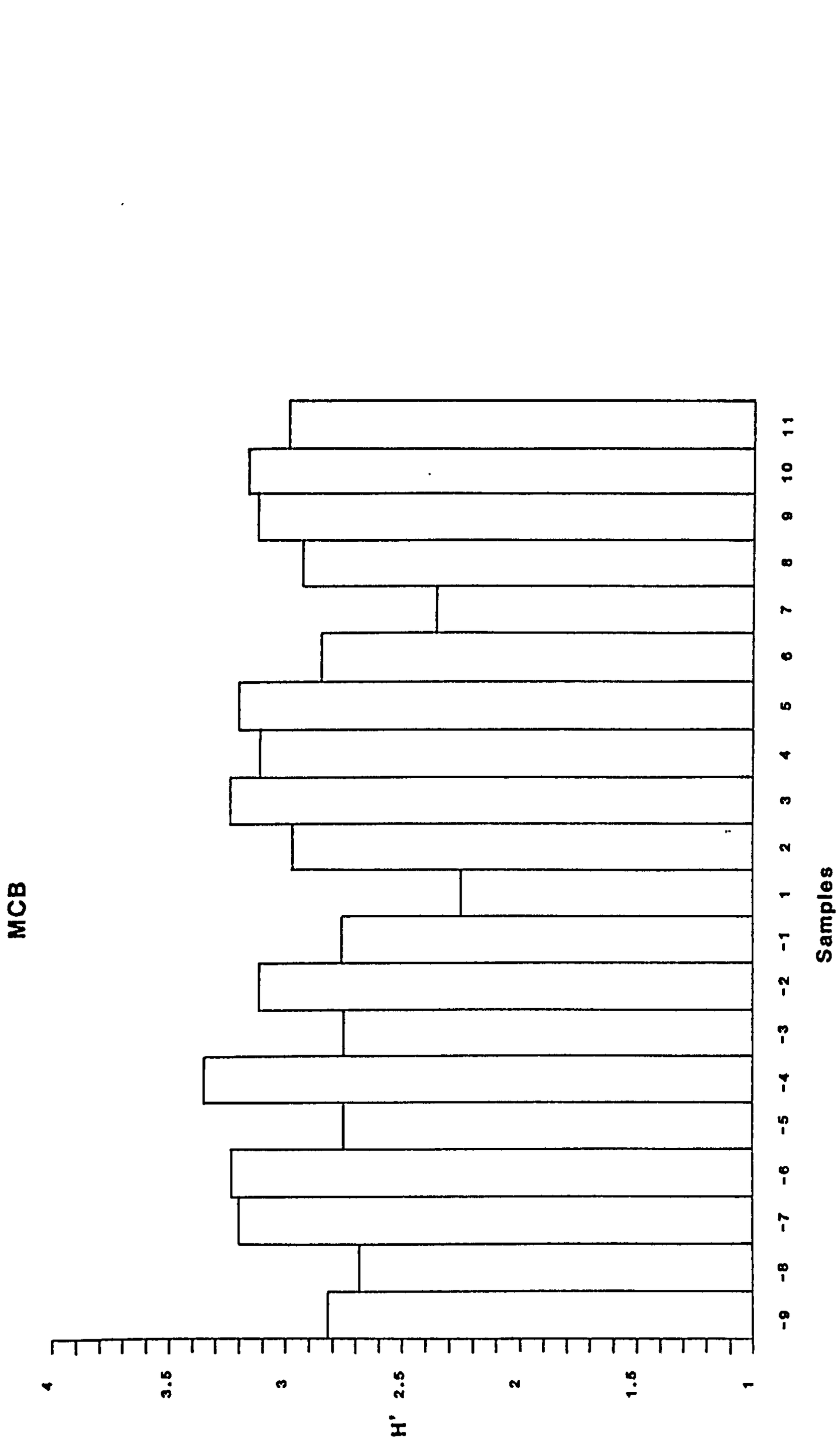

Figure 7.19 Species diversity for dinoflagellate cysts from section MCB samples based on Shannon index values (H'). See Fig. 7.18 for explanation of abbreviated sample numbering system.

nor to lithology. However, these measures of diversity do show a striking relationship to the feature of particular interest within this section, the Mid-Cenomanian non-sequence, Carter and Hart (1977). Within this study and others (Ditchfield, 1990) the term Mid-Cenomanian break (MCB) has been informally used to refer to the Mid-Cenomanian non-sequence of Carter and Hart (1977). Values of species diversity of the pre-MCB samples are distinctly higher [55 (59.22) 63] than those for the post-MCB samples [44 (53.09) 58]. Also, the values of total palynomorphs are higher for pre-MCB samples [57 (62.3) 67] than post-MCB samples [47 (55.9) 61]. Thus, pre-MCB samples contain a more diverse palynomorph assemblage than post-MCB samples.

H' - Shannon Index

Figure 7.19 displays the H' values of the MCB section which range between 2.25 (2.93) 3.35 implying a very diverse assemblage. This high diversity is also shown by the overall richness of the samples as detailed previously. The high Shannon index diversity values of this section are similar to those of the TBB section. Distribution of the H' values show some broad similarities to the distribution of number of dinoflagellate cysts per gramme of sediment (Figure 8.20), caused by the fact that they are both affected by the Mid-Cenomanian non-sequence (Carter and Hart, 1977). H' values are not linked in any way to lithology. The most striking feature of the Shannon diversity indices for the MCB section is that they successfully identify the presence of the Mid-Cenomanian non-sequence (Carter and Hart, 1977). Pre-MCB values range between 2.74 (2.98) 3.35 and post-MCB values between 2.25 (2.91) 3.23. This confidently indicates that the pre-MCB samples record a more diverse assemblage than that of post-MCB. It must be said however, that diversity values derived from the Shannon index method do not delineate the higher diversity of the pre-MCB samples in comparison to the post-MCB samples quite as successfully as the overall richness (S) method.

7.4.2. Cluster analysis D - Dice co-efficient

Calculations based on the Dice co-efficient matrices are displayed as a dendrogram, Figure 7.20. As can be seen from this diagram, cluster analysis successfully groups the MCB samples into two associations.

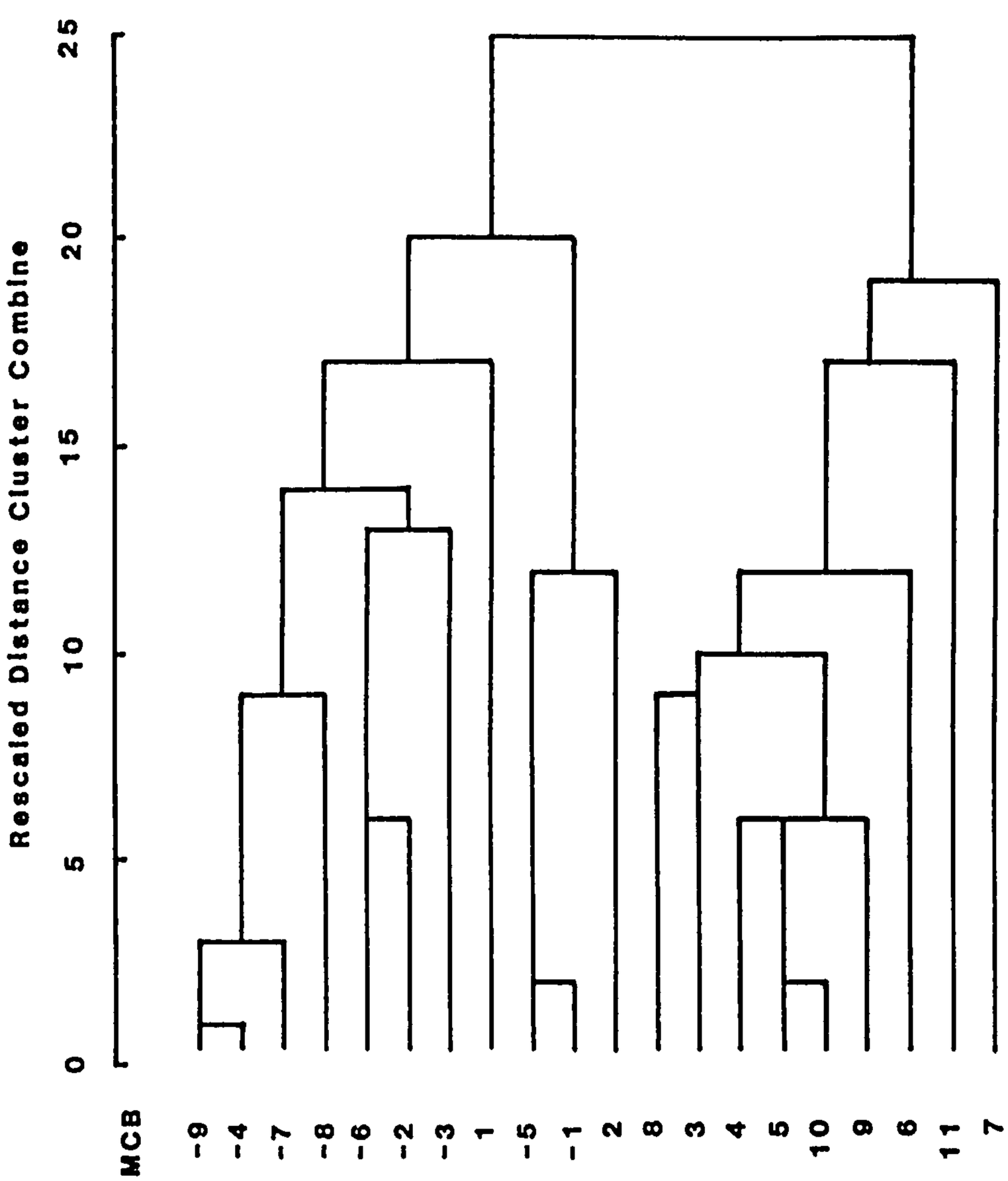

Figure 7.20 Dendrogram based on Cluster analysis of section MCB samples. See Fig. 7.18 for explanation of abbreviated sample numbering system.

Both associations are delimited at extremely similar confidence levels. These two associations are almost identical to those of the pre and post -MCB assemblages divided on the basis of the presence of the Mid-Cenomanian non-sequence, Carter and Hart (1977). The only slight deviation from this is that the two lowest samples within the post-MCB assemblage (MCB 0 --> 0.5 and MCB 0.5 --> 1) are included within the lower pre-MCB assemblage by the cluster analysis.

7.5. Section SFE, South Ferriby

7.5.1. Diversity

S - Overall Richness

A total of 19 samples from this section were processed for palynological analysis, but only four (SFE 18, 17, 16, 15) yielded any palynomorphs. All other samples were barren. As can be seen from Figure 7.21, these 4 productive SFE samples record a very restricted diversity assemblage. Number of dinoflagellate cysts species and total palynomorphs present are well below average, 22 (36.75) 44 and 24 (39.75) 48 respectively. Therefore, the SFE section records the lowest diversity of all sections studied herein. This characteristic of low diversity is further evidence in the support of the theory that the SFE section records a stressed assemblage.

H' - Shannon Index

Figure 7.22 displays the H' values of the four productive SFE samples. H' values range from 2.27 (2.45) 2.81 and are anomalously higher than is expected based on the overall diversity values. However this can be explained by the fact that Shannon index calculations take sample abundance into consideration. Thus, because of the extremely high numbers of cysts within these samples, higher than those recorded elsewhere in this analysis, Shannon index values are artificially raised. The trends identified by this statistical analysis add more evidence that the SFE section records a stressed, low diversity palynological assemblage.

7.5.2. Cluster analysis D - Dice co-efficient

A dendrogram based on the Dice co-efficient matrices of the four

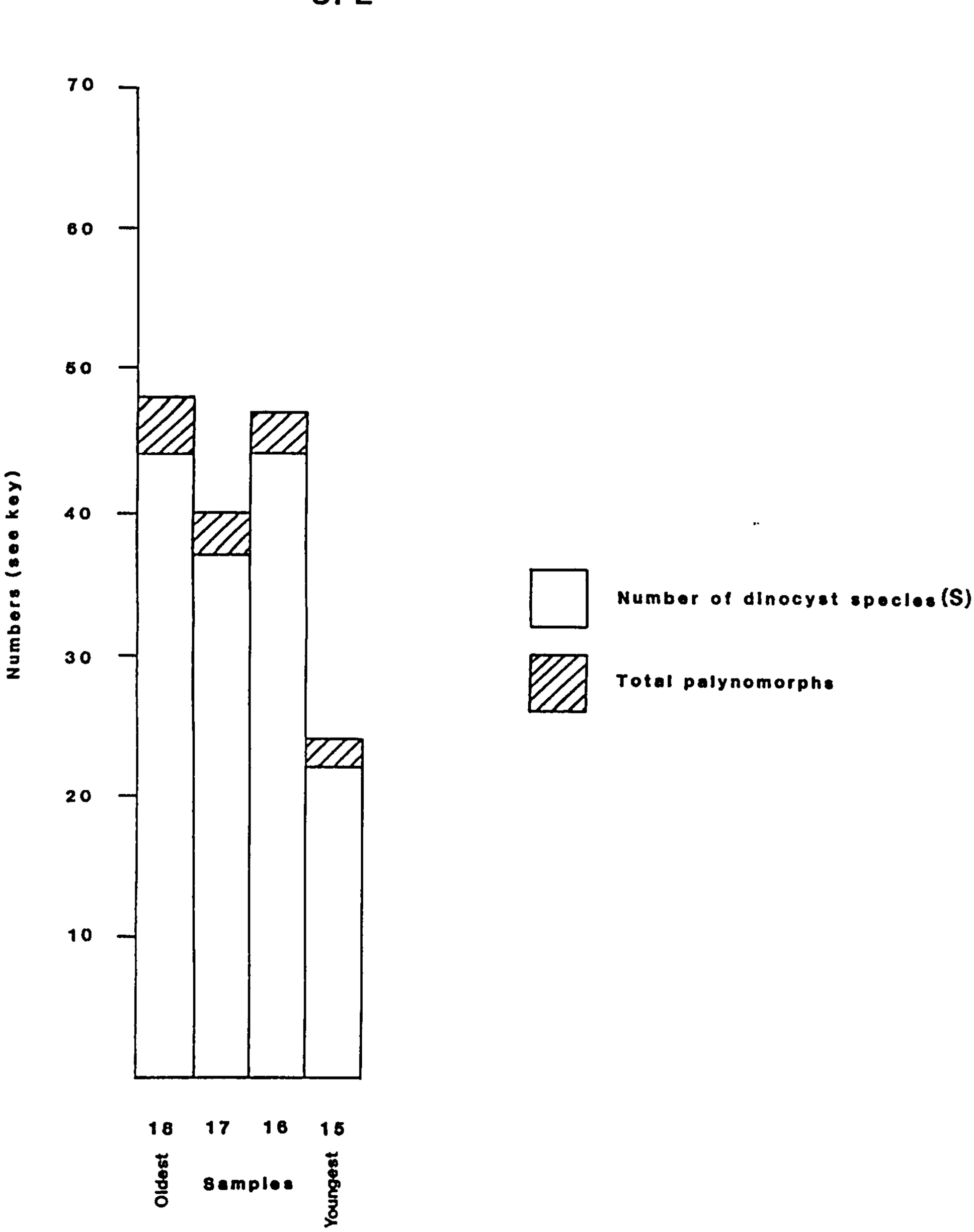

Figure 7.21 Species diversity for section SFE samples based on overall richness index values (S).

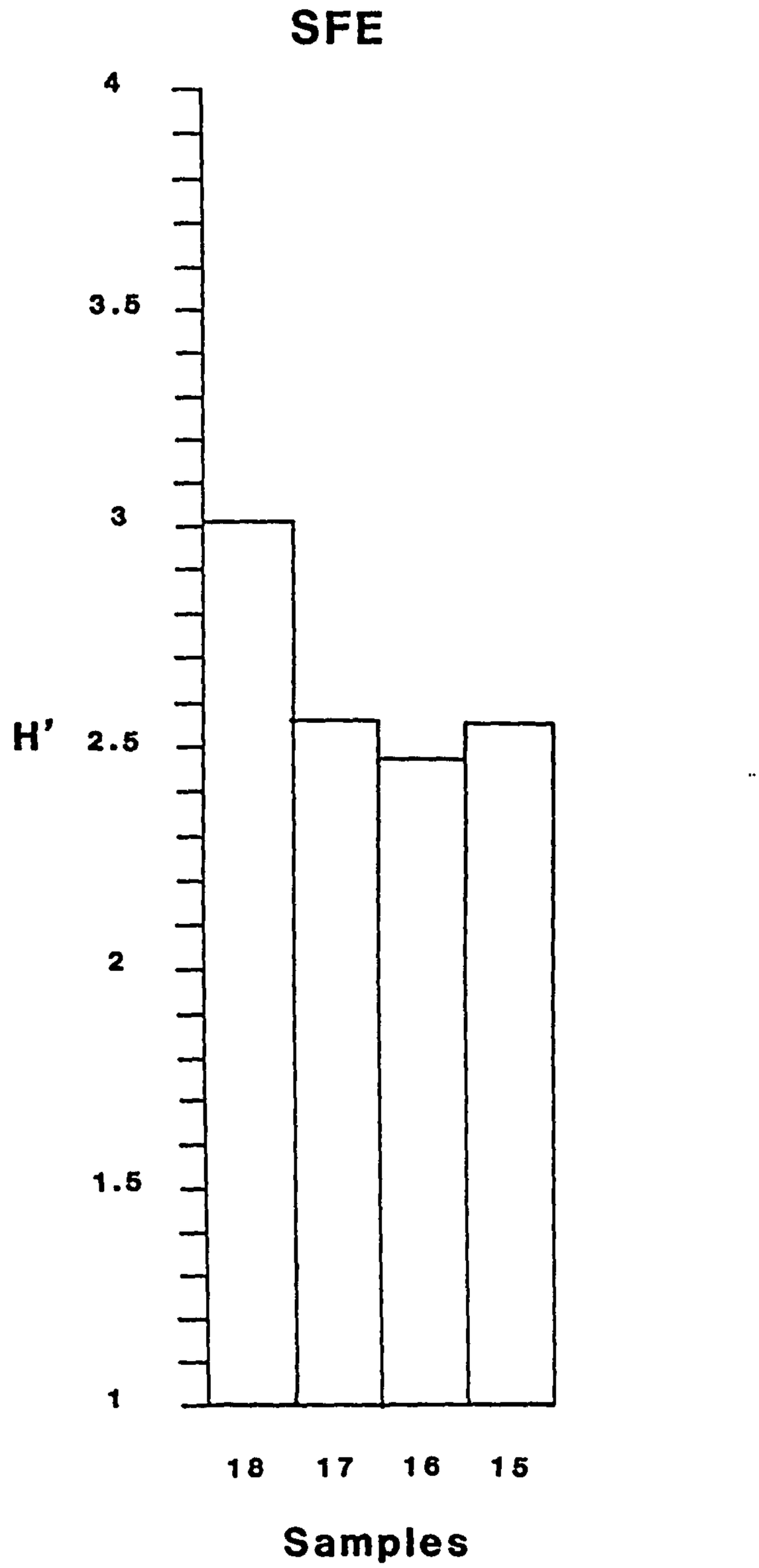

Figure 7.22 Species diversity for dinoflagellate cysts from section SFE samples based on Shannon index values (H').

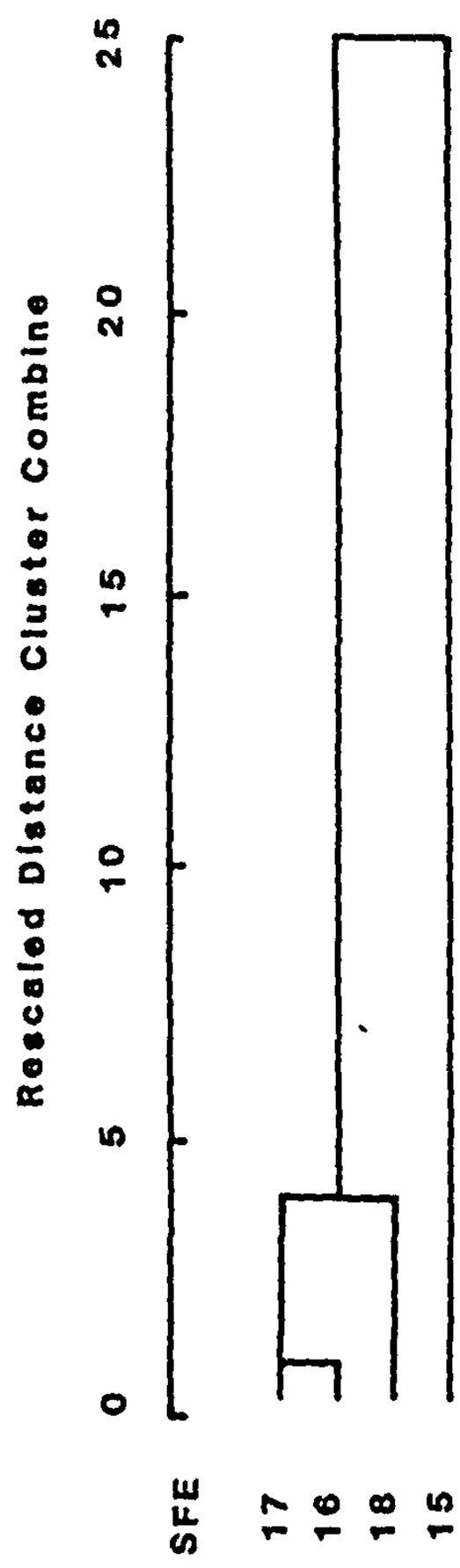

Figure 7.23 Dendrogram based on Cluster analysis of section SFE samples.

productive SFE samples is shown in Figure 7.23. Samples SFE 17 and 16 are closely linked at a high confidence level and indeed, their palynological appearance "down the microscope" (style of preservation and cyst content) imply that they are indeed very similar. In contrast, SFE 15 is strongly isolated due to its extreme dissimilarity to all other productive SFE samples, a feature also apparent from its preservational and palynological characteristics observed under the microscope. All these characteristics identified by the Dice co-efficient calculations are highly relevant to the interpretation that the SFE section records a stressed palynological assemblage, see Chapter 8 for more details.

Chapter 8

PALYNOLOGICAL RESULTS

8.1. Introduction

The sections investigated herein (Site 3a, TBB, MCB and SFE) yield well preserved, abundant and diverse dinoflagellate cyst assemblages with very minor percentages of spores and pollen, all of which indicate a Cenomanian age. This age is implied when comparisons are made to the known dinoflagellate cyst biostratigraphy of the Anglo-Paris Basin, as discussed previously in the Chapter 6 (Cookson and Hughes, 1964; Davey *et al.*, 1966; Clarke and Verdier, 1967; Davey, 1969a, 1970; Marshall, 1983; Marshall and Batten, 1988; Tocher and Jarvis, 1987; Jarvis *et al.*, 1987; Jarvis *et al.*, 1988a, 1988b; Leary *et al.*, 1989; Davey and Verdier, 1973, 1976; Verdier, 1975; Fauconnier, 1975, 1977; Foucher and Taugourdeau, 1975; Foucher, 1979, 1980, 1981, 1983; Harker and Sarjeant, 1975; Costa and Davey, 1992).

Because of the considerable wealth of knowledge on the dinoflagellate cyst biostratigraphy of the Cenomanian of the Anglo-Paris Basin, this study is not biostratigraphically orientated, as has been discussed in Chapter 1. Instead, particular features identified from other geological disciplines (micropalaeontology, sedimentology, stable isotope analysis etc.) as outlined in Chapter 2 are investigated with respect to palynology.

In the interpretation of dinoflagellate cyst abundance within the chalk and marl deposits investigated herein, the necessary assumption is made that a linear relationship exists between sediment thickness and sedimentation rate. Also, the effects of compaction, diagenesis and bioturbation on dinoflagellate cyst abundance are discounted as in the case of three of the four sections investigated (Site 3a, TBB and MCB), the effects of these post-depositional features are minimal. As it is not known whether the sedimentation and compaction rates for chalk and marl lithologies are the same or not, it is therefore assumed herein that they are indeed equal. Obviously, these assumptions are all unlikely to be true, however, this assumption-based argument is unavoidable.

The terrestrial component of the samples is not discussed in detail due to the small percentages of such palynomorphs present. The

terrestrial portion found, represented by spores (Plates 25-27), pollen (mainly bisaccate) (Plate 28), plant cuticles and tracheids only amounts to <2.5% of the overall palynomorph content. This very low percentage is considered to represent the more-or-less normal continuous "background" flux of terrestrial palynomorphs into the marine environment. Indeed, Habib and Miller (1989) stated that a sporomorph proportion of as much as 25% of the total palynomorph assemblage can be accounted for by background runoff from the neighbouring terrestrial source. Harker *et al.* (1990) also made reference to the low percentages of terrestrial taxa found occurring in dominantly marine palynomorph assemblages which can be regarded as standard runoff from the adjacent palaeocoastline.

The occurrence of acritarchs and fossil prasinophytes in each sample was noted in the form of their percentage presence or as presence/absence data. Acritarch species of the genera *Veryhachium* and *Michrystridium* are present in extremely low percentages (<1.2%) in the majority of samples from all sections examined. However, identification beyond the generic level was not attempted. Species of *Pterospermopsis* and *Tasmanites* are both present in almost negligible proportions (<0.3% for each group). Illustrations of all the above groups are given in Plates 29 and 30.

The percentage occurrence and varying morphology of organic foraminiferal test linings found are also documented. Such linings appear to be a cosmopolitan feature of almost all samples examined. However, only foraminiferal linings of six chambers or more were included (Traverse and Ginsburg, 1966). The term "microforaminifera" was applied to such foraminiferal linings by Traverse and Ginsberg (1966) because the best preserved linings are very often those of small Foraminifera. Pantic and Bajraktarevic (1988) have proposed the name "palynoforaminifera" for such preservation of foraminifera in palynological preparations of Mesozoic and Tertiary deposits. Within this study, three different types of foraminiferal lining morphologies were noticed; Type 1 (Pl. 31, Figs 1,2) is both trochospiral and planispiral, Type 2 (Pl. 31, Figs 3,4) is biserial and Type 3 (Pl. 31, Figs 5,6) appear branched.

Palynofacies analysis was carried out in the investigation of two sections (sections TBB and SFE), using the Bujak *et al.* (1977a) classification scheme which involves the identification of four

different kerogen types. Phyrogen (palynomorphs and plant cuticle), hylogen (structured non-opaque woody material), melanogen (unstructured opaque material) and amorphogen (structureless "fluffy" amorphous algal material). Bujak *et al.* (1977b) attached palaeoenvironmental significance to their kerogen types (Bujak *et al.*, 1977a) as follows. Phyrogen occurs in all environments, both terrestrial and marine. Hylogen predominates in shallow-water deposits. The kerogen type melanogen predominates in shallow water deposits. Finally, amorphogen is common in marine deposits and is generally absent from non-marine facies.

Estimations of the relative percentages of palynofacies types present within the unoxidised palynological preparations were made. This involves a semi-qualitative approach of averaging the relative percentage presence of each of the palynofacies types occurring in ten randomly selected fields of view of each sample. Such relative percentage values of palynofacies types present classify the identified palynofacies association.

8.2. Site 3a section

This section records a dominantly marine palynomorph assemblage, indicating open marine conditions. The marine component (dinoflagellate cysts, acritarchs, pterospermopsis and tasmanites) of the palynomorphs present varies between 97.5 - 99.66%; whereas the terrestrial percentages (spores and pollen) are very low indeed (0.34 - 2.5%). The dinoflagellate cyst associations present within Site 3a are very similar to dinoflagellate associations identified by Harker *et al.* (1990), subgroups A3, 5A and 5B, which are indicative of normal open marine conditions (see Appendix 6).

Dinoflagellate cyst species present indicate that this section is within the Middle Cenomanian *Epelidosphaeridia spinosa* subzone of Davey (1970). A range chart of all palynomorphs recorded within this section is given in Figure 8.1, and Appendix 1 contains all numerical raw data produced from counts.

Number of dinoflagellate cysts per gramme of sediment of this section indicates a moderate to high abundance, as values vary between 52 - 552 (Figure 8.2). However, samples from this site were processed and prepared without the benefit of quantitative aliquot slides. Laterly, in order to give some idea on the palynological abundance of this section, aliquot slides were made after the strewn slides had been prepared. For consistency, aliquot slides were made from the remaining residue which was made up to the same volume as that used for the other sections. Thus, the residues from this section, diluted by the prior removal of amounts necessary to make strewn mount slides, give artificially lower numbers of cysts per gramme of sediment than would otherwise be expected.

However, even bearing this limitation in mind, the variation in abundance values of these samples, measured as number of dinoflagellate cysts per gramme of sediment, shows a strong correlation to lithology. Marl samples consistently yield more abundant assemblages (224-552 dinoflagellate cysts/gm.) than do chalk samples (52-418 dinoflagellate cysts/gm.), see Figure 8.2. It can therefore be concluded that marl deposition records a more abundant situation than does chalk deposition, with respect to dinoflagellate cysts.

Dinoflagellate cyst species diversity levels for this section shown in Figures 8.3a and 8.3b, are discussed in greater

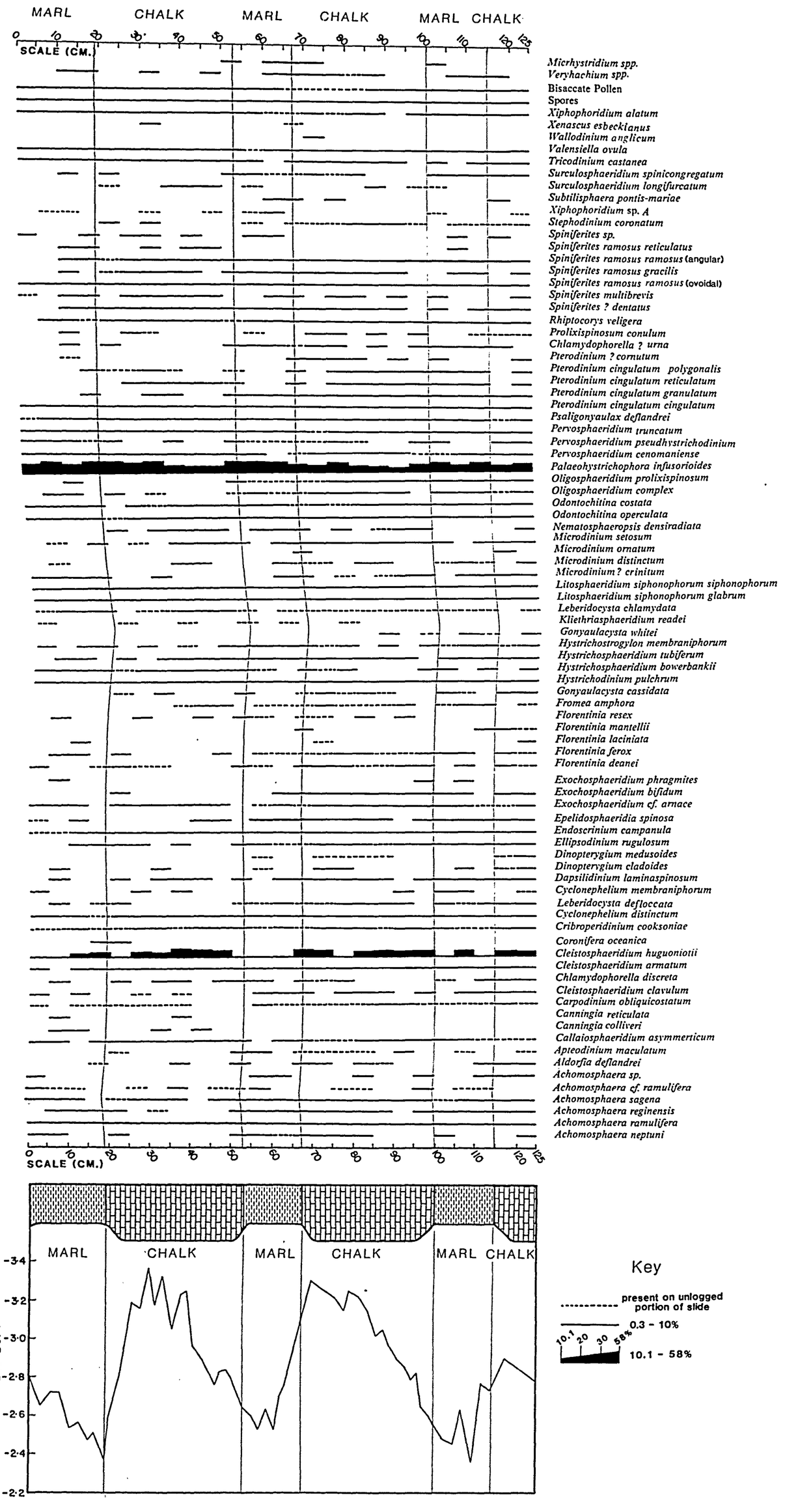

Figure 8.1 Range chart of the dinoflagellate cyst species and other palynomorph taxa of Site 3a together with $\delta^{18}O$ signature from Ditchfield and Marshall (1989).

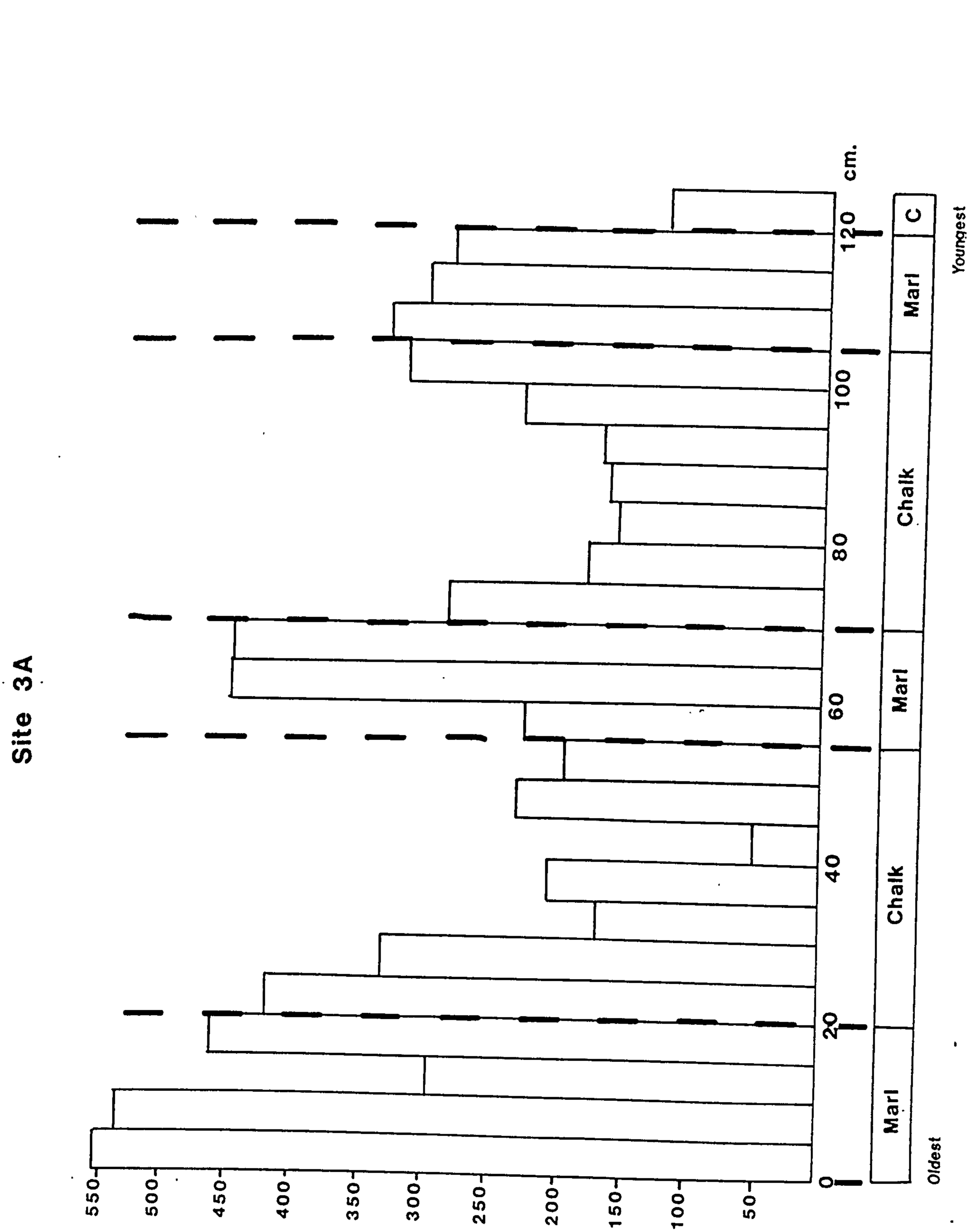

Figure 8.2 Abundance values for Site 3a samples based on number of dinoflagellate cysts per gramme of sediment.

detail in the Chapter 7. In summary however, both measurements of diversity indicate that the majority of samples within this section record a moderately diverse dinoflagellate assemblage, with a minor number indicating lower diversity levels. However, this variation in diversity levels cannot be linked to differing lithology nor to any of the particular features under investigation within this section which have been substantiated by other statistical analysis of the dinoflagellate cyst assemblages. The levels of diversity are consistent with moderate relative diversity levels of cyst communities A and E of Goodman (1979) which are typical of a more offshore palaeoenvironment.

Examination of the range chart (Figure 8.1) will show that the assemblages are dominated by *Palaeohystrichophora infusorioides* (Pl. 17, Fig. 1-3) (21-65%), with significant contributions of *Cleistosphaeridium huguoniotii* (Pl. 3, Figs 9,10) (9-25%), *Achomosphaera* spp. (Pl. 1, Figs 1-10) (3-9%), *Spiniferites* spp. (Pl. 20, Figs 1-8; Pl. 21, Figs 1-3) (2-9%) and *Cyclonephelium distinctum* Deflandre and Cookson 1955 (Pl. 6, Fig. 1) (1-6%). The remaining species, which usually represent <1% of the assemblage vary only slightly within the section, some range through-out and others have a very sporadic/patchy distribution, with every gradation in between.

The percentage distribution of some dinoflagellate cyst species exhibit a strong correlation to lithology as can be seen in Figures 8.4 to 8.8. Numbers of the species *P. infusorioides* increase markedly in marl samples when compared to their numbers in chalk samples (Figure 8.4). Conversely, species such as *C. huguoniotii, C. distinctum, Achomosphaera* spp., *Spiniferites* spp., *Callaiosphaeridium asymmetricum* (Deflandre and Courtville) Davey and Williams 1966a (Pl. 2, Fig. 3), *Cribroperidinium cooksoniae* Norvick 1976 (Pl. 4, Figs 1-7), *Hystrichodinium pulchrum* Deflandre 1935 (Pl. 10, Fig. 5; Pl. 11, Fig. 5) and *Pterodinium cingulatum* subspecies (Pl. 18, Figs 5-9; Pl. 19, Figs 1-5) (Figures 8.5 to 8.8) all increase in numbers in chalk samples.

It is realised that because the dinoflagellate cyst assemblages are dominated by one species, *P. infusorioides*, that its percentage distribution affects that of all other species. However, it is believed that distributions of some dinoflagellate cyst species as outlined above, are linked to the type of sediment being deposited.

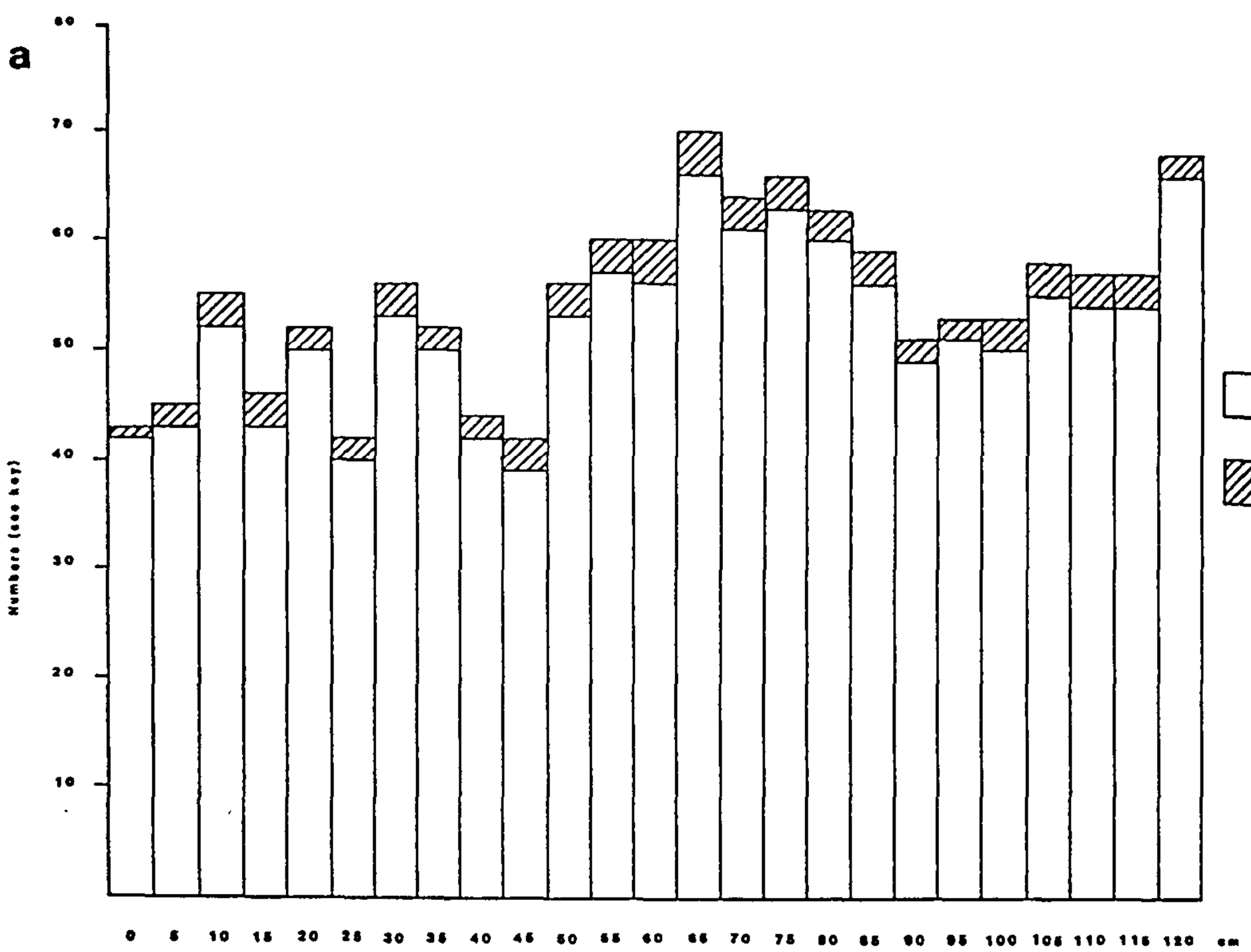

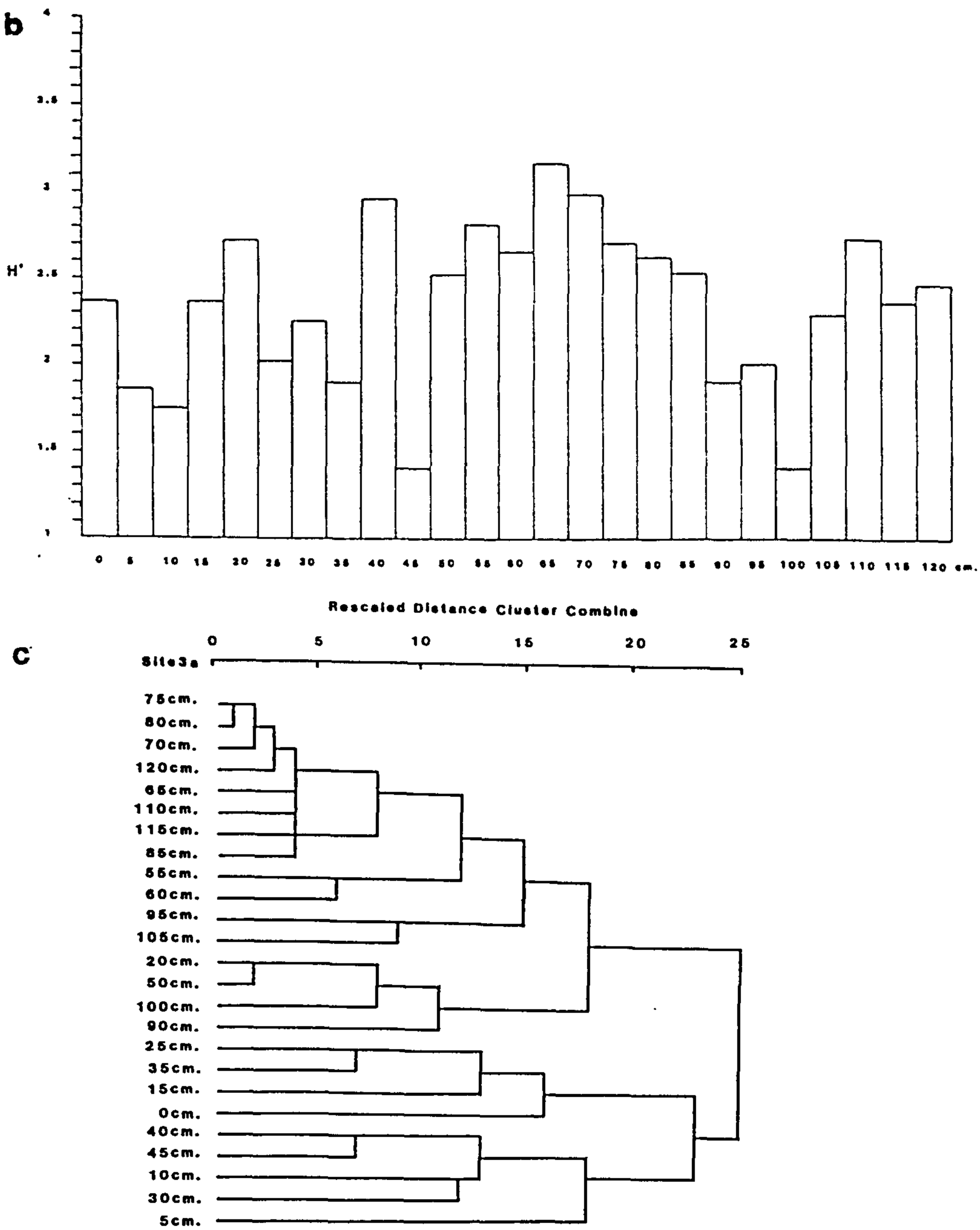

Figure 8.3 Summary of statistical analyses of Site 3a samples.
a. Overall species diversity index (S). b. Shannon species diversity index (H'). c. Cluster analysis dendrogram.

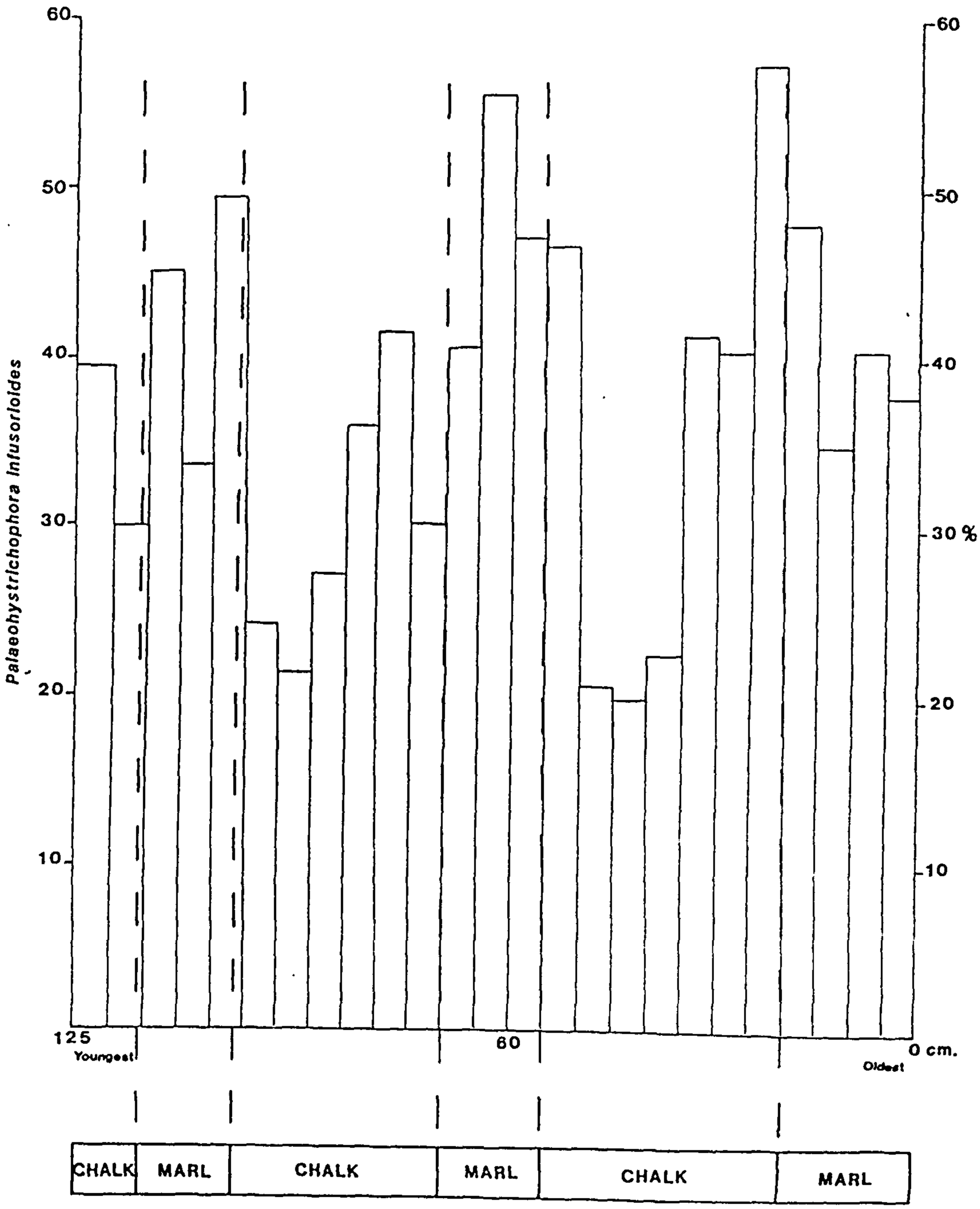

Figures 8.4 Percentage distribution of dinoflagellate cyst species within section Site 3a sample which show a relationship to lithology.

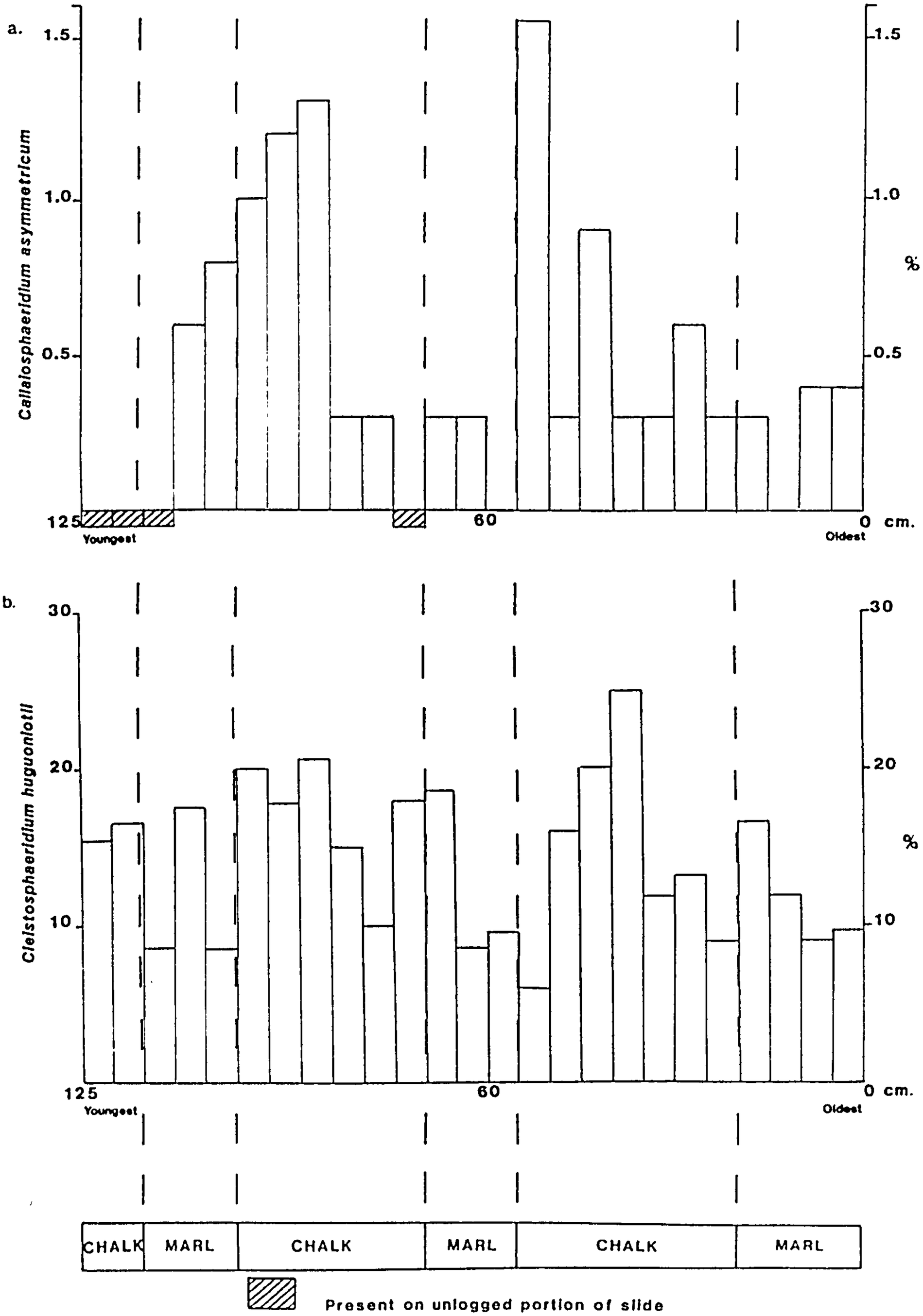

Figure 8.5 Percentage distribution of dinoflagellate cyst species within section Site 3a sample which show a relationship to lithology.

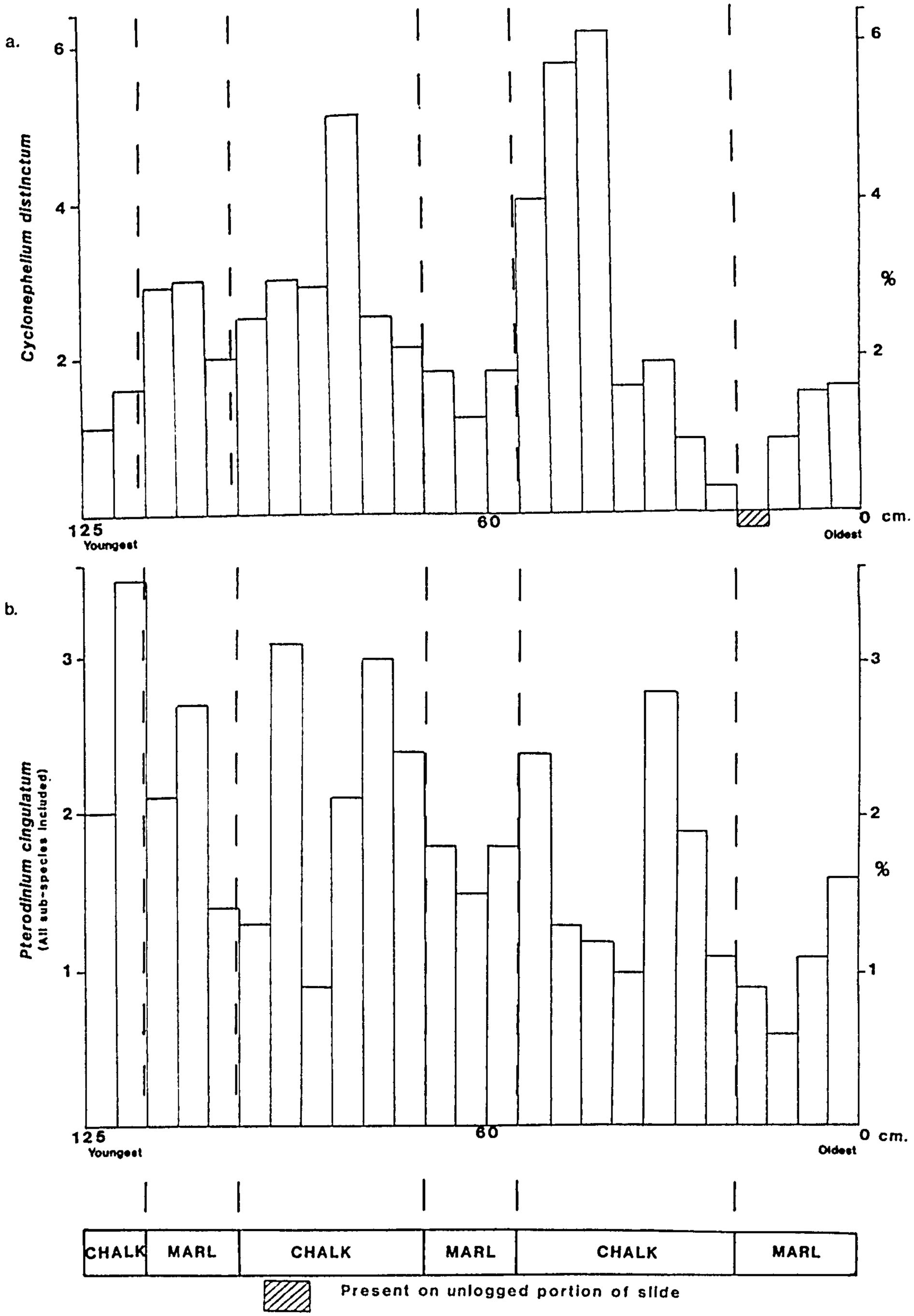

Figure 8.6 Percentage distribution of dinoflagellate cyst species within section Site 3a sample which show a relationship to lithology.

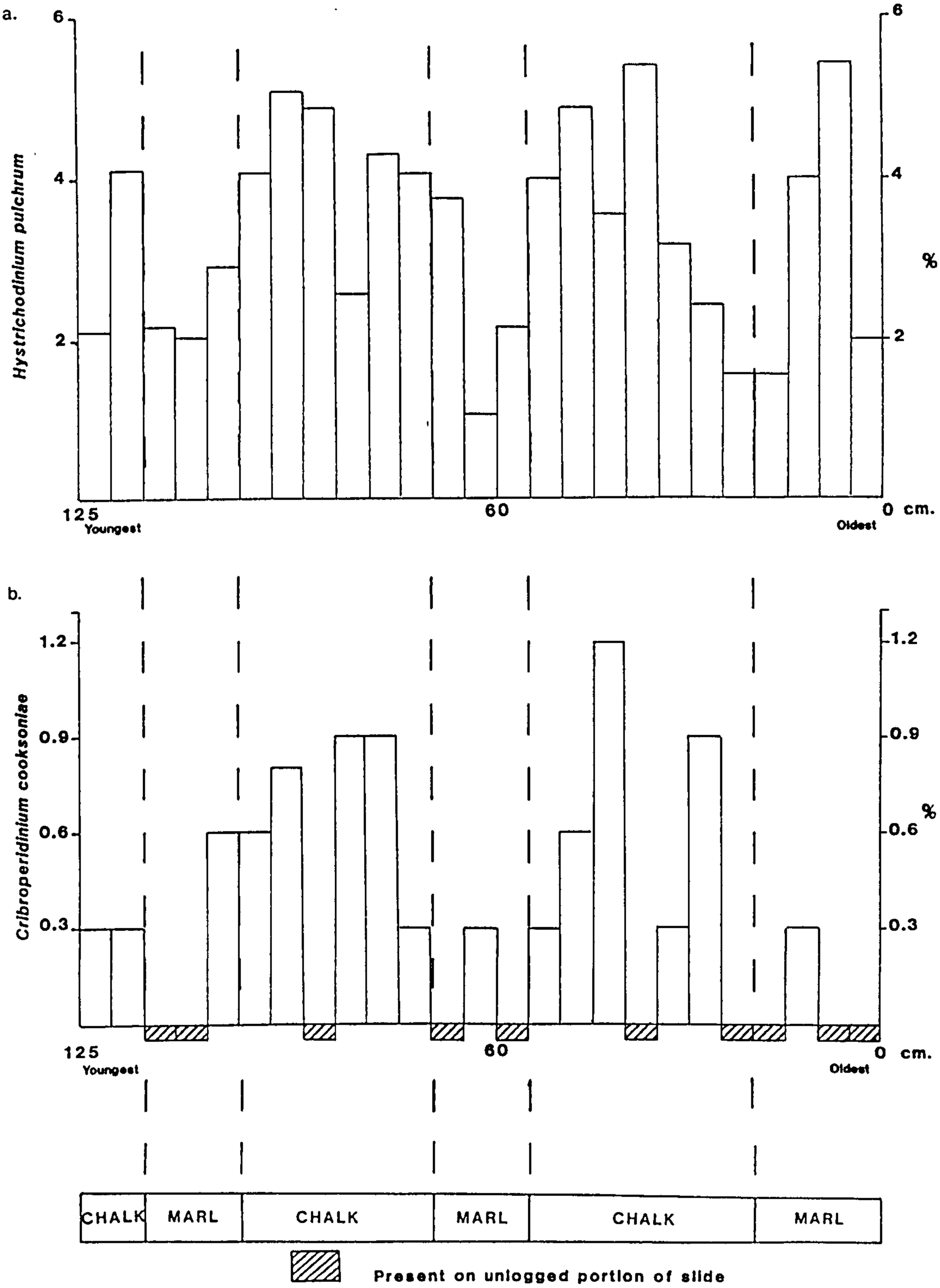

Figure 8.7 Percentage distribution of dinoflagellate cyst species within section Site 3a sample which show a relationship to lithology.

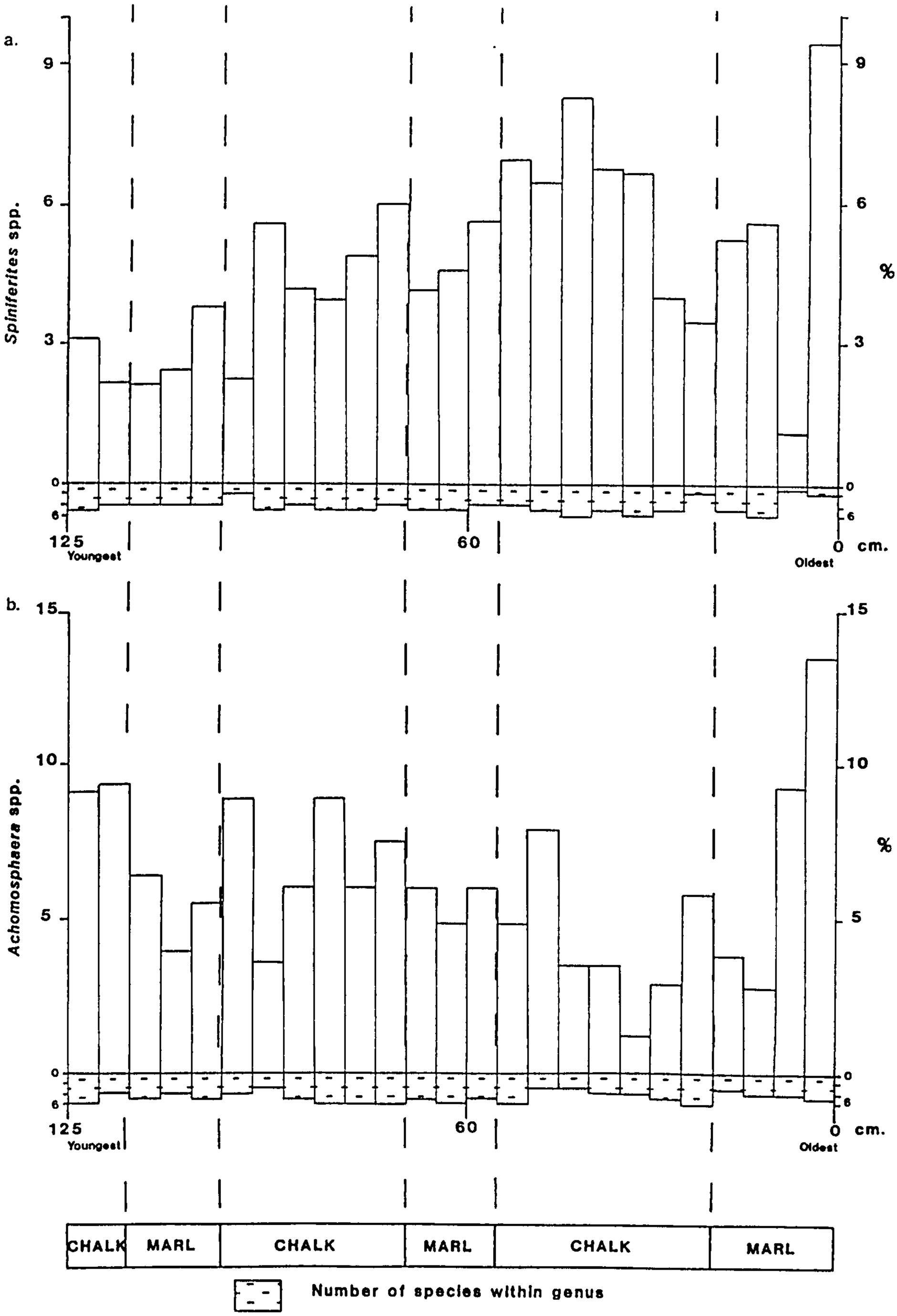

Figure 8.8 Percentage distribution of dinoflagellate cyst species within section Site 3a sample which show a relationship to lithology.

Ditchfield and Marshall (1989) investigated the stable isotopic variation of the rhythmically bedded chalks and marls of Site 3a. This revealed that there is a cyclical variation in the oxygen isotope composition of the carbonate component, which can be explained by palaeotemperature fluctuations (Ditchfield and Marshall, 1989). Their analysis was carried out on the same section as examined palynologically herein, however, their samples were taken at a sampling interval of 2cm, an interval of less than the scale of rhythmic bedding. This stable isotopic analysis was carried out to investigate the lithological rhythmicity that characterises the Cenomanian chalk sequence of south-east England, as discussed in Chapter 2. This cyclicity may be caused by many mechanisms ranging from palaeoclimatical to tectonic, eustatic to Milankovitch forcing (Einsele, 1982; Eder, 1982; Hallam, 1986; Read *et al.*, 1986; Barron *et al.*, 1985; Arthur *et al.*, 1986; Robinson, 1986b; Hart, 1987).

The oxygen and carbon signatures of Site 3a from Ditchfield and Marshall (1989) are shown in Figure 8.9. Examination of this figure shows that chalks ($\delta^{18}O$ -2.7°/oo to -3.3°/oo) and marls ($\delta^{18}O$ -2.3°/oo to -2.9°/oo) have different oxygen isotope composition which vary in a cyclical manner. The carbon isotope signature (Figure 8.9) shows no obvious lithologically related trends and all $\delta^{13}C$ values fall within the expected range of normal marine carbonates (Hudson, 1977).

Ditchfield and Marshall (1989) have discounted the effects of diagenesis, variations in the water chemistry and different nannofossil compositions as possible causes of the isotopic variation. It therefore seems likely that the variation in $\delta^{18}O$ values is due to primary temperature control, Ditchfield and Marshall (1989). Calculations carried out (Ditchfield and Marshall, 1989) imply that the marl samples yield an average temperature of formation of 23°C, and chalks give a mean temperature of formation of 25°C. Extreme values of palaeotemperatures are 22°C for marls and 26.5°C for chalks. Therefore, chalks are interpreted as recording higher surface water temperature conditions than marl deposits. Ditchfield and Marshall (1989) infer that this variation in sea-surface temperature, which at a maximum varies as much as 4.5°C from chalks to marls, could be due to variations in insolation levels which are caused by orbital forcing (Berger, 1983).

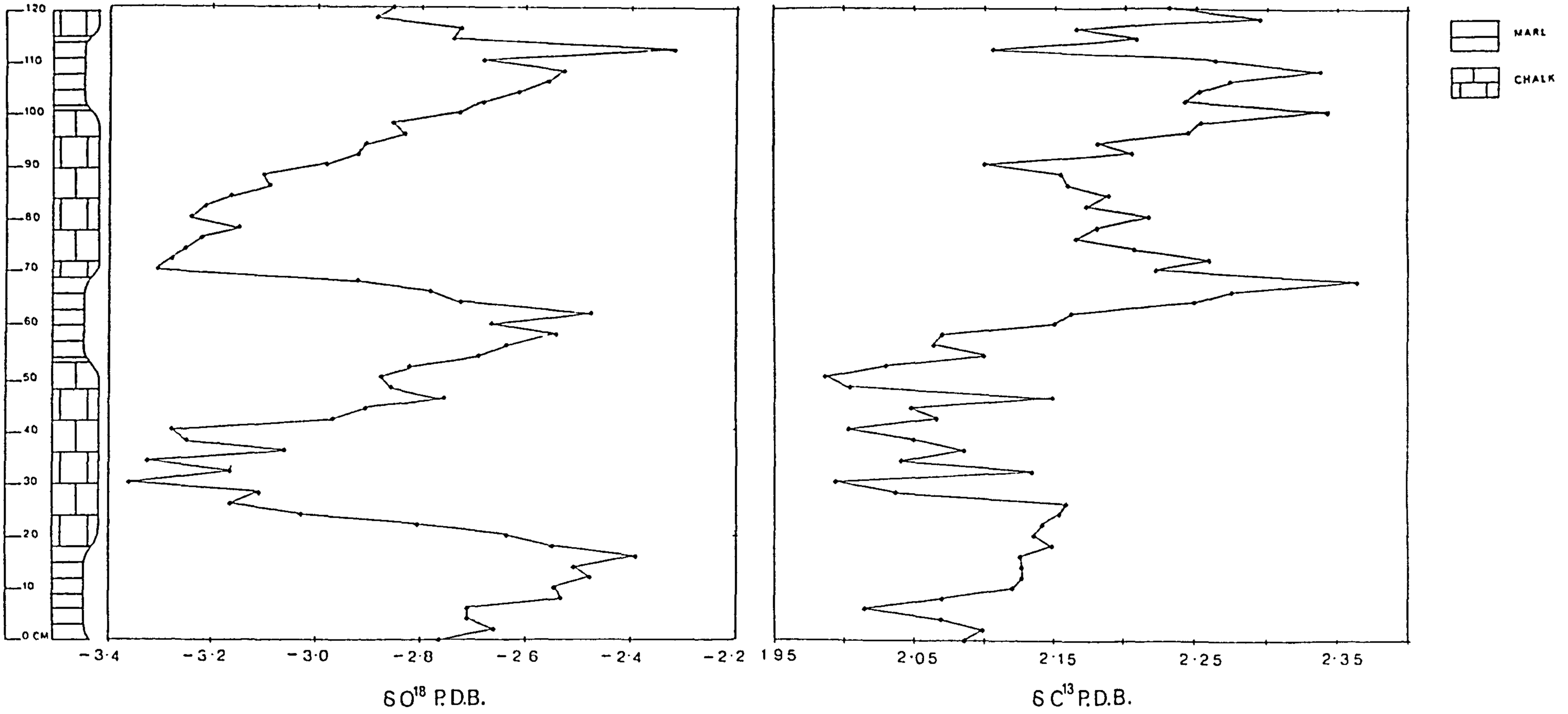

Figure 8.9 Oxygen and Carbon stable isotopic composition of Site 3a samples, from Ditchfield and Marshall (1989).

Jeans *et al.* (1991) have also recognised that trends within the $\delta^{13}C$ values of foraminifera of chalk-marl couplets within of the *Plenus* Marls sequence of Dover reflect a primary signal which is most probably controlled by variations in palaeotemperature. Periods of marl deposition are also interpreted by Jeans *et al.* (1991) as reflecting lower palaeotemperatures than those of chalk deposition.

As documented previously, some dinoflagellate cyst species show percentage distributions which are related to lithology. From the oxygen isotopic composition of the Site 3a (Ditchfield and Marshall, 1989), the distribution of such dinoflagellate species may be linked to palaeotemperature. Therefore, *P. infusorioides* (Figure 8.4) present in higher numbers in marl deposits than in chalks may now be interpreted as a slightly cooler water cyst (in comparison to chalks), favouring average palaeotemperatures of 23°C, and capable of withstanding 22°C. Those cysts found to increase numerically in chalks (*C. huguoniotii, C. distinctum, C. asymmetricum, C. cooksoniae, H. pulchrum, P. cingulatum* subspecies, *Achomosphaera* spp. and *Spiniferites* spp.) (Figures 8.5 to 8.8) can be interpreted as slightly warmer water species. Such dinoflagellate cyst species may be interpreted as favouring mean palaeotemperatures of 25°C and as high as 26.5°C.

It can be further concluded that the suite of dinoflagellate cyst species encountered in Site 3a can be inferred, from the work of Ditchfield and Marshall (1989), to have existed in a water mass niche experiencing a range of sea-surface palaeotemperature of 22 to 26.5°C.

In order to investigate further the features identified by Ditchfield and Marshall (1989) as outlined above, two methods of multivariate analysis were employed to the palynological data of Site 3a; Fast fourier transform (FFT), a method of spectral analysis and Autocorrelation. A detailed documentation of these methods is given in Chapter 7. However, in summary, such techniques enable the identification of otherwise hidden trends or cycles in multivariate data sets such as those produced herein.

Methods of spectral analysis treat such multivariate data sets as time series. However, in such stratigraphical time series the relationship between sediment thickness and time is not accurately known. Therefore, in order to analyse such time series as these in a mathematical manner, many inherent limitations need to be realised.

For example, the results of compaction, diagenesis, bioturbation, and variable sedimentation rate cannot be accounted for, but all result in the fact that the relationship between sediment thickness and time is non-linear.

In the study of the Pleistocene, such use of spectral analysis has great potential in the investigation of Milankovitch cyclicity (Anderson, 1984; Imbrie *et al.*, 1984; Imbrie, 1985). Milankovitch (1941) suggested that glacial/interglacial transitions which characterise the Pleistocene, are the result of periodic variations in the Earth's orbital elements. These variations comprise the precessional cycle (21,000 year cycle), the Earth's obliquity periodicity (40,000 year cycle) and the eccentricity cycle (100,000 year cycle), Lockwood (1980). Olsen (1986) has applied fourier analysis in the investigation of Milankovitch cyclicity within Triassic lake sediments of North America.

The application of FFT proved successful in the identification of cyclicity of differing frequencies within the thirty-one data sets examined, for more details see Chapter 7. These data sets fall into two groups, the first based on the percentage presence of twenty individual dinoflagellate species which occur through-out the section and the second on morphological groupings of cysts. This second category, that of the morphological groups comprises thirty-two data sets under the following headings. Number of individual data sets within each group is given in brackets after each category heading.

Peridinioid cysts (1)

Gonyaulacoid cysts (1)

P cyst and G cyst groups (Evitt, 1985) (10)

Cyst complexes (2)

Archaeopyle type (5)

Cyst morphology (10)

Number of species recorded in the count (a) (1)

Total number of palynomorphs recorded on slide (b) (1)

b/a (as above) (1)

Examination of the frequency 'v' amplitude spectra outputs of the FFT programme in Figures 7.4 to 7.14 and in the summary Figures 8.10 and 8.11, shows that 38% of all data sets exhibited a cycle frequency representing a sediment thickness of 20 and 40 cm., and an

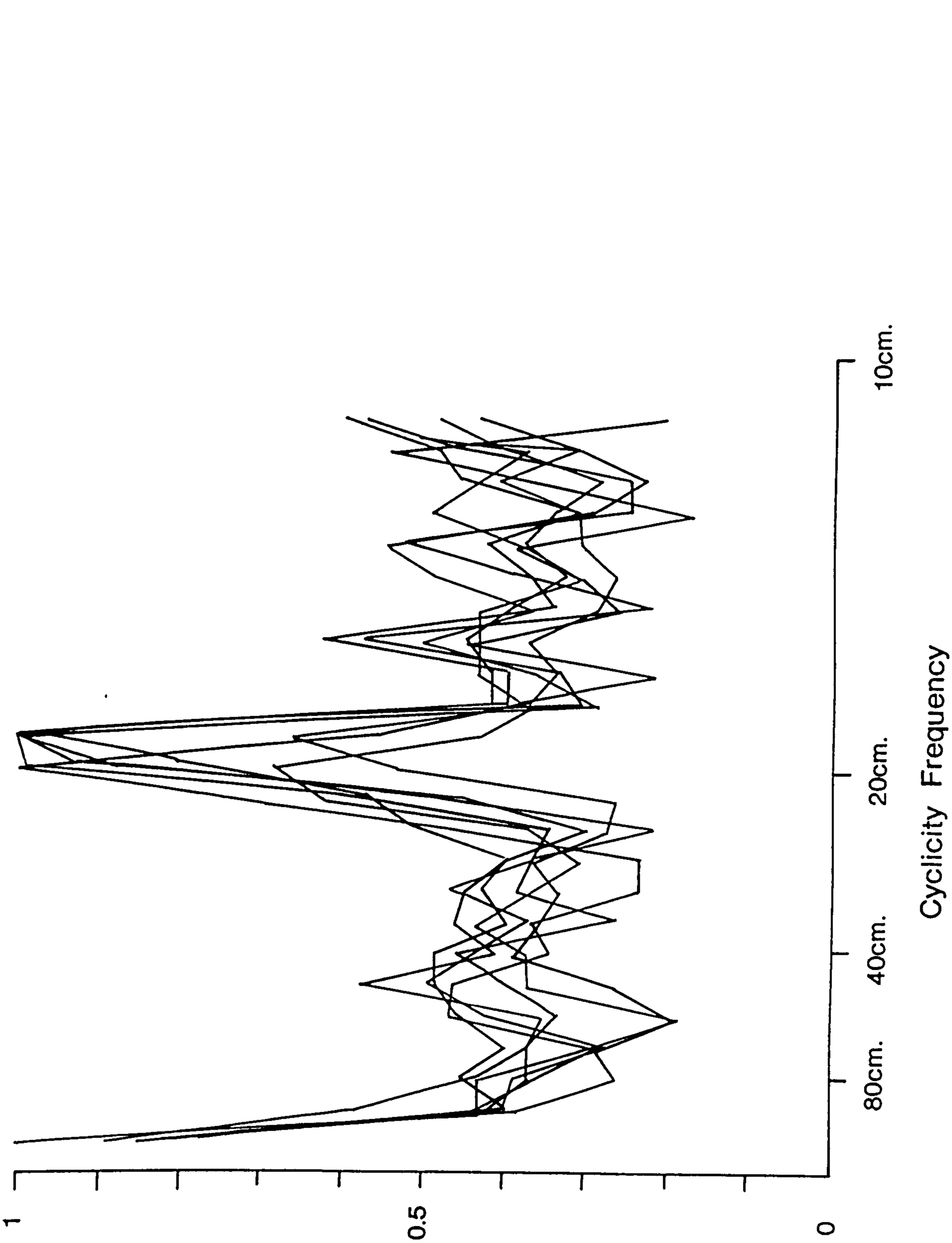

Figure 8.10 Composite frequency (f) 'v' amplitude (a) spectra produced from six individual plots of f 'v' a spectra which exhibit 20 cm. cyclicity frequency.

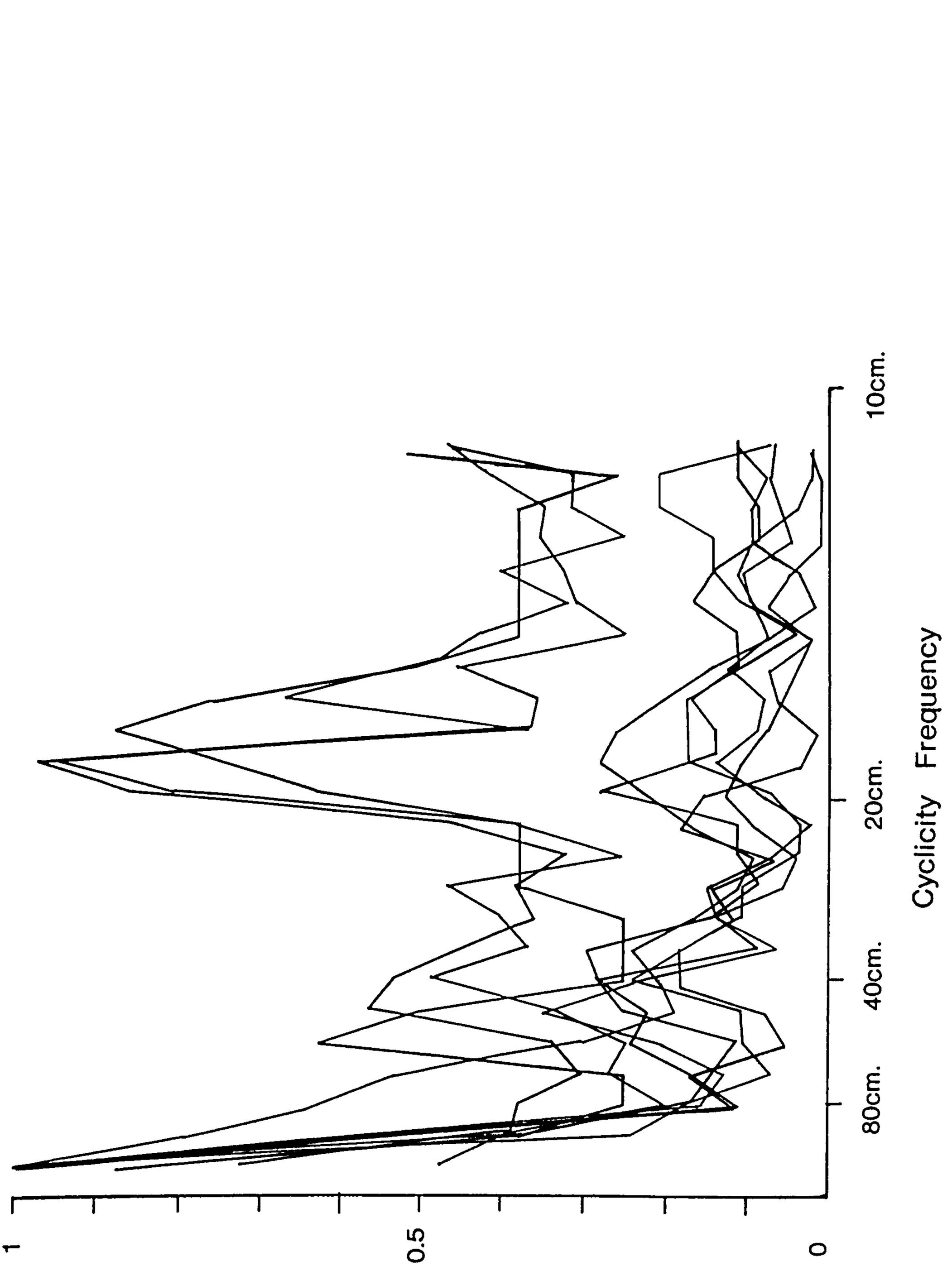

Figure 8.11 Composite frequency (f) 'v' amplitude (a) spectra produced from eight individual plots of f 'v' a spectra which exhibit 20 and 40cm. cyclicity frequencies.

almost equal percentage (34%) were found to record a periodicity which represents a 20cm. thickness of sediment. These results show that the dinoflagellate cyst distributions are influenced by lithology. Typical bed thickness of a marl is 20cm. and that of a chalk bed is typically 40cm (see Figure 3.5). Thus, the results of spectral analysis substantiate the conclusion derived independently, that distribution of dinoflagellate cyst species of Site 3a are related to lithological variation.

However, Gale (1989a) in an attempt at assessing the amount of time represented by individual rhythms has suggested that cyclicity of 40cm. sedimentary thickness within the Cenomanian represents the precessional cycle of 21,000 years (Milankovitch, 1941). This deduction was made by Gale (1989a) using the most complete composite sections available within the Cenomanian of the Anglo-Paris. Using a simplistic approach Gale (1989a), (in an extension of Hart, 1987) divided up the duration of the Cenomanian based on radiometric dates, by the total number of rhythms present.

Autocorrelation was carried out on the dinoflagellate cyst species assemblages of Site 3a. Details of the autocorrelation technique are given in Chapter 7. The same data sets as used in the fast fourier transform method were investigated. Unfortunately, due to the limitations caused by the small data set size, the results of autocorrelation proved spurious and therefore inconclusive and as a result they have not been included nor documented herein.

Cluster analysis was also employed in the investigation of the dinoflagellate cyst assemblages of Site 3a (Figure 8.3c); see Chapter 7. This analysis indicates that there is a very high degree of similarity between all the dinoflagellate cyst associations exhibited by Site 3a. Broadly speaking, cluster analysis of this section appears to identify two groups of samples, the first from 0cm. to 45cm. and the second from 50cm. to 120cm. However, these groupings are not interpreted further as they are not related in any way to lithology nor to any other feature or trend identified in the dinoflagellate analysis of Site 3a.

The palynological content of Site 3a is anomalous when compared to all other sections, in that it lacked a foraminiferal test lining content. Some individual chambers of foraminiferal tests were recorded, but none were sufficiently complete enough such that they

could be recorded (*i.e.* >6 chambers), see Traverse and Ginsburg (1966). The fact that only individual chambers were found probably indicates that this is an artifact introduced by processing bias.

8.3. TBB Section

This section records a dominantly marine palynomorph assemblage, indicative of an open marine situation. The dinoflagellate cyst associations recorded are strongly comparable to the subgroups A3, 5A and 5B of Harker *et al.* (1990) and are thought to indicate a marine situation with normal salinities (see Appendix 6). The marine palynomorphs present (dinoflagellate cyst, acritarchs, pterospermopsis and tasmanites) constitute between 98.98 - 99.83% of the assemblage with only an extremely minor terrestrial contribution (0.17 - 1.02%) of spores and pollen.

Dinoflagellate cyst species present within this section suggest assignment to the Middle Cenomanian *Epelidosphaeridia spinosa* subzone (Davey, 1970), on the basis of the almost consistent presence of *E. spinosa* and *P. cingulatum polygonalis* throughout the section. On the basis of lithostratigraphy however, the lower four samples (TBB -3 to TBB 1) are within the Lower Cenomanian, see Figure 3.7. However, considering the presence and distribution of such key dinoflagellate cysts, this section in its entirety is believed to be assignable to the Middle Cenomanian dinoflagellate cyst subzone (*E. spinosa)* of Davey (1970).

Appendix 2 contains all raw numerical data for this section and the range chart of the palynomorph content of section TBB is given in Figure 8.12. The content of the dinoflagellate cyst assemblage is extremely similar to that of Site 3a. As is typical of Cenomanian palynomorph assemblages, the species *P. infusorioides* dominates, representing between 21.6 and 61.6% of dinoflagellate species present. Considerable contributions are made by the following species; *C. huguoniotii* (8.4 - 51.6%); *Surculosphaeridium longifurcatum* (Firtion) Davey *et al.* 1966 (Pl. 22, Fig. 2) (0 - 7.6%); *Achomosphaera* spp. (1.1 - 9.6%); *Spiniferites* spp. (2.2 - 12.9%); *Litosphaeridium siphonophorum* subspecies (Pl. 12, Figs 1-6; Pl. 13, Figs 1-4) (1.5 - 6%). The remaining dinoflagellate cyst species typically represent 1% or less of the palynomorph content and display ranges which vary from through-out the section to only sporadic occurrences.

Counts of the number of dinoflagellate cysts per gramme of sediment imply that this is a abundant palynomorph assemblage. Values of number of dinoflagellate cysts per gramme of sediment vary from 198 - 630, see Figure 8.13. However, as can be seen in Figure

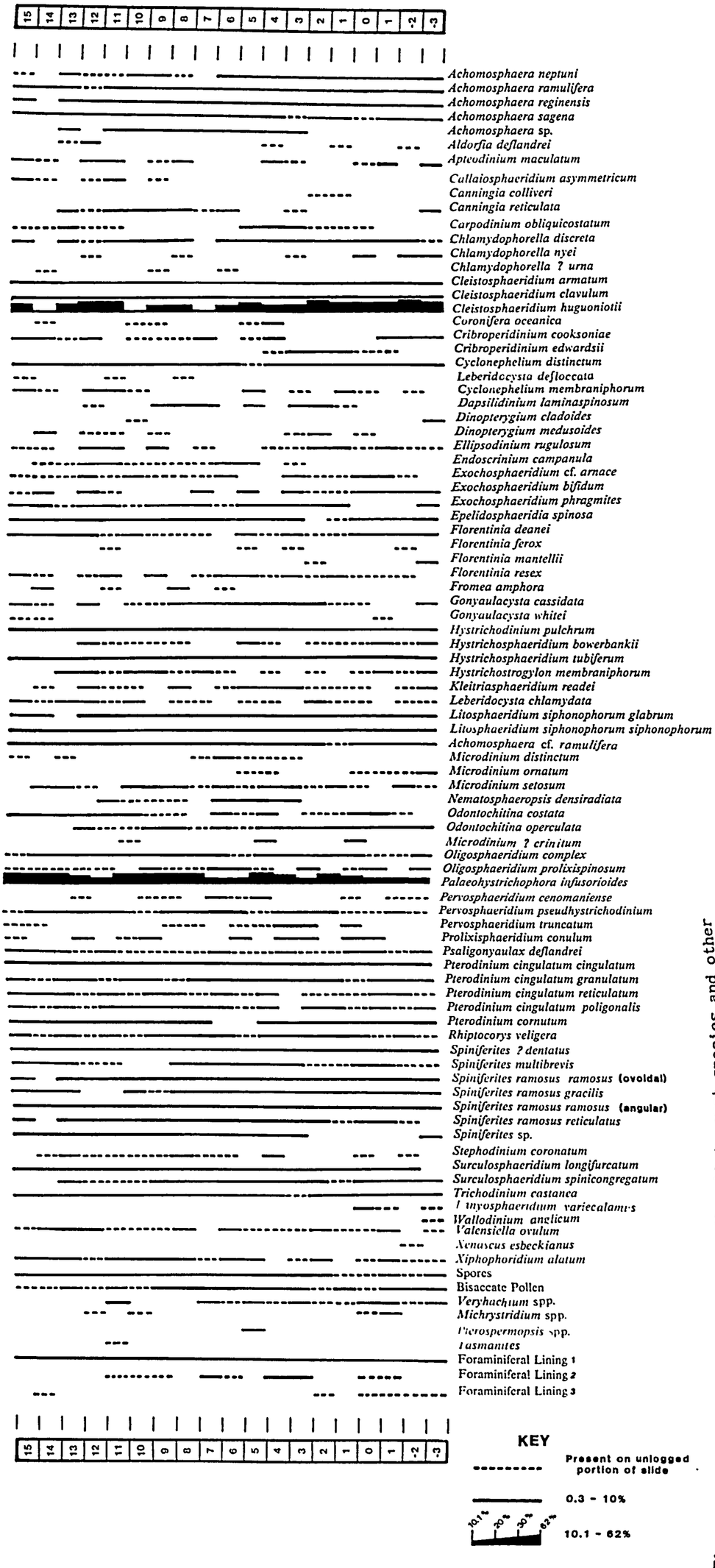

Figure 8.12 Range chart of the dinoflagellate cyst species and other palynomorph taxa of the TBB section.

8.13, it became apparent that certain samples (TBB -3, -1, 13 and 15) within this section which had been oxidised, yielded anomalously low values of abundance. In order to investigate this further, quantitative aliquot slides were subsequently made of the unoxidised portion of the remaining residues of these samples. As a result, it has been conclusively proven that oxidation causes considerable loss (up to 68%) of the palynomorph content of samples. Figure 8.13 shows uncorrected and corrected values of abundance based on whether samples have been oxidised or not. For more details see Chapter 4. It is believed that this loss is mechanical rather than chemical, due to the introduction of an extra stage of processing.

When comparison of abundance values is made to the lithological log of section TBB (Figure 3.8), it can be seen that there is a relationship between the number of dinoflagellate cysts per gramme of sediment and lithology. Marls consistently yield higher abundance values ($\bar{x}$ = 507 dinoflagellate cyst/gm.) than do both marly chalk ($\bar{x}$ = 417 dinoflagellate cysts/gm.) and chalk lithologies ($\bar{x}$ = 411 dinoflagellate cysts/gm.). Thus, analysis of the abundance signature of section TBB substantiates the evidence suggested by similar analysis of Site 3a, that marl deposits record period of higher abundance, than do both marly chalk and chalk lithologies.

Ditchfield (1990) investigated the carbon isotopic signature of the TBB section (Figure 8.14). This analysis was carried out to investigate the possible mechanisms causing the Mid-Cenomanian non-sequence of Carter and Hart (1977) which characterise this section and the next (section MCB). This identified a positive $\delta^{13}C$ excursion of up to +1.4 $^{o}/_{oo}$ relative to PDB. As can be seen in Figure 8.14, $\delta^{13}C$ values rise steadily from +1.6$^{o}/_{oo}$ (samples TBB -3 to 6) to +3.0$^{o}/_{oo}$ (sample TBB 7) and fall again to +1.8$^{o}/_{oo}$ (samples TBB 8 to 15). Ditchfield (1990) believes that the $\delta^{13}C$ excursion of section TBB represents a lowering of sea-level due to regression and a restriction of circulation between the Anglo-Paris Basin and the opening Atlantic ocean.

As has been mentioned previously in Chapter 2, the Cenomanian-Turonian boundary sequence of north-west Europe is associated with a $\delta^{13}C$ excursion (Schlanger *et al.*, 1987; Jarvis *et al.*, 1988a) exhibiting $\delta^{13}C$ values as high as +4$^{o}/_{oo}$ and +3.4$^{o}/_{oo}$, respectively. Obviously, when compared to such values, the $\delta^{13}C$

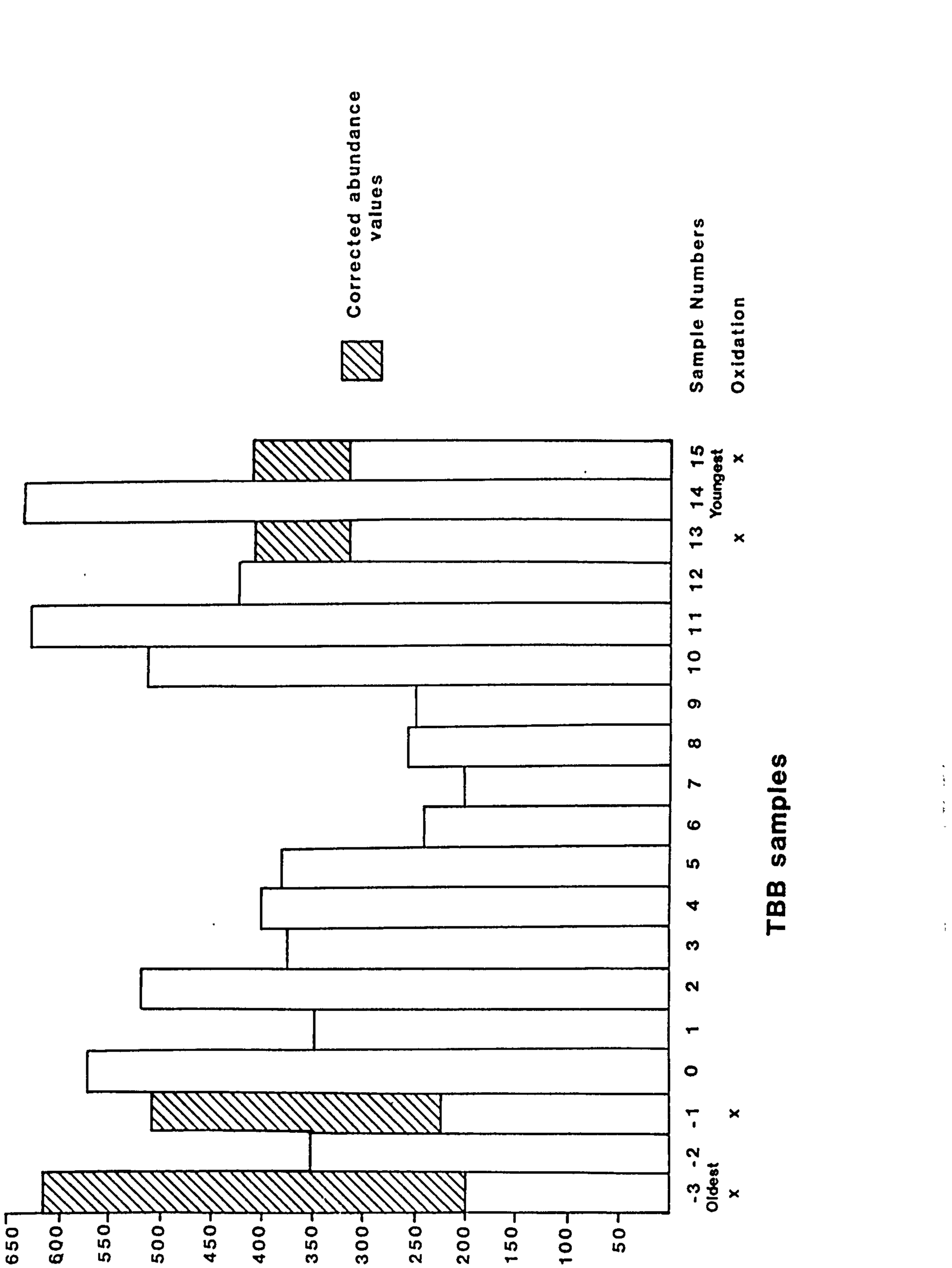

Figure 8.13 Abundance values for section TBB samples based on number of dinoflagellate cysts per gramme of sediment.

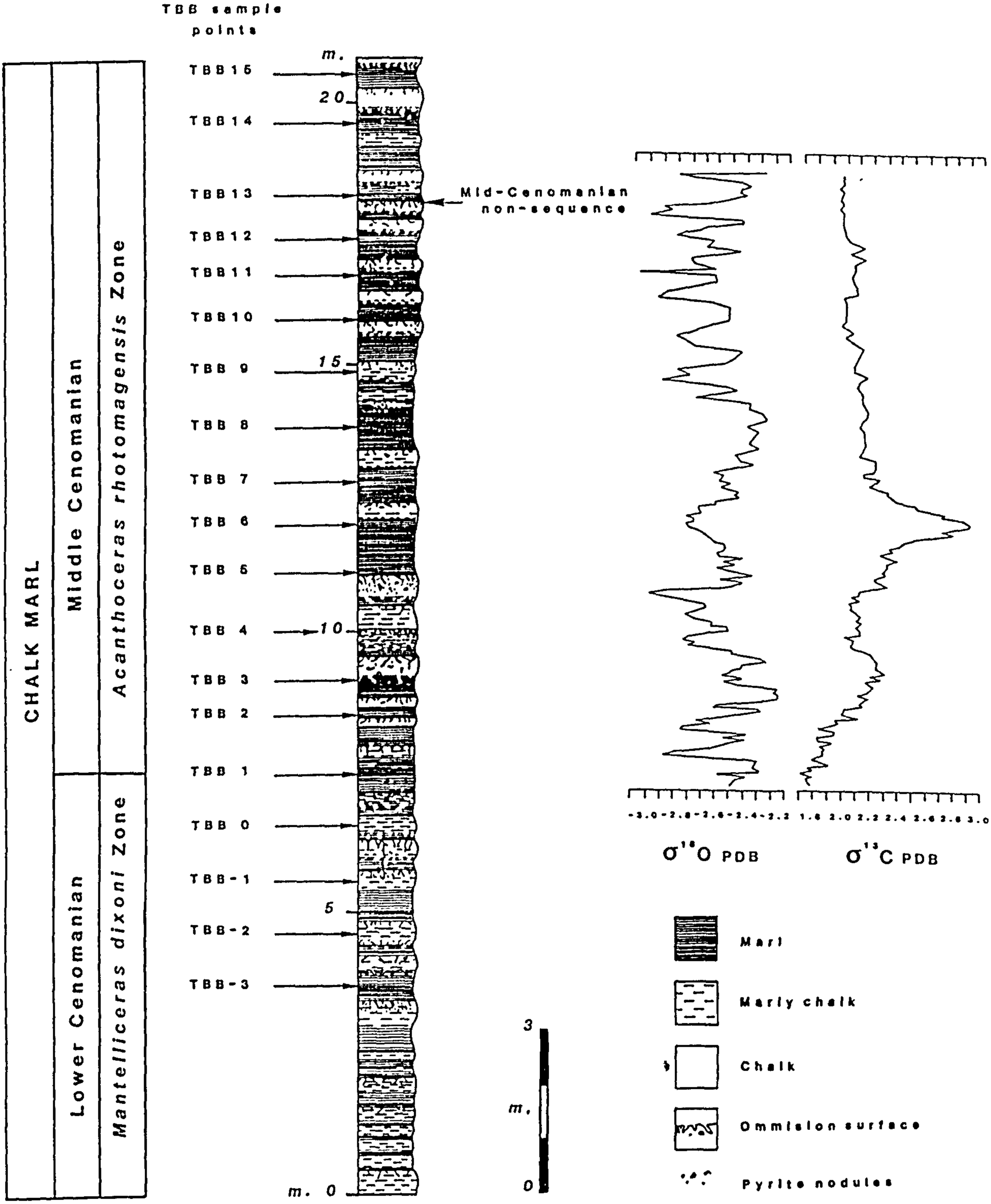

Figure 8.14 Carbon and Oxygen stable isotopic signatures for part of the TBB section, from Ditchfield (1990).

values as yielded by the TBB section are of a much lower magnitude, however, the overall profile of the signature is similar. Also, the TBB section does not record anoxic/dysaerobic conditions which characterise the Cenomanian-Turonian boundary event.

Gale (1989a) has noticed the presence in the Middle Cenomanian of a similar faunal association or 'pulse faunas' which characterise the Cenomanian-Turonian boundary event. Such 'pulse faunas' are a Boreal association of belemnites, brachiopods and bivalves. The foraminiferal content of this TBB section also displays features which can be linked to the $\delta^{13}C$ excursion, Leary (1989, *pers. comm.)*. Deeper dwelling planktonic foraminifera taxa (*Rotalipora* spp. and *Praeglobotruncana* spp.) decrease in size and become temporarily extinct at the peak of the $\delta^{13}C$ excursion after which they reappear again. *Hedbergella* spp. also decrease in size, but continue throughout the Middle Cenomanian. Benthonic foraminifera remain consistent and maintain high diversity levels during this time period. Also, there is a local flood of the planktonic foraminiferan *Favusella* at the level of the $\delta^{13}C$ excursion, Hart (1992, *pers. comm.*).

The distribution of the corrected values of abundance of section TBB (Figure 8.13) exhibit a trough centered on sample TBB 7. When compared to the $\delta^{13}C$ signature (Ditchfield, 1990) (Figure 8.14), there appears to be an inversely proportional relationship between δ^{13} values and numbers of dinoflagellate cyst per gramme of sediment. Therefore, samples exhibiting the positive δ^{13}excursion are marked by a period of reduced abundance of dinoflagellate cysts.

Section TBB records a higher species diversity assemblage than that of Site 3a. Species diversity levels present in this section compare with the high levels species diversity of cyst community B and A/B transition of Goodman (1979), which are indicative of a more offshore palaeoenvironment. Variations in species diversity are not related to abundance, as expressed by number of cysts per gramme of sediment, nor to lithology. However, both diversity indices used (see Chapter 7) indicate that species diversity of the dinoflagellate cyst assemblages of section TBB is linked to the fact that the section records a enrichment with respect to $\delta^{13}C$ in sample TBB 7. The distributions of these two species diversity indices (Figures 8.15a, 8.15b) exhibit lower than average values of species diversity in sample TBB 7. Indeed, the overall richness index of

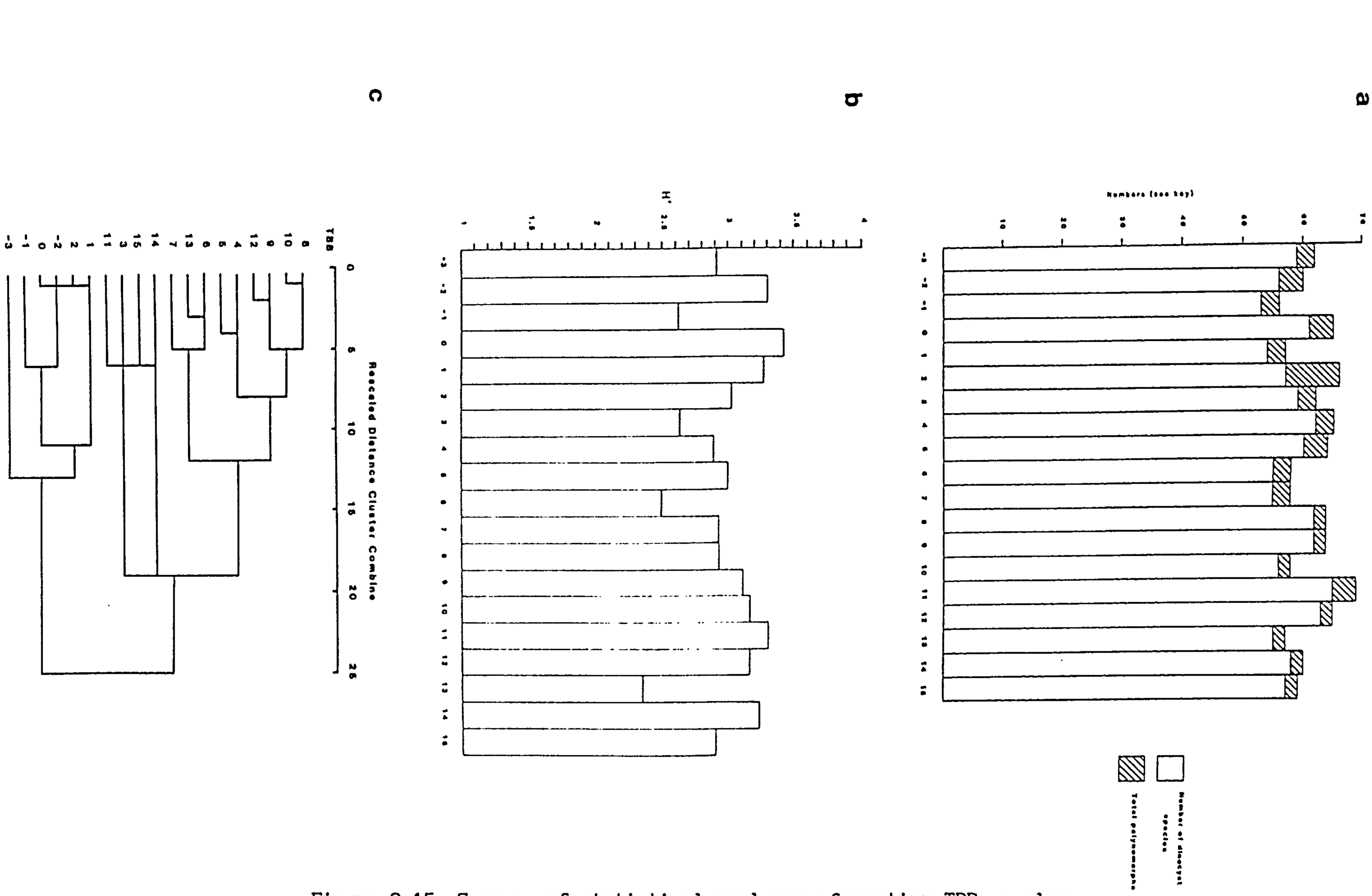

Figure 8.15 Summary of statistical analyses of section TBB samples. a. Overall richness species diversity index (S). b. Shannon species diversity index (H'). c. Cluster analysis dendrogram.

species diversity (S) indicates that pre-TBB 7 samples record a more diverse assemblage with a mean diversity value of 59.2, when compared to post-TBB 7 samples, which only reach an average species diversity level of 57.5. Thus, the presence of a $\delta^{13}C$ excursion within this section adversely affects species diversity and pre-TBB 7 samples record a more species diverse assemblage than post-TBB 7 samples.

The variations in both abundance and species diversity of dinoflagellate cysts as described above, are related to the peak in the $\delta^{13}C$ excursion which is present in the Middle Cenomanian TBB section. However, distributions of the individual species themselves are extremely uniform throughout the TBB section (Figure 8.12), and do not demonstrate such a relationship. This is confirmed by the cluster analysis method (Figure 8.15c). Because of this lack of variation in the ranges of dinoflagellate cyst species of section TBB, the theory that the $\delta^{13}C$ excursion is caused by a lowering of sea-level (Ditchfield, 1990) cannot be conclusively discussed. However, the fact that both abundance and species diversity are affected implies that somewhat adverse conditions affecting both dinoflagellate cyst numbers and species diversity prevailed within the water mass at this time. Thus, the dinoflagellate cyst assemblages of TBB section imply that there was a change in the water mass causing temporary unfavourable conditions, the forcing mechanism of which unfortunately remains unsure on the basis of palynological analysis alone.

Cluster analysis of the dinoflagellate cyst assemblages of this TBB section did not indicate the presence of similar associations associated with the presence of the $\delta^{13}C$ excursion. However, this method does identify the presence of two associations (Figure 8.15c), the first representing the lower 5m. of the section (samples TBB -3 to 2) and the second grouping the remaining upper 15m. of the section (samples TBB 3 to 15). The lower of these two associations (TBB -3 to TBB 2) is almost co-incident to the Lower Cenomanian part of this section (TTB -3 to TBB 1), see Figure 3.7. The Lower Cenomanian basal part of this section is defined solely on lithostratigraphy and is not biostratigraphically significant, based on the distribution and presence/absence of key dinflagellate cysts.

However, in order to further understand and interpret the associations identified by cluster analysis, an investigation into the palynofacies content of the section was undertaken. The decision

to perform such an investigation was a consequence of the recognition within the SFE section of a relationship between associations defined by cluster analysis and those distinguished by palynofacies analysis.

The palynofacies associations, as identified using Bujak *et al.* (1977a) and (1977b) tentatively correspond to the two associations identified by cluster analysis of section TBB. See Appendix 7 for relative palynofacies percentages of each individual sample and Figures 8.16 to 8.18 for photomicrographs of each sample. However, some samples within each of the associations deviate strongly from the overall palynofacies characteristics of that association, notably TBB 7, TBB 13 and TBB 15. Therefore, a definitive classification and delineation of these associations cannot strictly be defined. However, in the broadest of terms the following is a summary of the results of this technique:

Palynofacies association of samples TBB -3 to 2 (Figure 8.16)

Min	(Mean)	Max	
45	(48.17)	55%	Phyrogen
35	(39.17)	40%	Amorphogen
7	(9.17)	10%	Melanogen
1	(2.83)	5%	Hylogen

Palynofacies association of samples TBB 3 to 15 (Figures 8.17 & 8.18)

Min	(Mean)	Max	
55	(61.85)	70%	Phyrogen
15	(25.15)	35%	Amorphogen
9	(11.08)	15%	Melanogen
1	(2.69)	5%	Hylogen

This analysis has shown that the palynofacies of section TBB are dominated to a greater or lesser extent by phyrogen and have significant percentages of amorphogen, with minor percentages of both melanogen and hylogen. The palynofacies thus indicate that this section was deposited in a marine environment (Bujak *et al.*, 1977b). The particular kerogen types which vary noticeably from one association to the other are phyrogen and amorphogen, whereas the relative percentages of melanogen and hylogen remain fairly constant in both. There appears to be an inversely proportional relationship between amounts of phyrogen and amorphogen present. However, as the

Figure 8.16 (Page 262)

Palynofacies photomicrographs of TBB samples, magnification x112. See Appendix 7 for palynofacies percentages of each individual sample.

1 TBB-3

2 TBB-2

3 TBB-1

4 TBB 0

5 TBB 1

6 TBB 2

Figure 8.17 (Page 263)

Palynofacies photomicrographs of TBB samples, magnification x112. See Appendix 7 for palynofacies percentages of each individual sample.

1 TBB 3

2 TBB 4

3 TBB 5

4 TBB 6

5 TBB 7 ($\delta^{13}C$ excursion sample)

6 TBB 8

Figure 8.18 (Page 264)

Palynofacies photomicrographs of TBB samples, magnification x112. See Appendix 7 for palynofacies percentages of each individual sample.

1 TBB 9

2 TBB10

3 TBB11

4 TBB12

5 TBB13

6 TBB14

7 TBB15

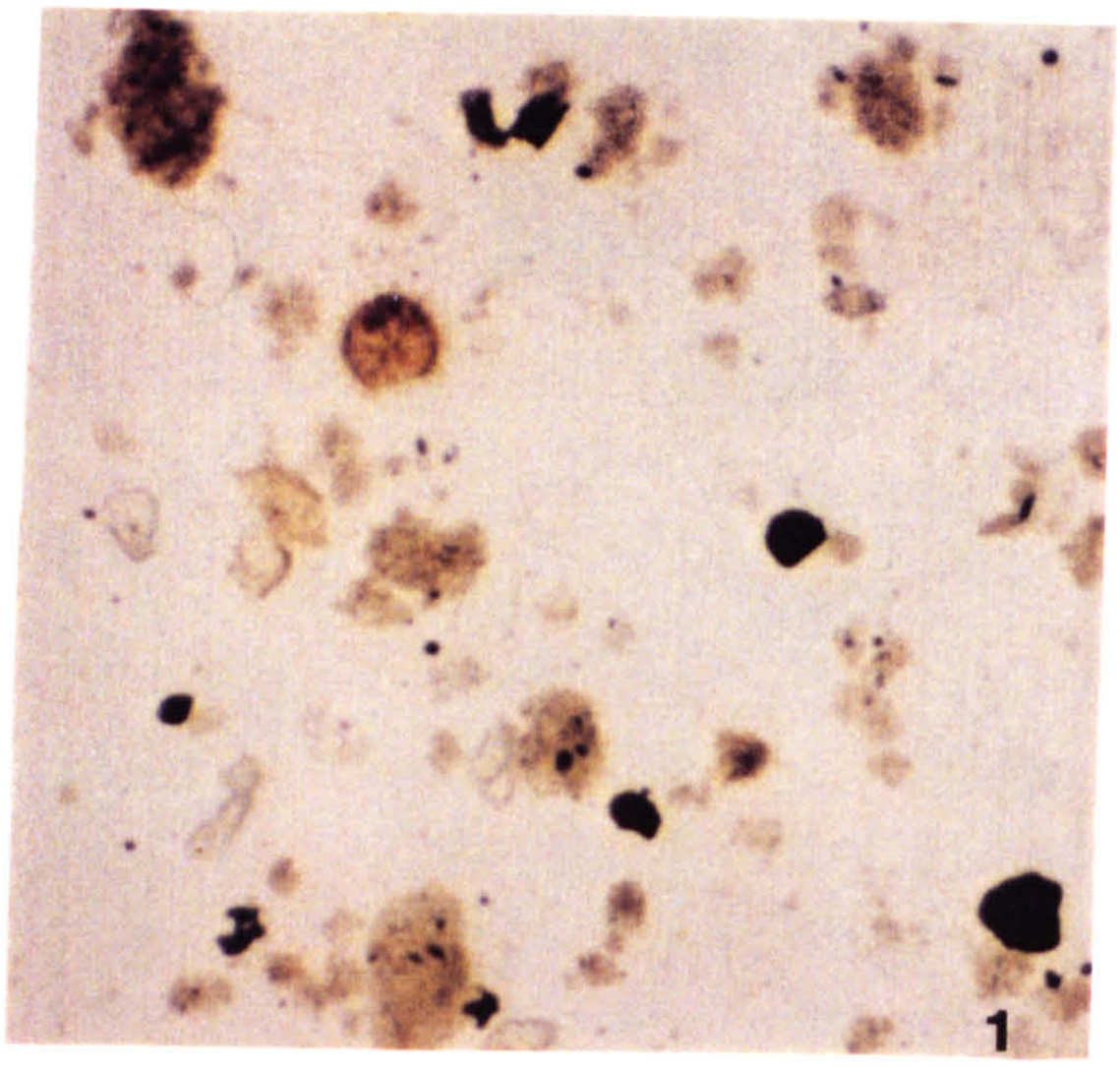

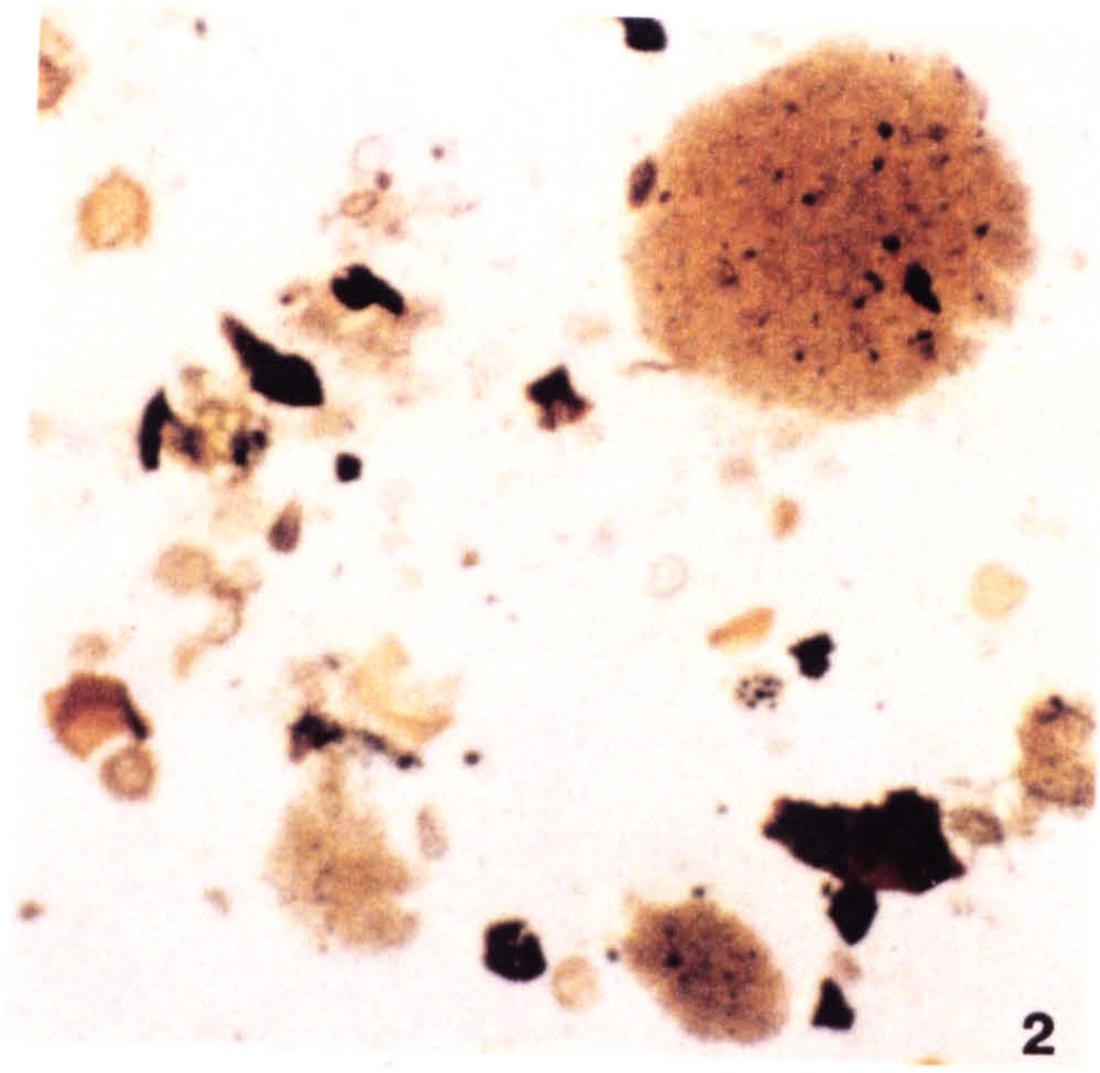

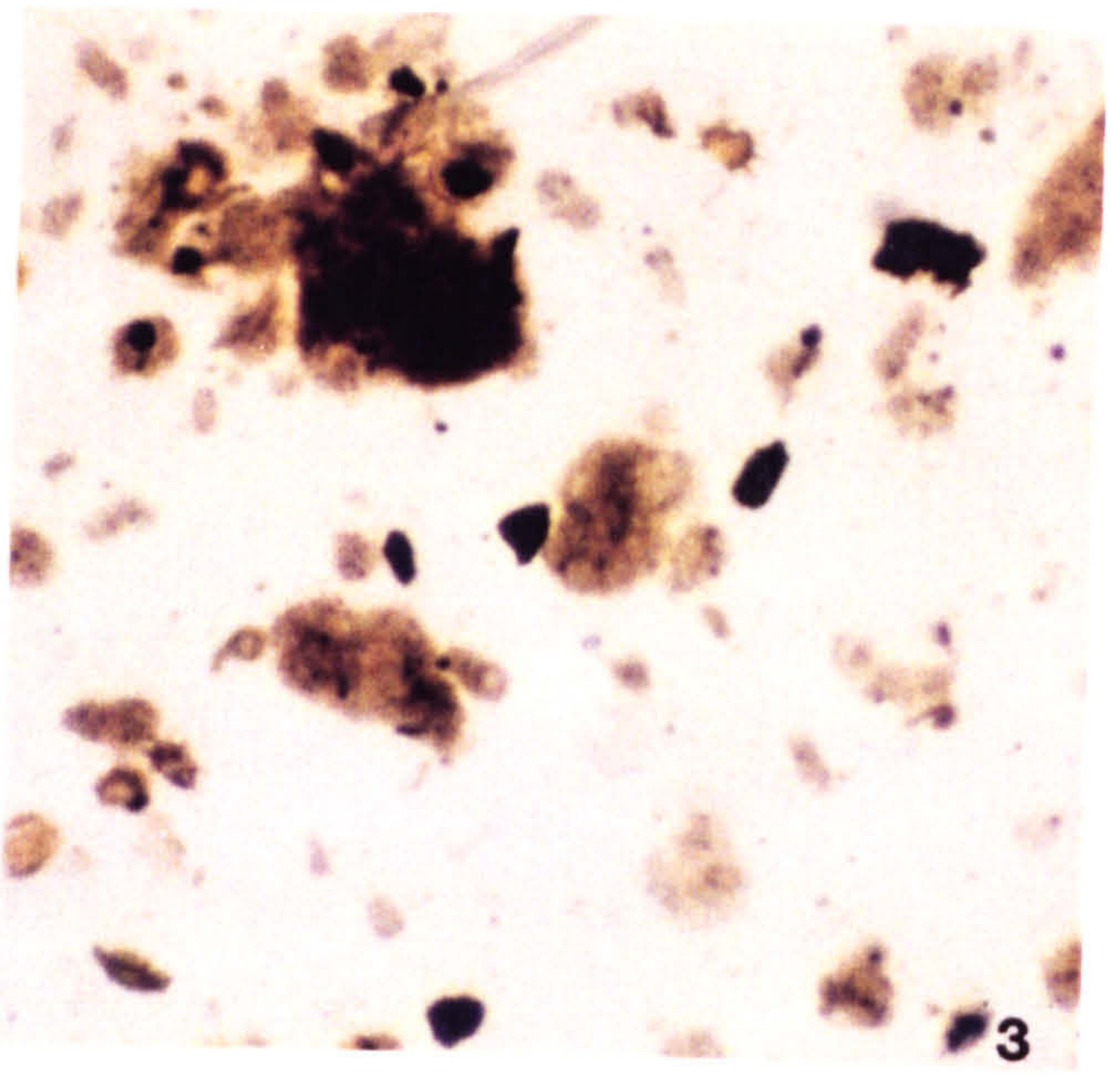

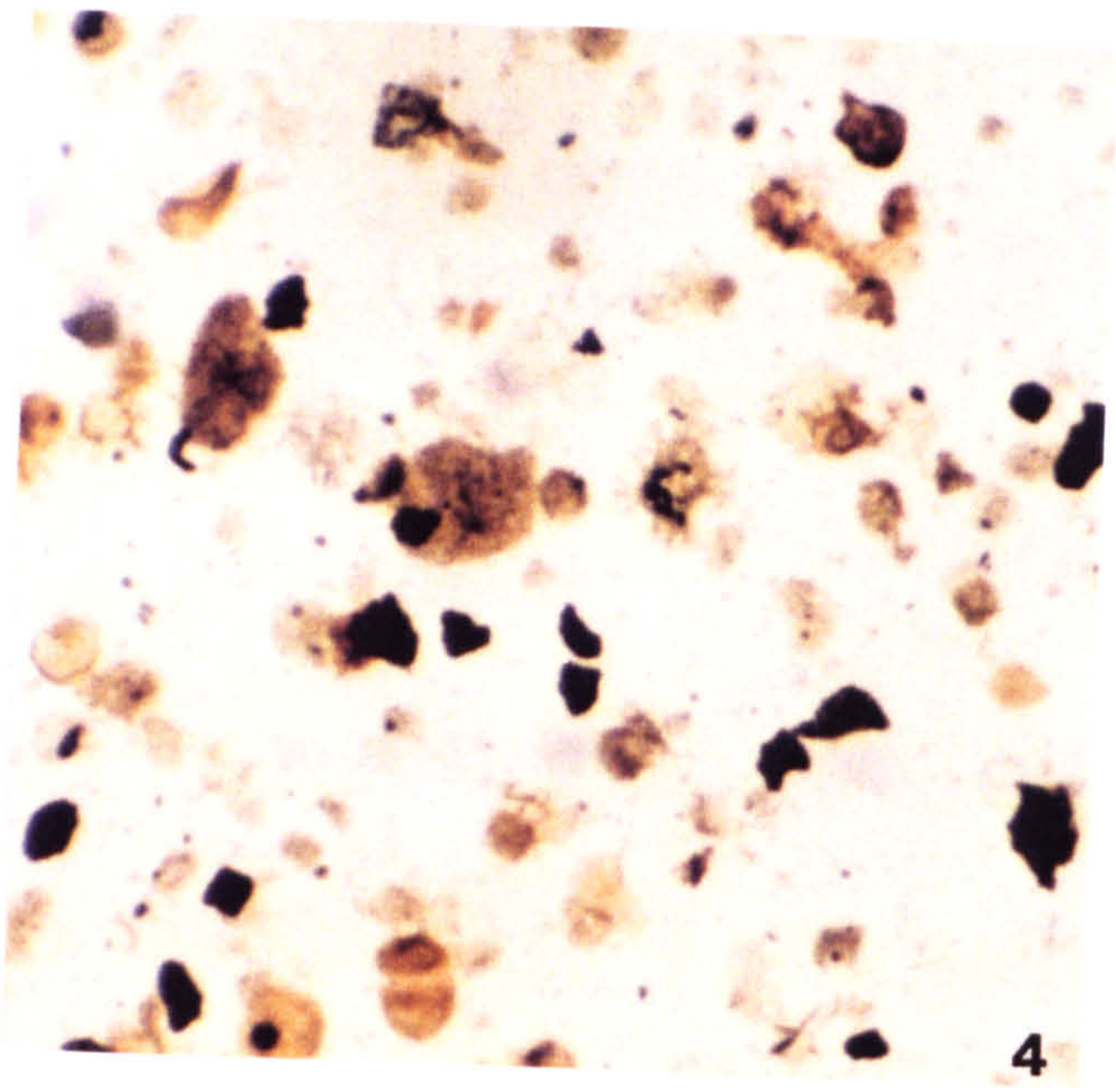

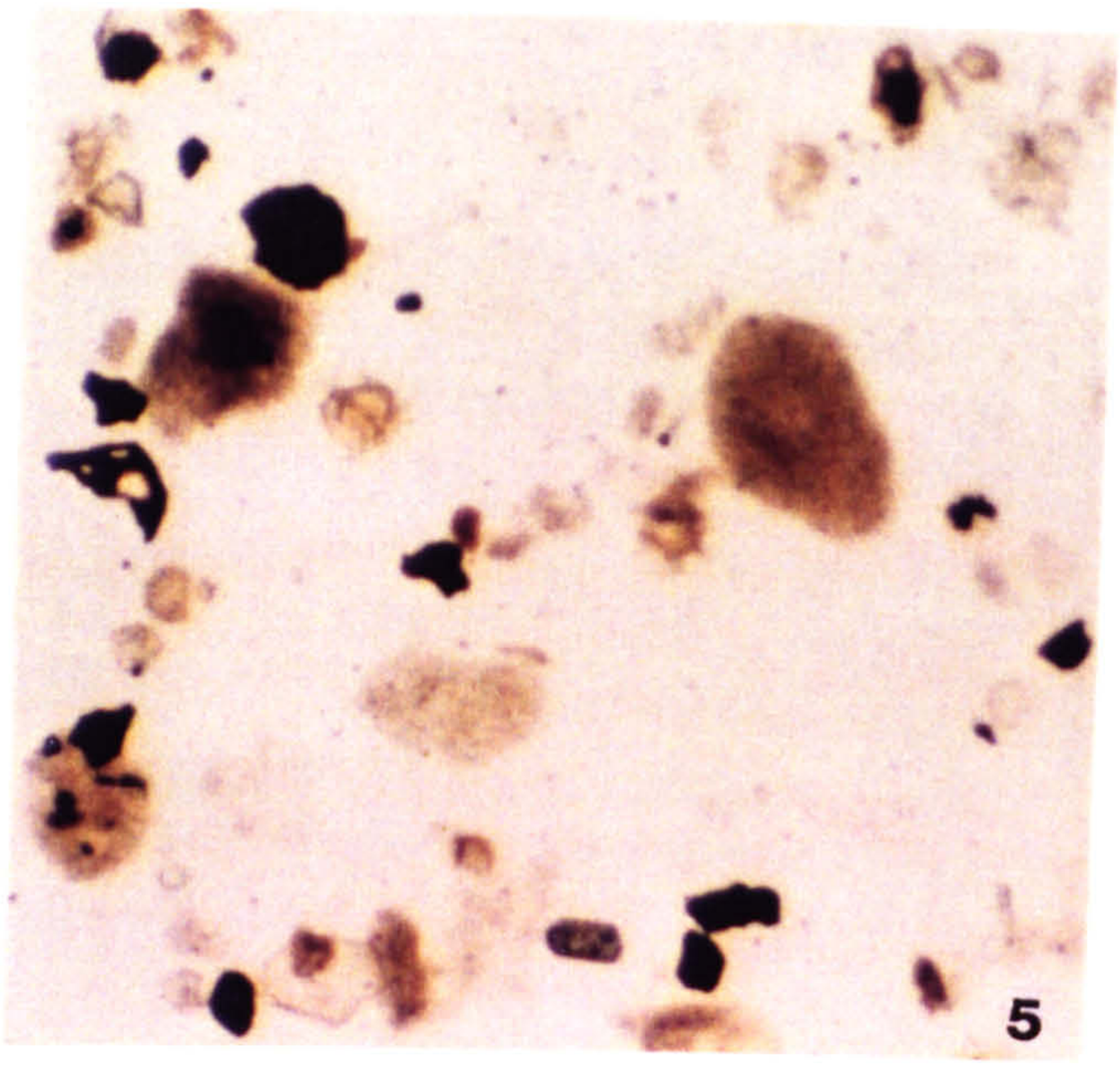

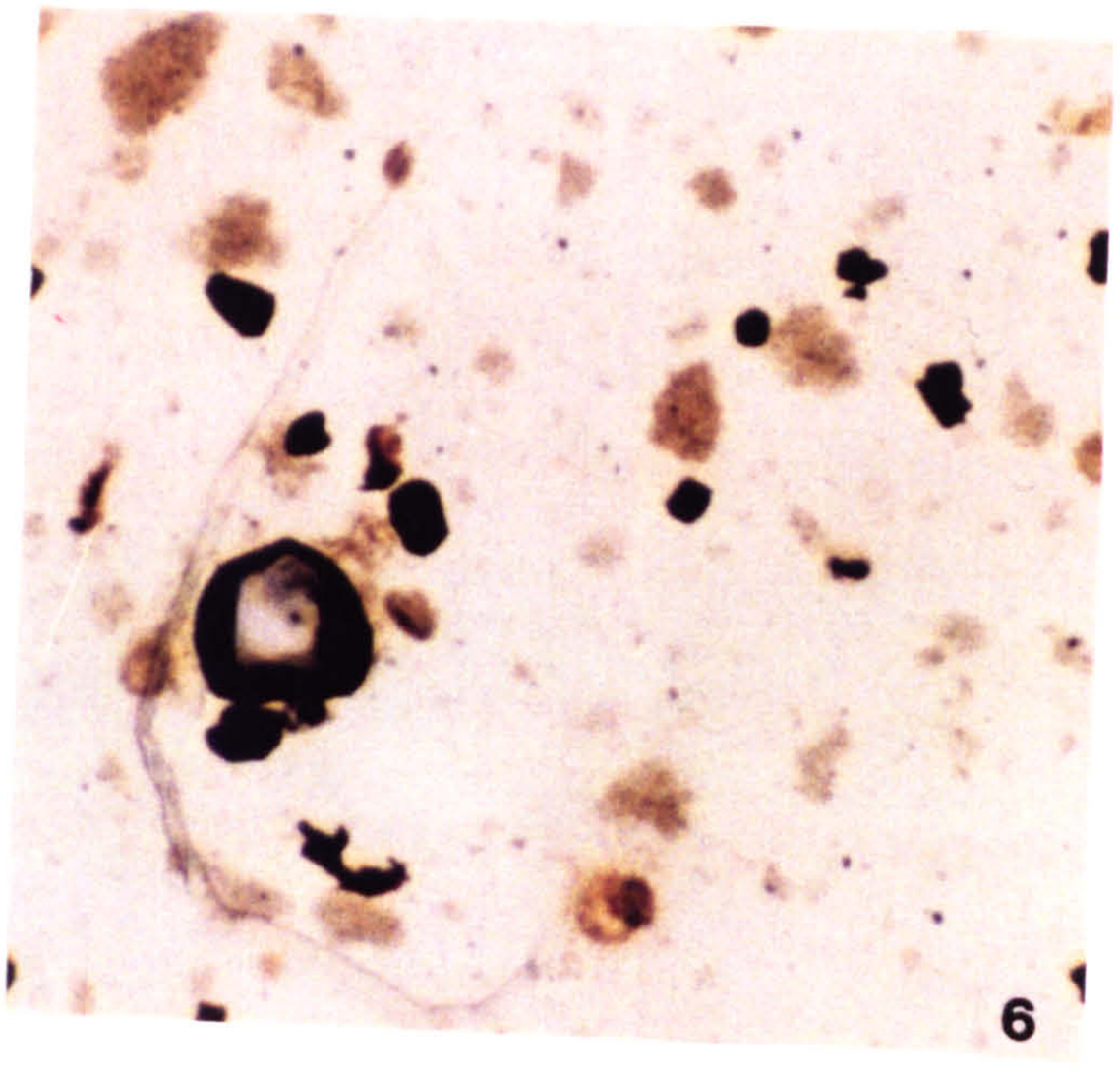

Figure 8.16

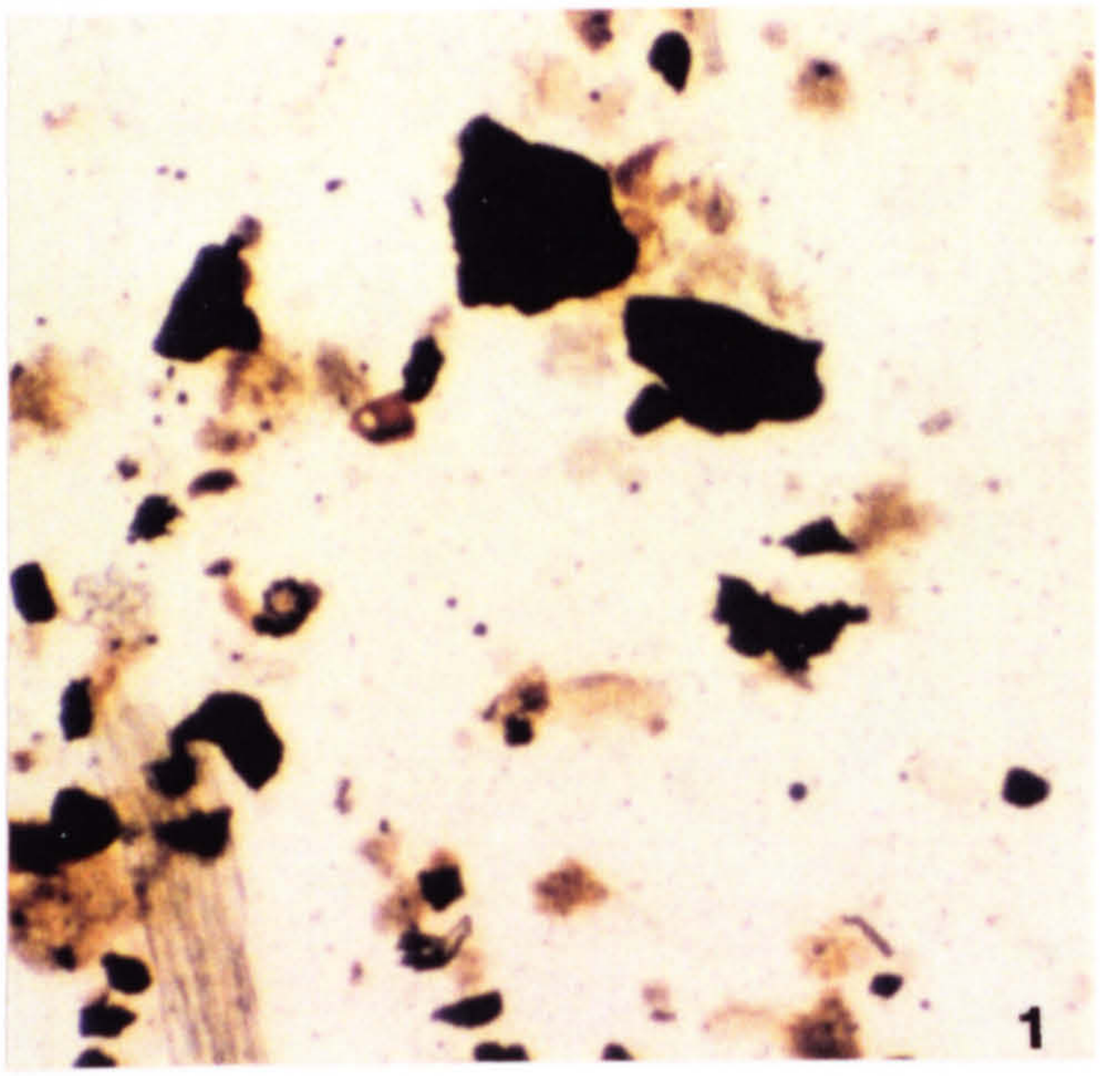

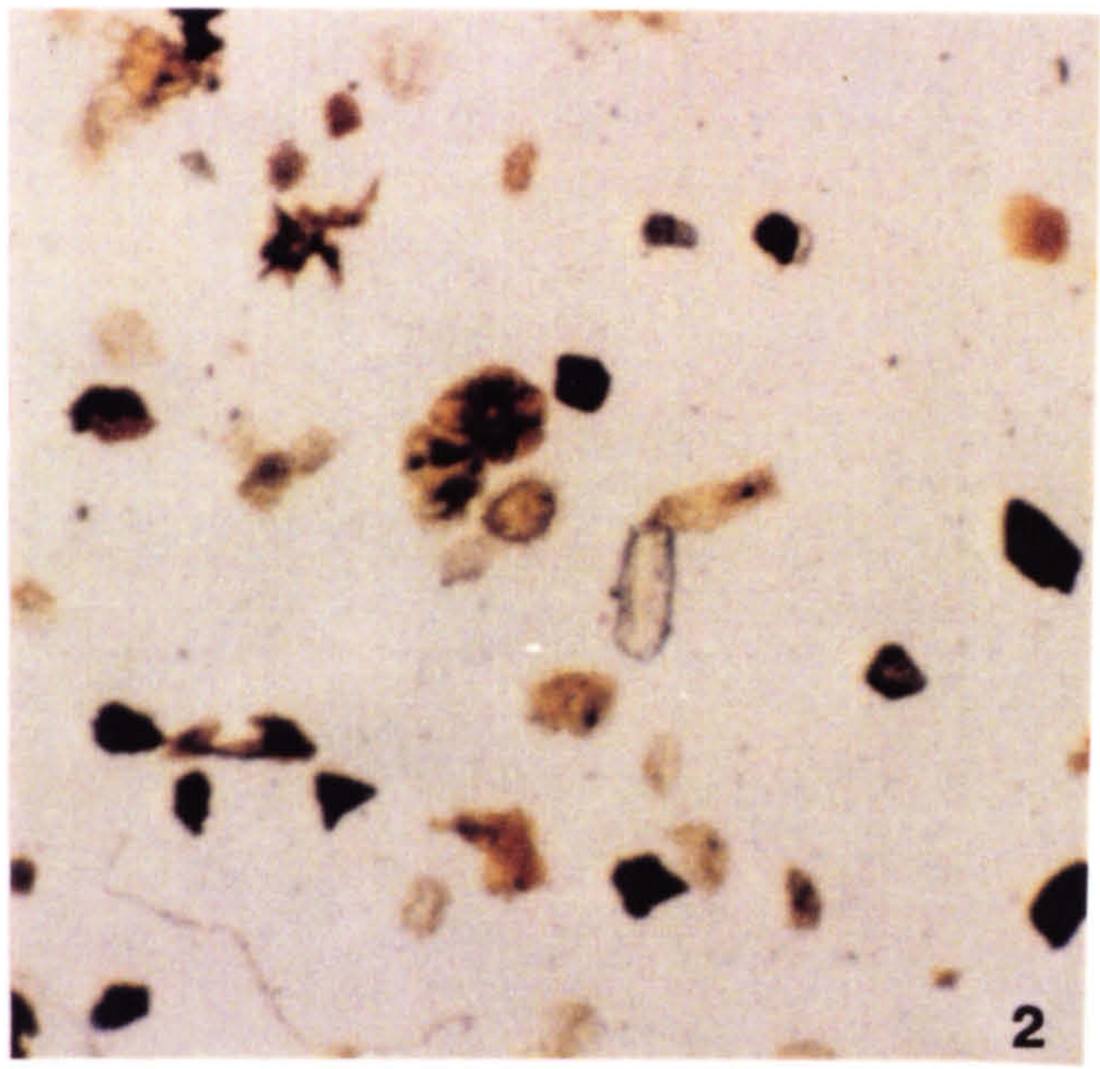

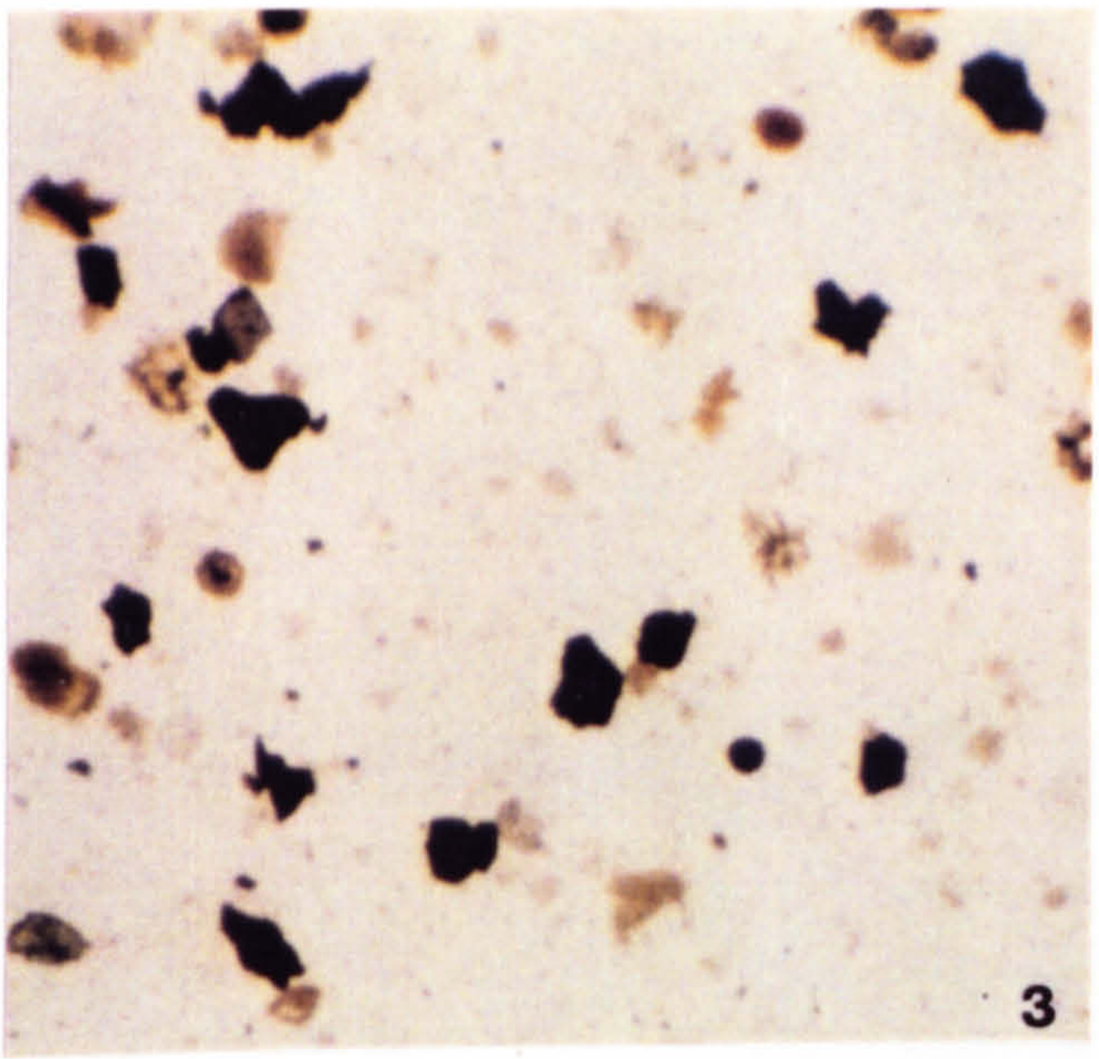

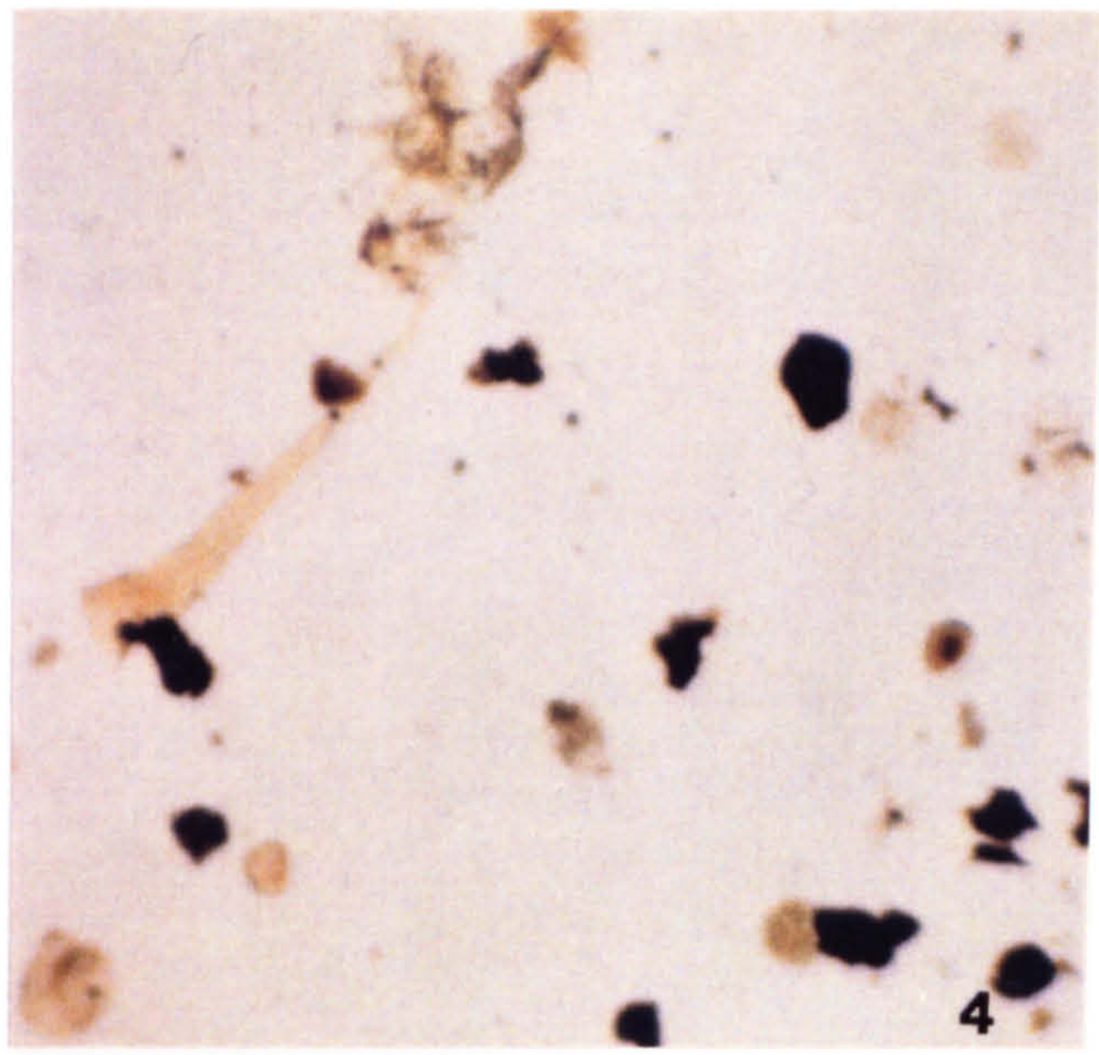

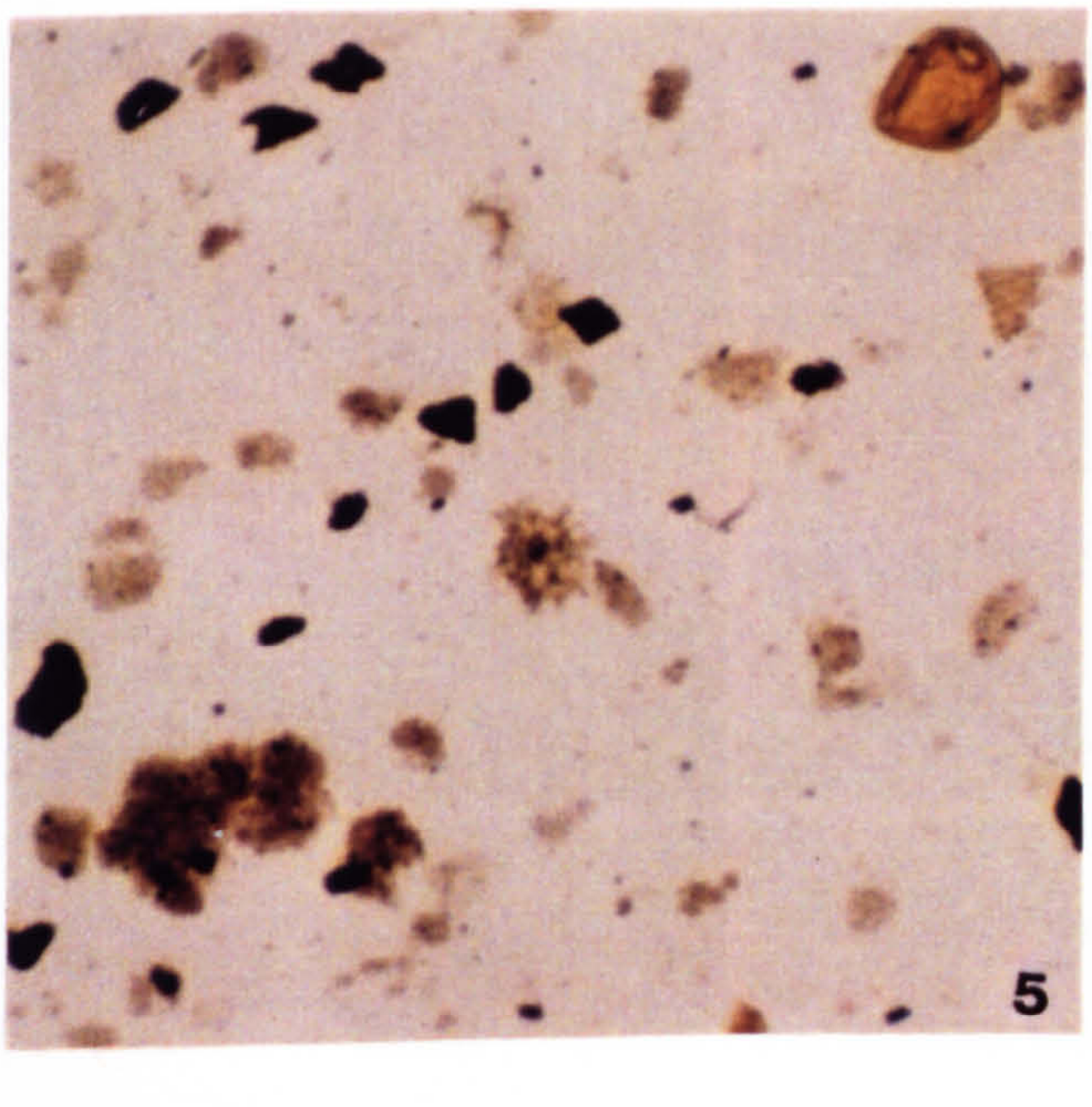

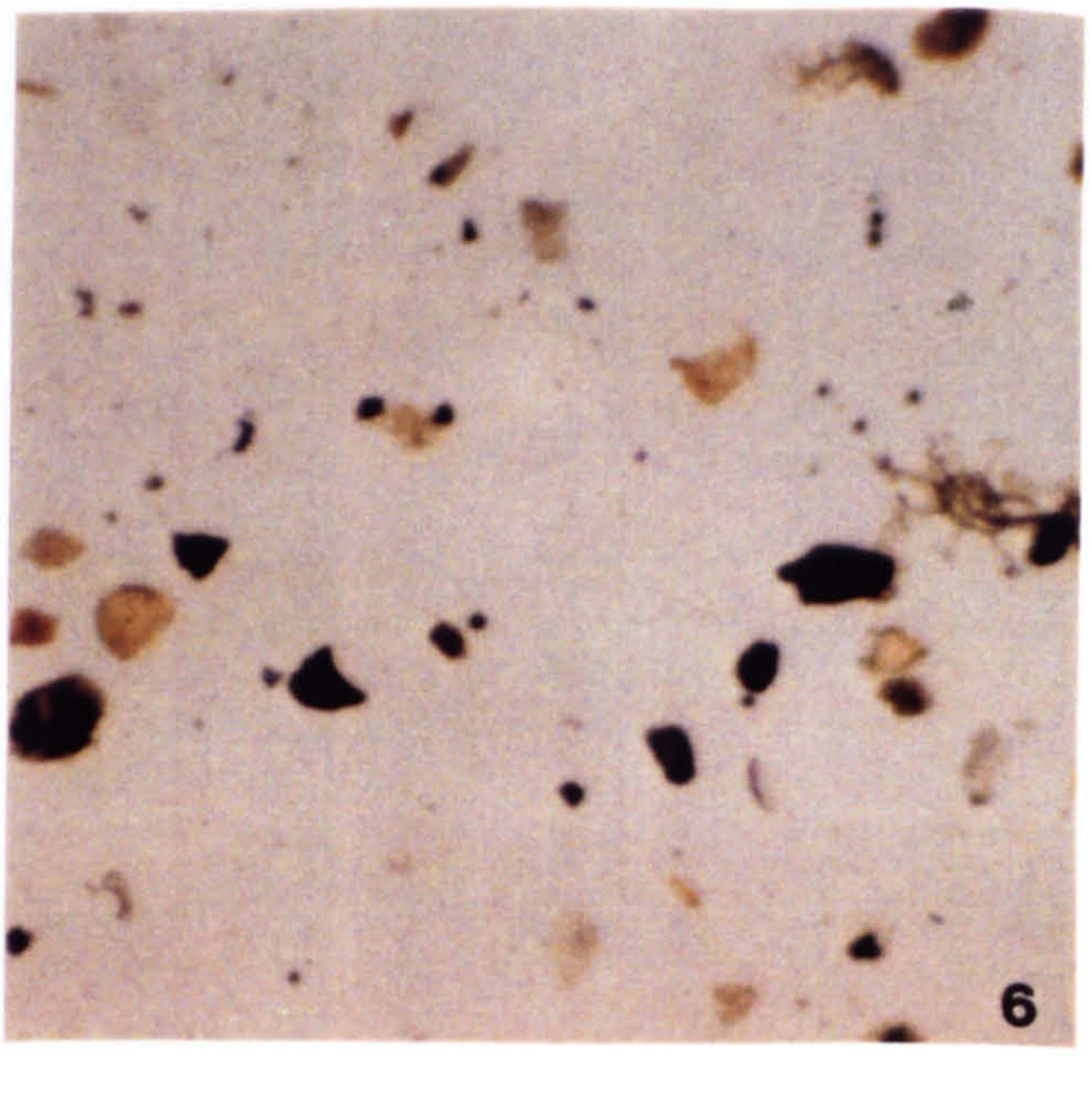

Figure 8.17

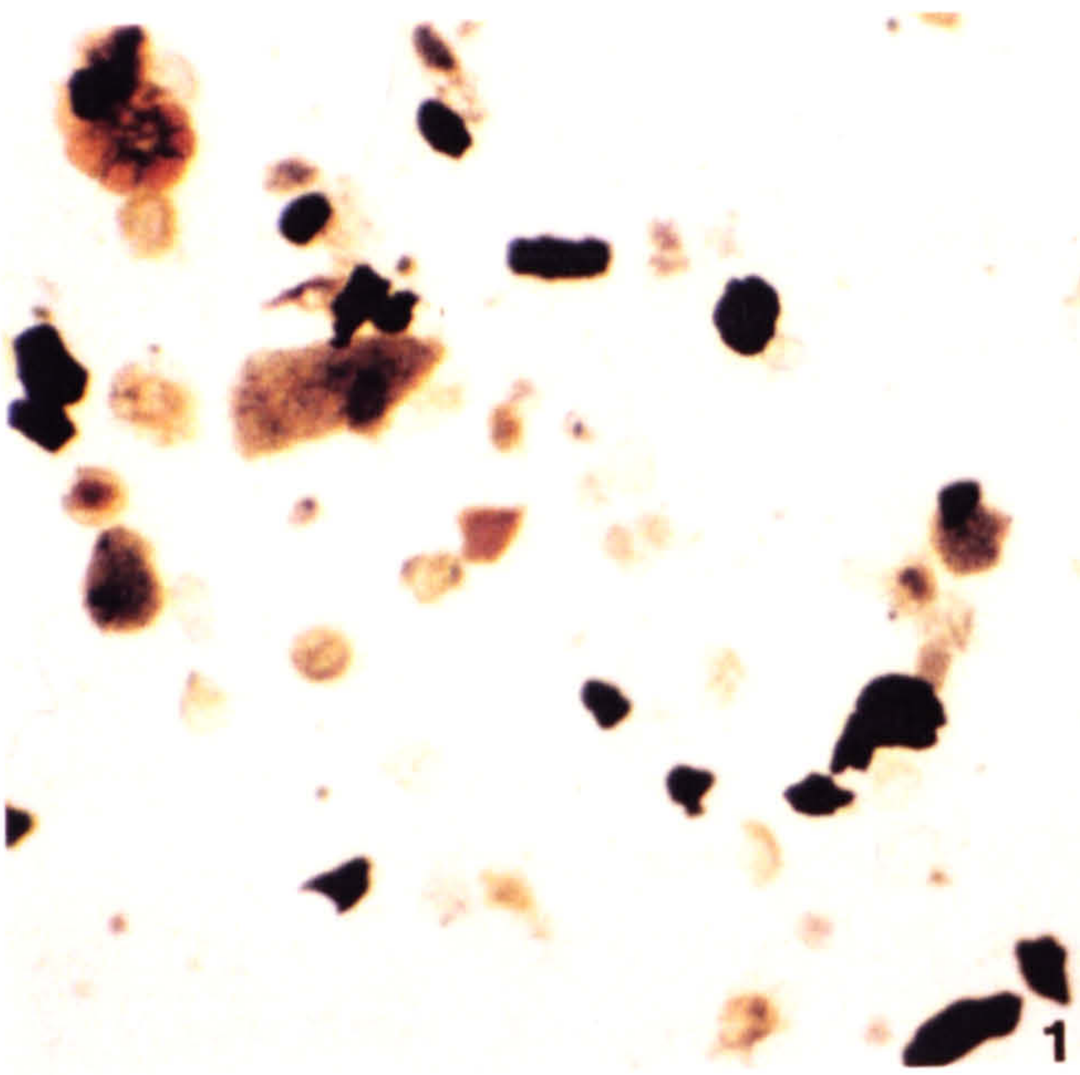

1

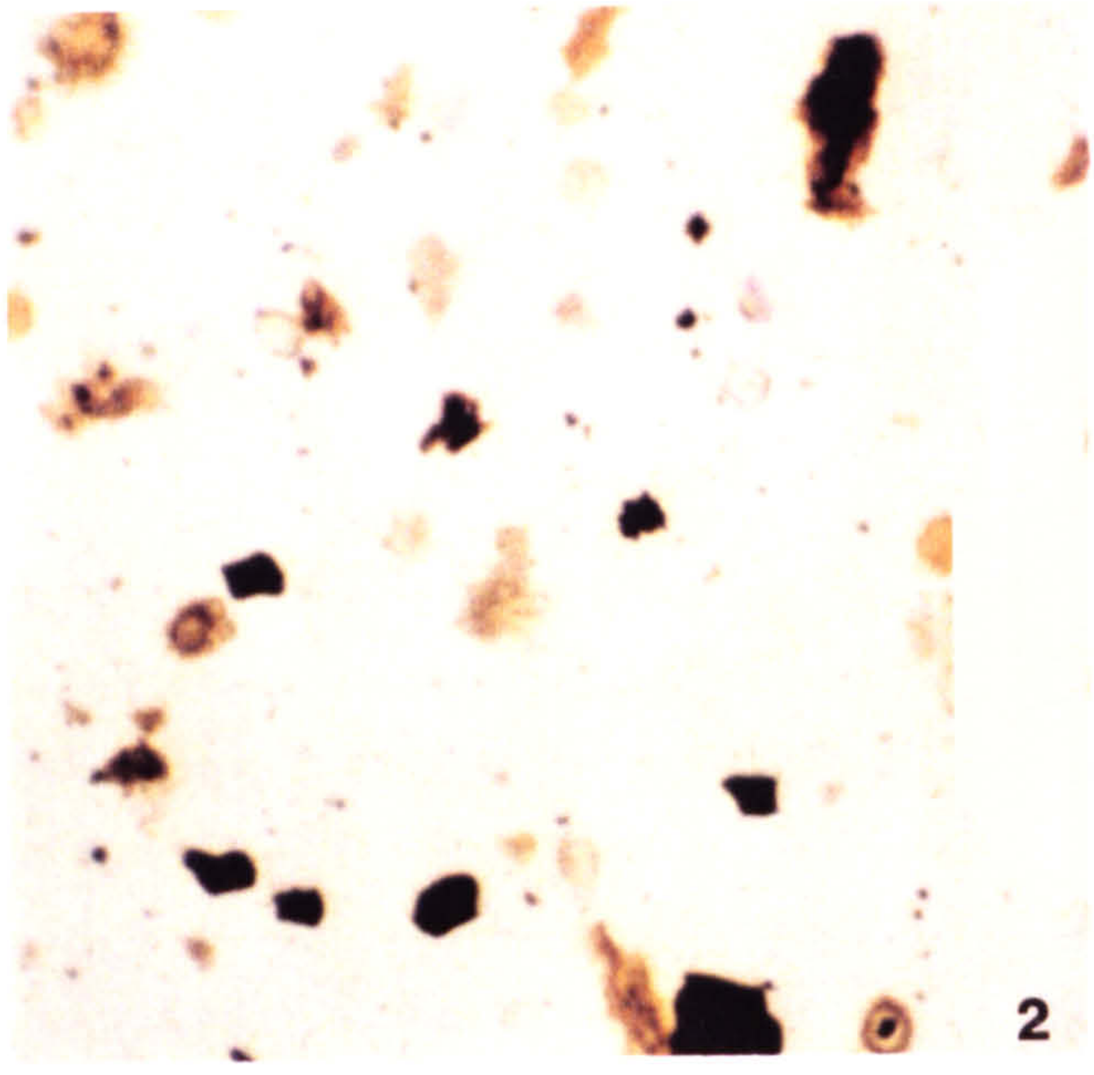

2

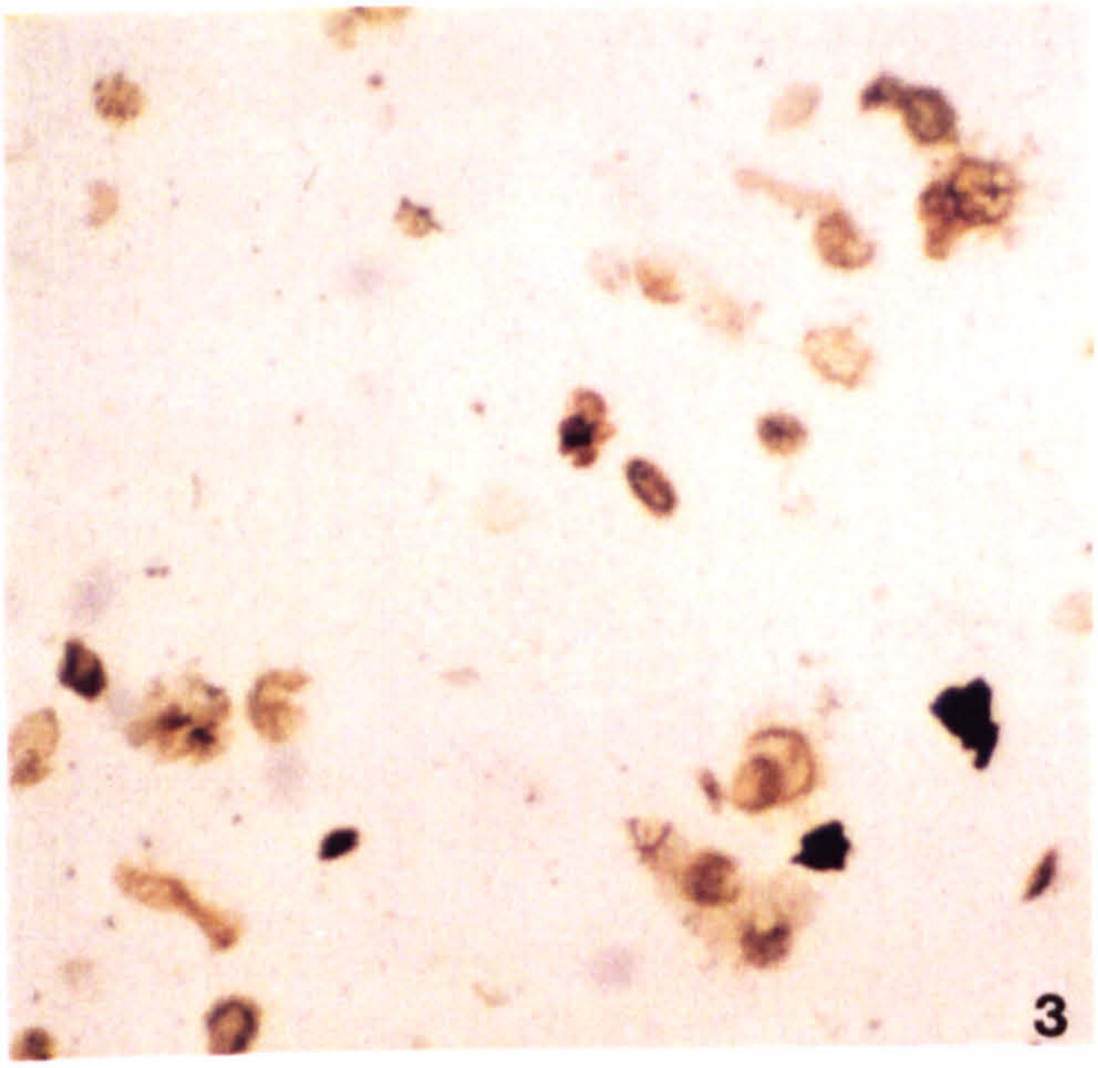

3

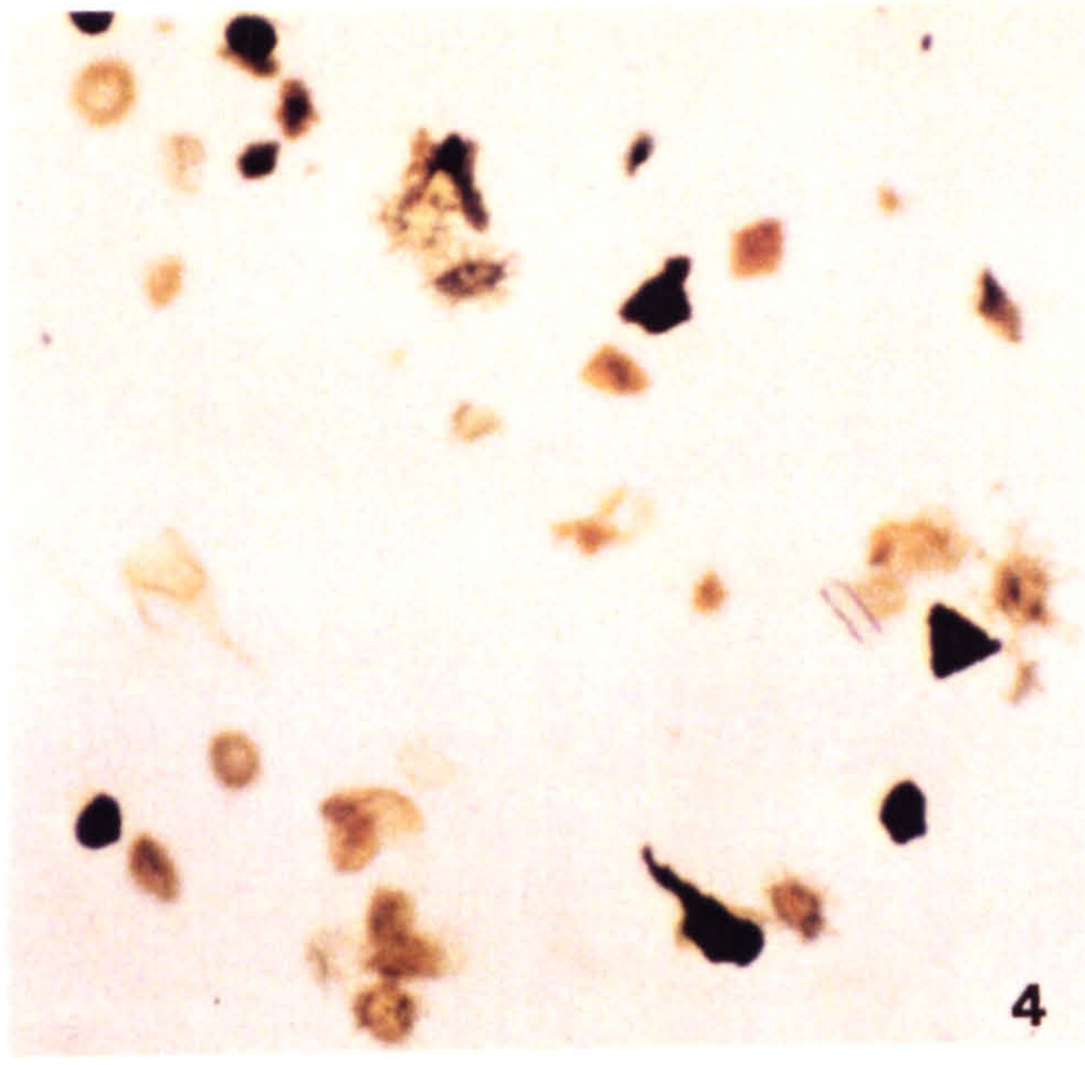

4

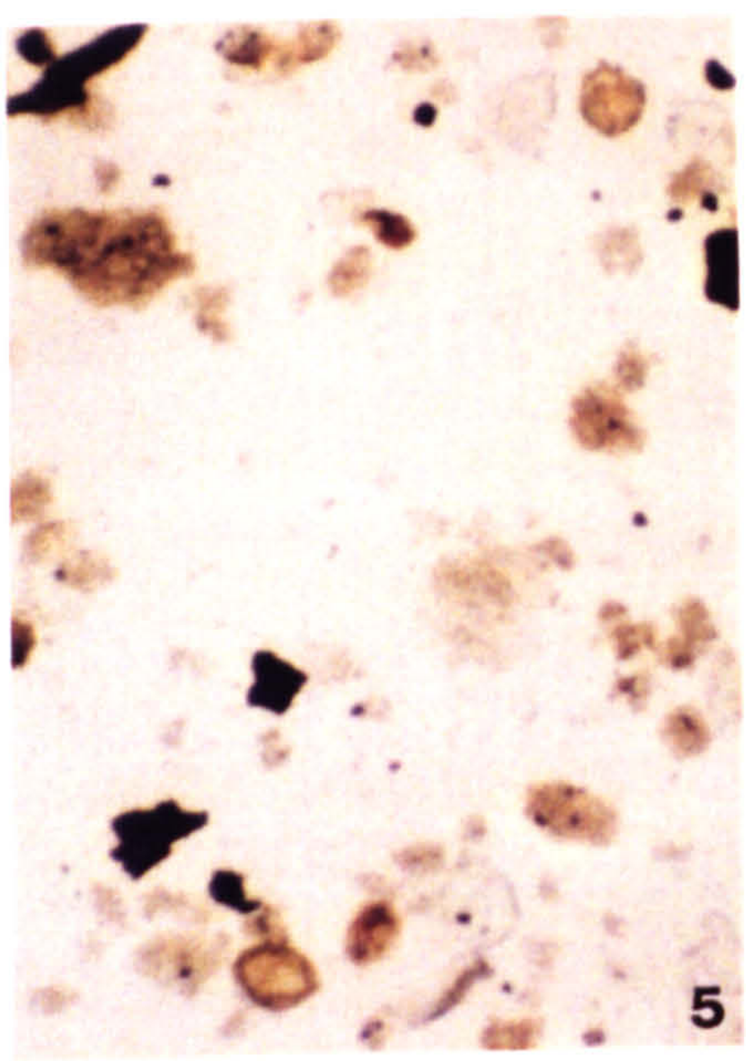

5

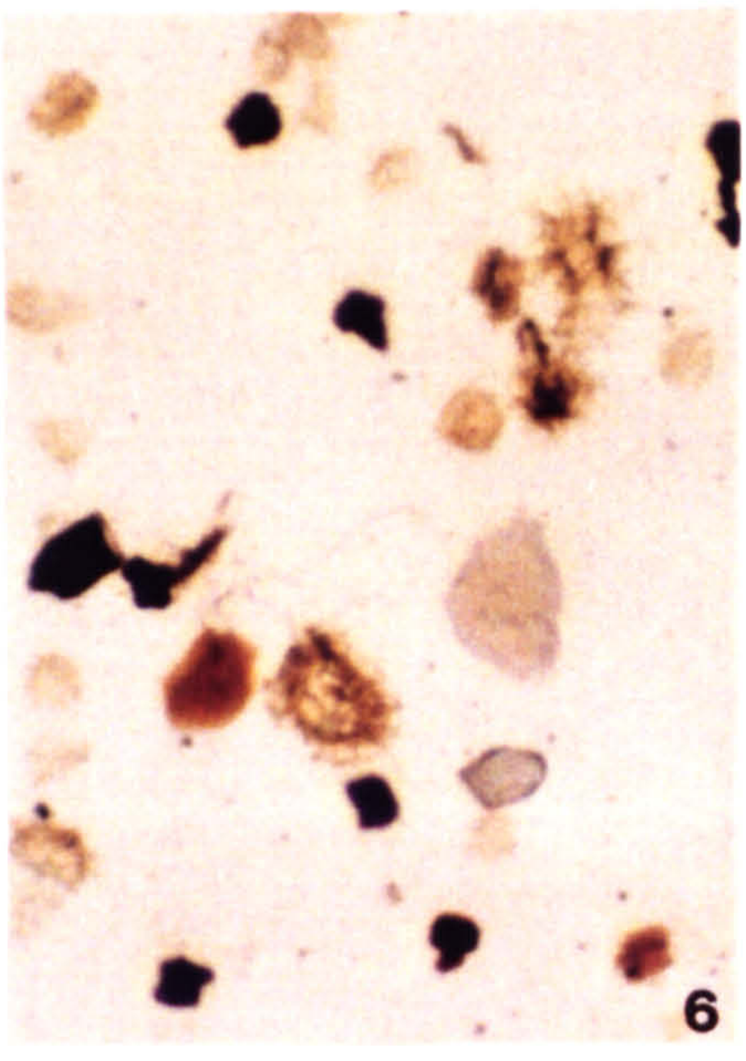

6

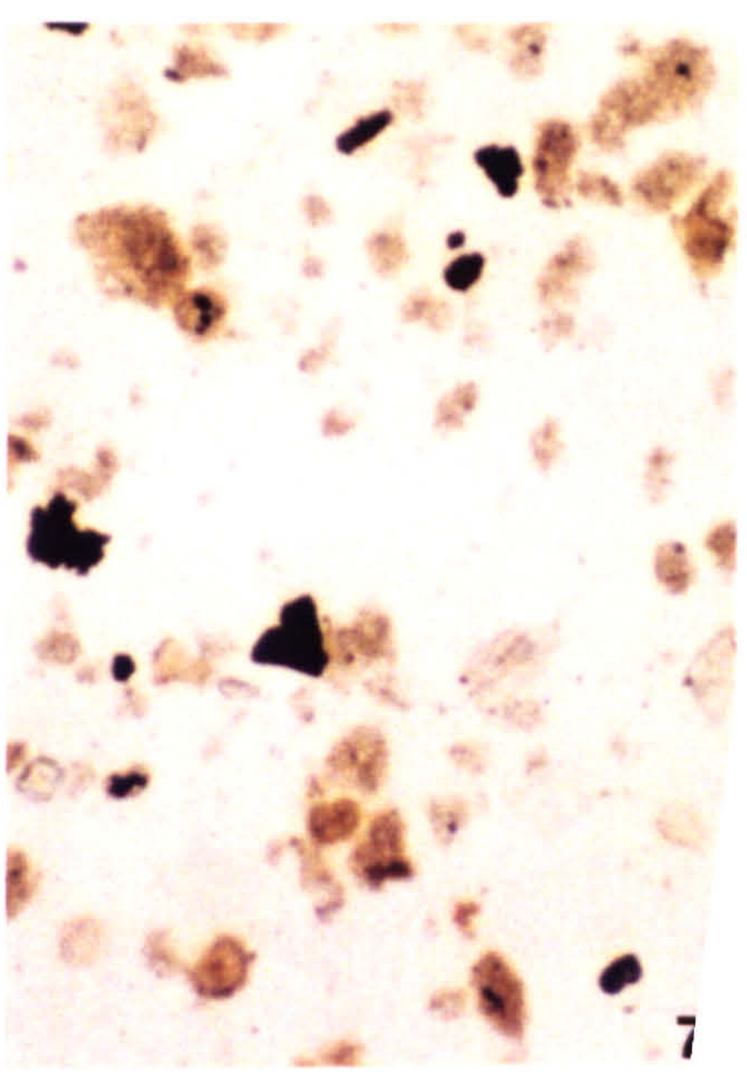

7

two associations, primarily identified by the cluster analysis technique, are only tentatively linked to slightly differing palynofacies associations, it is not felt that there is sufficient evidence on which to base any interpretation as to their possible mode of formation.

All three types of foraminiferal test linings are found commonly occurring in almost all samples of section TBB, see Figure 8.12. Type 1 (Pl. 31, Figs 1,2) is the most dominant form occurring in all samples, whereas Type 2 (Pl. 31, Figs 3,4) and Type 3 (Pl. 31, Figs 5,6) have more sporadic occurrences. The distribution of all types of foraminiferal test linings is random, and does not bear any relationship to any of the features previously discussed.

8.4. MCB Section

This section records a dominantly marine palynomorph assemblage indicative of open marine conditions of normal salinities. The dinoflagellate cyst associations present compare most closely to subgroups A3, 5A, and 5B of Harker *et al.* (1990), all of which are indicative of strongly marine conditions (see Appendix 6). The palynomorph content is heavily dominated by marine palynomorphs (dinoflagellates, acritarchs, pterospermopsis and tasmanites) representing between 98.84 - 99.84%, with only a minor contribution of terrestrial spores and pollen, 0.16 - 1.05%.

The dinoflagellate cyst species present indicate that they are representative of the Middle Cenomanian *Epelidosphaeridia spinosa* subzone (Davey, 1970). A range chart of the palynomorph content of this section is given in Figure 8.19. Appendix 3 contains all raw numerical data from this section.

Numbers of dinoflagellate cysts per gramme of sediment indicate that section MCB in general records an abundant assemblage (Figure 8.20). Numbers vary from 181 to 806 dinoflagellate cysts per gramme. Examination of Figure 8.20 shows that anomalously low values of abundance are associated with the particular feature which characterises this section, the Mid-Cenomanian non-sequence of Carter and Hart (1977) (Figure 3.9). For a more detailed documentation of the Mid-Cenomanian non-sequence (Carter and Hart, 1977), see Chapter 2. It is obvious that this non-sequence is marked by lower than average abundance levels of dinoflagellate cysts and thus, it is a period of time of decreased dinoflagellate cyst abundance within the water mass.

Average values of species diversity of section MCB as measured by the two diversity indices used (Figures 8.21a, 8.21b), indicate that this section records a highly diverse dinoflagellate assemblage. The species diversity levels exhibited by this section are similar to the high diversity levels of section TBB. When comparison is made to the diversity levels of the cyst communities identified by Goodman (1979), the species diversity levels present in this section are similar to B and A/B transition cyst communities. These cyst communities are interpreted by Goodman (1979) as representing a more offshore palaeoenvironment. The variation seen in species diversity is strongly influenced by the existence of the

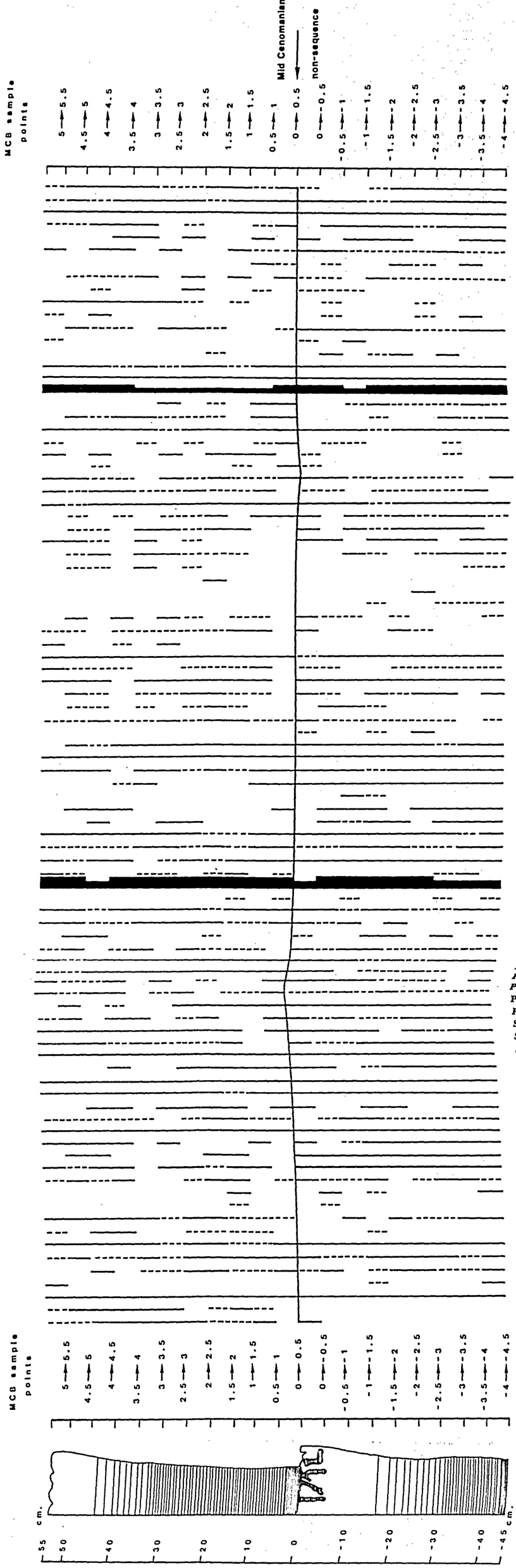

Figure 8.19 Range chart of the dinoflagellate cyst species and other palynomorph taxa of MCB section, together with the position of the Mid-Cenomanian non-sequence horizon.

Mid-Cenomanian non-sequence of Carter and Hart (1977), which distinguishes this sequence. The dinoflagellate cyst associations recorded by the samples which occur prior to the non-sequence (MCB -4.5 to 0cm.) exhibit consistently higher species diversity values than those occurring after the non-sequence (MCB 0 to 5.5 cm.).

As is typical of Cenomanian dinoflagellate cysts assemblages, this section is dominated by *P. infusorioides* (31.7 - 59.7%). Several species are present in considerable percentages; *C. huguoniotii* (14 - 32.3%); *C. distinctum* (0 - 3.8%); *L. siphonophorum* (Cookson and Eisenack) Davey and Williams 1966b subsp. *siphonophorum* Lucas Clark 1984 (Pl. 12, Figs 1-6) (1 - 5.3%); *Spiniferites* spp. (3 - 9.8%) and *Achomosphaera* spp. (1.3 - 5.4%). The remaining species which usually represent <3% of the dinoflagellate cyst population have variable distributions from those occurring consistently throughout the section to those with a patchy or an irregular presence.

The distribution and percentage presence of several dinoflagellate cyst species appears to be affected to varying degrees, by the presence of the Mid-Cenomanian non-sequence (Carter and Hart 1977). As can be seen from the range chart of species present within the MCB section (Figure 8.19), there is a gap in the distribution of several species before, during and after the non-sequence. The following species exhibit restricted distributions across the non-sequence horizon; *Carpodinium obliquicostatum* Cookson and Hughes 1964 (Pl. 2, Fig. 6), *Chlamydophorella discreta* Clarke and Verdier 1967 (Pl. 3, Fig. 1), *C. nyei* Cookson and Eisenack 1958 (Pl. 3, Fig. 2), *C. ? urna* Cookson and Eisenack 1960a (Pl. 3, Figs 3,4), *Coronifera oceanica* Cookson and Eisenack; emend. May 1980 (Pl. 3, Fig. 11), *C. cooksoniae, C. distinctum, Exochosphaeridium bifidum* (Clarke and Verdier) Clarke *et al.* 1968 (Pl 8, Fig. 5), *E. phragmites* Davey *et al.* 1966 (Pl. 8, Fig. 6), *Florentinia deanei* (Davey and Williams) Davey and Verdier 1973 (Pl. 9, Fig. 1), *F. ferox* (Deflandre) Duxbury 1980 (Pl. 9, Fig. 2), *Fromea amphora* Cookson and Eisenack 1958 (Pl. 9, Fig. 6), *Gonyaulacysta cassidata* (Pl. 10, Figs 1,2), *G. whitei* Sarjeant 1966 (Pl. 10, Figs 3,4), *Hystrichosphaeridium bowerbankii* Davey and Williams 1966b (Pl. 10, Fig. 6), *H. tubiferum* (Ehrenberg) Deflandre; emend. Davey and Williams 1966b (Pl. 10, Fig. 7), *Hystrichostrogylon membraniphorum* Agelopolos 1964 (Pl. 10, Fig. 8), *Kleithriasphaeridium readei* (Davey and Williams) Davey and Verdier 1976 (Pl. 11, Figs 2,3),

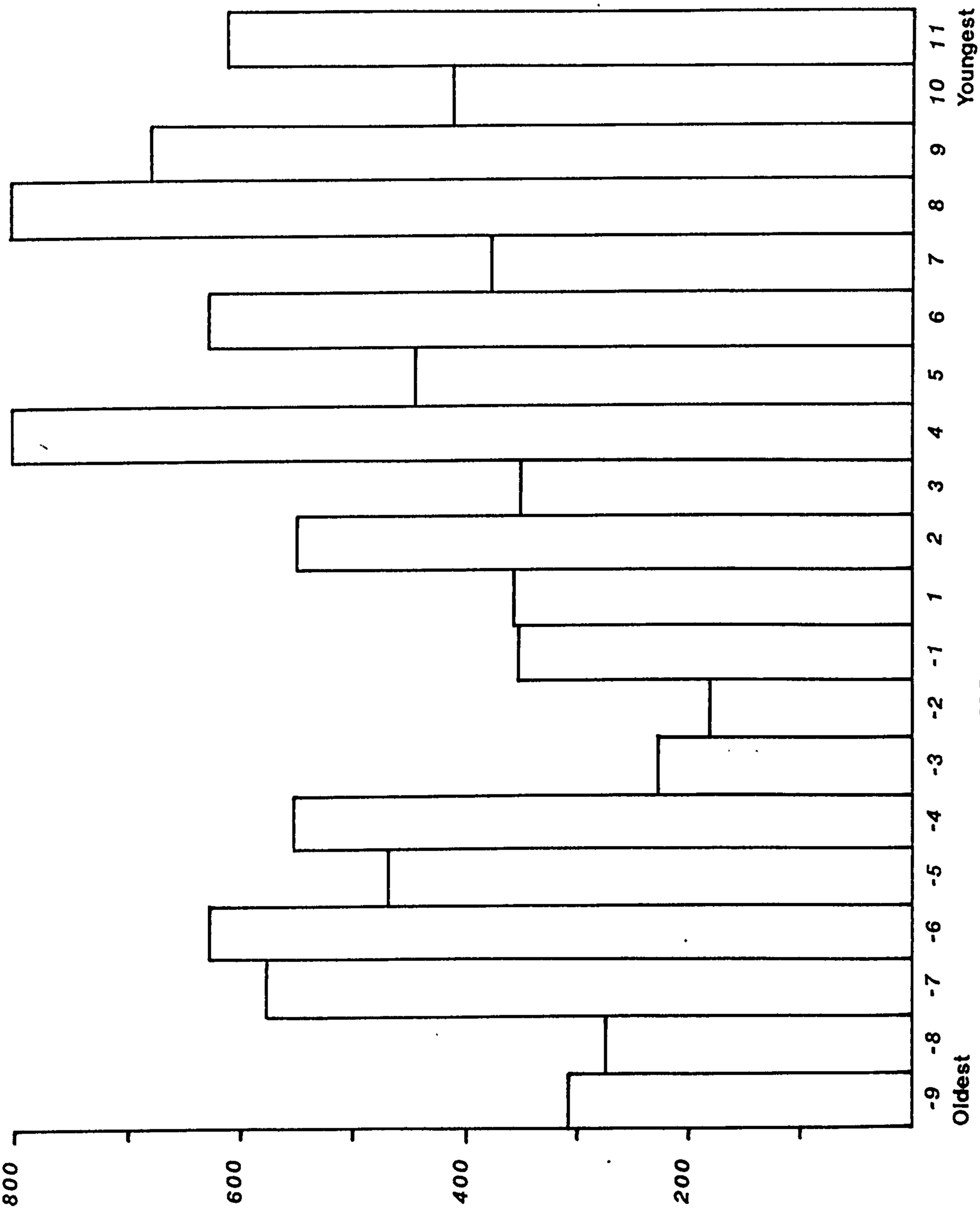

Figure 8.20 Abundance values for section MCB samples based on number of dinoflagellate cysts per gramme of sediment. See Fig. 7.18 for explanation of abbreviated sample numbering system.

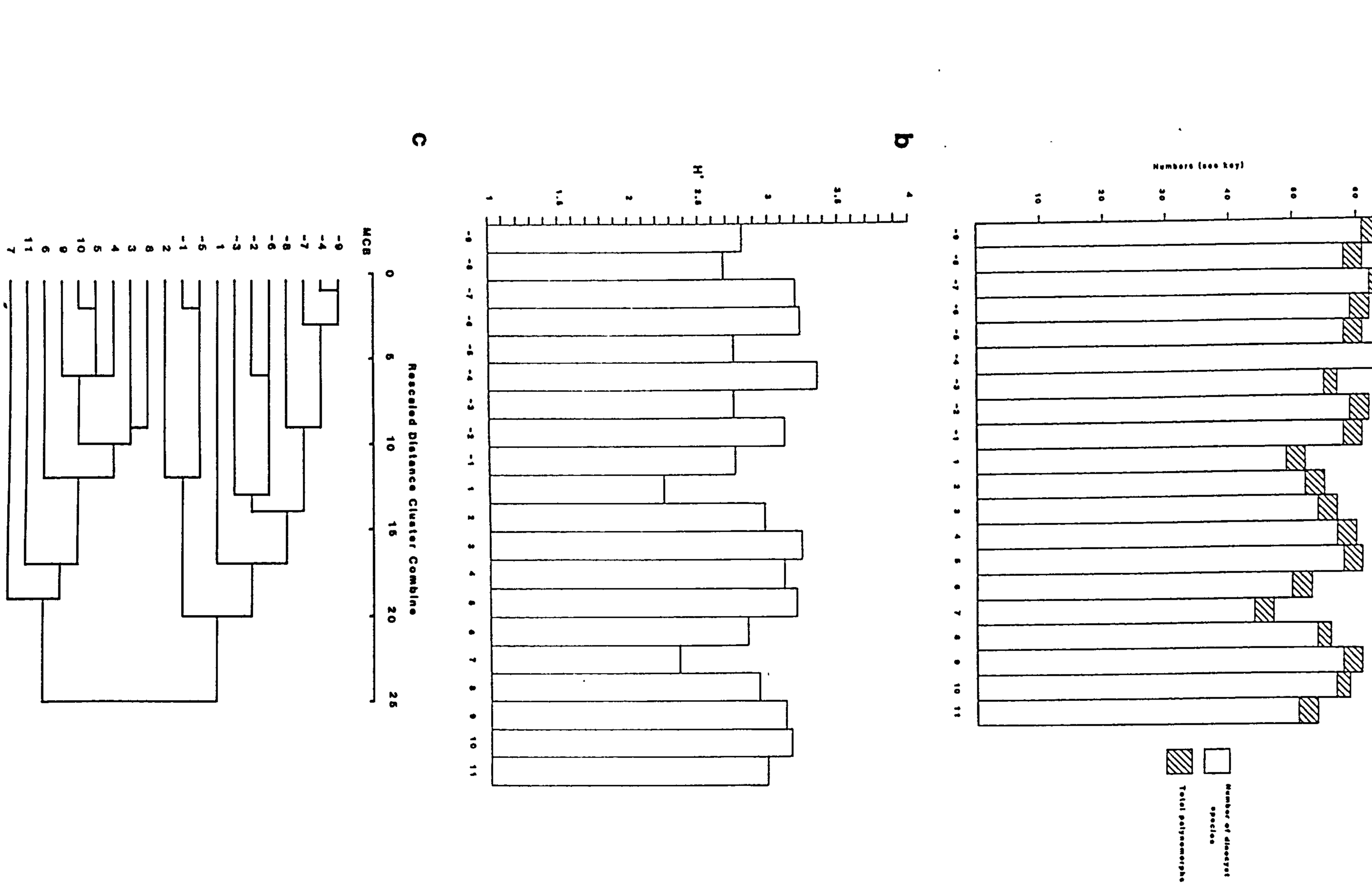

Figure 8.21 Summary of statistical analyses of section MCB samples. a. Overall richness species diversity index (S). b. Shannon species diversity index (H'). c. Cluster analysis dendrogram. See Fig. 7.18 for explanation of abbreviated sample numbering system.

Oligosphaeridium prolixispinosum Davey and Williams 1966b (Pl. 16, Fig. 6), *Psaligonyaulax deflandrei* Sarjeant; emend. Sarjeant 1982 (Pl. 18, Figs 3,4), *Spiniferites multibrevis* (Davey and Williams) Below 1982 (Pl. 20, Figs 3,4), *Tanyosphaeridium variecalamus* Davey and Williams 1966b (Pl. 22, Fig. 3), *Trichodinium castanea* (Deflandre) Clarke and Verdier 1967 (Pl. 22, Figs 5,6), *Xiphophoridium alatum* (Cookson and Eisenack) Sarjeant 1966 (Pl. 23, Figs 3,4). It can therefore be said that the Mid-Cenomanian non-sequence (Carter and Hart, 1977) causes serious perturbations to the dinoflagellate cyst assemblages of section MCB.

A number of species exhibit percentage presence variations which are linked to the presence of the non-sequence within section MCB. Most notable of these is that of *P. infusorioides* (Figure 8.22) which is present in significantly lower percentages [33.1 (41.55) 48.6%] in pre-non-sequence samples (MCB -4.5 to 0cm.) than in post-non-sequence samples (MCB 0 to 5.5cm.) where its percentage presence is consistently much higher [39.7 (49.87) 59.7%]. Two species which show the opposite trend to that of *P. infusorioides* and are present in somewhat higher percentages in pre-non-sequence samples are *C. huguoniotii* (Figure 8.23) and *C. distinctum* (Figure 8.24). As has been identified by the palynological analysis of Site 3a the distributions of these three dinoflagellate cysts are linked in such a way that an increase in the numbers of *P. infusorioides* is marked by a decrease of both *C. huguoniotii* and *C. distinctum*. It can therefore be said that there is an inversely proportional relationship between *P. infusorioides* and both *C. huguoniotii* and *C. distinctum*.

The application of cluster analysis to the palynomorph content of the section MCB has been very successful. The dendrogram based on the Dice co-efficients of section MCB (Figure 8.21c) shows that the section is divided into two associations which are delimited at similar confidence levels. The division between these two associations is almost exactly coincident with the Mid-Cenomanian non-sequence (Carter and Hart, 1977). Thus, as a result of the application of cluster analysis, it is evident that two distinct palynomorph assemblages exist. One characterises the pre-non-sequence period and the second distinguishes the post-non-sequence part of the section. However, there is slight discrepancy between the positioning of the division between the two statistical association (based on

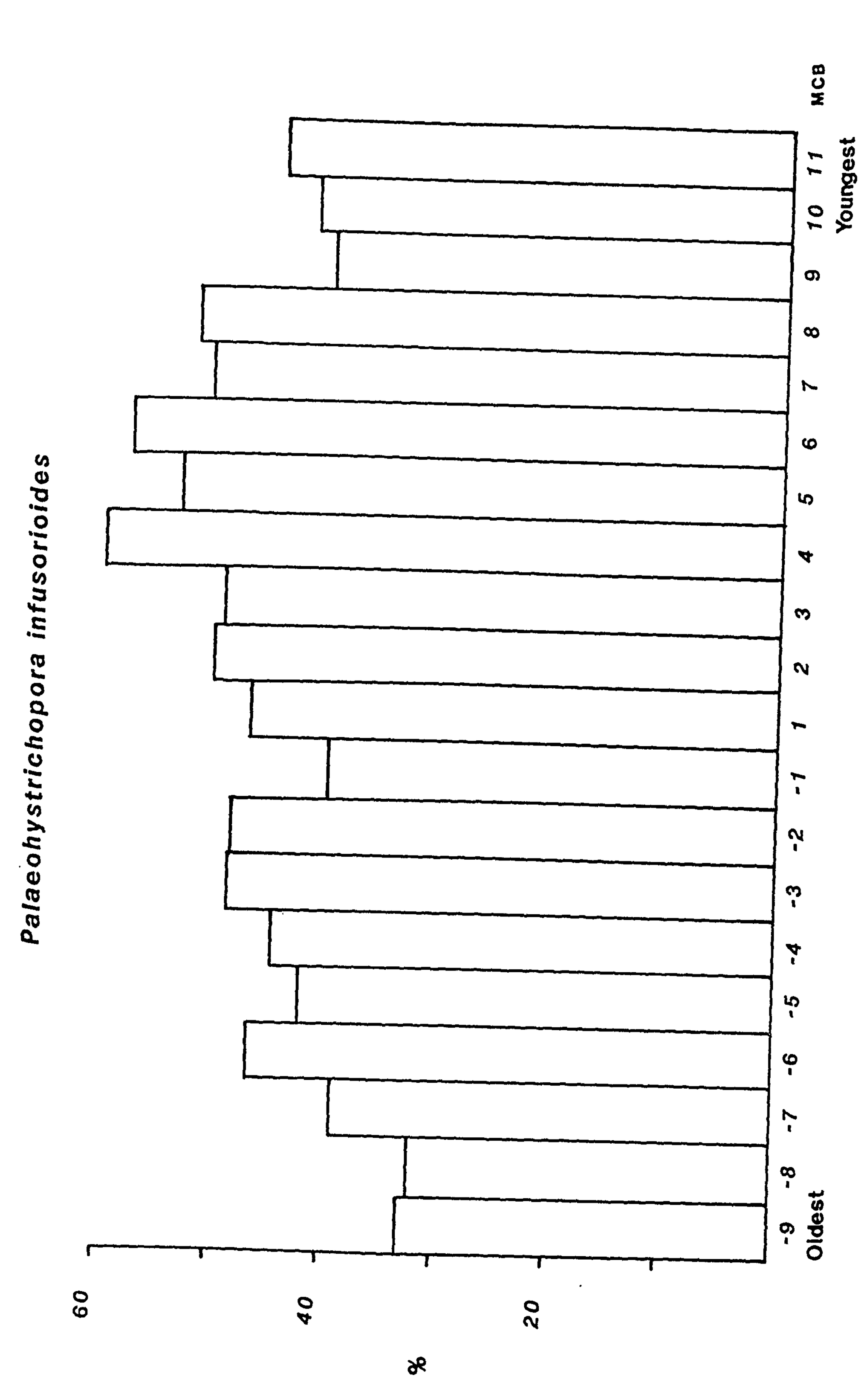

Figure 8.22 Percentage distribution of *Palaeohystrichophora infusorioides* within section MCB samples. See Fig. 7.18 for explanation of abbreviated sample numbering system.

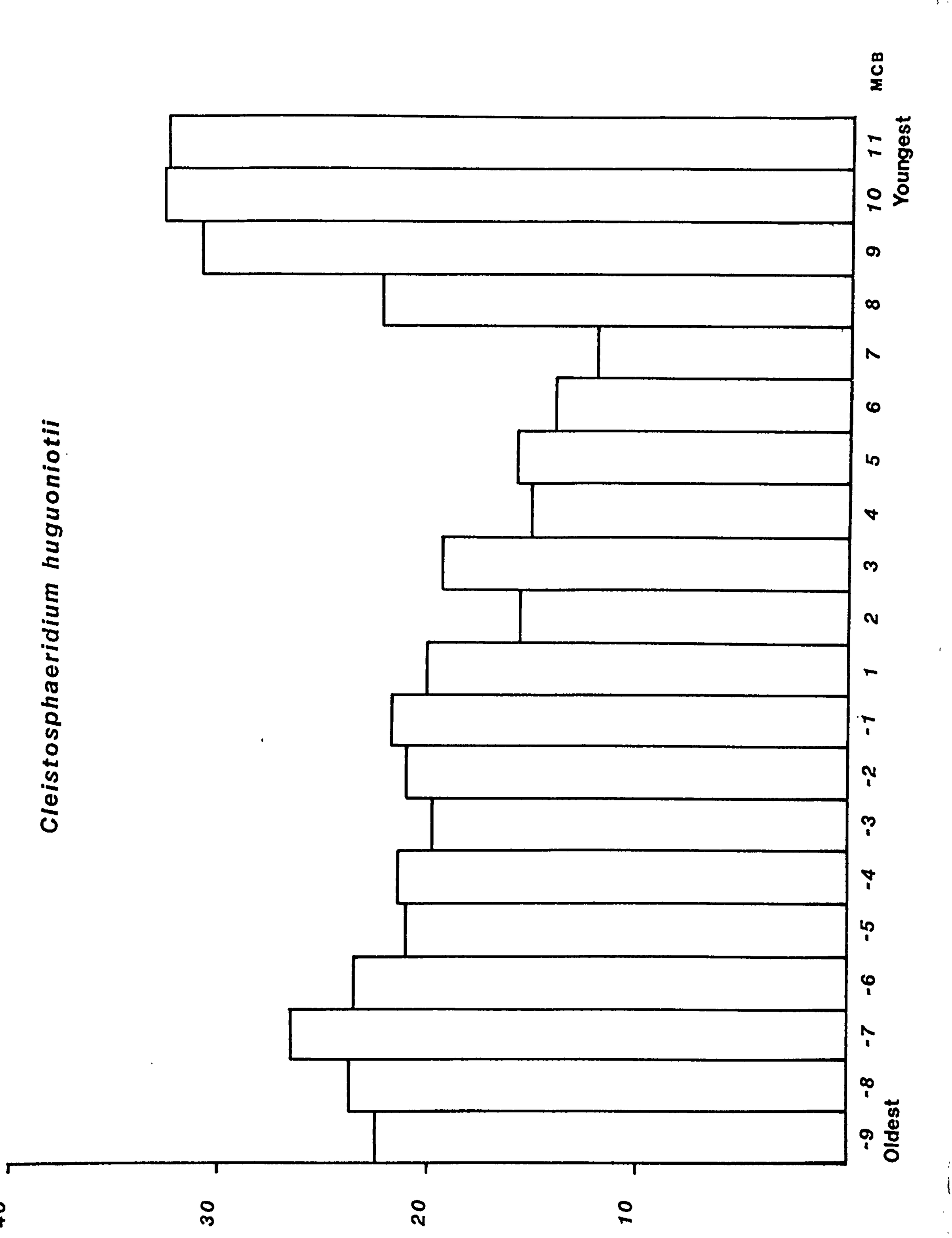

Figure 8.23 Percentage distribution of *Cleistosphaeridium huguoniotii* within the section MCB samples. See Fig. 7.18 for explanation of abbreviated sample numbering system.

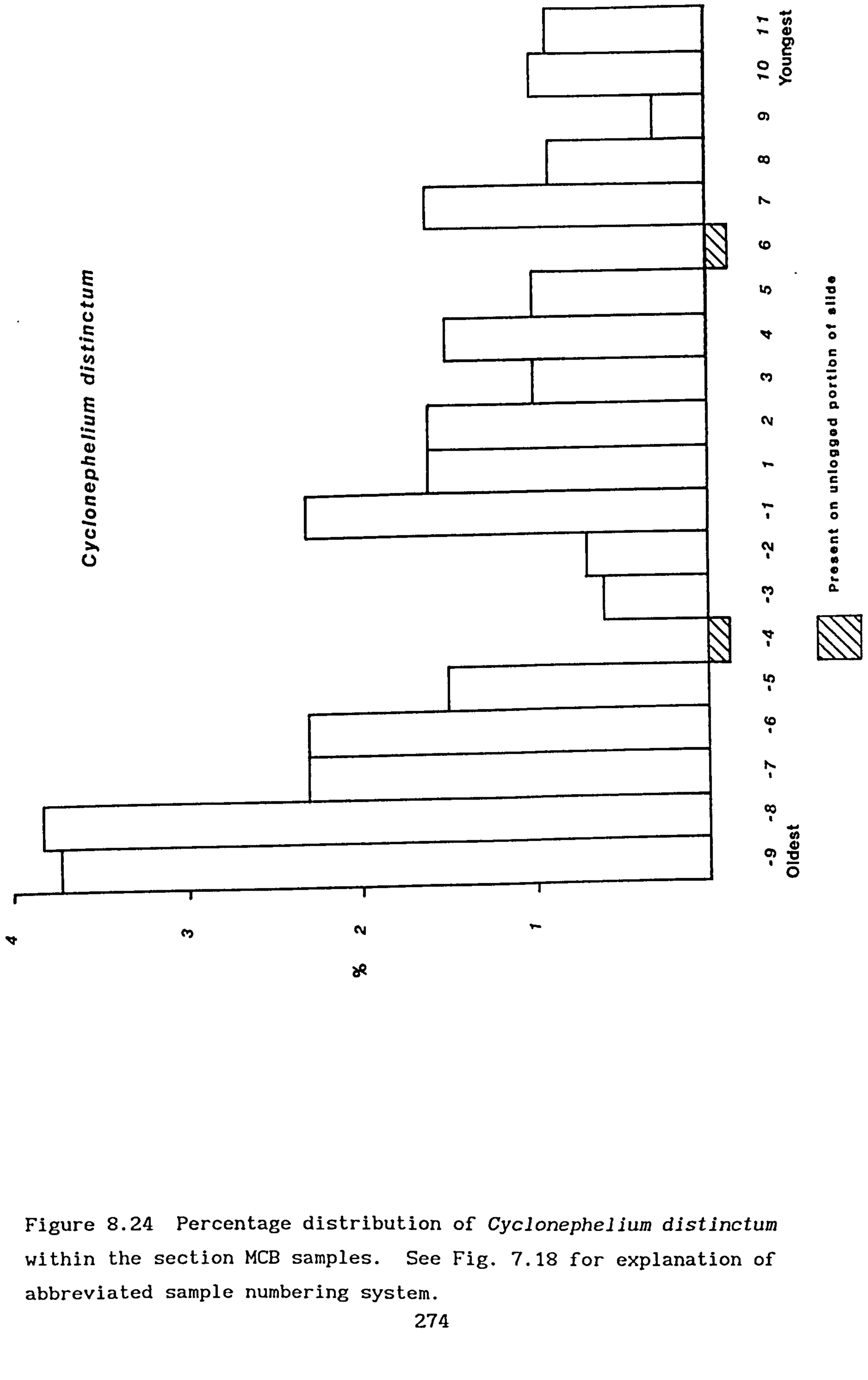

Figure 8.24 Percentage distribution of *Cyclonephelium distinctum* within the section MCB samples. See Fig. 7.18 for explanation of abbreviated sample numbering system.

palynological content) and the position of the Mid-Cenomanian non-sequence. On the basis of cluster analysis samples MCB 0 --> 0.5 and MCB 0.5 --> 1, the lowermost two samples which occur just above the non-sequence, are included in the pre-non-sequence palynomorph assemblage.

A possible explanation of this discrepancy can be suggested when comparison is made to the effect of the postulated oceanic anoxic event on the dinoflagellate cyst assemblage of the Cenomanian-Turonian boundary sequence of Dover (Jarvis *et al.*, 1988a). Within this event the dinoflagellate cysts are the second last of all microfossil groups examined (foraminifera, ostracods, calcareous nannofossils, dinoflagellate cysts) to be adversely affected by the expansion of the oxygen minimum zone (Jarvis *et al.*, 1988a) (nannofosslis are the last group to be affected). There therefore appears to be a lag period between the effect of a dramatic change in palaeo-oceanography of a basin such as this on the foraminiferal assemblage and its effect on the coeval dinoflagellate cyst assemblage. Thus, within the MCB section, the inclusion of the lowermost samples occurring after the non-sequence (MCB 0 --> 0.5 and MCB 0.5 --> 1) within the lower dinoflagellate association (identified by cluster analysis) can be explained on the basis that the dinoflagellate cyst associations were affected later than the foraminifera. However, it must be accepted that such a feature is hard to explain hydrodynamically.

The distribution of the three types of foraminiferal test linings (as identified herein) appears to show a correspondence to the positioning of the Mid-Cenomanian non-sequence (Carter and Hart, 1977). Post-non-sequence samples consistently yield more regular occurrences and more diverse types of foraminiferal linings than do pre-non-sequence samples. The distribution of Type 2 foraminiferal lining is restricted to post-non-sequence samples and that of Type 3 shows almost the same restricted distribution, with only two occurrences in the lower pre-non-sequence part of the section.

Carter and Hart (1977) interpreted the faunal non-sequence as being related to an increase in water depth of the Cenomanian sea, together with periodic changes between colder and warmer temperature water masses. The results of the analysis of the palynological content of this section cannot be used to substantiate the theory that the Mid-Cenomanian non-sequence is related to a deepening event within

the Mid-Cenomanian non-sequence is related to a deepening event within the basin. However, what the palynological analysis does suggest is the existence of two distinct palynological associations. These associations are divided by the non-sequence itself. When comparison is made to the conclusions of palynological analysis of Site 3a the following interpretations on section MCB can be made. The post-non-sequence association, because of the higher percentages of *P. infusorioides* is interpreted as a slightly colder water association than the pre-non-sequence assemblage, where numbers of warmer water dinoflagellate cyst species such as *C. huguoniotii* and *C. distinctum* increase. However, percentages of these dinoflagellate cyst species are sufficiently variable as to suggested there were no more than minor fluctuations in palaeotemperatures even within the two associations.

8.5. Section SFE, South Ferriby

A dominantly marine palynomorph assemblage is recorded in this section. The palynomorph content is heavily dominated by marine palynomorphs (dinoflagellate cysts, acritarchs, pterospermopsis) representing 97.47 - 99.67% and there is a minor proportion of terrestrial palynomorphs (spores and bisaccate pollen) of 0.33 - 2.53%.

Dinoflagellate cysts species present indicate that this section is of Late Cenomanian age and the assemblage present is comparable to the Late Cenomanian *Cleistosphaeridium huguoniotii* subzone (Davey, 1970). A range chart of all dinoflagellate cyst species present is given in Figure 8.25, and all raw numerical data for this section is given in Appendix 4.

Results of the quantitative analysis of section SFE reveals that only four samples (SFE 18, SFE 17, SFE 16 and SFE 15) of the nineteen examined yielded palynomorphs, all other samples are barren (Figure 3.12). Palynological preparations of the SFE samples below those that are productive (SFE 1-4, SFE 21-19) produce residues yielding all other kerogen types except palynomorphs (phyrogen). However, the preparations of the samples above the four productive samples (SFE 14-7) yield residues which are totally barren of any kerogen type.

The four productive samples yield very high numbers of dinoflagellate cysts per gramme of sediment (Figure 8.26). Abundance values range between 1,760 and 8,155 cysts/gm. These values are extremely high when compared to typical abundance levels (200-800 cysts/gm.) exhibited by other Cenomanian assemblages documented herein. The most abundant sample, SFE 17 (8,155 cysts/gm.) is that of the Black Band *sensu stricto* (Blake, 1878; Jefferies, 1963; Wood and Smith, 1978) (see Figure 3.12).

The four extremely abundant samples (SFE 18, SFE 17, SFE 16, SFE 15) are the result of one of two possibilities. The first is that they genuinely represent higher than average dinoflagellate abundance within the water mass. The second alternative, which is the more likely of the two, is that the four most abundant samples are the result of a condensed interval within the reduced *Plenus* Marls sequence of South Ferriby. The fact that the South Ferriby section records a condensed sequence of marly chalks has been identified by

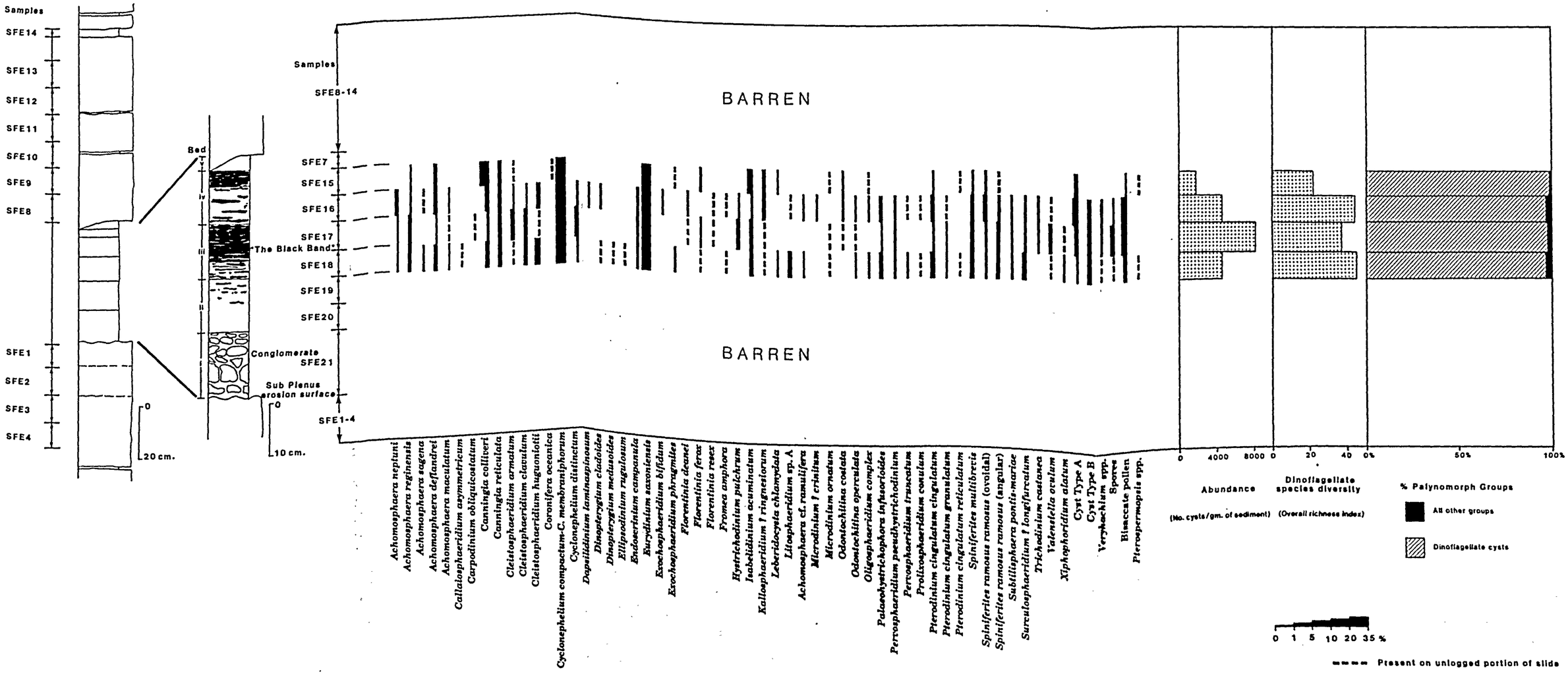

Figure 8.25 Range chart of the dinoflagellate cyst species and other palynomorph taxa of South Ferriby section (SFE), together with information on abundance, species diversity and % palynomorph groups.

Hart *et al.* (1991).

The productive samples of section SFE record low species diversity assemblages (Figures 8.27a, 8.27b). Values of species diversity of SFE samples are distinctly lower than normal values of species diversity exhibited by other Cenomanian samples examined within this study. Thus, it is apparent that the SFE section records a stressed environment which is typically indicated by lower species diversity levels as only a reduced number of highly adaptive species are present (Odum and Copeland, 1974; Davies *et al.*, 1982). The two lowest levels of species diversity (Figures 8.27a, 8.27b) are given by SFE 17 and SFE 15 both of which are black band horizons (Wood and Smith, 1978). There therefore appears to be a link between the anomalously low species diversity levels and these high organic content, dark marl deposits.

The dinoflagellate cyst assemblages of section SFE (Figure 8.28) are characterised by almost equal percentages of *Cyclonephelium compactum-membraniphorum* complex Marshall and Batten 1988 (24.1 - 28.3%) (Pl. 6, Figs 6-8) and *Eurydinium saxoniensis* Marshall and Batten (1988) (24 - 35%) (Pl. 8, Figs 1,2). *Canningia colliveri* Cookson and Eisenack 1960b (Pl. 2, Fig. 4) is present in minor percentages in samples SFE 18 - 16, but increases dramatically to represent 21% of the palynomorph assemblage in the last productive sample, SFE 15. The remaining dinoflagellate cyst species vary from 0.3 - 8.0% of the assemblage. There are very low percentages of *P. infusorioides* (0.6 - 2.5%), the species that dominates all other Cenomanian palynomorph assemblages examined within this study. Two unidentified palynomorphs, Cyst type A (Pl. 24, Figs 1-3) and ?Cyst type B (Pl. 23, Figs 4-6) are numerically quite common within the SFE section; 0.3 - 8% and 0 - 1.7% respectively. The former is likely to be a dinoflagellate cyst and the latter is of uncertain affinity.

Distinctively present within this uppermost Cenomanian palynomorph assemblage is the species *Litosphaeridium* sp. A. (Pl. 13, Figs 5-7). Marshall (1983) and Marshall and Batten (1988) recorded this species as occurring within Cenomanian-Turonian Black shale sequences of northern Europe. Marshall (1983) refers to this species as *Litosphaeridium chlidanum* n. sp. This species appears to have a restricted occurrence in Cenomanian-Turonian boundary sequences both herein within the South Ferriby section, South Humberside and sections

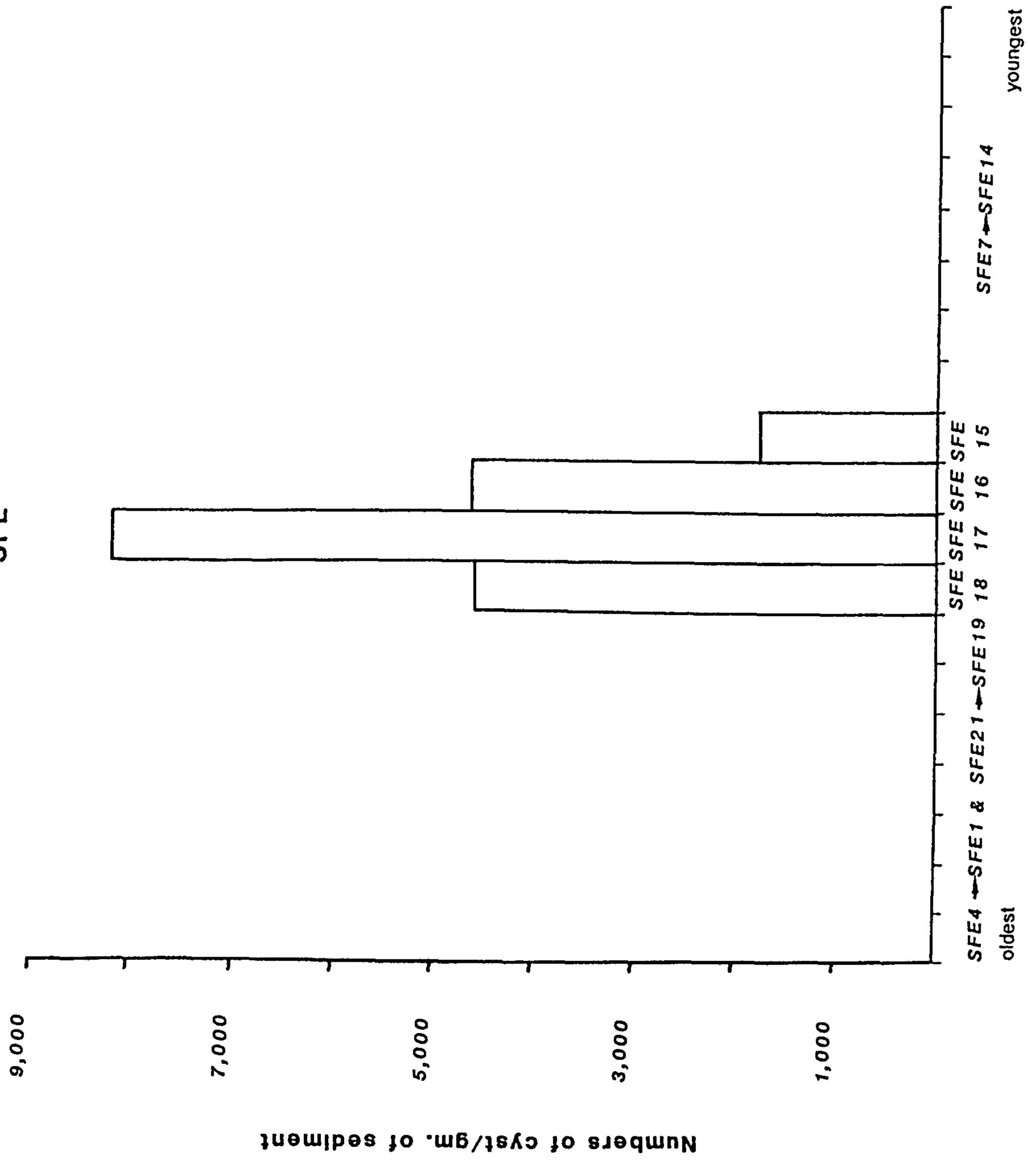

Figure 8.26 Abundance values for South Ferriby samples (SFE) based on number of dinoflagellate cysts per gramme of sediment.

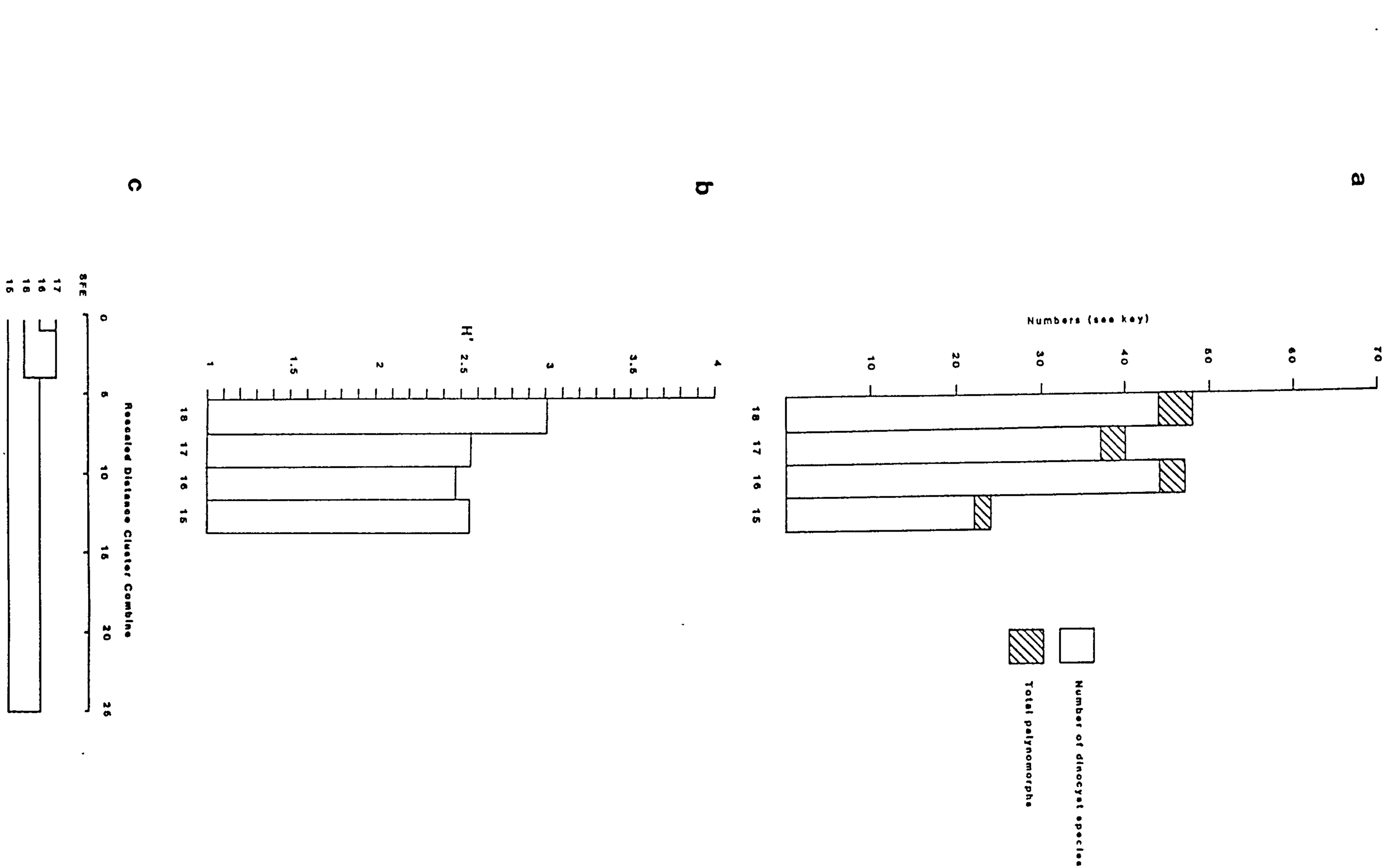

Figure 8.27 Summary of statistical analyses of South Ferriby samples (SFE). a. Overall richness species diversity index (S). b. Shannon species diversity index (H'). c. Cluster analysis dendrogram.

of south-east England. FitzPatrick (1990 *pers. comm.*) has noted this species as occurring in the lowermost, palynologically productive Turonian samples from south-east England. Hence, this species has great potential in the identification of uppermost Cenomanian - lowermost Turonian deposits elsewhere within the Anglo-Paris Basin and possibly on a broader scale, within northern Europe.

As can be seen from the list of species occurring in this section, see Appendix 4, and from examination of the range chart (Figure 8.25), together with features already outlined, such as extremely high abundance and very low species diversity, it can be seen that the SFE section records an atypical Cenomanian palynomorph assemblage.

When comparison is made to the palynomorph content of the Cenomanian-Turonian sequence at Dover investigated by Tocher *in* Jarvis *et al.*, 1988a, it appears that the palynomorph assemblage of the SFE section is quite dissimilar. The dinoflagellate cyst assemblages of the *Plenus* Marls sequence of Dover become increasingly more dominated by the species *Kallosphaeridium ? ringnesiorum* (Manum and Cookson) Helby 1987 (Pl. 11, Fig. 1). This species represents as much as 96% of the assemblage in Bed 6 (Jefferies, 1963). However, the upper beds (Beds 7-8, Jefferies, 1963) of the *Plenus* Marls and therefore of Latest Cenomanian age contain sparse to barren dinoflagellate cyst assemblages. Indeed, the dinoflagellate cyst assemblages do not recover until a considerable distance into the succeeding Turonian. The percentages of the cyst species *K. ? ringnesiorum* within the section SFE do not reach levels higher than 1.4%.

Within Jarvis *et al.* (1988a) comparison between the palynomorph content of the Dover sequence is made with other Cenomanian-Turonian sequences of *Plenus* Marl equivalents occurring elsewhere within the Anglo-Paris Basin. The palynomorph assemblages of Pas-de-Calais, the Isle of Wight and south-east Devon are documented by Foucher *in* Robaszynski *et al.*, 1980; Clarke and Verdier, 1967; Jarvis *et al.*, 1988a respectively and are typically dominated by *P. infusorioides* and *S. ramosus*. The Saumur section records a diverse but low abundance assemblage characterised by no one species dominating the assemblage, but which does contain *P. infusorioides* and *S. ramosus* (Foucher, *in* Robaszynski *et al.*, 1980). However, within the SFE section percentages of *P. infusorioides*, and *S. ramosus* (0.5 -

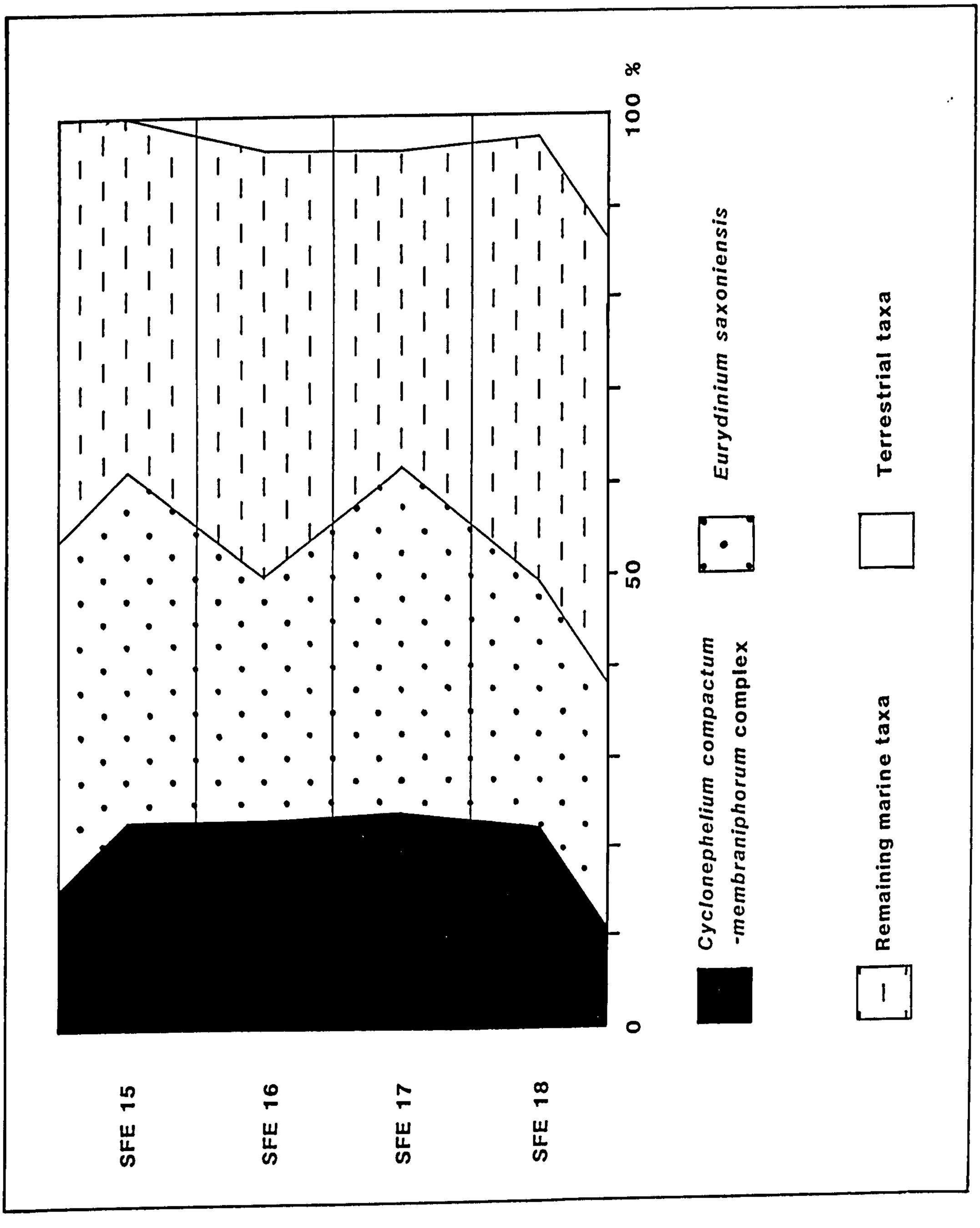

Figure 8.28 Relative percentages of dominant dinoflagellate cyst species within South Ferriby (SFE) samples.

2.4%) are very low indeed. Therefore, the dinoflagellate cyst assemblages exhibited by the SFE section are not similar to other sections within the Anglo-Paris Basin as outlined above.

Marshall and Batten (1988) examined the palynological content of two samples from the South Ferriby locality together with other sections within northern Europe which expose Cenomanian-Turonian black shale sequences. From this analysis two dinoflagellate cyst associations were identified, the *Spiniferites* association and the *Cyclonephelium/Eurydinium* association. The *Cyclonephelium/Eurydinium* association is equally dominated by *Eurydinium saxoniensis* and *Cyclonephelium compactum-membraniphorum* complex Marshall and Batten (1988),and has significant percentages of *Spiniferites* spp. with other species present in minor percentages. The palynological residue of this association is also distinctive, in that it is dominated by granular amorphous organic matter. The *Cyclonephelium/Eurydinium* association occurs within the SFE section examined herein and indeed, as documented previously, this association dominates the four productive samples. The presence of this association is interpreted by Marshall and Batten (1988) to represent deposition within a stressed environment due to the presence of a depleted level of oxygen which extended up into the water column. This depletion of oxygen is believed to be due to restricted circulation caused by periodic silling of the basin (Marshall and Batten, 1988).

Palynofacies analysis of the SFE section has revealed that there are distinct palynofacies associations present which are also identified and confirmed by cluster analysis (Figure 8.27c). The palynofacies associations of the SFE section are illustrated on Figure 8.29 and are classified using Bujak *et al.* (1977a) classification scheme as follows:

SFE 18	50% Phyrogen
	40% Amorphogen
	10% Melanogen
SFE 17 (Black Band)	35% Phyrogen
	60% Amorphogen
	5% Melanogen

SFE 16 50% Phyrogen
45% Amorphogen
5% Melanogen

SFE 15 95% Phyrogen
7% Amorphogen
3% Melanogen

The amorphogen component of the palynofacies is very distinctive within this section as it is present in considerably higher proportions in the Black Band sample (SFE 17) when compared to remaining SFE samples and to other Cenomanian palynological preparations examined within this study. This kerogen type gives the residue a characteristic "dirty" appearance. This particular kerogen type has been identified previously by other workers. Habib and Miller (1987) refer to it as an "amorphous debris facies". Habib (1982), in a investigation of black clay organic facies sedimentation of the Mesozoic of the North Atlantic identified a xenomorphic facies which is characterised by a predominance of well preserved amorphous debris and palynomorphs. This xenomorphic facies is characteristic of the Cenomanian deposits of the North Atlantic and is interpreted by Habib (1982) as having resulted from increased planktonic productivity and rapid sedimentation. Habib and Drugg (1987) further document this amorphous debris-rich xenomorphic facies as occurring in Cretaceous marine black clays in North America. Remarkably, although both are obviously highly organic, marly deposits, the localised upper black band of the South Ferriby section (SFE 15) yields a very "clean" residue in comparison to that of the Black Band (SFE 17) itself, see above palynofacies percentages. A possible explanation for the anomalously higher percentages of amorphogen present in sample SFE 17 is given below.

As is indicated by the dendrogram (Figure 8.27c) samples SFE 18 - 16 are grouped together at a high confidence interval and all these samples exhibit broadly similar palynofacies associations as can be seen from above classifications. The sample SFE 15 is identified by cluster analysis as being extremely dissimilar to the other three samples (SFE 18 - 16) and this is confirmed by the palynofacies type percentages as defined above.

Figure 8.29 (Page 287)

Palynofacies photomicrographs of South Ferriby (SFE) samples, magnification x337. See Chapter 8 for palynofacies percentages of each individual sample.

1 SFE 18

2 SFE 17 (Black Band sample)

3 SFE 16

4 SFE 15

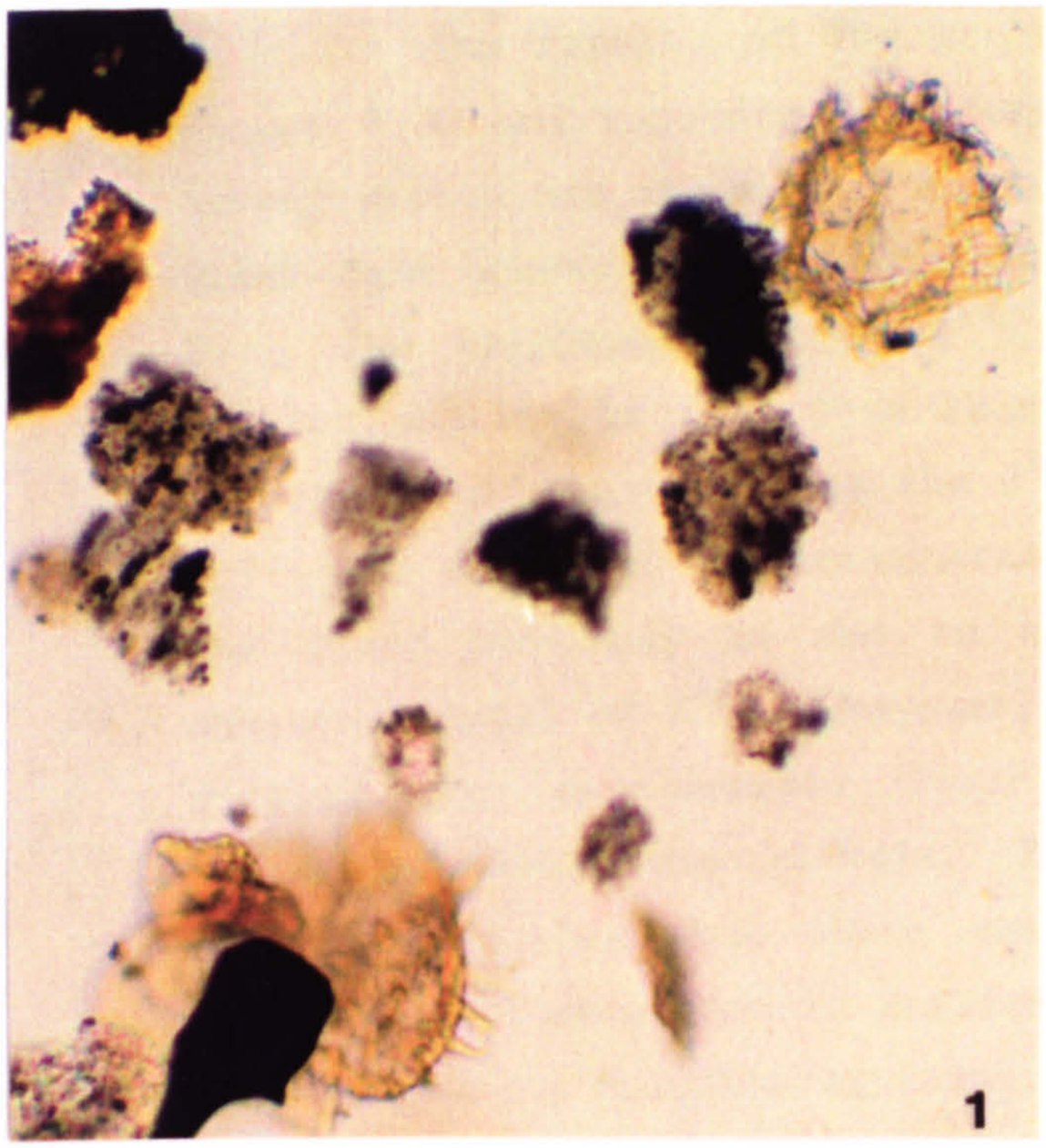

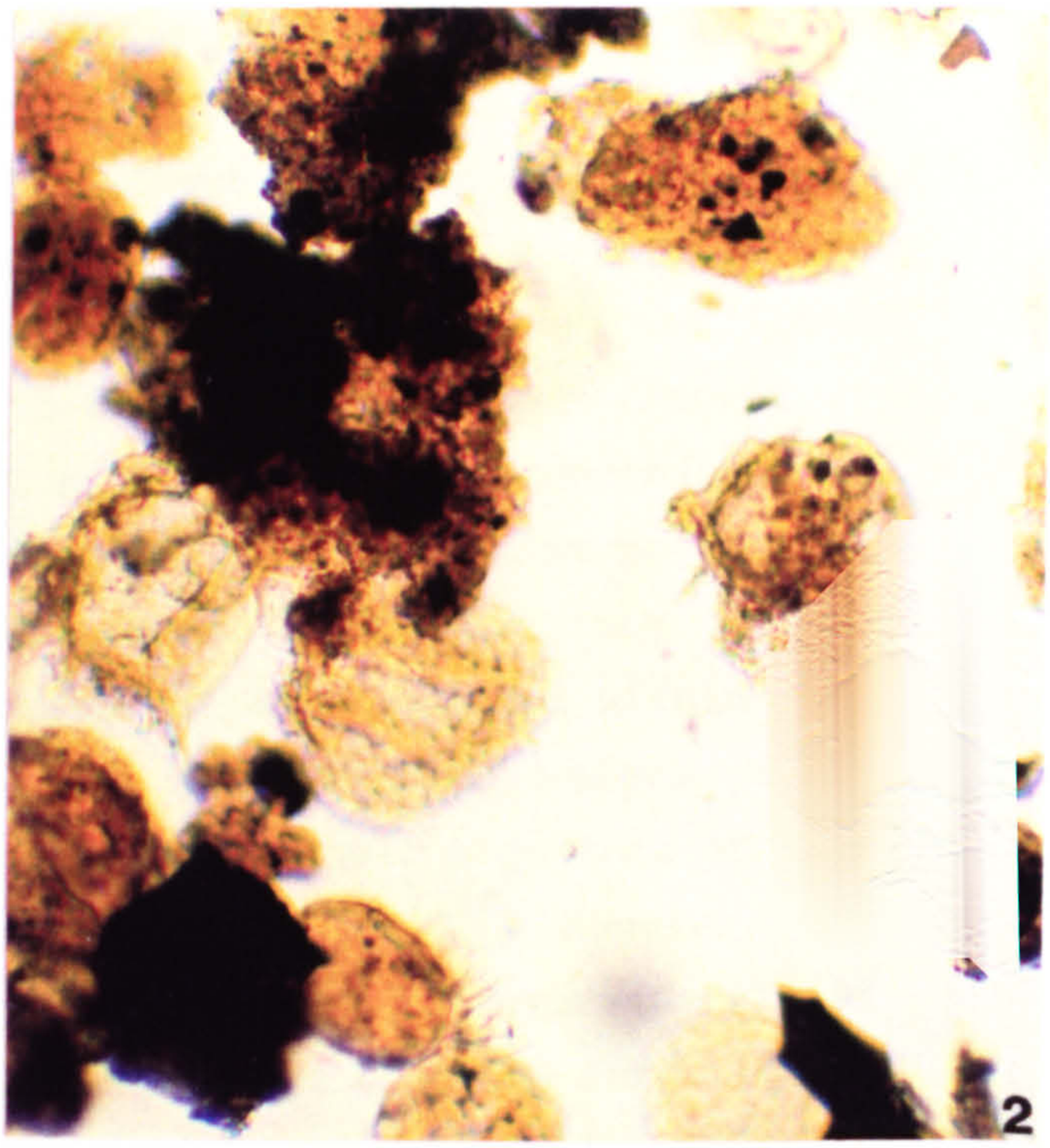

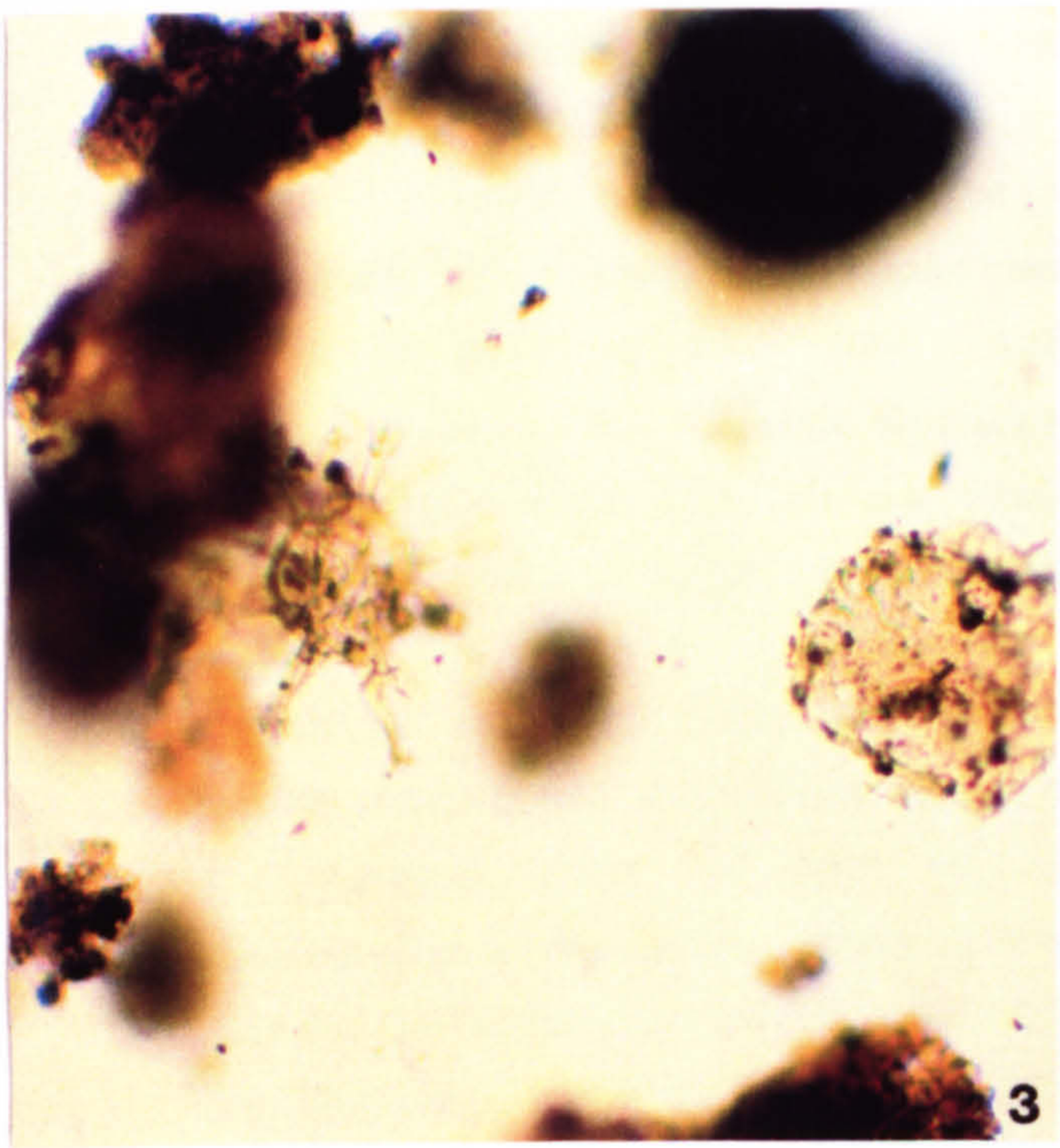

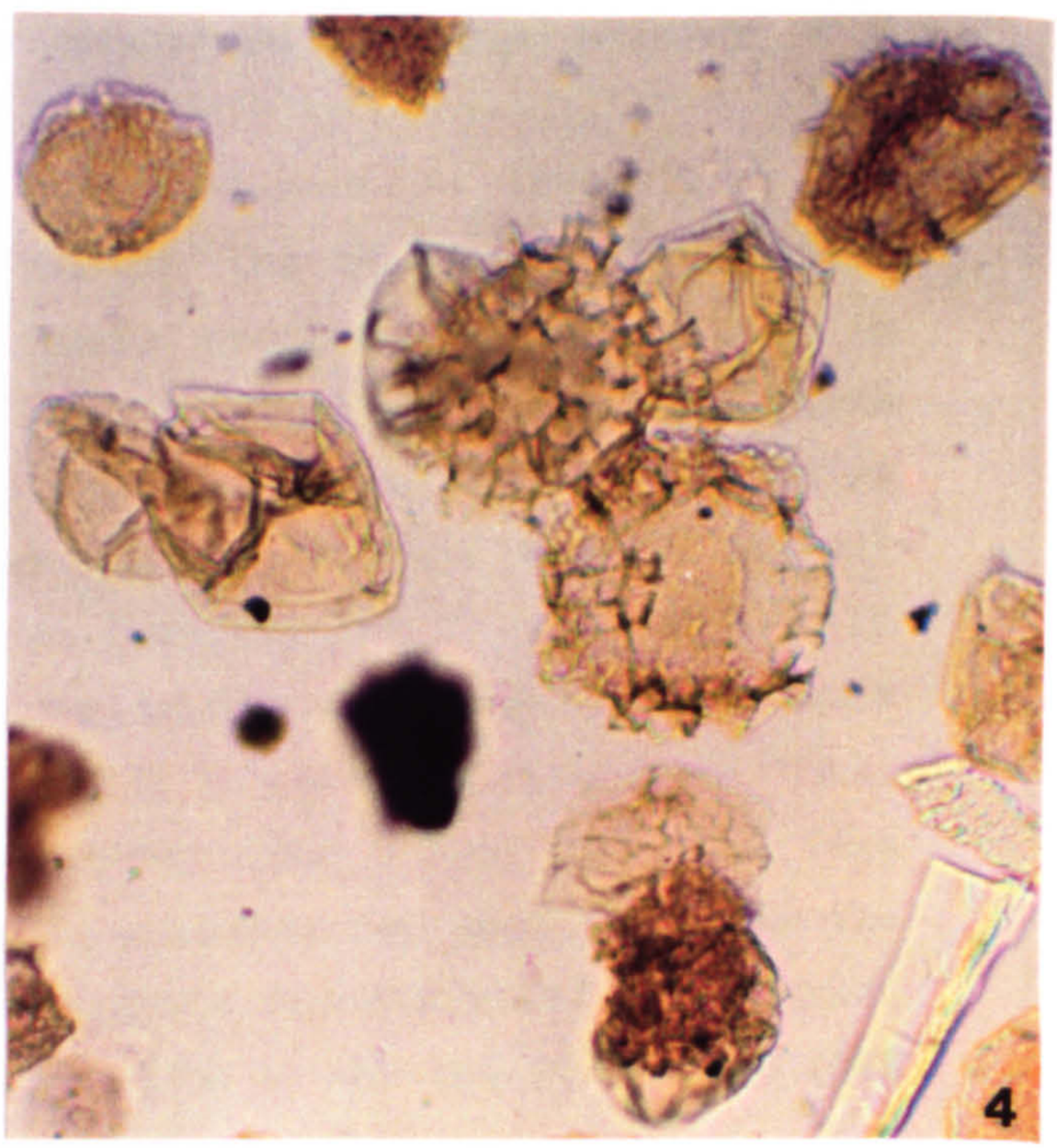

Figure 8.29

Hart *et al.* (1991) in an investigation of the late Cenomanian event of South Ferriby document the lithological, sedimentological, stable isotopic, rare earth geochemical, SEM investigation, foraminiferal and palynological analyses carried out on splits of the same samples.

The results of the stable isotope analysis can be seen in Figure 8.30 and Appendix 8 (Ditchfield *in* Hart *et al.*, 1991). This investigation has shown that a small $\delta^{13}C$ excursion occurs within the Black Band however, a maximum value of 4.17°/oo PDB is yielded by SFE 19. The magnitude of the $\delta^{13}C$ excursion exhibited by the South Ferriby section is much less than that observed at Dover (Jarvis *et al.*, 1988a). The fact that the $\delta^{13}C$ excursion does not correspond as one would expect to the concentration of organic matter as present in the Black Band may be due to methanogenesis, rather than due to enhanced burial of $\delta^{13}C$. However, values of $\delta^{13}C$ recorded within this section are considerably lower than the extreme values often associated with methanogenesis. The oxygen isotopic signature of this section indicates that there was a depletion of $\delta^{18}O$ however, the observed $\delta^{18}O$ excursion is smaller than that seen at Dover (Jarvis *et al.*, 1988a). A possible explanation for this is that the formation of burial cements and the overprinting effects of their isotopic signatures may have reduced the magnitude of any primary $\delta^{18}O$ excursion.

Rare earth geochemistry was performed to investigate the evidence of siderophile anomalies within the South Ferriby section (Orth *in* Hart *et al.*, 1991) and these results are illustrated in Figure 8.31. The element Iridium shows a broad maximum in the Black Band sample (SFE 17) but it shows a normal correlation to the clay content. When iridium is normalised against aluminum there is a small peak in the lower part of the section (samples SFE 1 - 4). The Mn/Ca ratio is reduced within the Black Band sample which may be the result of Mn depletion; a process often recorded in anoxic marine conditions. In summary, Orth *in* Hart *et al.* (1991) has shown that the late Cenomanian siderophile anomaly zone is probably represented within the hiatus between the top of the Ferriby Chalk Formation which is marked by the sub-*Plenus* erosion surface (post SFE 1) and the Black Band (SFE 17).

Investigations of the foraminiferal content of section SFE

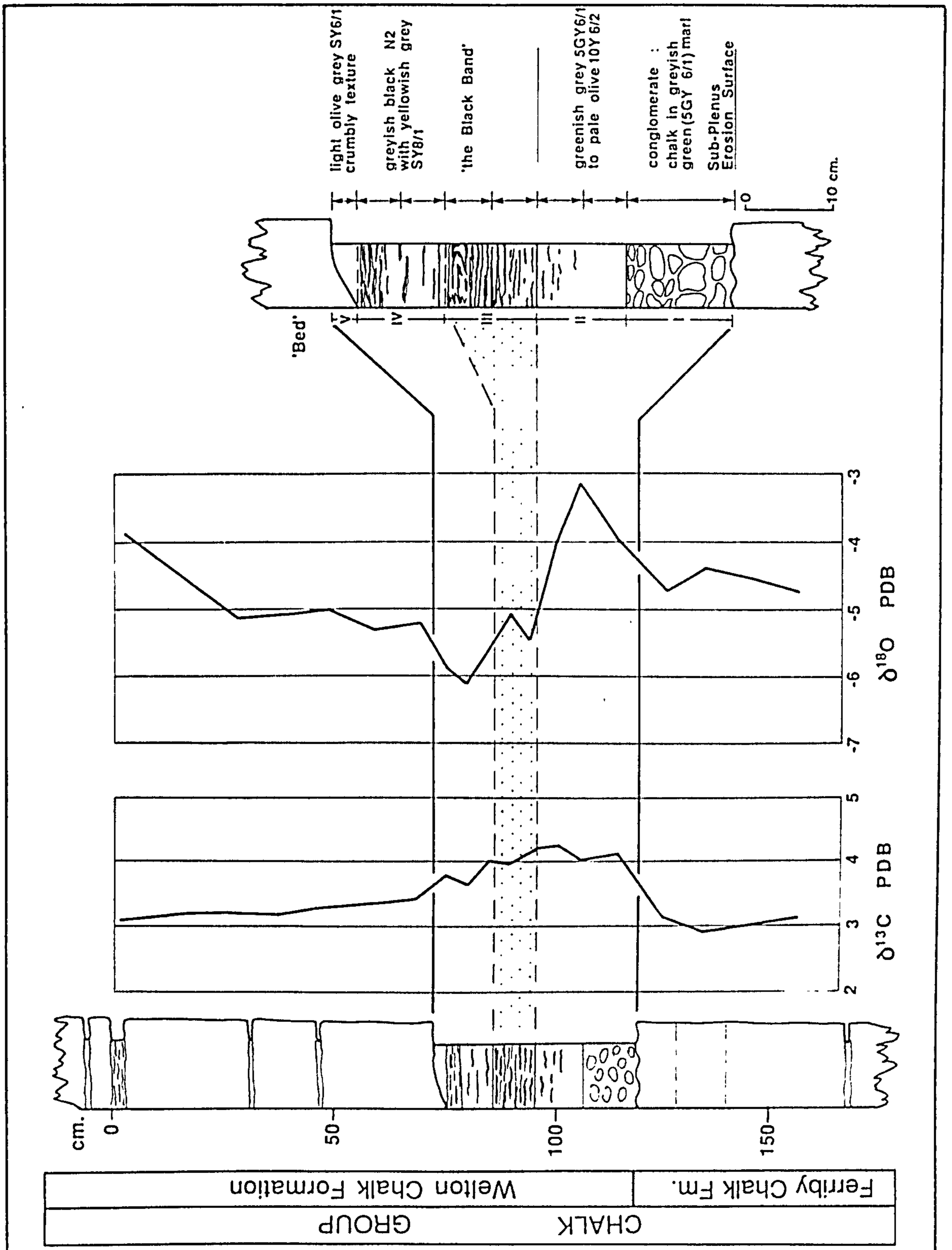

Figure 8.30 Carbon and oxygen stable isotope signatures for the South Ferriby section (SFE), from Hart *et al.*, (1991). (Rock colour references are taken from the Rock Color Chart).

have been carried out by Hart *et al.* (1991). Previously, Hart and Bigg (1981) documented the foraminiferal content of much of the key Upper Cretaceous Humberside sections. The extinction of *Rotalipora cushmani* (Morrow) occurs at the sub-*Plenus* erosion surface and this confirms the hiatus predicted by the rare earth geochemical data. There is a dominance of *Hedbergella/Whiteinella* fauna particularly in samples SFE 17 and SFE 18. The characteristic increase in small buliminids and simple agglutinated foraminifera is also present within the black mudstones of samples SFE 15 - SFE 19. There is almost complete extinction of typical Cenomanian benthonic foraminifera at the sub-*Plenus* erosion surface. However, during the succeeding latest Cenomanian and earliest Turonian (samples SFE 8 - SFE 14) the benthonics recover somewhat and this interval is characterised by a impoverished benthonic foraminifera fauna which is dominated by the species *Gavelinella berthelini* (Keller). These same samples are totally barren of both palynomorphs and any kerogen type. By comparison with other Cenomanian-Turonian boundary events worldwide (Jarvis *et al.*, 1988a; Eicher and Worstell, 1970; Koutsoukos, 1989; Koutsoukos *et al.*, 1990) the presence of the species *Gavelinella berthelini* (Keller) is interpreted as being characteristic of reduced oxygen conditions.

In summary, the South Ferriby section records an atypical uppermost Cenomanian palynomorph assemblage which is characterised by high abundance rates (measured as number of cysts per gramme), low species diversity and which is dominated equally by the dinoflagellate cyst species *Cyclonephelium compactum-membraniphorum* complex and *Eurydinium saxoniensis*. It is believed that this highly abundant palynomorph assemblage represents a condensed sequence which was originally deposited in a stressed environment within the water mass (Goodman, 1979). Such adverse conditions are believed to be the result of reduced oxygen levels within the Cenomanian sea due to restricted circulation which itself is possibly the consequence of barring of the basin during Late Cenomanian times. Restricted circulation could result in higher than normal amounts of the amorphogen kerogen type being deposited in the silled basin. However, it is not believed that the water mass experienced total anoxia as not all faunal and floral groups become extinct within the *Plenus* Marl sequence of South Ferriby. A more plausible situation is that there

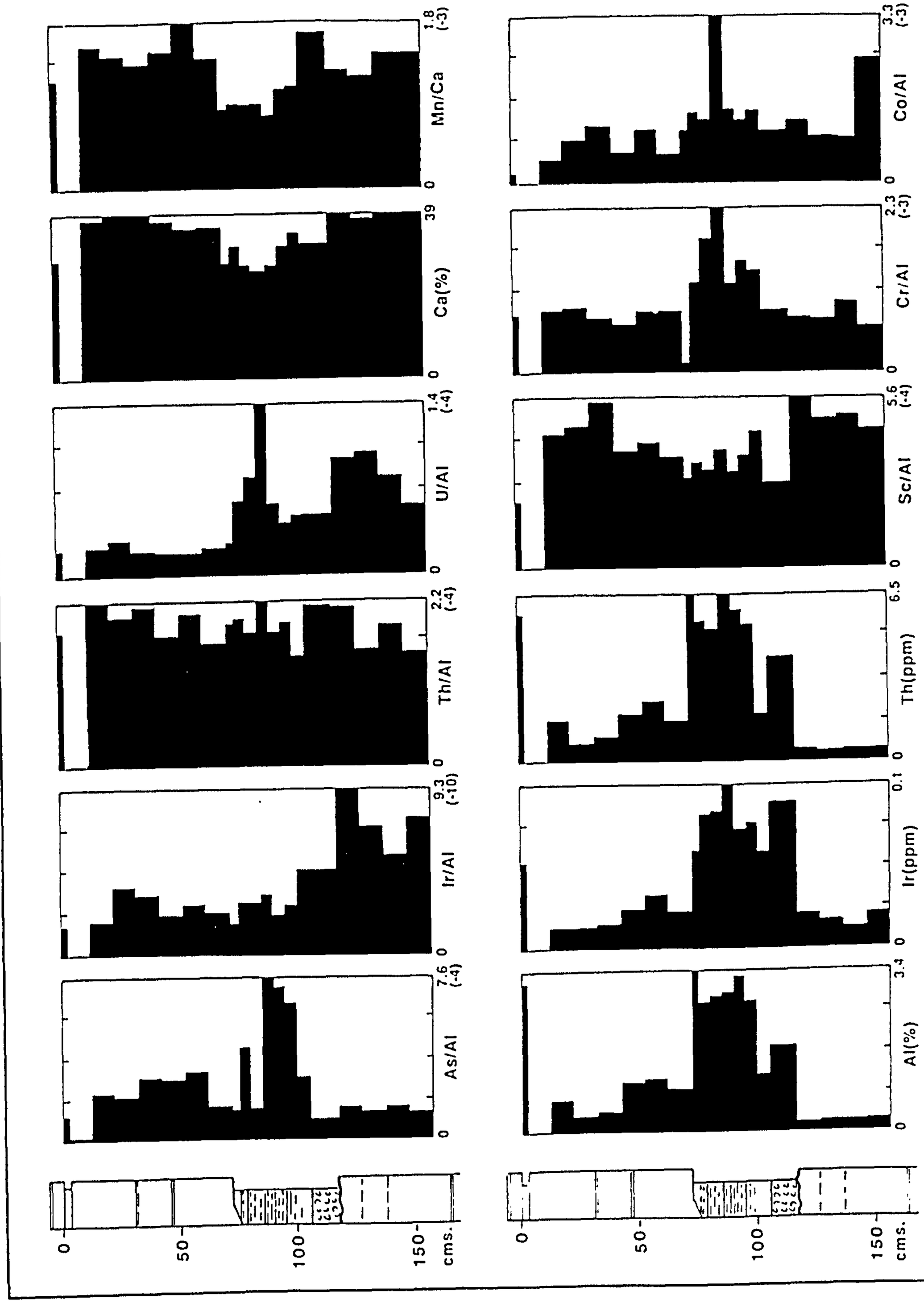

Figure 8.31 Rare earth geochemical data from the South Ferriby section (SFE), from Hart *et al.*, (1991).

was a reduction of the available oxygen within the water mass which affected successively higher levels in the water column as the oxygen minimum zone expanded, a mechanism which is much the same as that suggested by Jarvis *et al.*, 1988a. However, on the basis of palynological analysis alone, an interpretation into the overall forcing mechanism (eustacy, tectonism, palaeo-oceanographical change etc) within the basin cannot be conclusively made.

Chapter 9

CONCLUSIONS OF THE PALYNOLOGICAL ANALYSES

9.1. Overall conclusions

In consideration of the aims identified in Chapter 1, dealing with the reconstruction of the palaeo-oceanography and marine environmment of the Chalk sea, it is felt that much has been achieved. The strengths of this project are believed to be high resolution sampling, utilisation of statistical techniques and the application of a multidisclipinary approach. A summary now follows of the most important and salient points to be concluded from this study.

Key techniques, which measure very useful and meaningful parameters are the measurements of abundance and species diversity. These techniques have proven of great importance in the interpretation of palynological data herein. To exclude such techniques is to ignore easily acquired data.

The application of a quantitative technique necessary for abundance calculations does require the application of a somewhat non-standard processing procedure. This results in firstly, the need for a more rigorous approach to be applied to the processing of all samples to ensure quantitative consistency and secondly, the making of a second set of aliquot slides. Also, exclusion of an oxidation stage is advisable as it has been proven that oxidation introduces unwanted bias to the quantitative technique.

Species diversity has been measured by two indices; overall richness (S) and Shannon index (H'). Measurements of species diversity as calculated by both indices corresponded very well. However, because Shannon index calculations takes species abundance into account, the two indices are sometimes slightly at variance. In the analysis of the South Ferriby section the anomalously low levels of species diversity present have substantiated the interpretation that this section records a stressed environment (Odum and Copeland, 1974; Davies *et al.*, 1892).

More detailed statistical and spectral analysis techniques were employed to interpret properly the multivariate data sets produced by palynological analyses. The potential of these techniques is heightened by the fact that the majority of sections under

investigation are sampled at extremely small sampling intervals. The palynological analysis herein was carried out in order to further investigate features which characterise each section as identified by other geological disciplines (stable isotope, micropalaeontological and geochemical analyses). In the majority of cases the application of statistical techniques such as cluster analysis and fourier analysis has been useful in the investigation of similar trends within the palynological data. A summary of the success rate of the various statistical approaches used is as follows in Table 2

	SECTIONS							
	Site 3a		TBB		MCB		SFE	
STATISTICAL TECHNIQUES	Dino.	Palyfac.	Dino.	Palyfac.	Dino.	Palyfac.	Dino.	Palyfac.
Cluster	0%	N/A	0%	80%	100%	N/A	70%	100%
Fourier	100%	N/A	N/A		N/A		N/A	
Auto-Correlation	0%		N/A		N/A		N/A	

Dino. = Dinoflagellate cyst association

Palyfac. = Palynofacies association

N/A = Not applied

Table 2 Summary of success rates of the statistical techniques applied to palynological data.

Cluster analysis was carried out on the palynological data sets of all sections. As can be seen from Table 2 cluster analysis, on average has yielded mixed results but has been very successful in the verification and identification of some features. For example, cluster analysis confidently delimits two palynological associations within the MCB section which are caused by the presence of the Mid-Cenomanian non-sequence (Carter and Hart, 1977) which

characterises this section. The successful application of cluster analysis to palynofacies analysis was a somewhat unexpected outcome of this study (see section TBB and SFE for more details). It has been shown that this is a useful and valid approach and such application of this technique has great potential for future use.

Cluster analysis carried out in this study has shown that it is a moderately successful statistical technique, but some reservation must be exercised in its application as if it does not "fit" the data, then it can be ignored and *vice versa*.

Fourier analysis was only applied to the palynological data of one section (Site 3a) as this section was the only one under investigation from the aspect of the interpretation of its rhythmicity (both lithological and stable isotopical). This technique proved very successful indeed and as a result it is recognised as a valid technique for such investigation in the future.

The autocorrelation statistical technique was not successful. However, this is due to shortcomings in the nature of the palynological data, rather than any inherent flaw in the technique itself.

There now follows a brief summary of the most important conclusions from all the sections investigated.

9.2. Site 3a section

The marl lithology is consistently more abundant palynologically than coeval chalk deposits. This implies that marls in comparison to chalks, record a time within the water mass when more dinoflagellate cysts were available to be incorporated within the sediment.

From comparison with the stable isotope analysis of Ditchfield and Marshall (1989) it has been revealed that the distribution and relative abundance of some dinoflagellate cyst species is controlled by palaeotemperature. The cyst *P. infusorioides* increases in numbers in chalks and is interpreted as a colder water cyst present in waters which experienced palaeotemperatures as low as 22°C and with an average of 23°C. Conversely, numbers of the cysts *C. huguoniotii* and *C. distinctum* increase in marl samples. These species are interpreted as being warmer water dinoflagellate cysts favouring palaeo-oceanographical surface water temperatures averaging 25°C, but

capable of withstanding palaeotemperatures of 26.5°C. Other dinoflagellate cysts which are probably warmer species flourishing in similar palaeotemperatures are *C. asymmetricum, C. cooksoniae, H. pulchrum* and *P. cingulatum* subspp. The whole suite of dinoflagellate cyst present in Site 3a samples are interpreted as favouring sea surface palaeotemperatures of between 22 - 26.5°C.

There is a an inversely proportional relationship between the distribution and relative percentages of the dinoflagellate cyst species *P. infusorioides* and the two species *C. huguoniotii* and *C. distinctum*. Whether this relationship is independent of the influence of palaeotemperature or not cannot be concluded or refuted.

The distribution and percentage presence of dinoflagellate cyst species is linked to lithology which is due to the fact that differing lithologies are dependent on slightly different palaeotemperatures. This link between lithology and dinoflagellate cysts is further substantiated by the support of fourier analysis which picks out a cyclicity or periodicity within the palynological data sets investigated. The identified periodicity is coincident with the typical bed thickness of marls which are typically 20cm. thick and chalks of 40cm. thickness. The influence of lithology is believed to be the most important controlling factor within this section (Site 3a). However, what is forcing this lithological rhythmicity is not alluded to on the basis of the palynological analysis herein. Also, the palynological data neither refutes nor substantiates the Milankovitch forcing mechanism theory which Robinson (1986b), Hart (1987) and Gale (1989a) maintain causes the lithological rhythmicity present in the Cenomanian of the Anglo-Paris Basin.

9.3. Section TBB

During the investigation of the abundance of the samples from this section it became obvious that oxidation results in loss of palynomorph residue, as much as 68% loss in some cases. This is caused by a mechanical loss due to the introduction of an extra stage of processing and sieving in the preparation of the oxidised samples which the other non-oxidised samples did not undergo.

Marl deposits consistently record higher abundance values, as indicated by number of cysts per gramme of sediment than chalk

lithologies. Thus, this confirms the similar result concluded from the analysis of Site 3a.

The distributions of both abundance and species diversity values exhibit troughs which correspond to the peak in the $\delta^{13}C$ values (sample TBB 7), Ditchfield (1990). The overall richness index of species diversity implies that samples TBB -3 to TBB 7, which are those sampling the pre-$\delta^{13}C$ excursion portion of the sequence record a higher species diverse dinoflagellate assemblage than those samples which occur after the $\delta^{13}C$ excursion (samples TBB 8 to TBB 15).

However, the distribution and relative percentages of individual dinoflagellate species are extremely uniform throughout this section and thus, do not show any relationship to the $\delta^{13}C$ excursion. Nevertheless, because both species diversity and abundance do show such a relationship it can therefore be concluded that marginally adverse conditions were present in the water mass at the time of the $\delta^{13}C$ excursion.

When the results of cluster analysis are compared to the palynofacies associations present in section TBB, it is obvious that there is some correspondence between the two. However, this correspondence is rather tenuous and it is therefore felt that there is not sufficient evidence to suggest a possible interpretation or cause. It should be appreciated however, that the variations within the palynofacies associations seen are all relatively minor and are all included within the limits of the marine palynofacies realm (Bujak *et al.*, 1977b).

9.4. Section MCB

The Mid-Cenomanian non-sequence of Carter and Hart (1977) is marked by low abundance levels of palynomorphs.

Variations in the species diversity values are linked to the Mid-Cenomanian non-sequence (Carter and Hart, 1977). The dinoflagellate cyst associations which occur prior to the non-sequence (samples MCB -4.5 to 0cm.) are consistently more diverse than those which occur after the non-sequence (samples MCB 0 to 5.5cm.).

The distribution of several dinoflagellate species are restricted (to varying degrees) across the non-sequence horizon. It can therefore be concluded that the forcing mechanism causing this

non-sequence resulted in major perturbations to the dinoflagellate cyst populations. A number of dinoflagellate cysts also display variations in their percentage presence which are appear to be linked to the non-sequence. For example *P. infusorioides* is present in significantly lower percentages in samples occurring prior to the non-sequence when compared to those occurring after it. Conversely, the percentage presence of both *C. huguoniotii* and *C. distinctum* are noticeably higher in pre-non-sequence samples than in post-non-sequence samples.

These results, together with corroborating evidence from the palynological analysis of Site 3a suggests that pre-non-sequence samples record a warmer water dinoflagellate association than the post-non-sequence samples which are interpreted as recording a slightly colder water assemblage. Unfortunately, a further interpretation as to the possible forcing mechanism causing such variations in the palaeotemperatures is not possible on the basis of palynological analysis alone. Therefore, the palynological data of section MCB cannot be used to substantiate or refute the theory that the Mid-Cenomanian non-sequence is linked to a deepening event (Carter and Hart, 1977). However, the application of cluster analysis is very conclusive in the identification of two distinct palynological associations, one which characterises the pre-non-sequence samples and the other distinguishing the post-non-sequence part of the section.

The distribution of the three types of foraminiferal test linings as identified herein, shows a correspondence to the positioning of the Mid-Cenomanian non-sequence.

9.5. Section SFE, South Ferriby

The palynological analysis of this section has revealed that it records an atypical dinoflagellate assemblage.

Only four samples examined yield palynologically productive residues. However, these four samples are extremely abundant, especially the Black Band sample (SFE 17) which contains 8,155 dinoflagellate cysts per gramme of sediment. Such high abundance levels are interpreted as having resulted from a condensing of the *Plenus* Marls sequence together with possible anomalous preservation in dysaerobic conditions.

The productive samples exhibit low levels of dinoflagellate species diversity. This implies that the South Ferriby section records a stressed environment, as Odum and Copeland (1974) and Davies *et al.* (1982) state that only a few highly adaptive species are capable of dominating in a stressed ecosystem.

Anomalously low percentages of *P. infusorioides* are present in this section which is the species which dominates all other Cenomanian sections examined herein. Instead, the palynomorph assemblage is dominated almost equally by *E. saxoniensis* and *C. compactum-membraniphorum* complex, which constitute an assemblage previously identified by Marshall and Batten (1988). It is interpreted that these dinoflagellate cysts are indicative of stressed palaeoenvironmental conditions.

There is a diagnostic occurrence within this section of a new species of *Litosphaeridium*, *Litosphaeridium* sp. A. It appears that this species occurs uniquely in deposits of latest Cenomanian (as documented herein) to earliest Turonian age (FitzPatrick, *pers. comm.*, 1990). Thus, this cyst is a potential index dinoflagellate for the identification of Cenomanian-Turonian boundary sequence within the Anglo-Paris Basin and possibly elsewhere in northern Europe.

Cluster analysis of the South Ferriby section substantiates the results of palynofacies analysis. The palynofacies of three of the productive SFE samples (SFE 18, 17 and 16) contains anomalously high values of the amorphogen kerogen type, when compared to other palynological preparations of Cenomanian material. Such high levels of amorphogen present can be explained by the theory which now follows.

The South Ferriby section records an atypical palynomorph assemblage which was deposited in a stressed palaeoenvironment caused by dysaerobic conditions. Such conditions are interpreted to have arisen due to restricted circulation within the basin, which itself is interpreted as being due to temporary barring of the basin. However, whatever larger scale mechanism caused this palaeo-oceanographical situation is not concluded from the palynological analysis.

9.6. Final comment

The following points are believed to be the most important conclusions to be drawn from this analysis.

1. The introduction of an oxidation stage within the palynological processing of samples results in the mechanical loss of palynomorphs.

2. The percentage presence of certain dinoflagellate cysts is under palaeotemperature control. It is therefore recognised that *P. infusorioides* is a slightly colder water cyst than *C. huguoniotii* and *C. distinctum*, both of which appear to be slightly warmer water cysts. There also appears to be a inversely proportional relationship in the percentage distributions of these dinoflagellate three cysts (*ie. P. infusorioides* 'v' *C. huguoniotii* and *C. distinctum*) and this relationship is believed to be caused by variations in palaeotemperature.

3. Marls samples consistently yield more abundant palynological residues, based on number of dinoflagellate cyst per gramme of sediment, than do those of chalks and marly chalks.

4. There appears to be two palynological associations present within the Middle Cenomanian of south-east England. The division of these two associations is coincident with the positioning of the Mid-Cenomanian non-sequence of Carter and Hart (1977).

5. The South Ferriby section records an atypical Cenomanian palynomorph assemblage, caused by stressed palaeoenvironmental conditions. The dinoflagellate species *Litosphaeridium* sp. A appears to be indicative of a latest Cenomanian - earliest Turonian age.

6. The application of statistical techniques to complex and large palynological data sets is an extremely useful and valid approach in the attempt to reconstruct palaeoenvironments.

9.7. Future work

The following are points which, if they had been carried out would have enhanced this project further. However, due to time constraints, unfortunately, they were never investigated further. Therefore, they are identified here for the benefit of similar future work.

1. Similar methods of statistical analysis as those applied to the dinoflagellate cyst distributions, should be carried out to investigate further the parameter of abundance, based on number of dinoflagellate cysts per gramme of sediment.

2. The R-mode of cluster analysis, based on the similarity between species present within each individual sample should be investigated. This may have lead to the identification of dinoflagellate cyst species associations within individual samples. However, because the distributions of the species presented herein, was so uniform throughout all sections investigated, perhaps this technique would not have yielded any significantly new nor previously unapparent information.

3. The investigation of palynofacies was carried-out under semi-quantitative techniques, which yielded interesting results as a consequence of the comparison of palynofacies associations with associations identified by cluster analysis. However, the validity of this technique is in question as it is extremely subjective and cannot be statistically tested as it is not sufficiently mathematically based. Therefore, in future palynofacies investigations, it would be extremely useful to apply point-counting techniques to properly quantify the percentage presence of palynofacies types.

REFERENCES

AGELOPOULOS, J. 1964. *Hystrichostrogylon membraniphorum* n.g.n.sp. aus dem Heiligenhafener Kieselton (Eozän). *Neues Jahrbuch für Geologie und Paläontologie, Monasthefte,* pp. 673-675.

AKSU, A.E., de VERNAL, A. and MUDIE, P.J. 1989. High-resolution foraminifer, palynologic, and stable isotopic records of the Upper Pleistocene sediments from the Labrador Sea: paleoclimatic and paleoceanographic trends. *In* Srivastava, S.P., Arthur, M., Clement, B. *et al. Proceedings of the Ocean Drilling Program, Scientific Reports,* vol. 105, pp. 617-652.

ALBERTI, G. 1961. Zur Kenntnis mesozoischer und alttertiärer Dinoflagellaten und Hystrichopshaerideen von Nord- und Mitteldeutschland sowie einigen anderen europäischen Gebieten. *Palaeontographica, Abt. A,* vol. 166, pp. 1-58, pls 1-12.

ANDERSON, R.Y. 1984. Orbital forcing of evaporite sedimentation, *In* Berger, A. and Imbrie, J., Hays G., Kukla, G. and Saltzman, B. (eds), Milankovitch and Climate. *NATO ASI Series C,* 126, vol. 1, D. Reidel, Dordrecht, Netherlands, pp. 147.

ARTHUR, M.A., BOTTJER, D.J., DEAN, W.E., FISCHER, A.G., HATTIN D.E., KAUFFMAN, E.G., PRATT, L.M. and SCHOLLE, P.A. 1986. Rhythmic bedding in Upper Cretaceous pelagic carbonate sequences: Varying sedimentary response to climatic forcing. *Geology,* vol. 14, pp. 153-156.

ARTHUR, M.A., SCHLANGER, S.O. and JENKYNS, H.C. 1987. The Cenomanian-Turonian anoxic event, II. Palaeooceanographic controls on organic-matter production and preservation *In* Brooks, J. and Fleet, A.J., (eds), Marine petroleum source rocks. *Special Publications of the Geological Society of London,* vol. 26, pp. 401-420.

BACKHOUSE, J. 1988. Late Jurassic and Early Cretaceous palynology of the Perth Basin, Western Australia. *Geological Survey of Western Australia, Bulletin* 135, pp. 1-233, pls 1-51.

BALECH, E. 1974. El género "*Protoperidinium*" Burgh 1881 ("*Peridinium*" Ehrenberg, 1831, partim). *Revista de Museo Ciencias natural de Hidrobiologia,* vol. 4, no. 1, pp. 1-79.

BALTEŞ, N. 1963. Dinoflagellate şi Hystrichosphaeride cretacice din Platforma moezica. *Petrol şi Gaze,* vol. 14, pp. 581-589, pls 1-8.

BALTEŞ, N. 1967. Albian microplankton from the Moesic Platform, Rumania. *Micropaleontology,* vol. 13, no. 3, pp. 327-336, pls 1-4.

BARROIS, C. 1876. Récherches sur le terrain Crétacé Supérieur de l'Angleterre et de l'Irelande. *Mémoires de la Société géologique du Nord,* vol. 1, 232pp.

BARRON, E.J., ARTHUR, M.A. and KAUFFMAN, E.G. 1985. Cretaceous rhythmic bedding sequences: a plausible link between orbital variations and climate. *Earth and Planetary Science Letters,* vol. 72, pp. 327-340.

BARSS, M.S. and WILLIAMS, G.L. 1973. Palynology and nannofossil processing techniques. *Geological Survey of Canada, Paper* 73-26, pp. 1-25.

BELOW, R. 1981. Dinoflagellaten-Zysten aus dem oberen Hauterive bis Cenoman Süd West-Marokkos. *Palaeontographica, Abt.B,* vol. 176, pp. 1-145, pls 1-15.

BELOW, R. 1982. Scolochorate Zysten der Gonyaulacaceae (Dinophyceae) aus der Unterkreide Marokkos. *Palaeontographica, Abt. B,* vol. 182, pp. 1-51, pls 1-9.

BELOW, R. 1987. Evolution und Systematik von Dinoflagellaten-Zysten

aus der Ordnung Peridiniales I. Allgmeine Grundlagen und Subfamilie Rhaetogonyaulacoideae (Familie Peridiniaceae). *Palaeontographica, Abt. B,* vol. 205, pp. 1-178, pls 1-26.

BENSON, D.G. 1976. Dinoflagellate taxonomy and biostratigraphy at the Cretaceous-Tertiary boundary, Ropunds Bay, Maryland. *Tulane Studies in Geology and Paleontology,* vol. 12, pp. 169-233.

BERGER, A.L. 1983. Long term variations of caloric insolation resulting from the earth's orbital elements. *Quaternary Research,* vol. 9, pp. 139-167.

BINT, A.N. 1986. Fossil Ceratiaceae: A restudy and new taxa from the mid-Cretaceous of the Western Interior, U.S.A. *Palynology,* vol. 10, pp. 135-182, pls 1-9.

BIRKELUND, T., HANCOCK, J.M., HART, M.B., RAWSON, P.F., REMANE, J., ROBASZYNSKI, F., SCHMID, F. and SURLYK, F. 1984. Cretaceous stage boundaries - Proposals. *Bulletin of the Geological Society of Denmark,* vol. 33, pp. 3-20.

BLAKE, J.F. 1878. On the chalk of Yorkshire. *Proceedings of the Geologists' Association,* vol. 5, pp. 232-270.

BOULTER, M.C. and HUBBARD, R.N.L.B. 1982. Objective paleoecological and biostratigraphic interpretation of Tertiary palynological data by multivariate statistical analysis. *Palynology,* vol. 6, pp. 55-68.

BOWERBANK, J.S. 1841a. On the siliceous bodies of the Chalk, Greensand and Oolite. *Proceedings of the Geological Society, London,* vol. 3, pp. 278-281.

BOWERBANK, J.S. 1841b. On the siliceous bodies of the Chalk, Greensand and Oolite. *The Microscopie Journal and Structural Record,* vol. 1, pp. 99-103, pp. 113-115, pp. 131-135.

BOWERBANK, J.S. 1841c. On the siliceous bodies of the Chalk,

Greensand and Oolite. *Transactions of the Geological Society, London,* vol. 6, pp. 181-194.

BRIDEAUX, W.W. 1971a. Recurrent species groupings in fossil microplankton assemblages. *Palaeogeography, Palaeoclimatology, Palaeoecology,* vol. 9, pp. 101-122.

BRIDEAUX, W.W. 1971b. Palynology of the Lower Colorado Group, central Alberta, Canada, I. Introductory remarks. Geology and microplankton studies. *Palaeontographica, Abt B,* vol. 135, pp. 53-114, pls 21-30.

BRIGHAM, E.O. 1974. *The Fast Fourier Transform.* New Jersey: Prentice-Hall. 1-252pp.

BRONN H.G. 1848. Handbuch einer Geschichte der Natur. *Index palaeontologicus.* Stuttgart. 1382pp.

BUJAK, J.P., BARSS, M.S. and WILLIAMS, G.L. 1977a. Offshore east Canada's organic type and color and hydrocarbon potential. Offshore Eastern Canada - Part I. *The Oil and Gas Journal,* April 4, 1977, pp. 198- 202.

BUJAK, J.P., BARSS, M.S. and WILLIAMS, G.L. 1977b. Organic type and color and hydrocarbon potential. Offshore Eastern Canada - Part II. *The Oil and Gas Journal,* April 11, 1977, pp. 96-100.

BUJAK, J.P., DOWNIE, C., EATON, G.L. and WILLIAMS, G.L. 1980. Taxonomy of some Eocene dinoflagellate cyst species from southern England, *In* Bujak, J.P., Downie, C., Eaton, G.L. and Williams, G.L., Dinoflagellate cysts and acritarch from the Eocene of southern England. *The Palaeontological Association, Special Papers in Palaeontology,* vol. 24, pp. 26-36.

BURGESS, J.D. 1971. Palynological interpretation of Frontier environments in central Wyoming. *Geoscience and Man,* vol. 3, pp. 69-82, pl. 1.

BURNABY, T.P. 1962. The palaeoecology of the foraminifera of the Chalk Marl. *Palaeontology,* vol. 4, pp. 599-608.

BUZAS, M.A. 1979. The Measurement of Diversity, *In* Lipps, J.H., Burger, W.H., Buzas, M.A., Douglas, R.G. and Ross, C.A. Foraminiferal ecology and paleoecology. *Society of Economic Paleontologists and Mineralogists,* Short Course Notes, no. 6, pp. 3-10.

CARTER, D.J. and HART, M.B. 1977. Aspects of mid-Cretaceous stratigraphical micropalaeontology. *Bulletin of the British Museum (Natural History) Geology,* vol. 29, no. 1, pp. 1-135.

CLAPARÈDE, E. and LACHMANN, J. 1859. Êtudes sur les Infusoires et les Rhizopodes. *Mémoir de l'Institut National de Génévois,* vol. 6, pp. 392-484 (1858).

CLARKE, R.F.A., DAVEY, R.J., SARJEANT, W.A.S. and VERDIER, J.-P. 1968. A note on the nomenclature of some Upper Cretaceous and Eocene dinoflagellate taxa. *Taxon,* vol. 17, pp. 181-183.

CLARKE , R.F.A. and VERDIER, J.-P. 1967. An investigation of microplankton assemblages from the Chalk of the Isle of Wight, England. *Verhandelingen der Koninklijke Nederlandsche Akademie van Wetenschappen, Afdeeling Natuurkunde, Eerste Reeks,* vol. 24, pp. 1-96, pls 1-17.

COOKSON, I.C. and EISENACK, G 1958. Microplankton from Australian and New Guinea Upper Mesozoic sediments. *Proceedings of the Royal Society of Victoria*, vol. 70, no. 1, pp. 19-70, pls 1-12.

COOKSON, I.C. and EISENACK, G. 1960a. Microplankton from Australian Cretaceous sediments. *Micropaleontology*, vol. 6, no. 1, pp. 1-18, pls 13.

COOKSON, I.C. and EISENACK, G. 1960b. Upper Mesozoic microplankton from Australia and New Guinea. *Palaeontology,* vol. 2, no. 1, pp. 243-261, pls 37-39

COOKSON, I.C. and EISENACK, G. 1962. Additional microplankton from Australian Cretaceous sediments. *Micropaleontology,* vol. 8, no. 4, pp. 485-507, pls 1-7.

COOKSON, I.C. and EISENACK, G. 1969. Some microplankton from two bores at Balcatta, Western Australia. *Journal of the Royal Society of Western Australia,* vol. 52, pp. 3-8.

COOKSON, I.C. and EISENACK, G. 1970. Cretaceous microplankton from the Eucla Basin, Western Australia. *Proceedings of the Royal Society of Victoria,* vol. 83, no. 2, pp. 137-157, pls 10-14.

COOKSON, I.C. and EISENACK, G. 1974. Mikroplankton aus australischen Mesozoischen und Tertiären sedimenten. *Palaeontographica, Abt. b,* vol. 148, pp. 44-93, pls 20-29.

COOKSON, I.C. and HUGHES, N.F. 1964. Microplankton from the Cambridge Greensand (mid-Cretaceous). *Palaeontology*, vol. 7, no. 1, pp. 37-59, pls 5-11.

CORFIELD, R.M., HALL, M.A. and BRASIER, M.D. 1990. Stable isotope evidence for foraminiferal habits during the development of the Cenomanian/Turonian oceanic anoxic event. *Geology*, vol. 18, pp. 175-178.

CORRADINI, D. 1973. Non-calcareous microplankton from the Upper Cretaceous of the Northern Appennines. *Bolletino della Societá Paleontological Italiana,* vol. 11, pp. 119-197, pls 19-39.

COSTA, L.I. and DAVEY, R.J. 1992. Dinoflagellate cysts of the Cretaceous System, *in* Powell, A.J. (ed.), *A Stratigraphical Index of Dinoflagellate Cyst,* London: Chapman and Hall, pp. 99-157.

CRUMIÈRE, J-P., CRUMIÈRE-AIRAUD, C., ESPITALIÉ, J. and COTILLON, P. 1990. Global and regional controls on potential source-rock deposition and preservation: The Cenomanian-Turonian oceanic anoxic event (CTOAE) on the European Tethyan margin (southeastern

France) *In* Huc, A.Y. (ed.), Deposition of Organic Facies. *American Association of Petroleum Geologists, Studies in Geology,* No. 30, pp. 107-118.

DAKYNS, J.R., FOX-STRANGWAYS, C. and CAMERON, A.G. 1886. The geology of the country between York and Hull. *Memoirs of the Geological Survey U.K.* + 54pp.

DALE, B. 1976. Cyst formation, sedimentation and preservation: factors affecting dinoflagellate assemblages in Recent sediments from Trondheimsfjord, Norway. *Review of Palaeobotany and Palynology,* vol. 22, pp. 39-60, pl. 1.

DALE, B. 1983. Dinoflagellate resting cysts: "benthic plankton". *In* Fryxell, G.A. (ed.) *Survival strategies of the algae.* Cambridge: Cambridge University Press, pp. 69-136.

DAVEY, R.J. 1969a. Non-calcareous microplankton from the Cenomanian of England, northern France and North America, Part I. *Bulletin of the British Museum (Natural History) Geology,* vol. 17, pp. 103-180, pls 1-11.

DAVEY, R.J. 1969b. Some dinoflagellate cysts from the Upper Cretaceous of northern Natal, South Africa. *Palaeontologia Africana,* vol. 12, pp. 1-23, pls 1-4.

DAVEY, R.J. 1970. Non-calcareous microplankton from the Cenomanian of England, northern France and North America, Part II. *Bulletin of the British Museum (Natural History) Geology,* vol. 18, no. 8, pp. 333-397, pls 1-9.

DAVEY, R.J. 1971. Palynology and palaeoenvironmental studies with special reference to the Continental Shelf facies of South Africa. *Proceedings of the Second Planktonics Conference, Roma,* pp. 331-397.

DAVEY, R.J. 1974. Dinoflagellate cysts from the Barremian of the Speeton Clay, England, *in Symposium on Stratigraphic Palynology,*

Birbal Sahni Institute of Palaeobotany, Special Publication, no. 3, pp. 41-75, pls 1-9.

DAVEY, R.J. 1975. A dinoflagellate cyst assemblage from the Late Cretaceous of Ghana. *Proceedings of the* 5th *West African Colloquium on Microplankton*, Series 7, no. 5, pp. 150-173, pls 1-3.

DAVEY, R.J. 1978. Marine Cretaceous palynology of Site 361, D.S.D.P. Leg 40, off southwestern Africa. *In* Bolli, H.M., Ryan, W.B.F., *et al.*, *Initial Reports of the Deep Sea Drilling Project*, vol. 40, Washington D.C.: U.S. Government Printing Office, pp. 883-913, pls 1-9.

DAVEY, R.J. 1982. Dinocyst stratigraphy of the latest Jurassic to Early Cretaceous of the Haldager No. 1 borehole, Denmark. *Geological Survey of Denmark, Series* B, No. 6, pp. 1-57, pls 1-10.

DAVEY, R.J., DOWNIE, C., SARJEANT, W.A.S., WILLIAMS, G.L. 1966. Studies on Mesozoic and Cainozoic dinoflagellate cysts. *Bulletin of the British Museum of Natural History* (*Geology*), *Supplement* 3, pp. 1-248, pls 1-26.

DAVEY, R.J., DOWNIE, C., SARJEANT, W.A.S., WILLIAMS, G.L. 1969. Generic reallocations *In* Davey, R.J., Downie, C., Sarjeant, W.A.S. and Williams, G.L., Appendix to "Studies on Mesozoic and Cainozoic dinoflagellate cysts". *Bulletin of the British Museum of Natural History (Geology)*, Appendix to Supplement 3, pp. 1-24.

DAVEY, R.J. and ROGERS, J. 1975. Palynomorph distribution in Recent offshore sediments along two traverses off South West Africa. *Marine Geology*, vol. 18, pp. 213-225.

DAVEY, R.J. and VERDIER, J.-P. 1971. An investigation of microplankton assemblages from the Albian of the Paris Basin. *Verhandelingen der Koninklijke Nrderlandsche Akademie van Wetenschappen, Afdeling Natuurkunde, Eerste Reeks*, vol. 26, pp.

1-85, pls 1-7.

DAVEY, R.J. and VERDIER, J.-P. 1973. An investigation of microplankton assemblages from the Albian (Vraconian) sediments. *Revista Española Micropaleontología*, vol. 5, pp. 173-212, pls 1-5.

DAVEY, R.J. and VERDIER, J.-P. 1976. A review of certain non-tabulate Cretaceous hystrichospherid dinocysts. *Review of Palaeobotany and Palynology*, vol. 17, pp. 623-653, pls 91-93.

DAVEY, R.J. and WILLIAMS, G.L. 1966a. The genera *Hystrichosphaera* and *Achomosphaera*, *in* Davey, R.J., Downie, C., Sarjeant, W.A.S., Williams, G.L., Studies on Mesozoic and Cainozoic dinoflagellate cysts. *Bulletin of the British Museum (Natural History) Geology*, Supplement 3, pp. 28-52.

DAVEY, R.J. and WILLIAMS, G.L. 1966b. The genus *Hystrichosphaeridium* and its allies; *in* Davey, R.J., Downie, C., Sarjeant, W.A.S. and Williams, G.L., Studies on Mesozoic and Cainozoic dinoflagellate cysts. *Bulletin of the British Museum (Natural History) Geology*, *Supplement* 3, pp. 53- 106.

DAVIES E.H., BUJAK, J.P.and WILLIAMS, G.L. 1982. The applications of dinoflagellates to palaeoenvironmental problems. *Proceedings of the Third North American Paleontological Convention*, vol. 1, pp. 125-131.

DEANE, H. 1849. On the occurrence of fossil Xanthidia and Polythalamia in Chalk. *Transactions of the Microscopical Society, London*, vol. 2, pp. 77-79.

De CONINICK, J. 1969. Dinophyceae et Acritarcha de l'Yprésien du Bassin belge. *Service Géologique de Belgique, Prof. Paper no.* 12, pp. 1-151, pls 1-22.

DEFLANDRE, G. 1935. Considérations biologiques sur les microorganisms d'origne planctonique conservés dans les silex da la craie. *Bulletin biologique de la France et de la Beligique*, vol. 69,

pp. 213-244, pls 5-9.

DEFLANDRE, G. 1936a. Les flagellés fossiles. Aperçu biologique et paléontologique. *Rôle Géologique; Actualités scientifiques et industrielles,* no. 335, pp. 1-97.

DEFLANDRE, G. 1936b. Microfossiles des silex crétacés. Première partie. Généralités. Flagellés. *Annales de paléontologie,* vol. 25, pp. 151-191, pls 1-10.

DEFLANDRE, G. 1937. Microfossiles des silex crétacés. Deuxième partie. Flagellés *incertae sedis* Hystrichosphaeridés. Sarcondinés. Organismes divers. *Annales de paléontologie,* vol. 26, pp. 51-103, pls 11-18.

DEFLANDRE, G. 1938. Microplancton ders mers jurassique conservé dans les marnes de Villers-sur-Mer (Calvados). Étude liminaire et considérations générales. *Travaux de la Station Zoologique de Wimereux,* vol. 13, pp. 147-200. pls 5-11.

DEFLANDRE, G. 1943. Sur quelque nouveax Dinoflagellés des silex crétacés. *Bulletin de la Société géologique de France,* vol. 13, pp. 499-509, pls 17.

DEFLANDRE, G. 1946. Hystrichosphaeridés II. Espéces du Secondaire et du Tertiaire; Fich. micropaléont. sér. 6. *Archives Originales Serv. Documentation, Centre National de la Recherche Scientifique,* no. 235, cards 860-1019.

DEFLANDRE, G. 1947. Sur quelque microorganismes planctoniques des Jurassiques. *Bulletin de l'Institut océanographique de Monaco,* No. 921, pp. 1-12, pls 1-23.

DEFLANDRE, G. 1964. Remarques sur la classification des Dinoflagellés fossiles, à propos d'*Evittodinium,* nouveau genre crétacé de la famille des Deflandreaceae. *Comptes rendus de l'Académie des sciences, Paris,* vol. 258, pp. 5027-5030.

DEFLANDRE, G. and COOKSON, I.C. 1955. Fossil microplankton from Australian Late Mesozoic and Tertiary sediments. *Australian Journal of Marine and Freshwater Research,* vol. 6, pp. 242-313, pls 1-9.

DEFLANDRE, G. and COURTVILLE, H. 1939. Note préliminaire sur les microfossiles des silex crétacés du Cambrésis. *Bulletin de la Société française de Microscopie*, vol. 8, pp. 95-106, pls 1-3.

DESTOMBES, J.P. and SHEPHARD-THORN, E.R. 1971. Geological investigation of the Channel Tunnel site investigation 1964-65. *Report of the Institute of Geological Sciences,* 71/11, 1-12pp.

de VERNAL, A. and HILLAIRE-MARCEL, C. 1987a. Paleoenvironments along the eastern Laurentide ice sheet margin and timing of the last ice maximum and retreat. *Géographie physique et Quaternaire,* vol. 41, pp. 265-277.

de VERNAL, A. and HILLAIRE-MARCEL, C. 1987b. Éléments d'une climatostratigraphie du Pléistocene moyen et tardif dans l'est du Canada par l'analyse palynologique et isotopique du forage 84-030-003, mer du Labrador. *Canadian Journal of Earth Sciences,* vol. 24, pp. 1886-1902

de VERNAL, A. HILLAIRE-MARCEL, C. AKSU, A.E. and MUDIE, P.J. 1987. Playnostratigraphy and chronostratigraphy of Baffin Bay deep sea cores: climatostratigraphic implications. *Palaeogeography, Palaeoclimatology and Palaeoecology,* vol. 61, pp. 97-105.

DIESING,C.M. 1866. Revisionen der Prothelminthen, Abteilung: Mastigophoren. *Sitzungsberichte der Akademie de Wissenschaften in Wien,* vol. 52, pp. 37-52.

DITCHFIELD, P. 1990. *Milankovitch cycles in Cenomanian Chalks of the Anglo-Paris Basin.* Unpublished Ph.D Thesis, University of Liverpool.

DITCHFIELD, P. and MARSHALL, J.D. 1989. Isotopic variation in

rhythmically bedded chalks: palaeotemperature variation in the Upper Cretaceous. *Geology,* vol. 17, pp. 842-845.

DITCHFIELD, P., MITCHELL, S.F., PAUL, C.R.C., MARSHALL, J.D. and GALE, A.S. *in prep.* A carbon stable isotope excursion in the early Middle Cenomanian of northwest Europe.

DIXON, F. 1850. *The Geology and fossils of the Tertiary and Cretaceous formations of Sussex.* London: Longman, Brown, Green and Longmans. 1-422pp.

DODGE, J.D. 1965. Chromosome structure in the dinoflagellates and the problem of the mesokaryotic cell. *Excerpta Medica International Congress,* vol. 91, pp. 264-265.

DÖRHÖFER, G. and DAVIES, E.H. 1980. Evolution of archaeopyle and tabulation in Rhaetogonyaulacinean dinoflagellate cysts. *Royal Ontario Museum, Life Sciences Miscellaneous Publications,* pp. 1-91, pls 1-40.

DODSWORTH, P. 1990. *The geology of the Chalk Group of the southern east Midlands shelf and a detailed review of the Plenus Marl of the area.* Unpublished undergraduate project, Polytechnic South West.

DOWKER, G. 1870. On the Chalk of Thanet, Kent and its connection with the Chalk of east Kent. *Geological Magazine,* vol. 7, pp. 466-472.

DOWNIE, C., HUSSAIN, M.A. and WILLIAMS, G.L. 1971. Dinoflagellate cyst and acritarch associations in the Paleogene of southeast England. *Geoscience and Man,* vol. 3, pp. 29-35, pls 1-2.

DOWNIE, C. and SARJEANT, W.A.S. 1963. On the interpretation and status of some hystrichosphere genera. *Palaeontology.* vol. 6, pp. 83-96.

DUANE, A.M. 1988. *The palynology of cores from the Porcupine Basin,*

offshore western Ireland. Unpublished M.Sc. Thesis, University of Sheffield.

DUXBURY, S. 1977. A palynostratigraphy of the Barriasian to Barremian of the Speeton Clay of Speeton, England. *Palaeontographica, Abt. B,* vol. 160, pp. 17-67, pls 1-15.

DUXBURY, S. 1980. Barremian phytoplankton from Speeton, east Yorkshire. *Palaeontographica, Abt. B,* vol 173, pp. 107-146, pls 1-13.

DUXBURY, S. 1983. A study of dinoflagellate cysts and acritarchs from the Lower Greensand (Aptian to Lower Albian) of the Isle of Wight, southern England. *Palaeontographica, Abt.B,* vol. 186, pp. 18-80, pls 1-10.

EATON, G.L. 1976. Dinoflagellate cysts from the Bracklesham Beds (Eocene) of the Isle of Wight, Hampshire, southern England. *Bulletin of the British Museum (Natural History) Geology*, vol. 26, pp. 277-332. pls 1-21.

EDER, W. 1982. Diagenetic redistribution of carbonate, a process in forming limestone-marl alternations (Devonian and Carboniferous, Rheinisches Schiefergebirge, W. Germany). *In* Einsele, S. and Seilacher, A. (eds), *Cyclic and event stratigraphy,* New York, Springer-Verlag, pp. 98-112.

EHRENBERG, C.G. 1832. (separate 1830): Beiträge zur Kenntnis der Organisation der Infusorien und ihrer geographischen Verbreitung, besonders in Sibirien. *Abhandlungen der Preussischen Akademie der Wissenschaften,* 1830, pp. 1-88, pls 1-8.

EHRENBERG, C.G. 1838. Über das Massenverhältniss der jetzt lebenden Kiesel-Infusorien und über eins neues Infusorien-Conglomerat als Polischiefer von Jastraba in Ungarn. *Abhandlungen der Preussischen Akademie der Wissenschaften,* 1836, pp. 109-135, pls 1-2.

EHRENBERG, C.G. 1840. On numerous animals of the Chalk formation which are still to be found in a living state. *Transactions of the Royal Academy of Berlin for* 1840. Translatted by William Francis. 1-57pp.

EICHER, D.L. 1969. Palaeobathymetry of Cretaceous Greenhorn Sea in Eastern Colorado. *Bulletin of the American Association of Petroleum Geologists,* Tulsa, Oklahoma, vol. 53, pt. 5, pp. 1075-1090.

EICHER, D.L. and WORSTELL, P. 1970. Cenomanian and Turonian foraminifera from the Great Plains, United States. *Micropaleontology,* vol. 16, pp. 269-324.

EINSELE, S. 1982. Limestone-marl cycles (periodites): Diagenesis, significance, causes - A review. In Einsele, S. and Seilacher, A. (eds), *Cyclic and event stratification:* New York: Springer-Verlag, pp. 8-53.

EISENACK, A. 1958. Mikroplankton aus dem norddeutschen Apt. *Neues Jahrbuch für Geologie und Paläontologie, Abhandlungen,* vol. 106, pp. 383-422, pls 21-27.

EISENACK, A. 1963. Zur *Membranilarnax*-Frage. *Neues Jahrbuch für Geologie und Paläontologie, Monatshefte,* pp. 98-103.

EISENACK, A. and COOKSON, I.C. 1960. Microplankton from Australian Lower Cretaceous sediments. *Proceedings of the Royal Society of Victoria,* vol. 72, pp. 1-11, pls 1-3.

EISENACK, A. and KJELLSTRÖM, G. 1971. Katalog der fossilen Dinoflagellaten, Hystrichosphären und verwandten Mikrofossilien. Band II Dinoflagellaten. *E. Schweizerbart'sche Verlagsbuchhandlung, Stuttgart,* 1971, pp. 1-1130, pls 1-6.

EVITT, W.R. 1963. A discussion and proposals concerning fossil dinoflagellates, hystrichospheres, and acritarchs, I. *Proceedings of the National Academy of Sciences, Washington,* vol.

49, pp. 158-164.

EVITT, W.R. 1967. Dinoflagellate studies II. The archaeopyle. *Stanford University Publication, Geological Sciences,* vol. 10, no. 3, pp. 1-88.

EVITT, W.R. 1970. Dinoflagellates, a selective review. *Geoscience and Man,* vol. 1, pp. 29-45.

EVITT, W.R. 1985. *Sporopollenin Dinoflagellate Cysts. Their morphology and interpretation.* American Association of Stratigraphic Palynologists Foundation. Austin, Texas. 1-333pp.

FARRIMOND, P., EGLINGTON, G. BRASSELL, S.C. and JENKYNS H.C. 1990. The Cenomanian/Turonian anoxic event in Europe: an organic geochemical study. *Marine and Petroleum Geology,* vol. 7, pp. 75-88.

FAUCONNIER, D. 1975. Répartition des Péridiniens de l'Albien du bassin de Paris. Rôle stratigraphique et liaison avec le cadre sédimentologique. *Bulletin du Bureau de Recherches Géologique et Minières (deuxième série),* section 1, no. 4, pp. 235-273, pls 1,2.

FAUCONNIER, D. 1977. Les Dinoflagellés de l'Albien et du Cénomanien inférieur du Bassin de Paris. Répartition stratigraphique et relations avec la nature du dépôt. Thèse de Doctorat d'Université, Orléans. *Série "Documents" du Bureau de Recherches Géologique et Minières,* vol. 5, pp. 1-186. (1979)

FIRTION, F. 1952. Le Cénomanian inférieur du Nouvion-en-Thiérache examen micropaléontologique. *Annales de la Société Géologique du Nord,* vol. 72, pp. 150-164, pls 8-10.

FISCHER, A.G. and ARTHUR, M.A. 1977. Secular variation in the pelagic realm. *In* Cook, H.E. and Enos, P., (eds) Deep-water carbonate environments. *Special Publicationa of the Society of economic Palaeontologists and Mineralogists, Tulsa,* vol. 25, pp.

19-50.

FOLK, R.L. 1959. Prectical petrographic classification of limestones. *Bulletin of American Association of Petroleum Geologists,* vol. 43, pp. 1-38.

FOUCHER, J.-C. 1971. Étude micropaléontologique des silex coniaciens du puits 19 de Lens-Lievin (Pas-de-Calais). *Bulletin du Museum d'Histoire Naturelle, Paris,* vol. 21, pp. 77-157.

FOUCHER, J.-C. 1979. Distribution stratigraphique des kystes de dinoflagellés et des acritarches dans le Crétacé Supérieur du Bassin de Paris et de l'Europe septentrionale. *Palaeontographica, Abt. b.,* vol. 169, pp. 78-105.

FOUCHER J.-C. 1980. Dinoflagellés et Acritarches du Crétacé du Boulonnais. *In* Robaszynski, F., Améedro, F. (coord.) and Foucher, J.-C., Gaspard, D., Magniez-Jannin, H., Manivit, H. and Sornay, J. 1980. Synthèse biostratigraphique de l'Aptien au Santonien du Boulonnais a partir de sept groupes paléontologiques: foraminiféres, nannoplancton, dinoflagellés et macrofaunes. *Revue de Micropaléontologie,* vol. 22, no. 4, pp. 195-321.

FOUCHER, J.-C. 1981. Kystes de dinoflagellés du Crétacé Moyen Européen: proposition d'une echelle biostratigraphique pour le domaine Nord-occidental. *Cretaceous Research,* vol. 2, pp. 331-338.

FOUCHER, J.-C. 1983. Distribution des kystes de dinoflagellés dans le Crétacé Moyen et Supérieur du Bassin de Paris. *Cahiers de Micropaléontologie,* vol. 4, pp. 23-47, pls 1-3.

FOUCHER, J.C. and TAUGOURDEAU, Ph. 1975. Microfossiles de l'Albo-Cénomanian de Wissant (Pas-de-Calais). *Cahiers de Micropaléontologie,* vol. 1, pp. 1-30, pls 1-7.

FRITSCH F.E. 1929. Evolutionary sequence and affinities among

Protophyta. *Biological Reviews,* vol. 4, pp. 103-151.

GALE, A.S. 1989a. A Milankovitch scale for Cenomanian time. *Terra Nova,* vol. 1, pp. 420-425.

GALE, A.S. 1989b. Field Meeting at Folkestone Warren, 29th November, 1987. *Proceedings of the Geologists' Association,* vol. 100, pt. 1, pp. 73-82.

GERLACH, E. 1961. Mikrofossilien aus dem Oligozän und Miozän Nordwestdeutschlands, unter besonderer Berücksichtigung der Hystrichosphären und Dinoflagellaten. *Neues Jahrbuch für Geologie und Paläontologie, Abhandlungen,* vol. 112, pp. 143-228, pls 25-29.

GITMEZ, G.U. and SARJEANT, W.A.S. 1972. Dinoflagellate cysts and acritarchs from the Kimmeridgian (Upper Jurassic) of England, Scotland and France. *Bulletin of the British Museum (Natural History) Geology,* vol.21, pp. 171-257, pls 1-17.

GOCHT, H. 1959. Mikroplankton aus dem nordwestdeutschen Neokom (Teil II). *Paläontologische Zeitschrift,* vol. 33, pp. 50-89, pls 3-8.

GOODMAN, D.K. 1979. Dinoflagellate "communities" from the Lower Eocene Nanjemoy Formation of Maryland, U.S.A. *Palynology,* vol. 3, pp. 169-190.

HABIB, D. 1972. Dinoflagellate stratigraphy Leg 11, Deep Sea Drilling Projct. *In* Hollister, C.D., Ewing, J.I., *et al., Initial Reports of the Deep Sea Drilling Project,* vol.11, Washington D.C.: U.S. Government Printing Office, pp. 367-425, pls 1-22.

HABIB, D. and DRUGG, W.S. 1987. Palynology of Site 603 and 605, Leg 93, Deep Sea Drilling Project. *In* van Hinte, J.E., Wise S.W. *et al., Initial Reports of the Deep Sea Drilling Project,* vol. 93, Washington D.C.: U.S. Government Printing Office, pp. 751-775.

HABIB, D. and MILLER, J.A. 1989. Dinoflagellate species and organic

facies evidence of marine transgression and regression in the Atlantic Coastal Plain. *Palaeogeography, Palaeoclimatology, Palaeoecology,* vol. 74, pp. 23-47.

HAECKEL, E. 1894. Entwurf eines natürlichen System der Organismen auf Grund ihrer Stammesgeschichte. I: Systematische Phylogenie der Protisten und Pflanzen. *Reiner, Berlin,* 1-400pp.

HALLAM, A.A. 1986. The origin of minor limestone/shale cycles. *Geology,* vol. 14, pp. 121-127.

HANCOCK, J.M. 1976. The petrology of the Chalk. *Proceedings of the Geologists' Association,* vol. 86 (for 1975), pp. 499-535.

HANCOCK, J.M. 1989. Sea-level changes in the British region during the Late Cretaceous. *Proceedings of the Geologists' Association,* vol. 100, pt. 4, pp. 565-594.

HARKER, S.D. 1979. Archaeopyle formation in *Palaeohystrichophora infusorioides* Deflandre, 1935. *Neues Jahrbuch für Geologie und Paläontologie, Monatshefte,* pp. 369-377.

HARKER, S.D. and SARJEANT, W.A.S. 1975. The stratigraphic distribution of organic-walled dinoflagellate cysts in the Cretaceous and Tertiary. *Review of Palaeobotany and Palynology,* vol. 20, pp. 217-315.

HARKER, S.D., SARJEANT, W.A.S. and CALDWELL, W.G.E. 1990. Late Cretaceous (Campanian) organic-walled microplankton from the Interior Plains of Canada, Wyoming and Texas: biostratigraphy, palaeontology and palaeoenvironmental interpretation. *Palaeontographica, Abt B.,* vol. 219, pp. 1-243, pls 1-13.

HARLAND, R. 1973. Dinoflagellate cysts and acritarchs from the Bearpaw Formation (upper Campanian) of southern Alberta, Canada. *Palaeontology,* vol. 16, pt. 4, pp. 665-706, pls 84-88.

HARLAND, R. 1977. Recent and Late Quaternary (Flandrian and

Devensian) dinoflagellate cysts from marine continental shelf sediments around the British Isles. *Palaeontographica, Abt. B,* vol. 164, pp. 87-126.

HARLAND, R. 1983. Distribution maps of Recent dinoflagellate cyst in bottom sediments from the North Atlantic ocean and adjacent seas. *Palaeontology,* vol. 26, pt. 2, pp. 321-387.

HARLAND, R. 1984a. Quaternary dinoflagellate cysts from Holes 548 and 548A, Goban Spur (Deep Sea Drilling Project Leg 80). *In* Graciansky, P.C. de, Poag, C.W., *et al. Initial Reports of the Deep Sea Drilling Project,* Vol. 80, Washington D.C.: U.S. Government Printing Office, pp. 761-766.

HARLAND, R. 1984b. Quaternary dinoflagellate cysts from Hole 552A, Rockall Palteau, Deep Sea Drilling Project Leg 81. *In* Roberts, D.G., Schniter, D., *et al. Initial Reports of the Deep Sea Drilling Project,* Vol. 81, Washington D.C.: U.S. Government Printing Office, pp. 541-546.

HARLAND, R. 1988a. Quaternary dinoflagellate cyst biostratigraphy of the North Sea. *Palaeontology,* vol. 31, pt. 3, pp. 877-903. pls 78-82.

HARLAND, R. 1988b. Dinoflagellates, their cysts and Quaternary stratigraphy. *New Phytologist,* vol.108, pp. 111-120.

HARLAND, R. 1992. Dinoflagellate cyst biostratigraphy of the last 2.3Ma from the Rockall Plateau, northeast Atlantic Ocean. *Journal of the Geological Society, London,* vol. 149, pp. 7-12.

HART, M.B. 1987. Orbitally induced cycles in the chalk facies of the United Kingdom. *Cretaceous Research,* vol. 8, pp. 335-348.

HART, M.B. and BIGG, P.J. 1981. Anoxic events in the late Cretaceous chalk seas of North-West Europe. *In* Neale, J.W. and Brasier, M.D. (eds) *Microfossils from Recent and Fossil Shelf Seas.* Chichester: Horwood, pp. 177-185.

HART, M.B. and LEARY, P.N. 1989. The stratigraphic and palaeogeographic setting of the late Cenomanian 'anoxic' event. *Journal of the Geological Society, London,* vol. 146, pp. 305-310.

HART, M.B., DODSWORTH, P., DITCHFIELD, P.W., DUANE, A.M. and ORTH, C.J. 1991. The Late Cenomanian event in eastern England. *Historical Biology,* vol. 5, pp. 339-354.

HATTON, L., WORTHINGTON, M.H. and MAKIN, J. 1986. *Seismic Data Processing.* Oxford: Blackwell Scientific Publications. 1-177pp.

HELBY, R. 1987. *Muderongia* and related dinoflagellates of the latest Jurassic to Early Cretaceous of Australia, *in* Jell, P.A. (ed.), Studies in Australian Mesozoic Palynology. *Association of Australian Palaeontologists,* Memoir 4, pp. 297-336.

HELENES, J. 1984. Morphological analysis of Mesozoic-Cenozoic *Cribroperidinium* (Dinophyceae), and taxonomic implications. *Palynology,* vol. 8, pp. 107-137, pls 1-5.

HILLAIRE-MARCEL, C. and de VERNAL, A. 1989. Isotopic and palynologic records of the Late Pleistocene in eastern Canada and adjacent ocean basins. *Géographie physique et Quaternaire,* vol. 43, no. 3, pp. 263-290.

HILLAIRE-MARCEL, C., de VERNAL, A., AKSU, A. and MACKO, S. 1989. High-resolution isotopic and micropaleontological studies of Upper Pleistocene sediments at ODP Site 645, Baffin Bay. *In* Srivasta, S.P., Arthur, M., Clement, B. *et al. Proceeding of the Ocean Drilling Program, Scientific Reports,* vol. 105, pp. 599-616.

HUDSON, J.D. 1977. Stable isotopes and limestone lithification. *Journal of the Geological Society, London,* vol. 133, pp. 637-660.

HULTBERG, S.U. and MALMGREN, B.A. 1986. Dinoflagellate and planktonic foraminiferal paleobathymetrical indices in the Boreal uppermost

Cretaceous. *Micropaleontology,* vol. 32, no. 4, pp. 316-323.

IMBRIE, J. 1985. A theoretical framework for the Pleistocene ice ages. *Journal of the Geological Society, London,* vol. 142, pp. 943-953.

IMBRIE, J., HAYS, J.D., MARTINSON, D.G., McINTYRE, A., MIX, A.C., MORLEY, J.J., PISIAS, N.G., PRELL, W.L. and SHACKLETON, N.J. 1984. The orbital theory of Pleistocene climate: Support from a revised chronology of marine $\delta^{18}O$ record. *In* Milankovitch and Climate, Berger, A., Imbrie, J., Hays G., Kukla, G. and Saltzman, B. (eds), *NATO ASI Series* C, 126 , D. Reidel, Dordrecht, Netherlands, pp. 269-306.

JAIN, K.P. and MILLEPIED, P. 1973. Cretaceous microplankton from Senegal Basin, N.W. Africa. 1. Some new genera species and combinations of dinoflagellates. *Palaeobotanist,* vol. 20, pp. 22-32, pls 1-3.

JAN du CHÊNE, R., FAUCONNIER, D.C., FENTON, J.P.G. 1985. Problèmes taxonomique liés a la révision de l'espèce *"Gonyaulax" cornigera* Valensi, 1953, kyste fossiles de dinoflagellé. *Revue de Micropaléontologie,* vol. 28, pp. 109-124, pls 1-5.

JAN du CHÊNE, R., MASURE, E., BECHELER, I., BIFFI, U., de VAINS, G., FAUCONNIER, D., FERRARIO, R., FOUCHER, J.-Cl., GAILLARD, M., HOCHULI, P., LACHKAR, G., MICHOUX, D., MONTEIL, E., MORON, J.-M., RAUSCHER, R., RAYNAUD, J.-F., TAUGOURDEAU, J. and TURON, J.-L. 1986. Guide pratique pour la détermination de kystes de Dinoflagellés fossiles. Le complex *Gonyaulacysta. Bulletin* des *Centres de Recherches Exploration-Production Elf-Aquitaine,* Mémoir 12, pp. 1-479, pls 1-152.

JANSONIUS, J. 1986. Re-examination of Mesozoic Canadian dinoflagellate cysts published by S.A.J. Pocock (1962, 1972). *Palynology,* vol. 10, pp. 201-223, pls 1-6.

JARVIS, I., CARSON, G.A., COOPER, M.K.E., HART, M.B., LEARY, P.N.,

TOCHER, B.A., HORNE, D. and ROSSENFELD, A. 1988a. Microfossil assemblages and the Cenomanian-Turonian (Late Cretaceous) oceanic anoxic event. *Cretaceous Research,* vol. 9, pp. 3-103.

JARVIS, I., CARSON, G.A., HART, M.B., LEARY, P.N. and TOCHER, B.A. 1988b. The Cenomanian-Turonian (late Cretaceous) anoxic event in SW England: evidence from Hooden Cliffs, near Beer, SE Devon. *Newsletters on Stratrigraphy,* vol. 18, pt. 3, pp. 147-164.

JARVIS, I., LEARY, P.N. and TOCHER, B.A. 1987. Mid-Cretaceous (Albian-Turonian) stratigraphy of Shapwick Grange Quarry, S.E. Devon, England. *Mesozoic Research,* vol. 1, pt. 3, pp. 119-134.

JARVIS, I. and WOODROFF, P.B. 1984. Stratigraphy of the Cenomanian and basal Turonian (Upper Cretaceous) between Branscombe and Seaton, SE Devon, England. *Proceedings of the Geologists' Association,* vol. 95, pp. 193-215.

JEANS, C.V. 1968. The origin of the Montmorillonite of the European Chalk with special reference to the Lower Chalk of England. *Clay Minerals,* vol. 7, pp. 311-329.

JEANS, C.V. 1973. The Market-Weighton Structure: tectonics, sedimentation and diagenesis during the Cretaceous. *Proceedings of the Yorkshire Geological Society,* vol. 39, pp. 409-444.

JEANS, C.V. 1980. Early submarine lithification in the Red Chalk and Lower Chalk of eastern England: a bacterial control model and its implications. *Proceedings of the Yorkshire Geological Society,* vol. 43, pp. 81-157.

JEANS, C.V., LONG, D., HALL, M.A., BLAND, D.J. and CORNFORD, C. 1991. The geochemistry of the Plenus Marls at Dover, England: evidence of fluctuating oceanographic conditions and of glacial control during the development of the Cenomanian-Turonian $\delta^{13}C$ anomaly. *Geological Magazine,* vol. 128, pp. 603-632.

JEFFERIES, R.P.S. 1963. The stratigraphy of the *Actinocamax plenus*

Subzone (Turonian) in the Anglo-Paris Basin. *Proceedings of the Geologists' Association,* vol. 74, pt. 1, pp. 1-33.

JENKYNS, H.C. 1980. Cretaceous anoxic events: from continents to oceans. *Journal of the Geological Society, London,* vol. 137, pp. 171-188.

JUKES-BROWN. A.J. 1880. The subdivisions of the Chalk. *Geological Magazine,* vol. 7, pt.2, pp. 248-257.

JUKES-BROWN, A.J. and HILL, W. 1903. The Cretaceous rocks of Britain, Vol.II: The Lower and Middle Chalk of England. *Memoirs of the Geological Survey, U.K.,* VIII + 558pp.

KEMPTON, R.A. 1979. The structure of species abundance and measurement of its diversity. *Biometrics,* vol. 35, pp. 307-321.

KENNEDY, W.J. 1967a. Field meeting at Eastbourne, Sussex Lower Chalk sedimentation. *Proceedings of the Geologists' Association,* vol. 77, pp. 365-370.

KENNEDY, W.J. 1967b. Burrows and surface traces from the Lower Chalk of southern England. *Bulletin of the British Museum of Natural History (Geology),* vol. 80, pp. 127-167.

KENNEDY, W.J. 1969. The correlation of the Lower Chalk of south-east England. *Proceedings of the Geologists' Association,* vol. 80, pp. 459-560.

KLEMENT, K.W. 1960. Dinoflagellaten und Hystrichosphaerideen aus dem unteren und mittleren Malm Südwestdeutschlands. *Palaeontographica, Abt A,* vol. 114, pp. 1-104, pls 1-10.

KLUMPP, B. 1953. Beitrag zur Kenntnis der Mikrofossilien des mittleren und oberen Eozän. *Palaeontographica, Abt. A,* vol. 103, pp. 377-406, pls 16-20.

KJELLSTRÖM, G. 1973. Maastrichtian microplankton from Höllviken

Borehole no.1 in Scania, southern Sweden. Sveriges Geologiska Undersökning. *Afhandlingar Och Uppsatser Arsbok* 67, pp. 1-59.

KOUTSOUKOS, E.A.M. 1989. *Mid to Late Cretaceous microbiostratigraphy, palaeoecology and palaeogeography of the Sergipe Basin, northeastern Brazil*. Unpublished Ph.D. Thesis, Polytechnic South West.

KOUTSOUKOS, E.A.M., LEARY, P.N. and HART, M.B. 1990. Latest Cenomanian-earliest Turonian low-oxygen tolerant benthonic foraminifera: a case study from the Sergipe Basin (N.E. Brazil) and the western Anglo-Paris Basin (southern England). *Palaeogeography, Palaeoclimatology, Palaeoecology*, vol. 77, pp. 145-177.

KÖTHE, A. 1990. Paleogene dinoflagellates from northwest Germany - Biostratigraphy and paleoenvironment. *Geologische Jahrbuch Reihe A*, vol. 118, pp. 3-111, pls 1-27.

LEARY, P.N., CARSON, G.A., COOPER, M.K.E., HART, M.B., HORNE, D., JARVIS, I., ROSENFELD, A. and TOCHER, B.A. 1989. The biotic response to the late Cenomanian oceanic anoxic event; integreted evidence from Dover, SE England. *Journal of the Geological Society, London*, vol. 146, pp. 311-317.

LEARY, P.N. and WRAY, D.S. 1989. The foraminiferal assemblages across three Middle Turonian marl bands and a note on their genesis. *Journal of Micropalaeontology*, vol. 8, pt. 2, pp. 143-148.

LEFFINGWELL, H.A. and MORGAN, R.P. 1977. Restudy and comparison of the dinoflagellate cyst genus *Carpodinium* to that of *Prionodinium* n. gen. *Journal of Paleontology*, vol. 51, pp. 288-302, pls 1-4.

LEJEUNE-CARPENTIER, M. 1943. L'étude microscopique des silex. Une Hystrichosphaeridée à classer parmi les Péridiniens (Onzième note). *Annales de la Société géologique de Belgique*, vol. 67, pp. B22-B28.

LEJEUNE-CARPENTIER, M. and SARJEANT, W.A.S. 1983. Restudy of some smaller dinoflagellate cysts from the Upper Cretaceous of Belgium. *Annales de la Société géologique de Beligique,* vol. 106, pp. 1-17, pls 1-2.

LENTIN, J.K. and WILLIAMS, G.L. 1973. Fossil dinoflagellates: index to genera and species. *Geological Survey of Canada,* Paper no. 73-42, pp. 1-176.

LENTIN, J.K. and WILLIAMS, G.L. 1975. Fossil dinoflagellates: index to genera and species. Supplement 1. *Canadian Journal of Botany,* vol. 53, pp. 2147-2157.

LENTIN J.K. and WILLIAMS, G.L. 1976. A monograph of fossil peridinioid dinoflagellate cysts. *Bedford Institute of Oceanography, Report Series* BI-R-75-16, pp. 1-237.

LENTIN, I.C and WILLIAMS, G.L. 1977. Fossil dinoflagellate genus *Isabelidinium* nom. nov. *Palynology,* vol. 1, pp. 167-168.

LENTIN, J.K. and WILLIAMS, G.L. 1980. Dinoflagellate provincialism with emphasis on Campanian Peridiniaceans. *American Association of Stratigraphic Palynologists, Contribution Series,* No. 7, pp. 1-147.

LENTIN, J.K and WILLIAMS, G.L. 1981. Fossil dinoflagellates: index to genera and species, 1981 edition. *Bedford Institute of Oceanography, Report Series* BI-R-81-12, pp. 1-345.

LENTIN, J.K. and WILLIAMS, G.L. 1985. Fossil dinoflagellates: index to genera and species, 1985 edition. *Canadian Technical Report of Hydrography and Ocean Sciences,* no. 60, pp. 1-449.

LENTIN, J.K. and WILLIAMS, G.L. 1989. Fossil dinoflagellates: Index to genera and species, 1989 edition. *American Association of Stratigraphic Palynologists, Contributions Series,* No. 20, pp. 1-473

LIGHTHILL, M.J. 1958. *Introduction to Fourier Analysis and Generalised Functions.* Cambridge: Cambridge University Press. 1-79pp.

LINDEMANN, E. 1928. Abteilung Peridineae (Dinoflagellata). *In* Enger, A. (ed.), *Die Natürlichen Pflanzerfamilien Nebst ihren Gattungen und Wichtigeren Arter Insbesondere den Nutzpflanze,* vol. 2. Leipzig: Verlag von Wilheim Engelmann, pp. 3-104.

LOCKWOOD, J.G. 1980. Milankovitch theory and ice ages. *Progress in Physical Geography,* vol. 4, pp. 79-87.

LOEBLICH, A.R. Jr. and LOEBLICH, A.R. III. 1966. Index to the genera, subgenera, and sections of the Pyrrhophyta. *Studies in Tropical Oceanography, Miami,* no. 3, x + 94p, pl. 1.

LOEBLICH, A.R. Jr. and LOEBLICH, A.R. III. 1968. Index to the genera, subgenera, and sections of the Pyrrrophyta, II. *Journal of Paleontology,* vol. 42, pp. 210-213.

LOEBLICH, A.R. Jr. and TAPPAN, H. 1977. *Senegalidinium* Jain and Millepied, 1973, correct name for *Alterbia* Lentin and Williams, 1975, a dinoflagellate. *Micropaleontology,* vol. 23, pp. 368.

LOHMANN, H. 1904. Eier und sogenannte Cysten der Plankton-Expedition. Anhang: Cyphonautes. *Ergebnisse Plankton-Expedition. Humboldt-Stiftung, n. ser.,* vol. 4, pp. 1-60. Kiel

LONG, D., BENT, A., HARLAND, R., GREGORY, D.M., GRAHAM, D.K. and MORTON, A.C. 1986. Late Quaternary palaeontology, sedimentology and geochemistry of a vibrocore from the Witch Ground basin, central North Sea. *Marine Geology,* vol. 73, pp. 109-123.

LOTT, G.K. 1982. The sedimentation of the Lower Chalk (Middle-Upper Cenomanian) of Winterbourne Kingston borehole, Dorset. *In* Rhys, G.H., Lott, G.K. and Calver, M.A. (eds.), The Winterbourne Kingstone borehole, Dorset, England. *Report of the Institute of Geological Sciences,* No. 81/3, pp. 28-34.

LUCAS-CLARK, J. 1984. Morphology of species of *Litosphaeridium* (Cretaceous, Dinophyceae). *Palynology,* vol. 8, pp. 165-193, pls 1-5.

LUCAS-CLARK, J. 1987. *Wigginsiella* n. gen., *Spongodinium,* and *Apteodinium* as members of the *Aptiana-Ventriosum* complex (fossil Dinophyceae). *Palynology,* vol. 11, pp. 155-184, pls 1-5.

MAGURRAN, A.E. 1988. *Ecological Diversity and its measurement.* London: Croom Helm Ltd. 1-160pp.

MAIER, D. 1959. Plantonuntersuchungen in Tertiären und Quartären marinen Sedimenten. Ein Beitrag zur Systematik, Stratigraphie und Ökologie der Coccolithophorideen, Dinoflagellaten und Hystrichosphaerideen vom Oliozän bis zum Pleistozän. *Neues Jahrbuch für Geologie und Paläontologie, Abhandlungen,* vol. 107, pp. 278-340, pls 27-33

MANTELL, G.A. 1822. *The fossils of the South Downs, or Illustrations of the Geology of Sussex.* London: Lupton Relfe. 1-327pp.

MANTELL, G.A. 1845. Notes on a microscopical examination of the Chalk and Flint of south-east England, with remarks on the Animalculites of certain Tertiary and modern deposits. *Annual Magazine of Natural History,* London, vol.16, pp. 73-88.

MANTELL, G.A. 1850. *A pictorial atlas of fossil remains, consisting of coloured illustrations selected from Parkinson's "Organic remains of a former world", and Artis's "Antediluvian phytology",* Henry G. Bohn, London, xii + 207pp., 74pls.

MAO SHAOZHI and NORRIS, G. 1988. Late Cretaceous-Early Tertiary dinoflagellates and acritarchs from the Kashi area, Tarim Basin, Xinjiang Province, China. *Royal Ontario Museum, Life Sciences Contributions,* no. 150, pp. 1-93, pls 1-16.

MANUM, S. and COOKSON, I.C. 1964. Cretaceous microplankton in a

sample from Graham Island, Arctic Canada, collected during the second "Fram"-Expedition (1898-1902). With notes on microplankton from the Hassel Formation, Ellef Ringnes Island. *Schrifter utgitt av Det Norske Videnskaps-Akademi i Oslo, I. Mat-Naturv. Klasse, Ny Series* 17, pp. 1-35, pls 1-7.

MARGALEF, R. 1972. Homage to Evelyn Hutchinson, or why is there an upper limit to diversity. *Transactions of Connecticut Academy of Arts and Sciences,* vol. 1, pp. 211-235.

MARSHALL K.L. 1983. *Dinoflagellate cysts from the Cenomanian, Turonian and Coniacian of Germany and England.* Unpublished Ph.D. Theis, University of Aberdeen.

MARSHALL, K. L. and BATTEN, D.J. 1988. Dinoflagellate cyst associations in Cenomanian-Turonian "black shale" sequences of northern Europe. *Review of Palaeobotany and Palynology,* vol. 54, pp. 85-103, pls 1-3.

MAY, F.E. 1980. Dinoflagellate cysts of the Gymnodiniaceae, Peridiniaceae and Gonyaulacaceae from the Upper Cretaceous Monmouth Group, Atlantic Highlands, New Jersey. *Palaeontographica, Abt. B,* vol. 172, pp. 10-116, pls 1-23.

MEHROTRA, N.C. and SARJEANT, W.A.S. 1984. The dinoflagellate cyst genus *Polygonifera*; emendation and taxonomic stabilization. *Journal of Micropalaeontology,* vol. 3, no. 1, pp. 43-53, pls 1-2.

MEHROTRA, N.C. and SINHA, A.K. 1981. Further studies on microplanktons from the Sangchamalla Formation (Upper Flysch) of Malla Johar area in the Tethyan zone of Higher Kumaon Himalaya. *In* Sinha, A.K. (ed.). *Contemporary Geoscientific Researches in Himalaya, Dehra Dun, (India),* pp. 151-160.

MILANKOVITCH, M. 1941. Canon of Insolation and the Ice-Age Problem. *Königlich Serbische Akademie (Royal Serbian Academy, Special Publications, Science of Mathematical and Natural Sciences),* Belgrad, vol. 33. English translation by the Israel Program for

Science Translations, Jerusalem 1969. Washington D.C.: US Department of Commerce and National Science Foundation, Benny B. and Meroz I. (ed.), pp. 1-484.

MORGAN, R. 1980. Palynostratigraphy of the Australian Early and Middle Cretaceous. *Geological Survey of New South Wales, Palaeontology Memoir* 18, pp. 1-153, pls 1-38.

MORROW, A.L. 1934. Foraminifera and Ostrocoda from the Upper Cretaceous of Kansas. *Journal of Paleontology,* Menasha, Wisconsin, vol. 8, pt. 2, pp. 186-205, pls 29-31.

MORTIMORE, R.N. 1983. The Geology of Sussex, *in "Sussex : Environment, landscape, and society*". Geography Editorial Committee, University of Sussex, Alan Sutton, Gloucester, pp. 15-32.

MORTON. A.C., EVANS, D., HARLAND, R., KING, C. and RITCHIE, D.K. 1988. Volcanic ash in a cored borehole W of the Shetland Islands: evidence for Selandian (late Palaeocene) volcanism in the Faeroes region. *In* Morton, A.C. and Parson, L.M. (eds.). Early Tertiary Volcanism and Opening of the NE Atlantic. *Geological Society Special Publication* No. 39, pp. 263-269.

MORZADEC-KERFOURN, M.T. 1977. Les kystes de dinoflagellés dans les sédiments Récents le long des Côtes Bretonnes. *Revue de Micropaléontologie,* vol. 20, pp. 157-166.

MORZADEC-KERFOURN, M.T. 1979. Les kystes de dinoflagellés. In *Géologie Méditerranéenne, La mer Pélagienne,* 6, pp. 221-245.

NEALE, J.W. and SARJEANT, W.A.S. 1962. Microplankton from the Speeton Clay of Yorkshire. *Geological Magazine,* vol. 99, pp. 439-458, pls 19-20.

NORRIS, G. and SARJEANT, W.A.S., 1965. A descriptive index of genera of fossil Dinophyceae and Acritarcha. *New Zealand Geological Survey, Paleontology Bulletin,* no. 40, pp. 1-72.

NORVICK, M.S. 1976 *in* NORVICK, M.S. and BURGER, D., Mid-Cretaceous microplankton from Bathurst Island, *in* Palynology of the Cenomanian of Bathurst Island, Northern Territory, Australia. *Australian Bureau of Mineral Resources, Geology and Geophysics, Bulletin* 151, pp. 21-113.

ODUM, H.T. and COPELAND, B.J. 1974. Functional classification of the coastal ecosystems of the United States, *in* Odum, H.T., Copeland, B.J. and McMahon E.A., *Coastal Ecosystems of the United States,* vol. 1, pp. 5-84.

OLSEN, P.E. 1986. A 40-million-year lake record of Early Mesozoic Orbital climatic forcing. *Science,* vol. 234, pp. 842-848.

ORBIGNY, A.D. d' 1842-47. Pteropoda, Gasteropoda. *Paléontologie française, Terrains crétacés,* vol. 2, 456pp., Atlas 236 pls, table. (1842). Brachiopoda [includes Bivalvia]. *loc. ct.* vol. 4, 390pp., Atlas pls 490-599. (1847). Paris

ORBIGNY, A.D. d' 1852. *Cours élémentaire de paléontologie et de géologie stratigraphique,* vol. 2, pp. 268-949.

OSTENFELD, C.H. 1903. Phytoplankton from the sea around the Faeröes. *Botany of the Faeröes. II. Det Nordiske Forag. Copenhagen,* pp. 558-612.

PACEY, N.R. 1984. Bentonites in the Chalk of central eastern England and their relation to the opening of the northeast Altantic. *Earth and Planetary Science Letters,* vol. 67, pp. 48-60.

PANTIC, N. and BAJRAKTAREVIC, Z. 1988. "Nannoforaminifera" in palynological preparations and smear-slides from Mesozoic and Tertiay deposits in central and southeast Europe. *Revue de Paléobiologie,* Special volume no. 2, pt. II, pp. 953-959.

PASCHER, A. 1914. Über Flagellaten und Algen. *Bericht der Deutschen Botanischen Gesellschaft,* vol. 32, pp. 136-160.

PEET, R.K. 1974. The measurement of species diversity. *Annual Review of Ecological Systems,* vol. 5, pp. 285-307.

PHILLIPS, W. 1818. *A selection of facts from the best authorities arranged so as to form an outline of the geology of England and Wales.* London, pp. 38-50.

PHILLIPS, W. 1821. Remarks on the chalk cliffs in the neighbourhood of Dover and on the Blue Marle covering the Green Sand, near Folkestone. *Transactions of the Geological Society of London,* vol. 5, pp. 16-51.

PHIPPS, D. and PLAYFORD, G. 1984. Laboratory techniques for extraction of palynomorphs from sediments. *Papers, Department of Geology, University of Queensland,* vol. 11, pp. 1-23.

PIELOU, E.C. 1975. *Ecological Diversity.* New York: Wiley. 1-165pp.

POMEROL, B. 1984. *Geochimie des craies du bassin de Paris.* Thèses de doctorat d'État, Université Pierre et Marie Curie, 84-21. 1-540pp.

PRESS, W.H., FLANNERY, B.P., TEUKOLSKY, S.A. and VETTERLING, W.T. 1986. *Numerical Recipes.* Canbridge: Cambridge University Press. 1-818pp.

PRICE, F.G.H. 1877. On the beds between the Gault and Upper Cretaceous near Folkestone. *Quaterly Journal of the Geological Society of London,* vol. 33, pp. 431-448.

READ, J.F., GROTZINGER, J.P., BOVA, J.A. and KOERSCHNER, W.F. 1986. Models for the generation of carbonate cycles. *Geology,* vol. 14, pp. 107-110.

READE, REV. J.B. 1839. On some new organic remains in the flint of chalk. *Annals of Natural History,* vol. 2, pp. 191-198, pls 8,9.

REID, P.C. 1972. Dinoflagellate cyst distribution around the British Isles. *Journal of the Marine Biological Association, U.K.*, vol. 52, pp. 939-944.

REID, P.C. 1974. Peridiniacean and glenodiniacean dinoflagellate cysts from the British Isles. *Nova Hedwigia*, vol. 29, pp. 429-456.

REID, P.C. 1975. A regional sub-division of dinoflagellate cysts around the British Isles. *New Phytologist*, vol. 75, pp. 586-603.

REYMENT, R.A. and BENGTSON, P. 1985 (*compilers*). Mid-Cretaceous Events, report on results 1974-1983 by IGCP Project No. 58. *Publications from the Palaeontological Institution of the University of Uppsala*, Special volume 5, pp. 1-132.

ROBINSON, N.D. 1986a. Lithostratigraphy of the Chalk Group of the North Downs, southeast England. *Proceedings of the Geologists' Association*, vol. 97, Pt. 2, pp. 141-170.

ROBINSON, N.D. 1986b. Fining-upwards microrhythms with basal scour in the Chalk of Kent and Surrey, England and their stratigraphic importance. *Newsletters on Stratigraphy*, vol.17, (1), pp. 21-28.

Rock Color Chart, 1984 edition. *The Geological Society of America*, Colorado, U.S.A.

SAH, S.C.D., KAR, R.K. and SINGH, R.Y. 1970. Fossil microplankton from the Langpar Formation of Therriaghat, south Shillong Plateau, Assam, India. *Palaeobotanist, Lucknow*, vol. 18, pp. 143, pls 1-2.

SALUJHA, S.K. and KINDRA, G.S. 1981. Palynological fossils from the Langpar Formation exposed along South Shillong Front, Meghalaya, India. *Geoscience Journal*, vol. 2, pp. 43-62, pls 1-3.

SARJEANT, W.A.S. 1960. New hystrichospheres from the Upper Jurassic of Dorset. *Geological Magazine*, vol. 97, pp. 137-144, pl. 6.

SARJEANT, W.A.S. 1963. *Favilarnax,* new genus of Mesozoic hystrichospheres. *Journal of Paleontology,* vol. 37, pp. 719-721.

SARJEANT, W.A.S. 1966. Dinoflagellate cysts with *Gonyaulax*-type tabulation. *In* Davey, R.J., Downie, C., Sarjeant, W.A.S. and Williams, G.L., Studies on Mesozoic and Cainozoic dinoflagellate cysts. *Bulletin of the British Museum (Natural History) Geology, Supplement* 3, pp. 107-156.

SARJEANT, W.A.S. 1967a. The stratigraphical distribution of fossil dinoflagellates. *Review of Palaeobotany and Palynology,* vol. 1, pp. 323-343.

SARJEANT, W.A.S. 1967b. The genus *Palaeoperidinium* Deflandre (Dinophyceae). *Grana Palynologica,* vol. 7, pp. 243-258.

SARJEANT, W.A.S. 1970. The genus *Spiniferites* Mantell, 1850 (Dinophyceae). *Grana,* vol. 10, pp. 74-78.

SARJEANT, W.A.S., 1982. The dinoflagellate cysts of the *Gonyaulacysta* group: a morphological and taxonomic study. *American Association of Stratigraphic Palynologists, Contributions Series,* No. 9, pp. 1-80, pls 1-12.

SARJEANT, W.A.S. 1984a. A restudy of some dinoflagellate cysts and an acritarch from the Malm (Upper Jurassic) of southwest Germany. *Palaeontographica, Abt. B,* vol. 191, pp. 154-177, pls 1-4.

SARJEANT, W.A.S. 1984b. A restudy of some dinoflagellate cyst holotypes in the University of Kiel Collections V. The Danian (Palaeocene) Holotypes of Walter Wetzel (1952, 1955). *Meyniana,* vol. 36, pp. 121-171, pls 1-8.

SARJEANT, W.A.S. 1985a. The German Aptian dinoflagellate cysts of Eisenack (1958): a restudy. *Review of Palaeobotany and Palynology,* vol. 45, pp. 47-106, pls 1-10.

SARJEANT, W.A.S. 1985b. A restudy of some dinoflagellate cyst holotyes in the University of Kiel Collections: VI. Late Cretaceous dinoflagellate cysts and other palynomorphs in the O. Wetzel collection. *Meyniana,* vol. 37, pp. 129-185, pls 1-7.

SARJEANT, W.A.S. 1991. Henry Hopley White (1790-1877) and the early researches on Chalk "Xanthidia" by Clapham microscopists. *Journal of Micropalaeontology,* vol 10, pt. 1, pp. 83-93.

SCHLANGER, S.O., ARTHUR, M.A., JENKYNS, H.C. and SCHOLLE, P.A. 1987. The Cenomanian-Turonian Oceanic Anoxic Event, I : Stratigraphy and distribution of organic carbon-rich beds and the marine ^{13}C excursion. *In* Brooks, J and Fleet, A. (eds.) *Marine Petroleum Source Rocks. Geological Society Special Publications,* vol. 26, pp. 371-399.

SCHLANGER, S.O. and JENKYNS, H.C. 1976. Cretaceous oceanic anoxiv events: causes and consequences. *Geologie en Mijnbouw*, vol. 55, pp. 179-184.

SCHOLLE, P.A. 1974. Diagenesis of Upper Cretaceous chalks from England, Northern Ireland and the North Sea. *In* Hsü, K.H. and Jenkyns, H.C. (eds.). Pelagic Sediments: on land and under the sea. *Specical Publications. International Association of Sedimentologists,* vol. 1, pp. 177-210.

SCHOLLE, P.A. and ARTHUR, M.A. 1976. Carbon-isotopic fluctuations in Upper Cretaceous sediments: an indicator of paleo-oceanic circulation. *Geological Society of America, Abstracts with Programs,* vol. 8, pp. 1089.

SCHOLLE, P.A. and ARTHUR, M.A. 1980. Carbon isotope fluctuations in Cretaceous pelagic limestones: potential stratigraphic and petroleum exploration tool. *Bulletin of the American Association of Petroleum Geologists,* vol. 64, pp. 67-87.

SCULL, B.J., FLEIX, C.J., McCALEB, S.B. and SHAW, W.G. 1966. The inter-discipline approach to paleoenvironmental interpretations.

Transactions of the Gulf Coast Association Geological Societies, vol.16, pp. 81-117.

SPSS. 1975. *Statistical Package for the Social Sciences.* Second edition. Nie M.H. *et al.* New York: Mc Graw-Hill. 1-675pp.

STOKER, M.S., HARLAND, R. and GRAHAM, D.K. 1991. Glacially influenced basin plain sedimentation in the southern Faeroe-Shetland Channel, northwest United Kingdom continental margin. *Marine Geology,* vol. 100, pp. 185-199.

STOVER, L.E. and EVITT, W.R. 1978. Analysis of pre-Pleistocene organic-walled dinoflagellates. *Stanford University Publications,* vol.15, pp. 1-300.

STOVER, L.E. and WILLIAMS, G.L. 1987. Analyses of Mesozoic and Cenozoic organic-walled dinoflagellates 1977-1985. *American Association of Stratigraphic Palynologists, Contributions Series,* No. 18, pp. 1-243.

TOCHER, B.A. and JARVIS, I. 1987. Dinoflagellate cysts and stratigraphy of the Turonian (Upper Cretaceous) chalk near Beer, southeast Devon, England, *in* Hart, M.B. (ed.), *Micropalaeontology of Carbonate Environments.* Chichester: Horwood, pp. 138-175, pls 9.1-9.3.

TRAVERSE, A. and GINSBURG, R.N. 1966. Palynology of the surface sediments of Great Bahama Bank, as related to water movement and sedimentation. *Marine Geology,* vol. 4, pp. 417-459.

TURON, J.-L. and LONDEIX, L. 1988. Les assemblages de kystes de dinoflagellés en Méditerranée occidentale (Mer d'Alboran) mise en évidence de l'évolution des paléoenvironnements depuis le dernier maximum glaciaire. *Bulletin Centres Recherche Exploration-Production Elf-Aquitaine,* 12, pp. 313-344.

VALENSI, L. 1955a. Sur quelque microorganismes des silex crétacés du Magdalénien de Saint-Amand (Cher). *Bulletin de la Société*

géologique de France, sér. 6, vol. 5, pp. 35-40.

VALENSI, L. 1955b. Étude micropaléontlogique des silex du Magdalénien de Saint-Amand (Cher). *Société préhistorique française,* vol. 52, pp. 584-596, pls 1-5.

VERDIER, J.-P. 1975. Les kystes de dinoflagellés de la section de Wissant et leur distribution stratigraphique au Crétacé moyen. *Revue de Micropaléontologie,* vol. 17, pp. 191-197.

VOZZHENNIKOVA, T.F. 1967. Iskopaemye peridinei yurskikh, melovykh i paleogenovykh otlozheniy SSSR. *Akademiya Nauk SSSR, Sibirskoe Otdelenie, Instituta Geologii i Geofiziki, Trudy,* pp. 1-347, pls 1-121. (Fossil peridinians of the Jurassic, Cretaceous and Paleogene deposits of the USSR).

WALL, D. and DALE, B. 1968. Modern dinoflagellate cysts and evolution of the peridiniales. *Micropaleontology,* vol. 14, pp. 265-304, pls 1-4.

WALL, D., DALE, B., LOHMANN, G.P. and SMITH, W.K. 1977. The environmental and climatic distribution of dinoflagellate cysts in modern marine sediments from regions in the North and South Atlantic. *Marine Micropaleontology,* vol. 2, pp. 121-200.

WARREN, J.S. 1967. *Dinoflagellate and acritarchs from the Upper Jurassic and Lower Cretaceous rocks on the west side of the Sacramento Valley, California.* Unpublished Ph.D. thesis, Stanford University.

WETZEL, O. 1932. Die Typen der baltischen Geschiebefeuersteine, beurteilt nach ihrem Gehalt an Mikrofossilien. *Zeitschrift für Geschiebeforschung,* vol. 8, pp. 129-146, pls 1-3.

WETZEL, O, 1933a. Die in organischer Substanz erhaltenen Mikrofossilien des baltischen Kreide-Feuersteins mit einem sediment-petrographischen und stratigraphischen Anhang. *Palaeontographica, Abt. A,* vol. 77, pp. 141-188.

WETZEL, O, 1933b. Die in organischer Substanz erhaltenen Mikrofossilien des baltischen Kreide-Feuersteins mit einem sediment-petrographischen und stratigraphischen Anhang. *Palaeontographica, Abt. A,* vol. 78, pp. 1-110, pls 1-7.

WHITAKER, W. BRISTOW, H.W. and HUGHES, M. 1872. The geology of the London Basin Part I : The Chalk and the Eocene beds of the southern and western tracts. *Memoirs of the Geological Survey of England and Wales,* vol. 4, pp. 30-36.

WHITE, H.H. 1842. On fossil Xanthidia. *Microscopical Journal, London,* vol. 11, pp. 35-40, pl. 4

WILKINSON, S.J. 1849. On observations on Xanthidium, both fossil and recent. *Transactions of the Microscopical Society of London,* vol. 2, pp. 89-92, pl. 13.

WILLIAMS, D.B. 1971a. The distribution of marine dinoflagellates in relation to physical and chemical conditions. *In Micropaleontology of the Oceans*, Funnell, B.M. and Riedel, W.R. (eds). Cambrigde: Cambridge University Press, pp. 91-95.

WILLIAMS, D.B. 1971b. The occurrence of dinoflagellates in marine sediments. *In Micropaleontology of the Oceans*, Funnell, B.M. and Riedel, W.R. (eds). Cambridge: Cambridge University Press, pp. 231-243.

WILLIAMS, G.L. and DOWNIE, C. 1966. Further dinoflagellate cysts from the London Clay. *In* Davey, R.J., Downie, C., Sarjeant, W.A.S. and Williams, G.L., Studies on Mesozoic and Cainozoic dinoflagellate cysts. *Bulletin of the British Museum (Natural History) Geology, Supplement* 3, pp. 82-198.

WILLIAMS, G.L., SARJEANT, W.A.S. and KIDSON, E.J. 1978. A glossary of the terminology applied to dinoflagellate amphiesma and cysts and acritarchs: 1978 edition. *American Association of Stratigraphic Palynologists Contributions Series,* No.2A, pp. 1-121.

WILSON, G.J. 1974. *Upper Campanian and Maastrichtian dinoflagellate cysts from the Maastricht region and Denmark.* Unpublished Ph.D Thesis, University of Nottingham.

WHITAKER, W., BRISTOW, H.W. and Mc. HUGHES, T. 1872. The Geology of the London Basin. Part 1: The Chalk and the Eocene beds of the Southern and Western tracts. London: Longmans. *Memoirs of the Geological Survey of Great Britain,* vol. 4, pt. 1.

WHITHAM, F. 1991. The stratigraphy of the Upper Cretaceous Ferriby, Welton and Burnham formations north of the Humber, north-east England. *Proceedings of the Yorkshire Geological Society,* vol. 48, pp. 227-254.

WOOD, C.J. and SMITH, E.G. 1978. Lithostratigraphiacl classification of the Chalk in North Yorkshire, Humberside and Lincolnshire. *Proceedings of the Yorkshire Geological Society,* vol. 42, pt. 2, no. 14, pp. 263-287.

WOODWARD, S. 1833. *An outline of the geology of Norfolk.* Norwich: J. Stacy. 1-54pp.

WRIGHT, C.W. and WRIGHT, E.V. 1942. The Chalk of the Yorkshire Wolds. *Proceedings of the Geologists' Association,* vol. 53, pp. 112-127.

YU JINGXIAN and ZHANG WANGBING 1980. Upper Cretaceous dinoflagellate cysts and acritarchs of Western Xinjiang. *Bulletin Chinese Academy of Geological Sciences,* Series 1, vol. 2, no. 1, pp. 93-119, pls 1-6.

YUN, H.-S. 1981. Dinoflagellaten aus der Oberkreide (Santon) von Westfalen. *Palaeontographica Abt. B,* vol. 177, pp. 1-89, pls 1-16.

PLATES AND PHOTOGRAPHY

Introduction

The photomicrographs of all species recorded are arranged alphabetically, regardless of Family affinities. Information on slide identification for each specimen figured is given in the short-hand notation for each section studied; Site 3a, TBB, MCB, SFE, followed by the slide number. The exact location of each specimen on the relevant slide is given by an England Finder reference. The vast majority of specimens figured are from the standard strewn-mount slides. However, those taken from other slide types are indicated by the following suffixes: 'Al' indicating aliquot slide

'Ox' indicating oxidation slide

'Paly' indicating palynofacies slide

Greatest success in photography was achieved by keeping the light exposure level as constant as possible through-out at least one film, which yielded consistent results. Also, exposure level consistency within a film was achieved by keeping the magnification constant through-out.

In the majority of cases, ordinary transmitted light photography proved to be the most successful technique in attaining good photographic results. This technique involved the use of 35mm. colour film of 100ASA film speed. A Neutral density filter was employed to give the correct intensity of light. Exposure time varied between 0.3 to 0.5 of a second.

In the case of paler, more three dimensional specimens, the Nomarski interference contrast or Differential interference contrast method of light photography was employed. This technique involves the splitting of polarised light into two sets of components which travel through or are reflected from adjacent areas of the specimen. This results in a directional contrast which enhances the image. The stage may be rotated to yield the best image of the specimen. This photographic technique involves the use of 35mm. colour film of 200ASA film speed. The use of a blue filter gave the best light intensity. Exposures during this technique ranged between 1 to 3 seconds. Photomicrographs taken using this technique are indicated by the notation DIC.

Best photographic results were obtained by keeping conditions such as magnification, light exposure etc., as constant as possible through out one film and to a lesser extent, from film to film, as mentioned previously. As a consequence of this, processing and printing of the photomicrographs was relatively straight forward. This was an extremely desirable consequence, as the developing and printing of all films was carried out in a local "high street" photographic laboratory.

In the preparation of the plates, the decision was made to mount colour photomicrographs of the palynomorphs on different shades of coloured card. This was carried out in the hope of achieving the effect that the background of each individual photomicrograph would merge into the card background, such that one became indistinguishable from the other. During the course of plate preparation, it became obvious that this goal was impossible to achieve for all plates. Due to the necessary alphabetical ordering of palynomorphs, photomicrographs of several different shades of backgrounds had to be placed on the same plate. In retrospect, it is felt that plates would have been better prepared on white card, as in the preparation of standard black and white photomicrograph plates.

Plate 1

All photomicrographs taken at x 675 unless otherwise stated.

Fig. 1. *Achomosphaera neptuni* (Eisenack) Davey and Williams 1966a.
Dorsal view showing Type P archaeopyle.
MCB 1 --> 1.5 W22/3 x 1025 magnification

Fig. 2. *Achomosphaera ramulifera* (Deflandre) Evitt 1963.
Oblique dorsal view.
MCB -1 --> -1.5 G49 x 1025 magnification.

Fig. 3. *Achomosphaera reginensis* Corradini 1973.
Dorsal view. Faint parasutural lines are distinguishable, especially on the hypocyst. Note delicate nature of processes.
MCB -1.5 --> -2 O28/2 x 1025 magnification DIC

Figs 4-8. *Achomosphaera* cf. *ramulifera*
Figs 4,5. TBB -30x S29/4
4. Dorsal view. High focus shot showing process tip morphology.
5. Dorsal view. Low focus shot of same specimen showing precingular archaeopyle.
Figs 6,7. MCB 0 --> -0.5 U34/2
6. Dorsal view. High focus shot showing precingular archaeopyle and grapnel-like tips to paracingular processes.
7. Dorsal view. Low focus of same specimen showing process morphology of same specimen and broad membraneous base to paracingular processes.
Fig. 8. TBB -3 C45/3
Shows extreme development of apical, paracingular and antapical processes.

Figs 9,10. *Achomosphaera sagena* Davey and Williams 1966a
Fig. 9. TBB 130x M42
Oblique view showing dense reticulation of the periphragm extending into the base of some processes.
Fig. 10. Site 3A 0 W33
Dorsal view showing Type P archaeopyle and reticulated periphragm extending well into the processes.

NUMBERS

CUT OFF

IN

ORIGINAL

PLATE 1


1

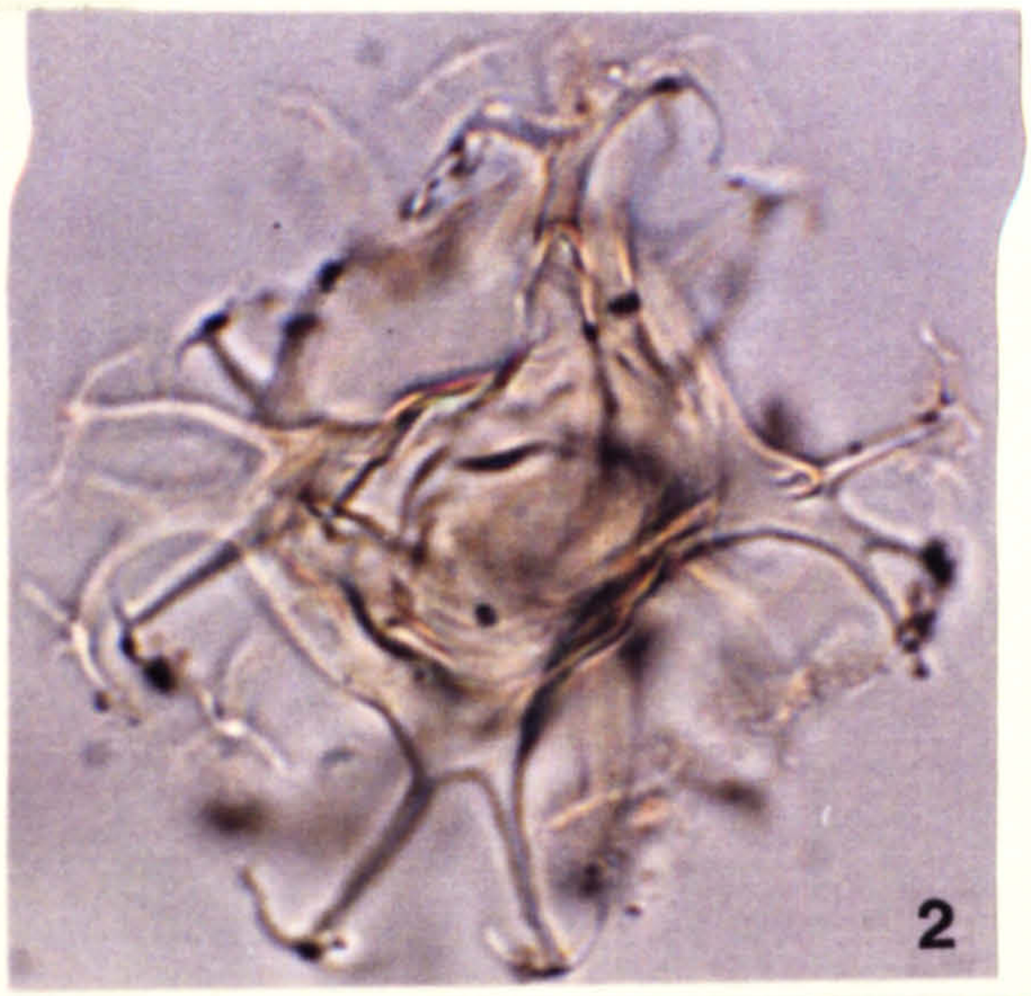
2

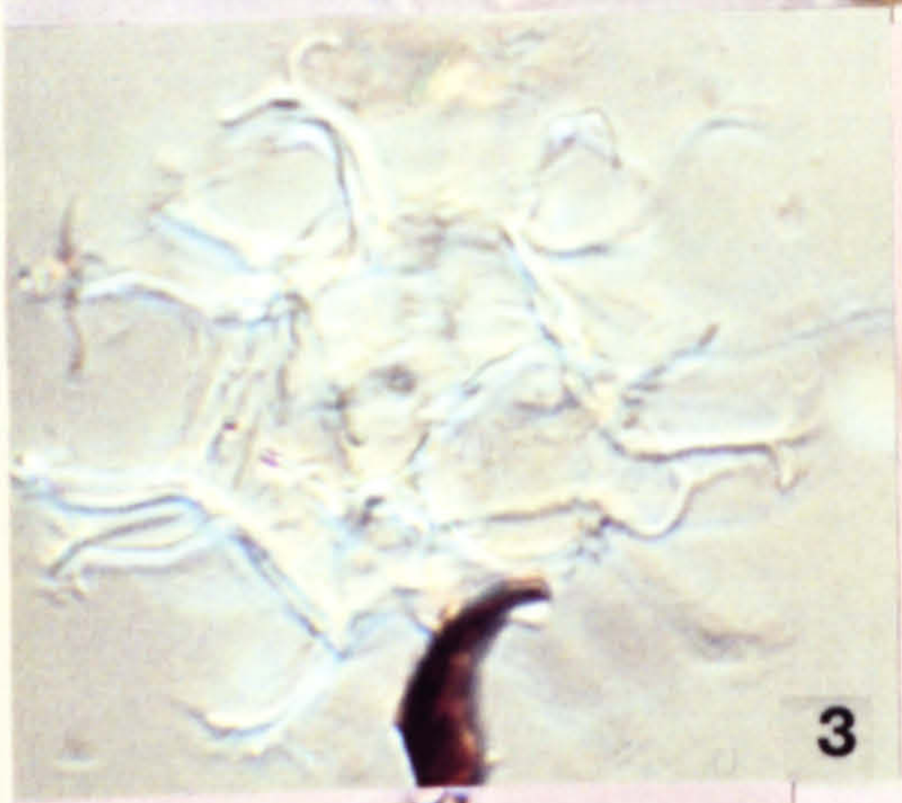
3


4


5


6


7

8


9

Plate 2

Fig. 1. *Apteodinium deflandrei* (Clarke and Verdier) emend. Lucas-Clark 1987
Dorsal view showing apical projection and Type P archaeopyle.
MCB 0 --> 0.5 U22/3 x 1025 magnification

Fig. 2. *Apteodinium maculatum* Eisenack and Cookson 1960
Left lateral oblique view, showing Type P archaeopyle
TBB W35 x 1025 magnification

Fig. 3. *Callaiosphaeridium asymmetricum* (Deflandre and Courtville) Davey and Williams 1966a
Oblique ?apical view showing large penitabular paracingular processes.
Site 3A 0 M25/2 x 675 magnification

Fig. 4. *Canningia colliveri* Cookson and Eisenack 1960b
Typical dorso-ventral compressional preservation showing zig-zag apical archaeopyle margin.
SFE 18A1 L55/1 x 675 magnification

Fig. 5. *Canningia reticulata* Cookson and Eisenack 1960b; emend. Helby 1987
Note dense granulation and zig-zag archaeopyle margin of cyst due to complete archaeopyle loss.
SFE 18A1 R30 x 900 magnification

Fig. 6. *Carpodinium obliquicostatum* Cookson and Hughes 1964
Site 3A 120 D45 x 1025 magnification
Dorsal view showing precingular archaeopyle and nature of parasutural ridges with their serrate to denticulate edges.

PLATE 2


1


2

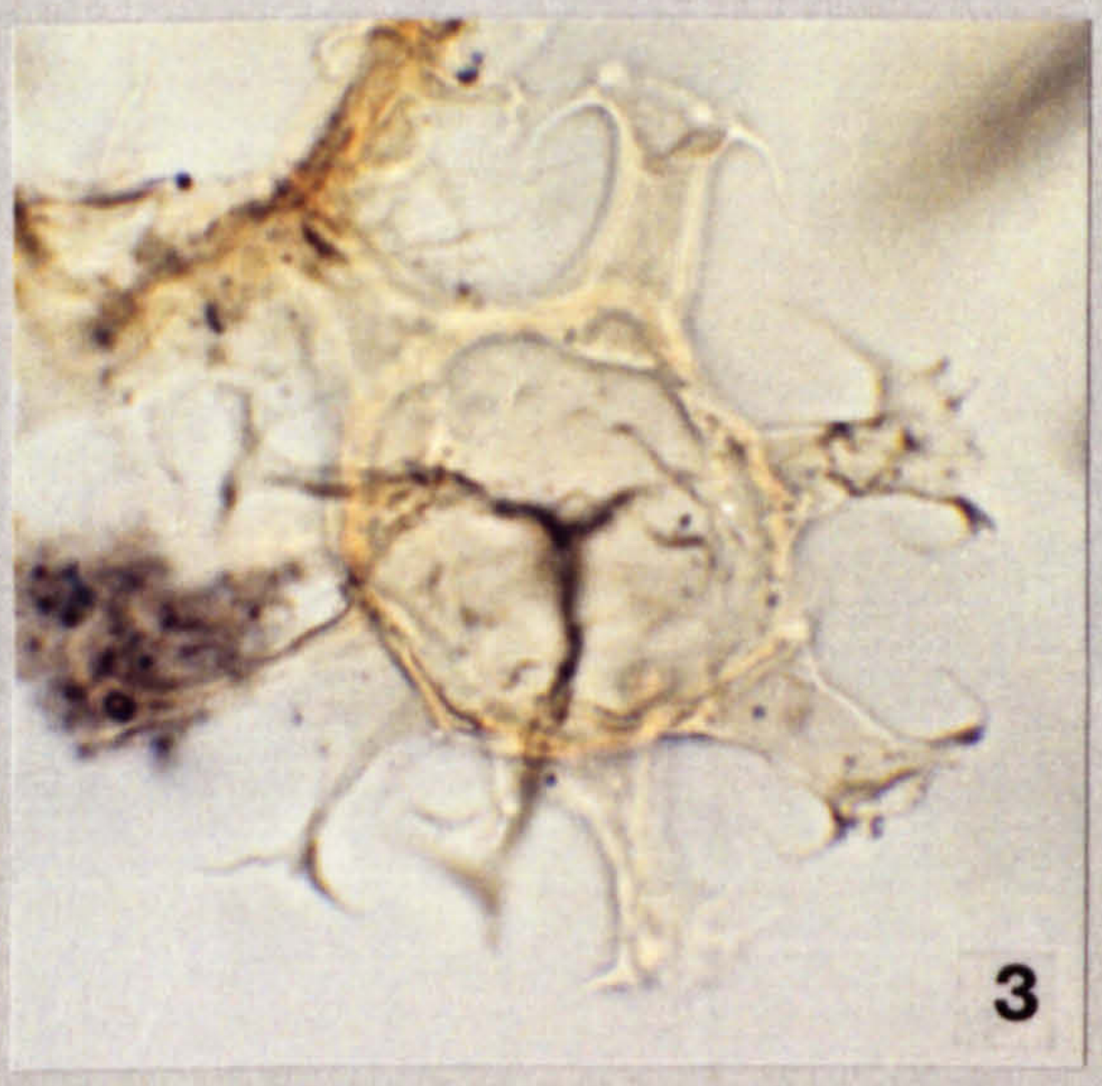
3


4

5


6

Plate 3

All photomicrographs taken at x 1025 magnification.

Fig. 1. *Chlamydophorella discreta* Clarke and Verdier 1967
Ventral view with faint traces of parasulcual area present.
MCB -4 --> -4.5 X47/1

Fig. 2. *Chlamydophorella neyi* Cookson and Eisenack 1958
Note distinguishing broad based apical horn and slight indication of paracingulum on outer margin of cyst.
MCB 5 --> 5.5 V39

Figs 3,4. *Chlamydophorella ? urna* Cookson and Eisenack 1960a
Fig. 3. Low focus shot with oblique view showing paracingulum.
Fig. 4. High focus shot showing ventral surface with paracingulum and parasulcus obvious.
TBB -2 C32/2

Figs 5,6. *Cleistosphaeridium armatum* (Deflandre) Davey 1969
Oblique views showing non-tabular processes.
Fig. 5. MCB 1.5 --> 2 W35
Fig. 6. Site 3A 0 M26

Figs 7,8. *Cleistosphaeridium clavulum* (Davey) Below 1982
Figs 7,8. Site 3A 85 P48/4
7. Shows the probable apical archaeopyle
8. Shows the general process morphology

Figs 9,10. *Cleistosphaeridium huguoniotii* (Valensi) Davey 1969
Figs 9,10. Site 3A 90 P39
9. Oblique apical view showing apical archaeopyle.
10. Oblique view showing process morphology.

Fig. 11. *Coronifera oceanica* Cookson and Eisenack; emend. May 1980
Oblique view showing faint paracingulum and distinctive large tubular antapical process.
Site 3A 60 F26

PLATE 3


1


2

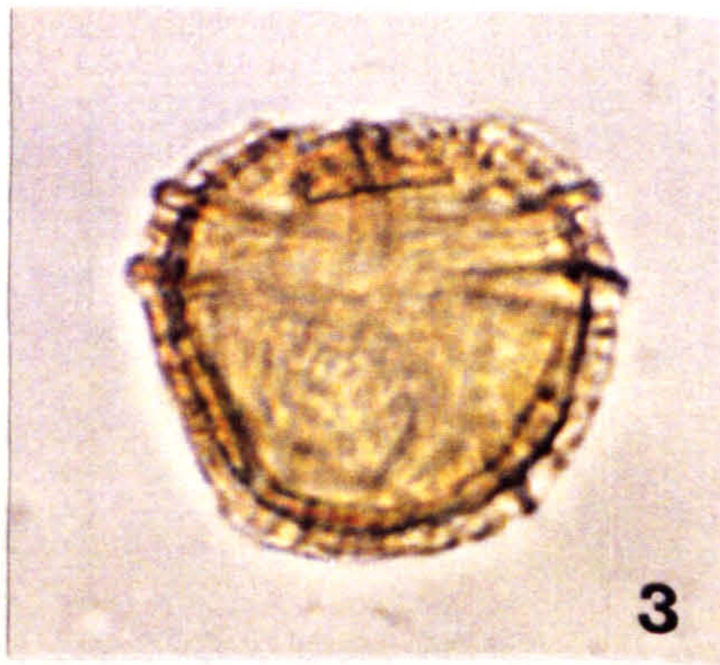
3

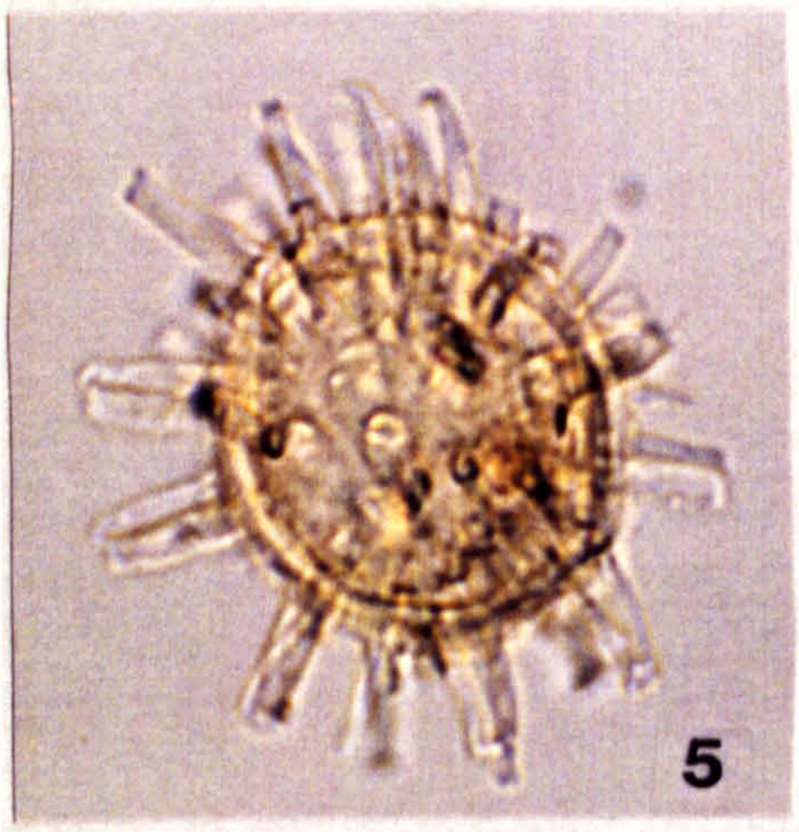
5


7


4

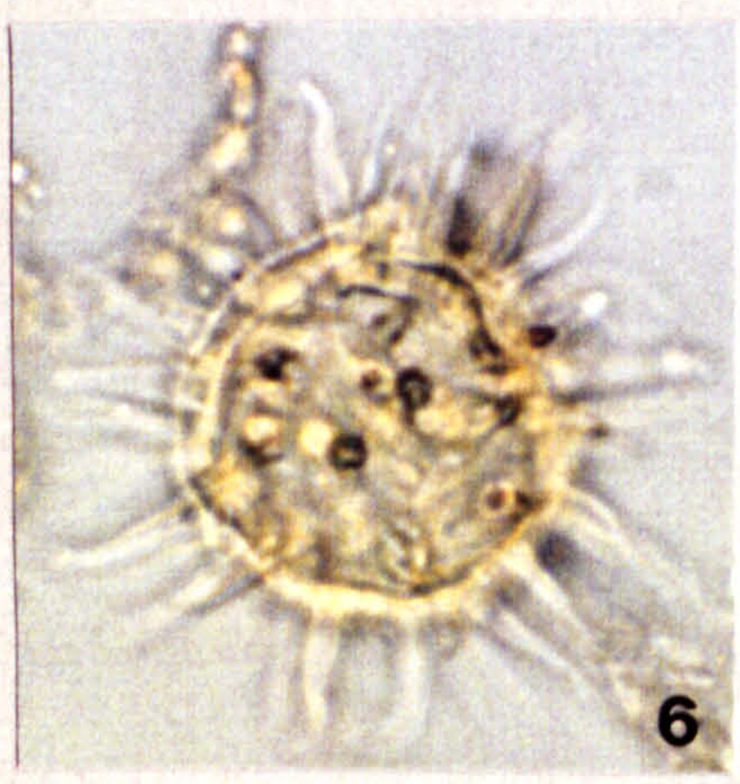
6


8


9

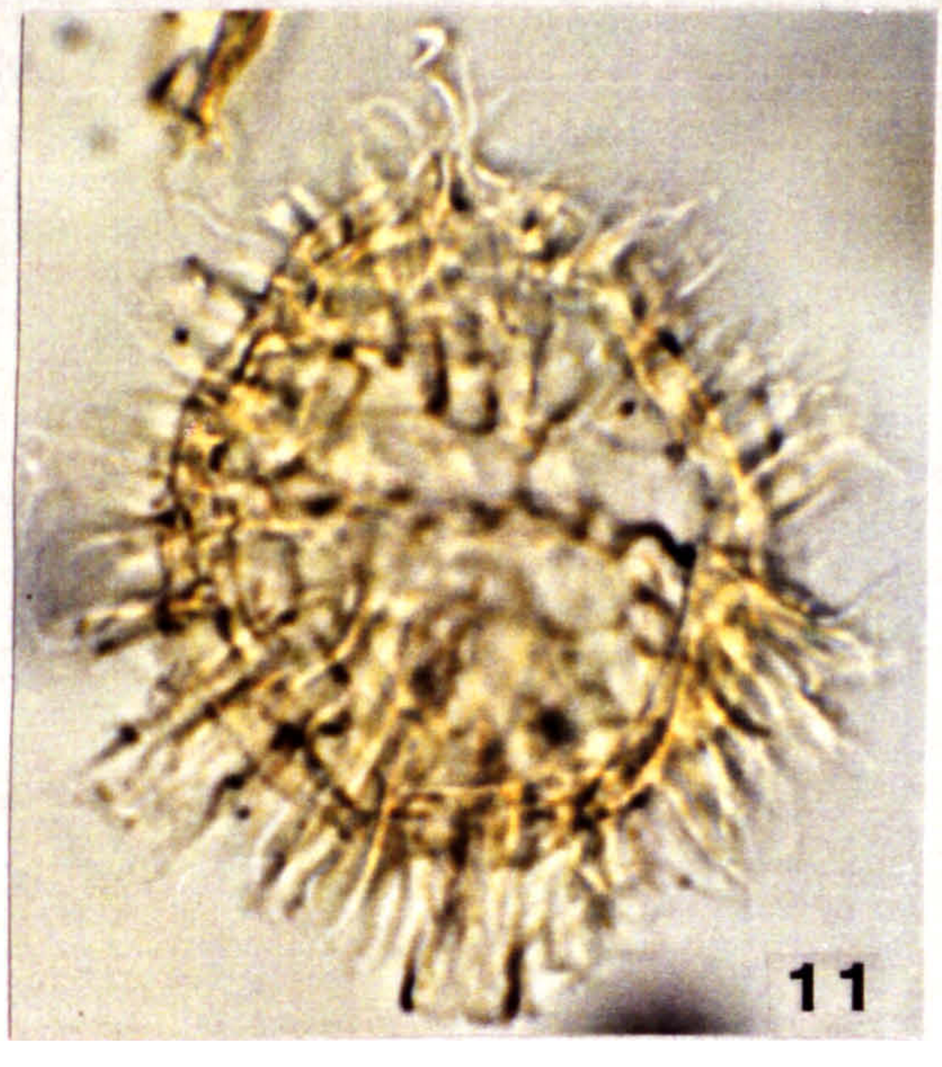
11

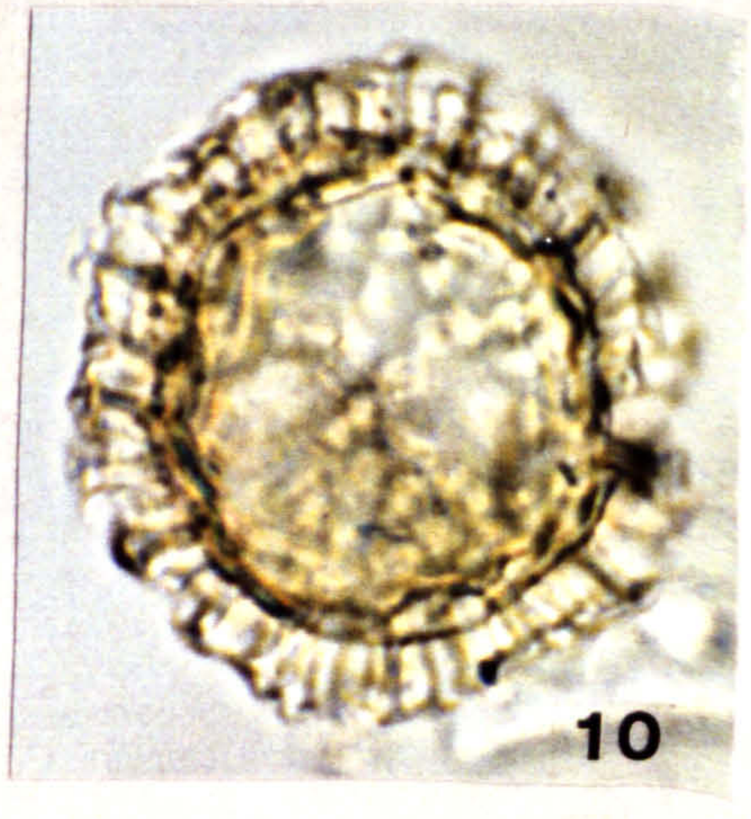
10

Plate 4

All photomicrographs taken at x 675 magnification.

Figs 1-7. *Cribroperidinium cooksoniae* Norvick 1976

Figs 1,2. Site 3A 85 H46/4

1. High focus, ventral view showing hypocystal paratabulation.

2. Low focus, dorsal view of the same specimen showing in place precingular archaeopyle, and double tram-line parasutural markings.

Fig. 3. TBB U32/1

3. Dorsal view showing enlarged precingular archaeopyle.

Figs 4,5. Site 3A 70A1 T46

4. High focus shot showing ventral surface with paratabulation and L-type parasulcal arrangement.

5. Low focus shot of dorsal surface of same specimen.

Figs 6,7. Site 3A 0 L36/4

6. High focus shot of dorsal view with enlarged precingular archaeopyle and large conical apical horn.

7. Low focus, ventral view of same specimen.

PLATE 4


1

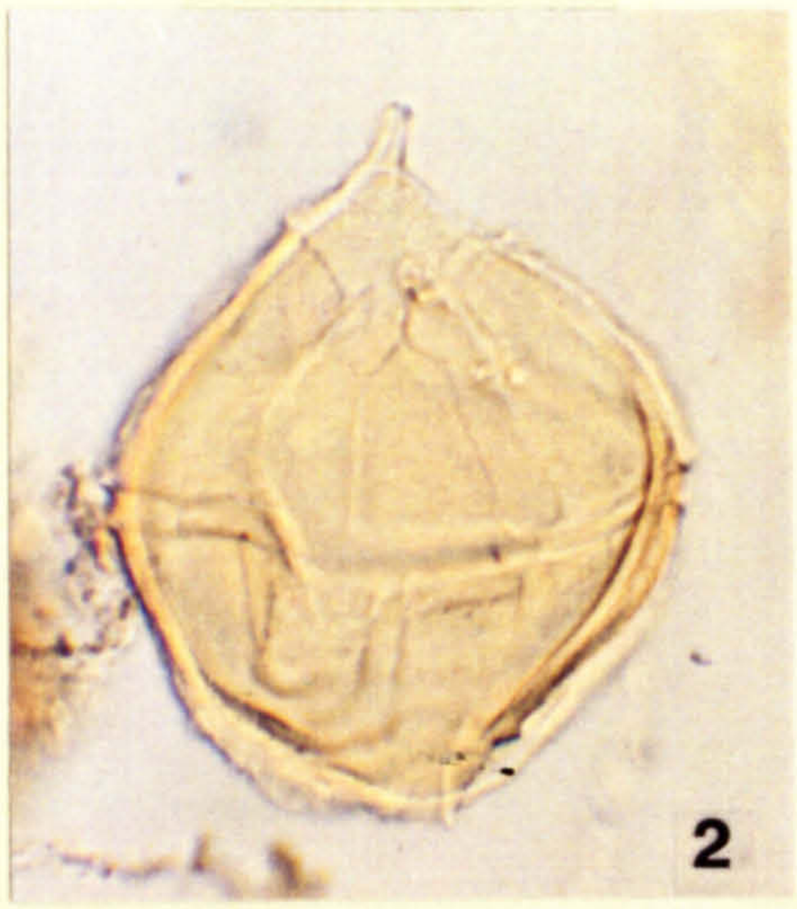
2

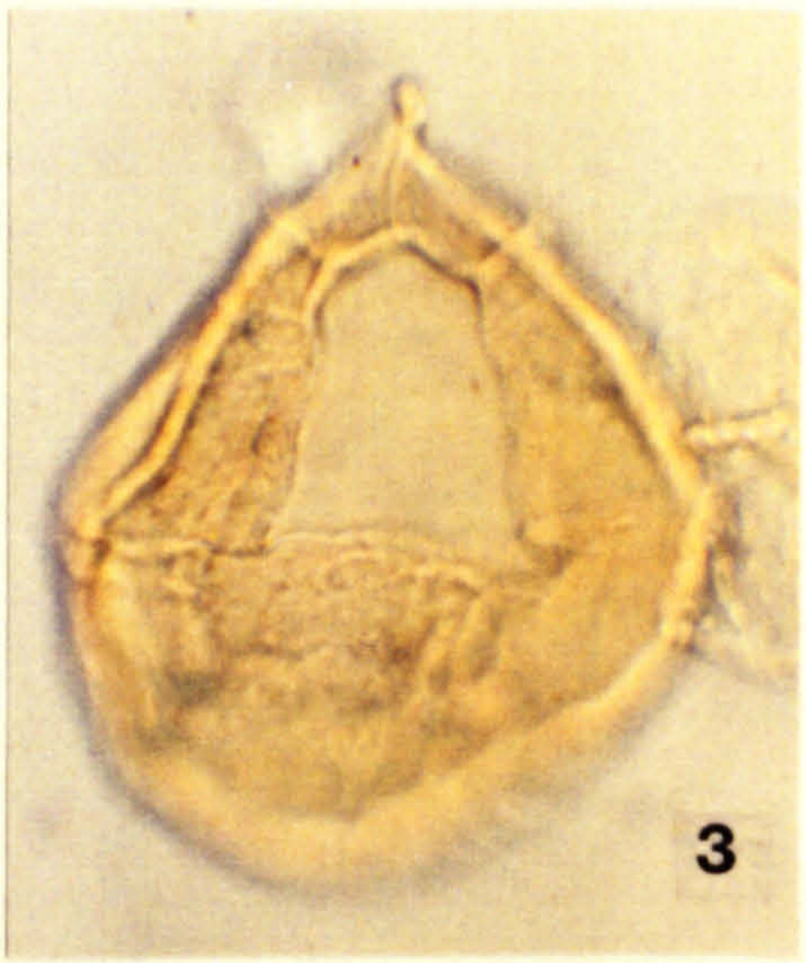
3


4


5

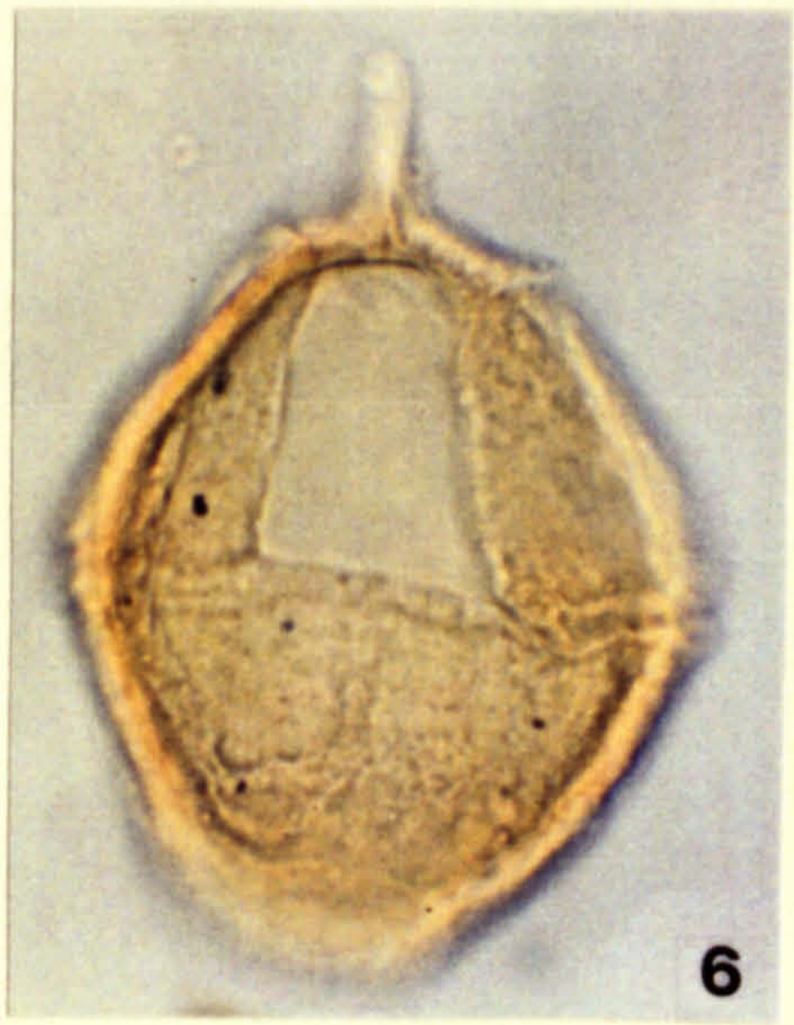
6


7

Plate 5

All photomicrographs taken at x 512 magnification.

Figs 1-6. *Cribroperidinium edwardsii* (Cookson and Eisenack) Davey 1969

Figs 1,2. TBB 2 H37

1. Strongly three-dimensional specimen. High focus, dorsal view showing enlarged Type P archaeopyle and indentation in parasulcal area.

Low focus, oblique dorsal-antapical view of same specimen showing sexiform antapical paraplate (1"").

Figs 3,4. TBB 0 W42

3. High focus, right lateral view showing enlarged precingular archaeopyle.

4. Low focus, left lateral view showing hypocystal paratabulation, especially postcingular paraplates and serrate nature of distal margin of parasutural ridges.

Figs 5,6. TBB 1 U43

5. Low focus, left lateral view showing pointed apical horn.

6. High focus shot of same specimen.

PLATE 5

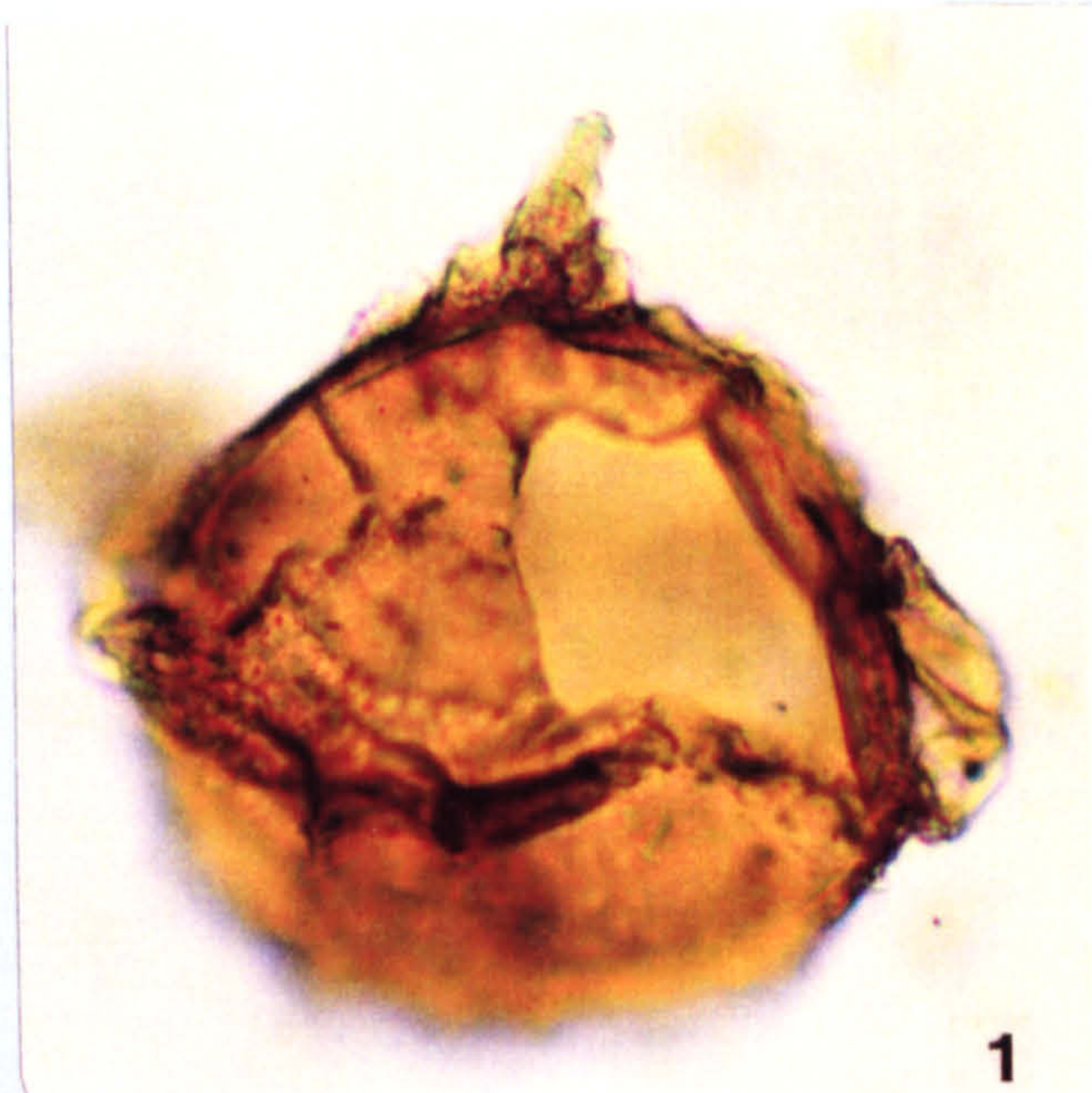
1

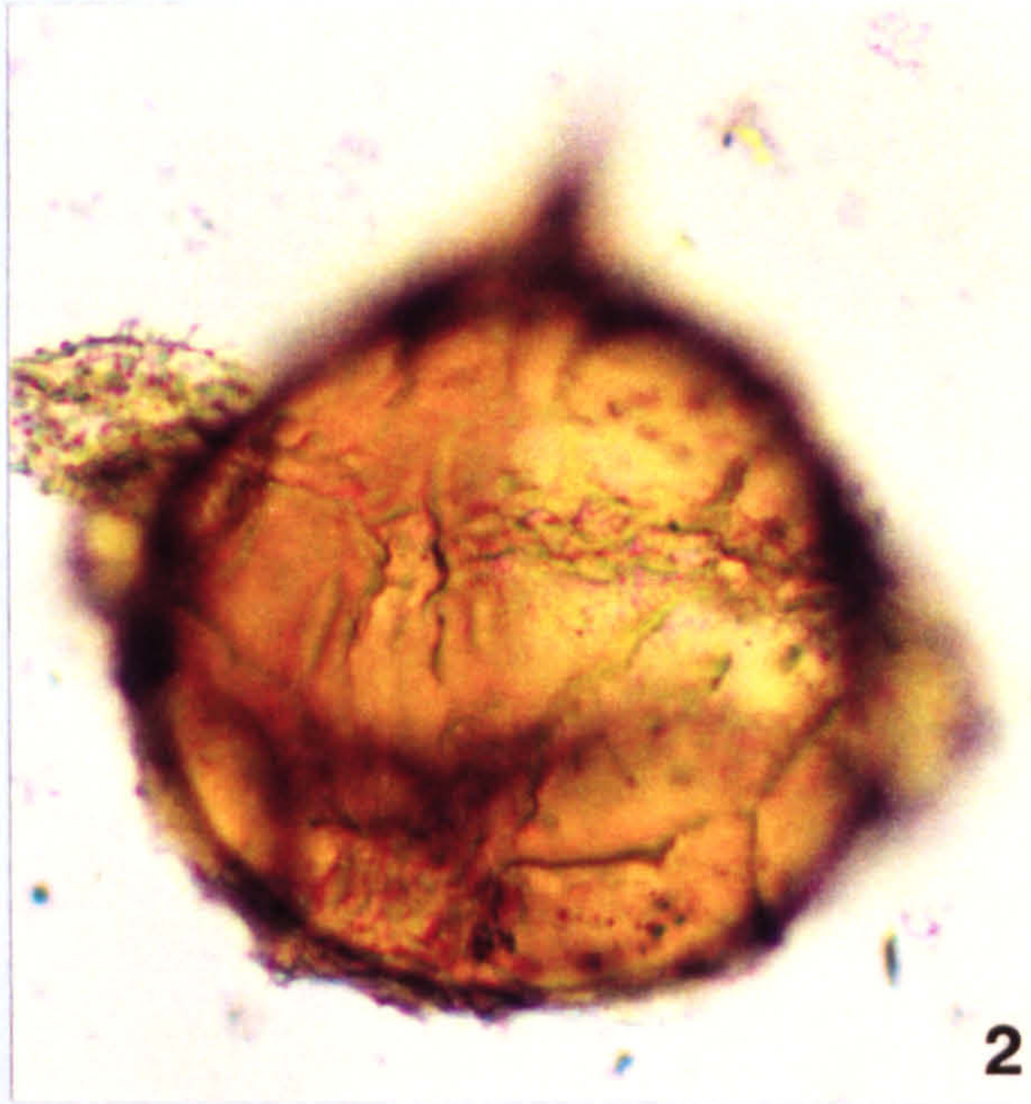
2

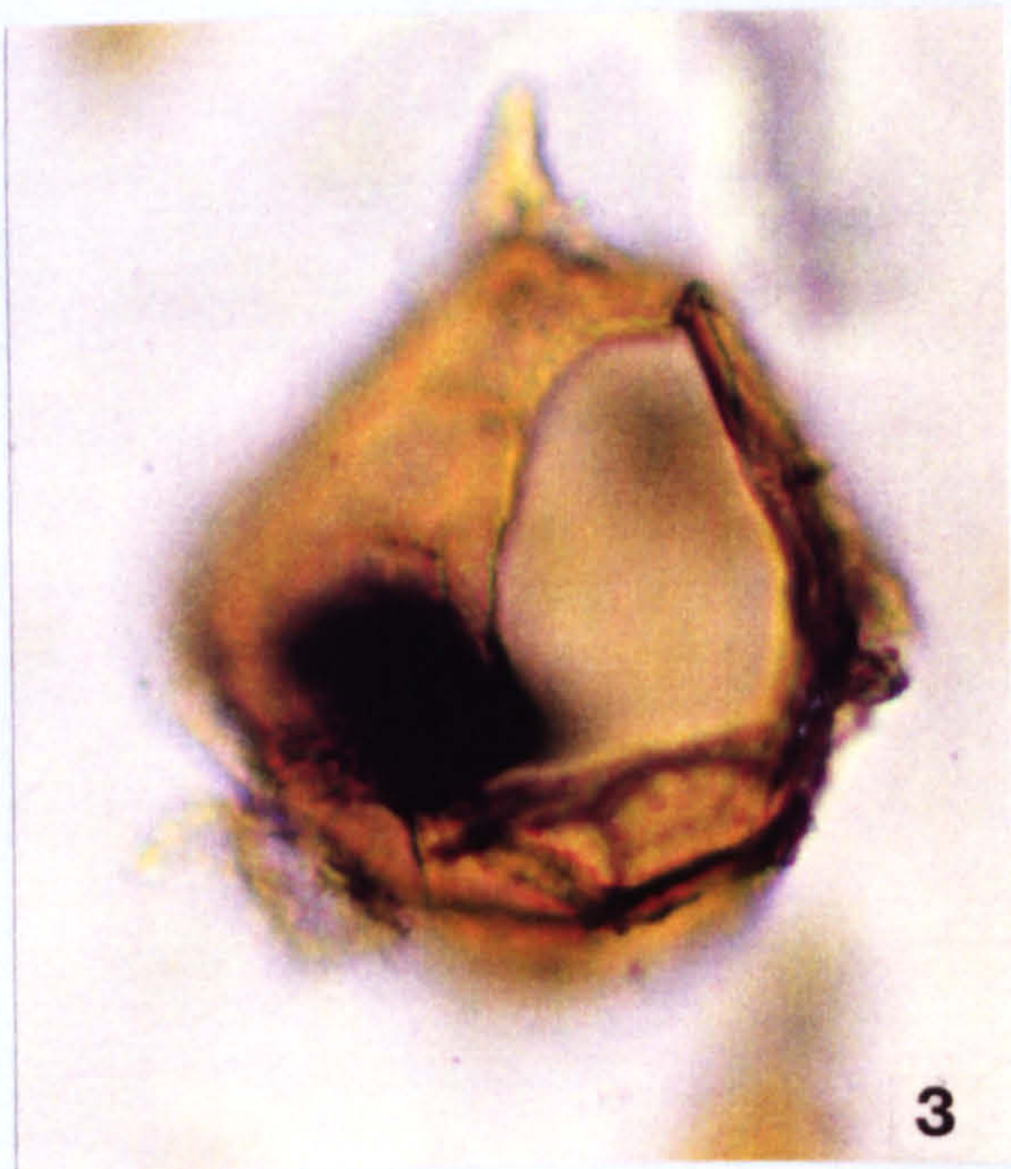
3

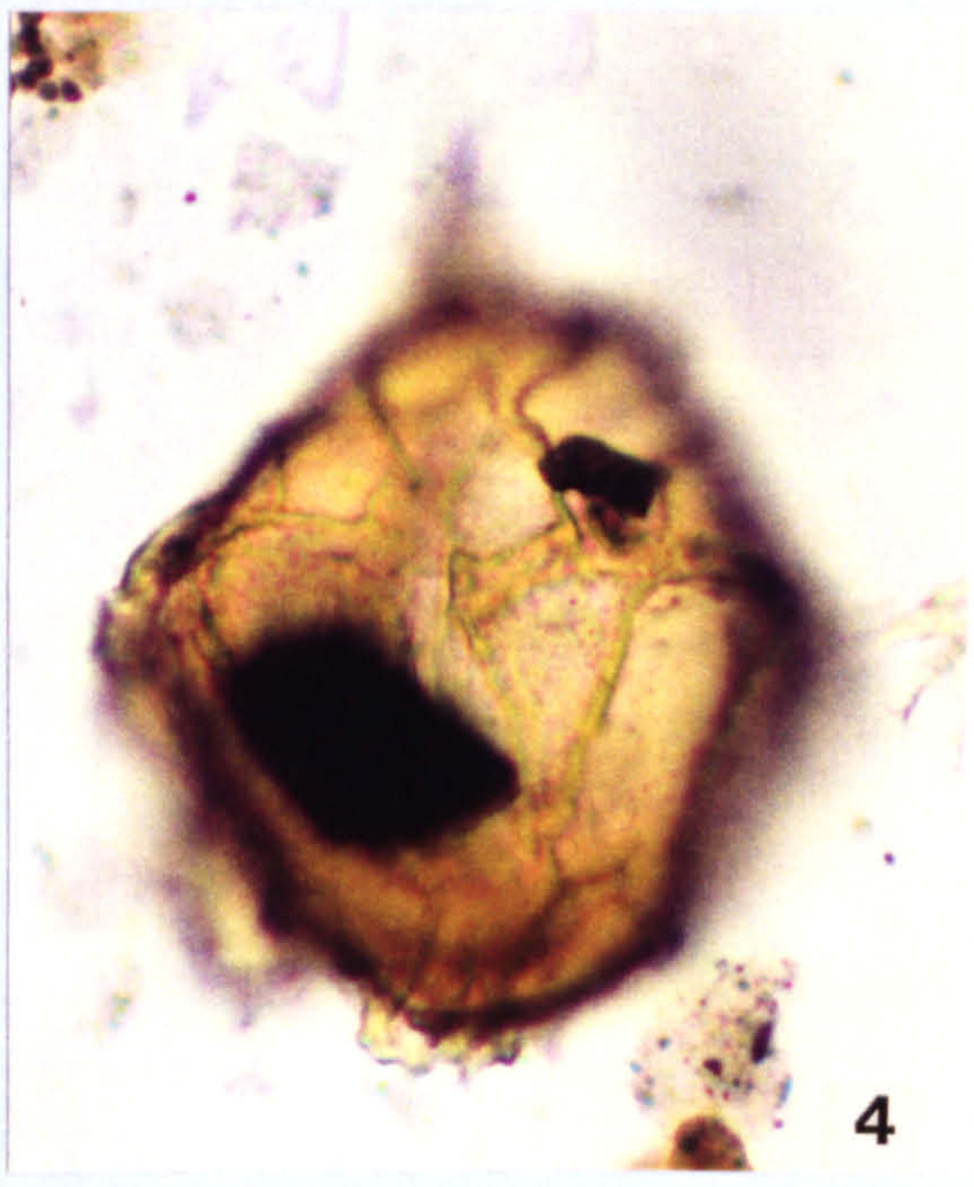
4

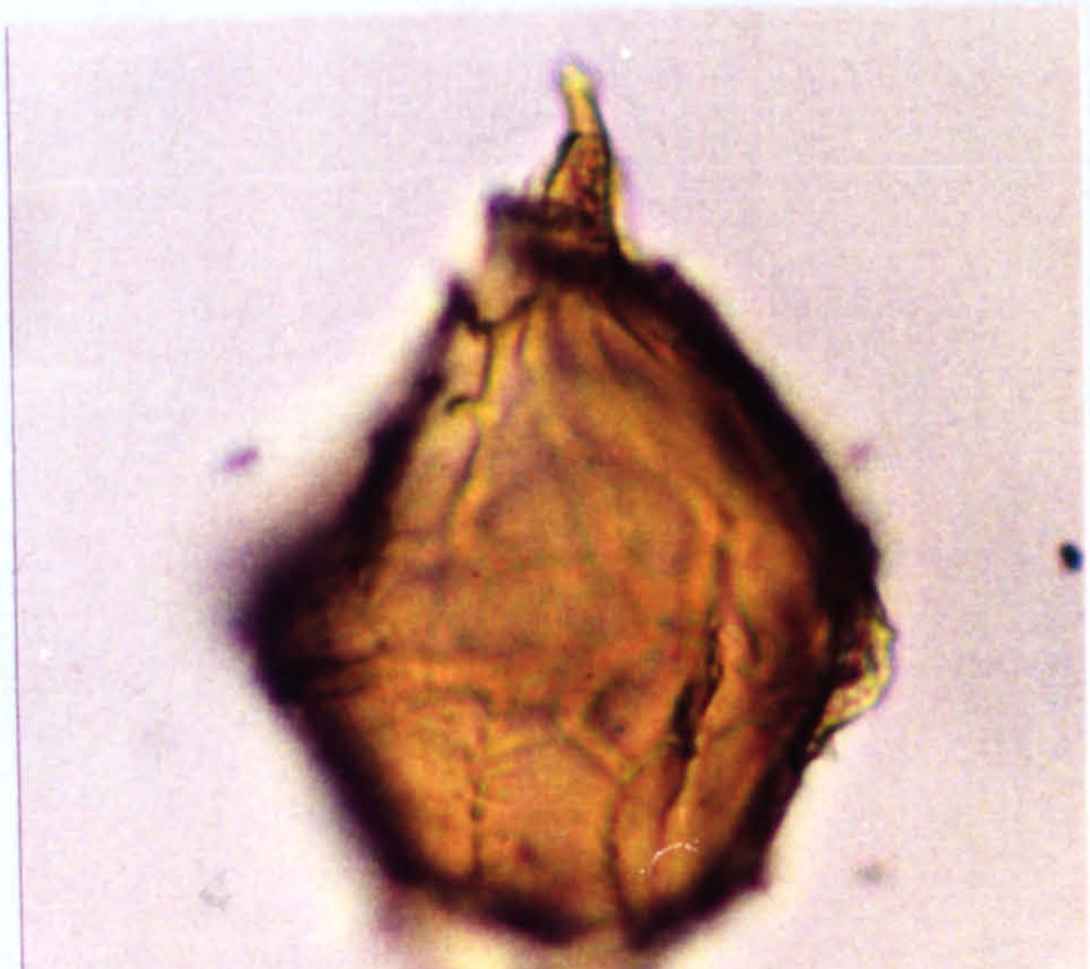

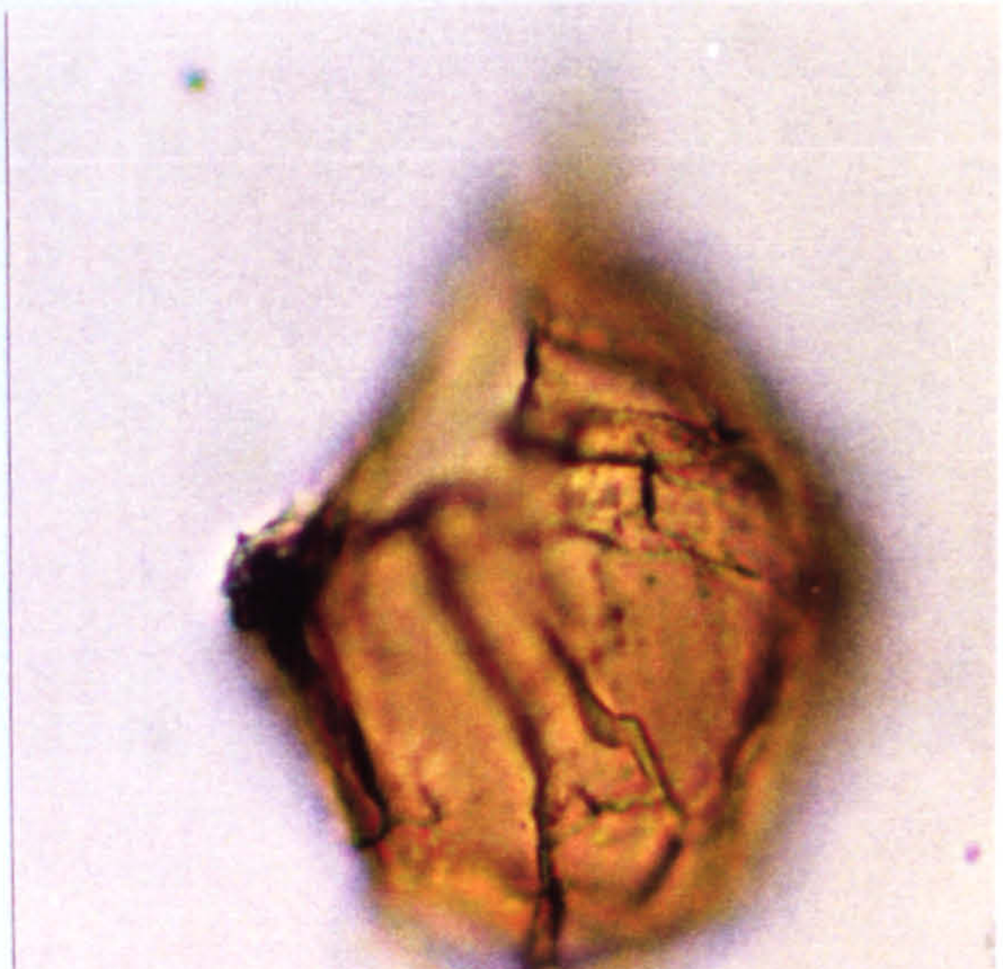

Plate 6

All photomicrographs taken at x 675 magnification.

Fig. 1. *Cyclonephelium distinctum* Deflandre and Cookson 1955

?Dorsal view showing zig-zag apical margin and simple, capitate and buccinate non-tabular processes. Note mid dorsal area is distinctively lacking in processes.

MCB -3.5 --> -4 G30/2

Figs 2-5. *Cyclonephelium membraniphorum* Cookson and Eisenack 1962

Figs 2,3. Site 3A 85 G44/1

2,3. Oblique view, showing box or funnel-shaped membranes which are non-tabular.

2. Low focus shot.

3. High focus shot.

Figs 4,5. Site 3A 85 S23/2

4. Low focus, ventral view showing clear paracingular and parasulcal paratabulation.

5. High focus shot of same specimen showing general morphology.

Figs 6-8. *Cyclonephelium compactum-membraniphorum* complex Marshall and Batten 1988

Fig. 6. SFE 15 K37/1

6. Oblique view, showing very low relief peripheral ornament and apical archaeopyle about to detach.

Fig. 7. SFE 15 K23/2

7. ?Dorsal view, showing moderate relief peripheral membranes similar to *C. compactum.* Also, zig-zag archaeopyle margin present.

Fig. 8. SFE 15 K41/1

8. Very high relief parasutural membranes approaching those exhibited by *C. membraniphorum.*

PLATE 6

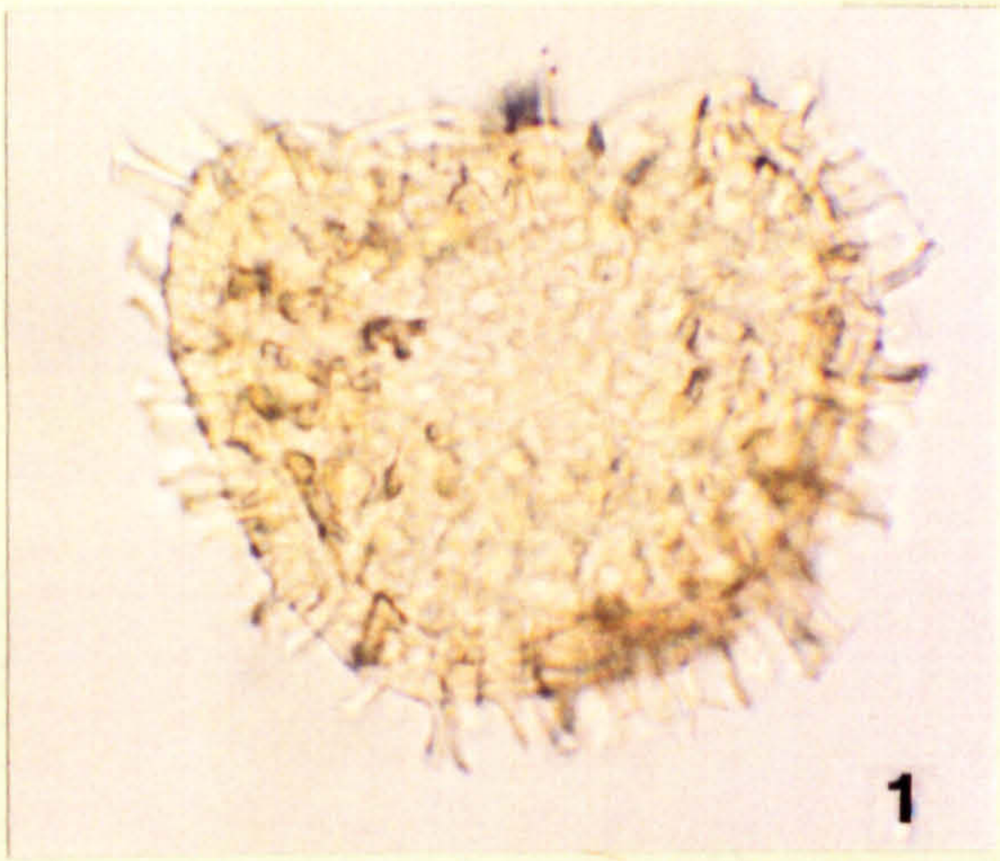
1

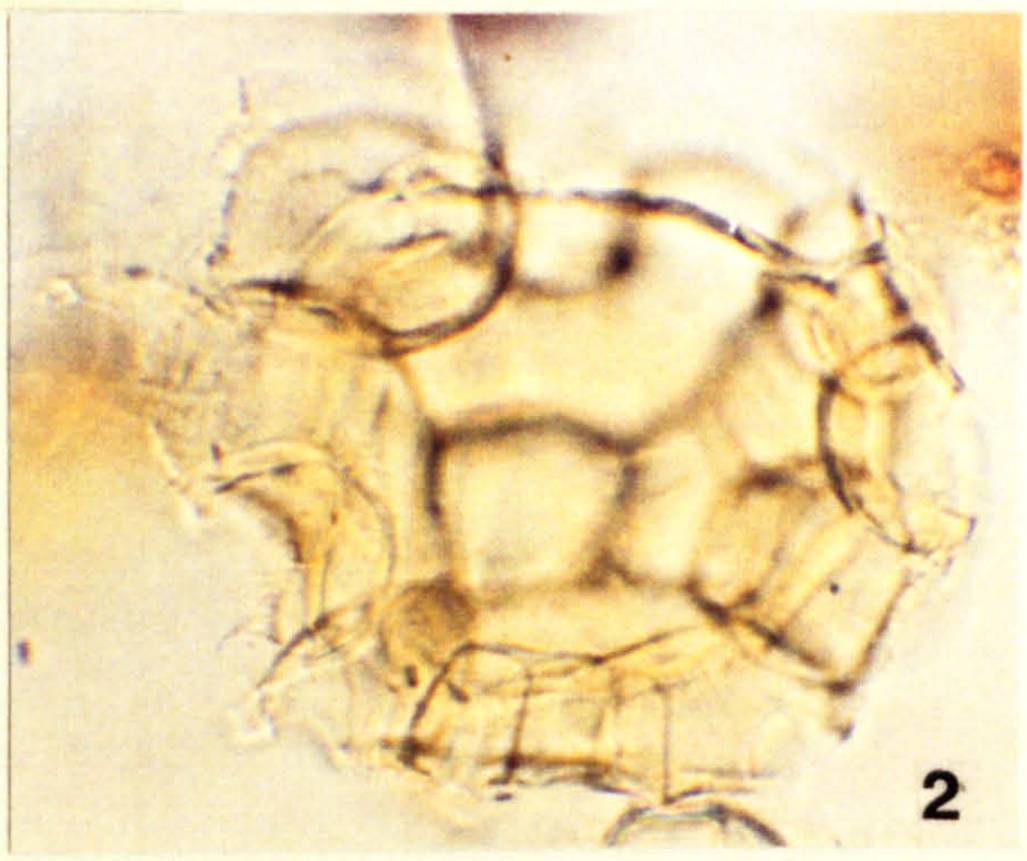
2

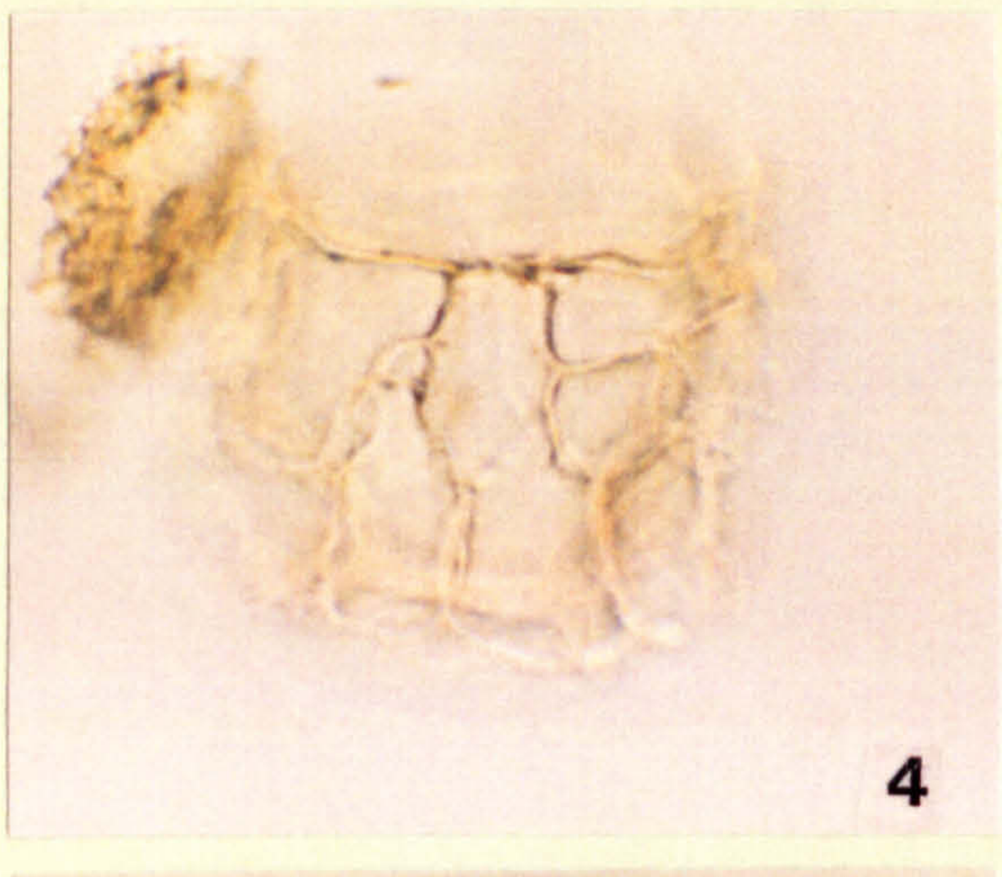
4


3

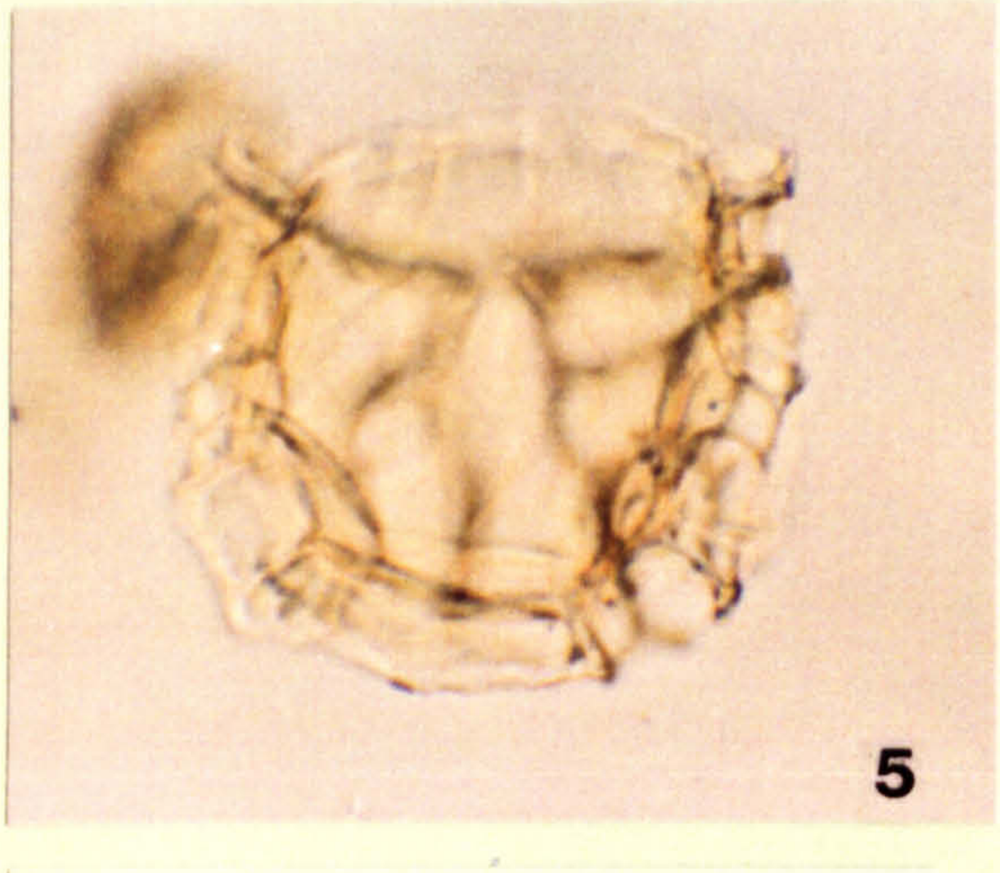
5

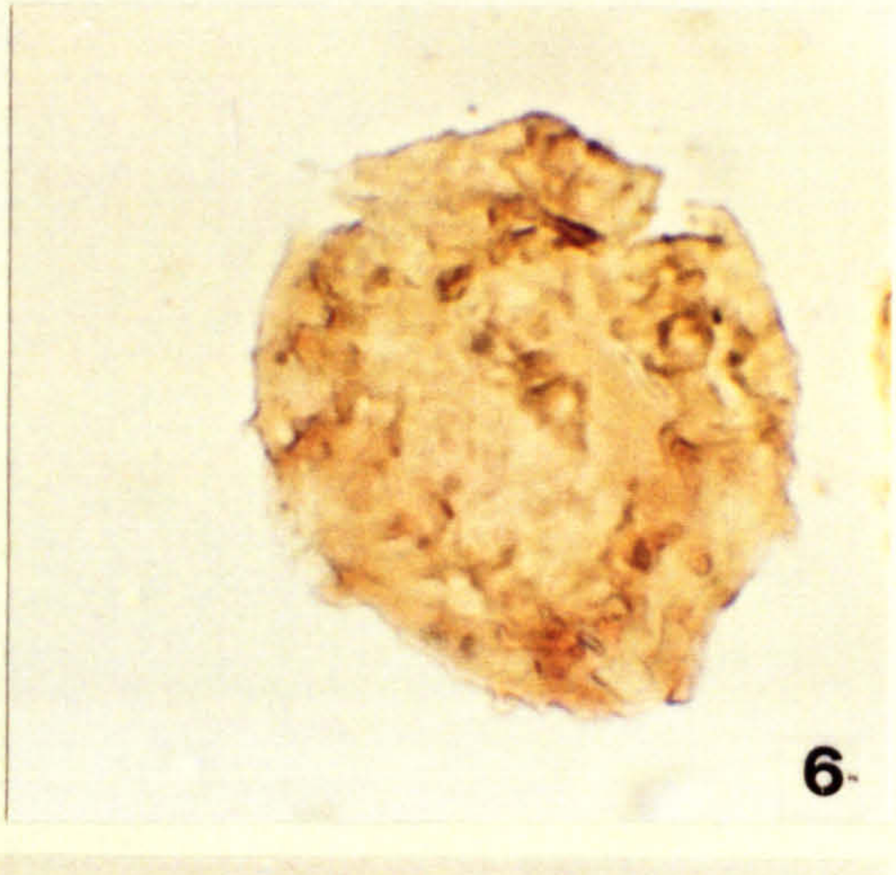
6

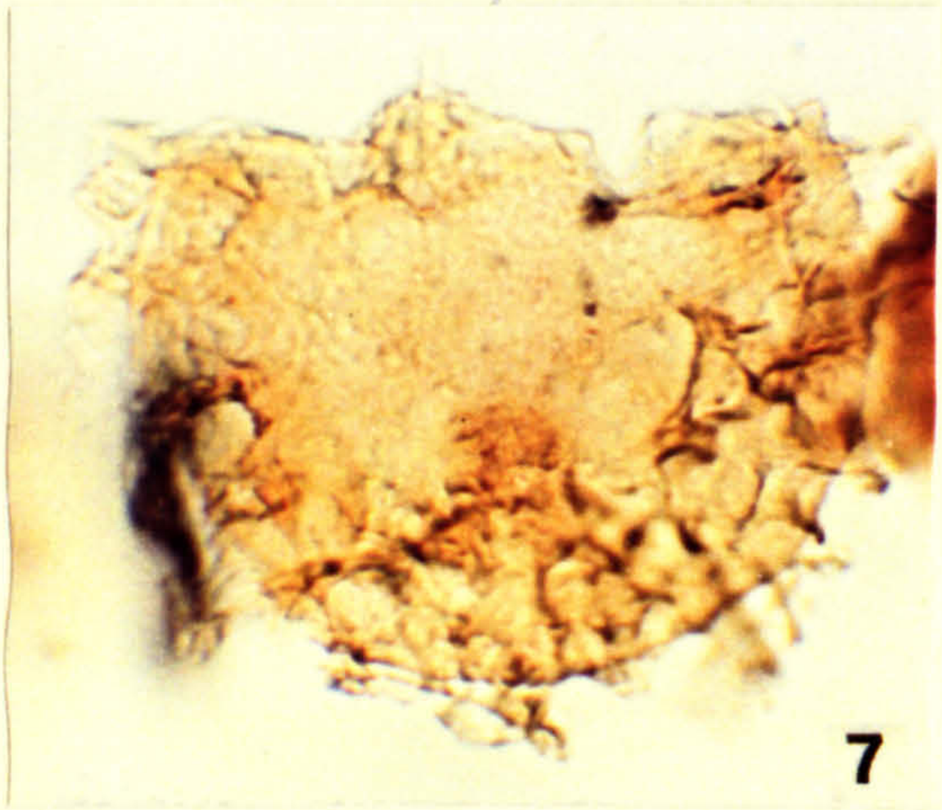
7

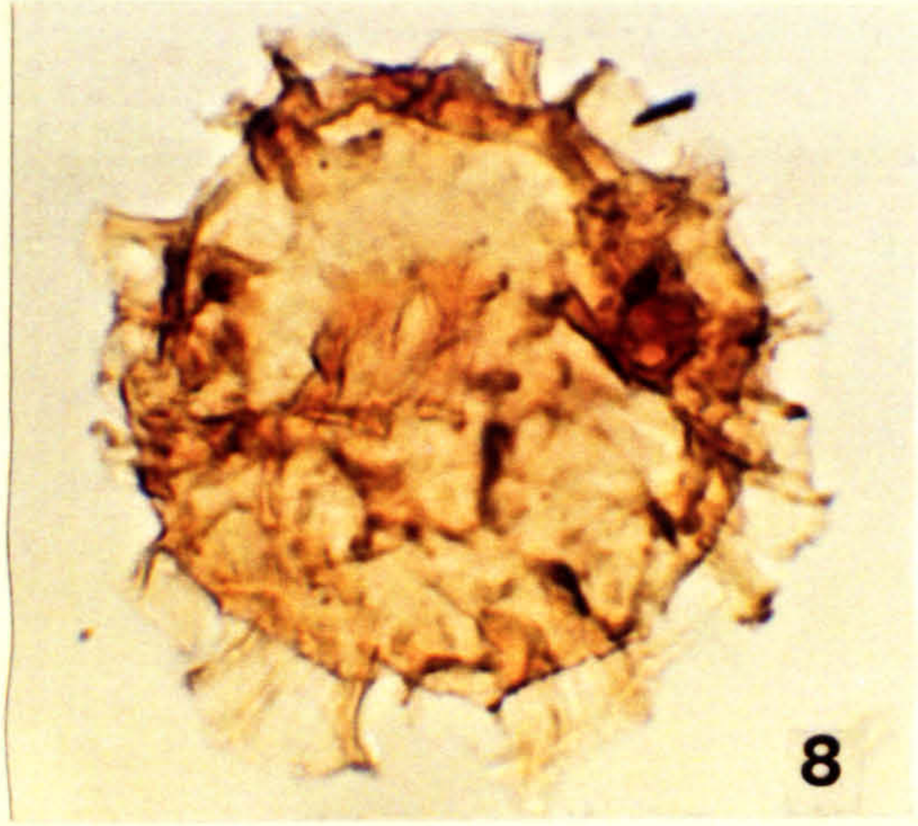
8

Plate 7

Fig. 1. *Dapsilidinium laminaspinosum* (Davey and Williams) Lentin and Williams 1981
Oblique view showing non-tabular hollow parallel-sided processes with flared margins.
MCB -4 --> -4.5 V44/4 x 1025 magnification. DIC

Fig.2. *Dinopterygium cladoides* Deflandre 1935
Oblique view showing elaborate parasutural septa.
Site 3A 0 L26/3 x 675 magnification

Fig. 3. *Dinopterygium medusoides* (Cookson and Eisenack) Stover and Evitt 1978
?Dorsal view showing strongly serrate parasutral septa and robust supporting processes.
TBB -3Paly R34 x 675 magnification

Fig. 4. *Ellipsoidinium rugulosum* Clarke and Verdier 1967
Lateral view, showing longitudinally parasutural ridges.
Site 3A 85 V43 x 1025 magnification

Figs 5,6. *Endoscrinium campanula* (Gocht) Vozzhennikova 1967
Fig. 5. MCB 2.5 --> 3 S35/2 x 675 magnification
Dorsal view showing precingular archaeopyle.
Fig. 6. TBB 12 M31 x 675 magnification
Right lateral view showing antapical pylome.

Figs 7,8. *Epelidosphaeridia spinosa* (Cookson and Hughes) Davey 1969
Fig. 7. MCB 5 --> 5.5 L34 x 1025 magnification
Dorsal surface with apical archaeopyle intact.
Fig. 8. MCB -3.5 --> -3 O33/2 x 1025 magnification.
Ventral surface showing paracingular and parasulcal areas, note left hypocystal projection.

PLATE 7

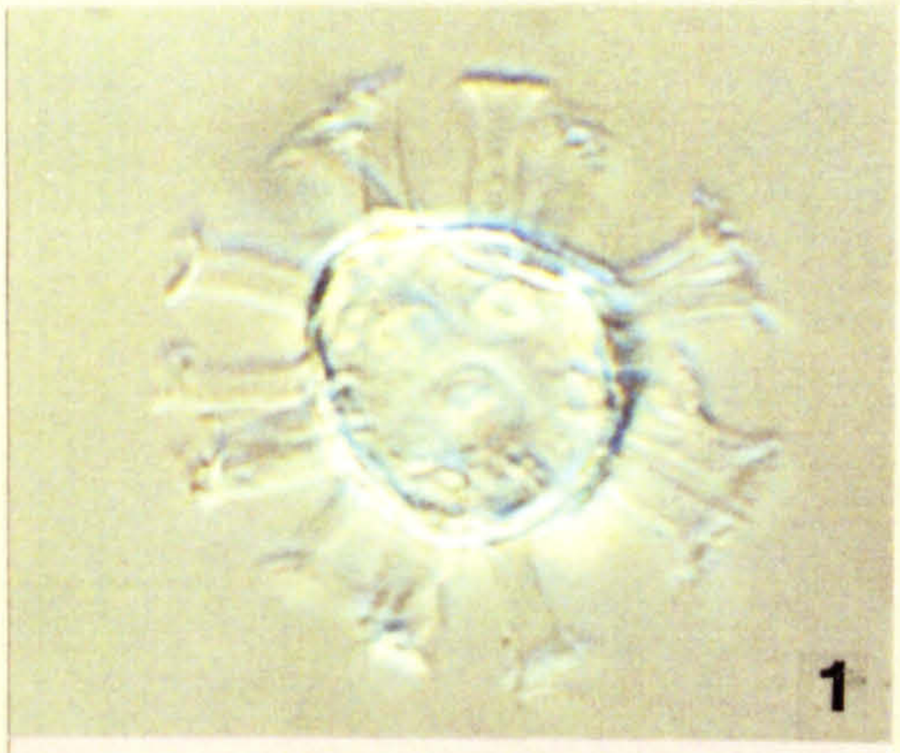
1


2

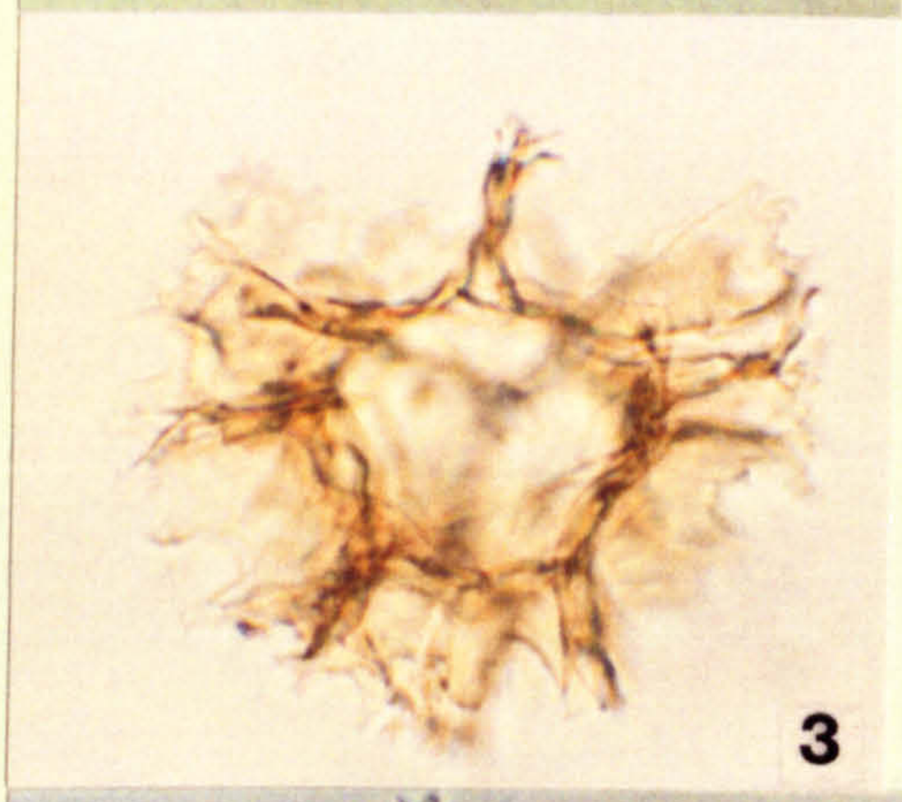
3

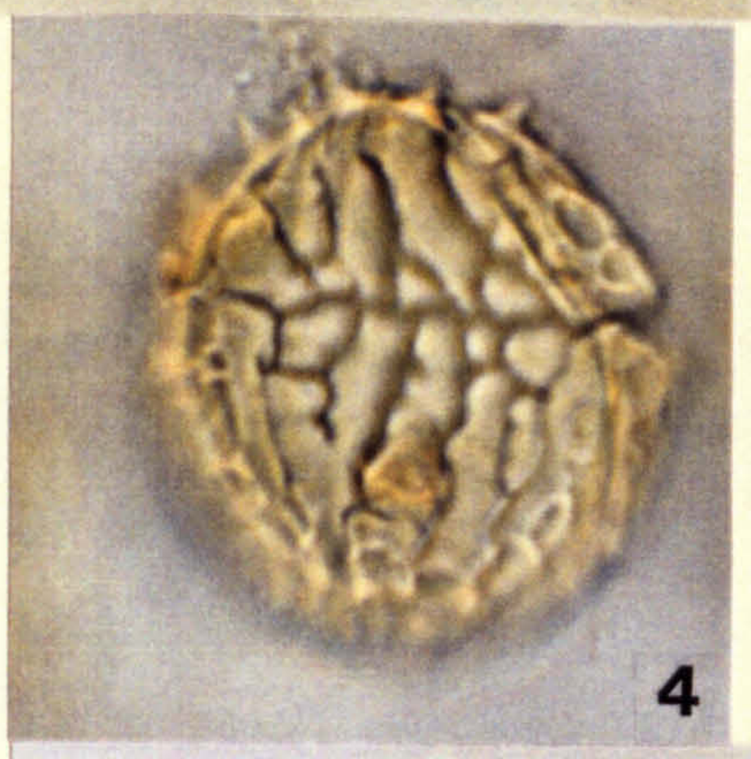
4

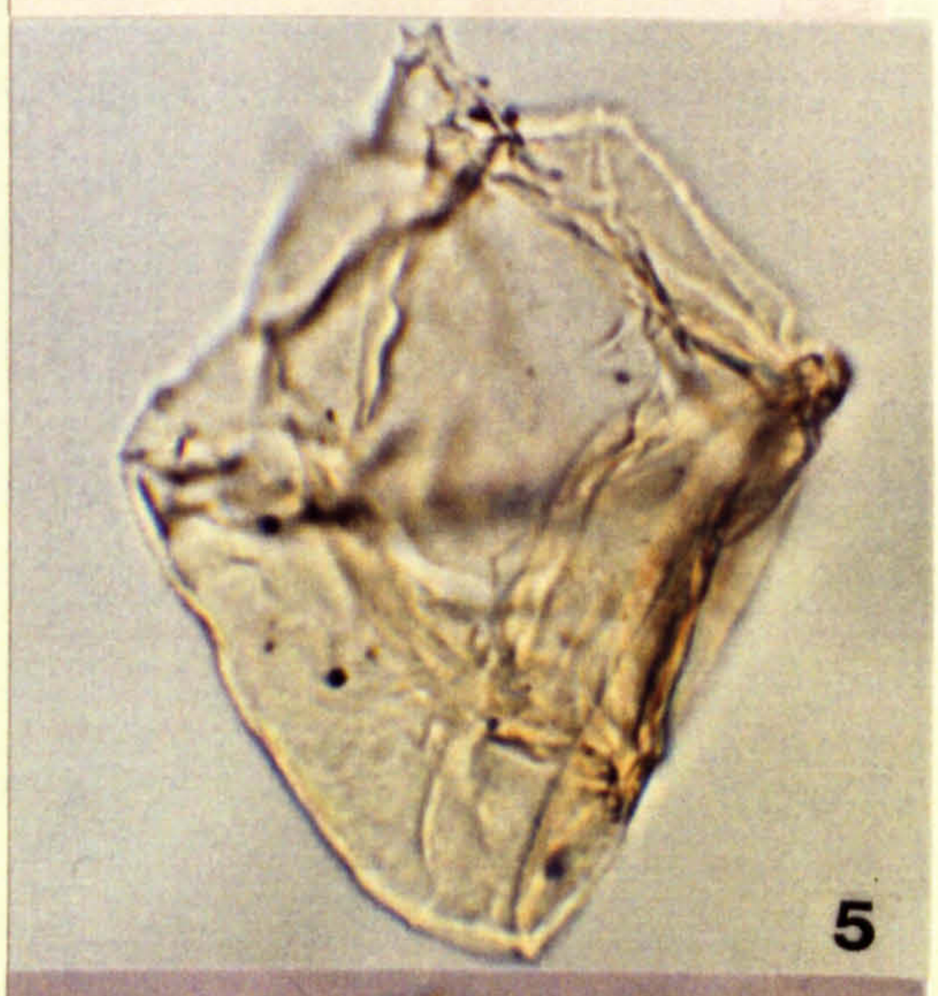
5

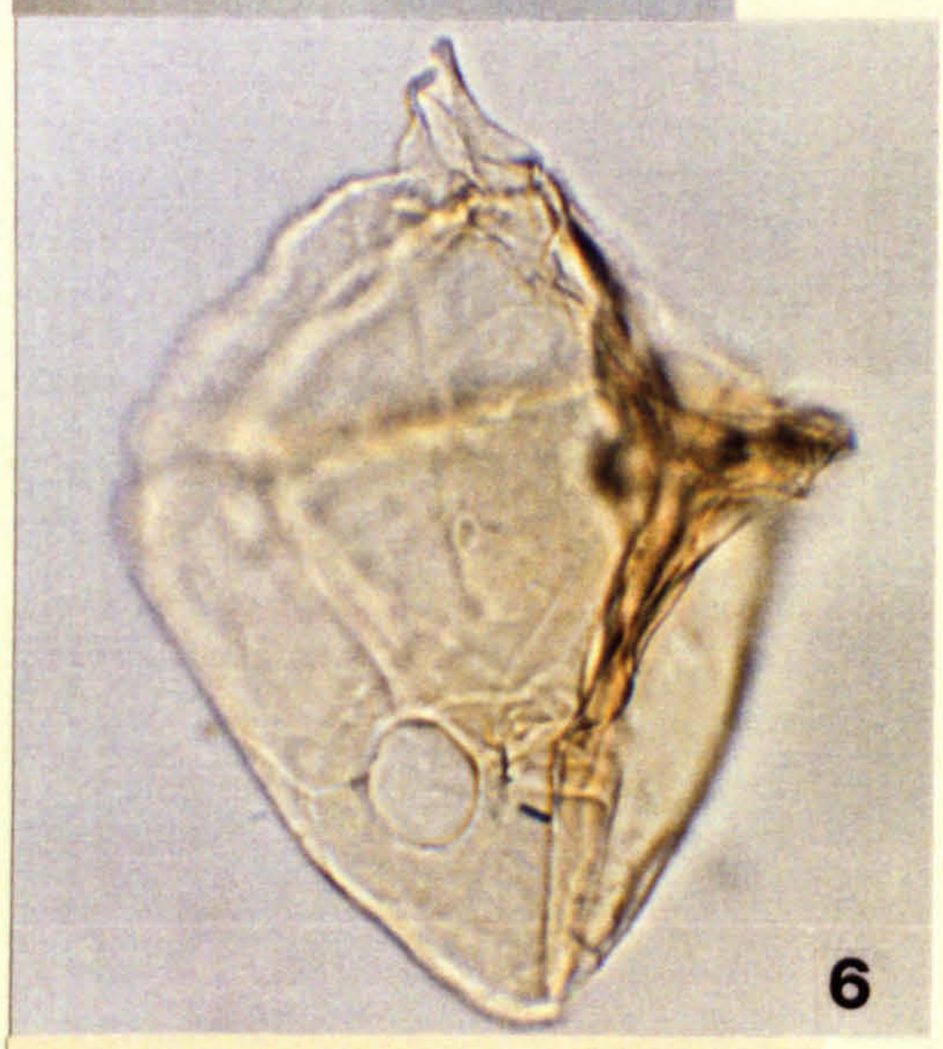
6

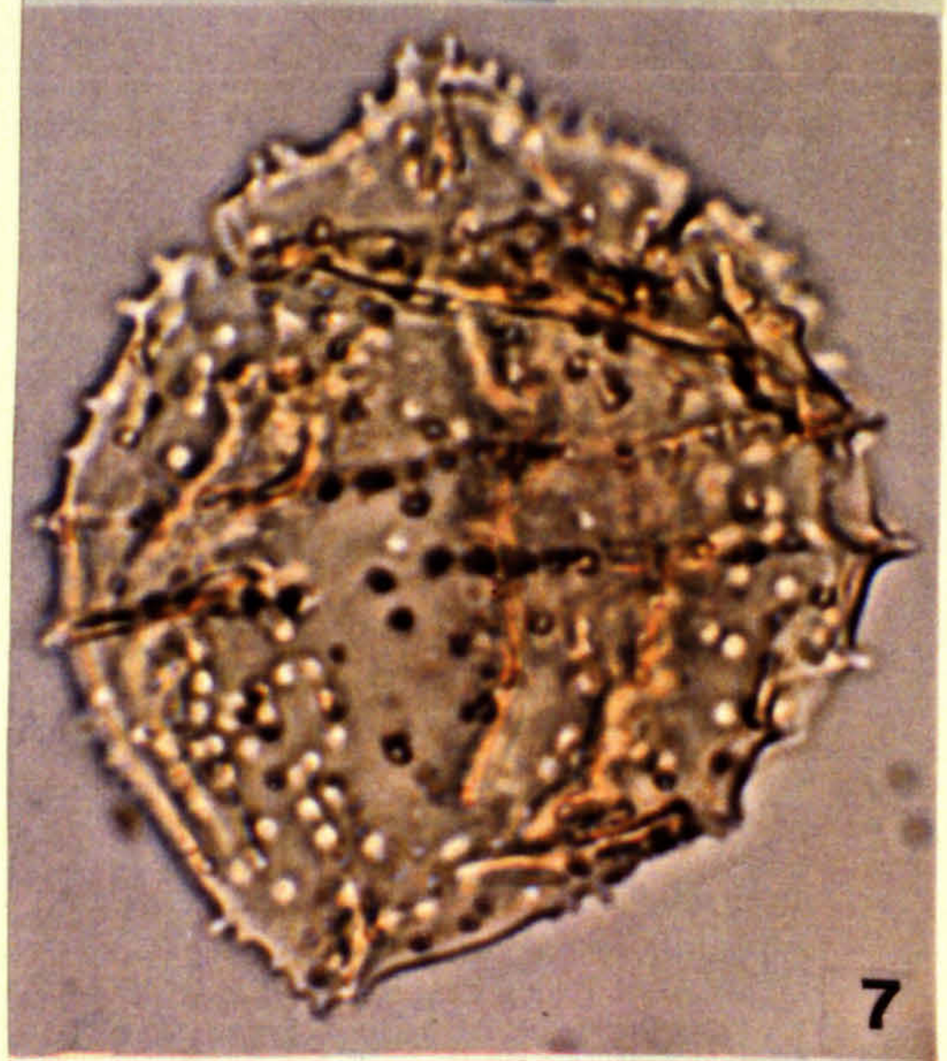
7

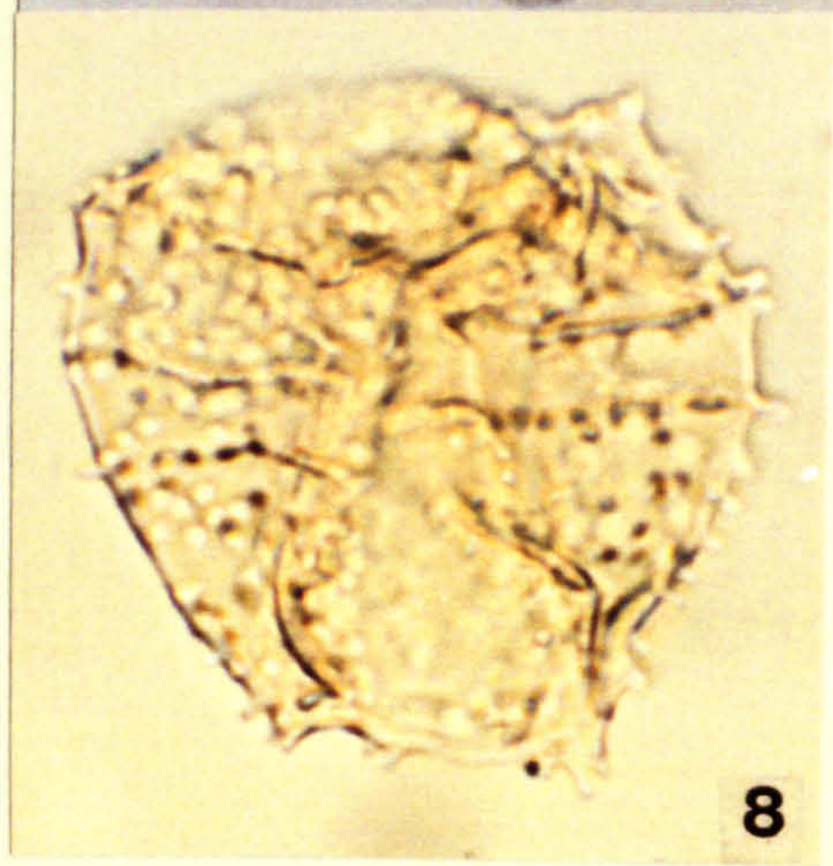
8

Plate 8

All photomicrographs taken at x 1025 magnification.

Figs 1,2. *Eurydinium saxoniense* Marshall and Batten 1988

Fig. 1. SFE 15 Q40

Oblique dorsal view with intercalary archaeopyle just detaching.

Fig. 2. SFE 15 Q43

Dorsal surface with intercalary archaeopyle still intact

Figs 3,4. *Exochosphaeridium* cf. *arnace*

Figs 3,4. Site 3A 85 L51

3. Apical view showing archaeopyle.

4. Shows dense delicate process morphology of same specimen.

Fig. 5. *Exochosphaeridium bifidum* (Clarke and Verdier) Clarke *et al.* 1968

Oblique view showing long, solid non-tabular processes. TBB -30x V31/3

Fig. 6. *Exochosphaeridium phragmites Davey et al.* 1966

Dorsal view with Type P archaeopyle.

Site 3A 85 E23/4

PLATE 8

1

2

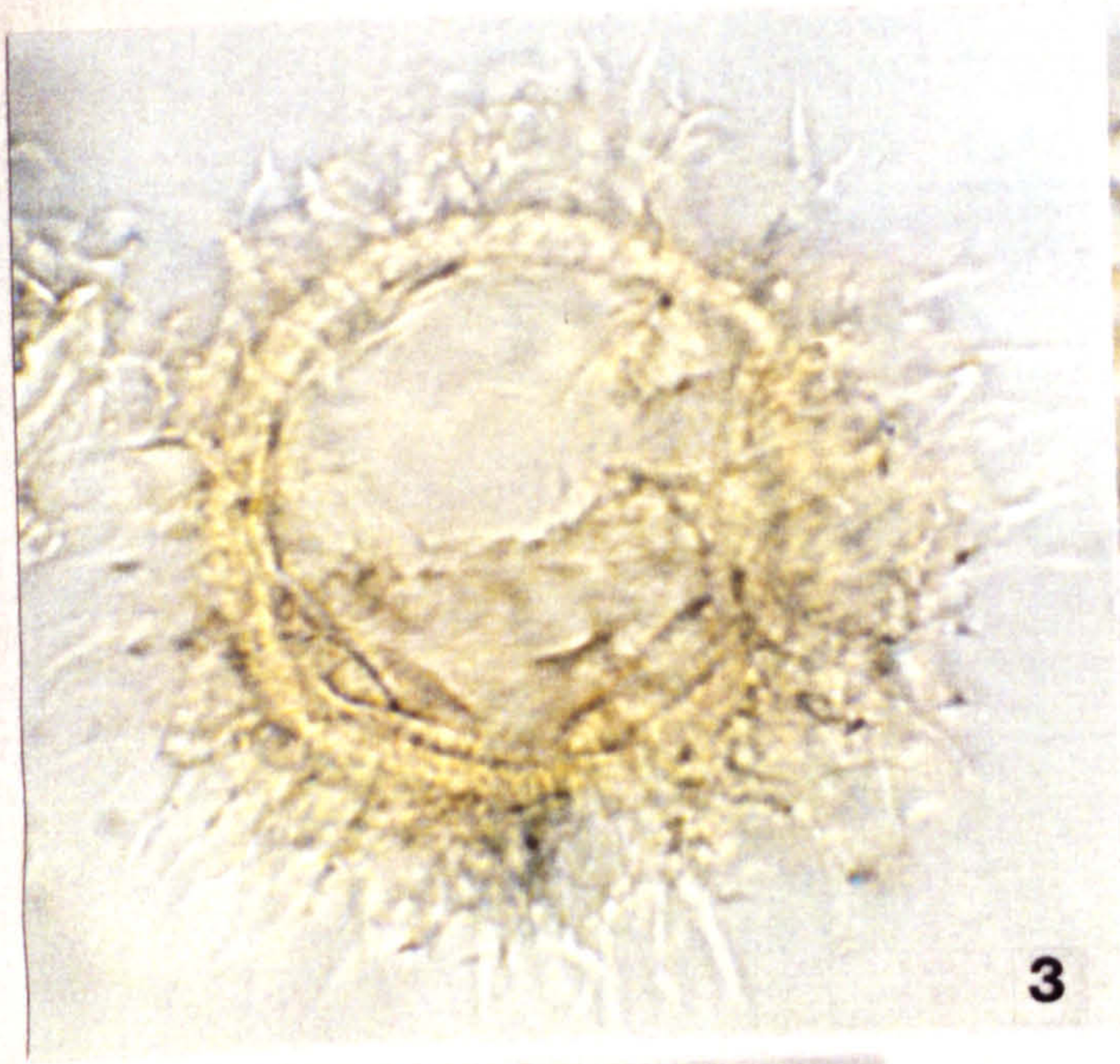

3

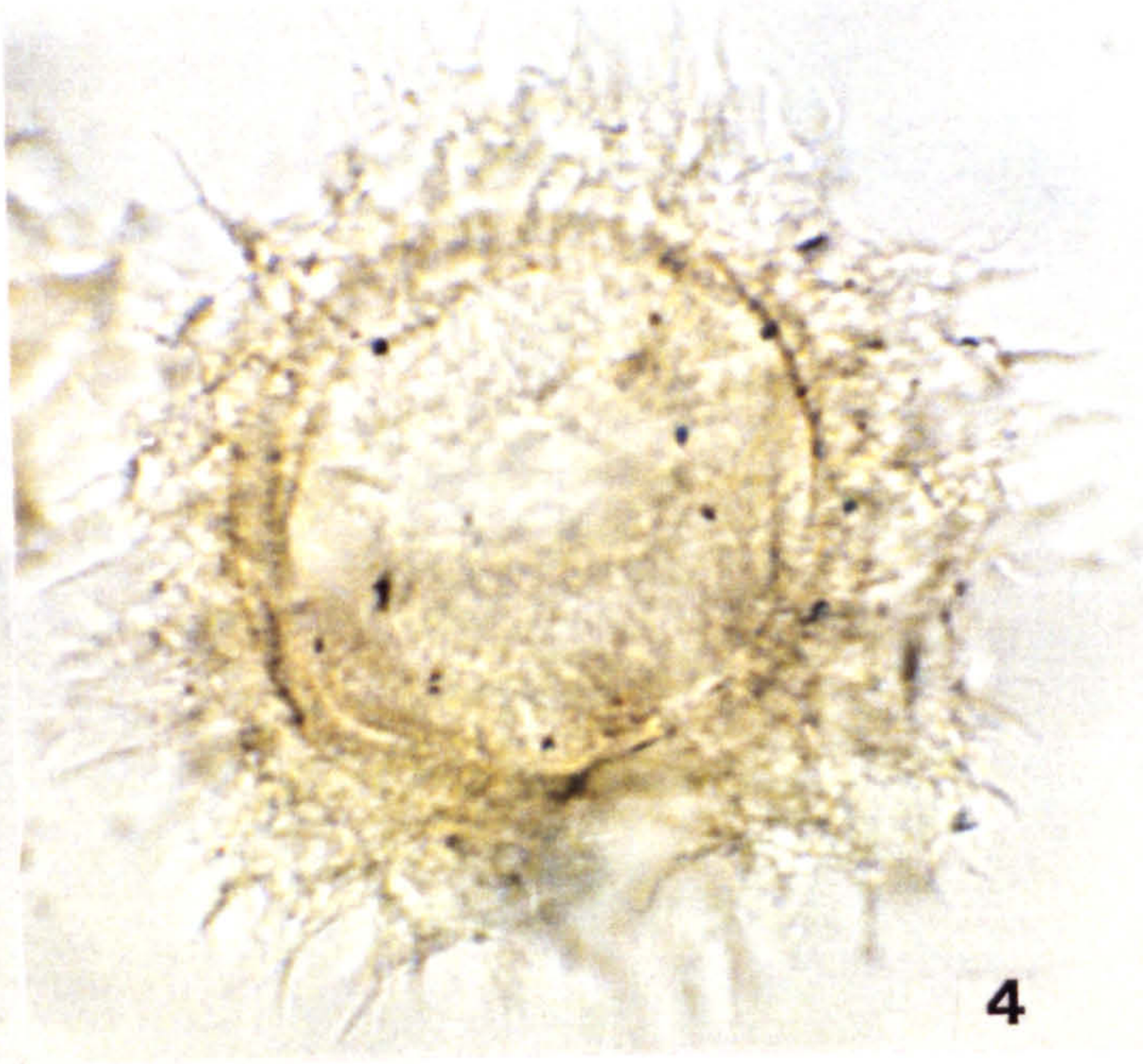

4

5

6

Plate 9

All photomicrographs taken at x 675 magnification, unless otherwise stated.

Fig. 1. *Florentinia deanei* (Davey and Williams) Davey and Verdier 1973
Dorso-ventral compressional preservation, showing diagnostic large antapical process.
Site 3A 0 J26

Fig. 2. *Florentinia ferox* (Deflandre) Duxbury 1980
Oblique apical view, showing compound, medianly bifurcate precingular processes.
Site 3A 0 J21/4 x 1025 magnification

Fig. 3. *Florentinia laciniata* Davey and Verdier 1973
Dorso-ventral orientation, showing large compound precingular and postcingualr, simple paracingular and parasulcal processes, and long sub-conical open antapical process.
MCB 1.5 --> 2 N41/1

Fig. 4. *Florentinia mantellii* (Davey and Williams) Davey and Verdier 1973
Oblique dorso-venmtal orientation, showing varied process morphology and large tapering antapical process.
Site 3A 0 X24/3

Fig. 5. *Florentinia resex* Davey and Verdier 1976
Oblique view showing variable process morphology.
Site 3A 85 M20/4

Fig. 6. *Fromea amphora* Cookson and Eisenack 1958
Arcuate transverse folds are common. (Note: cyst is orientated apex-antapex, right to left)
MCB 2 --> 2.5 Q24/2

PLATE 9

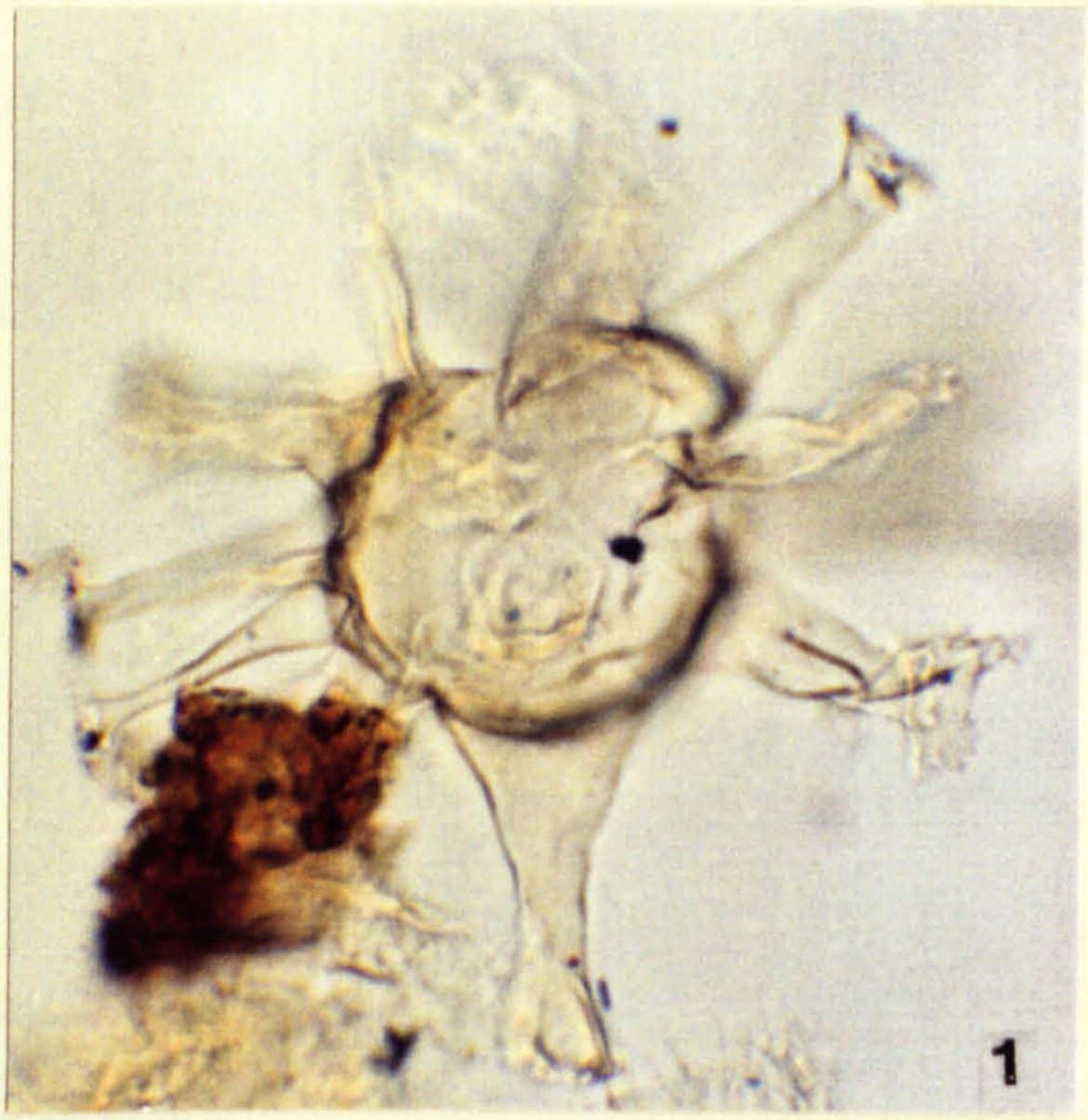
1


2

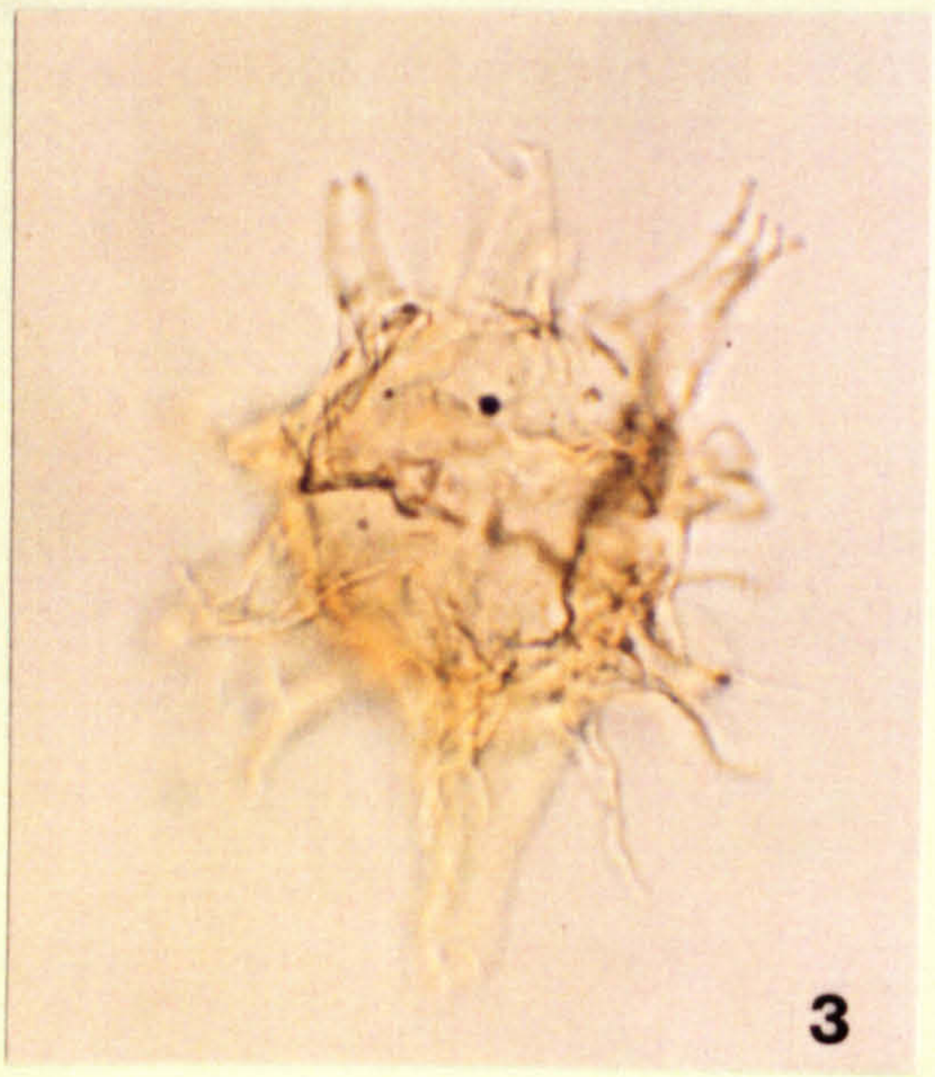
3

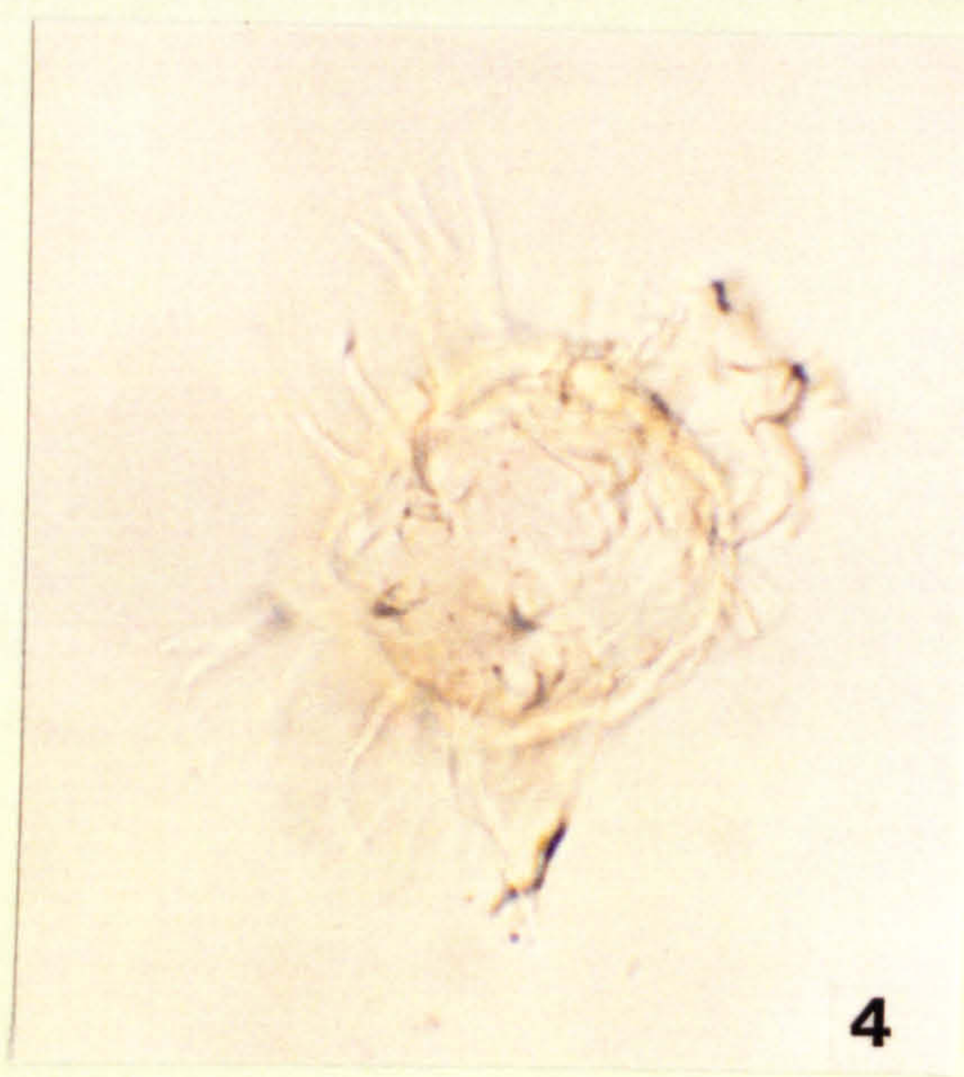
4

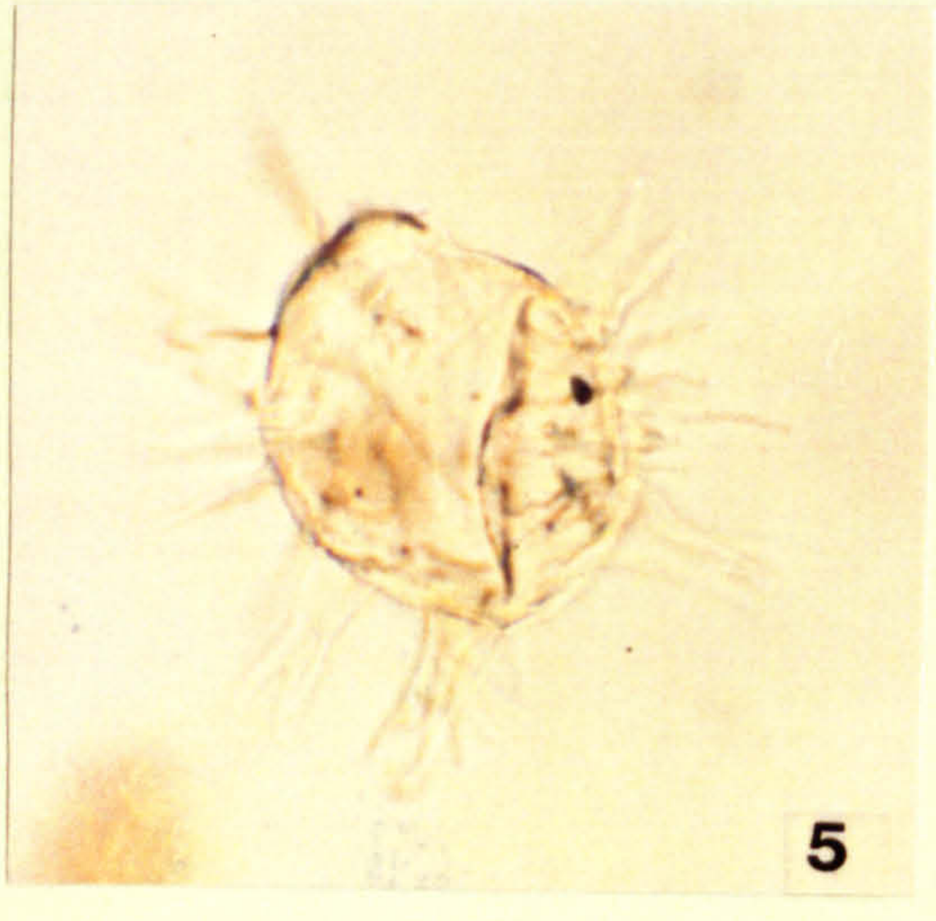
5

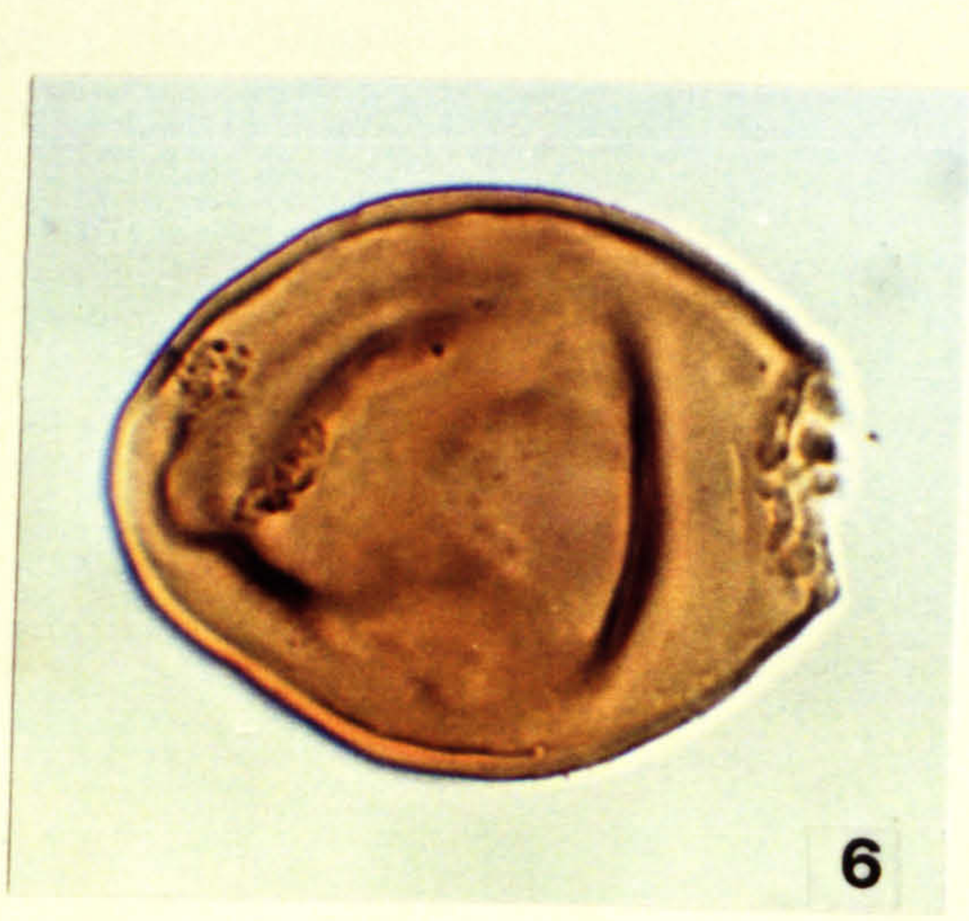
6

Plate 10

All photomicrographs taken at x 675 magnification, unless otherwise stated.

Fig. 1,2. *Gonyaulacysta cassidata* (Eisenack and Cookson) Sarjeant 1966
Figs 1,2. TBB -2 D28
1. Low focus, ventral view showing that epicyst is larger and more pointed (due to apical horn) than rounded hypocyst.
2. High focus, dorsal surface of same specimen showing Type P archaeopyle and machicolate margin of parasutural crest.

Figs 3,4. *Gonyaulacysta whitei* Sarjeant 1966
Figs 3,4. Site 3A 85 W42/3 x 1025 magnification
3. Low focus shot, showing general morphology and apical horn.
4. High focus, ventral view of same specimen showing S-Type parasulcal-paracingular arrangement.

Fig. 5. *Hystrichodinium pulchrum* Deflandre 1935
Dorsal view, showing Type P archaeopyle, paracingulum and long, distally recurved, non-tabular processes.
MCB 4.5 --> 5 N22

Fig. 6. *Hystrichosphaeridium bowerbankii* Davey and Williams 1966b
Dorso-ventral orientation, showing parallel-sided intratabular processes (distinctively including paracingulars) and circular mark at process bases.
MCB -3 --> -2.5 C27

Fig. 7. *Hystrichosphaeridium tubiferum* (Ehrenberg) Deflandre 1937; emend. Davey and Williams 1966b
Oblique view showing general morphology.
TBB -2 T36/2 x 1025 magnification

Fig. 8 *Hystrichostrogylon membraniphorum* Agelopolos 1964
Dorso-vental orientation, showing ventro-apical membrane.
MCB 4.5 --> 5 F40/3

Fig. 9. *Isabelidinium acuminatum* (Cookson and Eisenack) Stover and Evitt 1978
Dorsal view, showing apical horn and left antapical horn.
SFE 18A1 N2

PLATE 10


1


2

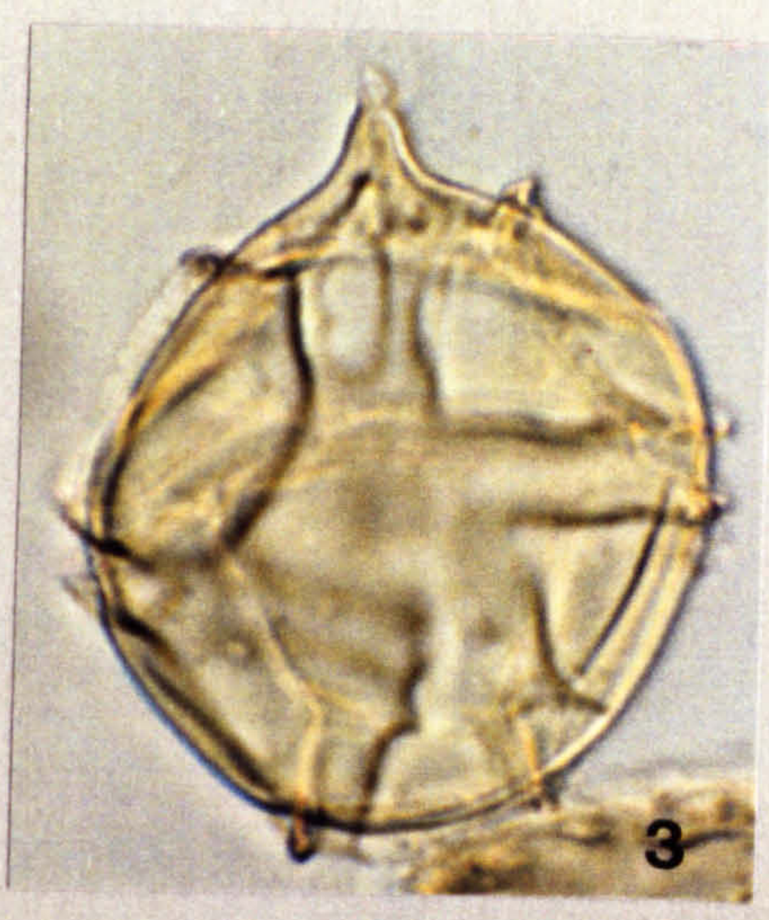
3

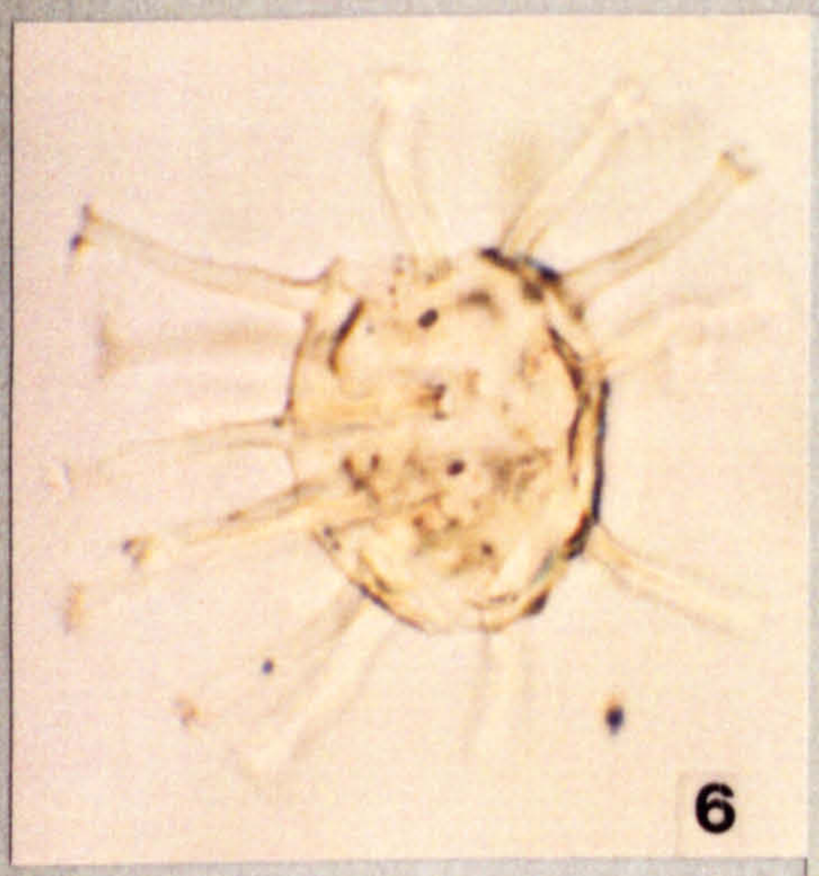
6

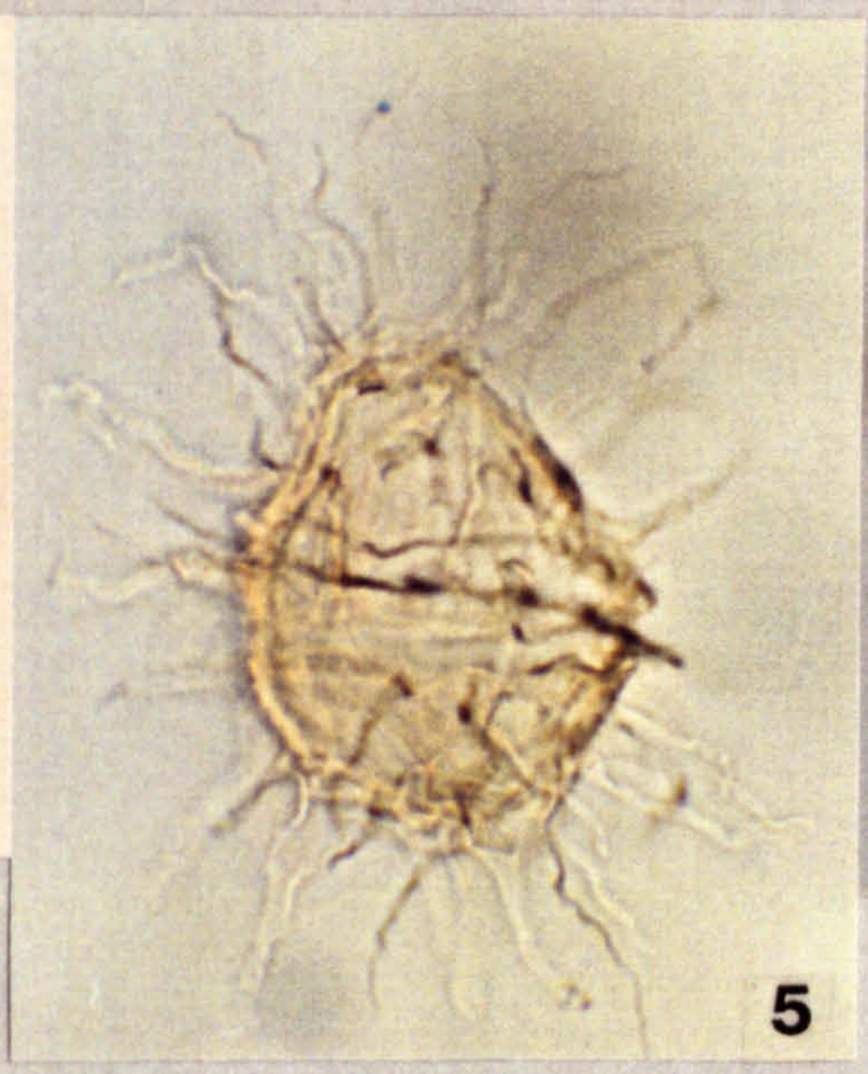
5

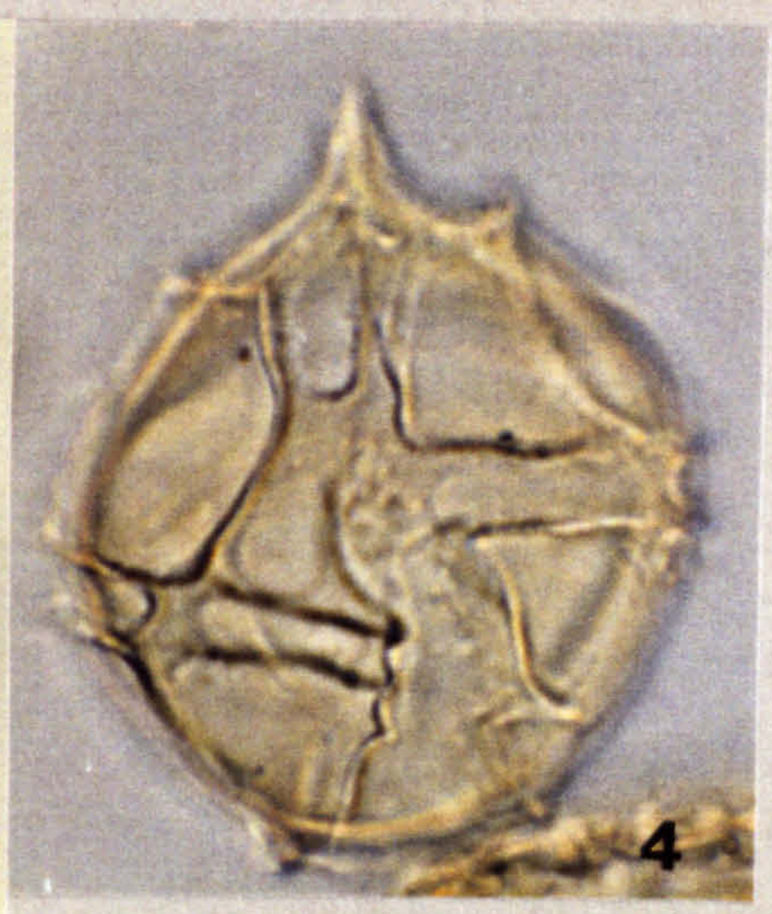
4

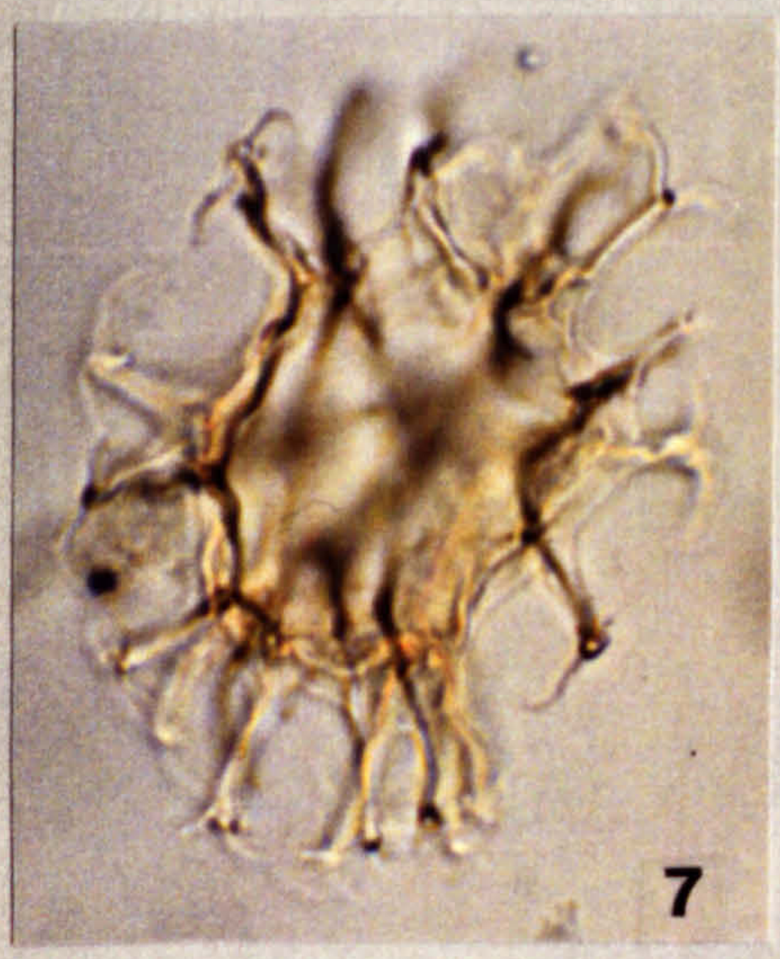
7

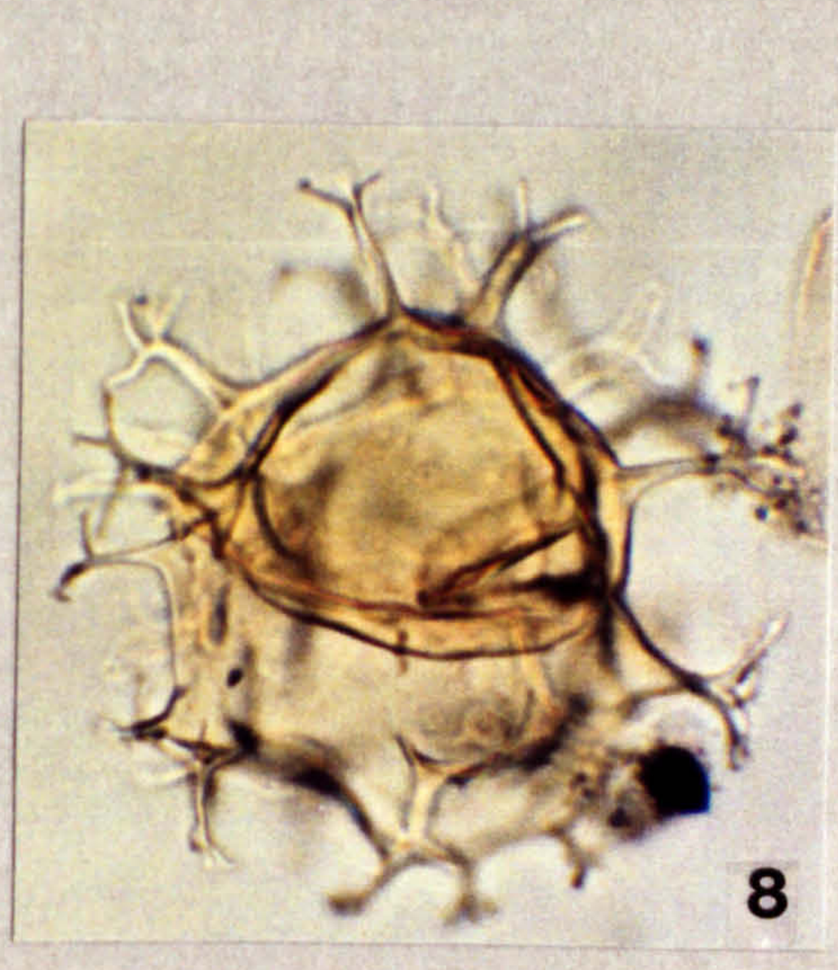
8


9

Plate 11

All photomicrographs taken at x 675 magnification, unless otherwise stated.

Fig. 1. *Kallosphaeridium ? ringnesiorum* (Manum and Cookson) Helby 1987
Ventral view, showing reticulate autophragm and adnate operculum.
SFE 18A1 T33/3

Figs 2,3. *Kleithriasphaeridium readei* (Davey and Williams) Davey and Verdier 1976
TBB 10 B39/3
2. High focus shot, showing P Type archaeopyle.
3. Low focus shot of same specimen, showing intratabular processes with their aculeate to secate distal margins.

Fig. 4. *Leberidocysta chlamydata* (Cookson and Eisenack) Stover and Evitt 1978
?Ventral view showing pericoel and densely verrucate central body.
MCB 4.5 --> 5 U16/1 x 1025 magnification

Fig. 5. *Hystrichodinium pulchrum* Deflandre 1935
Left lateral-dorsal view with precingular archaeopyle and paracingulum evident.
MCB 2 -->1.5A1 K25

Fig. 6. *Leberidocysta defloccata* (Davey and Verdier) Stover and Evitt 1978
Oblique view showing large pericoel development.
Site 3A 60 035/2 x 1025 magnification

PLATE 11

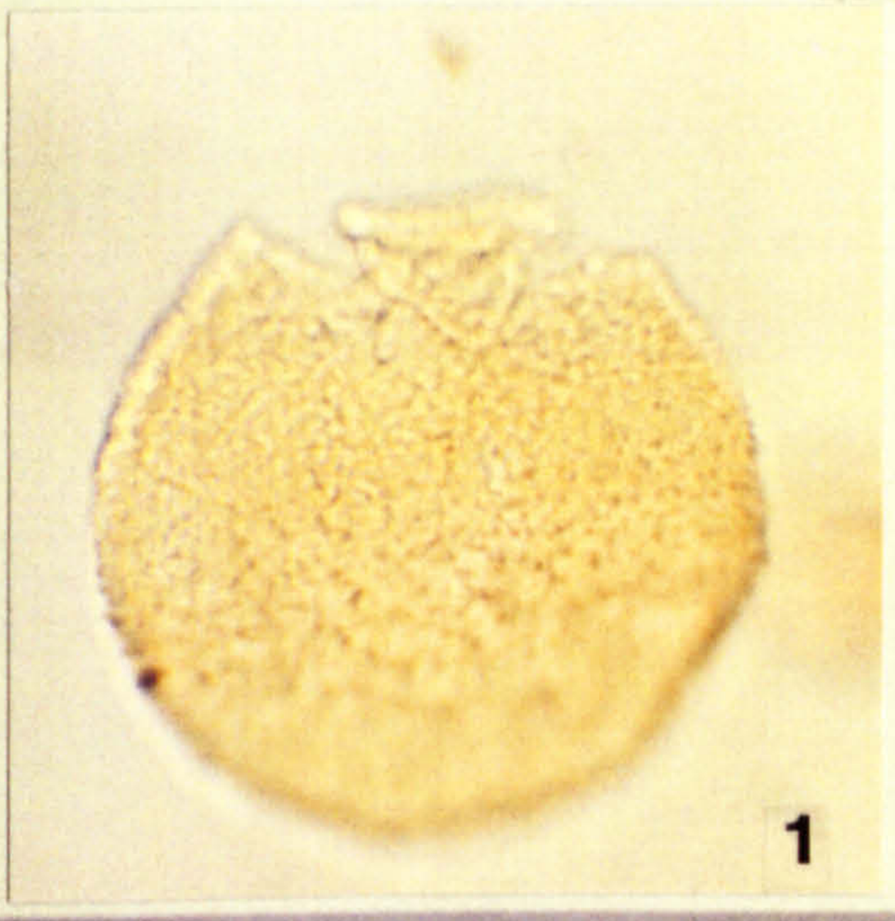
1

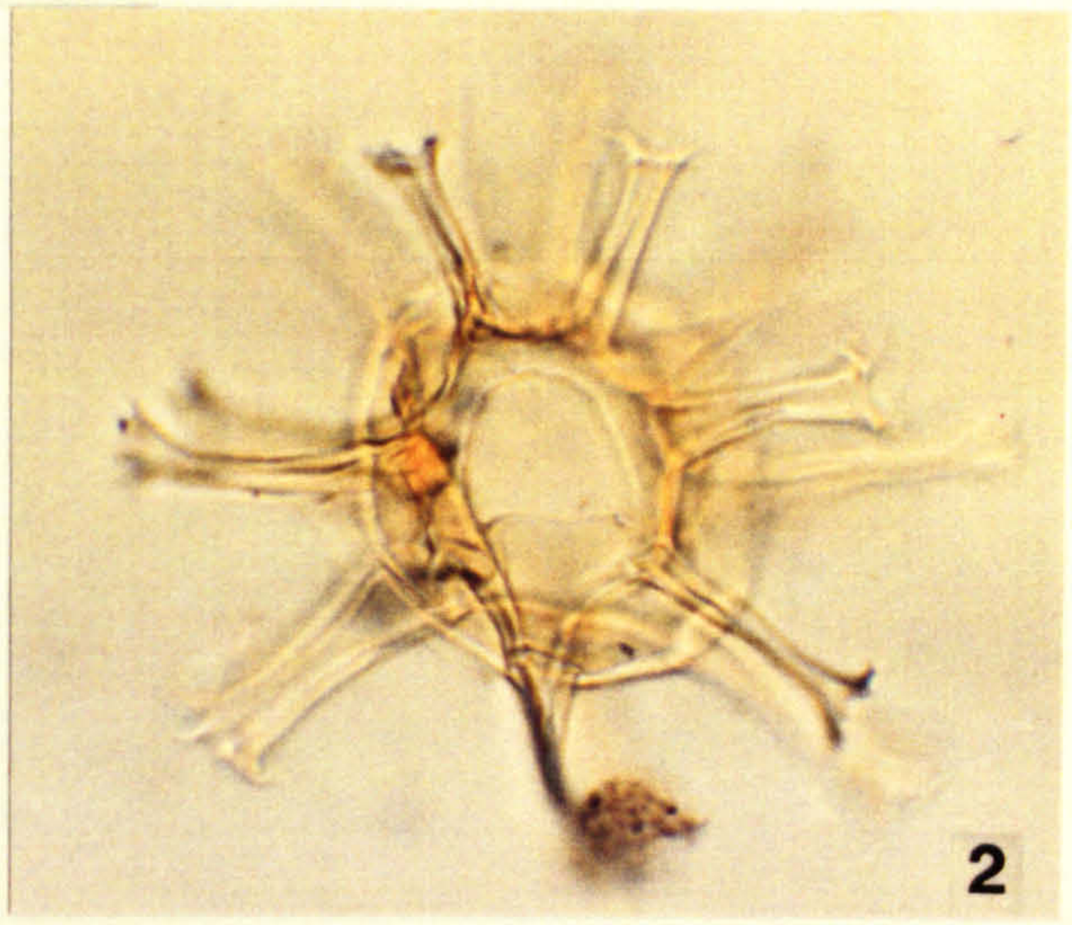
2


4

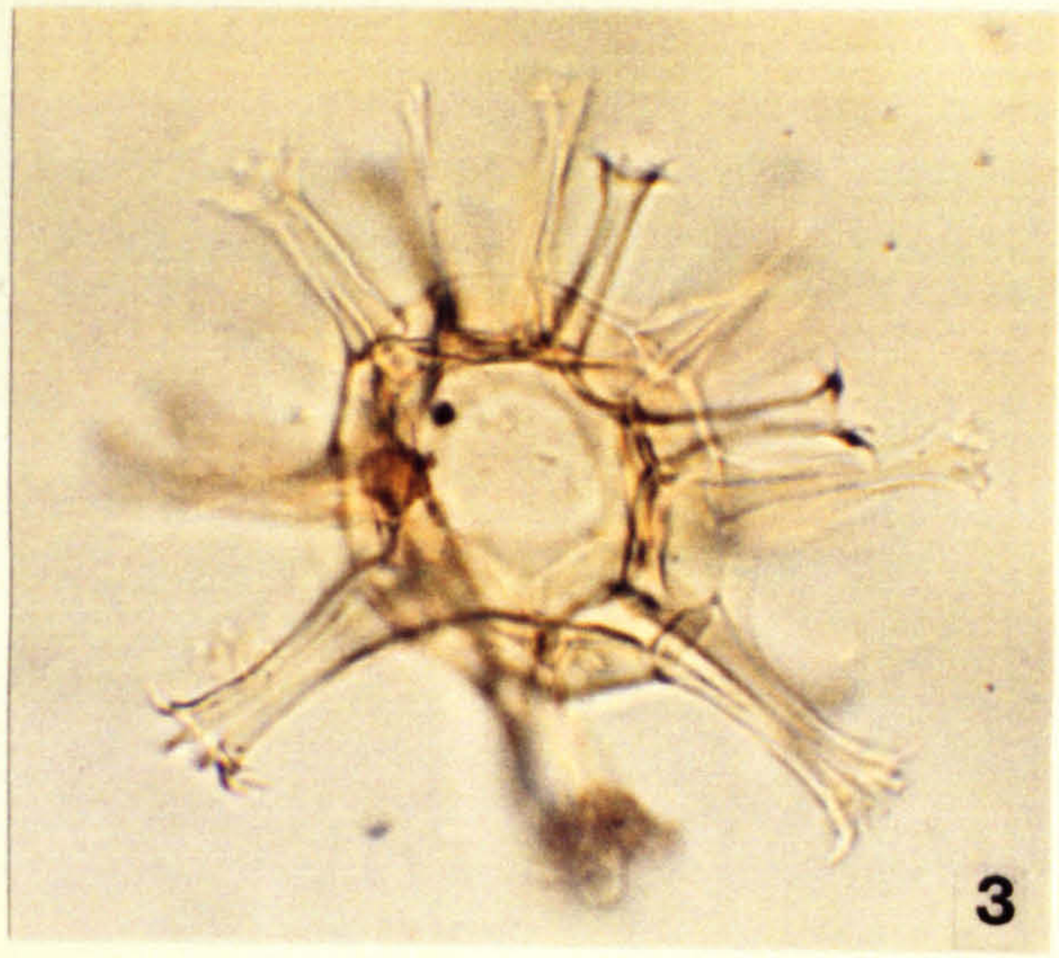
3

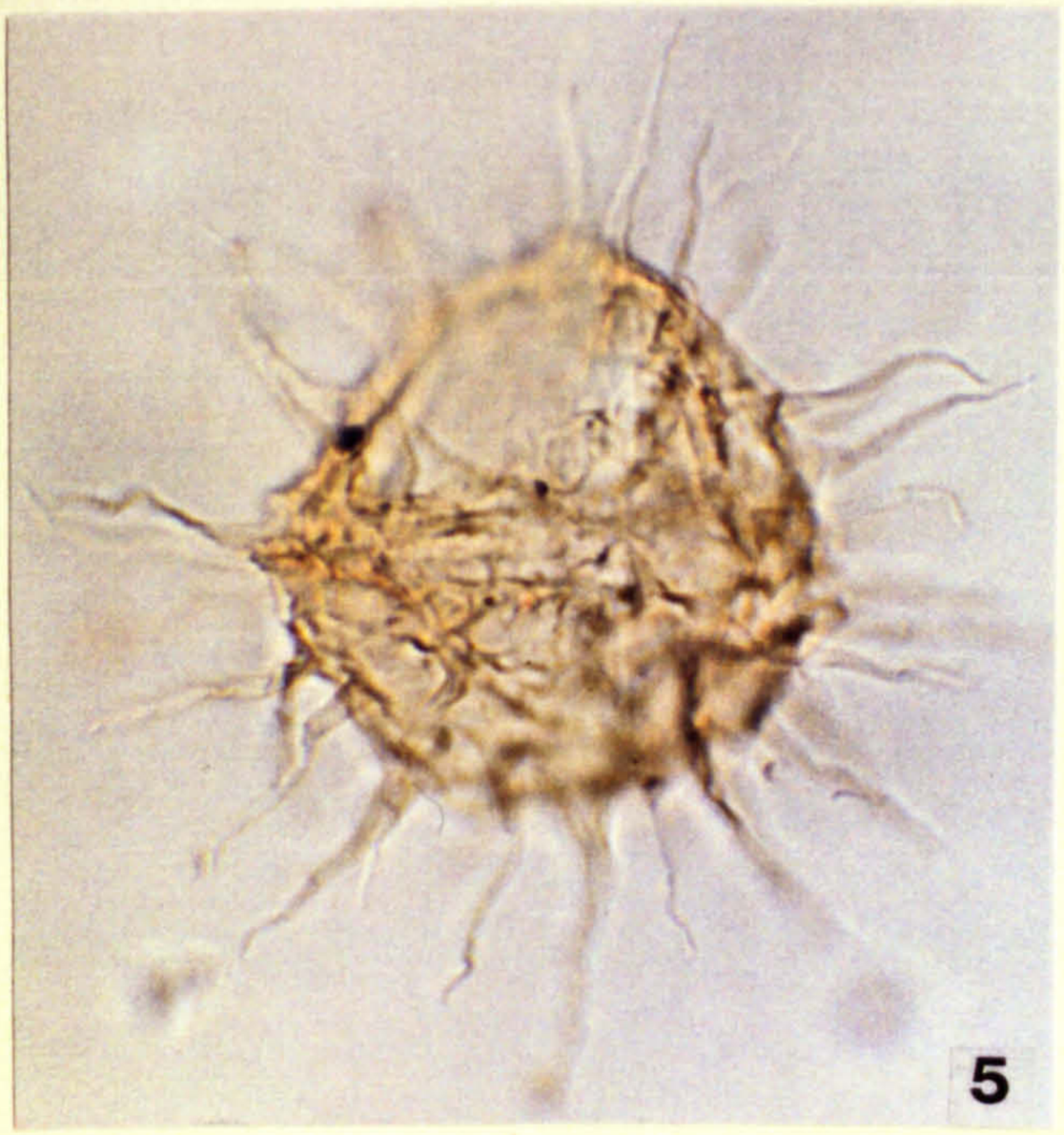
5


6

Plate 12

All photomicrographs taken at x 1025 magnification.

Figs 1-6. *Litosphaeridium siphonophorum* (Cookson and Eisenack) Davey and Williams 1966b; subspecies *siphonophorum* Lucas-Clark 1984

Fig. 1. Site 3A 85 V44/1

Lateral, dorso-ventral view showing in place apical archaeopyle carrying smaller conical apical processes and densely granular periphragm.

Fig. 2 Site 3A 20A1 T29

Apical view showing apical archaeopyle margin and lagenate process morphology.

Fig. 3. Site 3A 0 F28

Lateral, dorso-ventral view showing apical archaeopyle *in situ*. Process morphology is sub-conical to sub-cylindrical.

Fig. 4. TBB 10 045/1

Apical view, showing apical archaeopyle present and cylindrical processes.

Fig. 5. MCB 0.5 --> 0 Q28/1

Lateral dorso-ventral view showing apical archaeopyle just forming as archaeopyle sutures open up and dense periphragm reticulation. Process morphology is sub-cylindrical to cylindrical.

Fig. 6. Site 3A 0 G49

Lateral, dorso-ventral view showing apical archaeopyle and processes which are conical to sub-conical.

PLATE 12

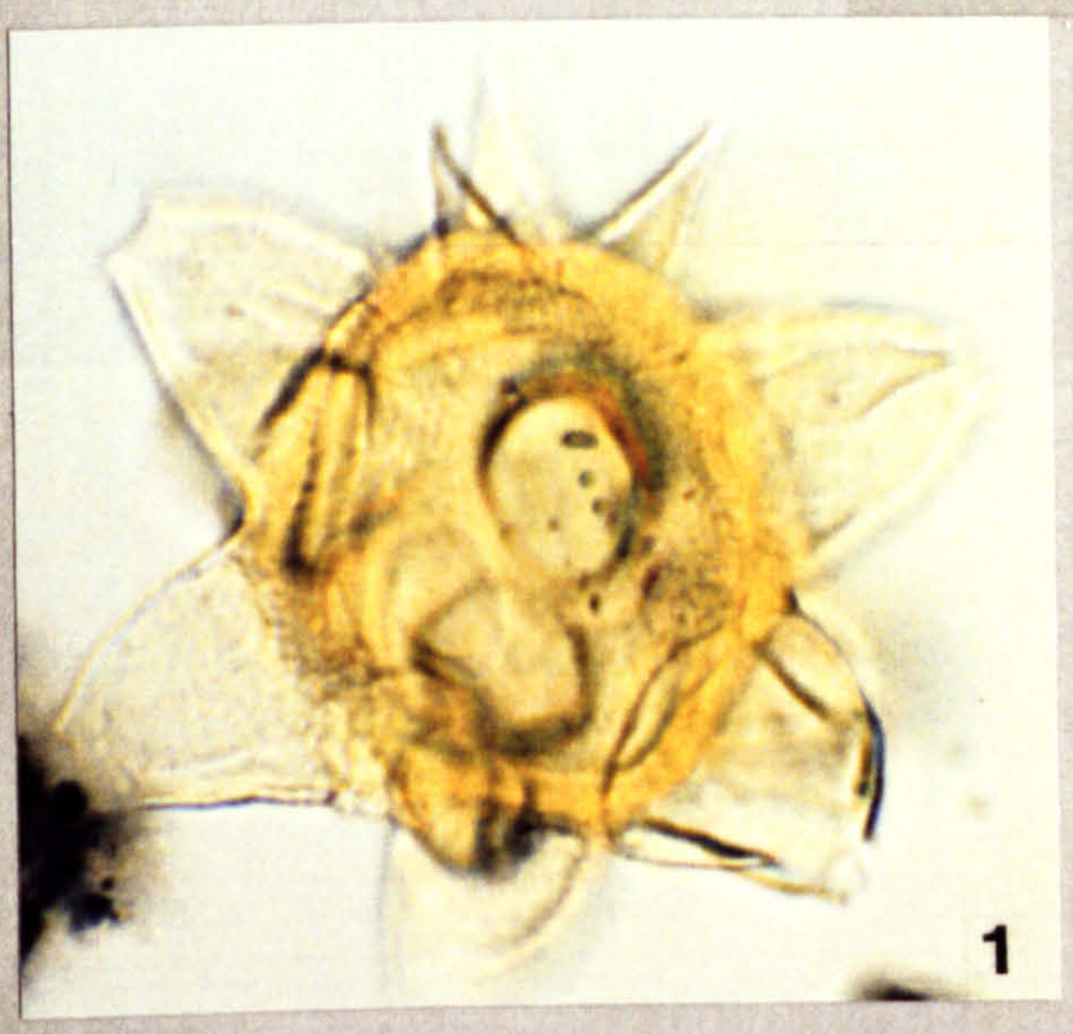
1

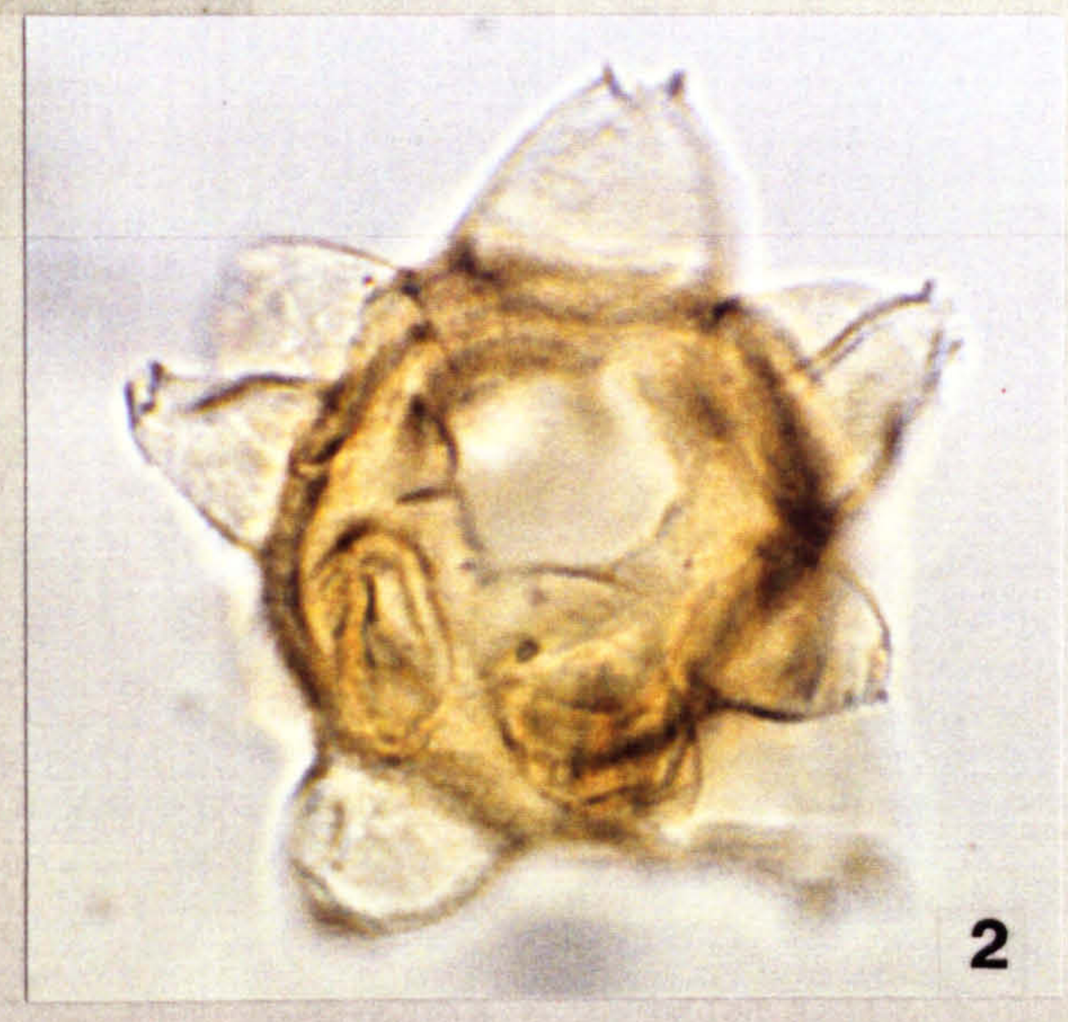
2

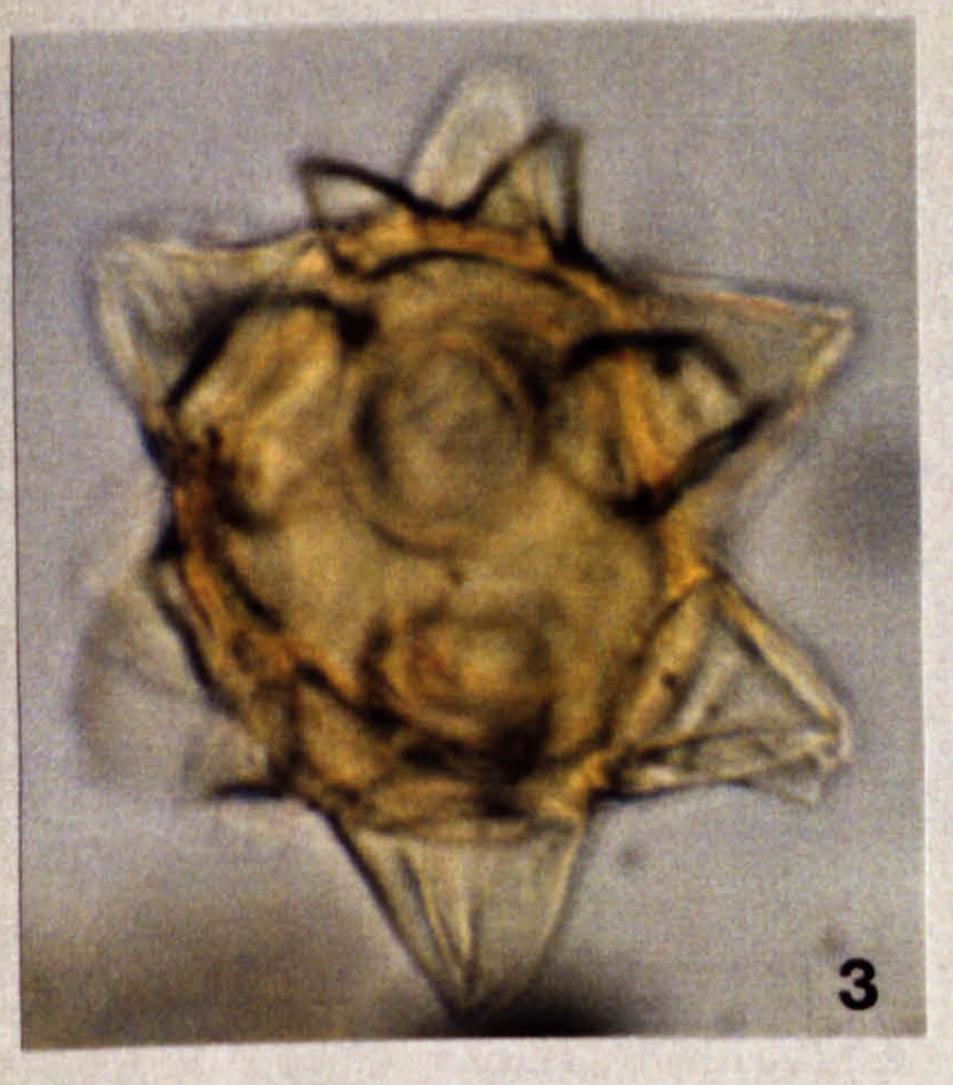
3

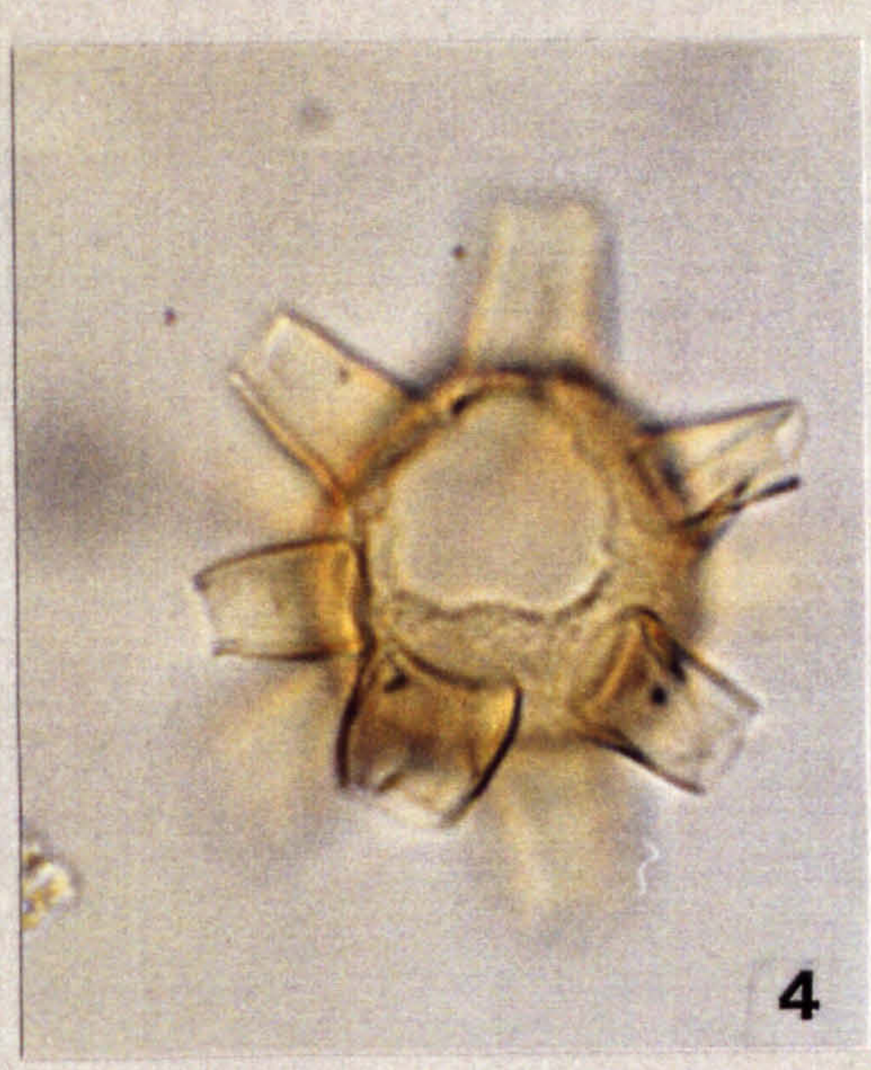
4

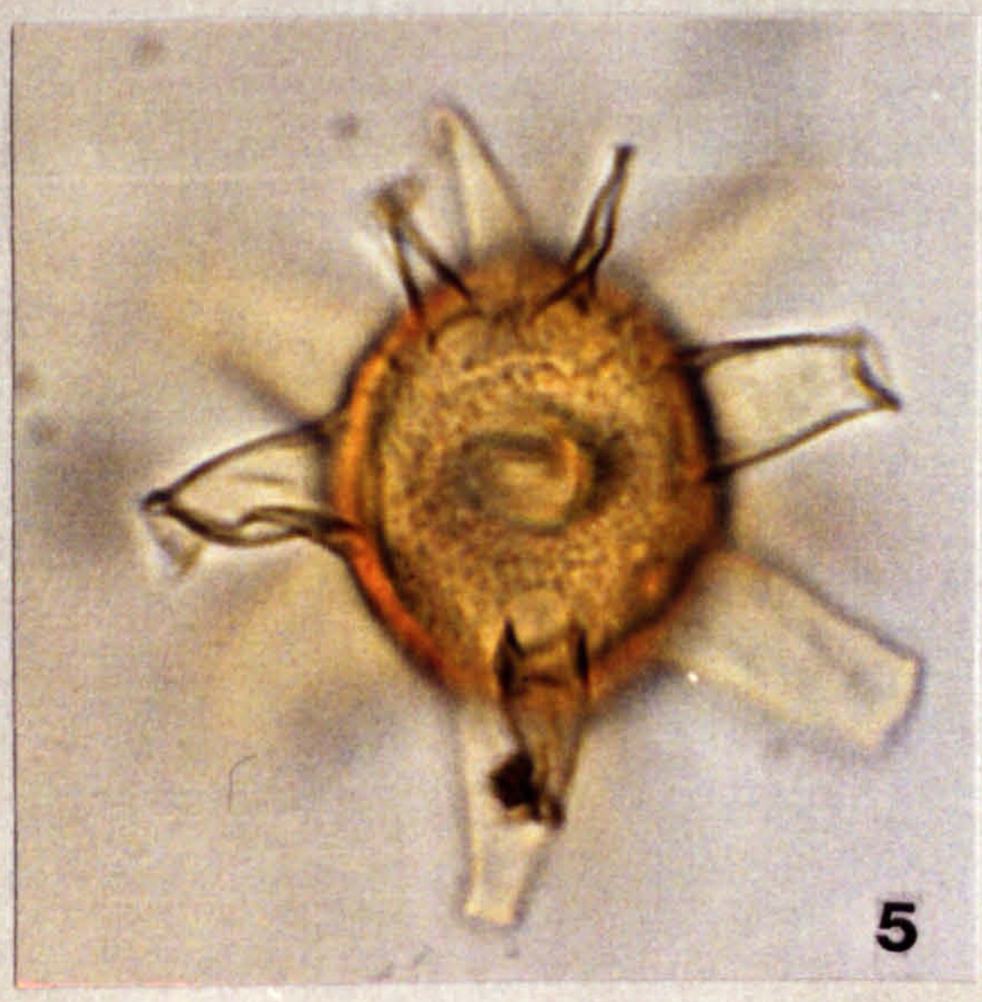
5

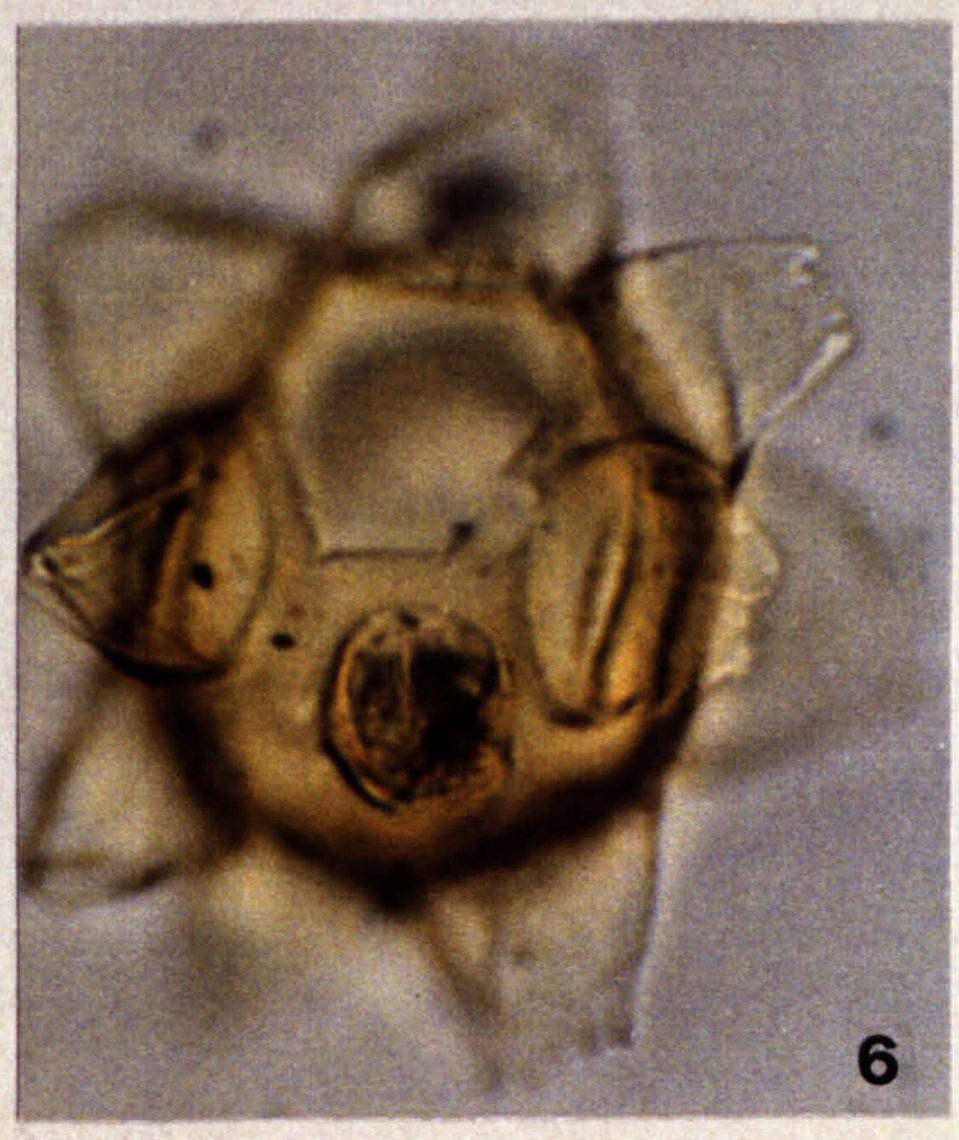
6

Plate 13

All photomicrographs taken at x 1025 magnification.

Figs 1-4. *Litosphaeridium siphonophorum* (Cookson and Eisenack) Davey and Williams 1966b; subspecies *glabrum* Lucas-Clark 1984

Fig. 1. Site 3A 85 X47
Apical view showing apical archaeopyle and sub-conical to sub-cylindrical process morphology .

Fig. 2. Site 3A 0 B33
Lateral dorso-ventral view, showing smooth periphragm and lagenate to bulbous process morphology, which display thickened distal tips.

Fig. 3. MCB -1.5 --> -2 M32/1. DIC
Lateral dorso-ventral view, showing apical archaeopyle and sub-conical processes.

Fig. 4. MCB -1 --> -1.5 R49 DIC
Lateral dorso-ventral view with conical process morphology present.

Figs 5-7. *Litosphaeridium* sp. A

Fig. 5. SFE 18A1 M50/2. DIC
Oblique view showing goblet-shaped process morphology and fine nature of cyst wall.

Fig. 6. SFE 18A1 P41/2. DIC

Fig. 7. SFE 18A1 M50/2
7. Oblique view showing apical archaeopyle margin evident towards top margin of cyst. Goblet-shaped processes obvious.

PLATE 13

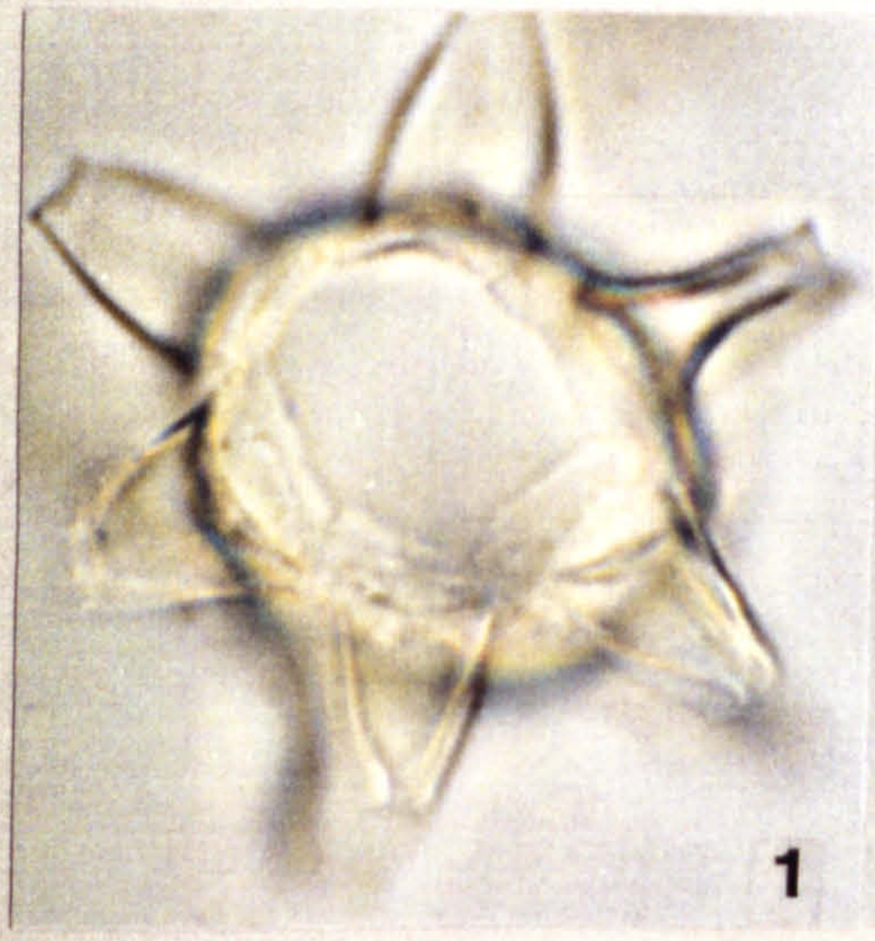

1

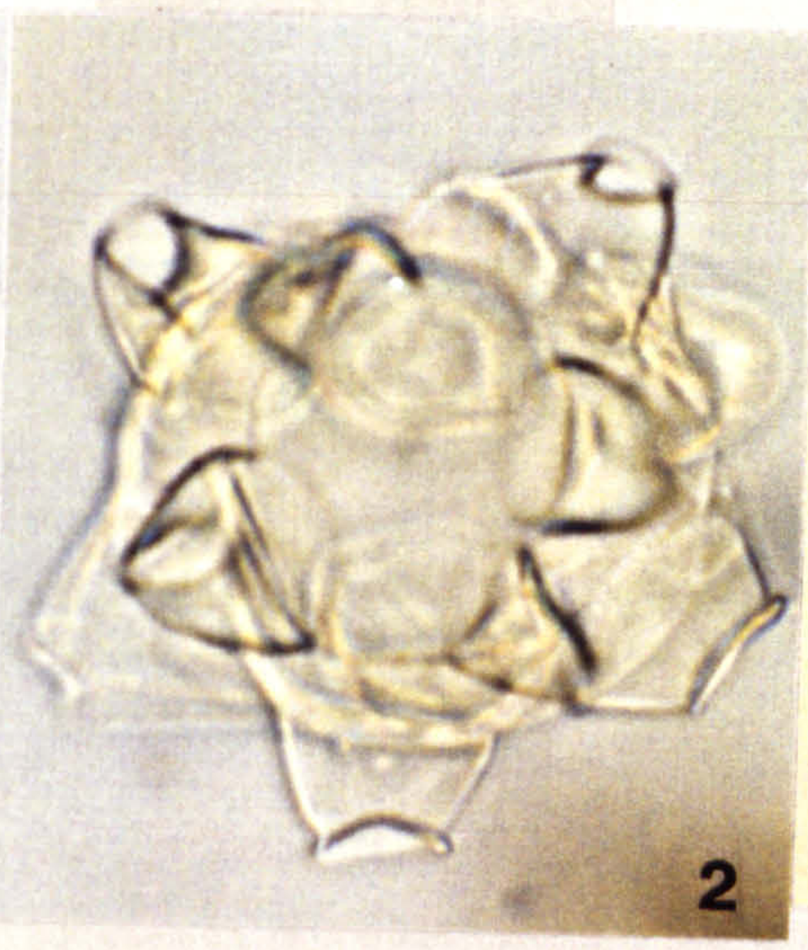

2

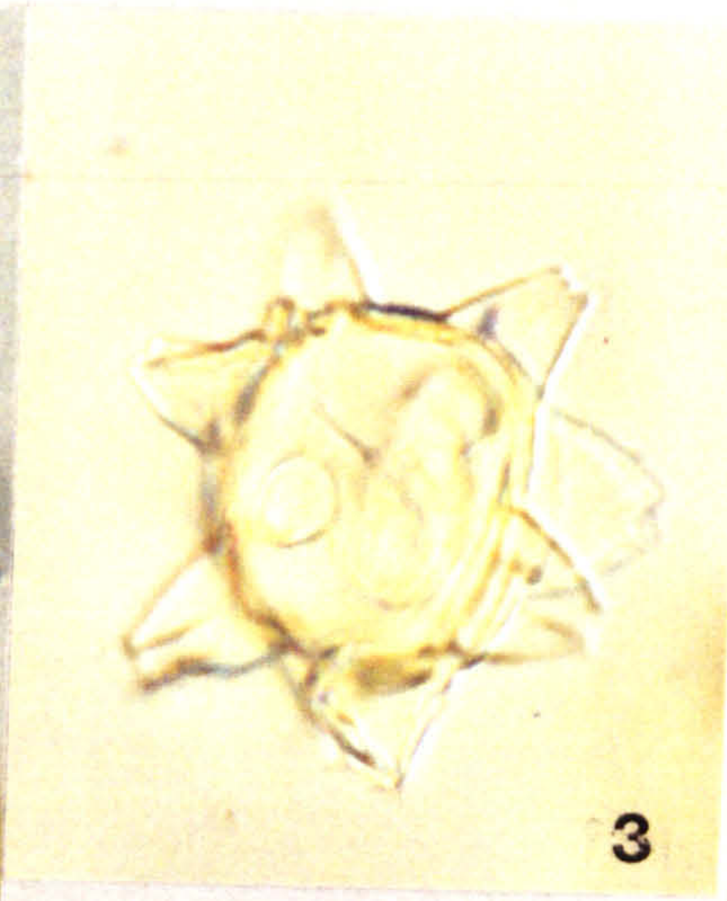

3

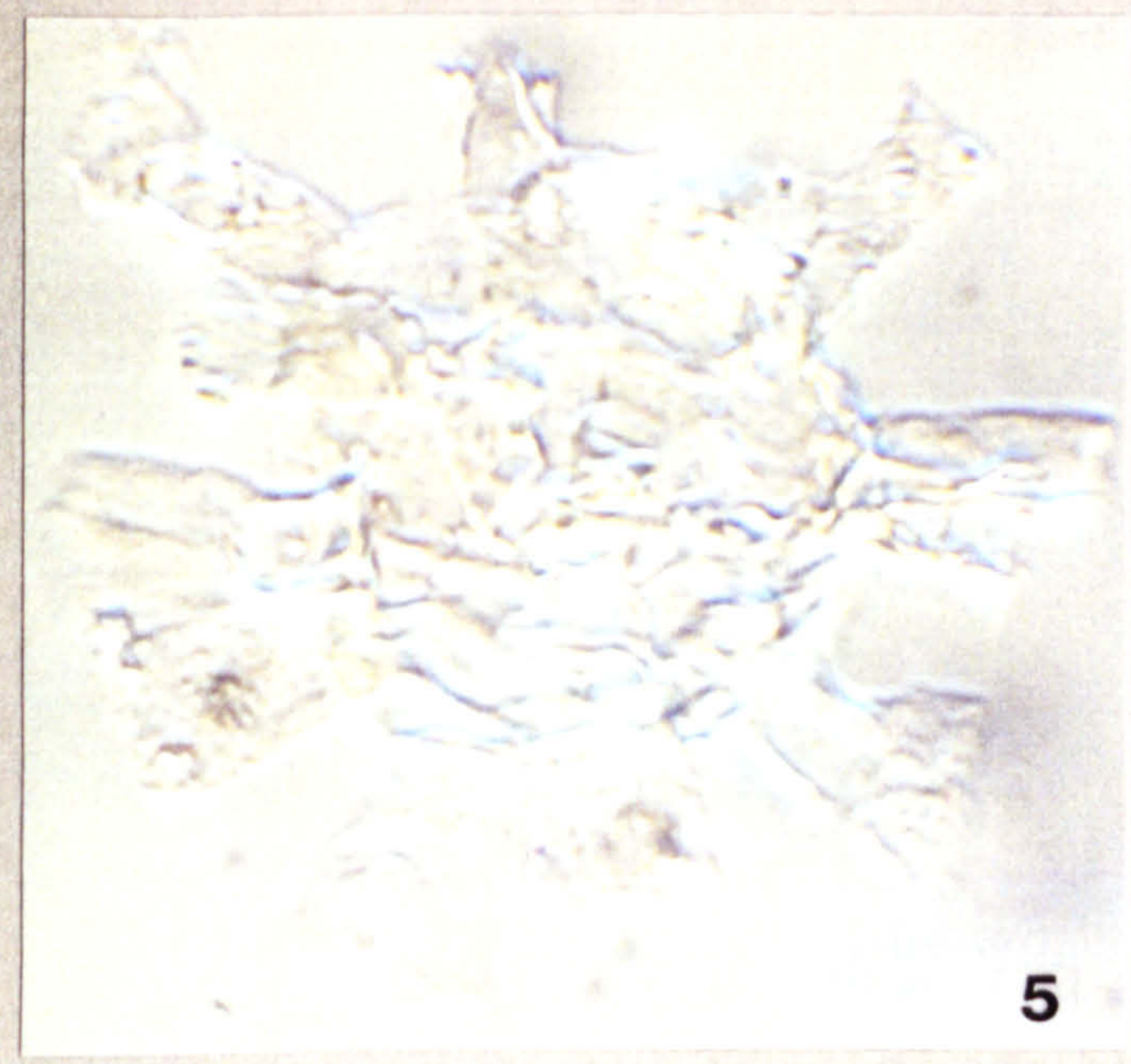

5

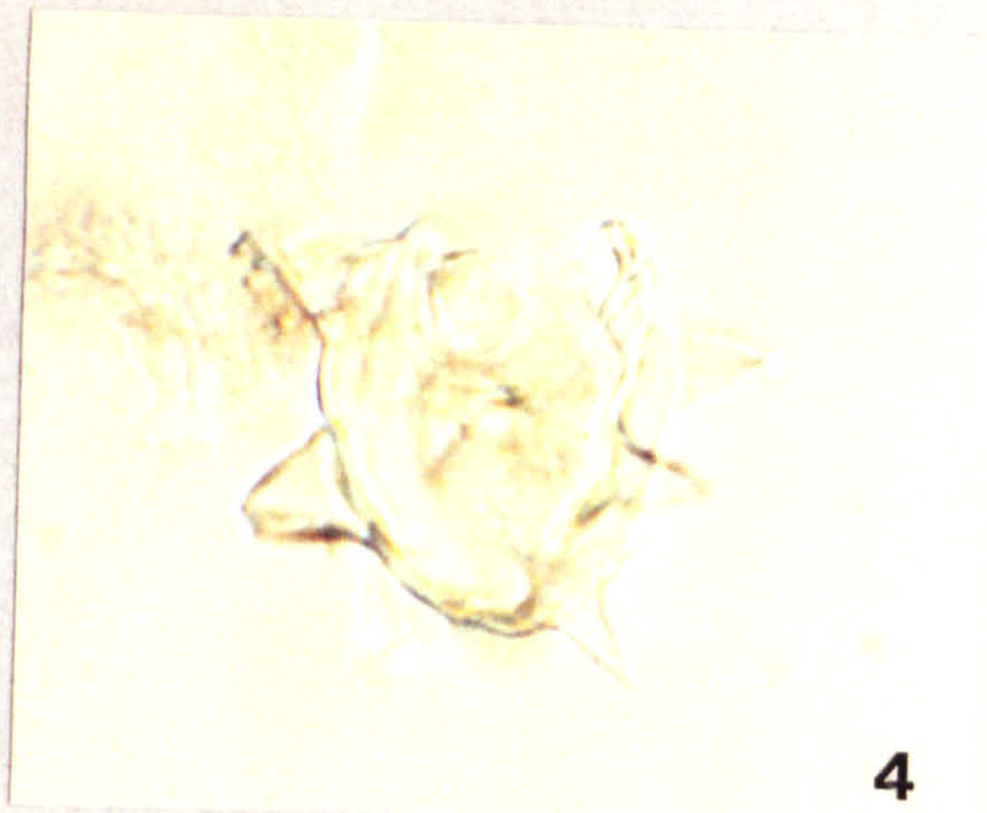

4

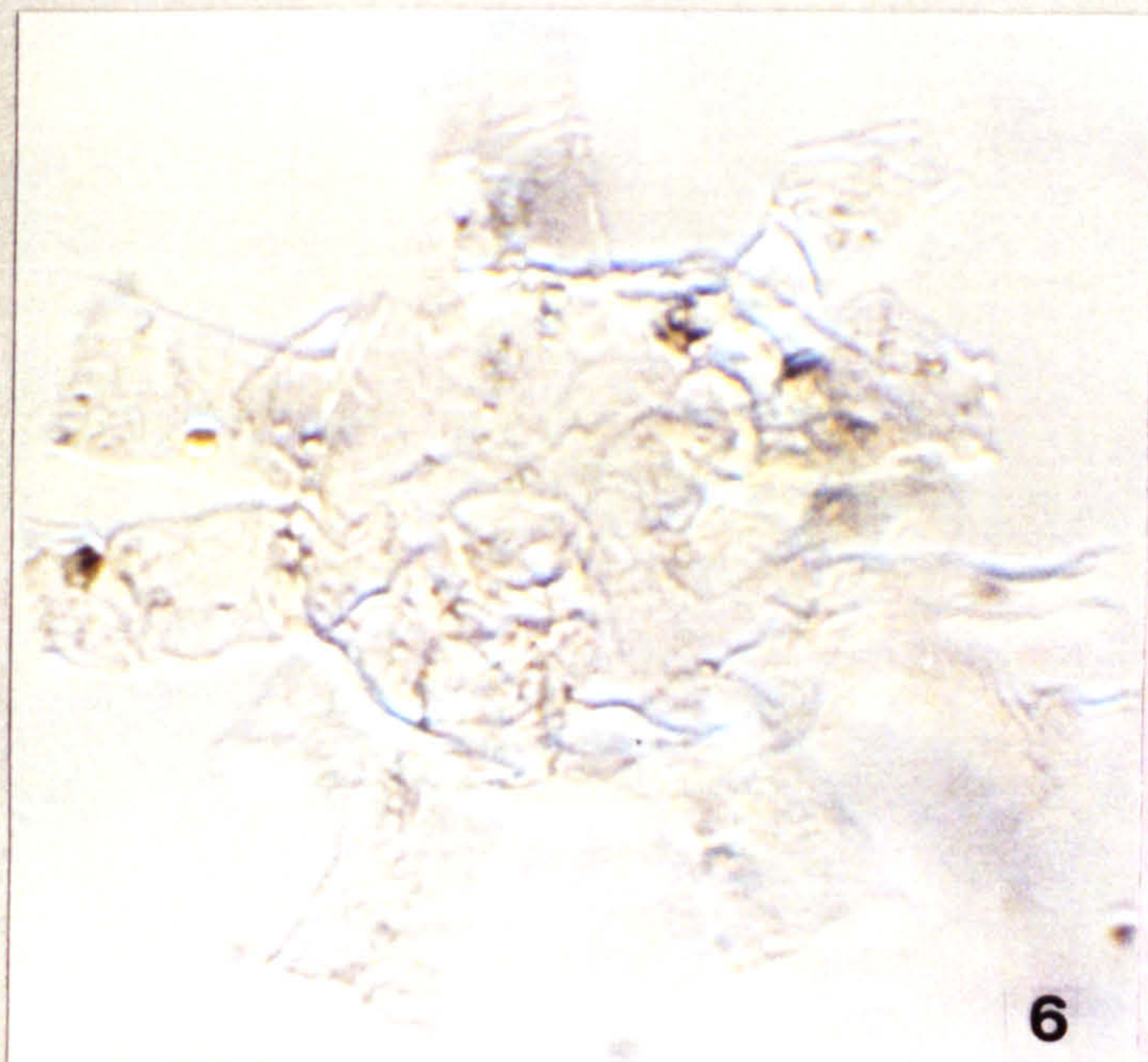

6

7

Plate 14

All photomicrographs taken at x 1025 magnification.

Figs 1,2. *Microdinium ? crinitum* Davey 1969
Site 3A 90 R23
1. Low focus shot of dorso-ventral orientatioin, showing granular autophragm and fibrous nature of processes.
2. High focus shot of same specimen, showing paracingulum, with individual paraplates obvious

Fig. 3. *Microdinium ornatum* Cookson and Eisenack 1960a
Dorsal view showing distinctive individual paracingular paraplates.

Figs 4,5. *Microdinium distinctum* Davey 1969
Site 3A 105 J38/2
4. Low focus, right lateral, ventral view showing parasulcus and paracingulum; the latter is diagnostically without individual paraplates.
5. High focus, dorsal view of same specimen, showing machicolate distal margin of parasutural crests.

Figs 6,7. *Microdinium setosum* Sarjeant 1966; emend. Below 1987
Fig. 6. Site 3A 90 H18/4
Dorsal view, showing paracingulum and denticulate to echinate distal margins of parasutural crests.
Fig. 7. Site 3A 90 F26/4
Ventral view showing paracingulum and parasulcus.

Figs 8,9. *Nematosphaeropsis densiradiata* (Cookson and Eisenack) Stover and Evitt 1978
TBB 6 V17
8. High focus oblique view of the trabeculae.
9. Low focus shot of the same specimen, showing general morphology.

PLATE 14


1


2

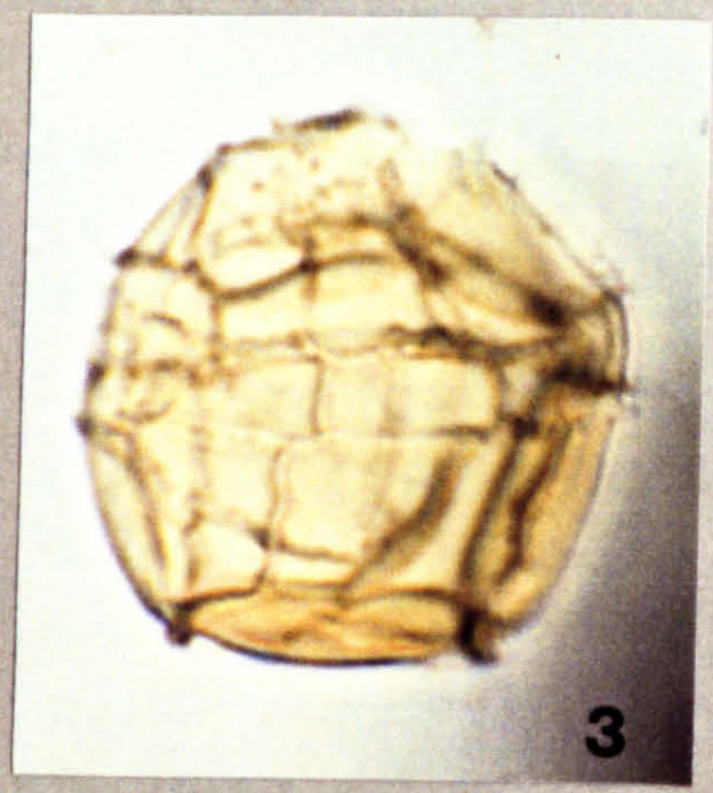
3


4

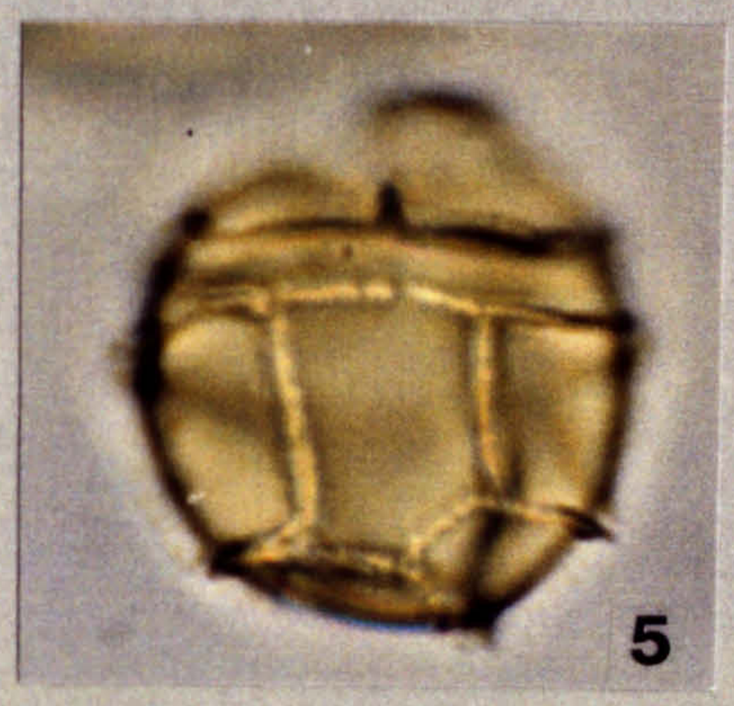
5

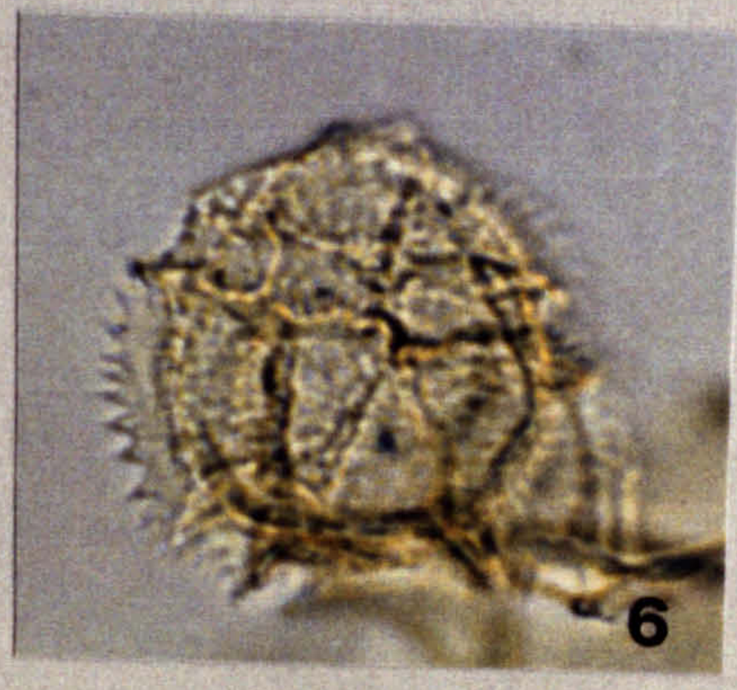
6

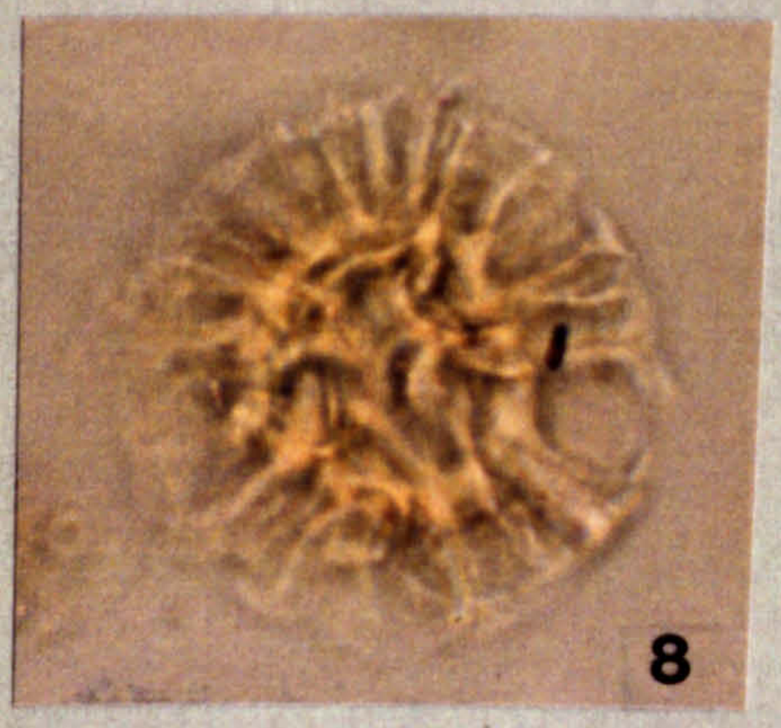
8

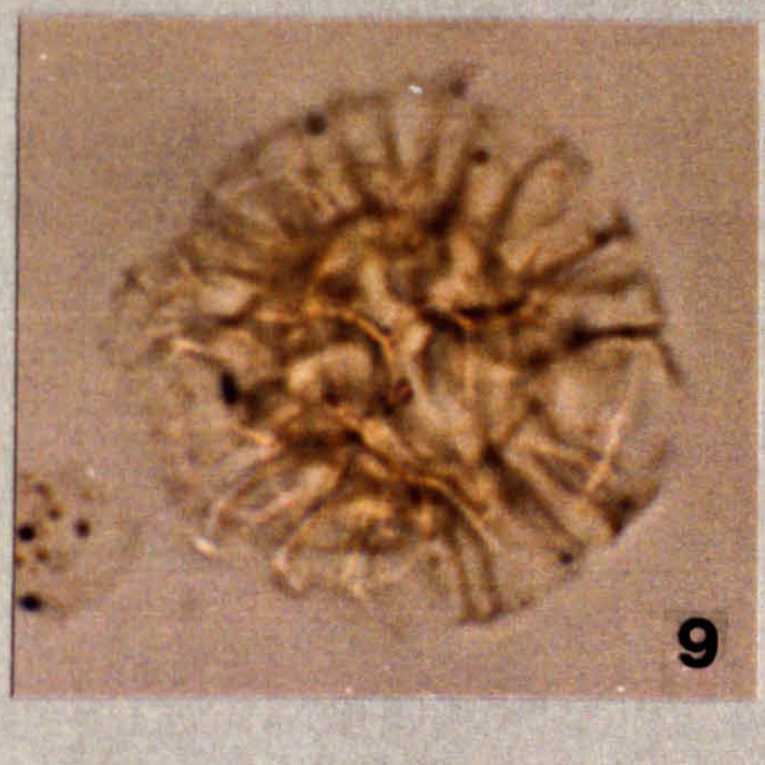
9


7

Plate 15

Figs 1-3. *Odontochitina costata* Alberti 1961; emend. Clarke and Verdier 1967

Fig. 1. MCB 4 --> 4.5 P29/3 x 512 magnification
Oblique dorso-ventral complete specimen, showing longitudinal ribs along horns and pylome in apical horn. Apical horn is folded back on itself.

Fig. 2. Site 3A 90 H20/4 x 338 magnification
Operculum with nipple-like extension of endocyst into the apical horn. Longitudinal ribs on horn are also obvious.

Fig. 3. Site 3A 85 S40 x 540 magnification
Ventral view of hypocyst showing longitudinal ribs on horns. The larger horn is the antapical horn.

Fig. 4. *Odontochitina operculata* (O. Wetzel) Deflandre and Cookson 1955
Complete specimen with badly folded antapical horn.
TBB 11 M47/3 x 338 magnification

PLATE 15

1

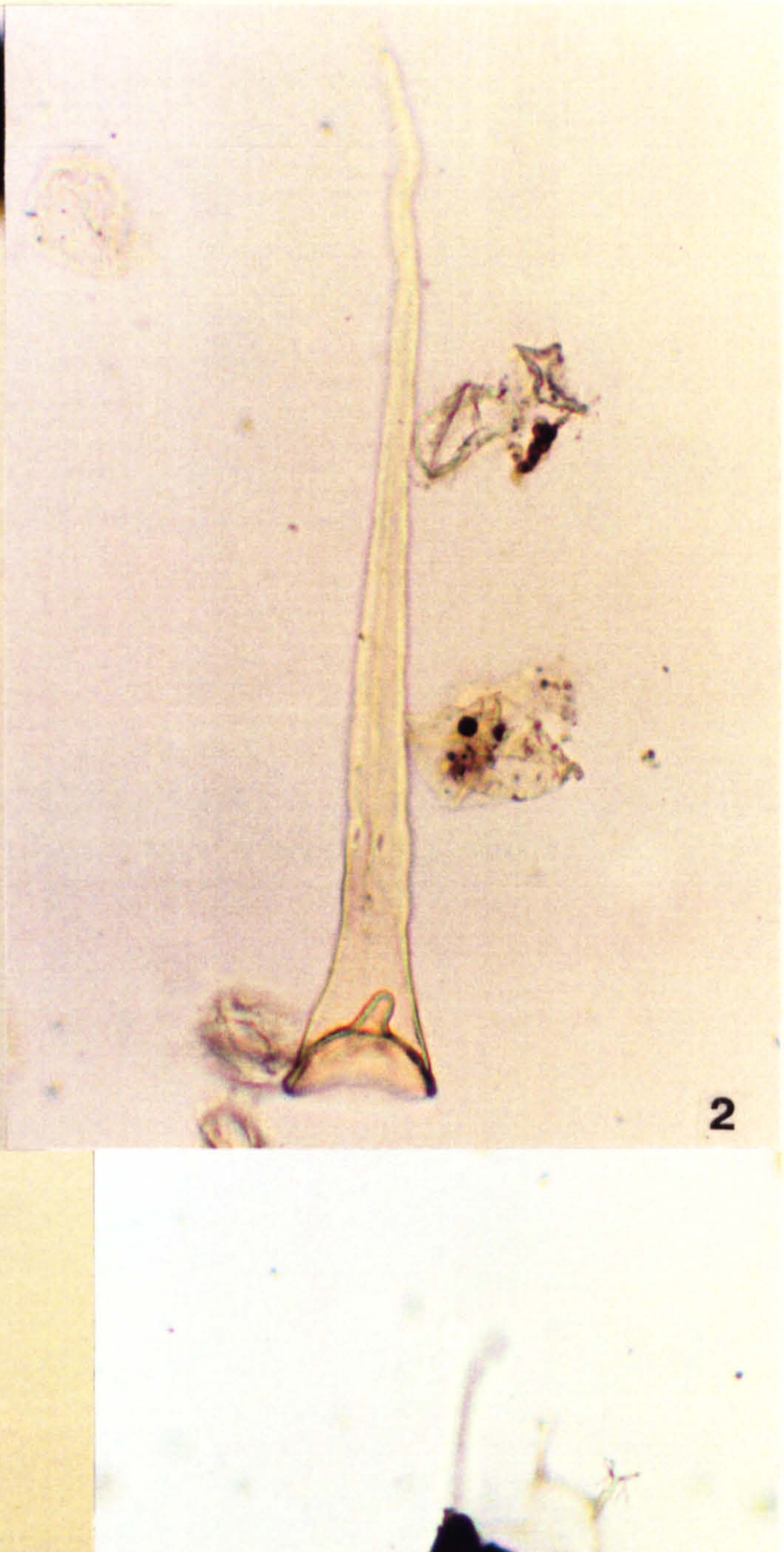

2

3

Plate 16

All photomicrographs taken at x 675 magnification.

Figs 1,2. *Odontochitina operculata* (O. Wetzel) Deflandre and Cookson 1955

Fig 1. Site 3A 85 P55

Operculum of *O. operculata*

Fig 2. Site 3A 60 M43

Hypocyst of *O. operculata* showing right lateral (shorter) and antapical (larger) horns.

Figs 3-5. *Oligosphaeridium complex* (White) Davey and Williams 1966b

Fig. 3. TBB 7 V33/2

Apical view of Large *O. complex* with apical archaeopyle margin evident.

Fig. 4. TBB 6 T17/4

Oblique dorso-ventral view of small *O. complex*.

Fig 5. TBB 6 U22/4

Operculum of large *O. complex*

Fig. 6. *Oligosphaeridium prolixispinosum* Davey and Williams 1966b

Dorso-ventral orientation with archaeopyle still intact.

Site 3A 85 D42/3

PLATE 16

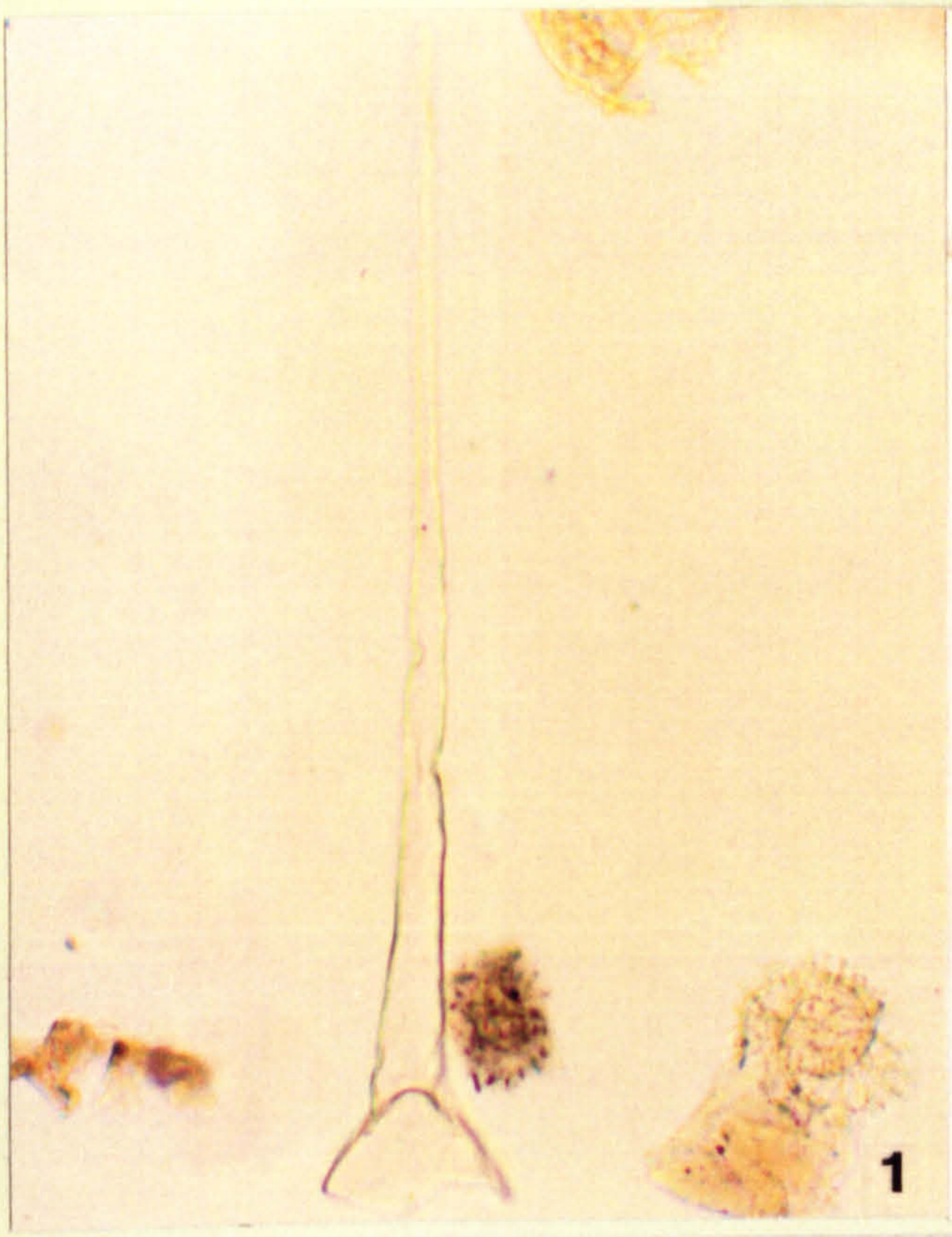
1


2


3

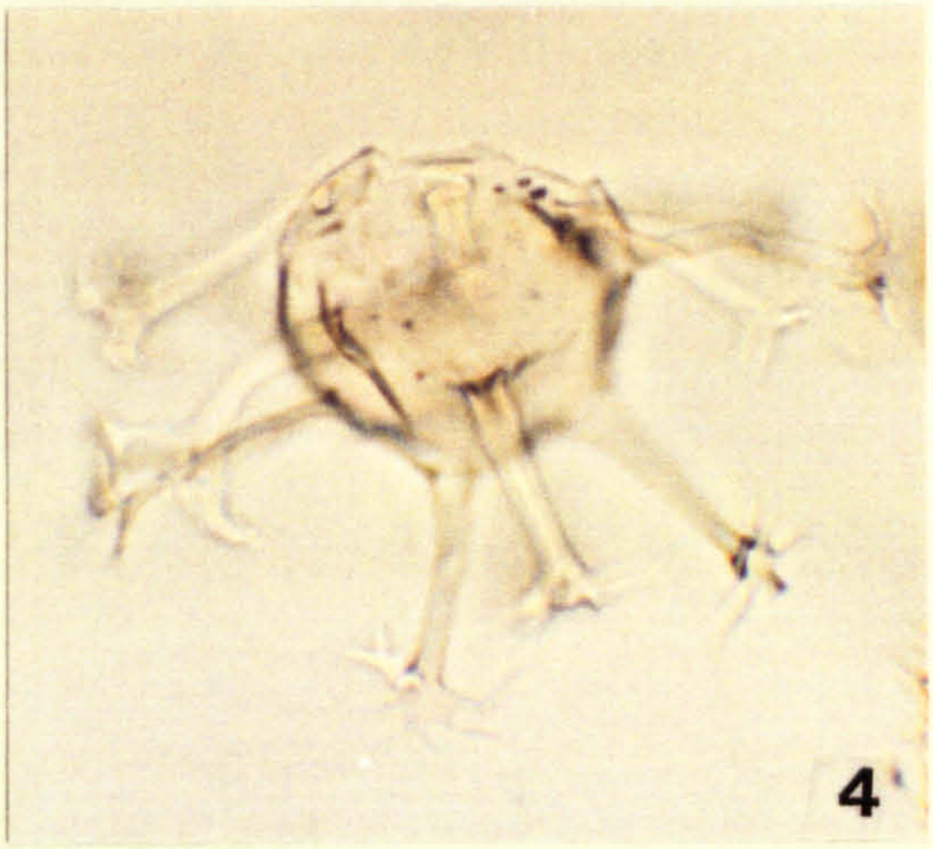
4


5

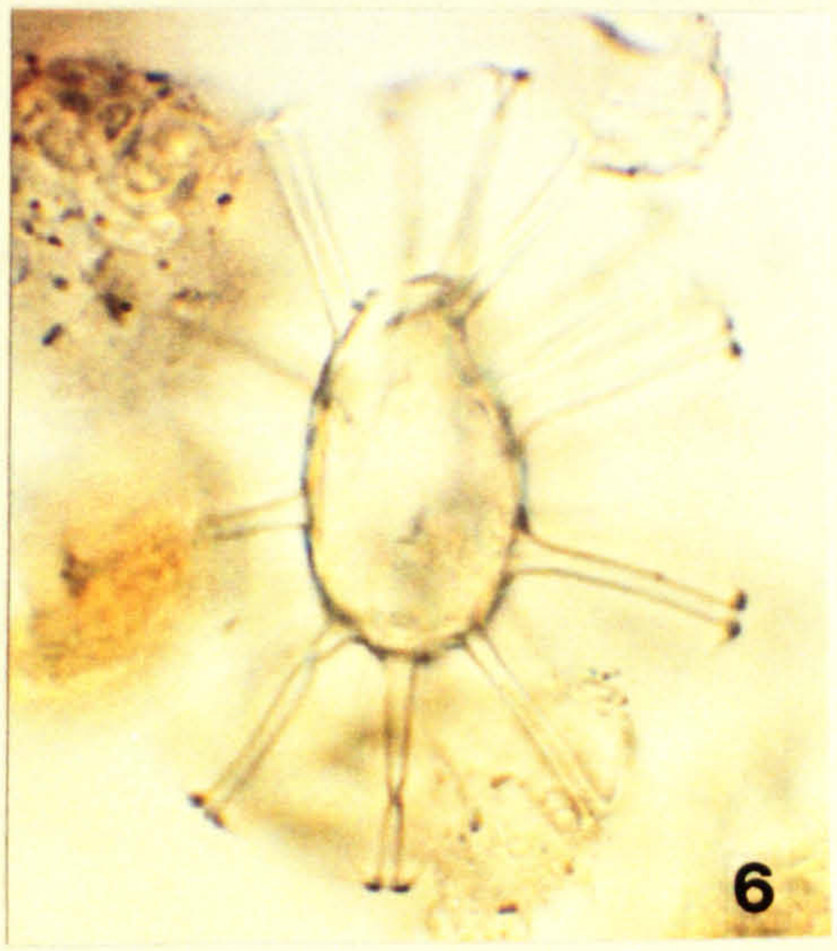
6

Plate 17

Figs 1-3. *Palaeohystrichophora infusorioides* Deflandre 1935

Fig. 1. MCB -2.5 --> -3 048/2 x 1025 magnification. DIC

1. Dorsal view, showing non-tabular short spines, and faint indication of a paracingulum.

Fig. 2. TBB 7 N33/1 x 1025 magnification. DIC

Fig. 3. TBB 14 N23 x 1025 magnification. DIC

3. Dorsal view of specimen carrying very few spines, which are confined to the paracingular, apical and antapical areas.

Fig. 4. *Pervosphaeridium cenomaniense* (Norvick) Below 1982

Oblique view, showing short non-tabular processes.

Site 3A 85 K47/1 x 675 magnification

Fig. 5. *Pervosphaeridium pseudhystrichodinium* (Deflandre) Yun 1981

Dorsal view showing 2P Type archaeopyle, and long non-tabular processes.

MCB 0 --> 0.5 R46/2 x 675 magnification

Fig. 6. *Pervosphaeridium truncatum* (Davey) Below 1982

Right lateral, dorsal view showing 2P archaeopyle and medium length non-tabular processes.

Site 3A 85 034 x 1025 magnification

PLATE 17

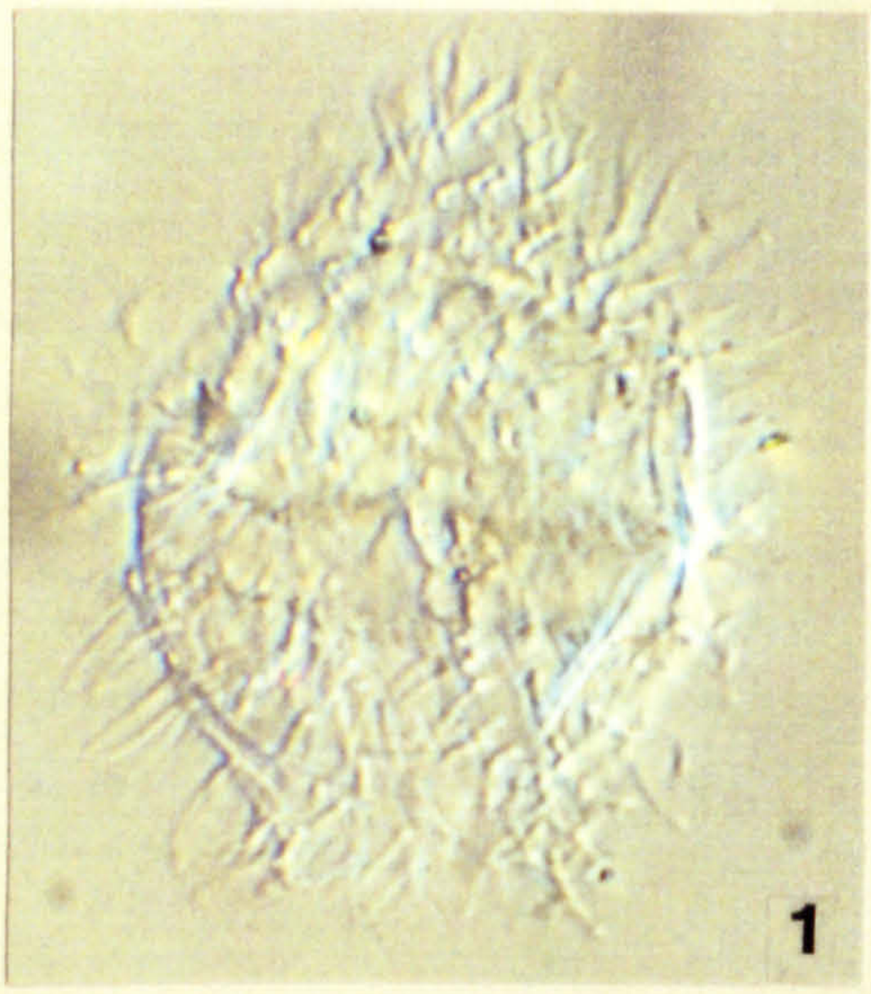
1


2

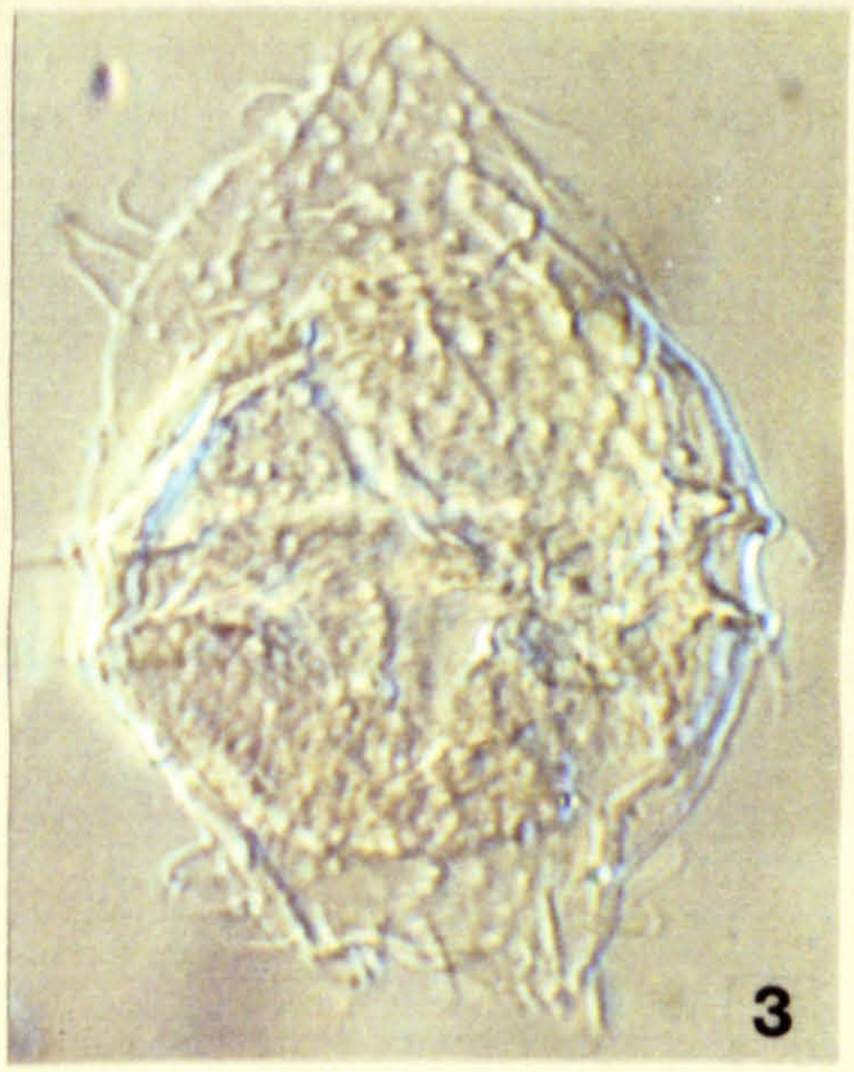
3


4

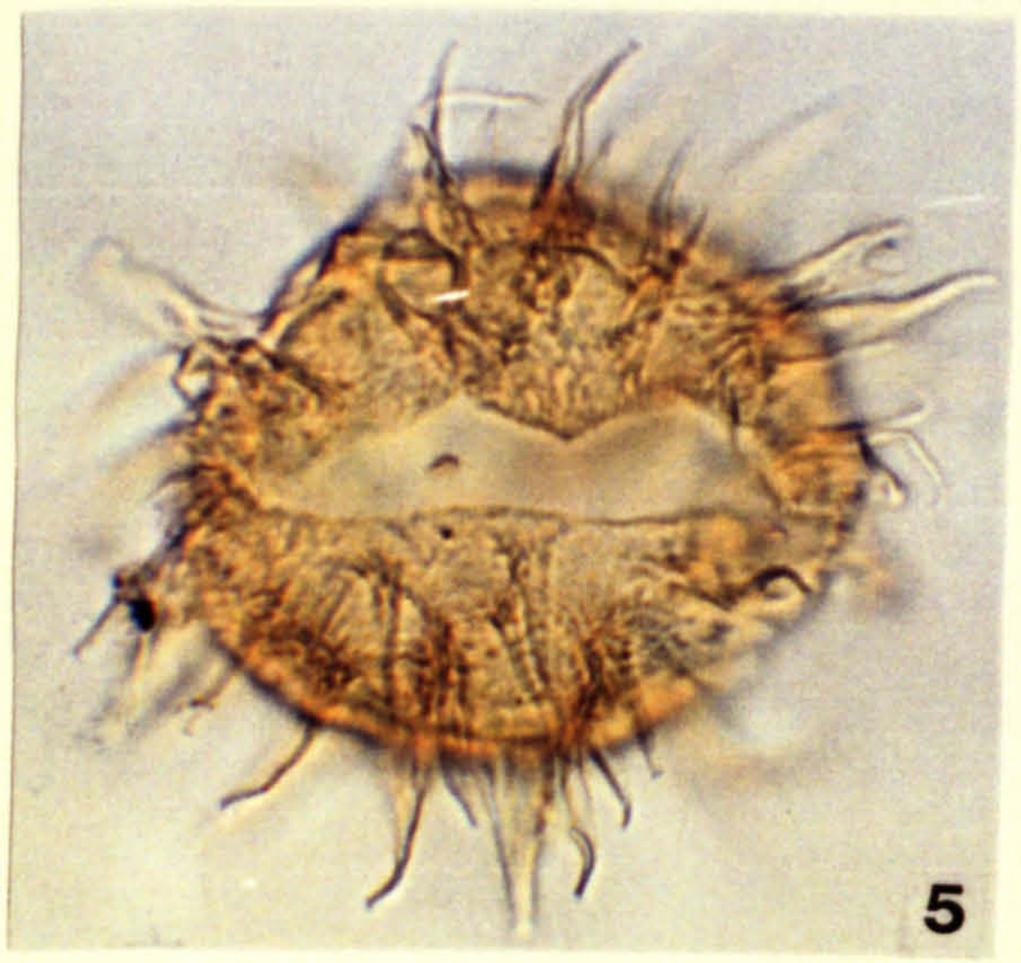
5

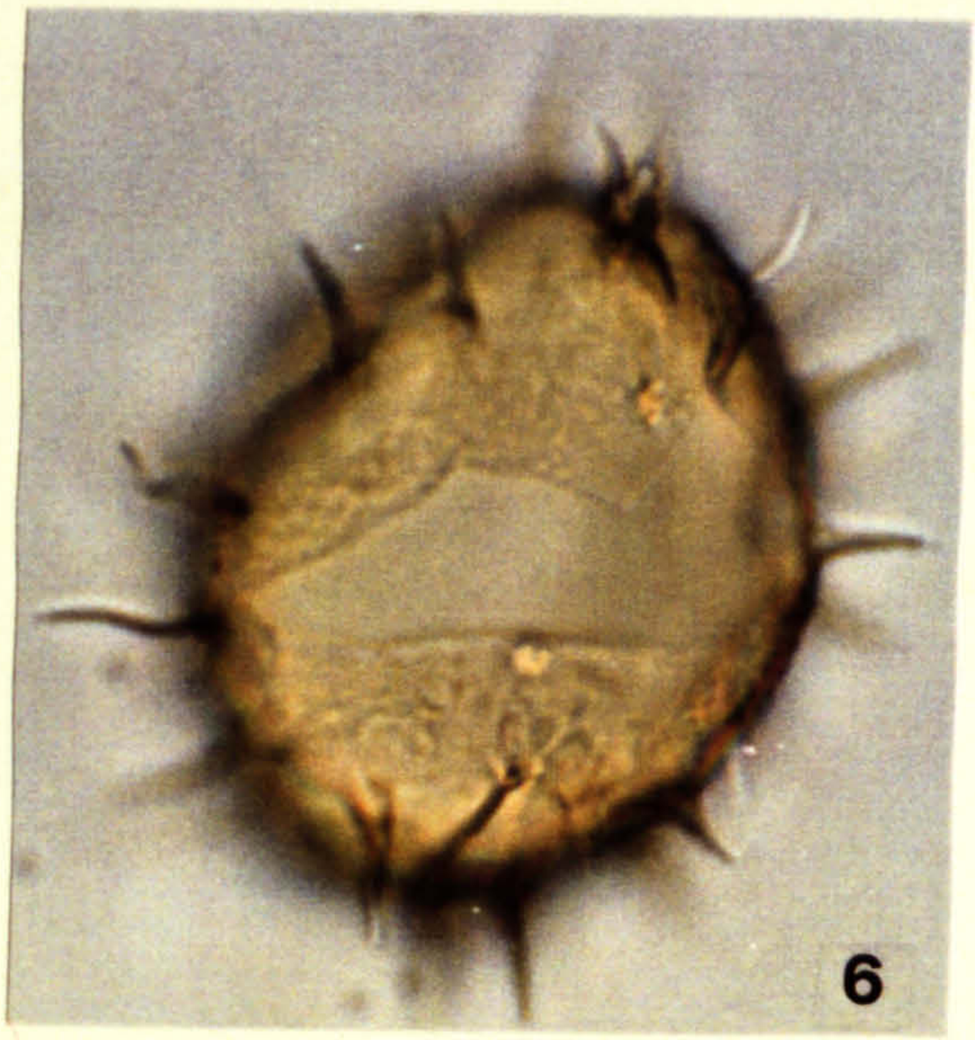
6

Plate 18

All photomicrographs taken at x 1025 magnification, unless otherwise stated.

Figs 1,2. *Prolixosphaeridium conulum* Davey 1969

Fig. 1. Site 3A 45A1 T41/1
Dorso-ventral view showing apical archaeopyle still intact.

Fig. 2. TBB 10 W42
Dorso-ventral view, showing densely granular autophragm, apical archaeopyle margin and acuminate processes.

Figs 3,4. *Psaligonyaulax deflandrei* Sarjeant 1966; emend. Sarjeant 1982
TBB -2 F33/4 x 675 magnification

3. Low focus, dorsal view with precingular archaeopyle.

4. High focus ventral view of same specimen showing S-type arrangement of paracingulum and parasulcus and parasutural crests.

Figs 5,6. *Pterodinium cingulatum* (O. Wetzel) subspecies *cingulatum* Below 1981
MCB 0.5 --> 1 P43/2

5. High focus shot of ventral surface and S-type ventral arrangement.

6. Low focus shot of dorsal surface of same specimen.

Figs 7,8. *Pterodinium cingulatum* (Clarke and Verdier) subspecies *granulatum* Lentin and Williams 1981
TBB -2 S29

7. High focus shot of ventral surface, showing S-type ventral arrangement and granulate endophragm.

8. Low focus, ventral view of same specimen, with reduced precingular archaeopyle obvious.

Fig. 9. *Pterodinium cingulatum* (Davey and Williams) subspecies *reticulatum* Lentin and Williams 1981
Site 3A 90 T46
Oblique dorso-ventral view showing parasutural crests.

PLATE 18


1


2

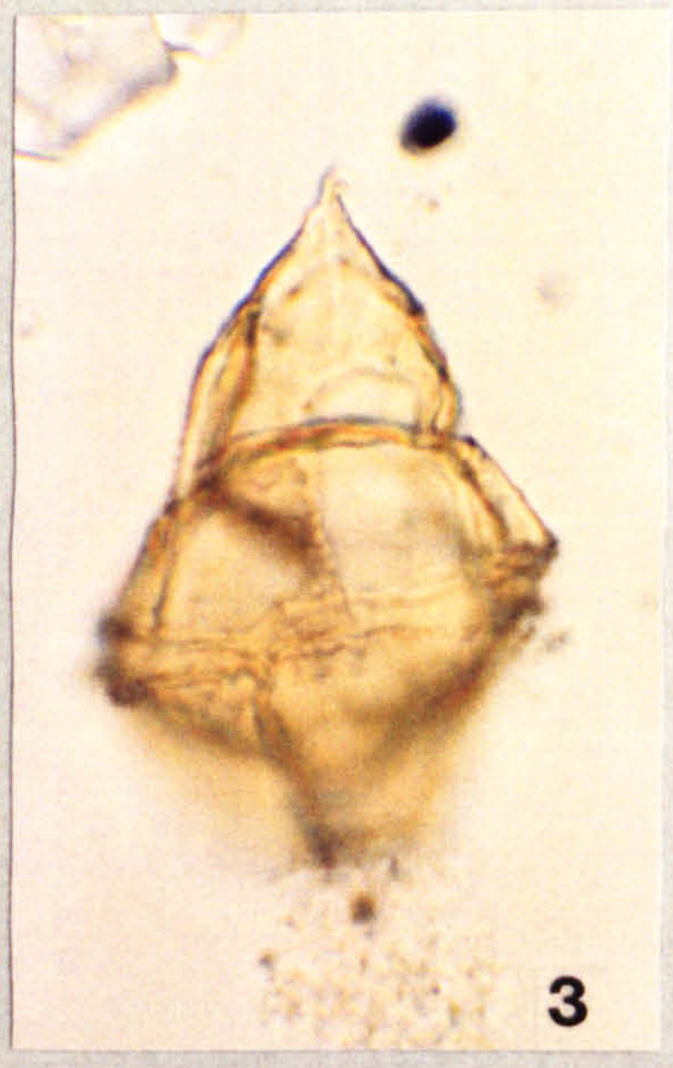
3


5

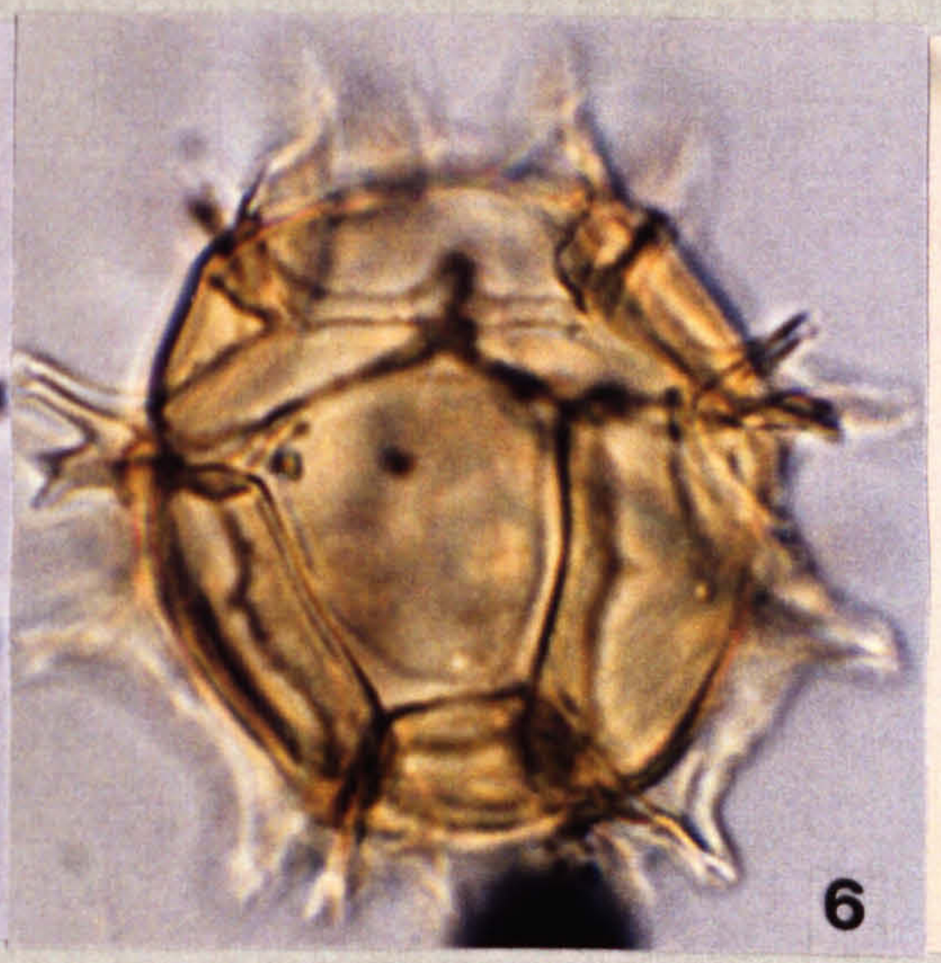
6


4


7


8


9

Plate 19

All photomicrographs taken at x 1025 magnification, unless otherwise stated.

Figs 1,2. *Pterodinium cingulatum* (Davey and Williams) subspecies *reticulatum* Lentin and Williams 1981
Site 3A 90 T46 (Same specimen as Pl. 18, Fig. 9)
Oblique dorso-ventral views, showing thick negative reticulate endophragm.

Figs 3-5. *Pterodinium cingulatum* (Clartke and Verdier) subspecies *polygonalis* Lentin and Williams 1973 *stat. nov.*
Fig. 3. Site 3A 85 C26
Oblique dorso-ventral view, showing polygonal nature of parasutural crests.
Fig. 4. MCB 2.5 --> 3 E41/2
Dorsal view showing precingular archaeopyle.
Fig. 5 MCB 0 --> -0.5 N23/1
Dorsal view, showing P Type archaeopyle still in place.

Figs 6,7. *Pterodinium ? cornutum* Cookson and Eisenack
MCB -3.5 --> -4 S15 x 1535 magnification
6. Low focus shot of ventral surface, showing S-type ventral arrangement.
7. High focus shot of dorsal surface of same specimen.

Figs 8,9. *Rhiptocorys veligera* (Deflandre) Lejeune-Carpentier 1983
Site 3A 85 053/3
8. Low focus shot of oblique ventral view, showing parasutural crest.
9. High focus shot of oblique dorsal view, showing large hypocyst in comparison to epicyst.

PLATE 19

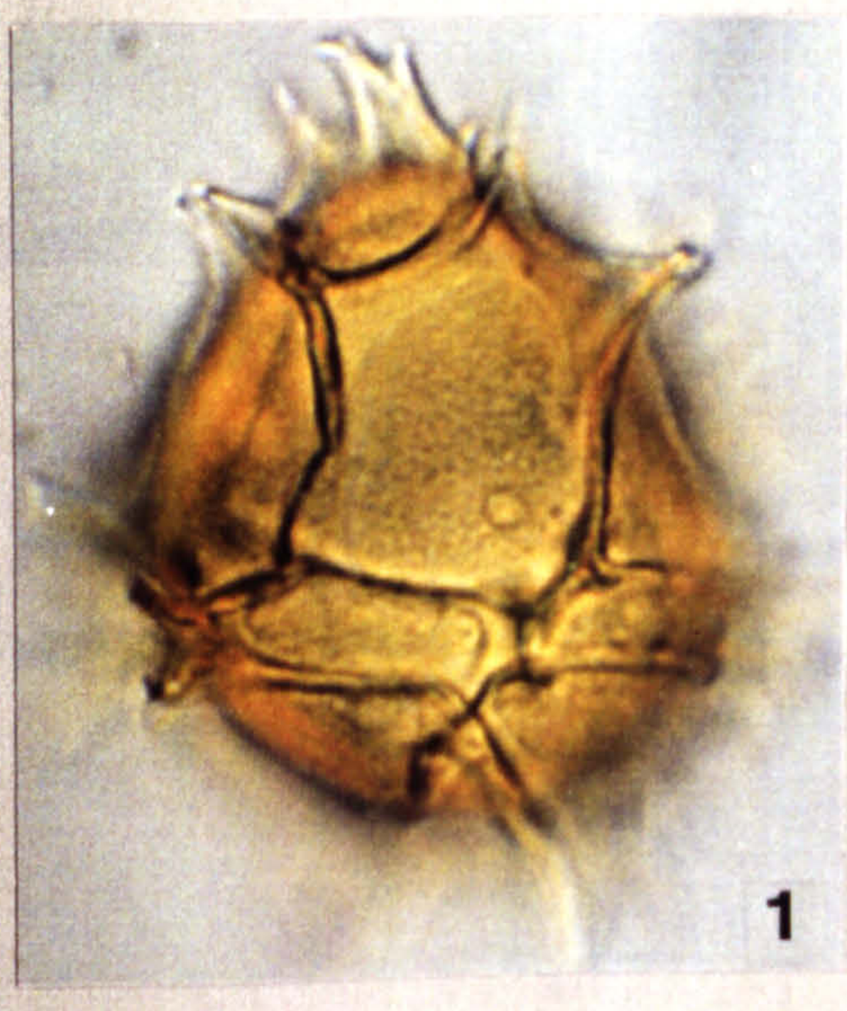
1


2

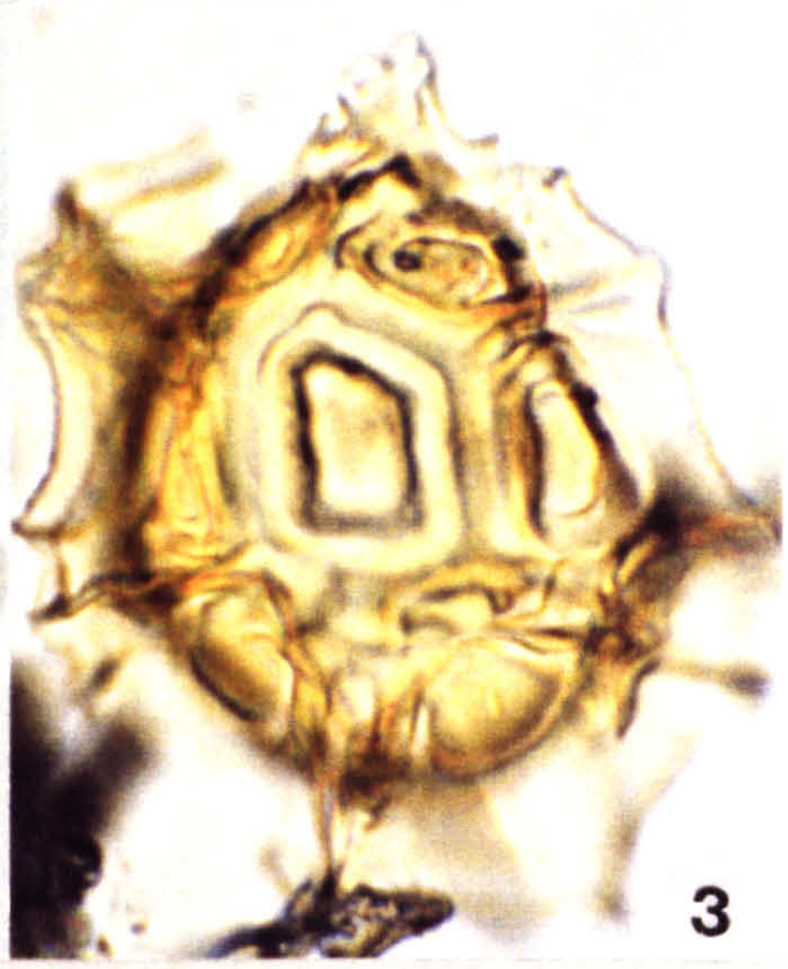
3

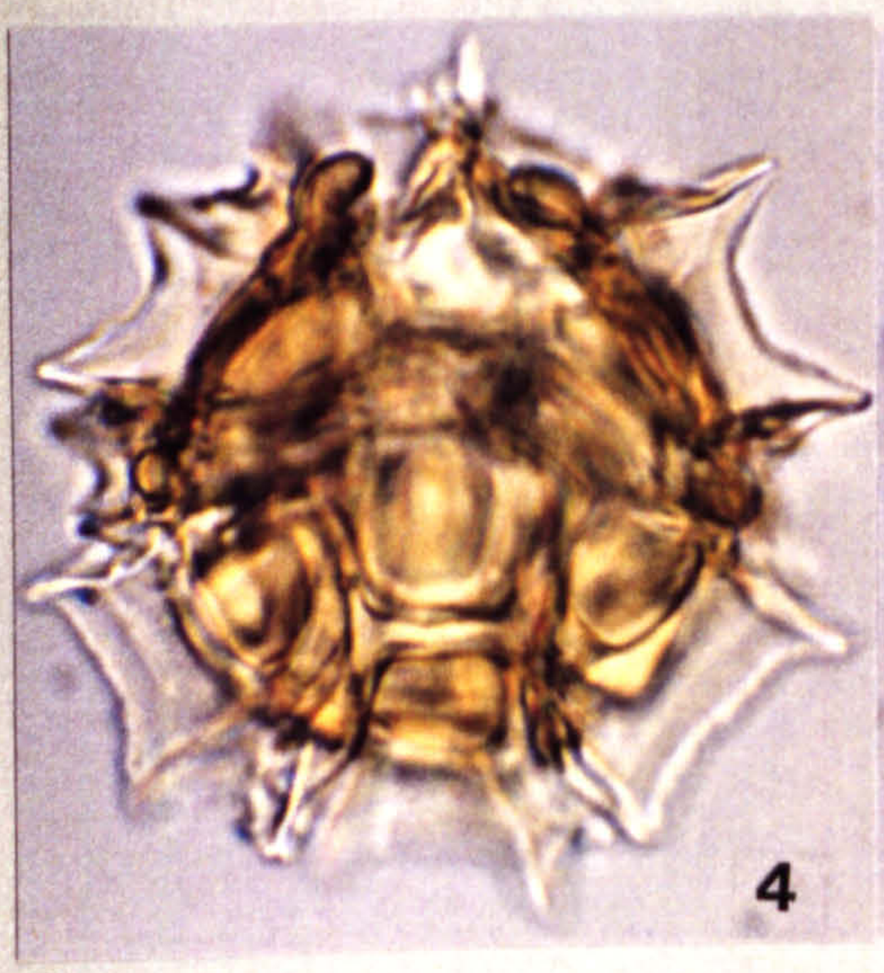
4

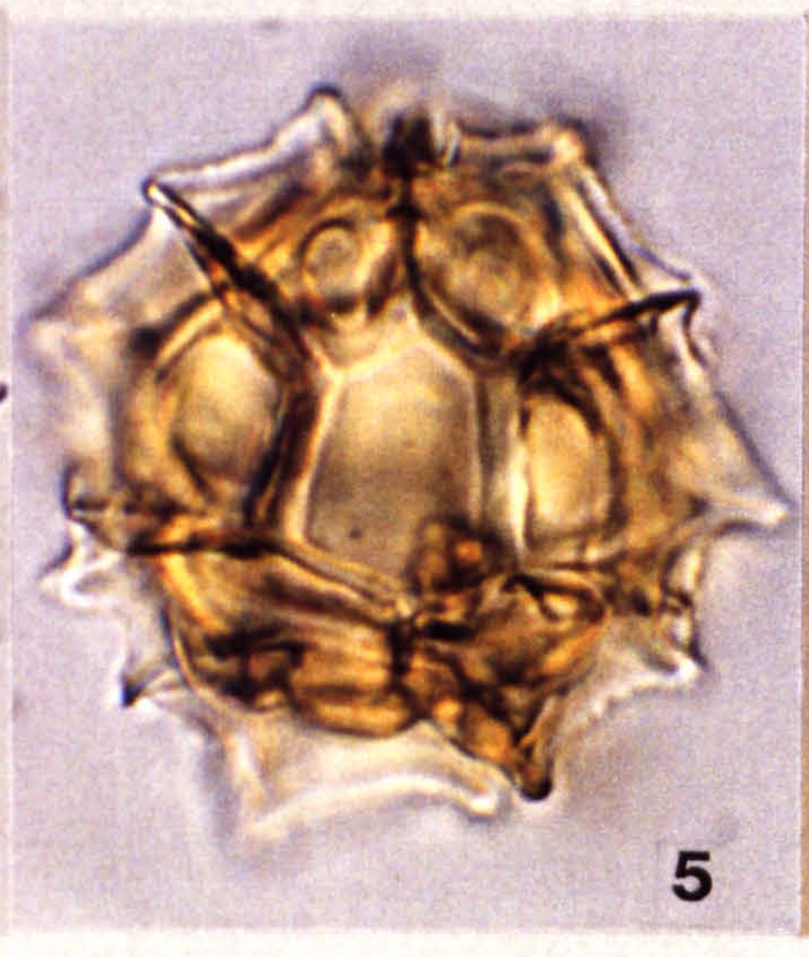
5

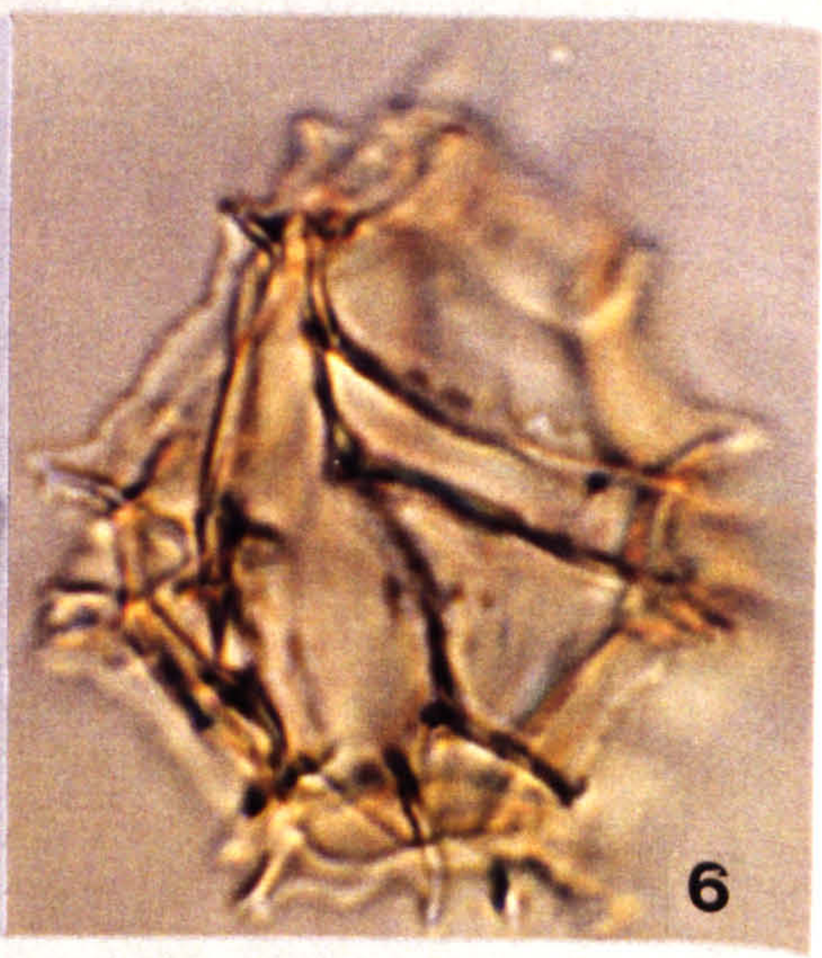
6

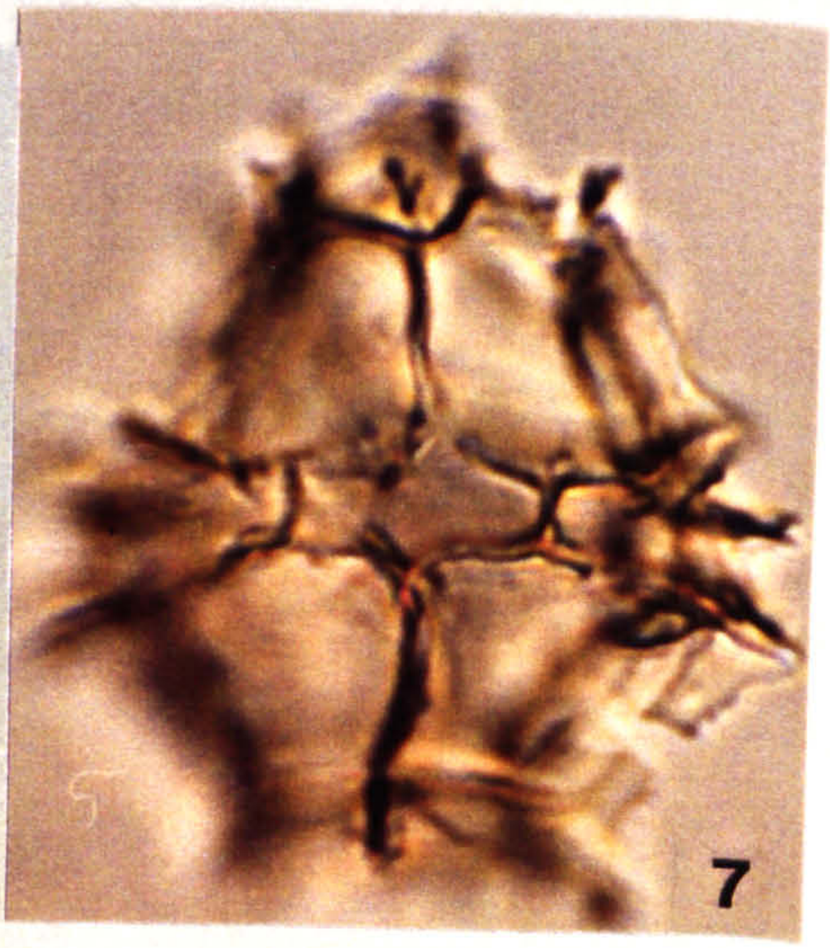
7

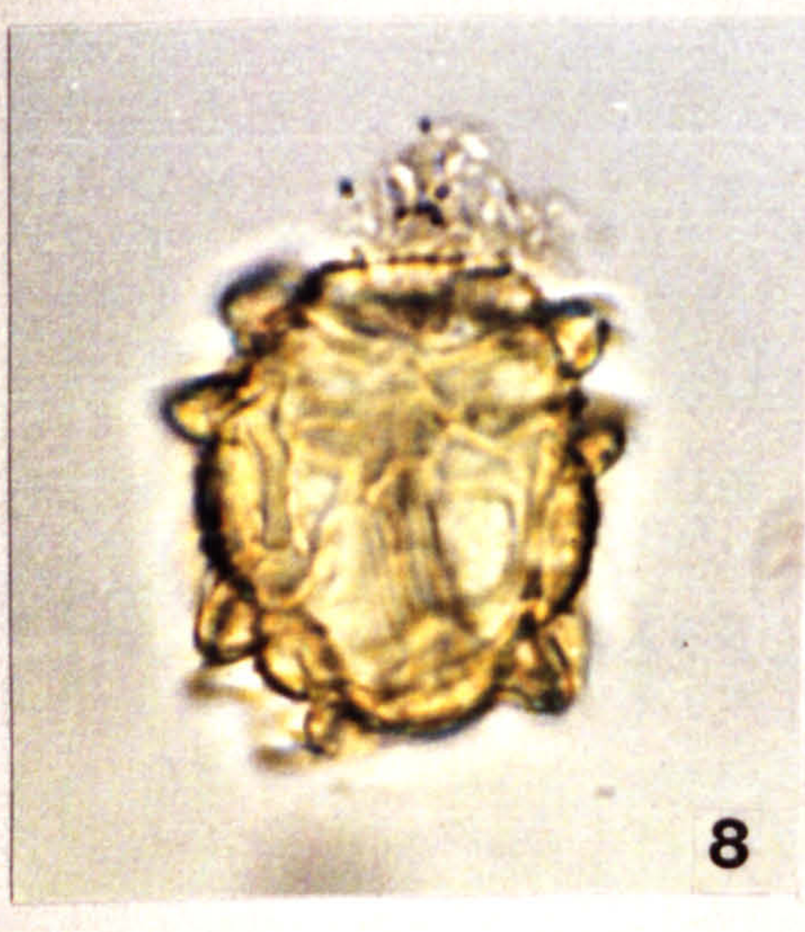
8


9

Plate 20

Figs 1,2. *Spiniferites ? dentatus* (Gocht) Lentin and Williams 1973

Site 3A 90 P39 x 1025 magnification

1. High focus shot of ventral surface, showing S-type ventral arrangement.

2. Low focus shot of dorsal surface of same specimen, showing reduced P-Type archaeopyle.

Figs 3,4. *Spiniferites multibrevis* (Davey and Williams) Below 1982

Site 3A 0 Q20/2 x 1025 magnification

3. Low focus shot of dorsal surface, showing reduced P-Type archaeopyle and short gonal and intergonal processes.

4. High focus shot of ventral surface of same specimen, showing S-type paracinguluar and parasulcal arrangement.

Figs 5-8. *Spiniferites ramosus* (Ehrenberg) Loeblich and Loeblich subspecies *ramosus* Davey and Williams 1966a

Figs 5,6. TBB4 N36/2 x 675 magnification

5. High focus shot of dorsal surface showing precingular archaeopyle of ovoidal-shaped group.

6. Low focus shot of ventral surface of same specimen.

Figs 7,8. Site 3A 0 S44 x 675 magnification

7. Low focus shot of dorsal surface, showing P-Type archaeopyle of angular-shaped group.

8. High focus shot, showing oblique view of same specimen.

PLATE 20

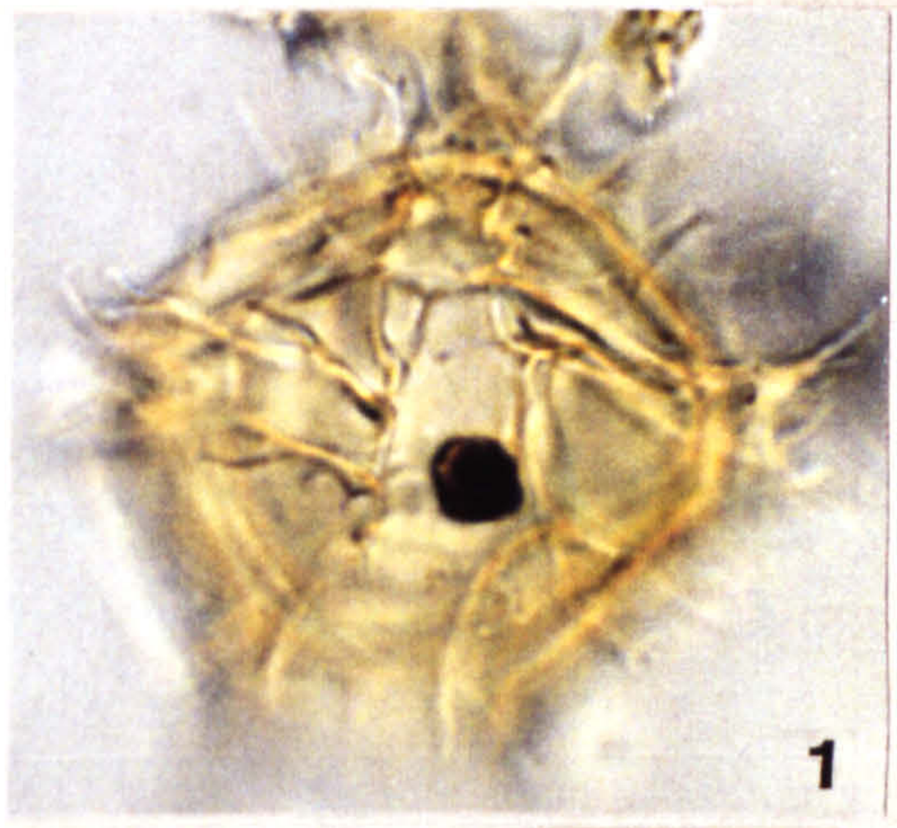
1

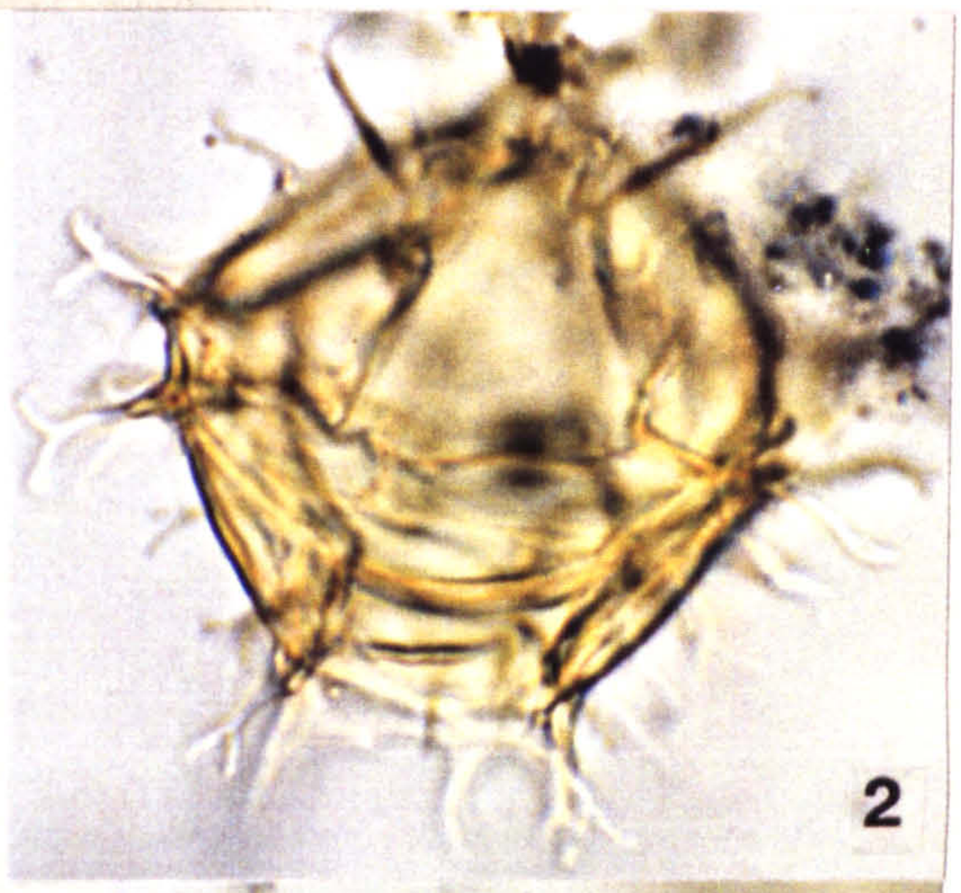
2

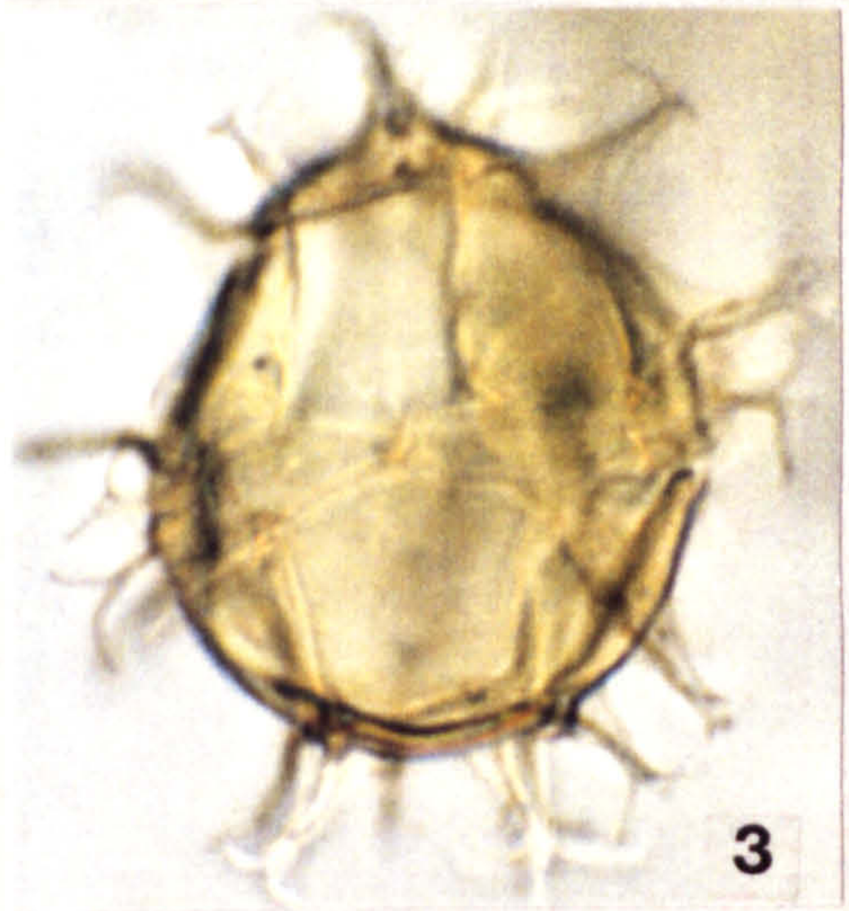
3

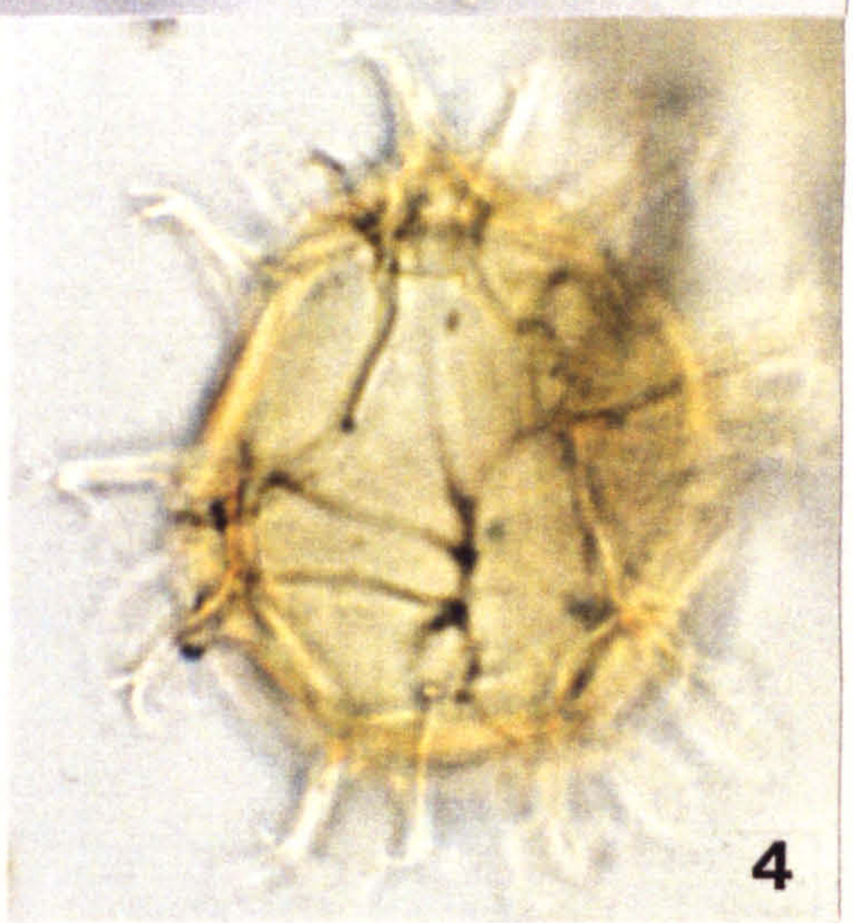
4

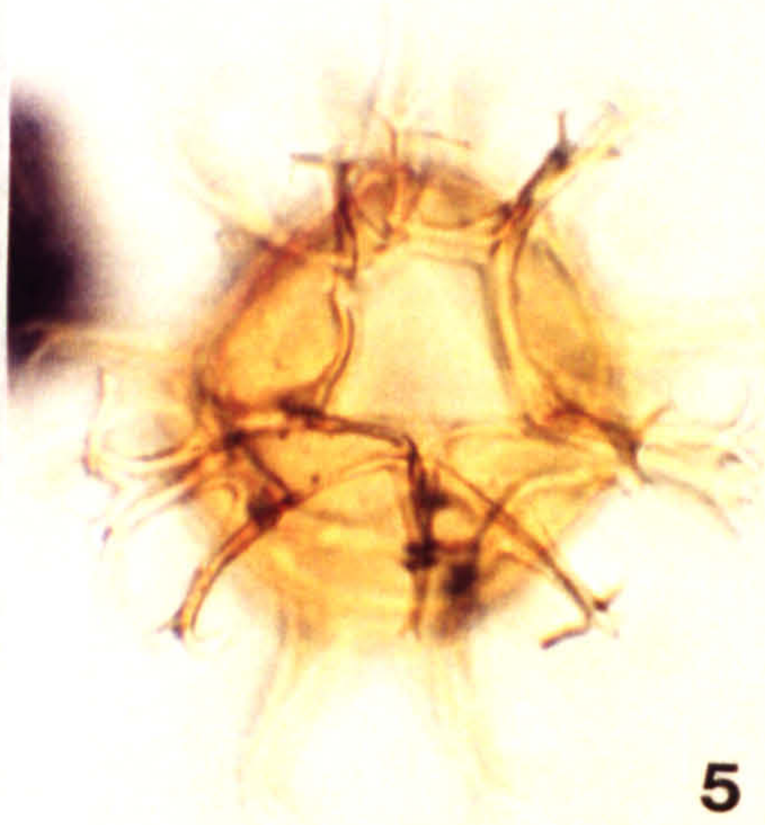
5


6

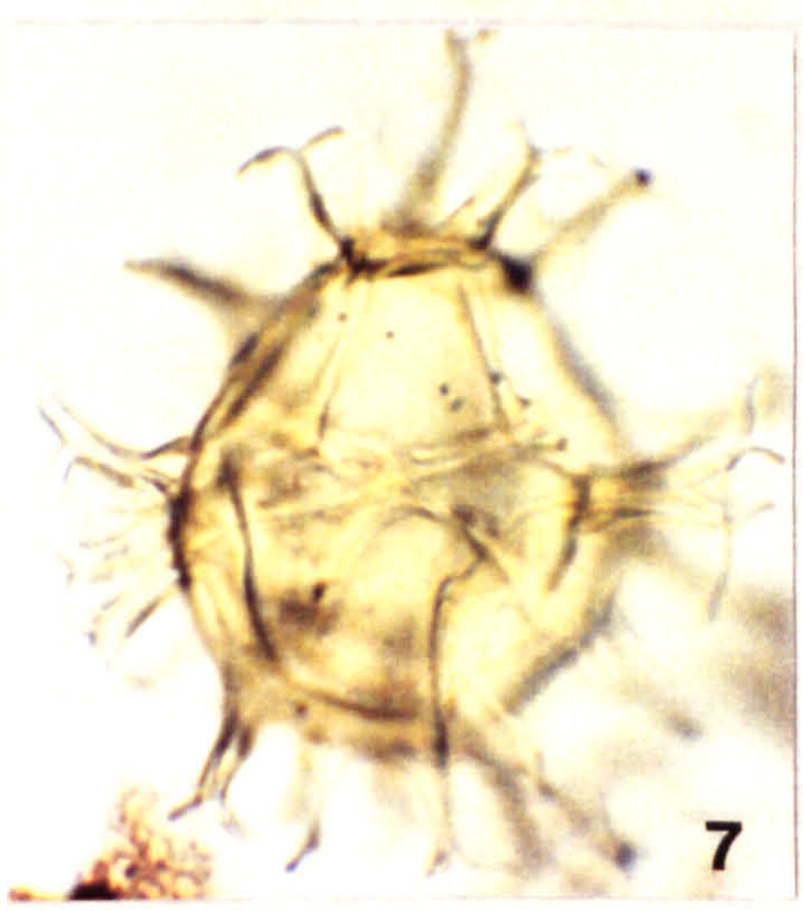
7


8

Plate 21

All photomicrographs taken at x 675 magnification, unless otherwise stated.

Figs 1,2. *Spiniferites ramosus* (Ehrenberg) Loeblich and Loeblich subspecies *reticulatus* (Davey and Williams) Lentin and Williams 1973
Site 3A 85 S27/4 x 1025 magnification
1. Low focus shot of dorsal surface, showing reticulate nature of endophragm.
2. High focus shot of dorsal surface of same specimen, showing reduced P-Type archaeopyle.

Fig 3. *Spiniferites ramosus* (Ehrenberg) Loeblich and Loeblich subspecies *gracilis* (Davey and Williams) Lentin and Williams 1973
Oblique dorso-ventral view, showing long, slender processes.
TBB -3Paly F35/4

Figs 4-6. *Stephodinium coronatum* Deflandre 1936a
Fig. 4. MCB -1.5 --> -2 032
Apical-antapical compressional view showing precingular archaeopyle and maximum pericoel development in the dorsal area.
Fig. 5 TBB4 V34/2
Dorsal view of dorso-ventral compression, showing precingular archaeopyle and apical horn.
Fig. 6. MCB -3 --> 3.5 U19
Dorso-ventral compression in dorsal view, showing precingular archaeopyle and large periocoel.

PLATE 21


1

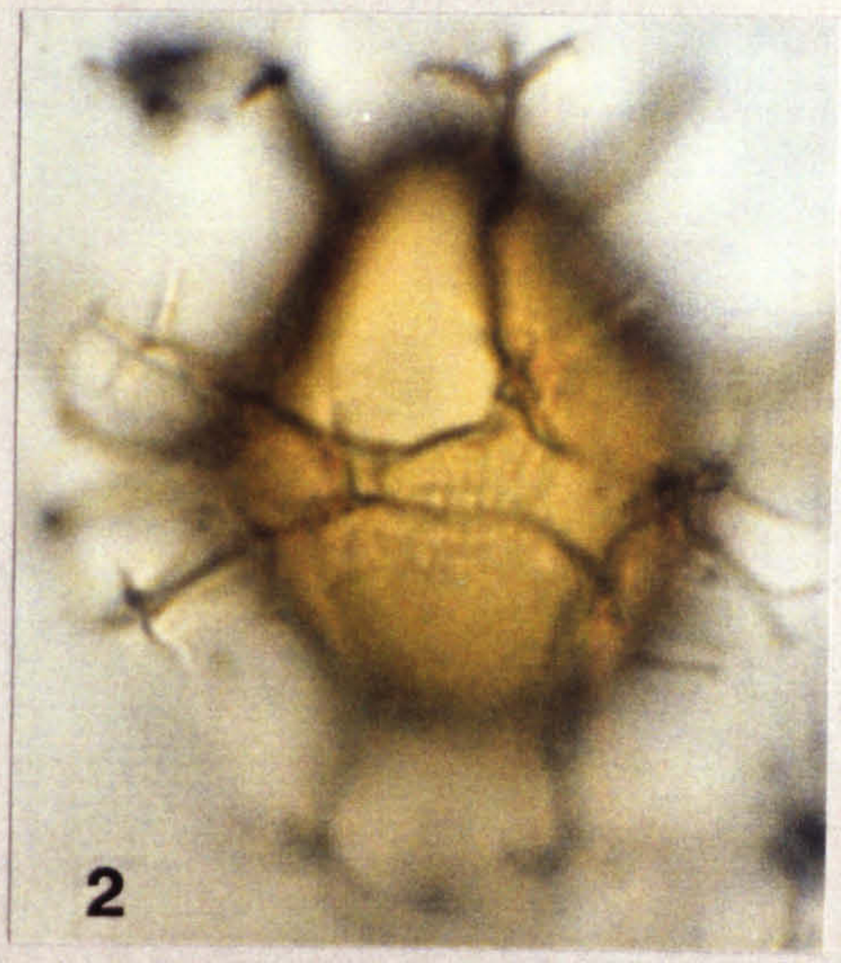
2

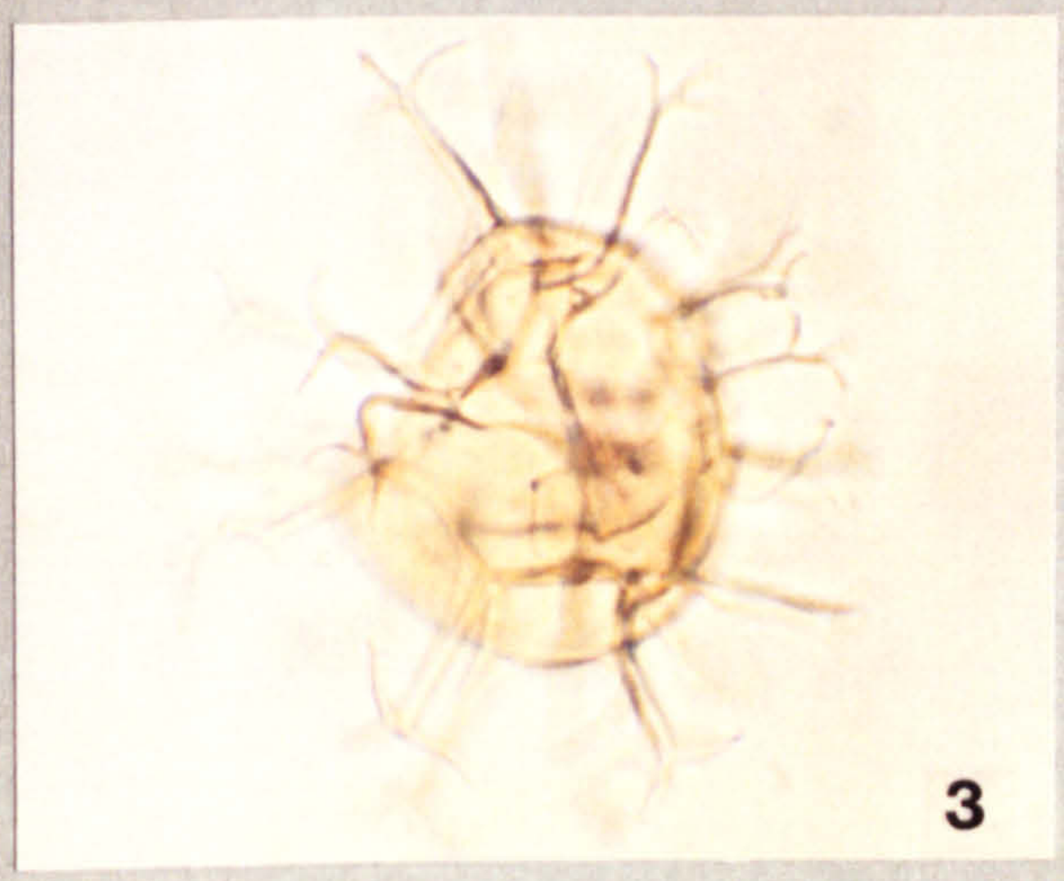
3

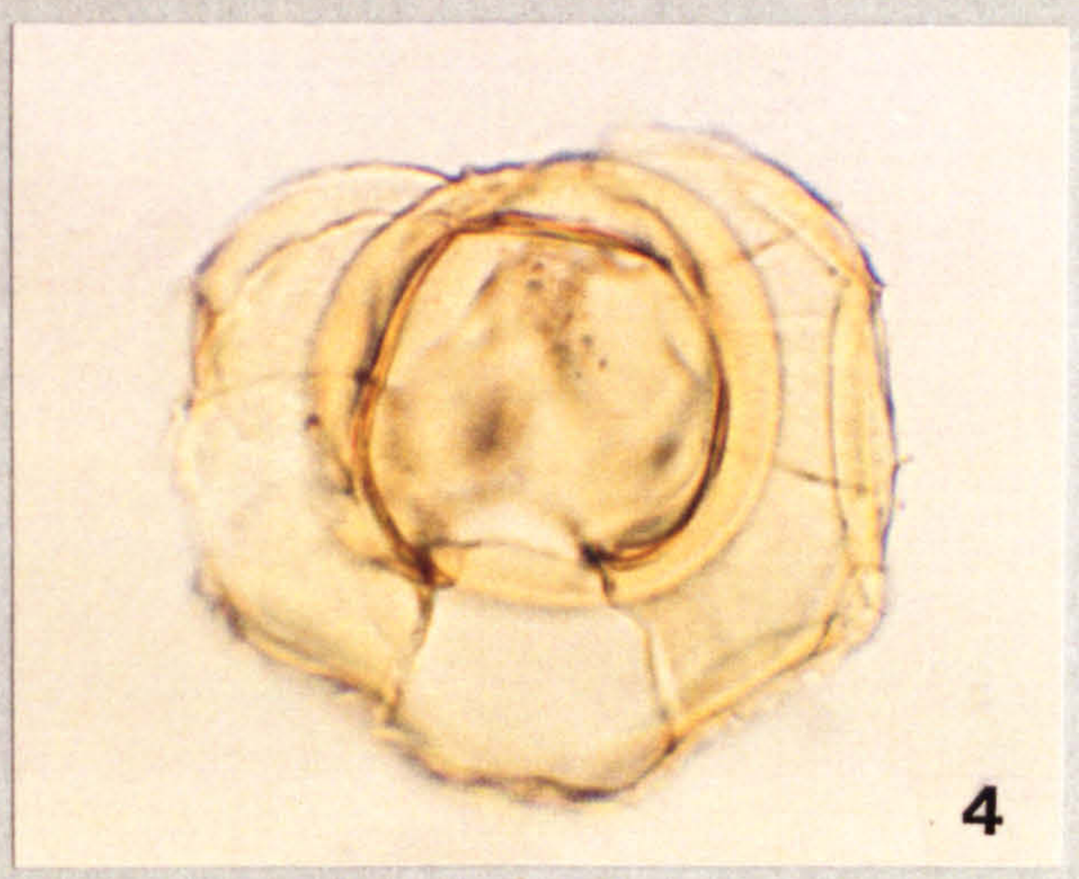
4

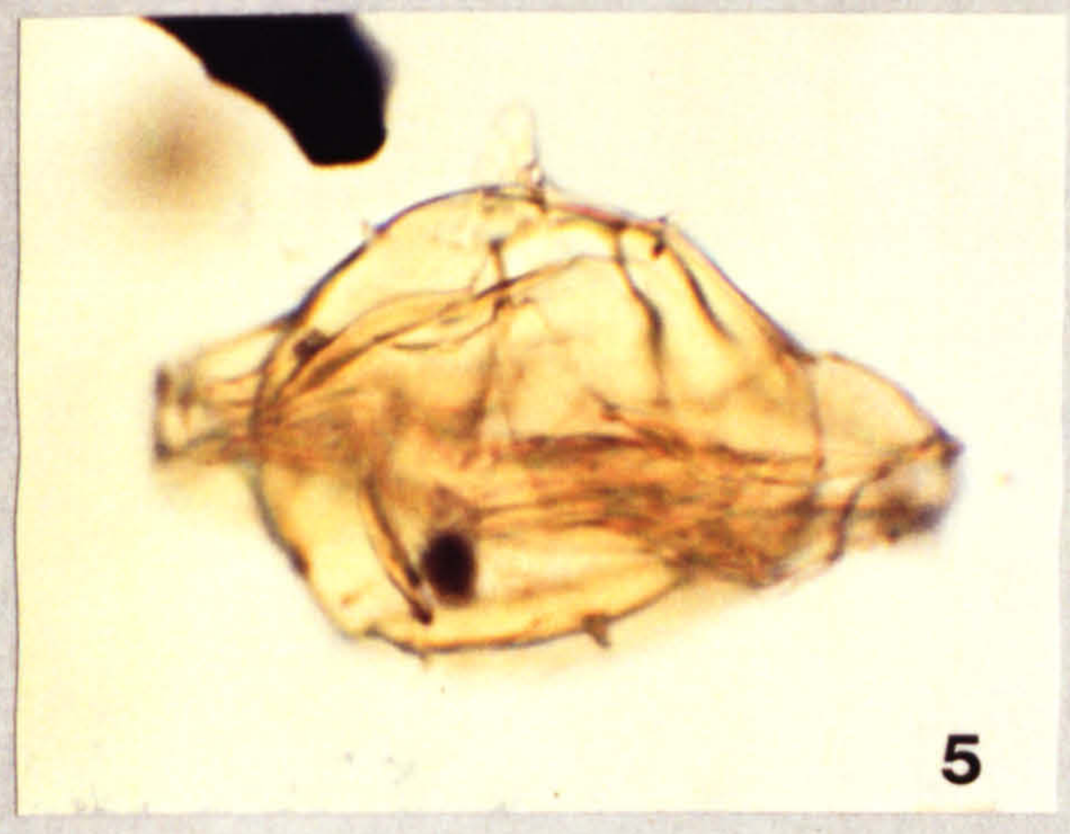
5

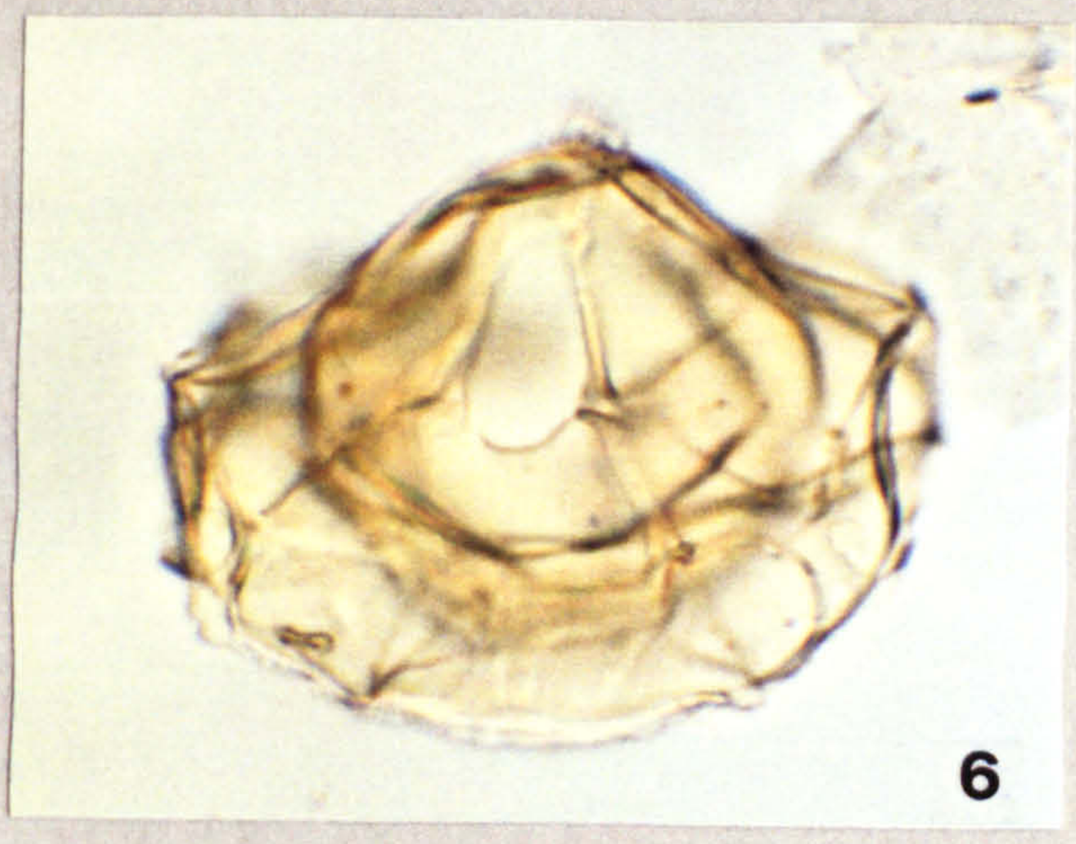
6

Plate 22

All photomicrographs taken at x 1025 magnification.

Fig. 1. *Subtilisphaera pontis-mariae* (Deflandre) Lentin and Williams 1976
?Ventral surface showing paracingulum, apical and antapical horns.
SFE 18A1 035/1

Fig. 2. *Surculosphaeridium longifurcatum* (Firtion) Davey *et al.* 1966
Dorso-venrtral orientation, showing apical margin and intratabular processes.
TBB 5 E45

Fig. 3. *Tanyosphaeridium variecalamus* Davey and Williams 1966
Dorso-ventral orientation, showing non-tabular, tubiform to buccinate processes.
MCB 4.5 --> 5 033 DIC

Fig. 4. *Surculosphaeridium spinicongregatum* Yun 1981
Oblique view, showing low relief, broad based processes.
TBB -2 T38/1

Figs 5,6. *Trichodinium castanea* (Deflandre) Clarke and Verdier 1967
Site 3A 0 E47/3
5. High focus shot of dorsal surface showing precingular archaeopyle and paracingular parasutures.
6. Low focus shot of ventral surface of same specimen.

Figs 7,8. *Valensiella ovulum* (Deflandre) Eisenack 1963
Site 3A 90 N33
7. Low focus, oblique orientation showing general morphology.
8. High focus of same specimen, showing an apical archaeopyle margin.

PLATE 22


1

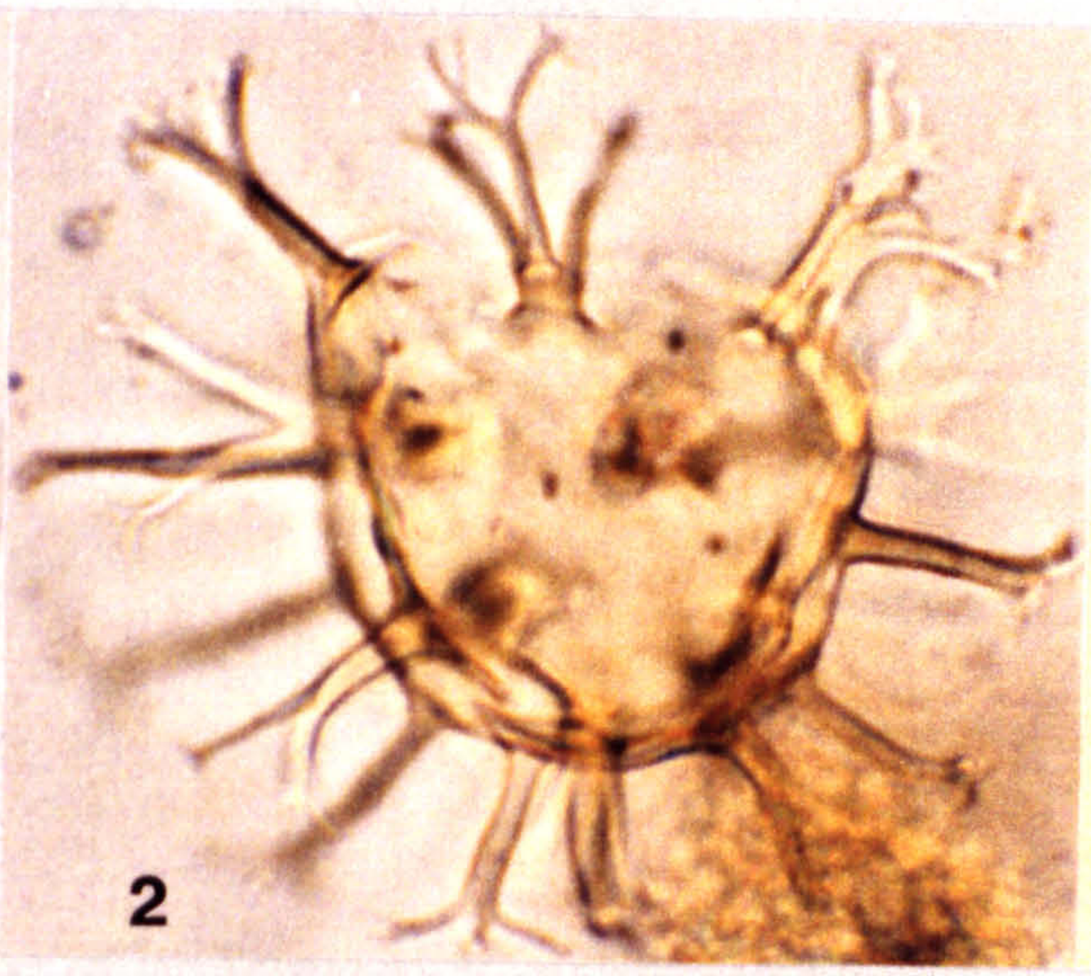
2


3


4

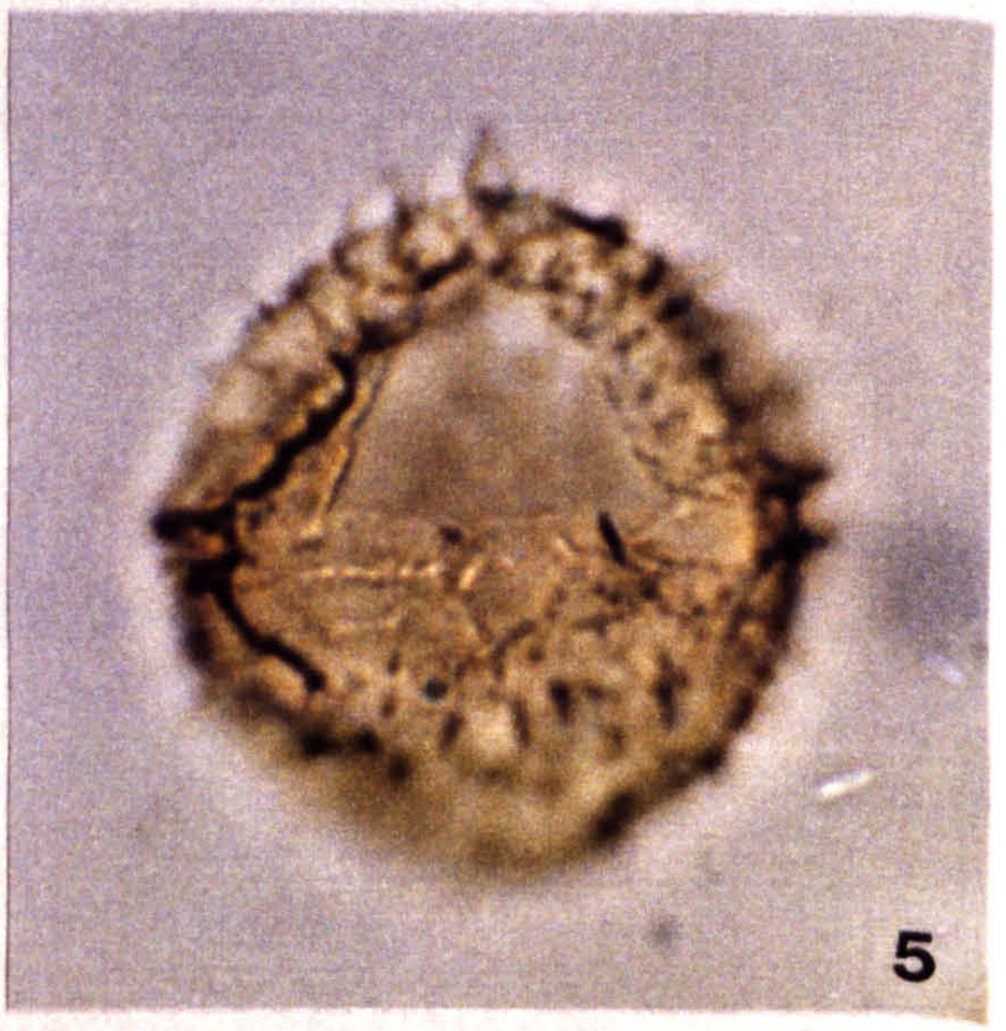
5


7


8

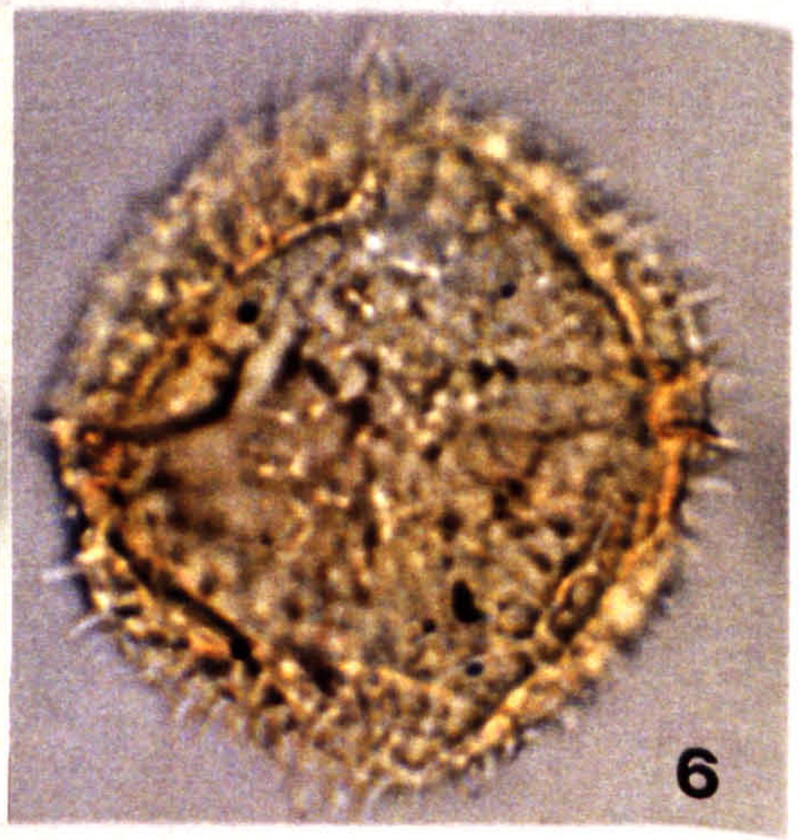
6

Plate 23

All photomicrographs taken at x 675 magnification.

Fig. 1. *Wallodinium anglicum* (Cookson and Hughes) Lentin and Williams 1973

?Left lateral view, showing lunate morphology of cyst, with maximum development of pericoel in the antapical and ?dorsal areas.

MCB -4 --> -4.5 J40/2

Fig. 2. *Xenascus esbeckianus* Yun 1981

Dorsal view, showing antapical and lateral horns.

MCB -0.5 --> -1 D34/2

Figs 3,4. *Xiphophoridium alatum* (Cookson and Eisenack) Sarjeant 1966

Fig. 3. Site 3A 0 R44/4

Dorso-ventral view, showing high parasutural flanges and presence of tubules.

Fig. 4. MCB 4.5 --> 5 S36

?Dorsal view with archaeopyle still in place, showing high parasutural flanges, themselves carrying spines.

Figs 5-7. *Xiphophoridium* sp. A

Fig. 5. Site 3A 90 P28

Apical-antapical compressional view, showing circumferential paracingular crests.

Fig. 6. Site 3A 60 M32

Dorso-ventral view, showing paracingular parasutural crests.

Fig. 7. Dorso-ventral view, showing high parasutural crests denoting the paratabulation.

PLATE 23

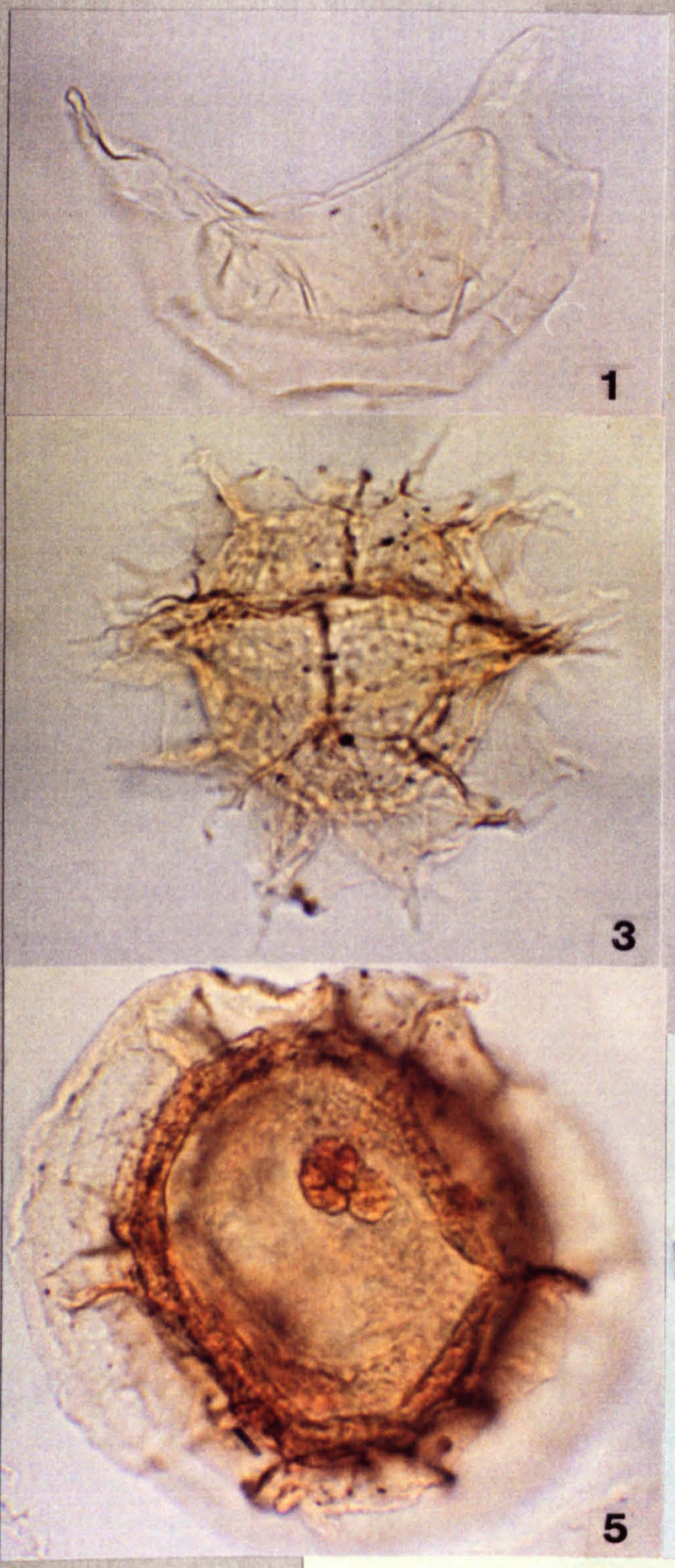
1

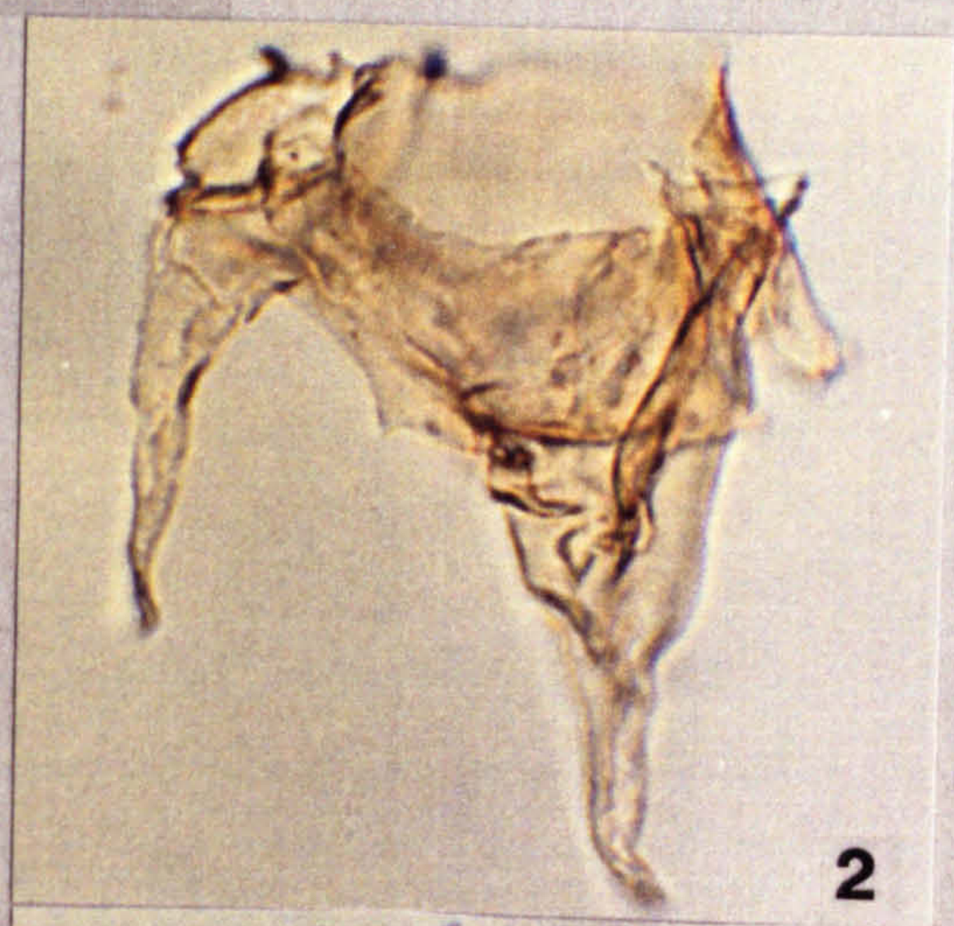
2

3

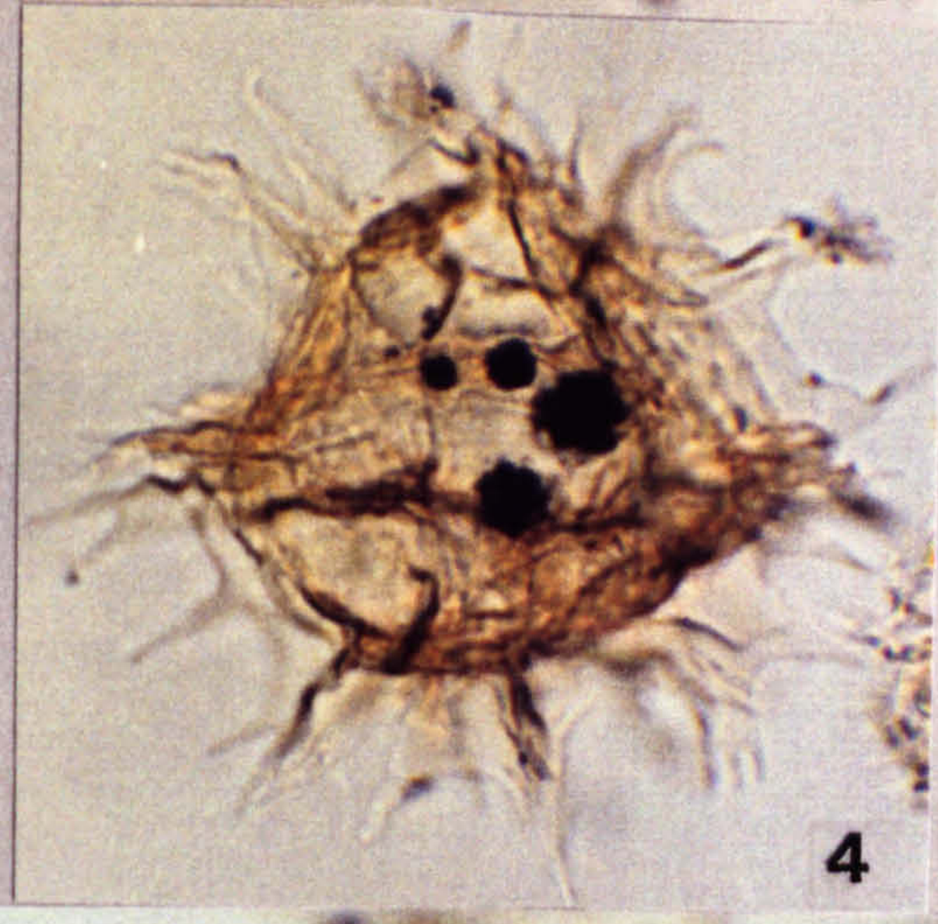
4

5


6

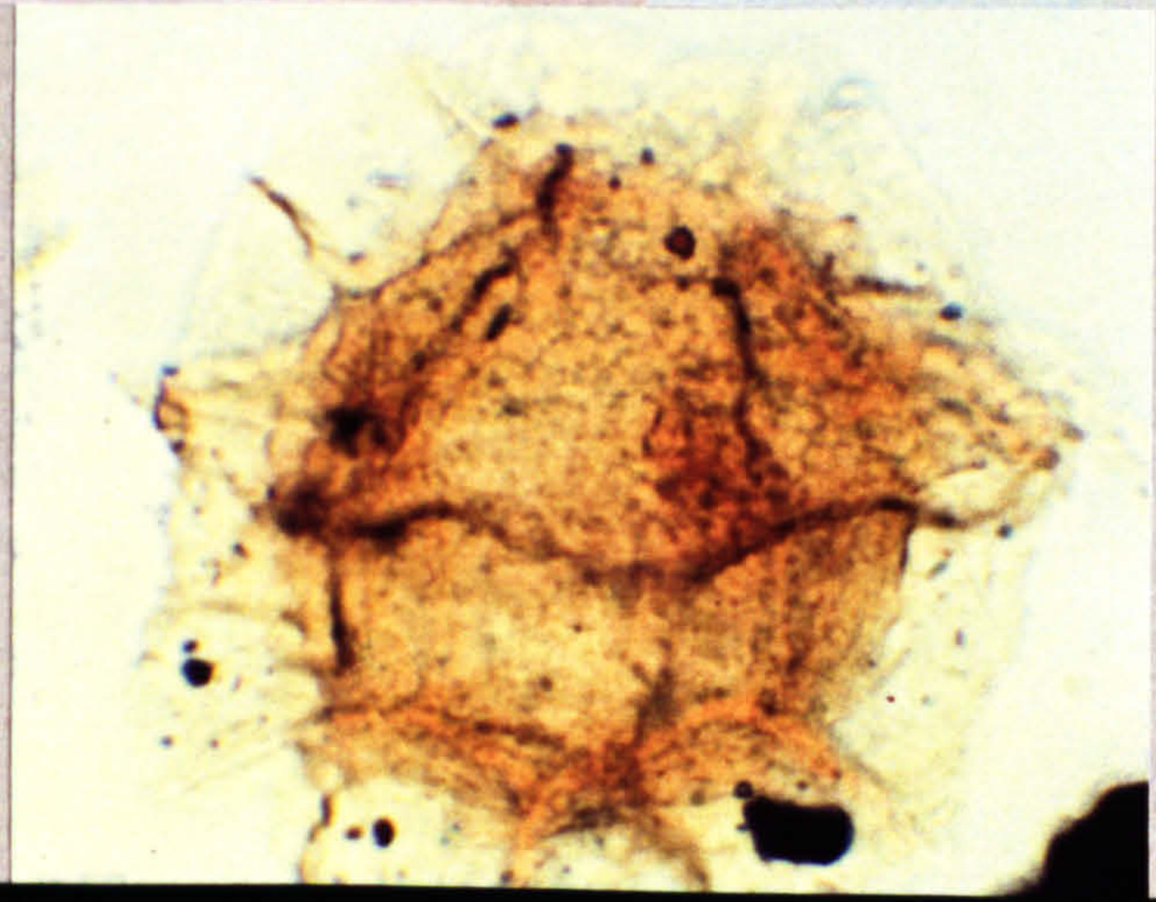

Plate 24

All photomicrographs taken at x 1025 magnification.

Figs 1-3. Cyst Type A

Fig. 1 SFE 15 P42/1

?Dorso-ventral compression, showing overall morphology of the cyst and reticulate nature of the wall surface.

Fig. 2. SFE 15 K36/2

?Dorso-ventral compressional orientation, showing longitudinal folds.

Fig. 3. SFE 15 K29

?Dorso-ventral view with longitudinal folds evident.

Figs 4-6. Cyst Type B

Fig. 4 SFE 18A1 R37/4

?Oblique view, showing bulbous nature of the ornament.

Figs 5,6. SFE 18A1 J33

5. Low focus shot of oblique view, showing the general morphology.

6. High focus of same specimen with bulbous ornament evident.

PLATE 24

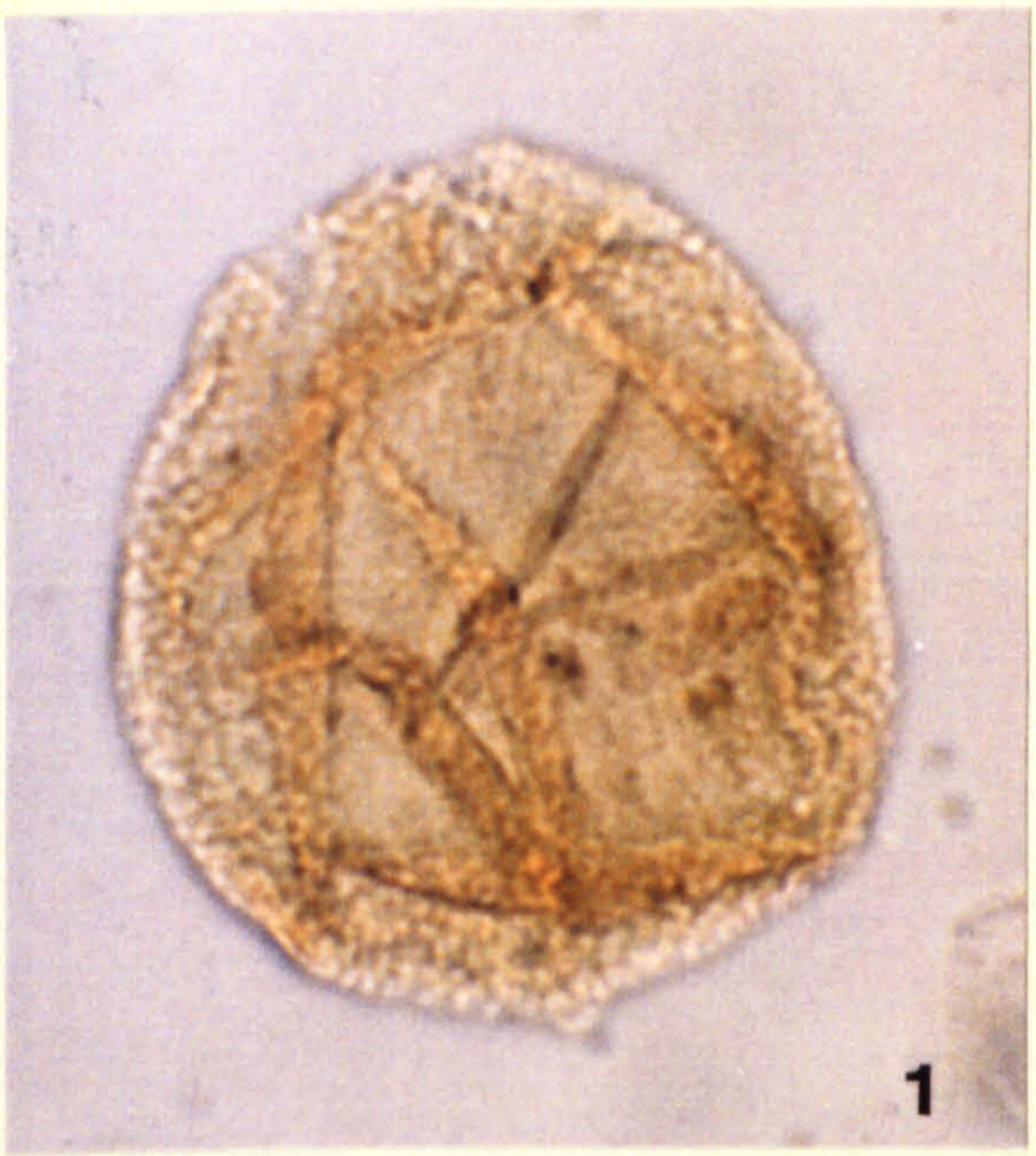
1

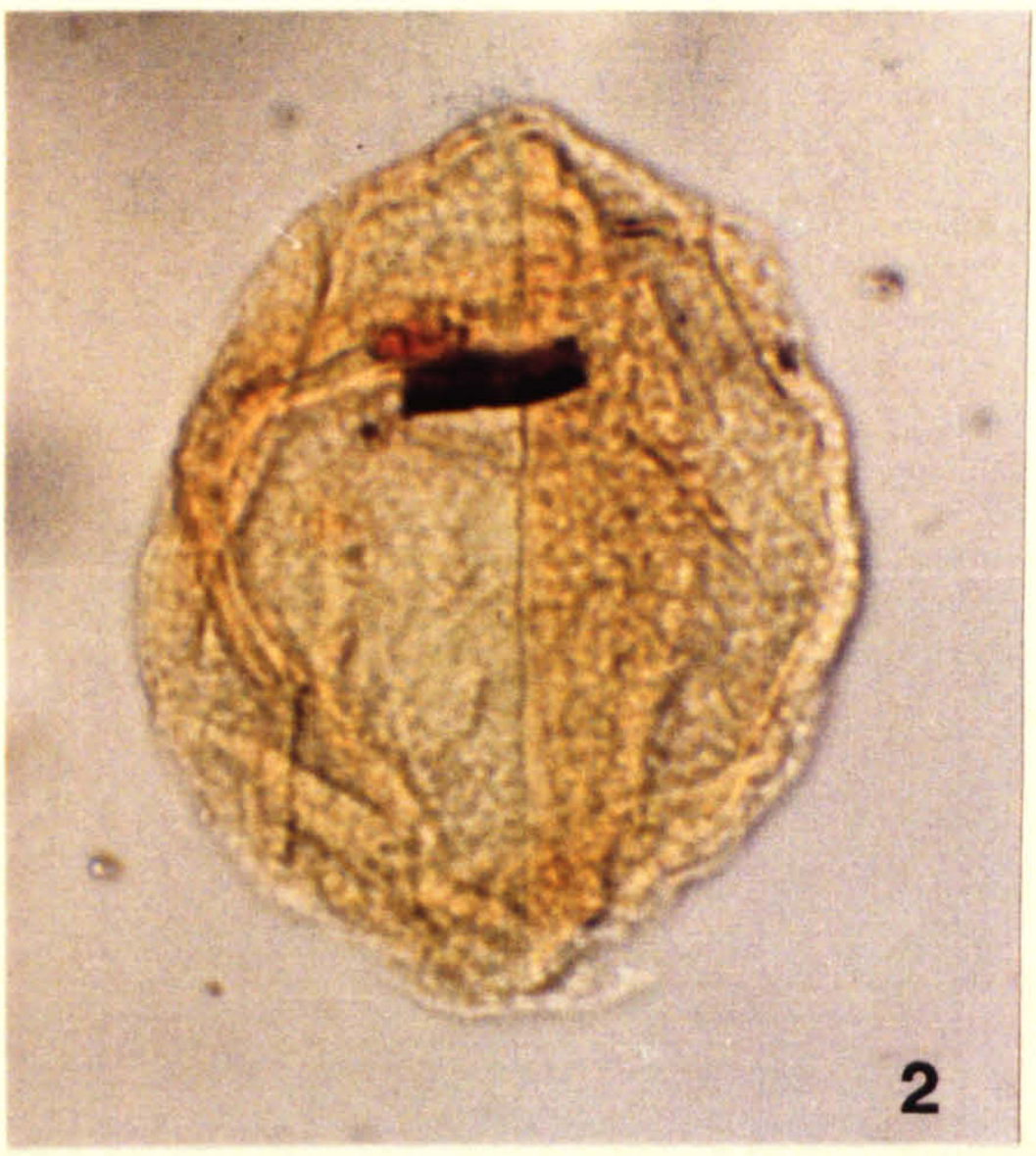
2

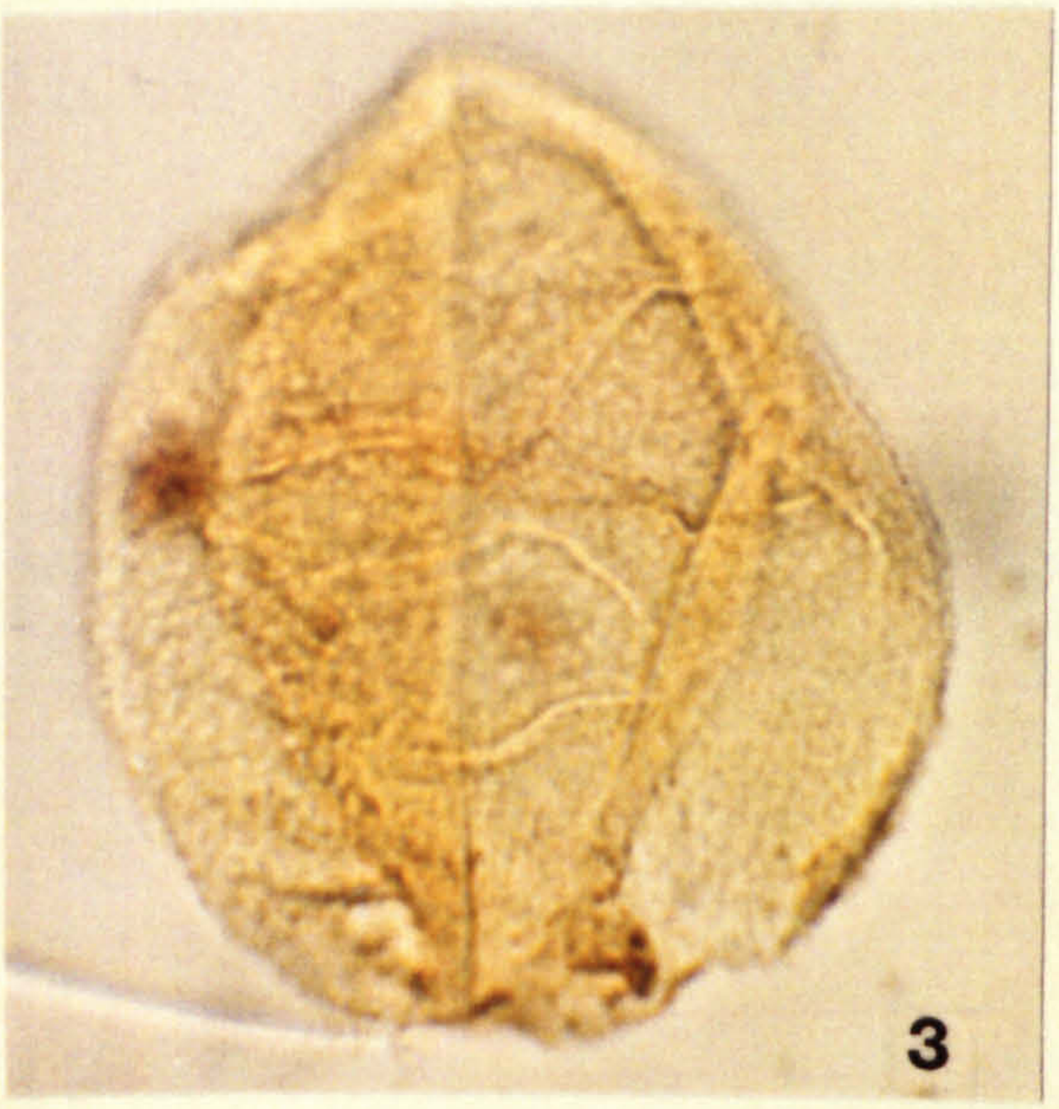
3

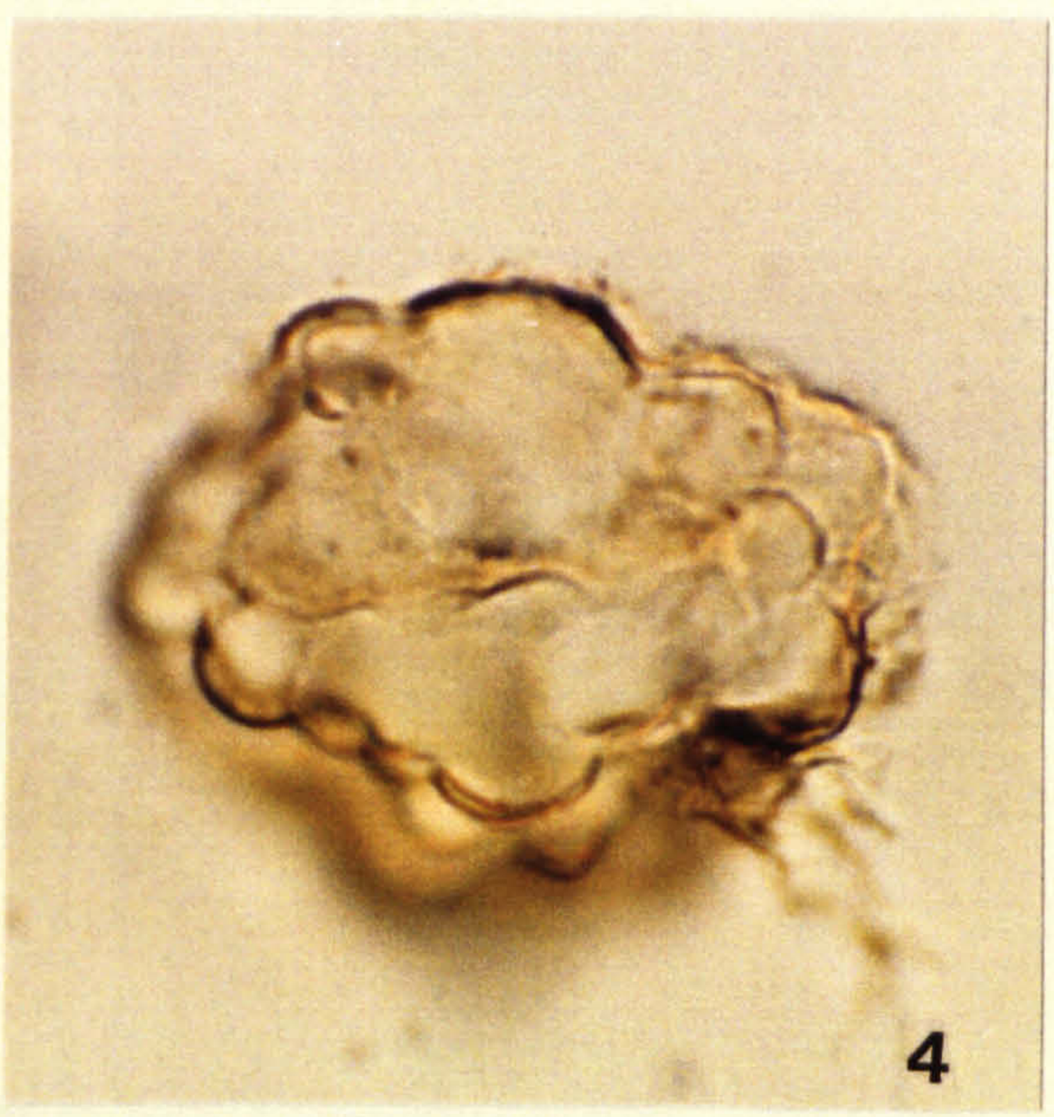
4

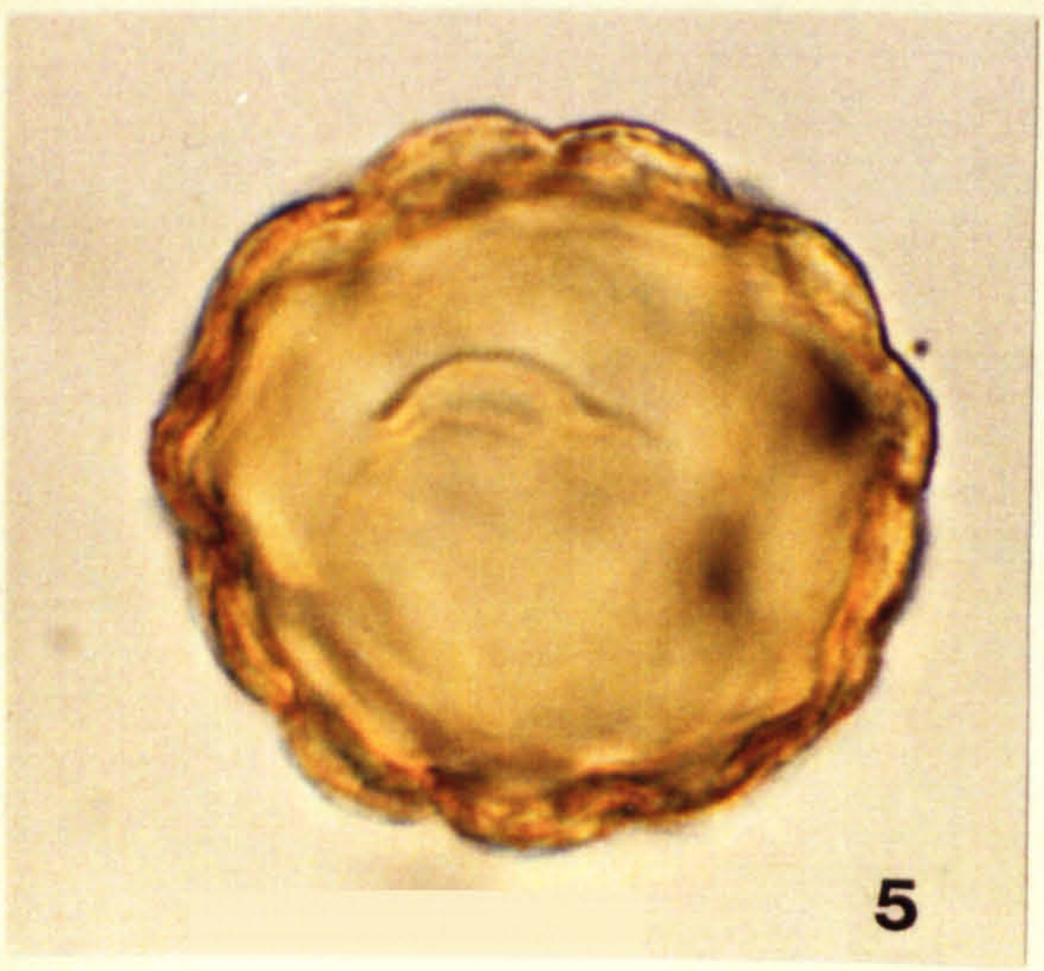
5

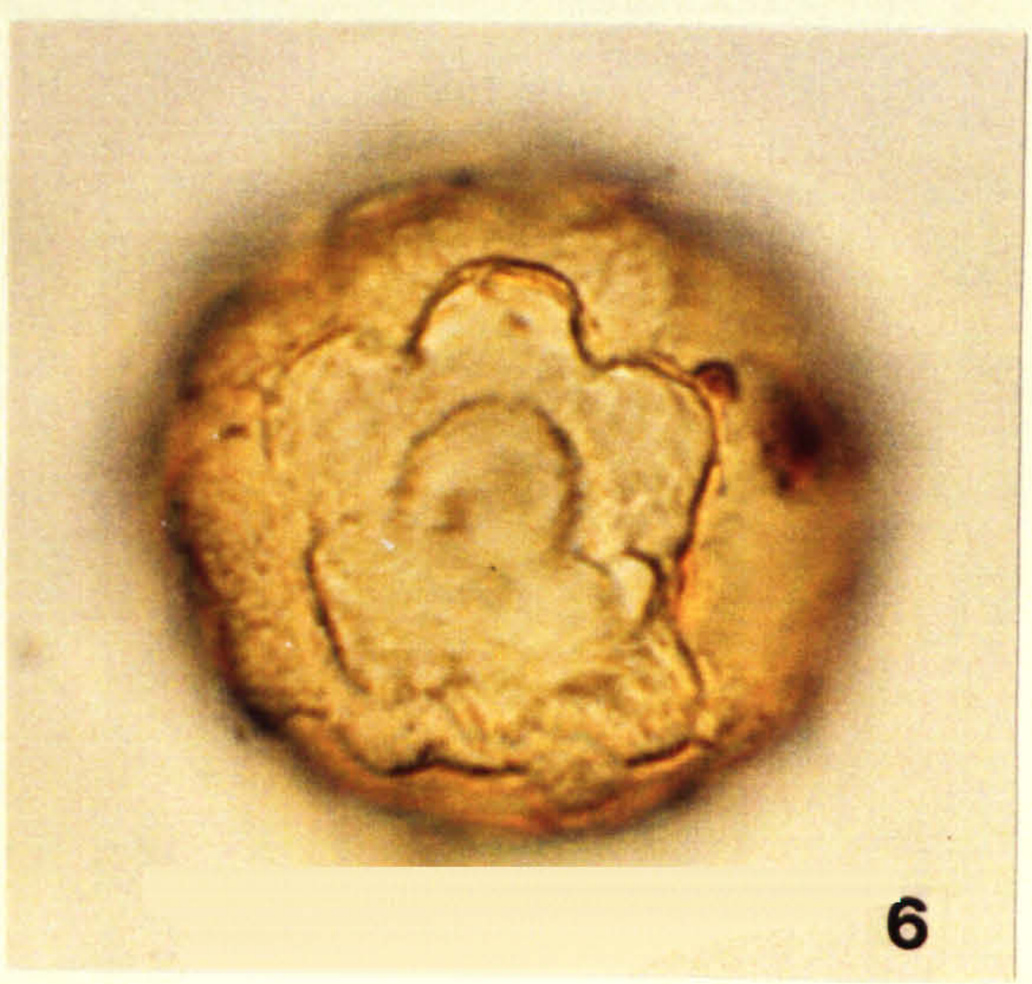
6

Plate 25

All photomicrographs taken at x 1025 magnification, unless otherwise stated.

Figs 1-8. Variation seen in spore morphology

Fig. 1. MCB -3.5 --> -4. T47/3 x 1535 magnification

Fig. 2. SFE 16A1 P45

Fig. 3. Site 3A 0 F26

Fig. 4. TBB -2 Q43

Fig. 5. Site 3A 0 W39/2

Fig. 6. TBB -30x M42/4

Fig. 7. Site 3A 60 O35/3

Fig. 8. MCB 1.5 --> 2A1 D41

PLATE 25

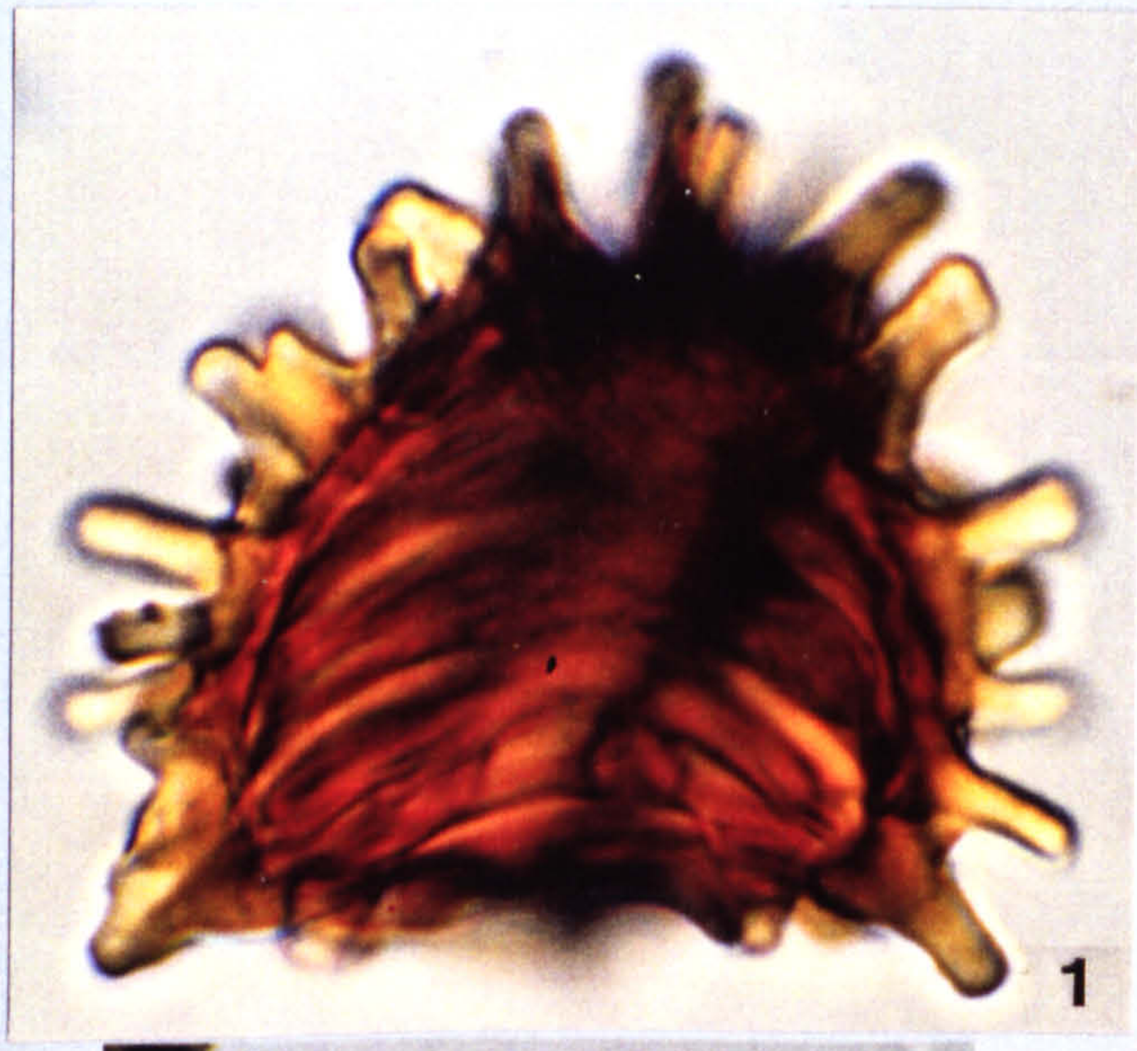
1

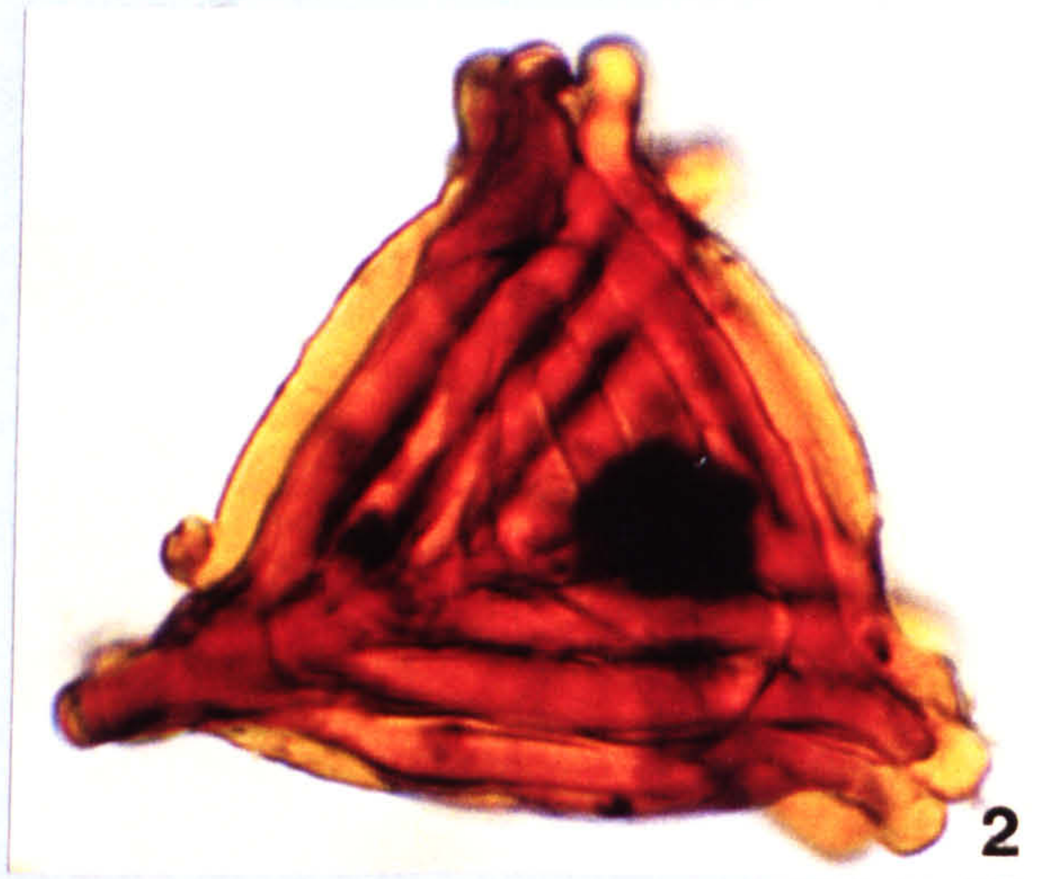
2

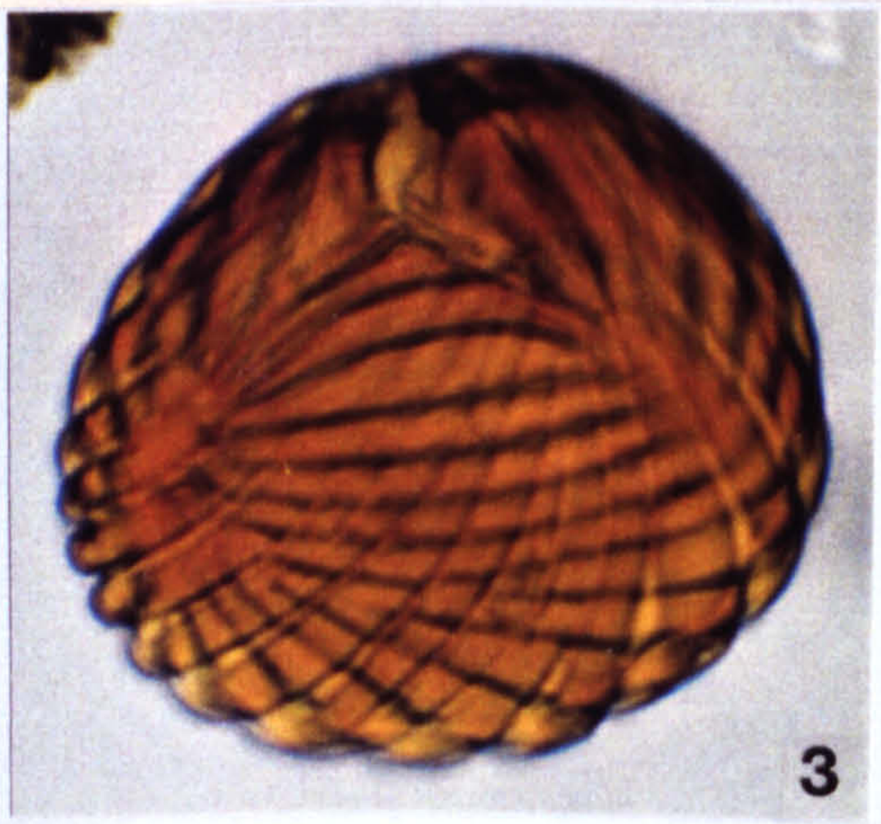
3


4


5


6

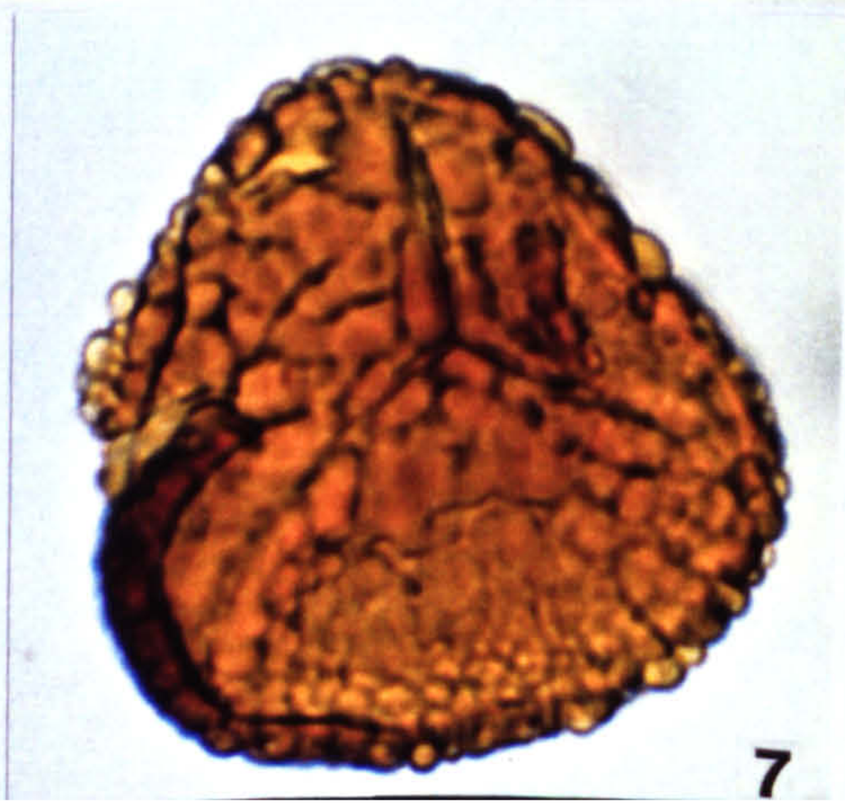
7

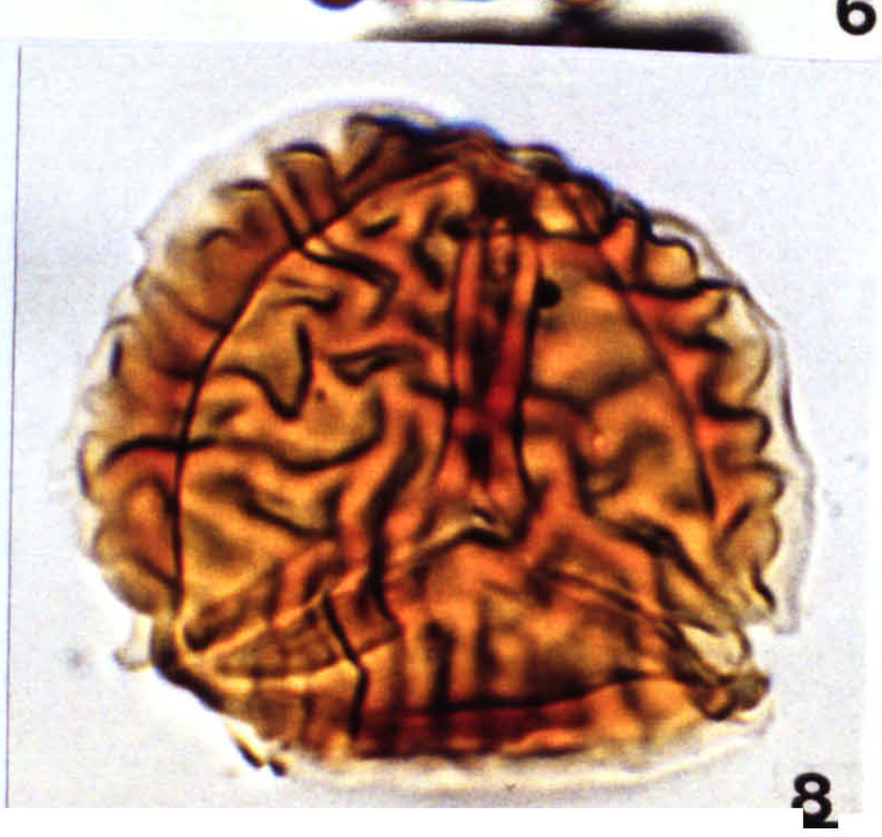
8

Plate 26

All photomicrographs taken at x 1025 magnification.

Figs 1-8. Variation seen in spore morphology

Fig. 1. Site 3A 85 E23/3

Fig. 2. Site 3A 105 A38/1

Fig. 3. Site 3A 85 D32/4

Fig. 4. Site 3A 120A1 A25/1

Fig. 5. Site 3A 0 N27

Fig. 6. MCB 4 --> 4.5 M28

Fig. 7. TBB 11 O50

Fig. 8. Spore tetrad Site 3A 85 L29

PLATE 26

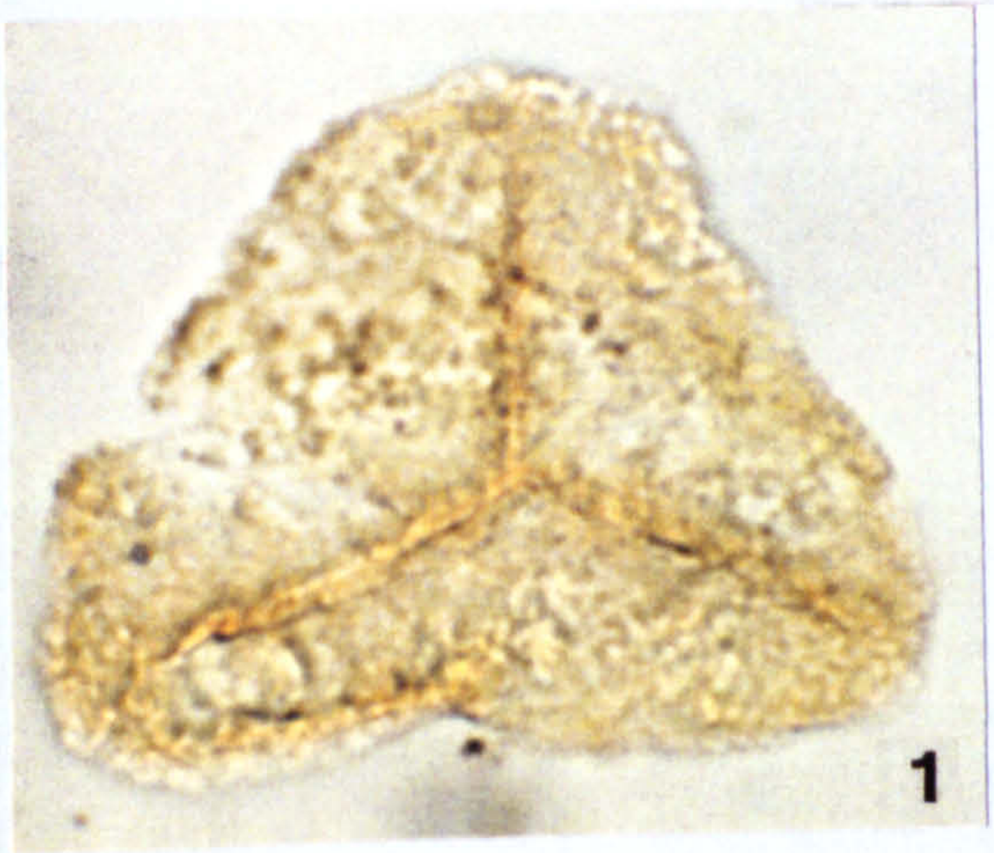
1

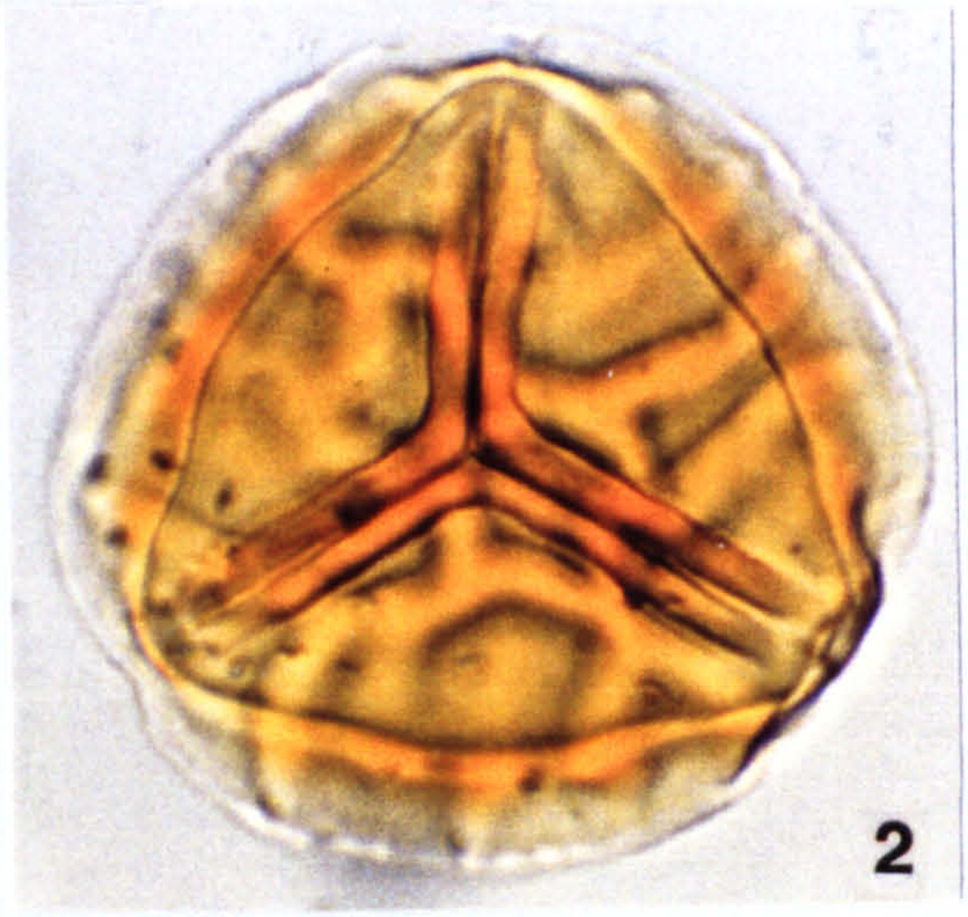
2


3

4

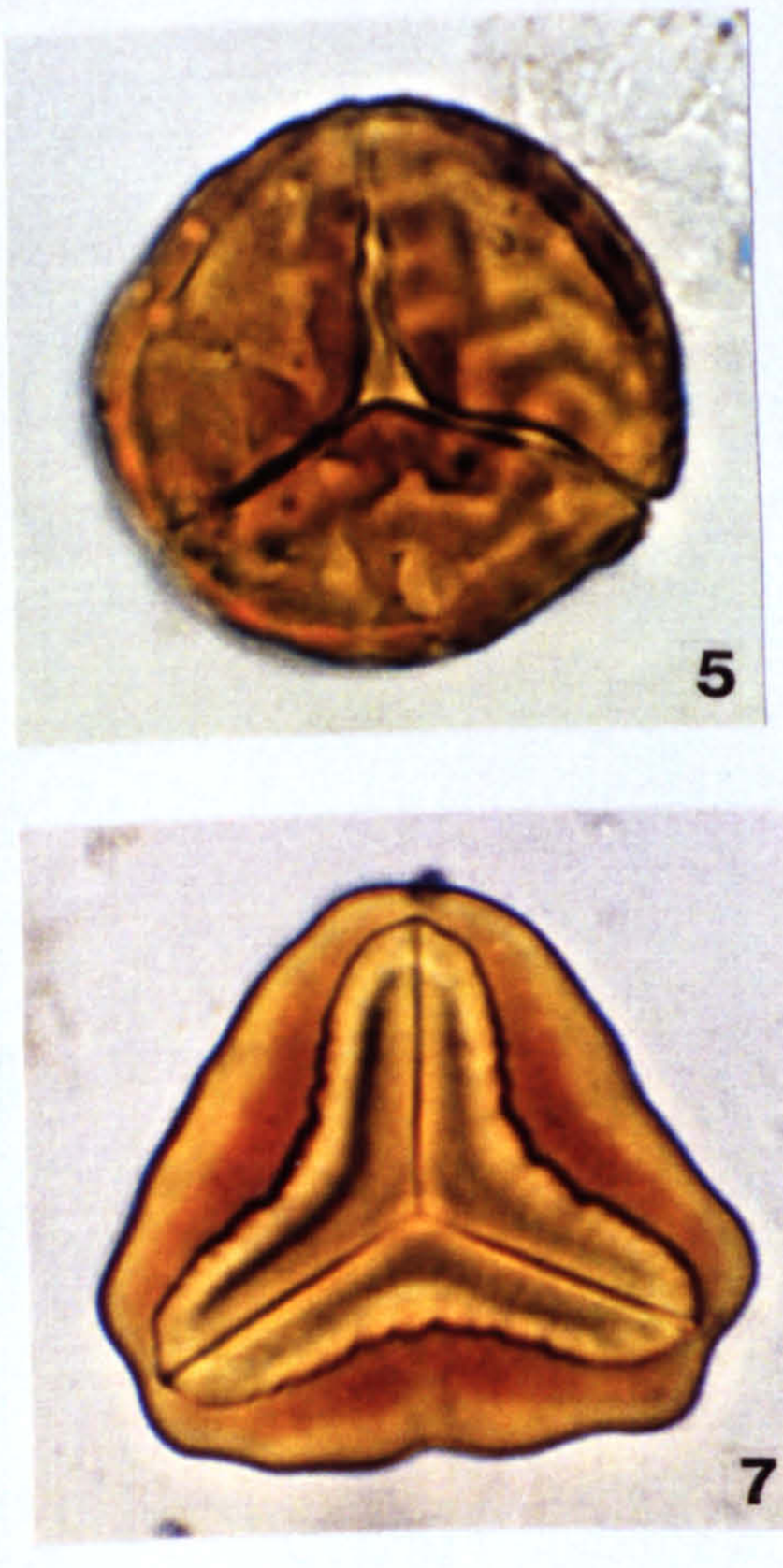
5

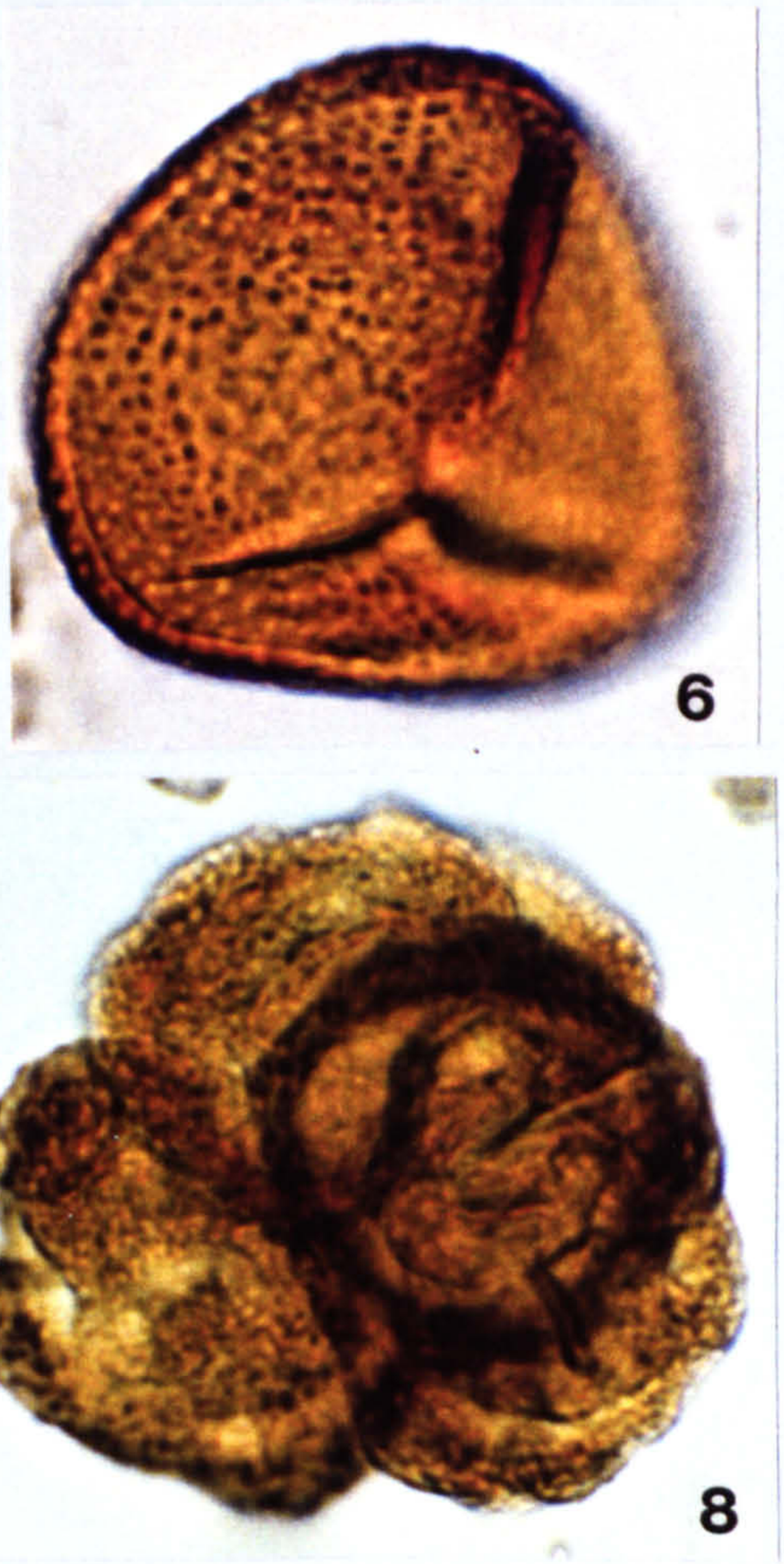
6

7

8

Plate 27

All photomicrographs taken at x 1025 magnification.

Figs 1-12. Variation seen in spore morphology

Fig. 1. Site 3A 60 G36

Fig. 2. Site 3A 60 V44

Fig. 3. MCB -4 --> -4.5 O26

Fig. 4. Site 3A 85 E23

Fig. 5. TBB 1 Q30

Fig. 6. Site 3A 85 B34/4

Fig. 7. TBB 14 K33/3

Fig. 8. MCB 0.5 --> 1 U35/2

Fig. 9. TBB 10 T35/2

Fig. 10. Site 3A 105 P22

Fig. 11. MCB 3.5 --> 4 H47

Fig. 12. Site 3A 60 K49/3

PLATE 27

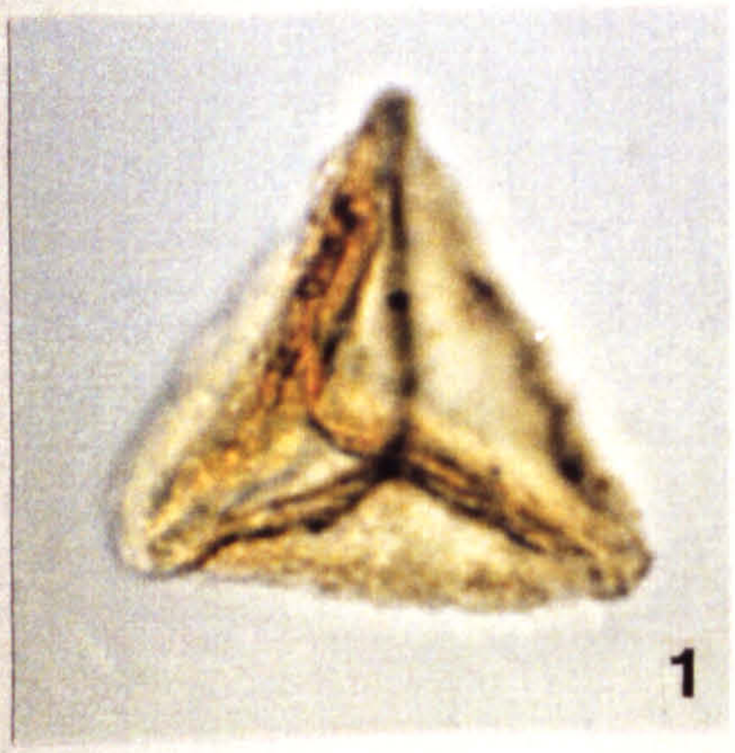
1

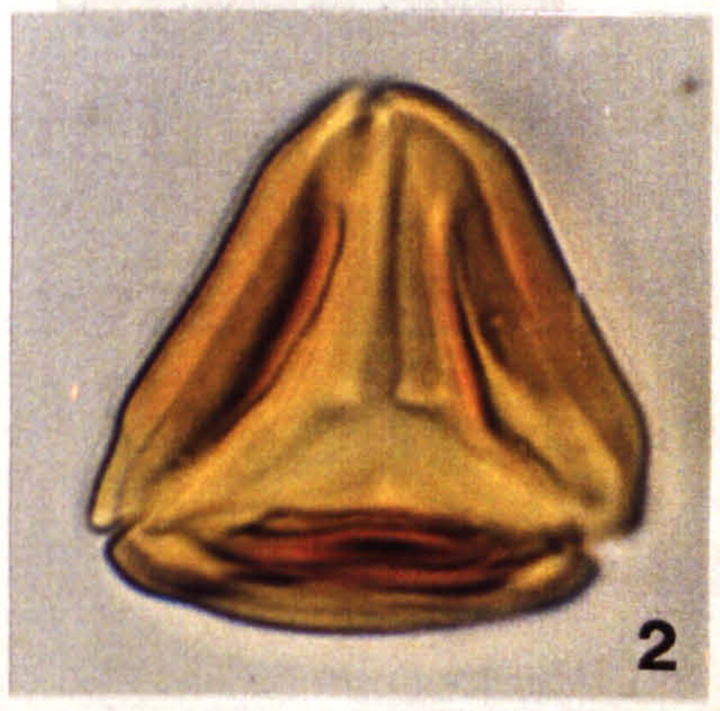
2

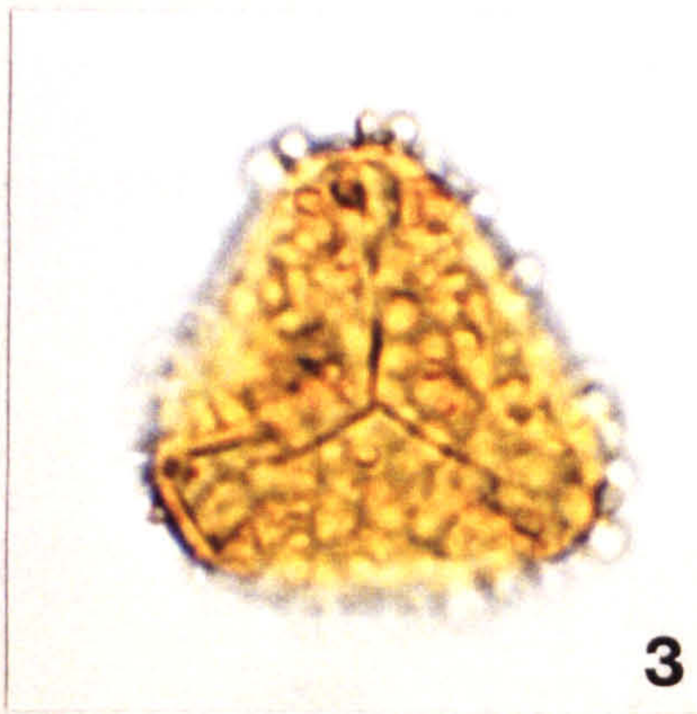
3


4


5

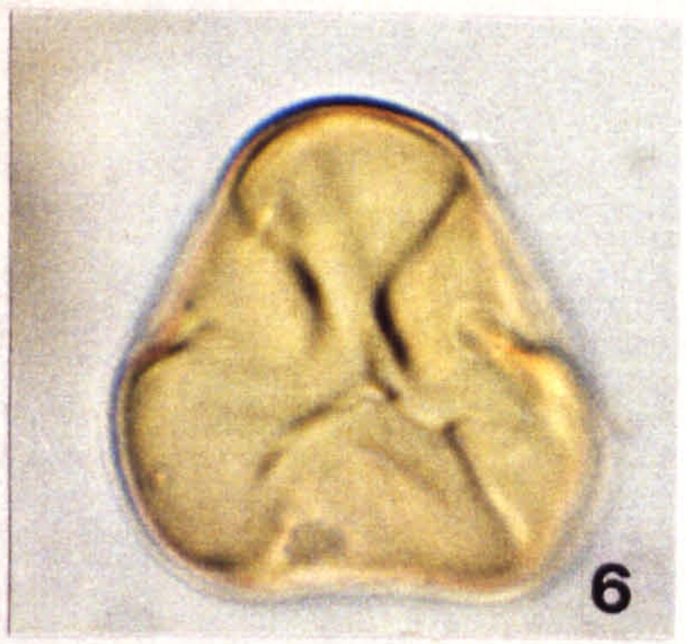
6


7

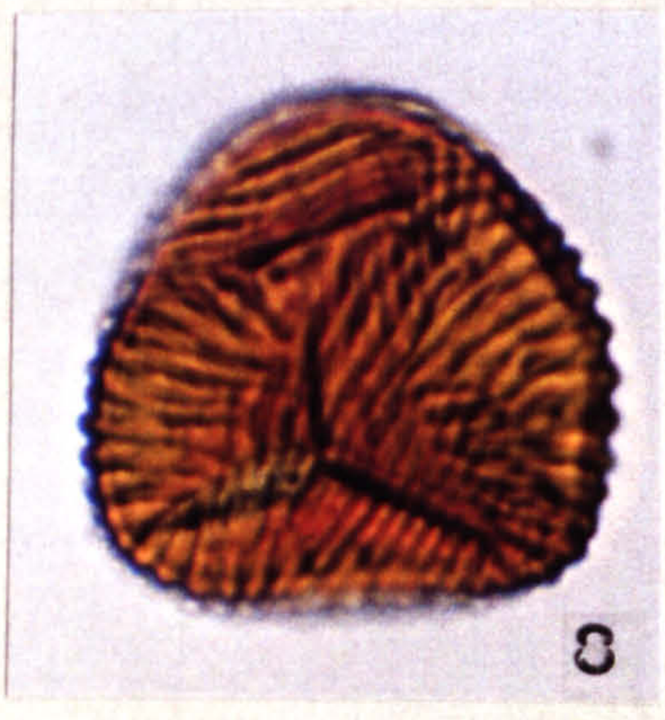
8


9

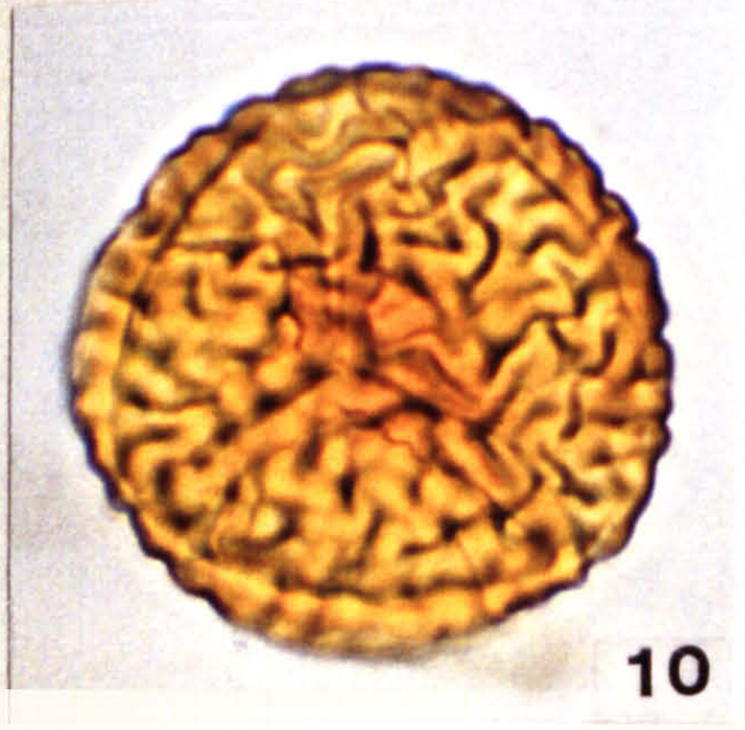
10

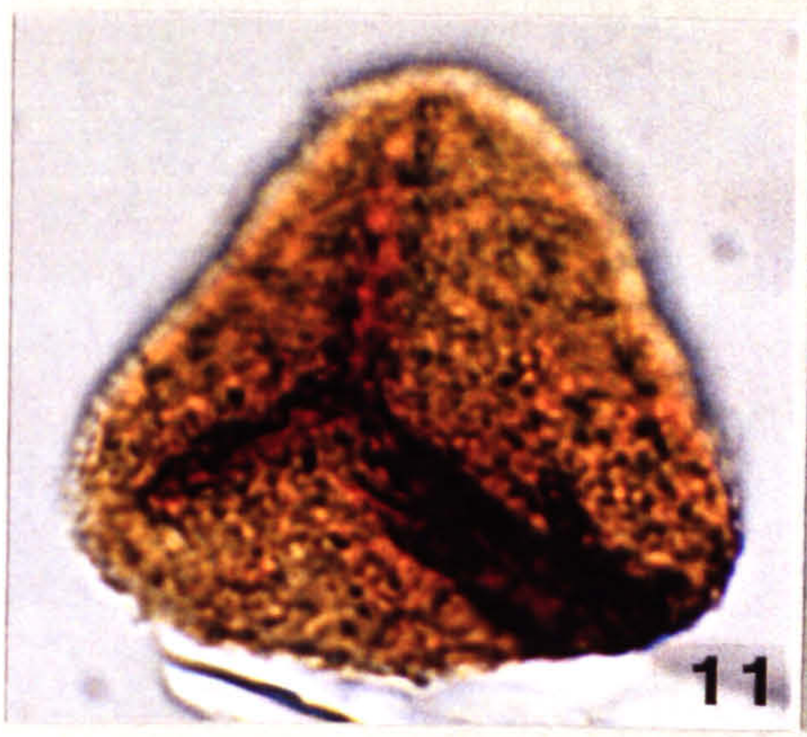
11

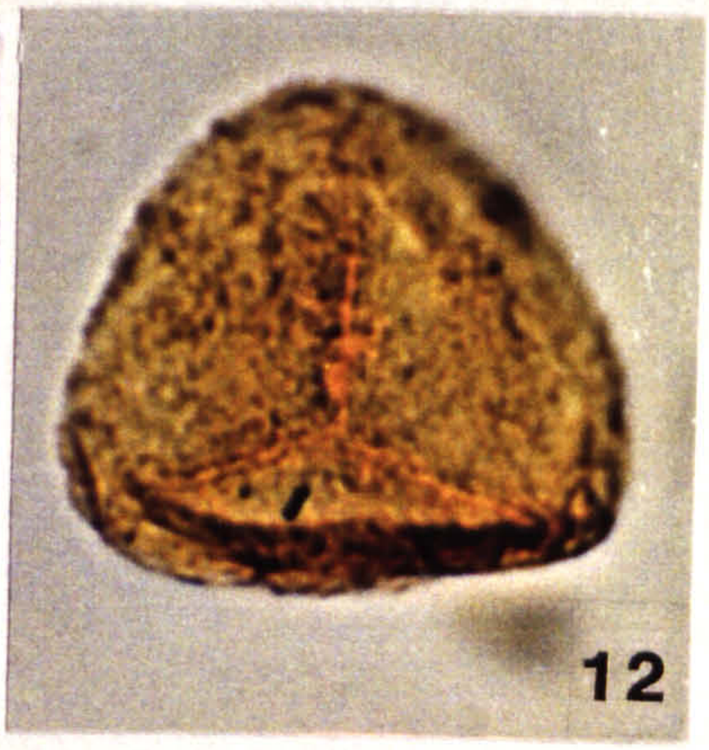
12

Plate 28

All photomicrographs taken at x 1025 magnification.

Figs 1-8. Variations seen in pollen morphology

Fig. 1. Bisaccate pollen
Site 3A 60 J21

Fig. 2. Bisaccate pollen
Site 3A 85 D21

Fig. 3. Bisaccate pollen
Site 3A 60 B30/2

Fig. 4. Bisaccate pollen
Site 3A 90 N24/2

Fig. 5. Bisaccate pollen
MCB -2.5 --> -3A1 Q28/4

Fig. 6. Bisaccate pollen
Site 3A 60 G32

Fig. 7. Bisaccate pollen
TBB -30x N30

Fig. 8. Triporate pollen
TBB 6 R19/2

PLATE 28

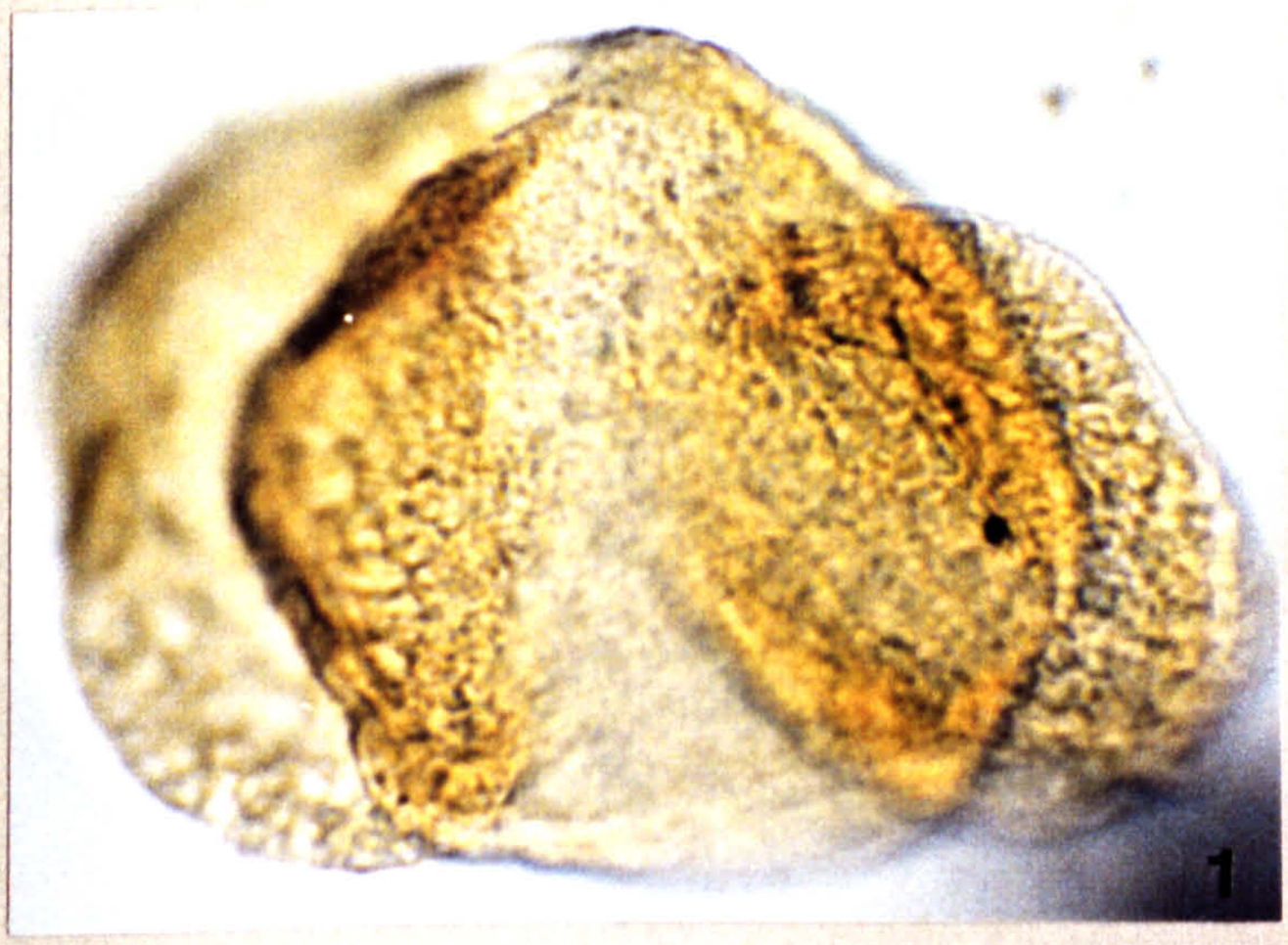
1


2

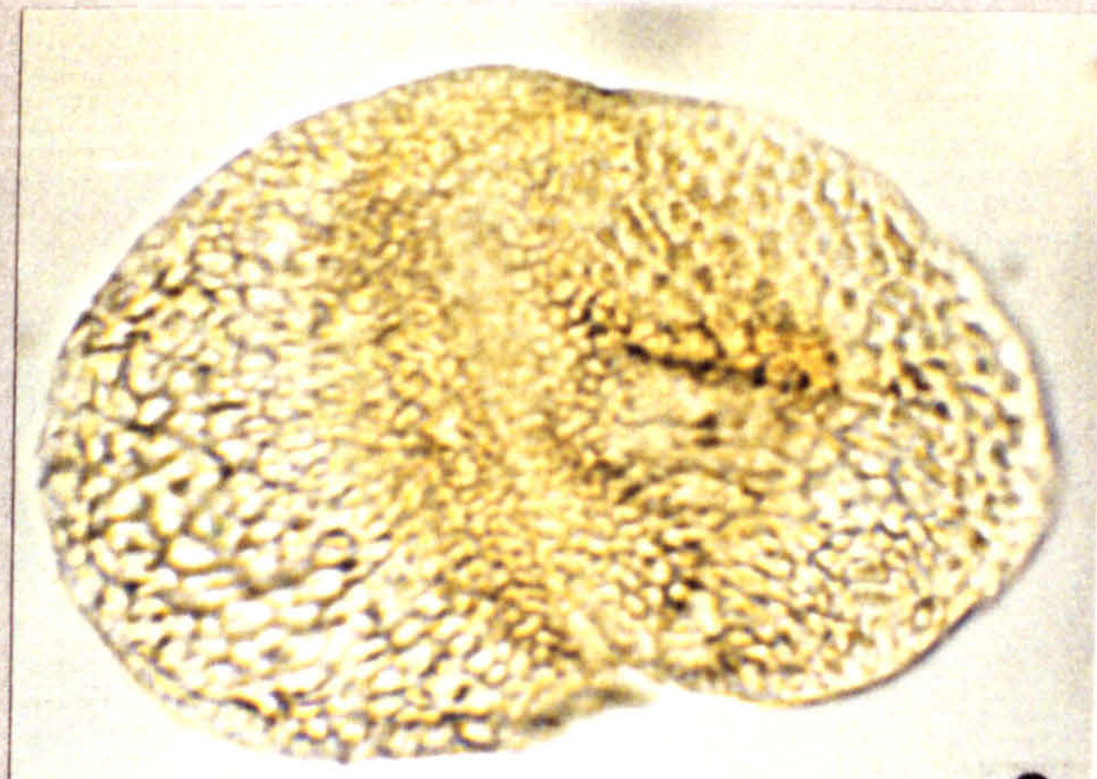
3


4


5


6

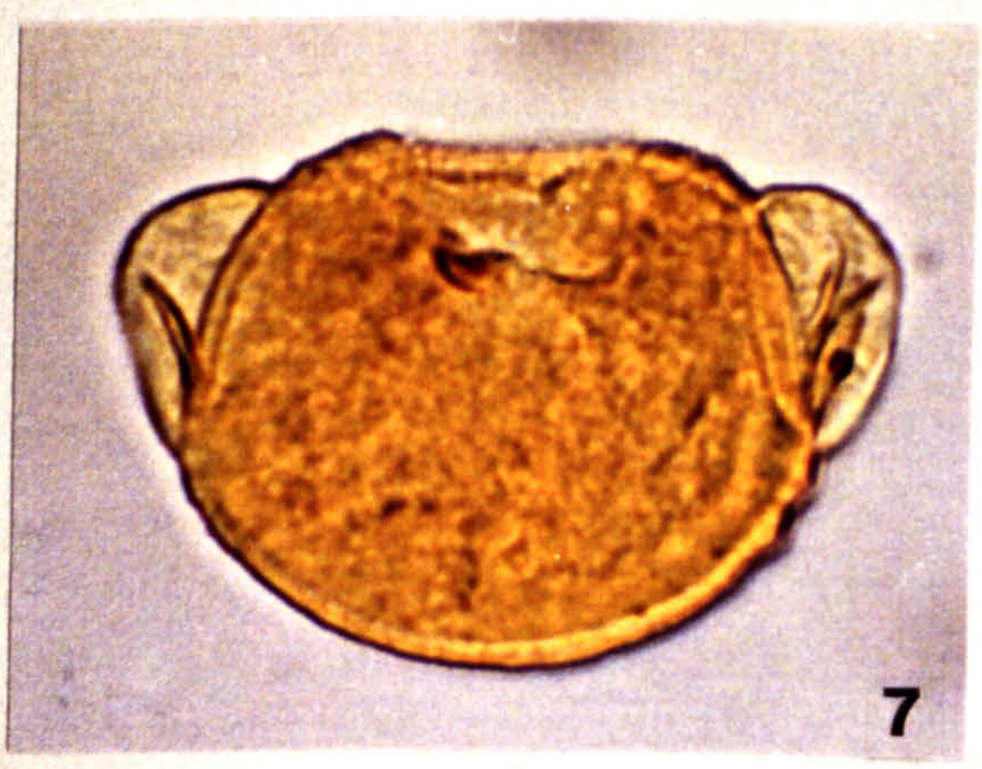
7

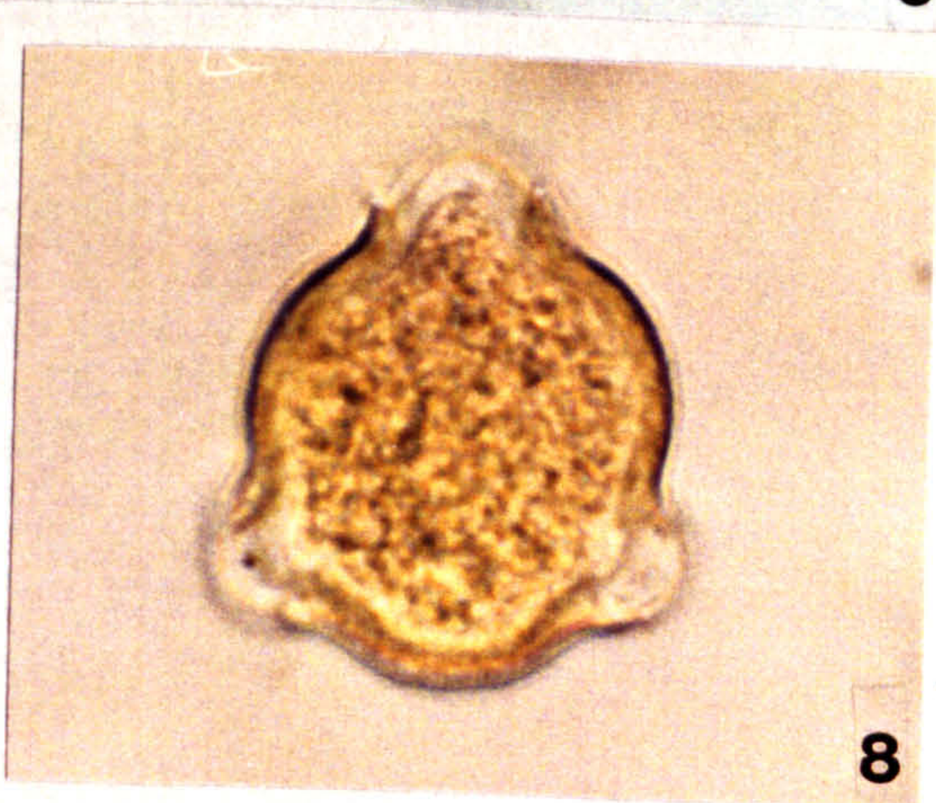
8

Plate 29

All photomicrographs taken at x 1025 magnification.

Figs 1-7. Variation seen in the Acritarch population

Fig. 1. *Tubulospina oblongata* Davey 1970
MCB 3.5 --> 3A1 Y40/2

Fig. 2. *Veryhachium* sp.
SFE 16A1 C40/3

Fig. 3. *Veryhachium* sp.
TBB -2 E43/3

Fig. 4. *Veryhachium* sp.
SFE 17 Q51

Fig. 5. *Veryhachium* sp.
TBB 0 N27

Fig. 6. *Michrystridium* sp.
TBB 10 G35

Fig. 7. *Michrystridium* sp.
Site 3A 0 T33 DIC.

PLATE 29

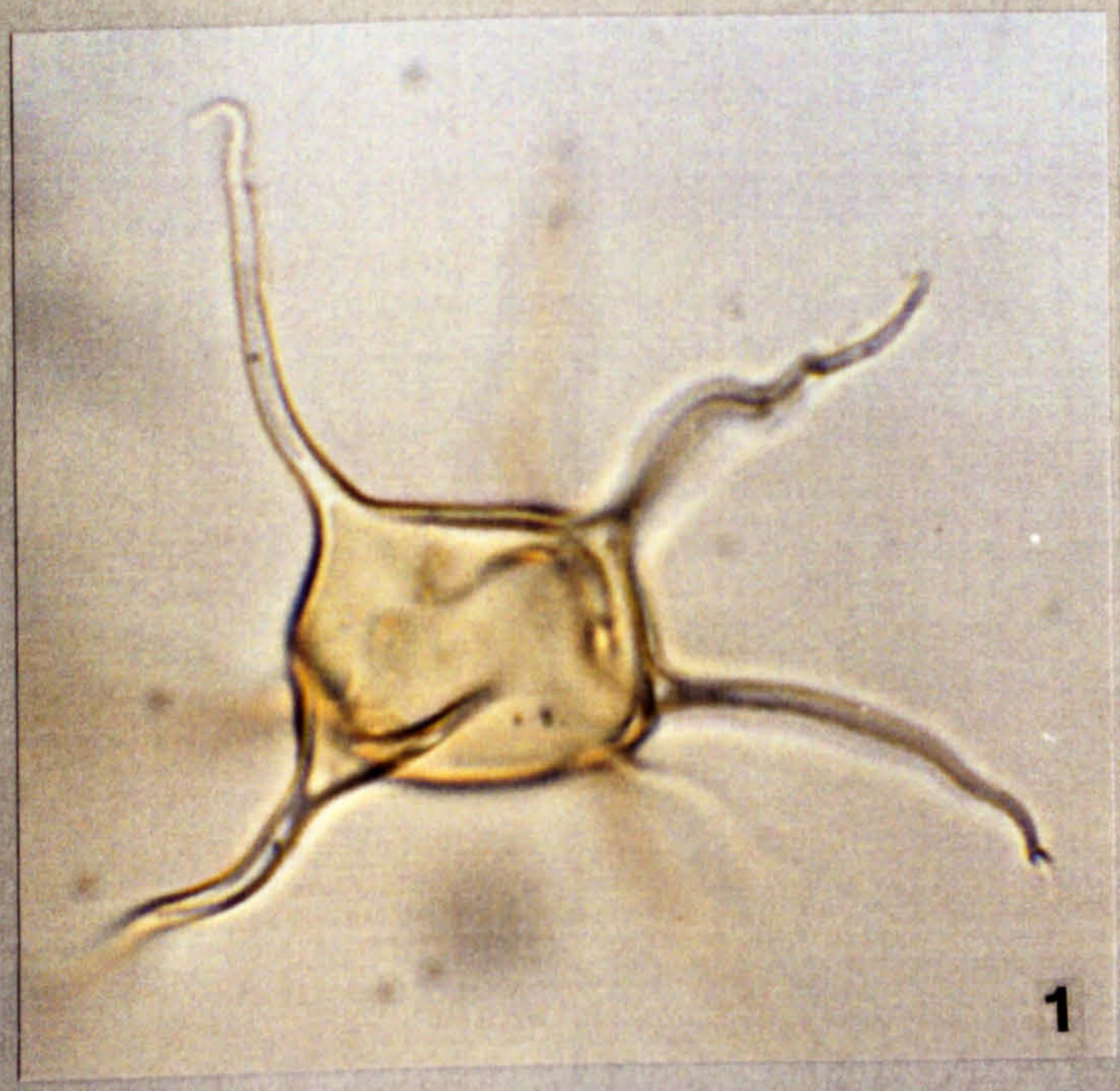
1

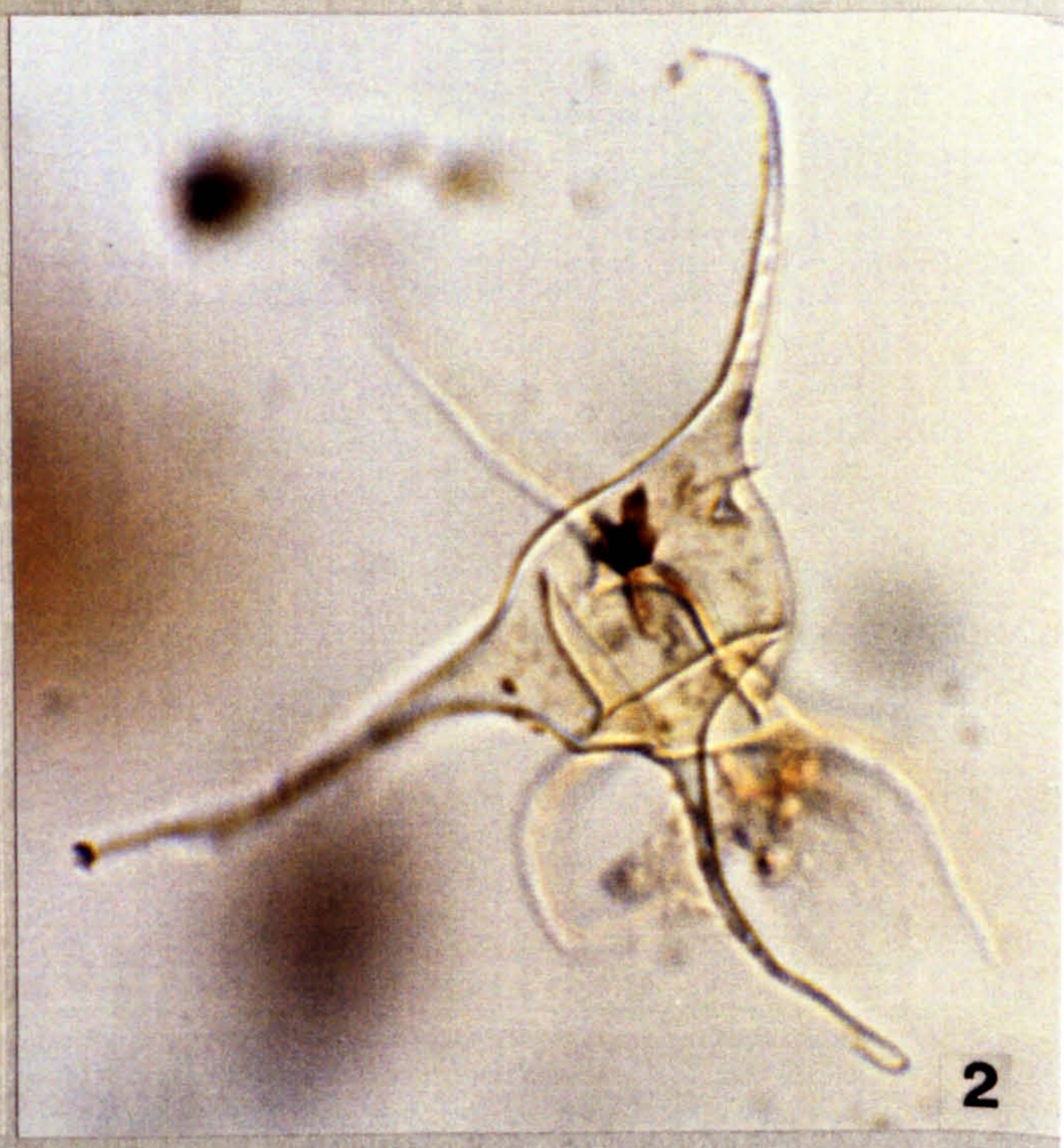
2

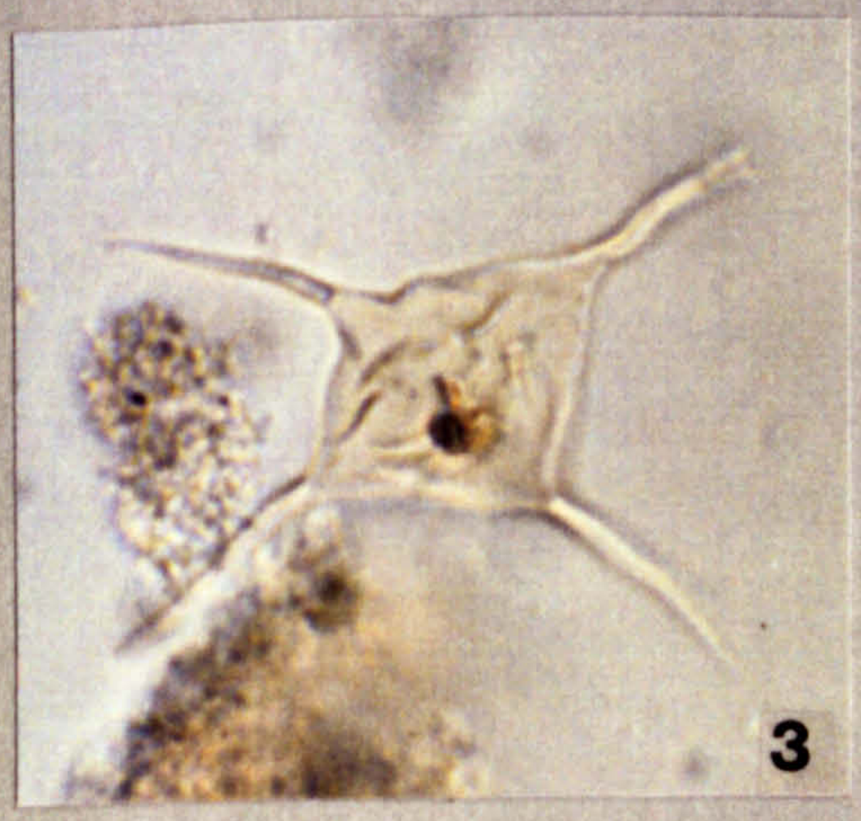
3


4

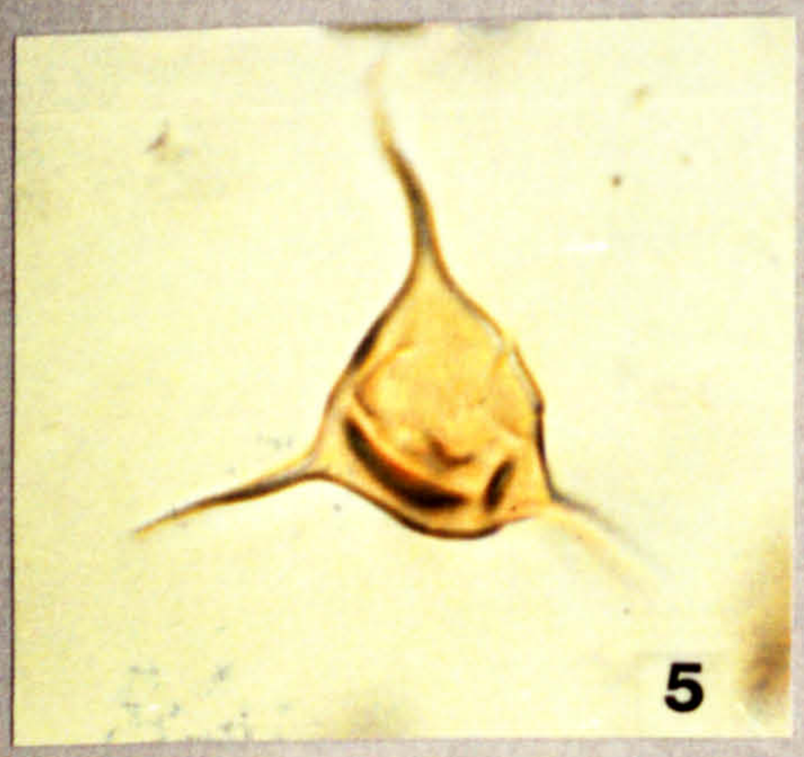
5

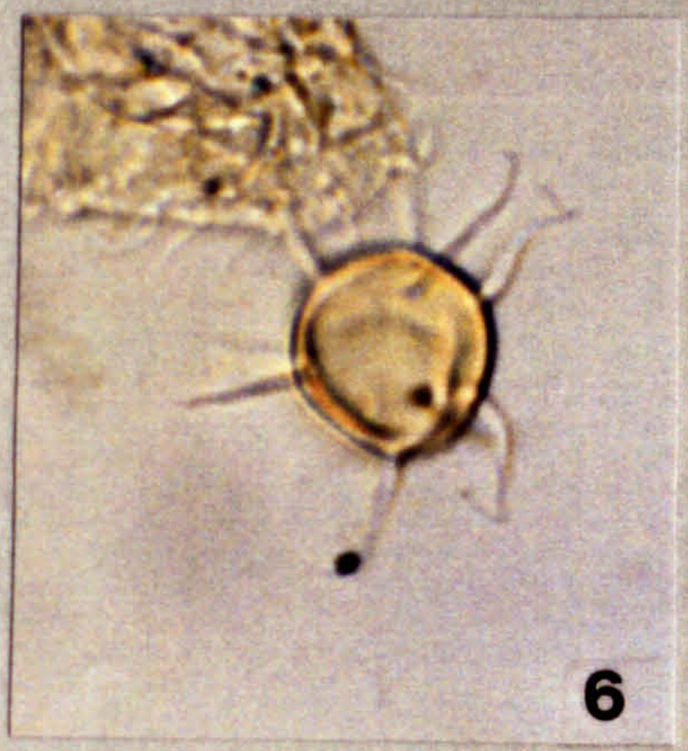
6

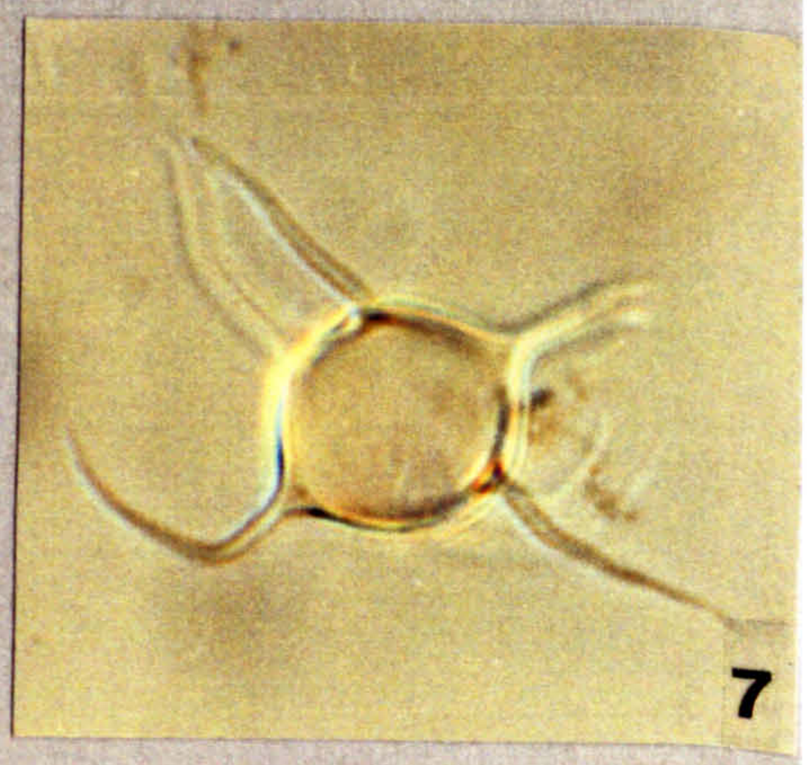
7

Plate 30

All photomicrographs taken at x 1025 magnification, unless otherwise stated.

Fig. 1-4. Some variation in *Pterospermopsis* spp. seen.

Fig. 1. MCB -1.5 --> -2 P41 x 675 magnification

Fig. 2. TBB 10A1 W26/2

Fig. 3. Site 3A 10A1 K47/2

Fig. 4. Site 3A 35A1 H40/2

Figs 5,6. Tasmanites sp.

TBB 11 T21/2

5. High focus shot.

6. Low focus shot of same specimen.

PLATE 30

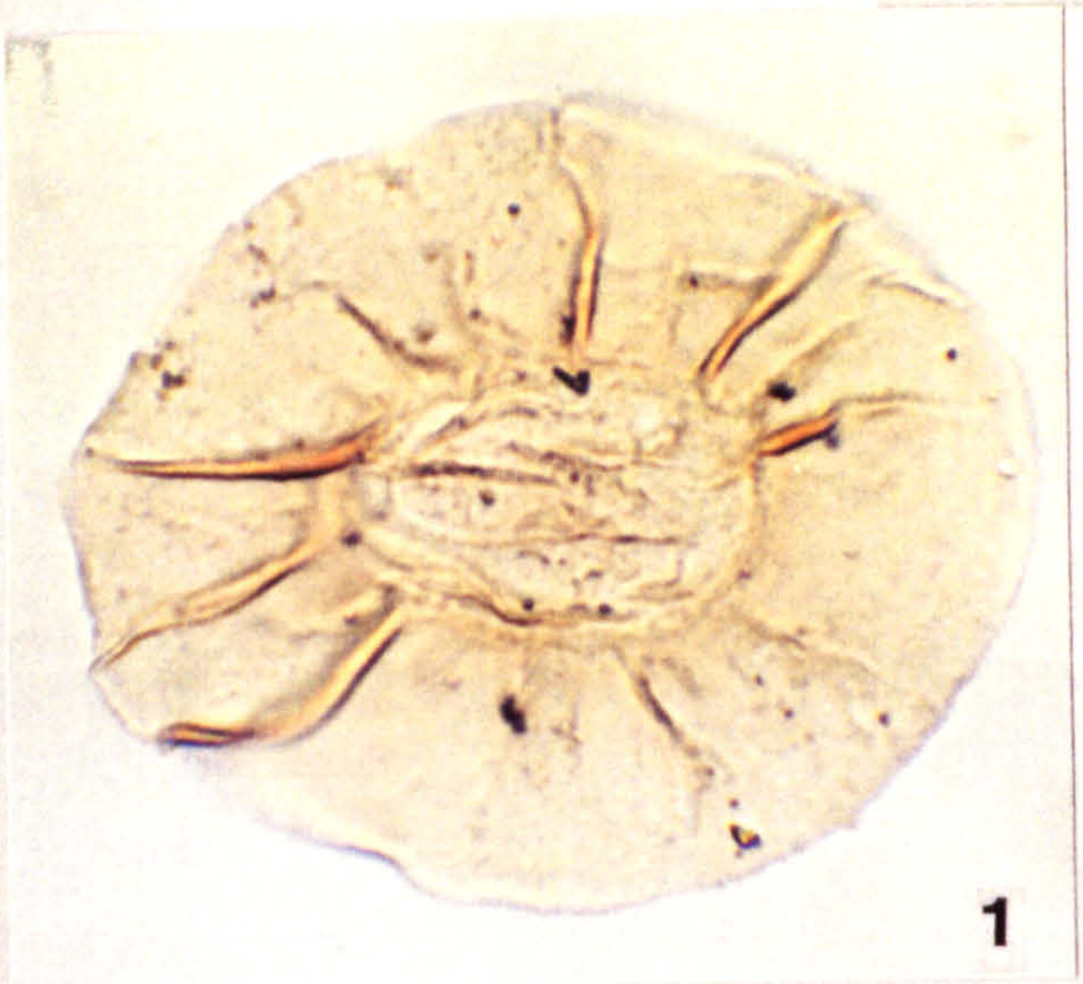
1

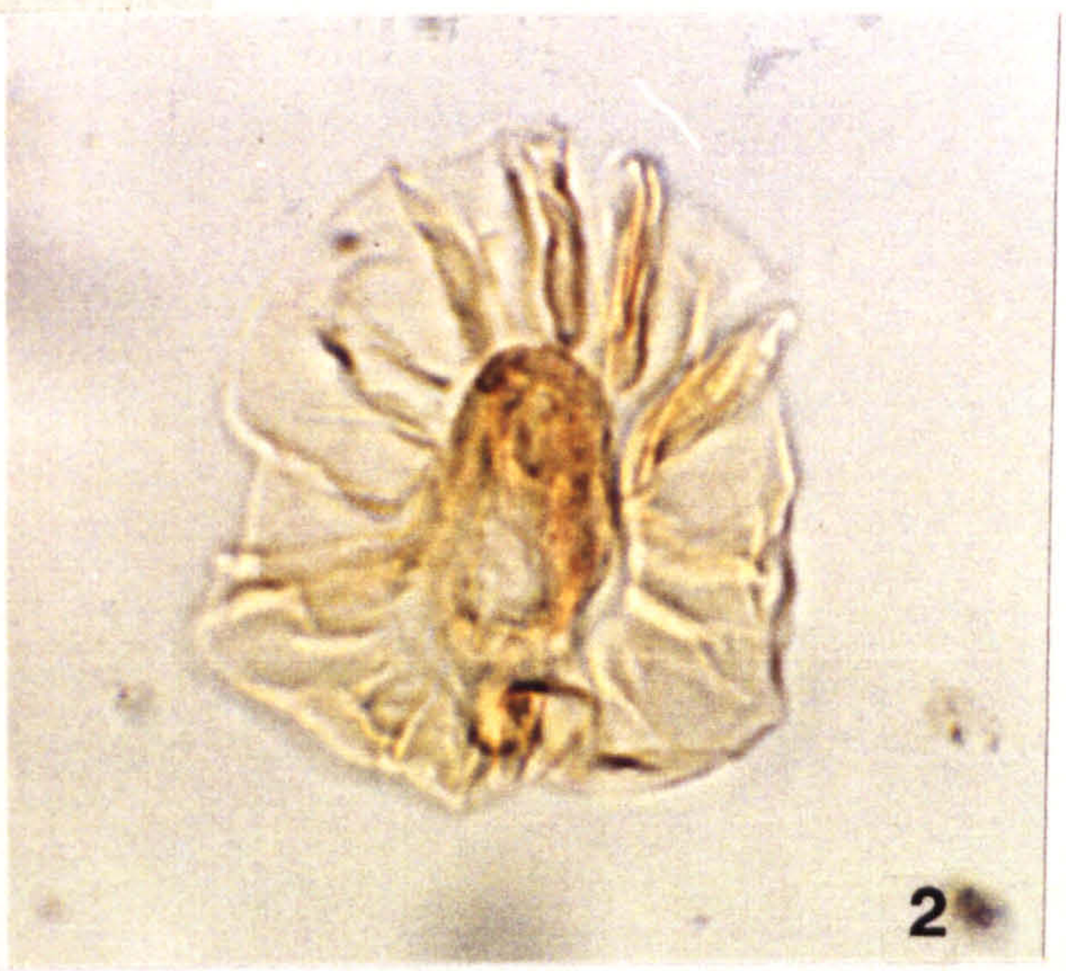
2


3

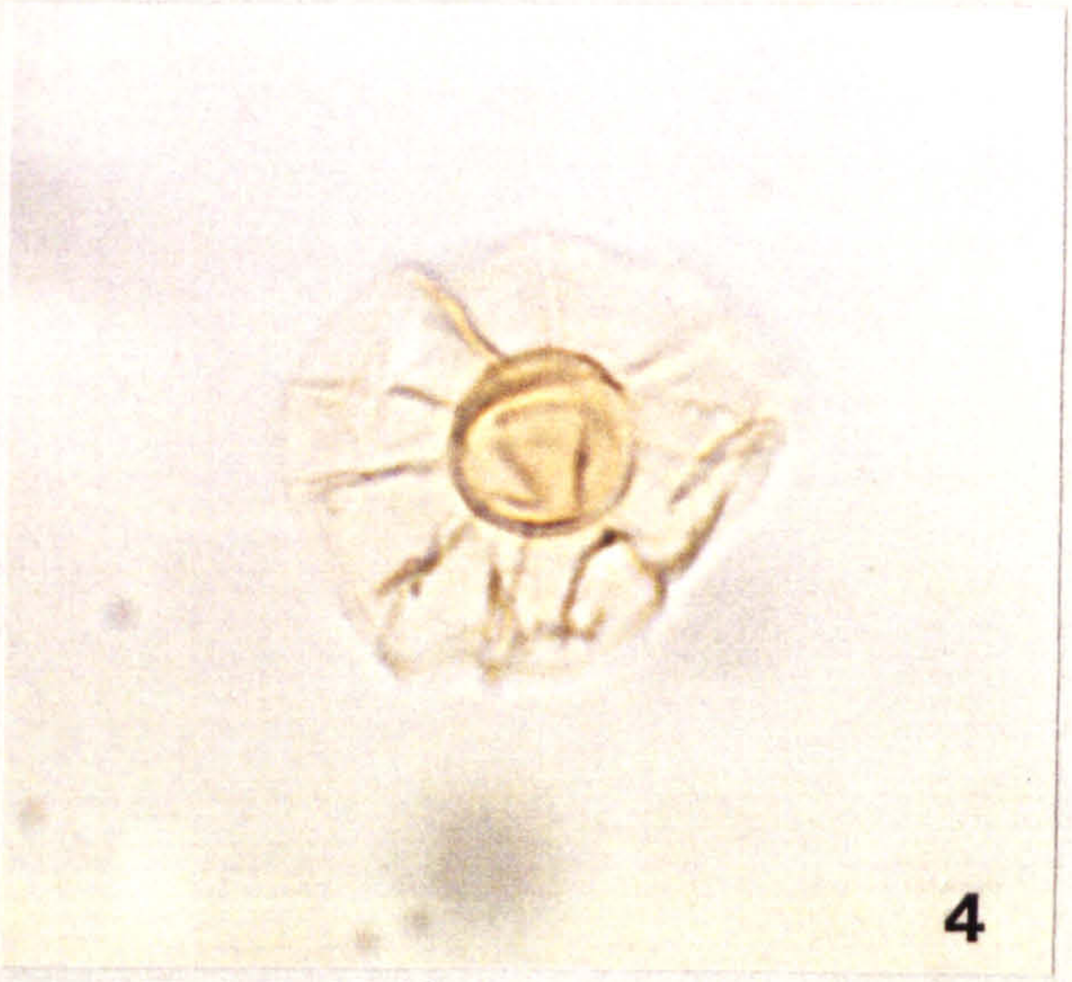
4

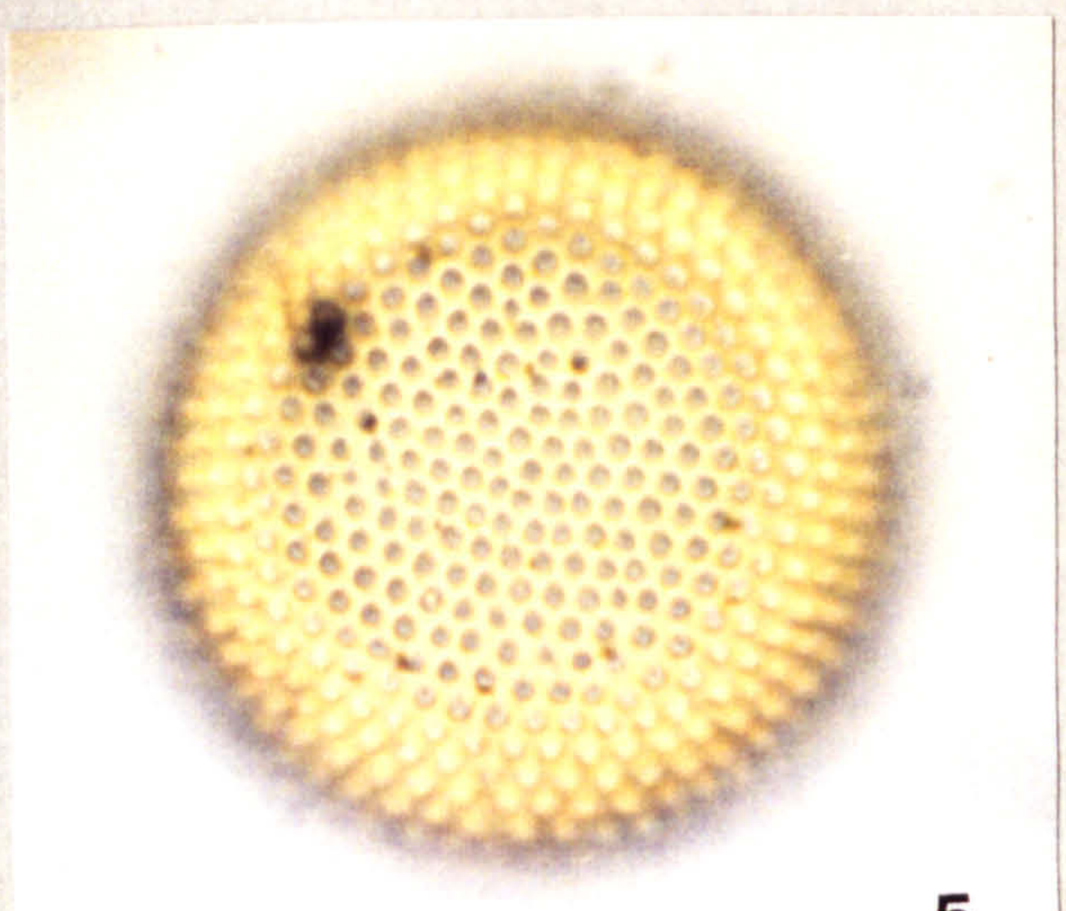
5

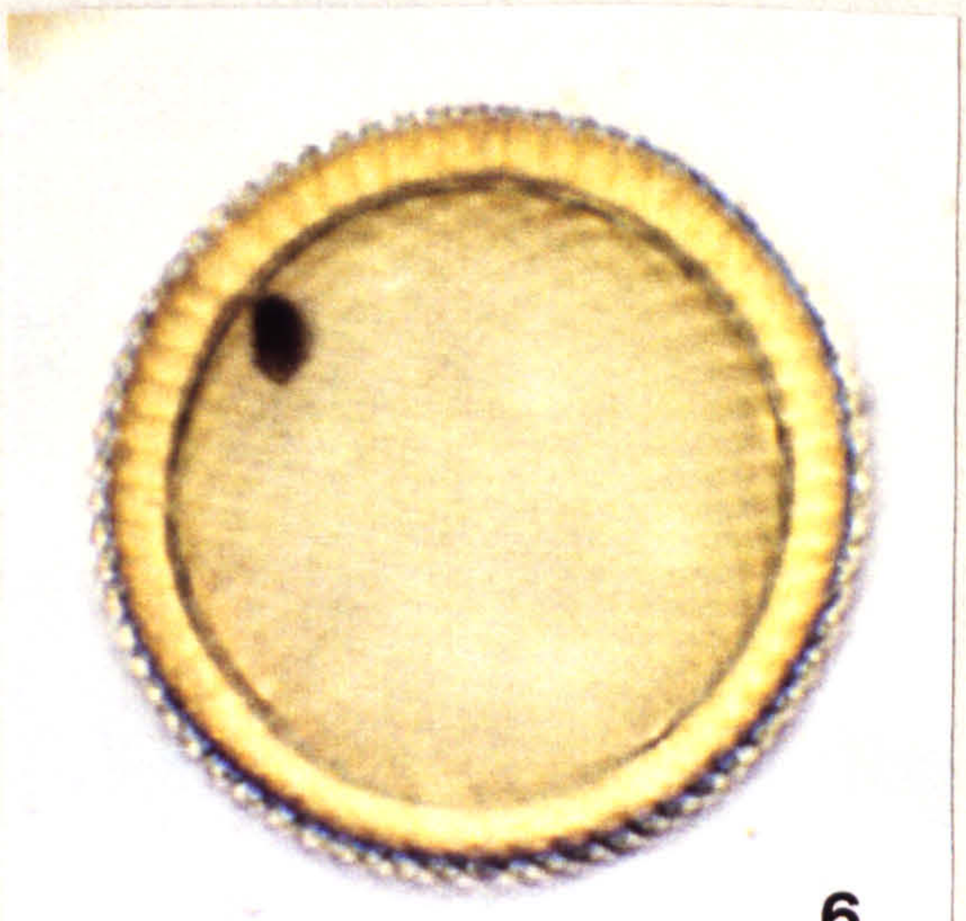
6

Plate 31

Figs 1-6. Some variation in the types of Foraminiferal linings seen.

Fig. 1. Foraminiferal lining Type 1. *Gavelinella* sp. (Hart, 1992 *pers comm.)*, a trochospiral form.
MCB 5 --> 4.5 G29/4 x 338 magnification

Fig. 2. Foraminiferal lining Type 1. Planispiral form.
TBB 3 H51/2 x 675 magnification

Figs 3,4. Foraminiferal lining Type 2. Biserial form.
Fig. 3. MCB 2 --> 2.5 D39 x 675 magnification
Fig. 4. TBB 0 X44/2 x 675 magnification

Figs 5,6. Foraminiferal lining Type 3. *Pleurostomella* spp. (Hart, 1992 *pers comm.)*, a branched form.
Fig. 5. MCB 4 --> 3.5 C33/4 x 338 magnification
Fig. 6. MCB 3 --> 3.5 V46 x 338 magnification

PLATE 31


1


2


3

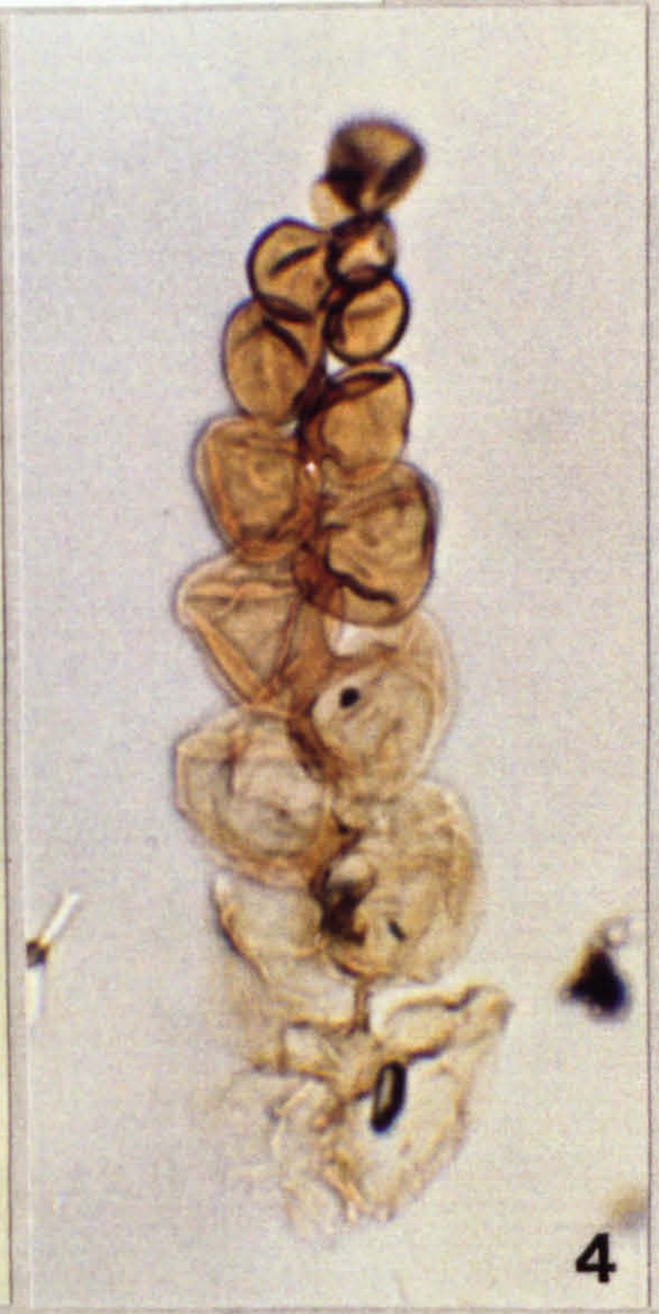
4


5

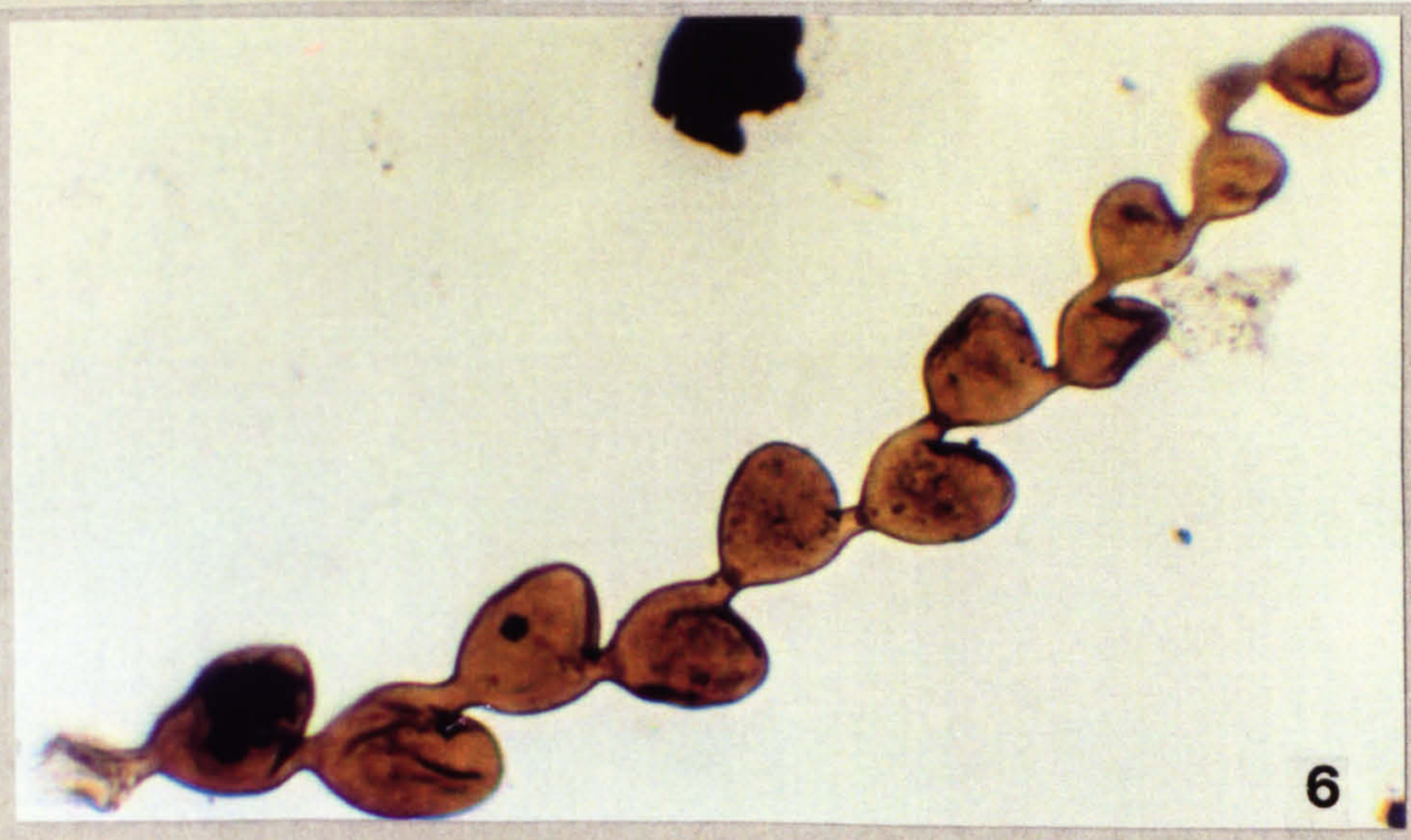
6

SITE 3A SECTION

Appendix 1. Raw numerical data of Site 3a samples. The figure "999" is used to indicate the presence of a palynomorph taxon on an unlogged portion of a slide.

sample number	0	5	10	15	20	25	30	35	40	45	50	55	60	65	70	75	80	85	90	95	100	105	110	115	120
sample number	0	5	10	15	20	25	30	35	40	45	50	55	60	65	70	75	80	85	90	95	11	12	13	14	16
A. neptuni	1	5	0	0	2	0	0	0	0	0	1	1	999	2	3	1	1	0	0	0	4	0	0	0	1
A. ramulifera	5	10	2	7	6	2	1	5	4	10	3	4	6	4	4	3	10	6	4	6	3	1	5	9	7
A. reginensis	2	7	1	2	9	4	1	2	7	14	6	8	6	9	9	8	10	3	0	3	3	5	4	7	12
A. sagena	10	2	6	2	3	2	2	3	1	1	6	6	3	5	9	4	6	10	13	14	10	7	9	11	11
A. sp	15	0	0	2	0	0	0	0	0	0	0	1	1	0	0	0	1	0	0	2	0	0	3	2	1
A. deflandrei	0	0	0	999	0	0	0	1	0	0	1	0	0	1	1	0	1	999	2	1	0	1	999	1	0
A. maculatum	0	0	0	0	999	0	0	0	0	0	1	2	0	999	999	999	999	0	1	0	0	999	0	0	999
C. asymmetricum	1	1	0	1	1	2	1	1	3	1	5	0	1	1	999	1	1	4	6	3	3	2	999	999	999
C. colliveri	0	1	6	0	0	0	1	0	1	0	0	0	0	0	0	0	0	0	0	0	0	0	0	0	0
C. reticulata	0	5	0	1	0	0	0	2	0	0	0	0	0	0	0	0	0	0	0	0	0	0	0	0	0
C. discreta	0	1	0	0	1	0	2	2	0	1	2	3	0	1	999	1	3	0	0	0	0	0	2	2	2
C. armatum	1	0	5	9	5	7	7	8	22	15	4	6	4	6	5	5	7	8	4	3	3	8	5	7	4
C. huguoniotii	24	24	39	62	32	42	38	76	69	51	20	33	28	61	61	34	50	64	85	63	30	55	29	51	52
C. clavulum	1	0	1	0	0	999	0	999	0	0	0	3	1	3	0	1	3	1	0	2	0	3	3	6	7
C. oceanica	0	0	3	1	0	0	0	0	0	0	0	0	0	0	0	0	0	0	0	0	0	0	0	0	0
C. cooksoniae	999	999	1	999	999	3	1	999	4	2	1	999	1	999	1	3	3	999	4	2	2	999	999	1	1
C. distinctum	4	4	3	999	1	3	6	5	21	18	13	6	4	6	7	9	17	9	14	8	7	10	10	5	4
C. defloccata	0	1	0	999	2	0	0	0	0	0	999	999	1	999	999	3	1	1	4	0	2	999	1	1	2
C. membraniphorum	1	0	0	0	0	1	0	1	0	0	0	0	0	0	0	0	0	0	4	0	1	1	0	0	999
D. laminaspinosum	0	2	0	0	3	0	3	1	1	0	1	0	1	10	6	6	4	5	999	1	3	1	3	3	5
D. cladoides	0	1	0	0	0	0	2	0	0	0	0	999	0	0	1	1	999	999	0	0	0	1	0	999	2
D. medusoides	0	0	0	0	0	0	0	0	0	0	0	999	0	0	999	999	999	999	0	0	0	0	0	999	2
E. rugulosum	0	0	3	1	1	2	0	2	0	0	1	2	999	999	2	1	3	999	10	6	1	5	1	2	1
E. campanula	999	999	2	5	3	2	1	1	2	1	2	4	2	3	2	4	2	8	6	1	1	6	1	3	1
E. spinosa	999	0	1	0	0	0	0	0	3	3	0	4	2	1	5	3	3	2	0	2	1	2	2	2	3
E. cf. arnace	3	4	1	4	1	3	1	3	0	1	999	1	999	1	2	3	3	2	7	5	4	3	999	999	1
E. bifidum	0	0	0	0	2	0	0	0	0	0	6	4	3	1	5	5	4	2	3	5	3	3	0	1	2
E. phragmites	0	1	0	0	0	0	0	0	0	0	0	0	0	0	0	0	0	0	0	2	0	2	0	0	0
F. deanei	2	0	0	999	1	999	999	0	0	0	1	999	0	1	1	1	999	999	1	1	3	0	0	1	999
F. ferox	0	1	1	0	1	0	0	0	1	0	999	999	999	999	2	2	999	999	2	3	0	2	1	5	2
F. laciniata	0	0	2	0	0	0	0	0	0	0	0	0	0	0	999	0	0	0	0	0	0	0	0	0	1
F. mantellii	0	0	0	0	0	0	0	0	0	0	0	0	0	1	0	0	0	0	0	0	0	0	1	1	999
F. resex	1	0	0	0	1	0	0	1	0	1	999	0	0	999	999	0	1	0	1	0	0	0	0	0	0
F. amphora	0	0	0	0	0	0	999	1	1	0	999	999	999	2	999	999	999	1	0	2	0	1	0	0	999
G. cassidata	0	0	0	0	999	0	1	0	0	0	1	0	0	999	1	999	1	999	0	0	1	999	0	1	1
H. pulchrum	5	14	13	5	5	8	10	16	12	15	13	8	3	12	14	15	8	15	24	13	10	7	8	13	8
H. bowerbankii	1	1	1	2	999	1	1	3	4	0	1	999	0	1	999	2	0	0	0	1	1	0	1	0	2
H. tubiferum	0	2	2	0	10	0	1	2	1	5	5	13	13	13	11	15	7	9	1	0	8	5	8	5	13
C. obliquicostatum	999	0	999	999	999	999	999	999	0	0	0	1	999	999	999	999	999	1	999	999	999	999	999	1	999
H. membraniphorum	2	0	1	2	0	1	0	999	0	1	3	1	1	2	999	1	0	1	0	4	0	4	4	999	2
K. readei	999	0	0	0	999	0	0	0	0	0	999	0	0	999	0	999	0	0	999	0	0	0	0	0	0
L. chlamydata	999	2	2	1	999	999	999	2	4	6	999	999	999	1	999	1	999	999	2	999	1	999	999	999	1
L. siphonophorum glabrum	1	0	3	8	8	5	2	4	5	2	5	5	6	6	3	1	1	2	4	2	3	4	5	6	3
L. siphonophorum siphonophorum	9	11	8	10	7	26	19	16	20	34	14	10	5	6	6	6	4	6	14	10	5	7	5	5	7
M. ?crinitum	4	2	4	2	0	0	2	0	0	0	0	0	1	1	0	999	0	999	8	2	0	1	2	2	1
M. distinctum	0	999	1	0	0	0	0	5	1	0	0	0	2	999	999	0	2	1	0	0	0	1	999	0	1
M. ornatum	0	0	0	0	0	0	0	0	0	0	0	0	0	1	0	0	0	0	0	0	0	0	0	1	0
M. setosum	999	0	4	0	999	0	4	4	4	1	0	3	2	2	7	1	1	2	8	1	5	0	2	1	3
N. densiradiata	0	0	0	0	1	0	4	3	1	1	0	1	1	1	0	1	0	999	1	1	0	0	0	0	1
O. operculata	3	4	0	7	999	7	3	4	3	5	2	1	4	2	1	1	2	5	11	7	2	2	6	4	3
O. costata	5	2	1	0	2	1	999	2	4	5	2	1	2	999	6	999	2	4	9	5	1	3	2	4	2
O. complex	0	1	3	0	2	0	999	0	0	0	999	1	999	999	2	1	3	1	3	0	2	4	1	999	2
O. prolixispinosum	0	0	0	0	999	0	0	0	0	0	1	999	999	999	1	1	1	1	10	5	1	3	3	3	2
P. infusorioides	93	109	113	178	204	129	132	69	67	59	152	162	182	134	103	142	120	85	101	77	177	111	154	93	143
P. cenomaniense	6	2	6	3	0	9	2	6	12	3	0	0	0	999	1	0	0	0	0	999	0	2	0	0	2
P. pseudhystrichodinium	1	1	2	999	4	0	0	1	0	0	1	999	999	999	999	1	999	0	0	3	2	0	0	1	2
P. truncatum	3	4	2	2	1	1	3	2	2	2	1	2	2	1	999	6	2	3	11	5	3	2	5	2	2
P. deflandrei	999	4	5	999	1	0	4	4	6	5	0	3	1	1	1	1	3	2	3	0	2	1	1	999	1
P. cingulatum cingulatum	4	3	2	2	4	6	7	1	4	4	7	4	4	3	6	6	5	2	13	3	3	5	4	8	5
P. cingulatum granulatum	0	0	0	1	0	0	2	2	0	0	1	2	1	3	2	4	2	1	2	1	1	4	3	2	2
P. cingulatum reticulatum	3	0	1	0	0	2	3	4	4	3	999	0	2	1	0	2	2	2	1	2	1	2	3	0	2
P. cingulatum polygonalis	0	0	0	2	999	999	1	999	0	0	1	0	0	1	999	2	999	2	999	0	2	0	0	0	2
P. cornutum	0	0	999	0	0	0	1	0	0	0	0	0	0	1	2	4	3	0	8	0	1	0	0	0	0
P. conulum	0	0	1	0	0	1	999	0	0	0	0	999	0	0	2	1	0	2	0	1	0	0	999	999	999
R. veligera	0	2	2	999	2	4	1	3	1	2	999	2	1	999	1	2	3	1	1	14	3	12	10	6	1
S. ?dentatus	0	0	8	4	10	2	4	6	6	9	7	6	2	6	5	2	5	5	2	0	5	0	4	4	4
S. multibrevis	999	0	2	3	0	3	4	3	3	3	0	0	1	1	0	1	1	0	3	0	1	0	0	0	1
S. ramosus ramosus (ovoidal)	21	3	3	1	2	5	3	6	4	4	7	8	1	4	8	6	2	4	11	5	5	2	1	1	3
S. ramosus gracilis	0	0	2	0	999	1	1	2	2	0	2	3	5	2	5	3	2	1	3	0	0	1	1	0	2
S. ramosus ramosus (angular)	0	0	3	6	999	2	2	3	2	2	7	1	4	1	2	4	3	3	8	2	2	1	1	1	1
S. ramosus reticulatus	0	0	2	3	0	0	4	0	8	2	0	0	0	0	0	0	0	0	0	0	0	3	0	0	0
S. sp.	2	0	0	2	0	1	3	0	3	0	0	1	2	1	0	0	0	0	0	6	0	1	0	1	0
S. coronatum	0	0	0	0	2	0	1	0	0	0	0	999	0	999	999	999	1	1	4	999	0	999	999	1	999
S. pontis-mariae	0	0	0	0	0	0	0	0	0	0	0	0	1	1	0	2	0	0	0	0	0	0	0	1	0
S. longifurcatum	0	0	0	0	999	0	0	3	1	1	1	0	999	0	0	0	0	1	0	999	0	0	0	0	0
S. spinicongregatum	0	0	1	0	2	0	0	0	0	0	4	3	999	999	2	999	1	0	0	0	2	2	5	2	2
T. castanea	5	4	7	11	2	4	9	3	4	6	2	3	0	4	3	2	6	3	5	0	2	0	3	2	7
V. ovulum	0	1	3	2	1	2	2	4	3	2	4	999	4	3	3	1	2	6	18	2	2	3	10	7	5
W. anglicum	0	0	0	0	0	0	0	0	0	0	0	0	0	2	0	0	0	0	0	0	0	0	0	0	0
X. esbeckianus	0	0	0	0	0	0	1	0	0	0	0	0	0	999	0	0	0	0	0	0	0	0	0	0	0
X. alatum	2	14	4	6	5	6	3	2	4	8	3	1	999	999	2	999	1	3	0	2	4	3	3	6	7
A. cf. ramulifera	1	999	999	0	0	999	0	1	0	999	999	1	0	0	0	999	999	0	0	1	0	999	999	0	0
G. whitei	0	0	0	0	0	0	0	0	0	0	0	0	0	0	0	0	0	1	0	999	0	1	999	0	1
Xiphophoricium sp. A	0	999	999	0	0	0	999	0	0	999	0	999	1	0	0	0	0	0	0	0	999	0	0	0	999
C. ?urna	0	0	2	0	2	0	0	0	0	0	1	1	4	999	1	2	0	6	0	4	2	4	4	2	0
Spores	2	1	8	5	1	9	4	2	3	4	1	4	3	1	2	1	2	3	4	4	6	4	3	6	1
Bisaccate pollen	0	1	3	2	1	2	4	1	5	1	2	1	2	999	999	999	1	1	11	3	4	4	1	1	1
Veryhachium spp.	999	0	1	2	0	0	2	0	0	1	0	0	1	1	4	2	999	1	0	0	0	1	1	1	0
Michrystridium spp.	0	0	0	0	0	0	0	0	0	0	1	3	1	1	0	0	0	0	0	0	3	0	0	0	0

TBB SECTION

sample number	-3	-2	-1	0	1	2	3	4	5	6	7	8	9	10	11	12	13	14	15
sample number	-3	-2	-1	0	1	2	3	4	5	6	7	8	9	10	11	12	13	14	15
A. neptuni	4	2	1	1	1	1	1	1	3	2	0	0	1	2	999	999	1	0	999
A. ramulifera	3	5	1	1	1	1	4	5	5	2	3	5	4	4	1	999	4	2	2
A. reginensis	14	3	1	1	1	1	17	10	14	10	8	14	8	7	4	3	1	0	3
A. sagena	6	1	0	0	0	0	3	2	5	3	2	1	2	1	3	3	5	1	3
A. sp	0	0	0	0	0	0	0	0	0	0	1	0	0	1	1	0	1	0	0
A. deflandrei	0	999	0	0	0	0	0	0	0	0	0	0	0	0	0	1	2	999	0
A. maculatum	1	0	0	0	0	0	0	0	1	0	0	1	999	0	1	0	0	0	2
C. asymmetricum	0	0	0	0	0	0	0	0	0	0	0	0	999	0	0	1	0	0	0
C. colliveri	0	0	0	0	0	0	0	0	0	0	0	0	0	0	1	999	0	0	0
C. reticulata	2	0	0	0	0	0	0	0	0	0	0	0	2	1	0	999	0	0	0
C. obliquicostatum	3	0	0	0	0	0	0	0	0	0	0	0	0	0	999	0	0	0	0
C. discreta	5	2	0	0	0	0	0	0	0	0	0	0	1	3	1	999	0	0	0
C. nyei	5	0	0	0	0	0	0	0	0	0	0	0	999	0	999	0	0	0	999
C. ?urna	0	0	0	0	0	0	0	0	0	999	0	0	999	0	0	0	0	0	1
C. armatum	11	4	0	0	0	0	0	0	0	17	5	6	9	12	4	3	4	2	4
C. clavulum	4	1	0	0	0	0	0	0	0	3	6	5	5	5	2	4	2	1	2
C. huguoniotii	102	140	0	0	0	0	0	0	0	0	0	0	0	0	0	0	0	0	0
C. oceanica	0	0	0	0	0	0	0	0	0	0	0	0	0	0	0	0	0	0	0
C. cooksoniae	1	1	0	0	0	0	0	0	0	0	0	0	0	0	0	0	0	0	0
C. edwardsii	999	999	0	0	0	0	0	0	0	0	0	0	0	0	0	0	0	0	0
C. distinctum	2	0	0	0	0	0	0	0	0	0	0	0	0	0	0	0	0	0	0
L. defloccata	0	0	0	0	0	0	0	0	0	0	0	0	0	0	0	0	0	0	0
C. membraniphorum	0	999	0	0	0	0	0	0	0	0	0	0	0	0	0	0	0	0	0
D. laminaspinosum	1	0	0	0	0	0	0	0	0	0	0	0	0	0	0	0	0	0	0
D. cladoides	2	0	0	0	0	0	0	0	0	0	0	0	0	0	0	0	0	0	0
D. medusoides	0	0	0	0	0	0	0	0	0	0	0	0	0	0	0	0	0	0	0
E. rugulosum	999	999	0	0	0	0	0	0	0	0	0	0	0	0	0	0	0	0	0
E. campanula	0	0	0	0	0	0	0	0	0	0	0	0	0	0	0	0	0	0	0
E. cf. arnace	0	999	0	0	0	0	0	0	0	0	0	0	0	0	0	0	0	0	0
E. bifidum	3	1	0	0	0	0	0	0	0	0	0	0	0	0	0	0	0	0	0
E. phragmites	1	0	0	0	0	0	0	0	0	0	0	0	0	0	0	0	0	0	0
E. spinosa	3	3	0	0	0	0	0	0	0	0	0	0	0	0	0	0	0	0	0
E. deanei	1	1	0	0	0	0	0	0	0	0	0	0	0	0	0	0	0	0	0
F. ferox	0	999	0	0	0	0	0	0	0	0	0	0	0	0	0	0	0	0	0
F. mantellii	1	0	0	0	0	0	0	0	0	0	0	0	0	0	0	0	0	0	0
F. resex	0	999	0	0	0	0	0	0	0	0	0	0	0	0	0	0	0	0	0
F. amphora	0	0	0	0	0	0	0	0	0	0	0	0	0	0	0	0	0	0	0
G. cassidata	2	0	0	0	0	0	0	0	0	0	0	0	0	0	0	0	0	0	0
G. whitei	0	0	0	0	0	0	0	0	0	0	0	0	0	0	0	0	0	0	0
H. pulchrum	6	2	0	0	0	0	0	0	0	0	0	0	0	0	0	0	0	0	0
H. bowerbankii	1	999	0	0	0	0	0	0	0	0	0	0	0	0	0	0	0	0	0
H. tubiferum	21	6	0	0	0	0	0	0	0	0	0	0	0	0	0	0	0	0	0
H. membraniphorum	2	999	0	0	0	0	0	0	0	0	0	0	0	0	0	0	0	0	0
K. readei	2	999	0	0	0	0	0	0	0	0	0	0	0	0	0	0	0	0	0
L. chlamydata	999	999	0	0	0	0	0	0	0	0	0	0	0	0	0	0	0	0	0
L. siphonophorum glabrum	7	3	0	0	0	0	0	0	0	0	0	0	0	0	0	0	0	0	0
L. siphonophorum siphonophorum	2	2	0	0	0	0	0	0	0	0	0	0	0	0	0	0	0	0	0
A. cf. ramulifera	1	1	0	0	0	0	0	0	0	0	0	0	0	0	0	0	0	0	0
M. ?crinitum	999	1	0	0	0	0	0	0	0	0	0	0	0	0	0	0	0	0	0
M. distinctum	0	0	0	0	0	0	0	0	0	0	0	0	0	0	0	0	0	0	0
N. ornatum	1	999	0	0	0	0	0	0	0	0	0	0	0	0	0	0	0	0	0
M. setosum	999	4	0	0	0	0	0	0	0	0	0	0	0	0	0	0	0	0	0
N. densiradiata	0	0	0	0	0	0	0	0	0	0	0	0	0	0	0	0	0	0	0
O. costata	0	999	0	0	0	0	0	0	0	0	0	0	0	0	0	0	0	0	0
O. operculata	2	1	0	0	0	0	0	0	0	0	0	0	0	0	0	0	0	0	0
O. complex	3	999	0	0	0	0	0	0	0	0	0	0	0	0	0	0	0	0	0
O. prolixispinosum	3	0	0	0	0	0	0	0	0	0	0	0	0	0	0	0	0	0	0
P. infusoroides	**80**	**84**	0	0	0	0	0	0	0	0	0	0	0	0	0	0	0	0	0
P. cenomanense	999	999	0	0	0	0	0	0	0	0	0	0	0	0	0	0	0	0	0
P. pseudhystrichodinium	999	1	0	0	0	0	0	0	0	0	0	0	0	0	0	0	0	0	0
P. truncatum	0	0	0	0	0	0	0	0	0	0	0	0	0	0	0	0	0	0	0
P. conulum	999	0	0	0	0	0	0	0	0	0	0	0	0	0	0	0	0	0	0
P. deflandrei	1	999	0	0	0	0	0	0	0	0	0	0	0	0	0	0	0	0	0
P. cingulatum cingulatum	4	6	0	0	0	0	0	0	0	0	0	0	0	0	0	0	0	0	0
P. cingulatum granulatum	2	2	0	0	0	0	0	0	0	0	0	0	0	0	0	0	0	0	0
P. cingulatum reticulatum	999	1	0	0	0	0	0	0	0	0	0	0	0	0	0	0	0	0	0
P. cingulatum polygonalis	1	999	0	0	0	0	0	0	0	0	0	0	0	0	0	0	0	0	0
P. cornutum	1	1	0	0	0	0	0	0	0	0	0	0	0	0	0	0	0	0	0
R. veligera	999	6	0	0	0	0	0	0	0	0	0	0	0	0	0	0	0	0	0
S. ?dentatus	6	4	0	0	0	0	0	0	0	0	0	0	0	0	0	0	0	0	0
S. multibrevis	999	999	0	0	0	0	0	0	0	0	0	0	0	0	0	0	0	0	0
S. ramosus ramosus (ovoidal)	7	4	0	0	0	0	0	0	0	0	0	0	0	0	0	0	0	0	0
S. ramosus gracilis	3	1	0	0	0	0	0	0	0	0	0	0	0	0	0	0	0	0	0
S. ramosus ramosus (angular)	7	10	0	0	0	0	0	0	0	0	0	0	0	0	0	0	0	0	0
S. ramosus reticulatus	0	999	0	0	0	0	0	0	0	0	0	0	0	0	0	0	0	0	0
S. sp.	2	0	0	0	0	0	0	0	0	0	0	0	0	0	0	0	0	0	0
S. coronatum	0	999	0	0	0	0	0	0	0	0	0	0	0	0	0	0	0	0	0
S. longifurcatum	0	2	0	0	0	0	0	0	0	0	0	0	0	0	0	0	0	0	0
S. spinicongregatum	1	3	0	0	0	0	0	0	0	0	0	0	0	0	0	0	0	0	0
I. castanea	4	8	0	0	0	0	0	0	0	0	0	0	0	0	0	0	0	0	0
V. ovulum	999	0	0	0	0	0	0	0	0	0	0	0	0	0	0	0	0	0	0
X. esbeckianus	0	999	0	0	0	0	0	0	0	0	0	0	0	0	0	0	0	0	0
X. alatum	999	999	0	0	0	0	0	0	0	0	0	0	0	0	0	0	0	0	0
W. anglicum	999	0	0	0	0	0	0	0	0	0	0	0	0	0	0	0	0	0	0
T. variecalamus	999	0	0	0	0	0	0	0	0	0	0	0	0	0	0	0	0	0	0
Spores	1	999	0	0	0	0	0	0	0	0	0	0	0	0	0	0	0	0	0
Bisaccate pollen	1	2	0	0	0	0	0	0	0	0	0	0	0	0	0	0	0	0	0
Verrychium spp.	1	999	0	0	0	0	0	0	0	0	0	0	0	0	0	0	0	0	0
Michrystridium spp.	0	1	0	0	0	0	0	0	0	0	0	0	0	0	0	0	0	0	0
Pterospermopsis spp.	0	0	0	0	0	0	0	0	0	0	0	0	0	0	0	0	0	0	0
Tasmanites spp.	0	0	0	0	0	0	0	0	0	0	0	0	0	0	0	0	0	0	0
Foram. lining type 1	2	1	0	0	0	0	0	0	0	0	0	0	0	0	0	0	0	0	0
Foram. lining type 2	0	0	0	0	0	0	0	0	0	0	0	0	0	0	0	0	0	0	0
Foram. lining type 3	999	999	0	0	0	0	0	0	0	0	0	0	0	0	0	0	0	0	0

Appendix 2. Raw numerical data of section TBB samples. The figure "999" is used to indicate the presence of a palynomorph taxon on an unlogged portion of a slide.

Appendix 3. Raw numerical data of section MCB samples. The figure "999" is used to indicate the presence of a palynomorph taxon on an unlogged portion of a slide.

MCB SECTION

sample number	-9	-8	-7	-6	-5	-4	-3	-2	-1	1	2	3	4	5	6	7	8	9	10	11
sample number	-9	-8	-7	-6	-5	-4	-3	-2	-1	1	2	3	4	5	6	7	8	9	10	11
A. neptuni	1	2	2	2	4	999	0	0	999	1	999	2	1	999	999	2	2	2	1	999
A. ramulifera	4	1	4	1	2	999	2	1	2	3	4	1	999	2	3	2	3	999	1	999
A. reginensis	12	10	7	7	9	3	1	2	2	2	4	2	2	5	5	8	5	2	5	9
A. sagena	1	2	1	999	1	1	1	1	0	1	999	0	0	999	0	2	1	1	999	999
A. sp	1	1	0	0	1	2	3	0	3	0	1	0	0	1	0	1	1	0	0	0
A. deflandrei	999	999	1	999	999	999	999	1	2	999	999	1	0	0	1	0	1	1	0	1
A. maculatum	0	1	0	999	1	0	0	999	0	999	1	0	0	0	0	0	0	0	0	0
C. asymmetricum	999	999	999	999	999	2	0	999	999	1	0	1	0	1	0	1	999	999	999	0
C. colliveri	0	0	0	0	0	0	999	999	999	0	999	0	0	1	0	0	0	999	0	0
C. reticulata	0	0	0	999	0	0	0	999	0	0	0	999	0	999	1	1	1	4	1	2
C. obliquicostatum	0	1	0	999	0	0	0	999	0	0	0	0	0	0	0	0	0	1	0	999
C. discreta	3	1	999	999	2	3	3	4	3	999	0	0	999	1	2	0	999	999	1	0
C. nyei	3	0	0	0	0	0	1	0	999	0	0	0	0	0	0	0	0	0	0	999
C. ?urna	0	0	1	0	1	999	0	2	0	0	0	0	999	0	0	0	0	0	0	0
C. armatum	5	5	4	3	3	4	3	1	5	2	5	999	2	3	999	5	999	3	1	2
C. clavulum	4	4	1	4	2	3	4	3	4	5	1	6	1	4	4	4	2	1	2	1
C. huguoniotii	79	75	82	72	68	68	66	65	74	63	49	60	50	49	45	38	72	97	102	114
C. oceanica	999	1	999	999	999	1	999	0	0	1	1	0	999	0	1	0	0	0	0	0
C. cooksoniae	1	999	1	0	0	999	0	0	0	1	1	0	999	999	999	1	1	999	1	0
C. distinctum	13	12	7	7	5	999	2	2	5	5	5	3	5	1	999	5	3	1	3	3
C. membraniphorum	0	0	999	0	0	0	999	999	0	1	999	0	0	999	0	999	0	0	0	999
D. laminaspinosum	0	0	999	0	0	0	0	0	999	0	1	1	1	0	1	0	0	1	0	1
D. medusoides	0	0	0	0	0	0	0	0	999	1	0	999	0	0	0	0	0	999	0	0
E. rugulosum	1	0	999	999	999	999	999	1	1	2	999	999	1	999	2	0	999	999	1	1
E. campanula	0	2	999	999	999	999	0	999	999	0	1	999	999	1	999	999	1	3	999	2
E. cf. arnace	999	2	1	999	1	999	1	0	1	1	1	0	1	999	999	0	999	0	999	0
E. bifidum	0	2	1	1	2	999	1	0	1	0	0	1	1	999	1	2	0	999	999	0
E. phragmites	1	2	0	1	1	1	0	1	1	0	0	0	0	999	0	2	0	999	1	1
E. spinosa	6	7	8	6	4	999	5	4	11	8	4	1	5	4	5	4	4	5	999	6
F. deanei	999	1	2	999	0	999	1	0	0	0	0	999	999	999	2	2	0	1	999	0
F. ferox	999	999	0	0	0	0	0	0	0	0	0	0	0	999	0	2	0	999	999	0
F. laciniata	0	0	0	0	0	0	0	0	0	0	0	0	1	0	0	0	0	0	0	0
F. mantellii	0	0	0	1	0	0	0	0	0	0	0	0	0	0	0	0	0	0	0	0
F. resex	999	999	999	0	0	999	0	0	0	0	0	0	0	0	0	0	0	0	0	0
F. amphora	999	0	0	0	999	0	999	999	1	0	999	999	0	999	1	0	1	0	1	0
G. cassidata	0	0	0	999	1	0	0	0	1	0	1	1	999	999	999	999	999	0	999	999
G. whitei	0	0	0	0	0	0	0	0	0	0	0	0	0	0	1	0	999	0	0	1
H. pulchrum	4	9	2	3	4	1	2	3	999	3	1	2	5	2	4	4	3	7	9	6
H. bowerbankii	999	999	999	999	999	0	0	999	999	0	1	999	999	999	0	0	999	999	999	1
H. tubiferum	6	4	3	3	3	2	2	1	1	0	4	5	4	3	3	2	0	2	2	1
H. membraniphorum	3	0	1	1	999	1	0	999	1	0	999	999	1	1	999	999	0	999	1	0
K. readei	0	0	0	0	0	999	1	1	0	0	0	999	1	999	0	999	0	999	999	0
L. chlamydata	999	0	999	999	999	999	999	999	1	999	999	1	1	999	1	999	999	2	999	999
L. defloccata	0	0	0	1	0	999	0	0	999	0	0	0	0	0	0	0	0	0	0	0
L. siphonophorum glabrum	4	4	999	2	2	6	3	1	5	3	1	3	1	1	1	1	1	999	2	0
L. siphonophorum siphonophorum	5	2	7	12	6	17	13	10	6	7	7	12	12	12	10	4	6	3	4	8
A. cf. ramulifera	2	1	1	3	3	999	2	5	3	3	2	999	1	999	3	2	0	1	2	4
M. ?crinitum	3	4	4	5	6	5	2	1	2	2	1	0	0	0	0	1	999	0	0	0
M. distinctum	0	0	0	0	0	999	2	0	0	0	0	0	0	0	0	0	0	0	0	0
M. setosum	2	1	1	1	0	1	1	1	0	1	0	0	0	0	0	0	1	2	1	0
N. densiradiata	1	2	1	0	1	1	999	2	0	0	0	0	0	1	1	0	0	1	0	0
O. costata	1	999	3	1	2	1	3	1	4	3	1	999	999	2	1	4	1	2	2	1
O. operculata	2	2	999	999	3	1	2	999	999	1	2	999	1	999	1	1	999	999	999	999
O. complex	3	2	2	3	3	3	1	4	2	1	1	1	999	2	999	0	1	1	999	1
O. prolixispinosum	0	1	999	0	0	0	0	0	0	999	0	2	999	0	999	999	0	0	999	1
P. infusorioides	117	101	122	142	135	142	162	149	135	143	173	152	198	164	186	159	168	125	131	157
P. cenomaniense	999	0	999	0	0	0	999	0	0	2	0	999	0	0	0	0	0	0	0	0
P. pseudhystrichodinium	2	1	999	999	1	1	999	1	4	2	1	1	999	2	1	9	2	999	1	1
P. truncatum	0	999	0	0	1	0	1	999	1	2	999	999	1	2	1	1	999	999	1	1
P. conulum	999	0	1	0	1	1	0	0	999	0	0	0	999	0	0	0	0	1	1	0
P. deflandrei	999	999	2	999	999	4	2	999	4	0	999	999	999	1	0	1	999	0	1	999
P. cingulatum cingulatum	2	3	1	999	2	999	3	4	5	2	4	4	2	6	5	3	2	5	999	3
P. cingulatum granulatum	1	0	999	1	999	999	0	1	1	1	1	1	2	2	2	0	1	1	999	999
P. cingulatum reticulatum	1	0	999	999	999	1	1	1	1	1	0	0	999	0	1	0	1	999	999	1
P. cingulatum polygonalis	999	999	999	999	1	999	2	999	999	1	999	999	0	1	999	0	2	1	999	1
P. cornutum	1	4	2	2	3	5	2	2	4	3	1	2	1	2	0	0	999	0	1	0
R. veligera	1	2	2	1	999	999	2	999	2	1	0	0	1	999	0	2	1	0	1	999
S. ?dentatus	3	1	999	2	0	1	2	4	3	2	0	4	2	5	2	1	1	3	1	1
S. multibrevis	2	1	6	1	4	1	999	999	1	0	0	3	999	999	999	1	999	2	2	1
S. ramosus ramosus (ovoidal)	11	4	1	2	3	1	8	8	5	6	7	9	5	5	5	9	5	7	6	5
S. ramosus gracilis	5	1	1	1	1	999	0	2	1	1	3	2	1	1	0	0	2	0	0	0
S. ramosus ramosus (angular)	7	5	5	2	4	4	4	2	4	7	2	4	8	8	5	12	9	6	7	6
S. ramosus reticulatus	3	4	3	1	1	2	1	5	2	2	1	999	1	1	2	1	1	2	3	1
S. sp.	2	2	0	0	3	3	0	0	2	1	0	2	1	3	2	0	2	1	0	0
S. coronatum	1	999	999	999	999	1	1	999	0	999	999	1	1	999	0	999	999	999	999	999
S. longifurcatum	4	3	2	1	4	1	1	2	4	5	9	7	1	4	7	9	10	7	5	1
S. spinicongregatum	1	1	1	1	1	1	999	0	1	0	1	0	0	0	2	0	1	1	1	1
T. variecalamus	1	1	2	1	1	3	2	2	2	0	0	3	2	0	0	0	0	1	1	0
T. castanea	3	3	2	1	5	3	4	1	3	0	3	3	999	3	1	0	2	2	999	3
V. ovulum	999	1	1	999	0	2	999	999	2	999	0	1	2	999	0	0	1	999	1	999
W. anglicum	1	0	0	0	0	999	0	1	0	0	0	1	0	0	0	0	0	0	0	0
X. esbeckianus	0	0	0	0	0	0	0	999	0	0	0	999	0	0	0	0	0	0	0	0
X. alatum	1	1	999	999	1	0	1	0	0	999	999	999	1	1	999	2	1	3	5	3
X. sp. A	0	0	0	0	0	999	0	0	0	0	999	999	999	999	0	0	1	1	0	999
Spores	5	6	6	2	3	5	7	5	5	1	999	999	3	2	999	3	1	2	2	1
Bisaccate pollen	1	999	1	3	3	1	999	999	4	1	2	4	1	2	999	1	999	999	2	999
Verybachium spp.	2	999	999	1	1	999	0	1	999	2	999	999	6	1	999	999	0	1	0	0
Pterospermopsis spp.	1	0	0	0	0	999	0	0	0	0	0	0	0	0	0	0	0	0	0	1
Foram. lining type 1	7	7	5	5	1	8	7	7	6	9	8	4	3	5	2	3	5	2	1	6
Foram. lining type 2	0	0	0	0	0	0	0	0	0	0	999	2	999	0	1	1	1	1	1	999
Foram. lining type 3	0	0	999	0	0	0	0	0	1	0	1	999	999	1	1	1	2	1	999	999

SFE SECTION

sample number	13	17	16	15

sample number	18	17	16	15
A. neptuni	3	1	4	0
A. reginensis	11	4	1	1
A. sagena	1	0	999	0
A. deflandrei	7	1	11	5
A. maculatum	1	999	1	0
C. asymmetricum	999	0	0	0
C. colliveri	4	1	11	78
C. reticulata	9	5	9	12
C. obliquicostatum	0	999	0	0
C. armatum	999	5	3	999
C. clavulum	6	6	3	0
C. nuguoniotii	24	22	14	0
C. oceanica	0	0	0	999
C. compactum-membraniphorum	78	102	88	94
C. distinctum	3	5	0	0
D. laminaspinosum	0	0	1	0
D. cladoides	999	0	1	0
D. meduscides	999	0	0	0
E. rugulosum	999	0	0	0
E. campanula	1	1	1	0
E. saxoniensis	78	126	81	130
E. bifidum	0	0	1	0
E. phragmites	1	0	0	0
E. deanei	0	999	2	999
E. ferox	999	1	1	2
E. resex	0	0	999	999
F. amphora	999	999	999	0
H. pulchrum	0	5	2	0
I. acuminatum	9	4	2	23
K. ringnesiorum	999	999	4	5
L. chlamydata	1	0	0	1
L. sp A.	11	0	999	0
A. cf. ramulifera	1	0	1	0
M. ?crinitum	0	0	1	0
M. ornatum	999	999	0	999
O. costata	0	999	1	0
O. operculata	1	999	2	999
O. complex	2	0	2	1
P. infusorioides	8	2	9	0
P. pseudhystrichodinium	1	2	1	0
P. truncatum	1	0	999	0
P. conulum	999	0	999	0
P. cingulatum cingulatum	8	2	9	3
P. cingulatum granulatum	3	1	999	0
P. cingulatum reticulatum	999	0	0	999
S. multicrevis	9	5	5	1
S. ramosus ramosus (ovoidal)	3	3	4	2
S. ramosus ramosus (angular)	5	4	2	999
S. pontis-mariae	3	2	1	0
S. longifurcatum	5	2	1	0
T. castanea	0	2	2	0
V. ovulum	999	4	999	0
X. alatum	1	999	0	0
Cyst type A	1	6	27	12
Cyst type B	4	6	5	0
Spores	999	5	2	0
Bisaccate pollen	15	22	18	1
Veryhachium spp.	999	3	3	0
Pterospermopsis spp.	999	0	0	999

Appendix 4. Raw numerical data of South Ferriby section (SFE) samples. The figure "999" is used to indicate the presence of a palynomorph taxon on an unlogged portion of a slide.

Appendix 5. Copy of Fast Fourier Transform programme written by R.E. Eddies, applied in the analysis of Site 3a samples.

```
      PARAMETER (PI=3.14159265)
      PARAMETER (IMAX=128)
      CHARACTER*1,ANSS,ANS
      DIMENSION DDATA(IMAX),AMP(IMAX),FREQ(IMAX),DATIN(2048)
      DIMENSION NDAT(128,16)
C     ***************************************************

C     THIS PROGRAM WILL CALCULATE THE AMPLITUDE SPECTRUM FOR ANY

C     PORTION OF A TIME SERIES, WHERE THE DATA SEGMENT IS A POWER OF

C     TWO. THE PROGRAM WILL ALSO CALCULATE THE AMPLITUDE SPECTRA OF

C     FURTHER WINDOWED SEGMENTS OF THE TIME SERIES.

C     THE SUBROUTINES 'REALFT' AND 'FOUR1' ARE TAKEN FROM

C     'Numerical Recipes',Press, W.H, Flannery,B.P.,
C      Teukolsky, S.A., Vetterling, W.T, 1986, Cambridge Press


C     ROD EDDIES, POLYTECHNIC SOUTH WEST,1988.

C     ***************************************************


      CHARACTER*16,FNAME,FFNAME
      CHARACTER*80,GTITLE
       PRINT *,'*************************************************'
       PRINT *,' '
       PRINT *,'    WELCOME TO THE FFQ.F77, A FORTRAN 77 COMPUTER '
       PRINT *,'    PROGRAM TO CACLULATE THE AMPLITUDE SPECTRUM OF  '
       PRINT *,'    SELECTED WINDOWS OF DATA FROM A SEISMIC TRACE OR'
       PRINT *,'    ANY OTHER TIME SERIES'
       PRINT *,'  '
      PRINT *,'*************************************************'


10     CALL GAPPER(5)

C      ----OPEN AN INPUT FILE CONTAINING THE INPUT DATA-------

       PRINT *,'PLEASE ENTER NAME OF FILE CONTAINING INPUT DATA'
       READ '(A12)',FNAME
       OPEN (9,FILE=FNAME)

       CALL GAPPER(5)

C      ----TELL THE PROGRAM WHERE TO START READING THE DATA---
C      ----IN THE INPUT ARRAY----------------------------


       PRINT *,'PLEASE ENTER THE ARRAY INDEX FOR WINDOW START'
       PRINT *,' '
       PRINT *,'THAT MEANS, TELL THE PROGRAM WHERE TO START'
```

```
      PRINT *,'READING THE DATA FOR THE FIRST WINDOW'



      READ*,NSTART

      CALL GAPPER(5)

C     ----TELL THE PROGRAM WHERE TO FINISH READING THE DATA-
C     ----IN THE INPUT ARRAY-----------------------------------

      PRINT *,'ARRAY INDEX FOR WINDOW END'
      PRINT *,' '
      PRINT *,'THAT MEANS TELL THE PROGRAM WHERE TO STOP'
      PRINT *,'READING THE DATA FOR THE FIRST WINDOW'

      READ*,NSTOP

      CALL GAPPER(5)

C     ----TELL THE PROGRAM WHAT THE SAMPLING INTERVAL IS----

      PRINT *,'PLEASE ENTER THE SAMPLING INTERVAL IN CENTIMETRES ?'
      READ*,SAMP

C     ----CALCULATE THE NYQUIST FREQUENCY FROM THE ---------
C     ----SAMPLING INTERVAL-----------------------------------



      FNYQ=(1/SAMP/2)


C     -----CALCULATE THE NUMBER OF DATA POINTS IN THE -------
C     ----CHOSEN WINDOW-----------------------------------

      N=NSTOP-NSTART
      NN=N/2


C     ----TELL THE COMPUTER HOW MANY WINDOWS----------------
C     -----ARE REQUIRED TO ANALYSE THE DATA SET-------------

      CALL GAPPER(5)


      PRINT *,'HOW MANY WINDOWS OF DATA WOULD YOU LIKE TO LOOK AT ?'
      READ*,NBIN

      CALL GAPPER(5)

      NDATA=NBIN*N
      NCOUNT=0

C     ----THE MAIN DO-LOOP NOW FOLLOWS, WHICH ALLOWS THE ---
C     ----REPEATED SPECTRAL ANALYSIS OF WINDOW AFTER--------
```

```
C       ----WINDOW-----------------------------------------

        NC=0
        KK=0
        KMEM=0




C       ----READ IN (FROM CHANNEL 9)  DATA POINTS-----------
C       -- this read loop is for 128*16 integers -------

        NSUM=0

        DO 111 K=1,128
                        READ(9,99)(NDAT(K,J),J=1,16)
111     CONTINUE

99      FORMAT(16I5)

        CLOSE(9)

C       -- CONVERT DATA TO REAL FORMAT --------

        DO 222 K=1,128

             DO 223 J=1,16
                NSUM=NSUM+1
                DATIN(NSUM)=REAL(NDAT(K,J))

223          CONTINUE

222     CONTINUE


C       --- REMOVE AVERAGE FROM DATA -----

        CALL AVRGE(DATIN,NSUM,XAV)

        DO 333 J=1,NSUM
        DATIN(J)=DATIN(J)-XAV
333     CONTINUE

C       ************************************************************
C
C       START OF THE MAIN FFT DO LOOP
C
C       ************************************************************

        DO 7 M=0,NDATA-N,N

        CALL GAPPER(5)
```

```
C       ----COUNT HOW MANY TIMES THE MAIN LOOP IS COMPLETED---

        NCOUNT=NCOUNT+1


        PRINT *,'_____________________________________________________'
```

```
        DO 1 J=1,N
        DDATA(J)=DATIN(J+NSTART-1+KK+M)

C       ----SET ALL THE VALUES OF THE AMPLITUDE ARRAY TO ZERO-

        AMP(J)=0.0000

1       CONTINUE

C       *** CALL THE FAST FOURIER SUBROUTINE 'REALFT' ********

C       ----THIS TRANSFORMS THE TIME DOMAIN DATA TO-----------
C       ----FREQUENCY DOMAIN DATA, THE FOURIER TRANSFORM------
C       ----RETURNING THE DATA IN COMPLEX FORMAT--------------


        CALL REALFT(DDATA,NN,1)

C       ----THE ZERO- FREQUENCY VALUE f0 IS CONTAINED---------
C       ----IN THE REAL PART OF THE FIRST COMPLEX DATA PAIR---
C       ----NO COMPLEX ARITHMETIC IS USED, THIS VALUE IS -----
C       ----FOUND IN THE FIRST COMPARTMENT OF THE DDATA ARRAY-


        AMP(1)=ABS(DDATA(1))

C       ----THE NYQUIST-FREQUENCY VALUE IS CONTAINED IN THE---
C       ----SECOND COMPARTMENT OF THE DDATA ARRAY-------------

        AMP(NN+1)=ABS(DDATA(2))


C       ----WITH THE EXCEPTION OF ZERO & NYQUIST FREQUENCIES--
C       ----THE PROGRAM WILL NOW COMBINE THE REAL AND---------
C       ----IMAGINARY PARTS OF THE FOURIER TRANSFORM FOR ALL--
C       ----OF THE OTHER REPRESENTED FREQUENCIES-------------
C       ----THIS WILL RESULT IN THE AMPLITUDE OR GAIN FOR-----
C       ----EACH FREQUENCY STORED IN THE ARRAY AMP-----------

        DO 3 J=2,2*NN-2,2

        AMP(J/2+1)=(DDATA(J+1)**2+DDATA(J+2)**2)**0.5

3       CONTINUE

C       ---- CALCULATE THE FREQUENCY VALUE FOR EACH
```

```
C       ---- AMPLITUDE VALUE


        FINT=REAL(FNYQ/NN)
        PRINT *,'FREQUENCY SPACING INTERVAL =',FINT
        KCOUNT=0

        DO 4 J=1,NN
        KCOUNT=KCOUNT+1
        FREQ(J+1)=REAL(FINT*KCOUNT)

4       CONTINUE
```

```
        CALL GAPPER(3)

        PRINT *,'  '
        PRINT *,'                                                    ******'
        PRINT *,'  AMPLITUDE SPECTRUM FOR WINDOW NUMBER ',NCOUNT
        PRINT *,'                                                    ******'
        PRINT *,'  '
        PRINT *,'  USING TIME SAMPLE POINTS ',M+1+KK+NSTART-1
     1  ,' TO',M+N+KK+NSTART-1
        PRINT *,'  '
        PRINT *,'  THE WINDOW IS ',NINT(SAMP*(N-1)),'cm in length'
        PRINT *,'  '

        NBEGIN=M+1+KK+NSTART-1
        NEND=M+N+KK+NSTART-1
```

```
        PRINT *,'  FROM ',NINT(SAMP*(NBEGIN-1)),'cm to',
     1 NINT(SAMP*(NEND-1)),'cm'


        CALL GAPPER(2)

        PRINT 100

100     FORMAT(8X,'AMPLITUDE',10X,'FREQUENCY (cycles per cm)')

        FREQ(1)=0.0

        DO 6 J=1,NN+1

        PRINT 101,AMP(J),FREQ(J)


6       CONTINUE


        CALL GAPPER(2)
        PRINT *,'Nyquist Frequency = ',NINT(FNYQ),' cycles per cm'
        CALL GAPPER(1)
        PRINT *,'Sampling interval = ',SAMP,' cm'
        PRINT *,'Sampling frequency = ',(FNYQ*2),' cm'
        CALL GAPPER(3)
        PRINT *,'_____________________________________________________'
101     FORMAT(8X,F8.3,13X,F8.3)
```

```
PRINT *,'do you want to write the amplitude spectrum to disk ?'

 READ '(A1)',ANSS

     IF(ANSS.EQ.('N').OR.ANSS.EQ.('n')) THEN

       GO TO 777

       ENDIF

       PRINT *,'enter name of file for amplitude spectrum '
       READ  '(A16)',FFNAME
       OPEN (8,FILE=FFNAME)

       PRINT *,'enter a header for the output file'
       READ '(A80)',GTITLE

       WRITE(8,'(A80)')GTITLE
       WRITE(8,103)

       DO 666 LL=1,NN+1
          WRITE(8,102)AMP(LL),FREQ(LL)
666    CONTINUE

       CLOSE(8)

777    CONTINUE

102          FORMAT(8X,F8.3,13X,F8.3)
103          FORMAT('        amplitude                    frequency (Hz)')

       KMEM=KK
       CALL GAPPER(10)
       PRINT *,'GAP DESIRED BETWEEN PREVIOUS + NEXT WINDOW ??'
       READ*,KK
       KK=KK+KMEM
       NC=1

7      CONTINUE

       PRINT *,'*** END OF PROGRAM ***'
       CALL GAPPER(4)
       PRINT *,'do you wish to process another file ?'
       READ '(A1)',ANS

       IF(ANS.EQ.('Y').OR.ANS.EQ.('y')) THEN

       GO TO 10

       ELSE

       CONTINUE

       ENDIF

       PRINT*,' OK, SEE YOU AROUND ANOTHER DAY, ANOTHER SESSION !'
```

```
      STOP
      END

      SUBROUTINE REALFT(DATA,N,ISIGN)
      REAL*8 WR,WI,WPR,WPI,WTEMP,THETA
      DIMENSION DATA(2*N)
      THETA=3.141592653589793/N
      C1=0.5
      IF(ISIGN.EQ.1) THEN
        C2=-0.5
        CALL FOUR1(DATA,N,+1)
      ELSE
        C2=0.5
        THETA=-THETA
      ENDIF
      WPR=-2.0*SIN(0.5*THETA)**2
      WPI=SIN(THETA)
      WR=1.0+WPR



      WI=WPI
      N2P3=2*N+3
      DO 11 I=2,N/2+1
         I1=2*I-1
         I2=I1+1
         I3=N2P3-I2
         I4=I3+1
         WRS=REAL(WR)
         WIS=REAL(WI)
         H1R=C1*(DATA(I1)+DATA(I3))
         H1I=C1*(DATA(I2)-DATA(I4))
         H2R=-C2*(DATA(I2)+DATA(I4))
         H2I=C2*(DATA(I1)-DATA(I3))
         DATA(I1)=H1R+WRS*H2R-WIS*H2I
         DATA(I2)=H1I+WRS*H2I+WIS*H2R
         DATA(I3)=H1R-WRS*H2R+WIS*H2I
         DATA(I4)=-H1I+WRS*H2I+WIS*H2R
         WTEMP=WR
         WR=WR*WPR-WI*WPI+WR
         WI=WI*WPR+WTEMP*WPI+WI
11       CONTINUE
         IF (ISIGN.EQ.1) THEN
         H1R=DATA(1)
         DATA(1)=H1R+DATA(2)
         DATA(2)=H1R-DATA(2)
         ELSE
         H1R=DATA(1)
         DATA(1)=C1*(H1R+DATA(2))
         DATA(2)=C1*(H1R-DATA(2))
         CALL FOUR1(DATA,N,-1)
         ENDIF
         RETURN
         END


      SUBROUTINE FOUR1(DATA,NN,ISIGN)
      REAL*8 WR,WI,WPR,WPI,WTEMP,THETA
      DIMENSION DATA(2*NN)
      N=2*NN
```

```
      J=1
      DO 11 I=1,N,2
      IF(J.GT.I) THEN
      TEMPR=DATA(J)
      TEMPI=DATA(J+1)
      DATA(J)=DATA(I)
      DATA(J+1)=DATA(I+1)
      DATA(I)=TEMPR
      DATA(I+1)=TEMPI
      ENDIF
      M=N/2
1     IF ((M.GE.2).AND.(J.GT.M)) THEN
      J=J-M
      M=M/2
      GO TO 1
      ENDIF
      J=J+M
11    CONTINUE
      MMAX=2
2     IF (N.GT.MMAX) THEN
      ISTEP=2*MMAX
      THETA=6.28318530717959/(ISIGN*MMAX)



      WPR=-2.0*SIN(0.5*THETA)**2
      WPI=SIN(THETA)
      WR=1.
      WI=0.
      DO 13 M=1,MMAX,2
      DO 12 I=M,N,ISTEP
      J=I+MMAX
      TEMPR=REAL(WR)*DATA(J)-REAL(WI)*DATA(J+1)
      TEMPI=REAL(WR)*DATA(J+1)+REAL(WI)*DATA(J)
      DATA(J)=DATA(I)-TEMPR
      DATA(J+1)=DATA(I+1)-TEMPI
      DATA(I)=DATA(I)+TEMPR
      DATA(I+1)=DATA(I+1)+TEMPI
12    CONTINUE
      WTEMP=WR
      WR=WR*WPR-WI*WPI+WR
      WI=WI*WPR+WTEMP*WPI+WI
13    CONTINUE
      MMAX=ISTEP
      GO TO 2
      ENDIF
      RETURN
      END

      SUBROUTINE GAPPER(NGAP)
      DO 1 J=1,NGAP
      PRINT *,' '
1     CONTINUE
      RETURN
      END


      SUBROUTINE AVRGE(VALUE,NNN,AV)
      DIMENSION VALUE(NNN)
```

Appendix 6

The following is a brief summary of the groups identified by cluster analysis by Harker *et al.* (1990) which are quoted in Chapter 8.

R-mode

Group A

Predominantly gonyaulacoid and gymnodinioid taxa, implying marine environment with normal or near-normal salinity.

Subgroup A3

1. Five chorate and proximachorate taxa, four of which are gonyaulacoid; *Tanyosphaeridium variecalamum, Spiniferites ramosus* var. *gracilis, Spiniferites ramosus* var. *multibrevis, Achomosphaera ramulifera,* and one peridinioid *Palaeohystrichophora infusorioides.*
2. This Subgroup occurs throughout the Austin and Taylor successions of Texas and many other successions in Canada.

Q-mode

Group 5

Contains all samples from Austin and Taylor successions in Texas. The microplankton assemblages are very varied, dominated by chorate and proximochorate species and containing few peridinioids. The terrsetrial component is low to very low, reflecting deposition at a considerable distance from and terrigenous source.

Subgroup 5A

1. This Subgroup consists of marl lithologies.
2. The microplankton assemblage contains a variety of gymnodinioid, ceratioid, chorate and proximochorate species from R-mode Subgroups A1, A2, A3, B1 and I1.
3. Common taxa include *Dinogymnium acuminatum, Dinogymnium digitus, Dinogymnium euclaensis, Odontochitina costata, Exochosphaeridium phragmites, T. variecalamum, S. ramosus* var. *ramosus, S. ramosus* var. *gracilis* and *P. infusorioides.*
4. A strong marine influence is further substantiated by the presence of numerous internal foraminiferal linings.
5. The terrestrial component is low with a small amount of plant

cuticle and low numbers of small spores and of inaperturate and bisaccate pollen grains.

6. Diversity and equitability values are high (mean diversity = 2.8, SD = 0.37; mean equitability = 0.68, SD = 0.07)

Sugroup 5B

1. This Subgroup consists of chalk and marl lithologies.

2. The microplankton assemblage consists of a variety of proximochorate, gymnodinioid, ceratioid and cavate spcies from R-mode Subgropups A1, A3, B1 and K2.

3. Common taxa include *Flerntinia truncigera, S. ramosus* var. *ramosus, S. ramosus* var. *gracilis, S. ramosus* var. *multibrevis, Achomosphaera ramulifera, Pervosphaeridium truncatum, Spinidinium echinoidcum, O. costata, Scnonisphaera rotundata.*

4. The presence of scolecodonts and internal foraminiferal linings gives further evidence of marine deposition.

5. The terrestrial component is very low, with little plant culticle and low numbers of small spores and inapeturate pollen grains.

6. Diversity and equitabllity values are high (mean diversity = 2.37, SD =0.08; mean equitability = 0.54, SD = 0.03)

Appendix 7

Palynofacies association of samples TBB -3 to TBB 2

	Phyrogen	Amorphogen	Melanogen	Hylogen
TBB -3	50%	40%	7%	3%
TBB -2	45%	40%	10%	5%
TBB -1	50%	40%	8%	2%
TBB 0	54%	35%	10%	1%
TBB 1	45%	40%	10%	5%
TBB 2	45%	40%	10%	5%

Palynofacies association of samples TBB 3 to TBB 15

	Phyrogen	Amorphogen	Melanogen	Hylogen
TBB 3	55%	25%	15%	5%
TBB 4	60%	28%	10%	2%
TBB 5	55%	30%	10%	5%
TBB 6	65%	15%	15%	5%
TBB 7	55%	34%	10%	1%
TBB 8	65%	25%	15%	5%
TBB 9	65%	23%	10%	2%
TBB 10	65%	23%	10%	2%
TBB 11	69%	25%	5%	1%
TBB 12	70%	15%	12%	3%
TBB 13	55%	35%	9%	1%
TBB 14	70%	15%	13%	2%
TBB 15	55%	34%	10%	1%

Appendix 8. Stable isotope data for South Ferriby samples (SFE), from Hart *et al.* (1991).

	A	B	C
1	Sample	C13 PDB	O18 PDB
2	SFE 1	3.122	-4.728
3	SFE 2	2.883	-4.324
4	SFE 3	3.004	-4.527
5	SFE 4	3.118	-4.757
6	SFE 7	3.695	-5.874
7	SFE 8	3.324	-5.189
8	SFE 9	3.248	-5.288
9	SFE 10	3.196	-4.975
10	SFE 11	3.075	-5.049
11	SFE 12	3.089	-5.082
12	SFE 13	3.059	-4.571
13	SFE 14	2.925	-3.853
14	SFE 15	3.563	-6.082
15	SFE 16	3.961	-5.511
16	SFE 17	3.899	-5.084
17	SFE 18	4.121	-5.391
18	SFE 19	4.171	-3.968
19	SFE 20	3.974	-3.144
20	SFE 21	4.056	-3.959

Historical Biology, 1991, Vol. 5, pp. 339–354
Reprints available directly from the publisher
Photocopying permitted by license only

THE LATE CENOMANIAN EVENT IN EASTERN ENGLAND

M.B. HART[1], P. DODSWORTH[2], P.W. DITCHFIELD[3], A.M. DUANE[1] and C.J. ORTH[4]

[1]*Department of Geological Sciences, Polytechnic South West, Drake Circus, Plymouth PL4 8AA, Devon, UK,* [2]*Centre for Palynological Studies, The University of Sheffield, Beaumont Building, Sheffield S3 7HF,* [3]*Department of Earth Sciences, University of Liverpool, PO Box 147, Liverpool L69 3BX, and* [4]*Los Alamos National Laboratory, Los Alamos, New Mexico 87545, USA*

(Received November 3, 1990)

The Cenomanian/Turonian boundary event has been fully documented from a series of localities between Flamborough Head in Humberside and Marham in Norfolk. The carbon isotope excursion can be identified and extrapolated to all the studied sections using bed-by-bed correlation. Evidence from studies of the isotope data, trace element geochemistry, and the micropalaeontology are presented. The famous "Black Band" is seen to change laterally into a "red" horizon and then a "green" horizon when traced southwards. This appears to represent the "feather-edge" of the anoxic event when traced towards a palaeo-high which is located in the region of the Wash. All the events, so-identified, can be correlated with the *A. plenus* Marl succession in southern England.

KEY WORDS: Cenomanian/Turonian boundary, anoxic event, isotope stratigraphy, geochemistry, Foraminifera, dinoflagellate cysts.

INTRODUCTION

The Late Cenomanian event is now regarded as one of the major global bioevents, ranking alongside the K/T boundary, Late Eocene event, and others on the Raup and Sepkoski (1984), 26 million year periodicity. Humberside (in eastern England) has, since the outset of interest in this event, been important as a key area, with South Ferriby quarry (Figures 1 and 2) accepted as a reference section. The work of Schlanger and Jenkyns (1976), Hart and Bigg (1981), Arthur *et al.* (1987) and Schlanger *et al.* (1987) has established the presence of a $\delta^{13}C$ isotope "spike" in the section, together with evidence of the palaeontological changes associated with the "Black Band". Following the work of Jarvis *et al.* (1988) on the micropalaeontological changes across the Late Cenomanian "anoxic event" it was decided to re-investigate the Humberside successions. In order to more closely calibrate the event, isotope (PWD) and rare earth geochemistry (CJO) determinations have been performed on splits of the *same* samples.

Field work by one of us (P.D.) in south Humberside and Lincolnshire has shown how the "Black Band" varies across a 100 mile (160 km) length of outcrop (Figure 1). Of particular significance is the quite clear thinning of the marl succession and its change from black to red to green across the area.

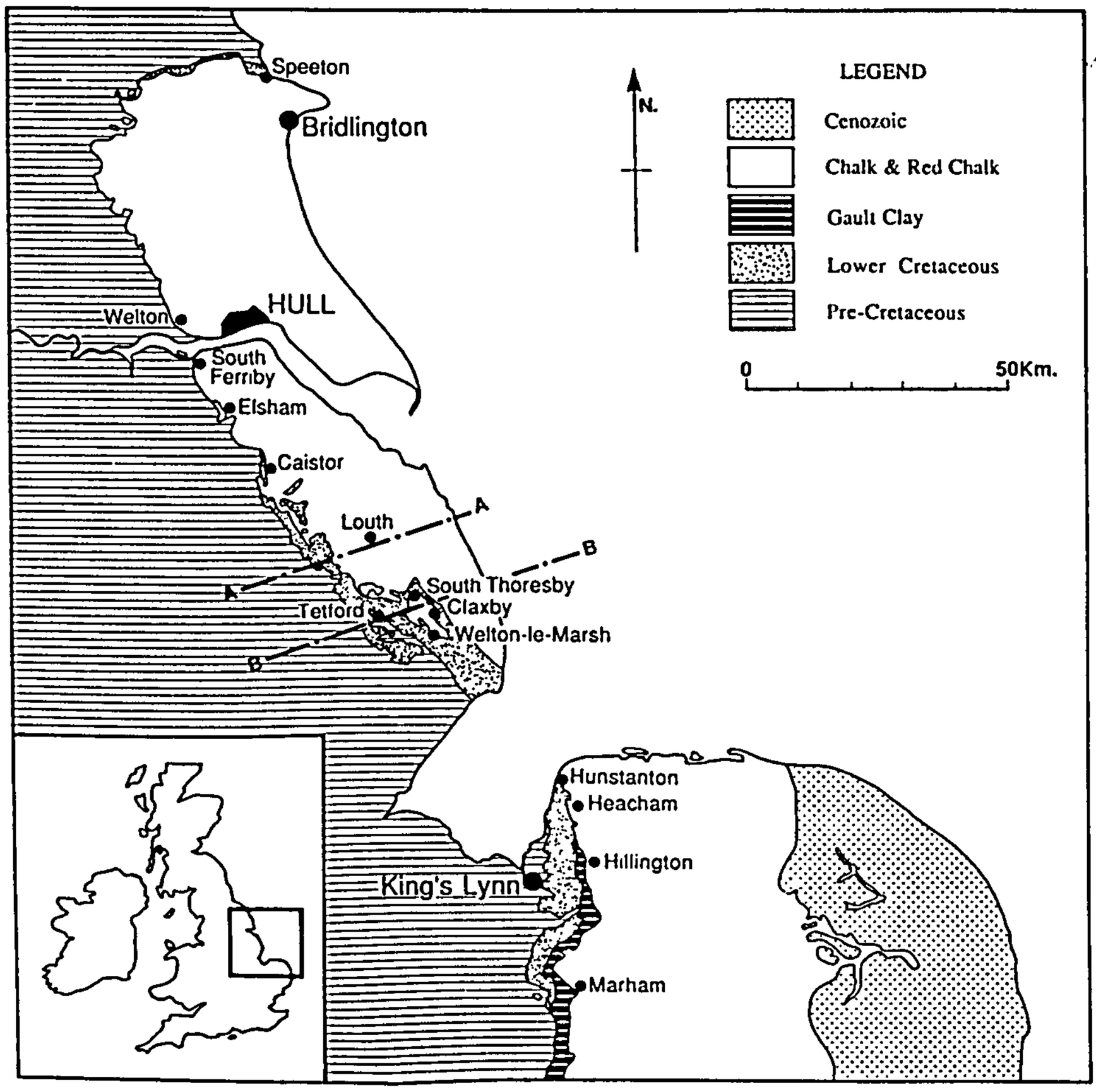

Figure 1 Locality map for sections discussed in the text. Line A–A marks the southern limit of the "Black Band". Between lines A–A and B–B the chalks and nodular chalks of the late Cenomanian event are dull red in colour, while south of line B–B the chalks at the same stratigraphic level are green.

FIELD DATA

The lower part of the Chalk Group of the East Midlands shelf is represented by a condensed sequence of marly chalks. The lithostratigraphic scheme used to subdivide the Anglo-Paris Basin succession of southern England cannot, therefore, be applied to this area. An alternative lithostratigraphy has been developed (Wood and Smith, 1978; Jeans, 1980) and this has been used throughout this study. The characteristic succession of the Plenus Marl Formation (Jefferies, 1962, 1963; Jarvis *et al.*, 1988) in southern England can be traced to Marham (Figures 1 and 2), while at Hillington (Norfolk) there is only a distinctive omission surface. From Heacham northwards the "Plenus Marl Formation" can be traced all the way to the coast at Speeton. The distinctive black, organic-rich mudstone, which gives the "Black Band" its name, only appears at Louth (West). A full account of this

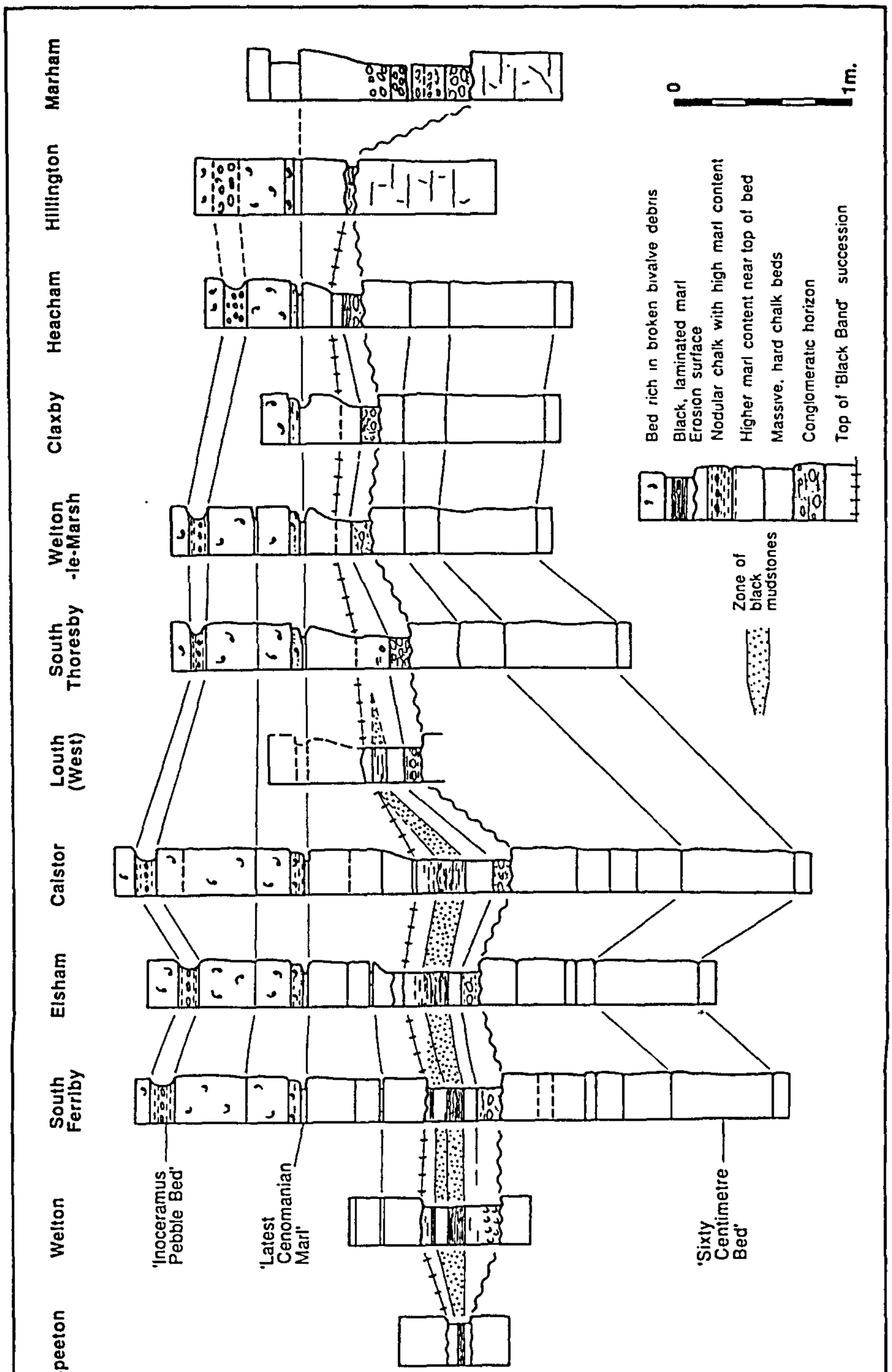

Figure 2 North–south correlation across Humberside, Lincolnshire and Norfolk. The boundaries shown on Figure 1 lie between Louth and South Thoresby (A–A) and between Welton-le-Marsh and Claxby (B–B).

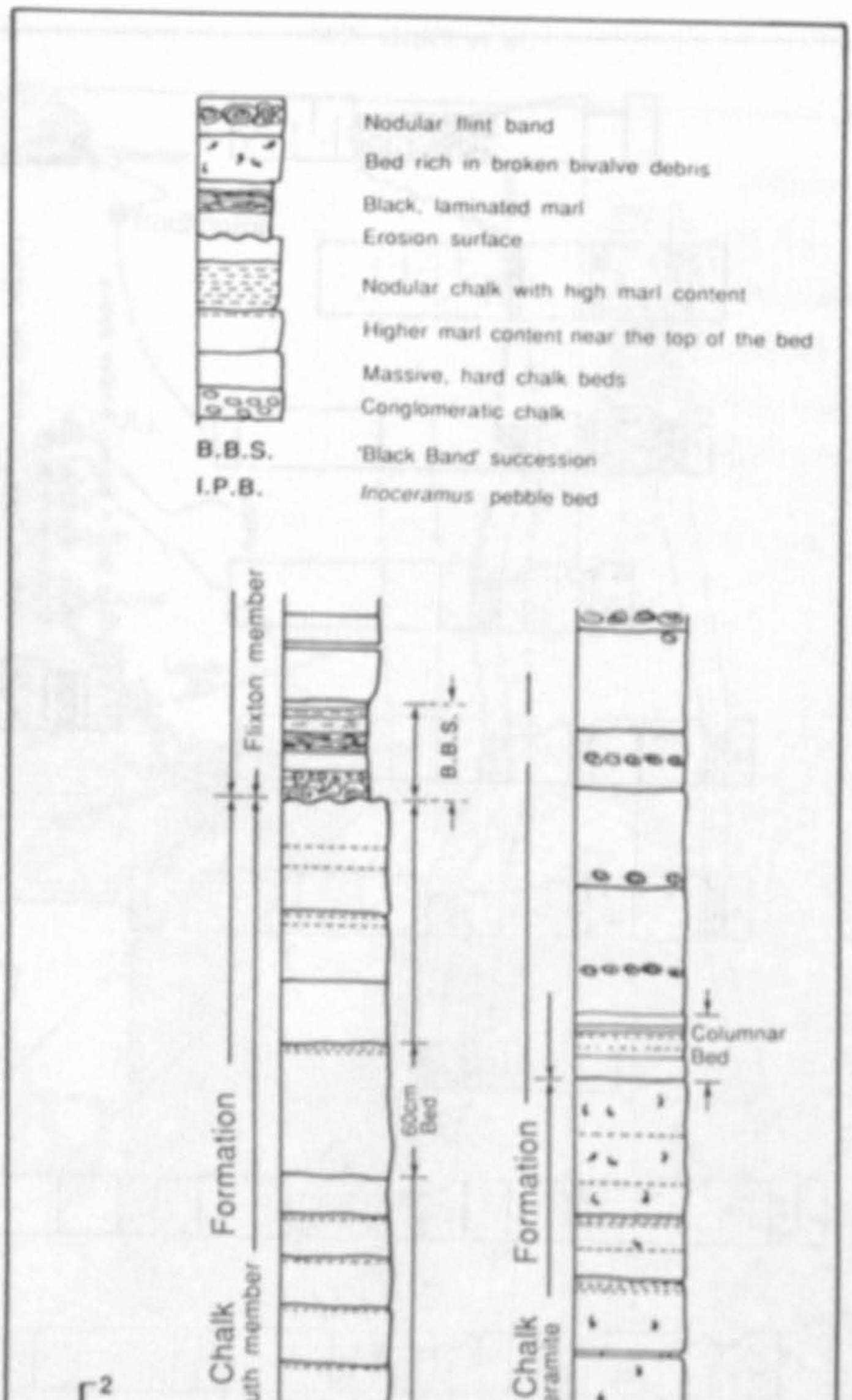

Figure 3 Part of the succession exposed in the South Ferriby Quarry with an explanation of the principal lithostratigraphical terms.

lithostratigraphical correlation is in preparation (by Dodsworth and Hart). The principal terms used are (Figure 3) the Ferriby Chalk Formation and the overlying Welton Chalk Formation.

The Louth Member (Ferriby Chalk Formation) is largely composed of massive, homogenous, chalks with thin intervening marls. Near the top of the member there is a relatively thick bed (on average 60 cm) of pure hard chalk. This bed can be correlated south from South Ferriby across much of the area shown in Figure 1 and there is no reason to suppose that its deposition was in any way diachronous. The position of the "60 cm bed" in the succession gives some indication of the amount of pre-Welton Chalk erosion there has been in the area. The Flixton Member constitutes the uppermost major upward-fining cycle proposed by Jeans (1980). There is a significant hiatus between the eroded top of the Louth Member and the overlying "Black Band" succession. A conglomerate of phosphatised chalk pebbles (indicative of long periods of exposure on the sea floor) rests on top of a slight angular unconformity (the sub-Plenus erosion surface).

The "Black Band" succession thins towards the south of the area, with the black organic-rich mudstones wedging out completely between Louth (West) and South Thoresby. It is important to note that the "Black Band" succession, shown in Figure 2, thins markedly towards Louth and the disappearance of the organic-rich mudstone is quite significant. This appears to be the feather-edge of the "oceanic anoxic event" and as such has not previously been described.

An over-simplified view of the "Black Band" as an homogenous, black mudstone seems to have been adopted by many authors. This view is refuted here. Careful examination of the main blackened horizon in the field, hand specimen, and thin section all reveal that the black marls are interlaminated with paler-coloured marls. Above and below the "Black Band", the proportion of these paler

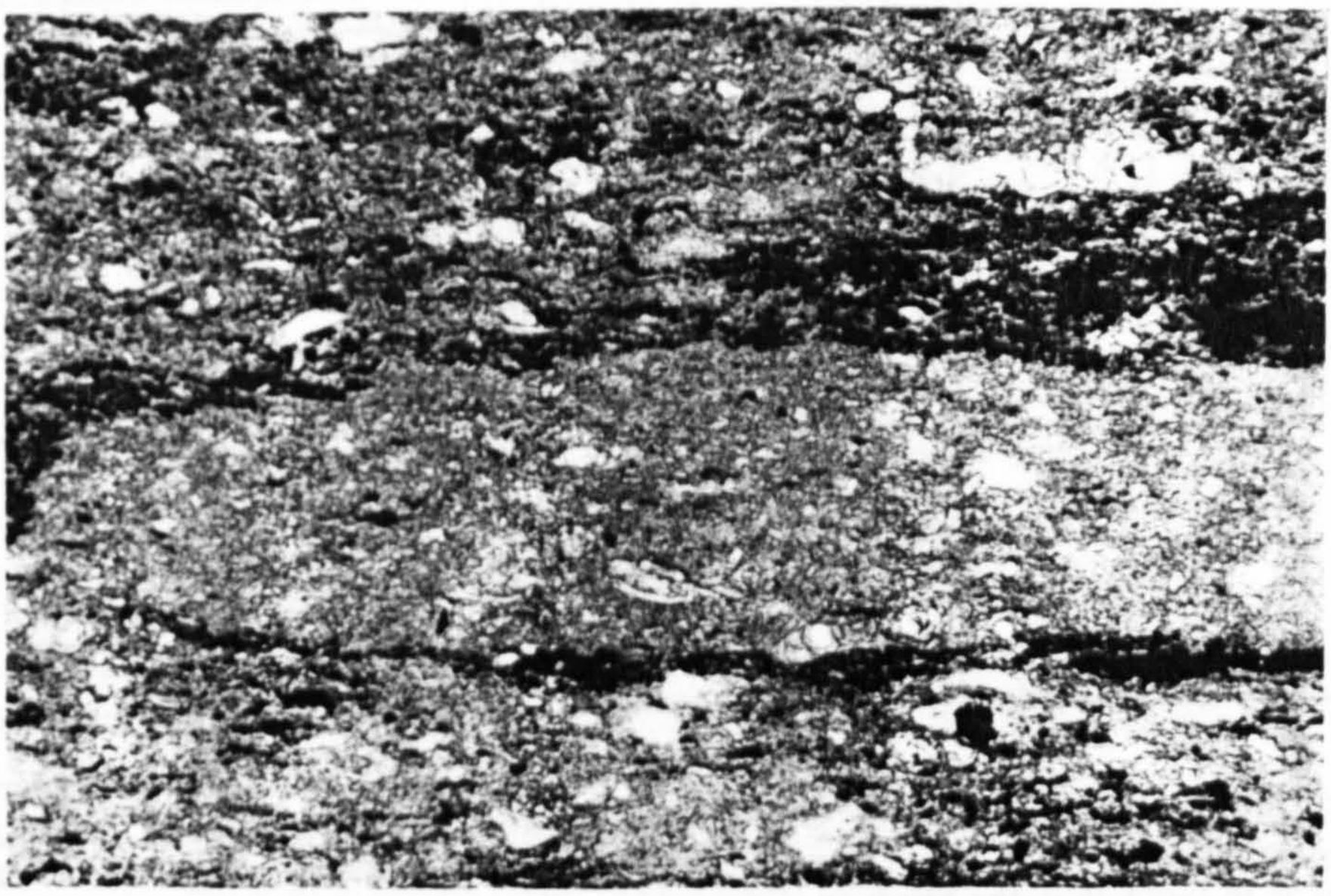

Figure 4 Part of the "Black Band" showing interlaminated pale cream mudstone and black organic-rich mudstone. A highly compressed, unidentifiable, foraminifer is visible in the upper right hand corner. This is sample SFE 17 and the field of view is 13 mm.

laminae becomes greater than that of the black laminae. At South Ferriby, a local, thinner laminated "Black Band" is developed at the top of Bed iv (Figure 2). Individual laminae have often been distorted and truncated by de-watering and compaction processes.

In places the original lamination has almost been destroyed by bioturbation (especially *Chondrites*). The black laminae are almost invariably associated with yellowish-grey marls (beds iii and iv) which are quite distinct from the greenish-grey and pale olive marls of beds i, ii and v. This "Black Band" facies wedges out southwards. At Louth (west) the black laminae are only poorly developed in the yellowish-grey marls of bed iii/iv.

ISOTOPE RECORD

There appears to be general agreement (Arthur *et al.*, 1987; Schlanger *et al.*, 1987; Hart and Leary, 1989) that the positive $\delta^{13}C$ isotope excursion in the latest Cenomanian–earliest Turonian is synchronous in many parts of the world. At South Ferriby, Schlanger *et al.* (1987) have shown the maximum values for $\delta^{13}C$ (+4‰ to +5‰ PDB) lie between bed i and the lower part of bed iii. The data (PWD) from the samples collected as part of this investigation are listed in Table 1 and shown in Figure 5.

Table 1 Carbon and oxygen isotope data from the South Ferriby sample suite.

South Ferriby

	A	B	C
1	Sample	C 13 PDB	O 18 PDB
2	SFE 1	3.122	−4.728
3	SFE 2	2.883	−4.324
4	SFE 3	3.004	−4.527
5	SFE 4	3.118	−4.757
6	SFE 7	3.695	−5.874
7	SFE 8	3.324	−5.189
8	SFE 9	3.248	−5.288
9	SFE 10	3.196	−4.975
10	SFE 11	3.075	−5.049
11	SFE 12	3.089	−5.082
12	SFE 13	3.059	−4.571
13	SFE 14	2.925	−3.853
14	SFE 15	3.563	−6.082
15	SFE 16	3.961	−5.511
16	SFE 17	3.899	−5.084
17	SFE 18	4.121	−5.391
18	SFE 19	4.171	−3.968
19	SFE 20	3.974	−3.144
20	SFE 21	4.056	−3.959

Figure 5 shows a small $\delta^{13}C$ excursion within the "Black Band" with a maximum value of 4.171‰ PDB within the upper part of bed ii (sample SFE 19). This is in fact below the black mudstone where the main concentration of organic matter would be expected. If that is the case then the carbon isotope excursion cannot be due to enhanced burial of $\delta^{13}C$ (i.e. organic matter) within the "Black Band" itself. The shift in $\delta^{13}C$ values may, therefore, be due to methanogenesis. In

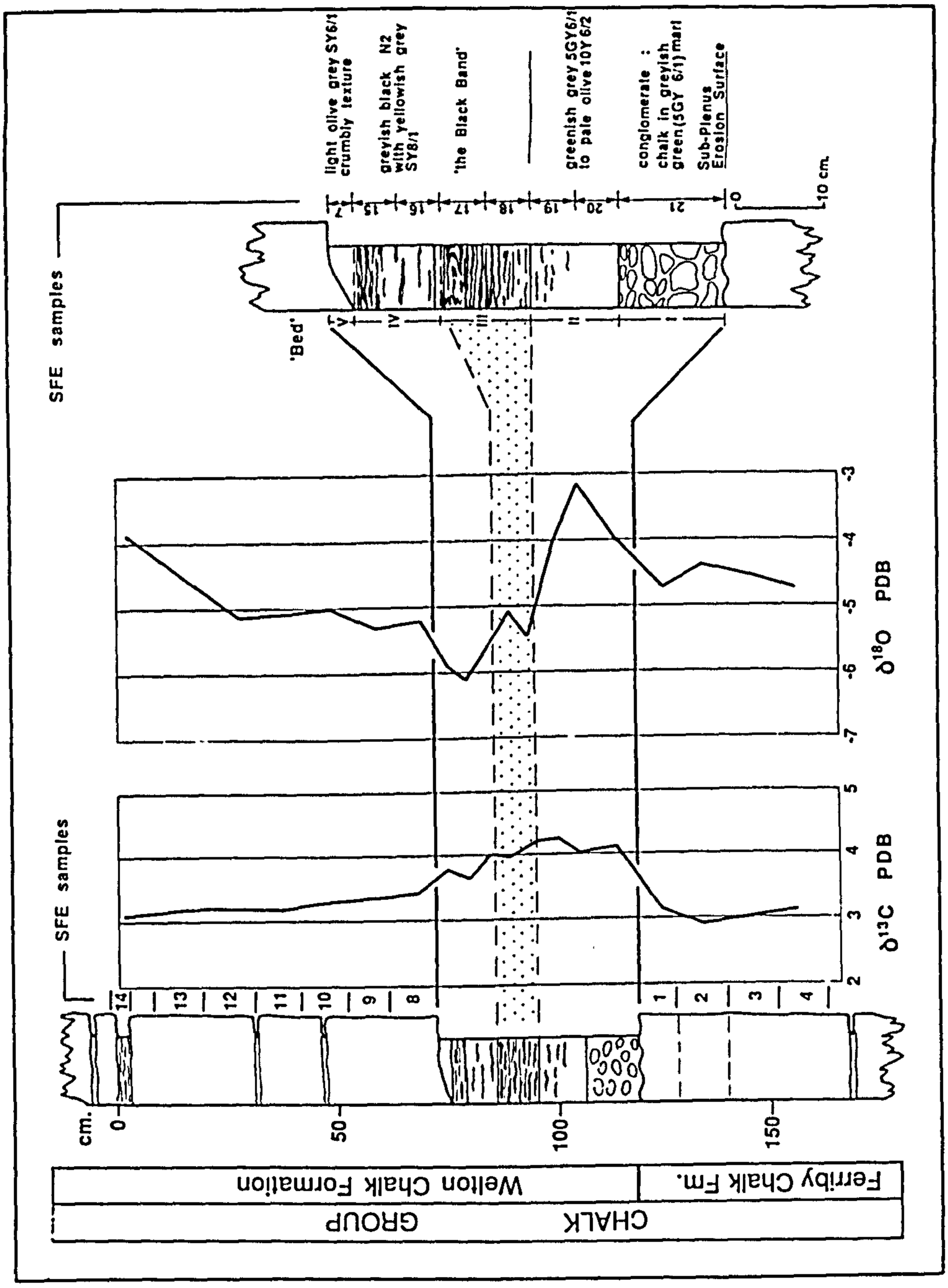

Figure 5 Carbon and oxygen isotope curves for the "Black Band" succession at South Ferriby.

this case $\delta^{13}C$-depleted methane might have migrated out of the system, leaving behind very $\delta^{13}C$ enriched bicarbonate which is then available for the formation of $\delta^{13}C$ enriched carbonate. The values of $\delta^{13}C$ recorded in this section are, however, considerably lower than the extreme values often associated with methanogenesis.

The oxygen isotope values are generally quite depleted in $\delta^{18}O$ and probably reflect the composition of burial cements. The least altered $\delta^{18}O$ values occur low in the succession and may reflect less intense burial diagenesis due to restricted permeability. The formation of burial cements and the overprinting effect of their isotopic signatures may have reduced the magnitude of any primary $\delta^{13}C$ excursion, and this may explain why the observed excursion is smaller than that seen at Dover.

RARE EARTH GEOCHEMISTRY

Sample splits have also been investigated for evidence of siderophile anomalies at the Los Alamos National Laboratory (CJO). The resulting data are presented in Figure 6.

Although Iridium shows a broad maximum in the "Black Band" it correlates with the aluminium (clay) content; a quite normal observation. Indeed SEM analysis by MBH and PD of a sample (SFE 20) from bed ii identifies a flake of montmorillonite with detectable levels of Iridium (using X-ray dispersive analysis equipment). When the Ir is normalized against Al there is a small excess near the bottom of the section (in the topmost bed(s) of the Louth Member, Ferriby Chalk Formation). Thorium, which is depleted in the better sections (Western Interior, USA), shows a pattern essentially identical to Ir. The Th/Al pattern is essentially flat. The peaks detected in the As/Al, U/Al, Co/Al, and possibly Cr/Al, are probably reflecting the higher organic content (see below).

The Mn/Ca ratio is enhanced in well-preserved or strong sites but in this section it is reduced within the "Black Band". This may be the result of Mn depletion; a process often recorded in anoxic marine environments.

The geochemical data presented here indicate that the Late Cenomanian siderophile anomaly zone is probably represented within the well-known (Hart and Bigg, 1981; Hart and Leary, 1989) hiatus between the top of the Louth Member and the "Black Band".

MICROPALAEONTOLOGY

Sample splits have been investigated for foraminifers, ostracods, calcareous nannofossils, and dinoflagellates. A more complete palaeontological account is in preparation and only a few general comments will be made here.

Samples have been processed for foraminifers, palynology, and ostracods. Thin sections have been made and rock fragments have been investigated under the SEM for information on calcareous nannofossils and evidence of diagenesis.

Palynology

Samples prepared for palynological investigation (AMD) have been investigated for both species content and, using the Aliquot Technique, for their quantitative distribution. A high number of cysts per gramme of sediment is taken to indicate

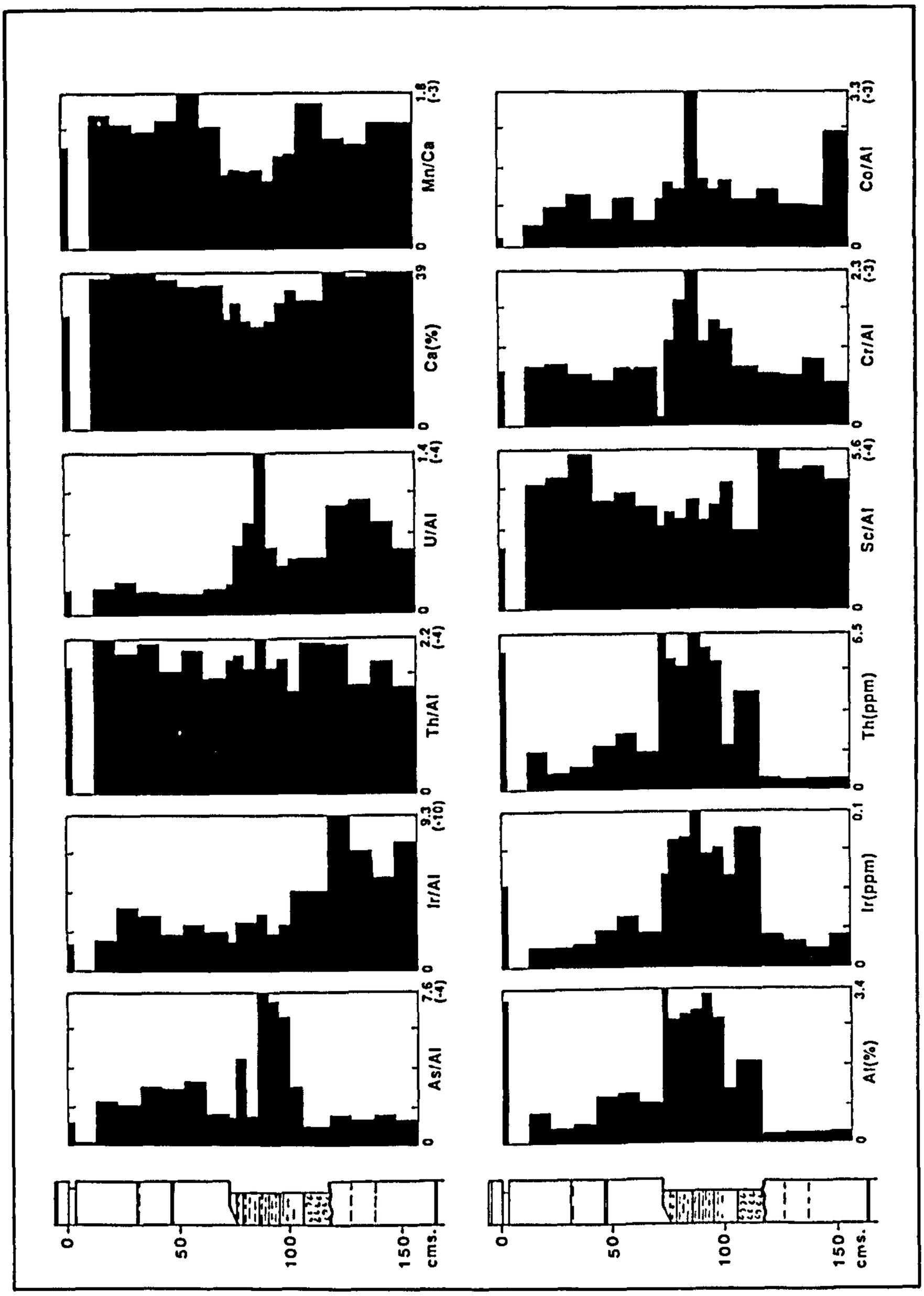

Figure 6 Rare earth geochemical data from the "Black Band" succession at South Ferriby.

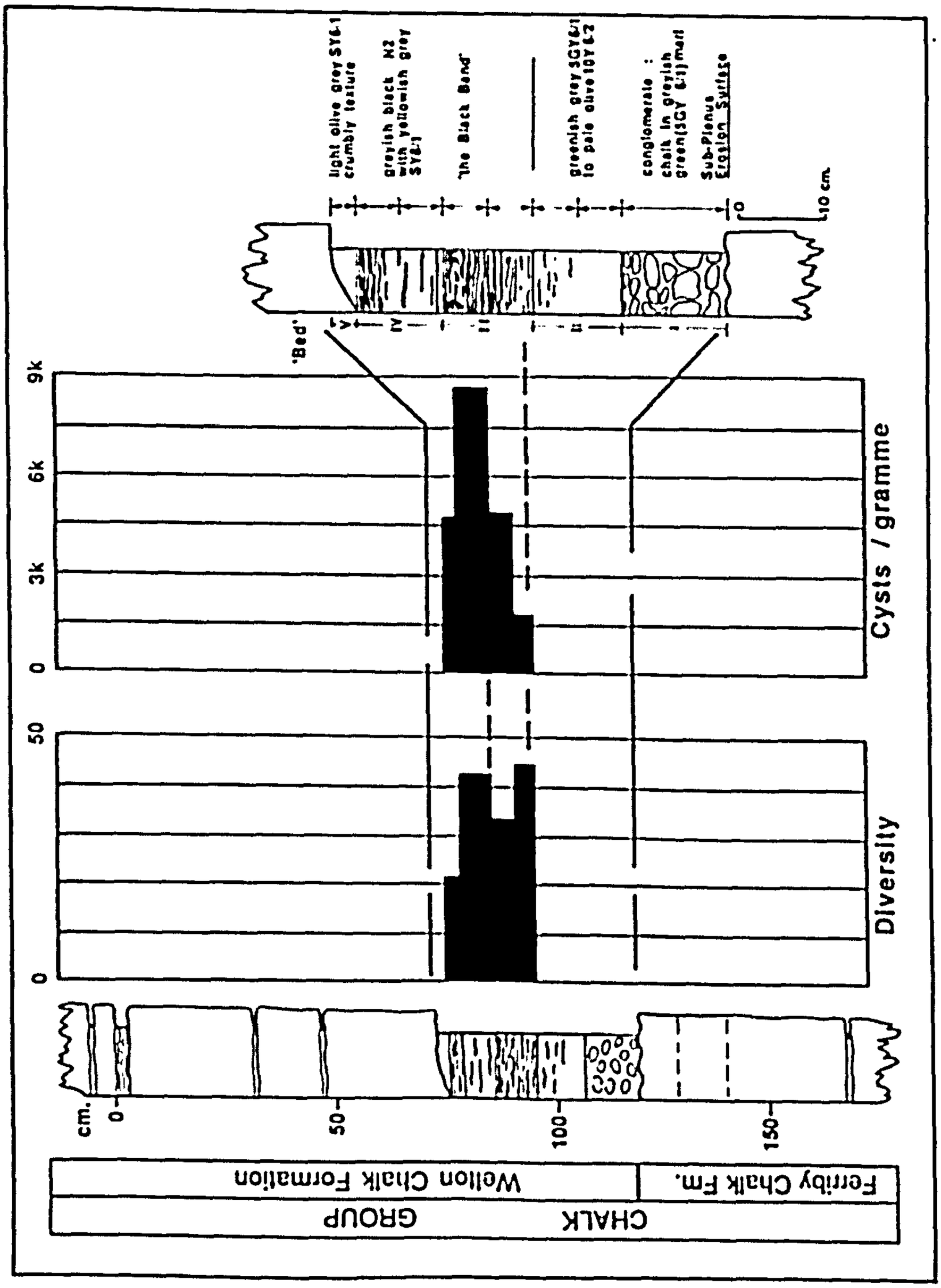

Figure 7 Palynological data from the "Black Band" succession at South Ferriby.

high levels of primary productivity in the water mass and vice versa. As indicated in Figure 7, the majority of samples are barren. Preservation of dinoflagellate cysts is thus restricted to the "Black Band" facies. The *average* abundance for a typical Cenomanian assemblage in southern England is 300–1200 cysts per gramme, somewhat lower than the values recorded in the "Black Band" facies. There must, therefore, have been exceptionally high productivity at this level or significantly enhanced levels of preservation. In the samples with extremely high values (SFE 15–SFE 18) dinoflagellates make up 97.34%–99.65% of the flora, the remainder being spores, bisaccate pollen and acritarchs. The terrestrially-derived component can be explained by normal run-off in a shelf environment or by simple rainfall. This set of results is in line with the data of Marshall and Batten (1988), although these authors only reported on the floral content of two samples from South Ferriby. Dinoflagellate cyst diversity (Figure 7), recorded by counts on standard strewn mount slides, ranges from 22 to 45 in the four productive samples. A typical Cenomanian assemblage yields 50–65 dinoflagellate cyst species, indicating a much lower level in the "Black Band" facies. SFE 15, in particular, has a very reduced assemblage. The flora is very restricted, being totally dominated by the *Cyclonephelium compactum-membraniphorum* complex and *Eurydinium saxoniensis*. Granular amorphous organic matter is quite common in sample SFE 17. Marshall and Batten (1988) concluded that this palynofacies represents a stressed environment with a low level of oxygen extending up into the water column. We confirm their suggestion that this distinctive palyno-horizon is primarily the result of abnormal preservational conditions at a time of otherwise reduced floras. The pattern of exctinctions/disappearances described by Tocher (in Jarvis *et al.*, 1988) from the Plenus Marl Formation at Dover is barely discernible here because of the distortion created by the barren samples and the exceptional preservation.

Foraminifera

The samples collected during this investigation have been investigated for foraminifera and the data so generated have been integrated with those of Hart and Bigg (1981). The extinction of *Rotalipora cushmani* (Morrow) is confirmed at the sub-plenus erosion surface. *Rotalipora greenhornensis* (Morrow) has never been recorded this far north in the UK and so can be left out of the discussion. In the Western Interior (USA) successions (e.g. Pueblo) *R. cushmani* disappears at, or about, the level of the lower (of two) geochemical anomalies (Orth *et al.*, 1988). In most UK successions (e.g. Dover, Eastbourne) *R. cushmani* extends above the sub-plenus erosion surface and the absence of this taxon at South Ferriby confirms the hiatus predicted from the geochemical data. The further work reported here has not clarified the position over the base of the *Praeglobotruncana helvetica* (Bolli) zone. The transitional forms of *Whiteinella* (?) *praehelvetica* (Trujillo) create an unrealiable datum at such a northerly palaeolatitude. The dominance of the *Hedbergella/Whiteinella* fauna at this level is confirmed, particularly in samples SFE 17 and SFE 18. The characteristic increase in small buliminids and simple agglutinated foraminifera is also confirmed within the black mudstones of samples SFE 15–SFE 19.

The near total loss of the typical Cenomanian benthonic fauna again occurs at the sub-plenus erosion surface. In southern England (Jefferies 1962, 1963; Carter and Hart, 1977; Jarvis *et al.*, 1988) this survives through to the top of Bed 1. The overlying very latest Cenomanian and earliest Turonian is characterised by an

impoverished benthonic fauna. *Gavelinella berthelini* (Keller) is by far the most abundant species and this morphotype is characteristic of reduced oxygen conditions at this stratigraphic level in SE England (Jarvis *et al.*, 1988), the Western Interior (Eicher and Worstell, 1970) and the Brazilian Continental Margin (Koutsoukos, 1989; Koutsoukos *et al.*, 1990).

SEM analysis

A considerable number of specimens have been investigated using a Link X-ray analysis system attached to a JEOL 35C SEM. This work has located the geochemical anomalies (in a semi-quantitative sense) and investigated diagenetic overprinting.

The "Black Band" itself (Figure 8) consists of finely disseminated clay minerals, which in the very organic-rich mudstones are devoid of visible calcareous fossils. In the more marly sediments (Figure 9) calcareous nannofossils are clearly visible and although slightly thickened by overgrowths, are still identifiable. This does not therefore, represent a residual clay that has formed by dissolution of a carbonate mud. The upper part of the Louth Member (Figure 10) shows a typical mud-free chalk rich in calcareous nannofossils, while those samples from the overlying *Inoceramus*-rich chalks (Figure 11) show a clean, porous, cement-free chalk that is almost entirely composed of calcareous nannofossils.

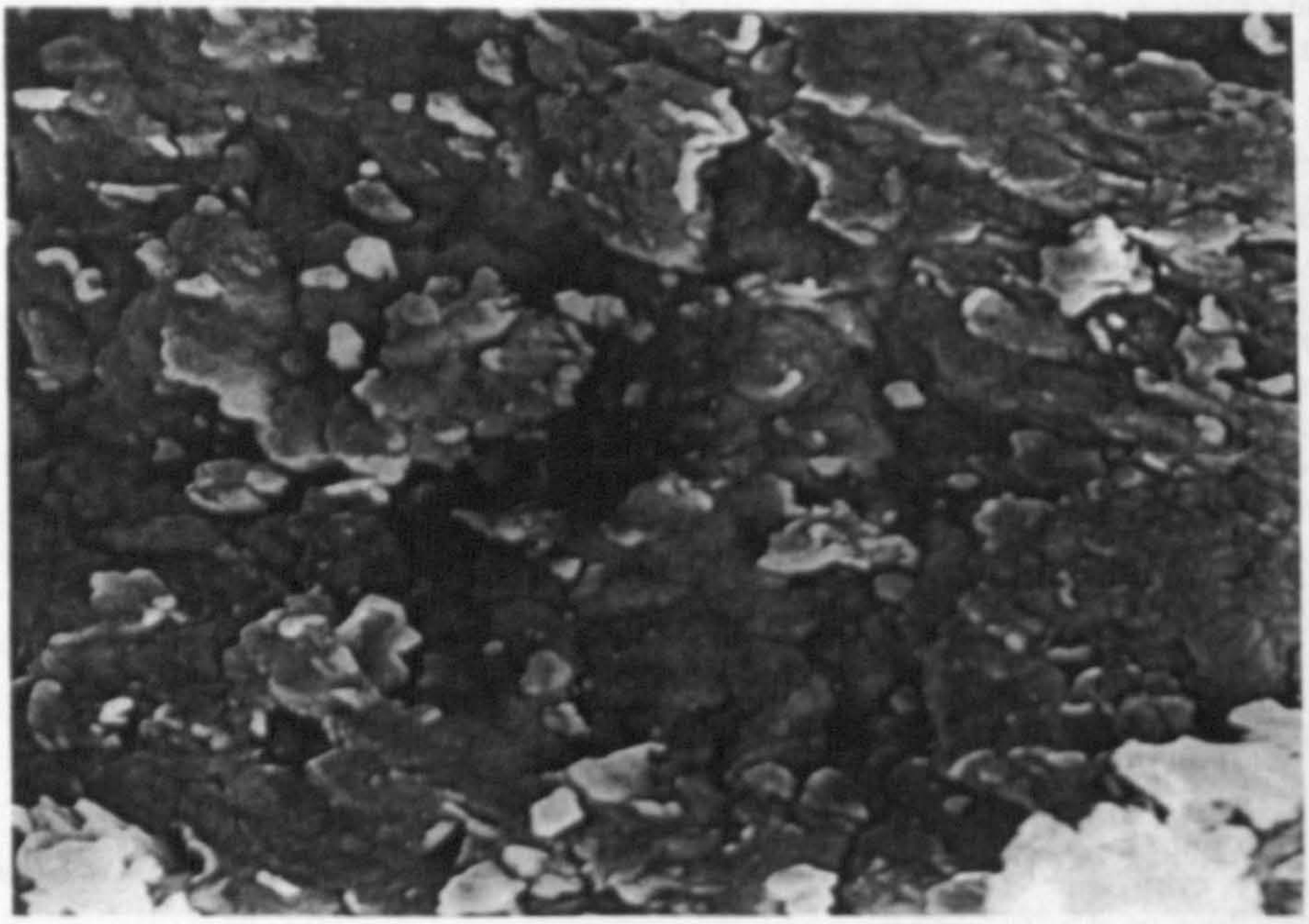

Figure 8 Finely laminated mudstone from South Ferriby (sample SFE 18). Field of view 25 μm.

Figure 9 Interbedded black/cream mudstones (Sample SFE 19) showing abundant calcareous nannofossils (*Haqius* sp. cf. *H. circumradiatus* (Stover)). Field of view 25 μm.

Figure 10 Sample SFE 4 from the upper part of the Louth Member showing abundant calcareous nannofossils, including *Cylindralithus coronatus* Bukry. Field of view 25 μm.

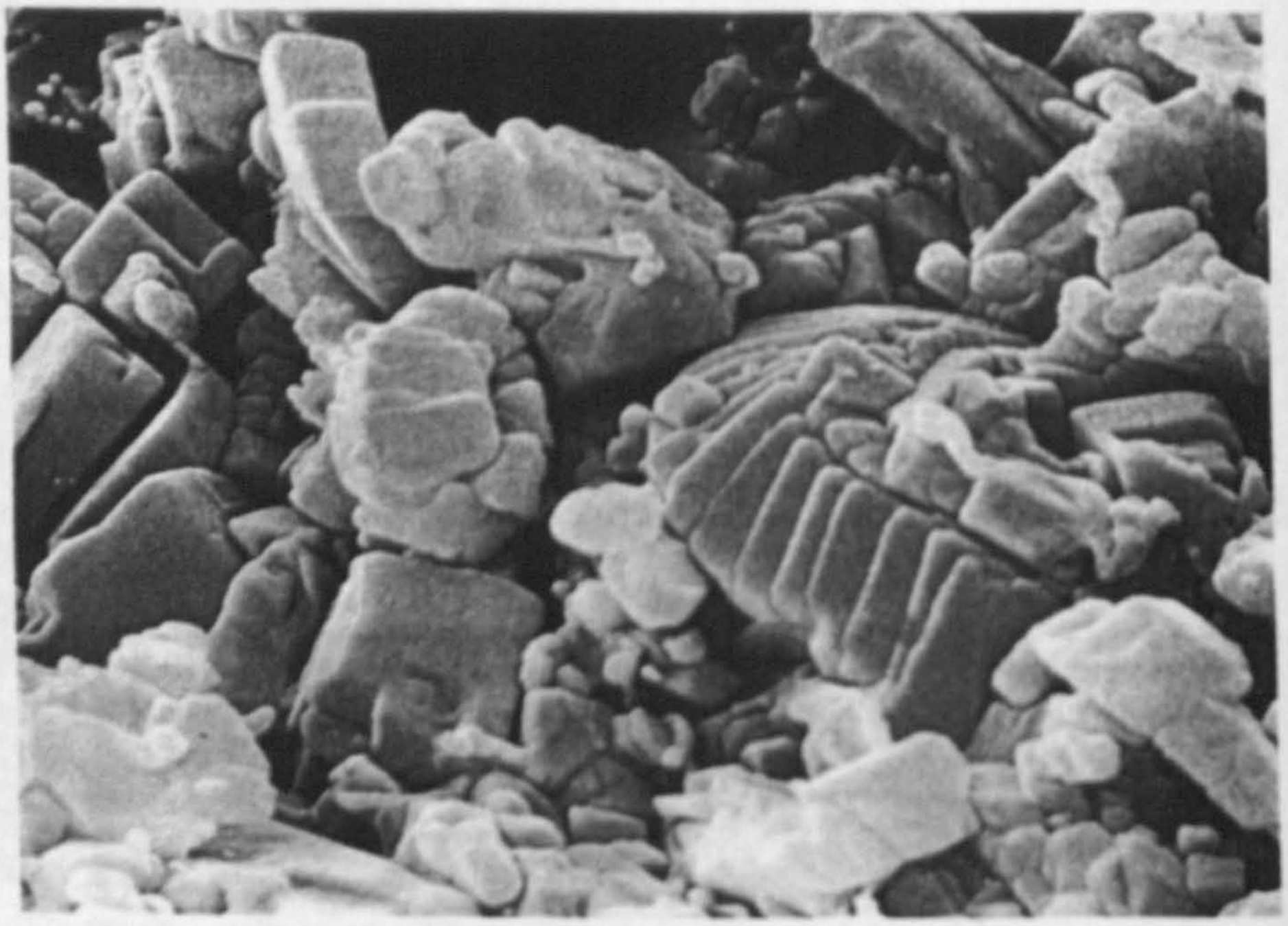

Figure 11 Sample SFE 13 from the *Inoceramus*-rich chalks above the extinction event. Field of view 20 μm.

SUMMARY

These new data from Humberside, it is hoped, will further refine our knowledge of the Late Cenomanian event. The presence of the well-known $\delta^{13}C$ isotopic excursion is confirmed. The micropalaeontological work reported here further refines our knowledge of the foraminiferal succession (*vide* Hart and Bigg, 1981) and provides floral data that confirm the "Black Band" as a horizon of exceptional preservation rather than enhanced productivity. The thinning of the "Black Band" across a depositional high (in North Norfolk) has been confirmed and its relationship to the Plenus Marls Formation explored. The gravity anomaly map of the UK quite clearly displays a feature trending E/W across N Norfolk in exactly the position required to separate the Plenus Marl Formation (Anglo-Paris Basin) and the "Black Band" (East Midlands Shelf). The correlations shown in Figure 2 are quite supportive of this model.

The detailed micropalaeontological work, currently in progress, will expand our knowledge of these successions considerably and the integration of the isotope and geochemical data will allow an independent inter-basinal correlation. The diagenesis of the succession (Jeans, 1980) and the resulting black/red/green mudstones that are contemporaneous with at least a part of the Plenus Marl Formation of Southern England indicates an interesting geochemical history (see Curtis, 1978, for possible models).

It is quite clear that the late Cenomanian global bioevent is only a part of a complex series of changes in the global environment at this level. Only very detailed work, such as that undertaken in Humberside and Lincolnshire, will advance our knowledge further.

Acknowledgements

The authors acknowledge the advice and co-operation of their colleagues in our various institutions. The work of M.B.H. and P.D. was supported by the Faculty of Science, Polytechnic South West. A.D. acknowledges the receipt of a Polytechnic South West research assistantship (1987–90); P.W.D. the receipt of a NERC studentship. Mr J. Abraham prepared the final diagrams while Ms M. Luscott-Evans typed the manuscript in its various stages of preparation.

References

Arthur M.A., Schlanger, S.O. and Jenkyns, H.C. (1987) The Cenomanian–Turonian Oceanic Anoxic Event, II. Palaeoceanographic controls on organic matter production and preservation. In *Marine Petroleum Source Rocks, Special Publication of the Geological Society of London*, edited by J. Brooks and A. Fleet, **26,** 401–420

Carter, D.J. and Hart, M.B. (1977) Aspects of mid-Cretaceous stratigraphical micropaleontology. *Bulletin British Museum Natural History (Geology)*, **29,** 1–135

Curtis, C.D. (1978) Possible links between sandstone diagenesis and depth-related geochemical reactions occurring in enclosing mudstones. *Journal of the Geological Society*, **135,** 107–117

Eicher, D.L. and Worstell, P. (1970) Cenomanian and Turonian foraminifera from the Great Plains, United States. *Micropaleontology*, **16,** 269–324

Funnel, B.M. (1987) Anoxic non-events; alternative explanations. In *Marine Petroleum Source Rocks*, edited by J. Brooks and A.J. Fleet, Geological Society, London, Special Publication, **26,** 421–422

Hancock, J.M. (1976) The petrology of the chalk. *Proceedings of Geological Association*, **86,** 499–535, for 1985

Hart, M.B. (1980) The recognition of mid-Cretaceous sea-level changes by means of Foraminifera. *Cretaceous Research*, **1,** 289–298

Hart, M.B. and Bigg, P.J. (1981) Anoxic events in the late Cretaceous chalk seas of North-West Europe. In *Microfossils of Recent and Fossil Shelf Seas*, edited by J.W. Neale and M.D. Brasier, Chichester, 177–185

Hart, M.B. and Leary, P.N. (1989) The stratigraphic and palaeogeographic setting of the late Cenomanian 'anoxic' event. *Journal of the Geological Society, London*, **146,** 305–310

Hays, J.D. and Pitman, W.C. (1973) Lithospheric plate motion, sea level changes and climatic and ecological consequences. *Nature*, **246,** 16–22

Jarvis, I., Carson, G.A., Cooper, K., Hart, M.B., Horne, D., Leary, P.N., Rosenfeld, A. and Tocher, B.A. (1988) Chalk microfossil assemblages and the Cenomanian-Turonian (late Cretaceous) oceanic anoxic event, new data from Dover, England. *Cretaceous Research*, **9,** 3–103

Jeans, C.V. (1973) The Market Weighton structure: tectonics, sedimentation and diagenesis during the Cretaceous. *Proceedings of the Yorkshire Geological Society*, **39,** 409–444

Jeans, C.V. (1980) Early submarine lithification in the Red Chalk and Lower Chalk of eastern England: a bacterial control model and its implications. *Proceedings of the Yorkshire Geological Society*, **43,** 81–157

Jefferies, R.P.S. (1962) The palaeoecology of the *Actinocamax plenus* subzone (lowest Turonian) in the Anglo-Paris Basin, *Palaeontology*, **4,** 609–647

Jefferies, R.P.S. (1963) The stratigraphy of the *Actinocamax plenus* subzone (lowest Turonian) in the Anglo Paris Basin, *Proceedings of the Geologists' Association*, **74** (1), pp 1–43

Leary, P.N. and Hart, M.B. (1989) The use of the ontogeny of deep water dwelling planktonic foraminifera to assess basin morphology, the development of water masses, eustasy and the position of the oxygen minimum zone in the water column. *Mesozoic Research*, **2,** 67–74

Koutsoukos, E.A.M. (1989) Mid to Late Cretaceous microbiostratigraphy, palaeo-ecology and palaeogeography of the Sergipe Basin, Northeastern Brazil. Unpublished Ph.D. Thesis, Polytechnic South West/CNAA, 2 vols

Koutsoukos, E.A.M., Leary, P.N. and Hart, M.B. (1990) Latest Cenomanian–earliest Turonian low-oxygen tolerant benthonic foraminifera: a case study from the Sergipe Basin (N.E. Brazil) and the western Anglo-Paris Basin (southern England). *Palaeogeography, Palaeoclimatology, Palaeoecology*, **77,** 145–177

Marshall, K.L. and Batten, D.J. (1988) Dinoflagellate cyst associations in Cenomanian–Turonian "Black Shale" sequences of northern Europe. *Review of Palaeobotany and Palynology*, **54,** 85–103

Orth, C.J., Attrep, M., Mao, X.Y., Kauffman, E.G., Diner, R. and Elder, W.P. (1988) Iridium abundance maxima in the Upper Cenomanian extinction interval. *Geophysical Research Letters*, **15,** 346–349

Raup, D.M. and Sepkoski, J.J. Jnr. (1984) Periodicity of extinctions in the geologic past. *Proceedings of the National Academy of Science*, 81, 801–805

Schlanger, S.O. and Jenkyns, H.C. (1976) Cretaceous oceanic anoxic events; causes and consequences. *Geol. Mijnbouw*, 55, 179–184

Schlanger, S.O., Arthur, M.A., Jenkyns, H.C. and Scholle, P.A. (1987) The Cenomanian-Turonian Oceanic Event, I. Stratigraphy and distributions of organic-rich beds and the marine 13C excursion. In *Marine Petroleum Source Rocks*, edited by J. Brooks and A. Fleet, *Geological Society of London Special Publication*, 26, 371–399

Vogt, P.R. (1989) Volcanogenic upwelling of anoxic nutrient-rich water: A possible factor in carbonate bank/reef demise and benthic faunal extinctions? *Bulletin, Geological Society of America*, 101, 1225–1245

Wood, C.J. and Smith, E.G. (1978) Lithostratigraphical classification of the Chalk in North Yorkshire, Humberside and Lincolnshire. *Proceedings of the Yorkshire Geological Society*, 42, 263–287